# Hadron models and related New Energy issues

edited by
F. Smarandache and V. Christianto

Including articles never before published

InfoLearnQuest, USA
November 2007
ISBN: 978-1-59973-042-4

# Hadron models and related New Energy issues

edited by
F. Smarandache & V. Christianto

InfoLearnQuest Publisher, USA
November 2007
ISBN: 978-1-59973-042-4

This book can be ordered in a paper bound reprint from:

**Books on Demand**
**ProQuest Information & Learning**
**(University of Microfilm International)**
300 N. Zeeb Road
P.O. Box 1346, Ann Arbor
MI 48106-1346, USA
Tel.: 1-800-521-0600 (Customer Service)
http://wwwlib.umi.com/bod/basic

Copyright 2007 by **InfoLearnQuest** and Authors for their papers.

Plenty of books can be downloaded from the following E-Library of Science:
http://www.gallup.unm.edu/~smarandache/eBooks-otherformats.htm

**Peer-reviewers of this book:**

1. **R.M. Kiehn** – Professor Emeritus, University of Houston, Houston.
2. **E. G. Bakhoum** – Professor of Electronics Engineering, University of West Florida; formerly Professor in Dept. of Electronic Engineering, New Jersey Institute of Technology, New Jersey.
3. **C. Castro** – Center for Theoretical Studies of Physical Systems, Clark Atlanta University, Atlanta, Georgia.

**ISBN: 978-1-59973-042-4**

**Standard Address Number: 297-5092**
**Printed in the United States of America**

# Hadron models and related New Energy issues

The present book covers a wide-range of issues from alternative hadron models to their likely implications in New Energy research, including alternative interpretation of low-energy reaction (coldfusion) phenomena.

The authors explored some new approaches to describe novel phenomena in particle physics. M Pitkanen introduces his nuclear string hypothesis derived from his Topological Geometrodynamics theory, while E. Goldfain discusses a number of nonlinear dynamics methods, including bifurcation, pattern formation (complex Ginzburg-Landau equation) to describe elementary particle masses. Fu Yuhua discusses a plausible method for prediction of phenomena related to New Energy development.

F. Smarandache discusses his unmatter hypothesis, and A. Yefremov *et al*. discuss Yang-Mills field from Quaternion Space Geometry. Diego Rapoport discusses theoretical link between Torsion fields and Hadronic Mechanic.

A.H. Phillips discusses semiconductor nanodevices, while V. and A. Boju discuss Digital Discrete and Combinatorial methods and their likely implications in New Energy research.

Pavel Pintr *et al*. describe planetary orbit distance from modified Schrödinger equation, and M. Pereira discusses his new Hypergeometrical description of Standard Model of elementary particles.

The present volume will be suitable for researchers interested in New Energy issues, in particular their link with alternative hadron models and interpretation.

While some of these discussions may be found a bit too theoretical, our view is that once these phenomena can be put into rigorous theoretical framework, thereafter more 'open-minded' physicists may be more ready to consider these New Energy methods more seriously. Our basic proposition in the present book is that considering these new theoretical insights, one can expect there are new methods to generate New Energy technologies which are clearly within reach of human knowledge in the coming years.

November 8th, 2007
FS & VC

## Preface

The work of the epistemologist T. Kuhn pointed out that science is a social construction, which integrates into the whole social fabric, interacting and integrating with it in the construction of a whole world view. Thus, it is part of a cultural system such as is the economy, politics, the arts, the legal systems, religions, etc. The validation of this system we know as science runs from the effectiveness of producing sustainability of its own existence: Cultural systems are autopoietic, they are self-producing. From time to time, this validation is called into question. Experiences may surprise some of the producers of this system; also, examination of the purported true world view can be pursued theoretically, and inconsistencies may appear which will lead to new theories. This will lead in some instances to the realization of new experiments which will be the framework for the validation or invalidation of this ideas. Whatever may be the contents of this cognitive system which we know as science (in fact it only exists as an ideal, we only know of the existence of the sciences, with no integration of them), one of the first clues to its validation stands in the fact that these self-producing systems, by consistence, should be able to persist in time: Humankind which produce these cognitive systems, should exist to produce them and be produced by them. This is starting to be perceived as barely possible. Cataclysmic climate changes are taking a serious toll of lifes and the validity of our world view is brought into question. The destruction of the world in which we live appears to be the cause of these changes.

In one side we have constructed cognitive systems which function in the only way they can, through languages, and in the other hand we are not far from our ancestors burning perishable material which has not been processed with any deep linguistic process, with the notable exception of the use of fission processes with their possible environmental impact that has not been solved yet. Some of the ideas being proposed is the use of biofuels, which itself is not sustainable with due integration of Humankind, and then by the validation criteria of a cultural system to be a life supporting view, it should be strategically discarded. Other ideas go back to the Tomahawk project of fusion, which started decades ago, and has produced no results till today.

None of these approaches take in account that the present frontier of knowledge of the science of physics is space and time. Of course, any physics student has heard about zero-point energies and the apparent existence of processes which do not conform to the present cognitive system. Governmental and private laboratories around the globe are carrying research in these processes.

This book is a small step in examining space and time structures, and

the claims that they may appear to be the source for the new self-producing energies we might be searching for. The theories we shall be presenting have evolved in the last two or three decades. Some of them have reached already the stage of industrial implementations. Others are original and in their initial stages of development.

Returning to our introductory words, no cognitive system stands as an eternal source of life and we intend by these contributions to invite others to examine the world in their own views and to participate in the construction of the ideas presented in this volume.

D.R.

# Contents


Peer-reviewers ii
Abstract iii
Preface by D. Rapoport iv
Contents vi
Foreword viii
Prologue: Socio-economic impact of New Energy technologies xi
Contributors to this volume xiv
Short biography of Contributors xv

## Free energy and Topological Geometrodynamics

1. Nuclear string hypothesis – M. Pitkanen 1
2. The notion of free-energy and many-sheeted Space-Time concept – M. Pitkanen 44
3. Prediction and calculation of New Energy development – Fu Yuhua 111
4. Some unsolved problems in the physics of elementary particle – V. Christianto & F. Smarandache (*PiP*, vol. 3 no. 4, 2007) 127
5. About some unsolved problems in physics – M. Pitkanen 132

## Beyond Standard Model, Unmatter and Yang-Mills Field

6. Bifurcations and pattern formation in particle physics: an introductory study – E. Goldfain (submitted to *APS conference,* 2008) 151
7. Dynamics of Neutrino oscillations and the Cosmological constant problem – E. Goldfain 168
8. Fractional dynamics and the Standard Model of Elementary particles – E. Goldfain (*Comm. In Nonlin. Science and Numerical. Simulation*, 2007) 176
9. A new possible form of Matter, Unmatter – formed by particles and anti-particles – F. Smarandache (*PiP*, vol. 1, 2005, www.ptep-online.com) 184
10. Verifying Unmatter by experiments, more types of Unmatter and a Quantum Chromodynamics formula – F. Smarandache (*Progress in Physics*, vol. 2, 2006, www.ptep-online.com) 189
11. Unmatter entities inside nuclei, predicted by the Brightsen Nucleon Cluster Model – F. Smarandache & Dmitri Rabounski (*Progress in Physics*, vol. 2, www.ptep-online.com) 198
12. Yang-Mills field from Quaternion space geometry, and its Klein-Gordon representation – A. Yefremov, F. Smarandache, V. Christianto (*Progress in Physics,* vol. 3 no. 3, 2007, www.ptep-online.com) 208
13. Numerical solution of radial biquaternion Klein-Gordon equation – V. Christianto & F. Smarandache (*Progress in Physics*, vol. 4 no. 1, Jan. 2008, www.ptep-online.com) 220
14. A new derivation of biquaternion Schrödinger equation and plausible implications – V. Christianto & F. Smarandache (*Progress in Physics*, vol. 3 no. 4, 2007, www.ptep-online.com) 223

15. An exact mapping from Navier-Stokes equation to Schrödinger equation via Riccati equation – V. Christianto & F. Smarandache (*Progress in Physics*, vol. 4 no. 1, Jan. 2008, www.ptep-online.com) 229
16. A note on possible translation of Schrodinger's uncertainty theorem into modern uncertainty notations – V. Christianto & F. Smarandache 233

**Torsion field, Astrophysics quantization, Mesoscopic physics, and Hypergeometrical universe**

17. Torsion fields, Brownian motions, Quantum and Hadronic mechanics – D. Rapoport 236
18. Distribution of distances in solar system – V. Perinova, A. Luks, and Pavel Pintr (CSF, 2007) 293
19. Nanotechnology and semiconductor nanodevices – A.H. Phillips 308
20. Digital, Discrete and Combinatorial Methods in an Euclidean or Riemannian context – V. Boju and A. Boju 332
21. The Hypergeometrical Standard Model – M. Pereira 382
22. Interpretation of solution of radial biquaternion Klein-Gordon equation, and comparison with EQPET/TSC model – V. Christianto & F. Smarandache 436
23. A note on computer solution of wireless energy transmitted using magnetic resonance – V. Christianto & F. Smarandache (*Progress in Physics*, vol. 4 no. 1, Jan. 2008, www.ptep-online.com) 439

**Index** 443

# Foreword

"*Any sufficiently advanced technology is indistinguishable from magic*," says Arthur Clarke. While his idiom may be true for most of advanced technologies surrounding our modern society, the notion of 'new energy' as described herein may have been around in the air for years, with scattering results, from just another obscure promise to really impressive results.

Yet in this book some authors have been invited to write on particular aspects of New Energy issues, especially those which may be related to (alternative) hadron models. In the light of the fact that most of 'New Energy' assessment belongs to two categories: either eulogizing the new method(s), or denouncing-style by 'conventional mainstream' physicists, in this book the authors offer some new *theoretical insights*, which may be found useful in order to understand these phenomena related to New Energy methods.

In the first chapter, M. Pitkanen discusses how coldfusion experiments (http://www.lenr-canr.org ) can be explained using *'nuclear string hypothesis'* based on his TGD theory (#1). Interestingly, a recent report explains that there are chemical reactions which remain rapid down to temperatures as low as a few kelvin.[1] In other chapter, he also discusses some critical issues of Free Energy technologies found in the literature (#2), in particular from the viewpoint of his Topological Geometrodynamics model (TGD). It seems to be the first attempt of its kind to put these technologies under rigorous framework. He also discusses a number of open problems in theoretical physics, in particular from the viewpoint of TGD theory (#5).

Fu Yuhua describes a plausible method to predict some phenomena which may affect New Energy development (#3).

Thereafter, E. Goldfain discusses a number of open problems in the present Standard Model of elementary particles, in particular from the viewpoint of nonlinear dynamics theory (bifurcation, pattern formation, complex Ginzburg-Landau *etc*.), which may open a new path to find 'untapped energy' hidden in the formation of elementary particles (#6, #7, #8). It seems more interesting to note that Goldfain's methods reveal hidden link between micro-systems and large scale systems. Although some physicists prefer to call this 'plausible' link as 'scale invariant principle' or 'scale relativistic principle', one can remember that the same principle has been known in the past century as '*Mach principle'* (i.e. the seemingly hidden connection between our Earth and galaxy rotation, especially in Newtonian rotating bucket experiment).[2] Alternatively, one can describe this 'hidden link' between micro-systems and macrosystems as '*scale-entanglement'*, as an equivalent term to 'quantum entanglement'.

In subsequent chapter, Perinova, Luks, and Pintr also describe how modified Schrödinger equation can describe planetary orbit distances around the Sun (#18), which seems to suggest that the same equation that was normally used to describe quantum phenomena at microscale can also be used to describe orbits at astrophysics scale. All of these aforementioned new methods may seem to reflect a Japanese *koan*:[3]

A thousand
kaleidoscopic world

inside
a light snow

the inside
is also

a light snow

(Ryokan)

F. Smarandache offers his new term '*unmatter*' which may be useful in describing some unexplained phenomena, in particular with regards to Brightsen's *closed-packed cluster* model of nuclei (#9, #10, #11). This model which seems quite similar to the *close-packed spheron* model by Linus Pauling in 60s, may offer a new thinking on nuclei structure.

A. Yefremov, F. Smarandache, and V Christianto discuss a new insight that Yang-Mills field can be viewed as pure geometrical aspect of quaternion space geometry, and its link to Klein-Gordon equation, in particular using biquaternion differential operator (#12, #13). They extend further to describe biquaternion Schrödinger equation (#14). Some unsolved problems in the elementary particle physics are also discussed (#4).

In the meantime, Diego Rapoport extends his *geometro-stochastic* theory of quantum mechanics and gravitation to the strong interactions, by including in his framework the theory of Hadronic Mechanics (#17). In this setting, it is derived as a group-theoretical modification of torsion, and the isotopic Santilli-Schrödinger equation is treated as torsion geometry with an associated diffusion process. Alike to Quantum Mechanics in which the Schrödinger wave function produces torsion, in Hadronic Mechanics the wave function of the composite also produces a torsion field. This sets in a general framework, ad-hoc models of fusion treated as diffusions in the already standard approach to the problem. As well, the association of torsion with kinetic theory and rotations is elaborated. The isotopic theory of the strong interactions due to Santilli has developed to include an

extension of Quantum Chemistry known as Hadronic Chemistry, which has lead to the development, already in an industrial level, of plasmas and of clean fuels.

A. Phillips discusses some new ideas with respect to nanotechnologies, which may be found useful in the context of new energy technologies (#19). Thereafter, V. Boju and A. Boju discuss a new concept called Digital, Discrete and Combinatorial Methods and their implications to New Energy research (#20).

M. Pereira describes how most experimental data can be explained using his hypergeometrical theory of Standard Model, despite his theory is a quite different from the standard theory of elementary particles (#21). The theory indicates the possibility of a paradigm shift from Nuclear Chemistry to Nonlinear Hadronics methods similar to the ones used in *nonlinear optics* using four dimensional phase-matching. For a recent conference on hyperbolic space, see [4].

Of course, some of these discussions may be found a bit too theoretical, but our view is that once these phenomena can be put into rigorous theoretical framework, thereafter more 'open-minded' physicists may be more ready to consider these New Energy methods more seriously. Our basic propositions in the present book is that considering these new theoretical insights, one can expect that there are new methods to generate New Energy technologies which are clearly within reach of human knowledge in the coming years.

We would like to extend our gratitude to D. Rabounski and L. Borissova for their kind permission to publish the articles from *Progress in Physics* Journal. And special thanks to all contributors for their creative efforts and permission to include their works in this volume; and also to Profs. R.M. Kiehn, Ezzat G. Bakhoum, and C. Castro for their kind willingness to proof-read and review this book. Also special thanks to numerous colleagues all over the world, who have shared ideas with us over these years.

October 29th, 2007
FS & VC

---

[1] See H. Sabbah *et al*., "Understanding reactivity at very low temperatures: The reactions of oxygen atoms with alkenes," *Science* magazine, vol. 317, July 6th, 2007, p.102. http://www.sciencemag.com.

[2] Another variation of this theme is known in ancient belief, saying that the galaxy center (called 'Hunab Ku', cf. Scott Hyman, 2005, http://www.achtphasen.net/index.php/2007/01/17/p153 ) is the center of creation and also affects the well-being of people in Earth. Interestingly, there is also a recent debate over the question whether the galaxy center affects climatic changes (www.physicalgeography.net/fundamentals/7y.html). For a recent reference of 'scale entanglement' term, see for instance: 'Multi-Scale Entanglement Renormalization Ansatz,' http://front.math.ucdavis.edu/0710.3829

[3] Quoted from an email to Sarfatti Physics Seminar, May 18, 2007, at 7:06 PM.

[4] *Science* magazine, "Geometry and imagination: In hyperbolic space, size matters," vol. 317, July 6th, 2007, p.38. http://www.sciencemag.com.

# Prologue: Socio-Economic impacts of New Energy technologies

As we all know, Energy is all as controversial as always, in particular if one uses this word in conjunction with 'new' or 'alternative' word, the resulting controversy become more adverse. Part of this controversy may come from the fact that most of 'alternative energy' technologies are not 'scalable' enough, i.e. they cannot compete with conventional ones in terms of massive implementation, for instance to replace energy use for mass-rapid transportation system.

Other controversy may take place because sometimes these new energy technologies have been implemented just for the hype purposes. For example, a '*solar-cell based reading-lamp'* may be not as useful as what its designer expects, because by the time there is enough 'solar energy' (at daylight) more people would prefer to read books or magazines without lamp at all. There are similar examples that the 'new energy' term has been used in conjunction with *'New Age'* philosophy or wherever *'back to nature'* jargon can be exploited solely for the hype purposes, instead of improving energy use efficiency at large-scale.

Nevertheless, if we call these 'new' unexplored alternative energy technologies as 'New Energy', it is by no means to indicate that we are promoting a *'free energy'* market. First of all, research on untapped energy technologies is likely to require a substantial amount of initial support, which may be quite similar or comparable to the amount needed to survey wells in conventional oil exploration. Therefore to discuss 'New Energy' issues is not the same as saying that these alternatives are 'costless' either to government, scientists or to the people, in particular at the initial phase of its development.

For comparison purpose, one may use the *'open source'* movement as analogue story. Despite the open-source movement (mostly was inspired by R. Stallman's GNU/GPL license) indicates that there is 'no (*or less*) license fee' required to purchase a particular computer software, there are remaining modification, scalability and other issues required to be considered before this 'open source' technology could be implemented in industrial scale. Continuing this analogue story, one may use the IT hardware(s) to indicate 'scale' of energy generating technologies, see Table 1.

Table 1. Comparison between IT hardware scale and Energy generation scale

| IT hardware 'scale' | Energy generation 'scale' | Implication to New Energy methods |
|---|---|---|
| PDA/mobile device | Mobile energy cells | - Fuel-cell based PDA, better reusable battery etc. |
| Standalone PC | Individual energy generator | - Wind-power home energy, solar-cell vehicle |
| LAN | Village-based energy generator | - Microhydro generator |
| Grid/MAN | National/city-wide energy | - Alteration or Combination of the above |

Note: LAN= local area network; MAN=metropolitan area network

It shall be clear therefore that perhaps there are not much choices available yet for Grid/National-wide energy supply system, therefore in the near future the existing method is likely to continue (unless someone can achieve a breakthrough in hotfusion/ITER[6] or using laser fusion method, see www.focusfusion.org). But, perhaps there are more choices and market for other energy applications (mobile energy cells, home-based energy, or village-based energy system). Most of the 'New Energy' methods discussed in this book may be more suitable for these (small-scale) applications (for instance, see paper by A.H. Phillips).

Furthermore, the production and distribution technologies given a 'New Energy' method is ready for full-scale implementation may be quite considerable,[5] let alone its socio-economic ramifications, such as costs required to change the present energy-generating technologies to the new-energy ones. For instance, while LNG (liquid natural gas) engine for vehicles (cars) has been already known since more than a decade ago, it is not so easy to implement the alternative LNG-based engine to replace the all-pervasive gasoline/diesel-driven engines.[7] Perhaps the only exceptional story in this regard is Brazil, which is able to alter their (transportation) energy mode from gasoline to renewable energy sources within a few decades.

But by then the question as to how to replicate this story to other (developing) countries may require not only 'ready-to-implement' New Energy technologies, but may also involve socio-economic aspects of the particular country. And also what are the critical success factors behind this exceptional story may require another intensive study.

These interesting issues, however, are beyond the scope of this book, which limits itself in particular to theoretical considerations of some hadron models and their plausible links to New Energy issues. In this regards, allow us to quote here a remark by Arthur Clarke: "*It is now beyond serious dispute that anomalous amount of energy are being produced from hydrogen by some unknown reaction*." [8]

Another limitation of this book is, of course, that we only discuss alternative energy issues from the viewpoints of physicists. Other viewpoints of renewable energy sources, for instance from biochemistry and biotechnology viewpoints which may prefer *synthetic biology* processes or using *isoprenoids,*[9] are outside the reach of this book. But perhaps this omitting is for a good reason, because some of these technologies will require special enzyme(s) as catalyst which is available only at considerable price, therefore these alternatives may not be an appropriate choice for developing countries.

As concluding note, the authors hope that the present book may inspire further study on how some of these New Energy ideas/technologies discussed herein can be implemented in more practical way in the near future.

October 29th, 2007
FS & VC

---

[5] An alternative method for distributing energy is using wireless technology, but thus far it remains in research stage, with ~40% efficiency. See A. Kurs *et al.,* "Wireless power transfer via strongly coupled magnetic resonance," *Science* magazine, vol. 317, July 6th, 2007, p.83. www.sciencemag.com

[6] It is known that the Hot Fusion method faces complicated problems caused by magnetohydro-dynamics (MHD) instability of plasma confinement.

[7] Considering the fact that technology choices are part of 'social construct' – at least in the sense of Habermas' viewpoint -, some researchers argue that the gasoline-engine is a good example of '*technological locked-in'* problem (while others may prefer '*technology inertia'* word).

[8] Clarke, A.C., "2001: The coming age of hydrogen power," *Infinite Energy* 4(22) (1998) p.15.

[9] *The Economist*, "Ethanol, schmethanol," Sept. 29th, 2007, p.80.

# Contributors to this volume


1. **M. Pitkanen** – Dept. of Physical Sciences, University of Helsinki, Finland
2. **E. Goldfain** – Photonic Center of Excellence, Welch Allyn Inc., NY, USA
3. **D. Rapoport** – Dept. of Sciences and Technology, Universidad Nacional de Quilmes, Buenos Aires, Argentina
4. **A.H. Phillips** – Faculty of Engineering, Ain-Shams University, Cairo
5. **Fu Yuhua** – China Offshore Oil Research Center, PO Box 4728, Beijing, 100027, China
6. **Fu Anjie** – Microsoft Research Asia, Beijing
7. **V. Boju** – Montreal Tech, Montreal, Qc, H3S 2W9, Canada
8. **A. Boju** – Montreal Tech, Montreal, Qc, H3S 2W9, Canada
9. **V. Perinova** – Laboratory of Quantum Optics, Olomouc, Czech Republic
10. **A. Luks** – Laboratory of Quantum Optics, Olomouc, Czech Republic
11. **Pavel Pintr** – Laboratory of Quantum Optics, Olomouc, Czech Republic
12. **M. Pereira** – *390 Greenwich Street,* NY, USA
13. **A. Yefremov** – Institute of Gravitation and Cosmology, People's Friendship University of Russia, Miklukho-Maklaya Str.6, Moscow
14. **D. Rabounski** – Chief Editor, *Progress in Physics* Journal
15. **F. Smarandache** – Chairman Dept. of Mathematics, University of New Mexico, Gallup, USA
16. **V. Christianto** – sciprint.org administrator, A free preprint service without hassles

# Short Biography of Contributors

- **M. Pitkanen** – has worked since 1978 as a free researcher developing a unified theory of fundamental interactions ("*Topological Geometro-dynamics*", PhD thesis 1982). TGD can be regarded either as a modification of general relativity providing a possible solution of the conceptual problems related to the definition of inertial and gravitational energies, or as a generalization of superstring models obtained by replacing strings with 3-dimensional light-like surfaces as basic objects. The first challenge has been the precise formulation of quantum TGD based on the generalization of the Einstein's geometrization program to infinite-dimensional context. The basic observation is that the mere existence requirement in infinite-dimensional context makes the geometry and thus physics highly unique. This program has turned out to require a fusion of several mathematical concepts such as infinite-dimensional geometry, p-adic number fields, classical number fields including quaternions and octonions, and certain von Neumann algebras known has hyperfinite factors of type II_1. One example about resulting fruitful interaction between quantum physics and number theory is a proposal for the proof of Riemann hypothesis relying on conformal invariance (M. Pitkänen (2003), "*A Strategy for Proving Riemann Hypothesis*", *Acta Math. Univ. Comeniae*, vol. 72). Second main challenge has been the deduction of the physical predictions of the theory, in particular the new physics predicted by the theory. During the last decade he has worked also with quantum theory of consciousness emerging as a generalization of quantum measurement theory aiming to resolve the difficult conceptual problems of the standard quantum measurement theory where observer still remains an outsider. The theory of consciousness is also an integral part of TGD proper. TGD forces also a generalization of the formalism of quantum mechanics itself by allowing dynamical and quantized Planck constant. The basic application is the modeling of living systems as macroscopic quantum systems on basis of new physics predicted by TGD. The book "Topological Geometrodynamics" [Luniver Press (2006)] is the latest - already slightly out of date - summary of TGD as a physical theory. The online books at his homepage http://www.helsinki.fi/~matpitka/ provide an overall view of the development of TGD.

- **E. Goldfain** – is a Senior Research and Development Scientist of Welch Allyn Inc., based in Photonics Center of Excellence, Skaneateles Falls, New York, USA. He has 10 patents on optical systems for ophthalmic and bio-medical applications, has published 8 papers in optical sciences and photonics, and 16 papers in theoretical physics. His research interests include opto-mechanical design/engineering for photonic devices; advanced research for novel bio-photonics technologies; and advanced research in theoretical physics (quantum field theory, particle physics, nonlinear science and chaos, quantum optics, nonlinear optics).

- **D. Rapoport** – received his Ph.D. in Tel Aviv, in Mathematical Physics, under the supervisions of Prof. S. Sternberg (Harvard and Tel Aviv) and Prof. Yuval Ne´eman (Tel Aviv, and Austin-Texas). Hold positions in Tel Aviv, Mexico, Rio de

Janeiro, Sao Paulo, Buenos Aires. Presently he is a full professor at the Universidad Nacional de Quilmes, Buenos Aires. Member of the Editorial Committees of Algebras, Groups and Geometries; Hadronic Journal; Hadronic Journal Supplements. Areas of interest: Quantum and Hadronic Mechanics, and Unification Theories through Torsion Geometries. General Systems theories and Autopoiesis. Cognitive Systems and Consciousness. Metascience.

- **A.H. Phillips** – is professor of physics at Faculty of Engineering, Ain Shams University, Cairo, and also a senior lecturer at Higher Institute for Computer Sciences and Information Systems. He also taught Physics courses at the Higher Institute for Engineering and Technology (New Cairo Academy for Sciences and Arta) 5th district, New Cairo city, Egypt. His scientific activities include examination of PhD theses from Austrian and Japanese universities (1998) and from University of Waterloo, Ontario, Canada (2006). He also had developed Physics Lab at Faculty of Engineering, Ain-Shams University, Cairo (funded by World Bank Load, No. 3137 EGT-1993). His research interests include: Quantum effect in mesoscopic superconductor-semiconductor quantum devices and quantum computer; investigation of quantum transport properties of some nanodevices such as quantum dot turnstile with oscillating barrier; spintronics and nanotronics. He has published 14 recent published papers (as a whole he has 60 published papers) in various journals, including *Egypt. J. Physics, Progress in Physics, I.J. of Nanoscience* etc.

- **Fu Yuhua** – is a Senior engineer in China offshore oil research center. He is also Senior research fellow of China Asia-Pacific economy development research center, and Secretary general in Beijing Relativity Theory Research Federation. His research interests include Physics, Mechanics, and Engineering. He is also a prolific writer, with a number of recent publications, including: [1] F. Smarandache, V. Christianto, Fu Yuhua, R. Khrapko, J. Hutchison*, Unfolding the Labyrinth: Open Problems in Physics, Mathematics, Astrophysics, and Other Areas of Science*, Hexis-Phoenix, 2006; [2] Fu Yuhua, On quantization in Astrophysics, in: *Quantization in Astrophysics, Brownian Motion, and Supersymmetry* (editors: Florentin Smarandache, V. Christianto), MathTiger - Chenai, India, 2007; [3] Fu Yuhua, A Unified Variational Principle for Quantization in *Dynamic Smarandache Multi-Space*, http://www.gallup.unm.edu/~smarandache/SE1.pdf; [4] Fu Yuhua, *A Revision to Godel's Incompleteness Theorem by Neutrosophy*, http://www.gallup.unm.edu/~smarandache/SE1.pdf; [5] Fu Yuhua, *Applications of Smarandache's notion to Physics and Conservation of Energy*, http://www.gallup.unm.edu/~smarandache/SE1.pdf

- **Valentin Boju** – is the director of MontrealTech Press ( P.O.Box 78574, Station Wilderton, Montreal, H3S 2W9, Canada, http://pages.videotron.com/nanotech). He was a Professor of Mathematics and director of Doctoral Thesis at Univ. of Craiova, Romania, until 2000. He left Romania for Canada, where he taught at MontrealTech, since 2001. In 2004, he was honored with the title of Officer of the Order "Cultural Merit", Category “Scientific Research”. His research work was primarily in the field of Combinatorial and Riemannian Geometry/Analysis. He discovered the QC-spaces (*Journal of Differential Geom*. 13,1978, #3, 373-383; see also Hwang Cheng Chung : Nanking University, China), as an application of

his method (V. Boju, *Contributions to the Differential Geometry of the gradient operator*. Ph.D. Thesis, Univ. of Bucharest) of Versor Type Functions (VTF). This method (Boju: TV-functions-Univ. of Craiova-1980), equation and hypothesis (co-author Louis Funar, Univ. of Grenoble: A note on the Bonnet-Myers theorem. *Zeitsch. Analysis Anwendungen,* 15, 1996, no. 2), are treated with brilliancy by D. Holcman (Weizmann Inst. of Sci., Rehovot) and C. C. Pugh (Univ. of Berkeley), to solve the problem of the Boundary between Compact and Noncompact Complete Riemann Manifolds (*Indiana Univ.Math.J*., 56, No. 1, 2007). The concepts of "Juxtaposition Combinatorial Measure" and "Generalized Hadwiger Numbers" have been introduced and studied in [V. Boju. Fonctions de juxtaposition, Invariants. In: Proceedings of the 13th NCGT, Univ. of Cluj, 1982, p. 36-37]. Another original method was presented in paper "Zones perturbatrices du mouvement ou de la structure d'un mobile", Polytechnic International Press, Montreal, 2001, pp. 540-543, which can model interesting phenomena such as Bermuda Triangle (http://en.wikipedia.org/wiki/Bermuda_Triangle). He further promoted the Biostatistics and Biomathematics as a discipline within the Department of Medicine of the University of Craiova (see Dr Petrica Badea, www.umfcv.ro/en/Departments/FacultyOfMedicine/Biostatistics/History.html). He was actively involved in coaching college students in problem solving and intuitive mathematics; see MontrealTech Campus programme, based on his books "Problems on Geometry of Differentiable Manifolds", Technical Publishing House, Bucharest (1978), 239 pages (with M. Popescu), "The Math Problems Notebook", Springer/Birkhäuser-Boston, (2007, with Louis Funar) and "Digital, Discrete and Combinatorial Methods in an Euclidean or Riemannian context and Programming Languages Appl.", MontrealTech Press, (2007). He is also a Quebecian music (St-Laurent Large River Blues, Harfang des Neiges, Lys Flower, Hymne du Québec, Symphonic Dance), a composer-author-interpreter (concerts publiques: Parcs Troie, Van Horne, Devonshire and the "Bistro Marseille"-Montreal, subvetionnés par le Gouvernement du Québec), and a member of SOCAN - Society of Composers, Authors and Music Publishers of Canada: http://www.soundclick.com/valentinmusicgroup**.**

- **Antoniu Boju** – (B.A.Sc - Computer Engineering, Concordia University, Montreal, 2003; Software Engineer MontrealTech) has discovered (with V.Boju) the L-K Digital Spaces (© 2005-2007, V. Boju and A. Boju: Digital, Discrete & Combinatorial Methods in an Euclidean or Riemann context and Programming Languages Appl., MontrealTech Press, 2007). He has developed with V.Boju C++, Python & Pascal adjacent Programs & Technologies (Copyright © 2005-2007, V. Boju and Antoniu Boju); also, for Juxtaposition Fractals. The concepts, properties and formulae such as (L; K)-Stability Formulae, (L; K)-Iso-Stable Digital Spaces, Iso-Stability Diophantine Equations; Topological and Metric Structure of (L; K)Digital Spaces, Hybrid Digital Spaces;the cap-polynomial and Polynomial growth of the Digital-Energetic-superstable-Levels; Asymptotic Dimension of Digital Spaces; Hybrid multi-type-CEBGU; the "enveloping mechanism" of Hybrid phenomenon; Super-Fractals; the natural mechanism of the phenomenon of (L; K)-stability, Inverse Quotient Curvature Coefficients were discovered (with V.Boju) by computer search, combinatorial techniques and computer-assisted proofs based on their original Computer Programs.

- **Vlasta Perinova**– is a professor of mathematical physics in the Laboratory of Quantum Optics, Olomouc, Czech Republic. She is an author and a coauthor of monographic chapters in *Modern Nonlinear Optics* (1993, 2001), and a coauthor of monographic chapters in *Progress in Optics* (1994, 2000, 2001). She published 200 scientific papers in mathematical and physical journals in the fields of nonlinear integral equations, application of mathematical statistics in medicine, and of quantum optics. She is a coauthor of a monograph *Phase in Optics* (World Scientific, Singapore, 1998).

- **Antonin Luks**– is a senior scientific worker in the Laboratory of Quantum optics, Olomouc, Czech Republic. He is a coauthor of monographic chapter in Moderm Nonlinear Optics (2001) and in Progress in Optics (1994, 2000, 2001). He published 120 scientific papers in the area of quantum optics. He is a coauthor of a monograph Phase in Optics (World Scientific, 1998).

- **Pavel Pintr** – is a research scientist in the Laboratory of Quantum Optics, Olomouc (2000-2005), Czech Republic, and also a photometry engineer at Koito Czech (2005-). His address is Svatovaclavska 2521, Zatec, 438 01, Czech Republic. Research activities include: Discretization in cosmic scales, Formation of planets in star systems, and polarization in optics. His recent publications include: (i) "The solar system from the quantization viewpoint," *Physica* (2003-2004) 42--43: 195-209; (ii) "Discretization of distances in the Solar system," *Chaos, Solitons & Fractals*, Vol. 34, Issue 3, November 2007, p. 669-676; (iii) "Allowed planetary orbits in the solar system," *Chaos, Solitons & Fractals*, In Press, Corrected Proof, Available online in http://www.sciencedirect.com. Next cooperation is with Dr. Mikula V. (NASA), prof. Perinova V., Dr. Luks A (UP. Olomouc), Dr. Kalenda P. (USMH AVÈR).

- **M. Pereira** – his broad background includes Physical Chemistry (UPenn-PhD), Molecular Biophysics (Assistant Professor at the Albert Einstein College of Medicine), Finance (NYU-MBA, Citigroup), Nuclear Physics (Instituto Tecnologico de Aeronautica (Brazil)-MSc). During his undergraduate electronic engineering education at the Instituto Tecnologico de Aeronautica, Dr. Pereira worked in Solid State Physics at the National Institute for Space Research. Upon graduation, Dr. Pereira joined the Institute for Advanced Studies (Brazil) where he developed research on the photophysics of ladder (IR + UV) and multiphoton absorption processes. Later he went to the University of Pennsylvania for a PhD in Physical Chemistry studying energy transfer mechanisms, rotational dynamics of small molecules, Raman scattering. At the University of Rochester, Dr. Pereira worked in Photonics and Molecular Biophysics. In Molecular Biophysics, Dr. Pereira studied deligation processes in hemoglobin, myoglobin using a novel (IR to UV) broadband femtosecond transient absorption spectrophotometer. Recently, Dr. Pereira work in the field of statistical arbitrage and derivative financial instruments.

- **A. Yefremov** – is head of Institute of Gravitation and Cosmology of People's Friendship University of Russia, Miklukho-Maklaya Str.6, Moscow. His research interests include the use of quaternion and biquaternion number in theoretical physics. In recent years he developed his own theory of Quaternion Relativity theory (Q-relativity in short) and this new theory has been presented in various

scientific journals, including *Gravitation and Cosmology* since 1996. He has also published a book discussing theoretical and mathematical aspects of this Quaternion Relativity theory.

- **D. Rabounski** – Editor in Chief of *Progress in Physics* Journal, USA. He is also active in research related to General Relativity theory, and also co-authored a book discussing '*Neutrosophic General Relativity*', with L. Borissova and F. Smarandache (Hexis-Phoenix, 2006).

- **F. Smarandache** – is Chairman, Dept. of Math & Sc., University of New Mexico, Gallup, USA. Born in December 10, 1954 in Balcesti, Romania, he has multiple abilities; with works embracing various aspects of mathematics, physics, painting, arts, philosophy. He developed some new branches in mathematics, including Neutrosophic Logic (NL), Neutrosophic Statistics, Multispace, and also Unified Fusion Theory which extends further Information Fusion theory. He is also frequently invited to be speaker in various conferences to give presentation of his theories, and has held conferences dedicated solely to Neutrosophic Logic. He has published numerous scientific papers and books. His recent work since 2002 includes a generalization of information fusion theory and Dempster-Shafer theory, to become Dezert-Smarandache theory (DSmT), can be found in: http://www.gallup.unm.edu/~smarandache/DSmT.htm.

- **V. Christianto** – is *sciprint.org* administrator and an independent researcher. His research interests include quantization in astrophysics; use of quaternion and biquaternion number in various aspects of theoretical physics; and computational methods in science. He has published more than 14 scientific papers (independently and with F. Smarandache and others), some of them can be found at *AFLB, EJTP*, and *Progress in Physics*, http://www.ptep-online.com. He also co-authored some books (independently and with F. Smarandache and others), including: (a) F. Smarandache, V. Christianto, *Multivalued Logic, Neutrosophy and Schrödinger equation*, Hexis-Phoenix, USA (March 2006); (b) F. Smarandache, V. Christianto, Fu Yuhua, R. Khrapko, J. Hutchison, *Unfolding the Labyrinth: Open Problems in Physics, Mathematics, Astrophysics, and Other Areas of Science*, Hexis-Phoenix, USA (Oct. 2006); (c) Florentin Smarandache, V. Christianto (editors), *Quantization in Astrophysics, Brownian Motion, and Supersymmetry*, MathTiger - Chenai, India (Jan. 2007).

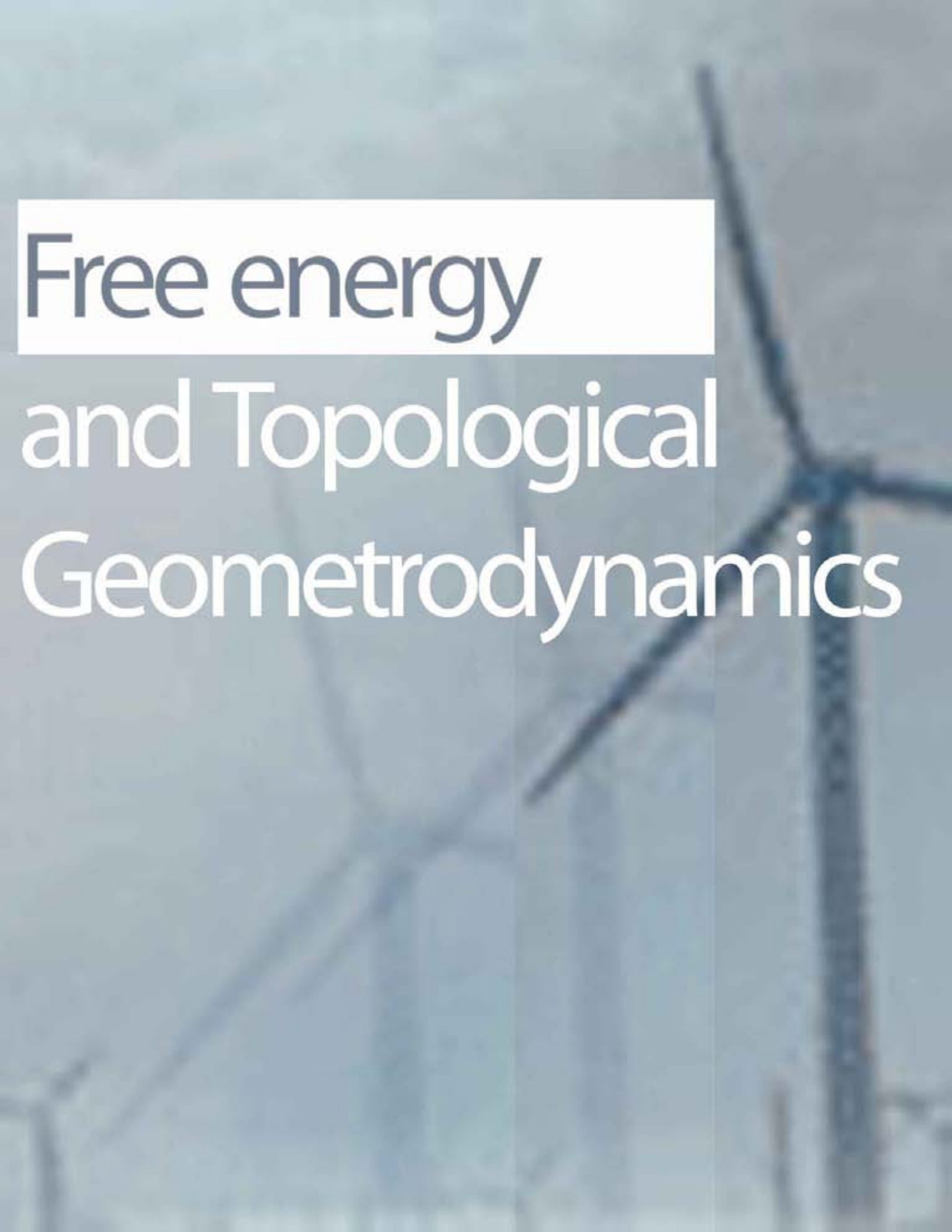

# Free energy and Topological Geometrodynamics

# Nuclear String Hypothesis

M. Pitkänen[1], April 8, 2007

[1] Department of Physical Sciences, High Energy Physics Division,
PL 64, FIN-00014, University of Helsinki, Finland.
matpitka@rock.helsinki.fi, http://www.physics.helsinki.fi/∼matpitka/.
Recent address: Puutarhurinkatu 10,10960, Hanko, Finland.

## Contents

**1 Introduction** **4**
- 1.1 $A > 4$ nuclei as nuclear strings consisting of $A \leq 4$ nuclei . . . 5
- 1.2 Bose-Einstein condensation of color bonds as a mechanism of nuclear binding . . . 5
- 1.3 Giant dipole resonance as de-coherence of Bose-Einstein condensate of color bonds . . . 6

**2 Some variants of the nuclear string hypothesis** **6**
- 2.1 Could linking of nuclear strings give rise to heavier stable nuclei? . . . 6
- 2.2 Nuclear strings as connected sums of shorter nuclear strings? 7
- 2.3 Is knotting of nuclear strings possible? . . . 7

**3 Could nuclear strings be connected sums of alpha strings and lighter nuclear strings?** **8**
- 3.1 Does the notion of elementary nucleus make sense? . . . 8
- 3.2 Stable nuclei need not fuse to form stable nuclei . . . 9
- 3.3 Formula for binding energy per nucleon as a test for the model 10
- 3.4 Decay characteristics and binding energies as signatures of the decomposition of nuclear string . . . 11
- 3.5 Are magic numbers additive? . . . 11
- 3.6 Stable nuclei as composites of lighter nuclei and necessity of tetra-neutron? . . . 12
- 3.7 What are the building blocks of nuclear strings? . . . 13
  - 3.7.1 Option Ia) . . . 13
  - 3.7.2 Option Ib) . . . 14
  - 3.7.3 Options IIa) and IIb) . . . 15

**4 Light nuclei as color bound Bose-Einstein condensates of $^4He$ nuclei** **16**
4.1 How to explain the maximum of $E_B$ for iron? . . . . . 16
4.2 Scaled up QCD with Bose-Einstein condensate of $^4He$ nuclei explains the growth of $E_B$ . . . . . 16
4.3 Why $E_B$ decreases for heavier nuclei? . . . . . 19
4.3.1 Fermi statistics as a reason for the reduction of the binding energy . . . . . 19
4.3.2 Could upper limit for the size of $^4He$ Bose-Einstein condensate explain the maximum of binding energy per nucleon? . . . . . 21

**5 What QCD binds nucleons to $A \leq 4$ nuclei?** **21**
5.1 The QCD associated with nuclei lighter than $^4He$ . . . . . 22
5.1.1 Various options to consider . . . . . 22
5.1.2 Option Ia): Ordinary nucleons and massless color bonds 22
5.1.3 Other options . . . . . 24
5.2 The QCD associated with $^4He$ . . . . . 25
5.3 What about tetra-neutron? . . . . . 26
5.4 What could be the general mass formula? . . . . . 27
5.5 Nuclear strings and cold fusion . . . . . 28
5.5.1 Signatures of cold fusion . . . . . 29
5.5.2 Could exotic deuterium make cold fusion possible? . . 30
5.5.3 About the phase transition transforming ordinary deuterium to exotic deuterium . . . . . 31
5.5.4 Exotic weak bosons seem to be necessary . . . . . 32
5.6 Strong force as a scaled and dark electro-weak force? . . . . . 33

**6 Giant dipole resonance as a dynamical signature for the existence of Bose-Einstein condensates?** **34**
6.1 De-coherence at the level of $^4He$ nuclear string . . . . . 35
6.2 De-coherence inside $^4He$ nuclei . . . . . 35
6.3 De-coherence inside $A = 3$ nuclei and pygmy resonances . . . 39

**Abstract**

Nuclear string hypothesis is one of the most dramatic almost-predictions of TGD. The hypothesis in its original form assumes that nucleons inside nucleus form closed nuclear strings with neighboring nuclei of the string connected by exotic meson bonds consisting of color magnetic flux tube with quark and anti-quark at its ends. The lengths of flux tubes correspond to the p-adic length scale of electron and therefore the mass scale of the exotic mesons is around 1 MeV in accordance with the general scale of nuclear binding energies. The long lengths of em flux tubes increase the distance between nucleons and reduce Coulomb repulsion. A fractally scaled up variant of ordinary QCD with respect to p-adic length scale would be in question and the usual wisdom about ordinary pions and other mesons as the origin of nuclear force would be simply wrong in TGD framework as the large mass scale of ordinary pion indeed suggests.

*1. $A > 4$ nuclei as nuclear strings consisting of $A \leq 4$ nuclei*

In this article a more refined version of nuclear string hypothesis is developed.

a) It is assumed $^4He$ nuclei and $A < 4$ nuclei and possibly also nucleons appear as basic building blocks of nuclear strings. $A \leq 4$ nuclei in turn can be regarded as strings of nucleons. Large number of stable lightest isotopes of form $A = 4n$ supports the hypothesis that the number of $^4He$ nuclei is maximal. Even the weak decay characteristics might be reduced to those for $A < 4$ nuclei using this hypothesis.

b) One can understand the behavior of nuclear binding energies surprisingly well from the assumptions that total *strong* binding energy associated with $A \leq 4$ building blocks is *additive* for nuclear strings.

c) In TGD framework tetra-neutron is interpreted as a variant of alpha particle obtained by replacing two meson-like stringy bonds connecting neighboring nucleons of the nuclear string with their negatively charged variants. For heavier nuclei tetra-neutron is needed as an additional building brick.

*2. Bose-Einstein condensation of color bonds as a mechanism of nuclear binding*

The attempt to understand the variation of the nuclear binding energy and its maximum for $Fe$ leads to a quantitative model of nuclei lighter than $Fe$ as color bound Bose-Einstein condensates of pion like colored states associated with color flux tubes connecting $^4He$ nuclei. The color contribution to the total binding energy is proportional to $n^2$, where $n$ is the number of color bonds. Fermi statistics explains the reduction of $E_B$ for the nuclei heavier than $Fe$. Detailed estimate favors harmonic oscillator model over free nucleon model with oscillator strength having interpretation in terms of string tension.

Fractal scaling argument allows to understand $^4He$ and lighter nuclei as strings of nucleons with nucleons bound together by color bonds. Three fractally scaled variants of QCD corresponding $A > 4$ , $A = 4$, and $A < 4$ nuclei are involved. The binding energies of also $A \leq 4$ are predicted surprisingly accurately by applying simple p-adic scaling to the model of binding energies of heavier nuclei.

*3. Giant dipole resonance as de-coherence of Bose-Einstein condensate of color bonds*

Giant resonances and so called pygmy resonances are interpreted in terms of de-coherence of the Bose-Einstein condensates associated with $A \leq 4$ nuclei and with the nuclear string formed from $A \leq 4$ nuclei. The splitting of the Bose-Einstein condensate to pieces costs a precisely defined energy. For $^4He$ de-coherence the model predicts singlet line at 12.74 MeV and triplet at $\sim$ 27 MeV spanning 4 MeV wide range.

The de-coherence at the level of nuclear string predicts 1 MeV wide bands 1.4 MeV above the basic lines. Bands decompose to lines with precisely predicted energies. Also these contribute to the width. The predictions are in rather good agreement with experimental values. The so called pygmy resonance appearing in neutron rich nuclei can be understood as a de-coherence for $A = 3$ nuclei. A doublet at $\sim$ 8 MeV and MeV spacing is predicted. The prediction for the position is correct.

# 1 Introduction

Nuclear string hypothesis [F8] is one of the most dramatic almost-predictions of TGD [TGDquant]. The hypothesis in its original form assumes that nucleons inside nucleus organize to closed nuclear strings with neighboring nuclei of the string connected by exotic meson bonds consisting of color magnetic flux tube with quark and anti-quark at its ends. The lengths of flux tubes correspond to the p-adic length scale of electron and therefore the mass scale of the exotic mesons is around 1 MeV in accordance with the general scale of nuclear binding energies. The long lengths of em flux tubes increase the distance between nucleons and reduce Coulomb repulsion. A fractally scaled up variant of ordinary QCD with respect to p-adic length scale would be in question and the usual wisdom about ordinary pions and other mesons as the origin of nuclear force would be simply wrong in TGD framework as the large mass scale of ordinary pion indeed suggests. The presence of exotic light mesons in nuclei has been proposed also by Illert [4] based on evidence for charge fractionization effects in nuclear decays.

### 1.1 $A > 4$ nuclei as nuclear strings consisting of $A \leq 4$ nuclei

In the sequel a more refined version of nuclear string hypothesis is developed.

a) The first refinement of the hypothesis is that $^4He$ nuclei and $A < 4$ nuclei and possibly also nucleons appear as basic building blocks of nuclear strings instead of nucleons which in turn can be regarded as strings of nucleons. Large number of stable lightest isotopes of form $A = 4n$ supports the hypothesis that the number of $^4He$ nuclei is maximal. One can hope that even also weak decay characteristics could be reduced to those for $A < 4$ nuclei using this hypothesis.

b) One can understand the behavior of nuclear binding energies surprisingly well from the assumptions that total *strong* binding energy associated with $A \leq 4$ building blocks is *additive* for nuclear strings and that the addition of neutrons tends to reduce Coulombic energy per string length by increasing the length of the nuclear string implying increase binding energy and stabilization of the nucleus. This picture does not explain the variation of binding energy per nucleon and its maximum appearing for $^{56}Fe$.

c) In TGD framework tetra-neutron [2, 3] is interpreted as a variant of alpha particle obtained by replacing two meson-like stringy bonds connecting neighboring nucleons of the nuclear string with their negatively charged variants [F8]. For heavier nuclei tetra-neutron is needed as an additional building brick and the local maxima of binding energy $E_B$ per nucleon as function of neutron number are consistent with the presence of tetra-neutrons. The additivity of magic numbers $2, 8, 20, 28, 50, 82, 126$ predicted by nuclear string hypothesis is also consistent with experimental facts and new magic numbers are predicted [5, 6].

### 1.2 Bose-Einstein condensation of color bonds as a mechanism of nuclear binding

The attempt to understand the variation of the nuclear binding energy and its maximum for $Fe$ leads to a quantitative model of nuclei lighter than $Fe$ as color bound Bose-Einstein condensates of $^4He$ nuclei or rather, of pion like colored states associated with color flux tubes connecting $^4He$ nuclei. The crucial element of the model is that color contribution to the binding energy is proportional to $n^2$ where $n$ is the number of color bonds. Fermi statistics explains the reduction of $E_B$ for the nuclei heavier than $Fe$. Detailed estimate favors harmonic oscillator model over free nucleon model with oscillator strength having interpretation in terms of string tension.

Fractal scaling argument allows to understand $^4He$ and lighter nuclei as

strings formed from nucleons with nucleons bound together by color bonds. Three fractally scaled variants of QCD corresponding $A > 4$ nuclei, $A = 4$ nuclei and $A < 4$ nuclei are thus involved. The binding energies of also lighter nuclei are predicted surprisingly accurately by applying simple p-adic scaling to the parameters of model for the electromagnetic and color binding energies in heavier nuclei.

### 1.3 Giant dipole resonance as de-coherence of Bose-Einstein condensate of color bonds

Giant (dipole) resonances [18, 19, 21], and so called pygmy resonances [22, 23] interpreted in terms of de-coherence of the Bose-Einstein condensates associated with $A \leq 4$ nuclei and with the nuclear string formed from $A \leq 4$ nuclei provide a unique test for the model. The key observation is that the splitting of the Bose-Einstein condensate to pieces costs a precisely defined energy due to the $n^2$ dependence of the total binding energy. For $^4He$ de-coherence the model predicts singlet line at 12.74 MeV and triplet (25.48, 27.30,29.12) MeV at $\sim 27$ MeV spanning 4 MeV wide range which is of the same order as the width of the giant dipole resonance for nuclei with full shells.

The de-coherence at the level of nuclear string predicts 1 MeV wide bands 1.4 MeV above the basic lines. Bands decompose to lines with precisely predicted energies. Also these contribute to the width. The predictions are in a surprisingly good agreement with experimental values. The so called pygmy resonance appearing in neutron rich nuclei can be understood as a de-coherence for $A = 3$ nuclei. A doublet (7.520,8.4600) MeV at $\sim 8$ MeV is predicted. At least the prediction for the position is correct.

## 2 Some variants of the nuclear string hypothesis

The basic assumptions of the nuclear string model could be made stronger in several testable ways. One can make several alternative hypothesis.

### 2.1 Could linking of nuclear strings give rise to heavier stable nuclei?

Nuclear strings $(Z_1, N_1)$ and $(Z_2, N_2)$ could link to form larger nuclei $(Z_1 + Z_2, N_1 + N_2)$. If one can neglect the interactions between linked nuclei, the properties of the resulting nuclei should be determined by those of composites. Linking should however be the confining interaction forbidding the

decay of the stable composite. The objection against this option is that it is difficult to characterize the constraint that strings are not allowed to touch and there is no good reason forbidding the touching.

The basic prediction would be that if the nuclei $(Z_1, N_1)$ and $(Z_2, N_2)$ which are stable, very long-lived, or possess exceptionally large binding energy then also the nucleus $(Z_1 + Z_2, N_1 + N_2)$ has this property. If the linked nuclear strings are essentially free then the expectation is that the half-life of a composite of unstable nuclei is that of the shorter lived nucleus. This kind of regularity would have been probably observed long time ago.

### 2.2 Nuclear strings as connected sums of shorter nuclear strings?

Nuclear strings can form connected sum of the shorter nuclear strings. Connected sum means that one deletes very short portions of nuclear string A and B and connects the resulting ends of string A and B together. In other words: A is inserted inside B or vice versa or A and B are cut to open strings and connected and closed again. This outcome would result when A and B touch each other at some point. If touching occurs at several points more complex fusion of nuclei to a larger nucleus to a composite occurs with piece of A followed by a piece of B followed... For this option there is a non-trivial interaction between strings and the properties of nuclei need not be simply additive but one might still hope that stable nuclei fuse to form stable nuclei. In particular, the prediction for the half-life based on binding by linking does not hold true anymore.

Classical picture would suggest that the two strings cannot rotate with respect to each other unless they correspond to rather simple symmetric configurations: this applies also to linked strings. If so then the relative angular momentum $L$ of nuclear strings vanishes and total angular momentum $J$ of the resulting nucleus satisfies $|J_1 - J_2| \leq J \leq J_1 + J_2$.

### 2.3 Is knotting of nuclear strings possible?

One can consider also the knotting of nuclear strings as a mechanism giving rise to exotic excitations of nuclear. Knots decompose to prime knots so that kind of prime nuclei identified in terms of prime knots might appear. Fractal thinking suggests an analogy with the poorly understood phenomenon of protein folding. It is known that proteins always end up to a unique highly folded configuration and one might think that also nuclear ground states correspond to unique configurations to which quantum system (also proteins

would be such if dark matter is present) ends up via quantum tunnelling unlike classical system which would stick into some valley representing a state of higher energy. The spin glass degeneracy suggests an fractal landscape of ground state configurations characterized by knotting and possibly also linking.

# 3 Could nuclear strings be connected sums of alpha strings and lighter nuclear strings?

The attempt to kill the composite string model leads to a stronger formulation in which nuclear string consists of alpha particles plus a minimum number of lighter nuclei. To test the basic predictions of the model I have used the rather old tables of [8] for binding energies of stable and long-lived isotopes and more modern tables [7] for basic data about isotopes known recently.

## 3.1 Does the notion of elementary nucleus make sense?

The simplest formulation of the model assumes some minimal set of *stable* "elementary nuclei" from which more complex *stable* nuclei can be constructed.

a) If heavier nuclei are formed by *linking* then alpha particle $^4He = (Z,N) = (2,2)$ suggests itself as the lightest stable composite allowing interpretation as a closed string. For connected sum option even single nucleon n or p can appear as a composite. This option turns out to be the more plausible one.

b) In the model based on linking $^6Li = (3,3)$ and $^7Li = (3,4)$ would also act as "elementary nuclei" as well as $^9Be = (4,5)$ and $^{10}Be = (4,6)$. For the model based on connected sum these nuclei might be regarded as composites $^6Li = (3,3) = (2,2) + (1,1)$, $^7Li = (3,4) = (2,2) + (1,2)$, $^9Be = (4,5) = 2 \times (2,2) + (0,1)$ and $^{10}Be = (4,6) = (2,2) + 2 \times (1,2)$. The study of binding energies supports the connected sum option.

b) $^{10}B$ has total nuclear spin $J = 3$ and $^{10}B = (5,5) = (3,3) + (2,2) =^6 Li +^4 He$ makes sense if the composites can be in relative $L = 2$ state ($^6Li$ has $J = 1$ and $^4He$ has $J = 0$). $^{11}B$ has $J = 3/2$ so that $^{11}B = (5,6) = (3,4) + (2,2) =^7 Li +^4 He$ makes sense because $^7Li$ has $J = 3/2$. For the model based on disjoint linking also $10^B$ would be also regarded as "elementary nucleus". This asymmetry disfavors the model based on linking.

### 3.2 Stable nuclei need not fuse to form stable nuclei

The question is whether the simplest model predicts stable nuclei which do not exist. In particular, are the linked $^4He$ composites stable? The simplest case corresponds to $^8B = (4,4) =^4 He +^4 He$ which is not stable against alpha decay. Thus stable nuclei need not fuse to form stable nuclei. On the other hand, the very instability against alpha decay suggests that $^4B$ can be indeed regarded as composite of two alpha particles. A good explanation for the instability against alpha decay is the exceptionally large binding energy $E = 7.07$ MeV per nucleon of alpha particle. The fact that the binding energy per nucleon for $^8Be$ is also exceptionally large and equal to 7.06 MeV $< E_B(^4He)$ supports the interpretation as a composite of alpha particles.

For heavier nuclei binding energy per nucleon increases and has maximum 8.78 MeV for Fe. This encourages to consider the possibility that alpha particle acts as a fundamental composite of nuclear strings with minimum number of lighter isotopes guaranteing correct neutron number. Indeed, the decomposition to a maximum number of alpha particles allows a qualitative understanding of binding energies assuming that additional contribution not larger than 1.8 MeV per nucleon is present.

The nuclei $^{12}C$, $^{16}O$, $^{20}Ne$, $^{24}Mg$, $^{28}Si$, $^{32}S$, $^{36}A$, and $^{40}Ca$ are lightest stable isotopes of form $(Z,Z) = n \times^4 He$, $n = 3,...,10$, for which $E_B$ is larger than for $^4He$. For the first four nuclei $E_B$ has a local maximum as function of $N$. For the remaining the maximum of $E_B$ is obtained for $(Z, Z+1)$. $^{44}Ti = (22,22)$ does not exist as a long-lived isotope whereas $^{45}Ti$ does. The addition of neutron could increase $E_B$ by increasing the length of nuclear string and thus reducing the Coulomb interaction energy per nucleon. This mechanism would provide an explanation also for neutron halos [1].

Also the fact that stable nuclei in general have $N \geq Z$ supports the view that $N = Z$ state corresponds to string consisting of alpha particles and that $N > Z$ states are obtained by adding something between. $N < Z$ states would necessarily contain at least one stable nucleus lighter than $^4He$ with smaller binding energy. $^3He$ is the only possible candidate as the only stable nucleus with $N < Z$. ($E_B(^2H) = 1.11$ MeV and $E_B(^3He) = 2.57$ MeV). Individual nucleons are also possible in principle but not favored. This together with increase of Coulomb interaction energy per nucleon due to the greater density of em charge per string length would explain their smaller binding energy and instability.

### 3.3 Formula for binding energy per nucleon as a test for the model

The study of $^8B$ inspires the hypothesis that the total binding energy for the nucleus $(Z_1+Z_2, N_1+N_2)$ is in the first approximation the sum of total binding energies of composites so that one would have for the binding energy per nucleon the prediction

$$E_B = \frac{A_1}{A_1+A_2} \times E_{B_1} + \frac{A_2}{A_1+A_2} \times E_{B_2}$$

in the case of 2-nucleus composite. The generalization to N-nucleus composite would be

$$E_B = \sum_k \frac{A_k}{\sum_r A_r} \times E_{B_k} \quad .$$

This prediction would apply also to the unstable composites. The increase of binding energy with the increase of nuclear weight indeed suggests a decomposition of nuclear string to a sequence alpha strings plus some minimum number of shorter strings.

The first objection is that for both $Li$, $B$, and $Be$ which all having two stable isotopes, the lighter stable isotope has a slightly smaller binding energy contrary to the expectation based on additivity of the total binding energy. This can be however understood in terms of the reduction of Coulomb energy per string length resulting in the addition of neutron (protons have larger average distance along nuclear string along mediating the electric flux) . The reduction of Coulomb energy per unit length of nuclear string could also partially explain why one has $E_B > E_B(^4He)$ for heavier nuclei.

The composition $^6Li = (3,3) = (2,2) + (1,1)$ predicts $E_B \simeq 5.0$ MeV not too far from 5.3 MeV. The decomposition $^7Li = (3,4) = (2,2) + (1,2)$ predicts $E_B = 5.2$ MeV to be compared with 5.6 MeV so that the agreement is satisfactory. The decomposition $^8Be = (4,4) = 2\times\ ^4He$ predicts $E_B =$ 7.07 MeV to be compared with the experimental value 7.06 MeV. $^9Be$ and $^{10}Be$ have $E_B = 6.46$ MeV and $E_B = 6.50$ MeV. The fact that binding energy slightly increases in addition of neutron can be understood since the addition of neutrons to $^8Be$ reduces the Coulomb interaction energy per unit length. Also neutron spin pairing reduces $E_B$. The additive formula for $E_B$ is satisfied with an accuracy better than 1 MeV also for $^{10}B$ and $^{11}B$.

### 3.4 Decay characteristics and binding energies as signatures of the decomposition of nuclear string

One might hope of reducing the weak decay characteristics to those of shortest unstable nuclear strings appearing in the decomposition. Alternatively, one could deduce the decomposition from the weak decay characteristics and binding energy using the previous formulas. The picture of nucleus as a string of alpha particles plus minimum number of lighter nuclei $^3He$ having $E_B = 2.57$ MeV, $^3H$ unstable against beta decay with half-life of 12.26 years and having $E_B = 2.83$ MeV, and $^2H$ having $E_B = 1.1$ MeV gives hopes of modelling weak decays in terms of decays for these light composites.

a) $\beta^-$ decay could be seen as a signature for the presence of $^3H$ string and alpha decay as a signature for the presence of $^4He$ string.

b) $\beta^+$ decay might be interpreted as a signature for the presence of $^3He$ string which decays to $^3H$ (the mass of $^3H$ is only .018 MeV higher than that of $^3He$). For instance, $^8B = (5,3) = (3,2) + (2,1) = {}^5Li + {}^3He$ suffers $\beta^+$ decay to $^8Be = (4,4)$ which in turn decays by alpha emission which suggests the re-arrangement to $(3,2) + (1,2) \to (2,2) + (2,2)$ maximizing binding energy.

c) Also individual nucleons can appear in the decomposition and give rise to $\beta^-$ and possible also $\beta^+$ decays.

### 3.5 Are magic numbers additive?

The magic numbers $2, 8, 20, 28, 50, 82, 126$ [5] for protons and neutrons are usually regarded as a support for the harmonic oscillator model. There are also other possible explanations for magic nuclei and there are deviations from the naive predictions. One can also consider several different criteria for what it is to be magic. Binding energy is the most natural criterion but need not always mean stability. For instance $^8B = (4,4) = {}^4He + {}^4He$ has high binding energy but is unstable against alpha decay.

Nuclear string model suggests that the fusion of magic nuclear strings by connected sum yields new kind of highly stable nuclei so that also $(Z_1 + Z_2, N_1 + N_2)$ is a magic nucleus if $(Z_i, N_i)$ is such. One has $N = 28 = 20 + 8$, $50 = 28 + 20 + 2$, and $N = 82 = 50 + 28 + 2 \times 2$. Also other magic numbers are predicted. There is evidence for them [6].

a) $^{16}O = (8,8)$ and $^{40}Ca = (20,20)$ corresponds to doubly magic nuclei and $^{60}Ni = (28,32) = (20,20) + (8,8) + {}^4 n$ has a local maximum of binding energy as function of neutron number. This is not true for $^{56}Ni$ so that the idea of magic nucleus in neutron sector is not supported by this case. The

explanation would be in terms of the reduction of $E_B$ due to the reduction of Coulomb energy per string length as neutrons are added.

b) Also $^{80}Kr = (36, 44) = (36, 36) +^4 n = (20, 20) + (8, 8) + (8, 8) +^4 n$ corresponds to a local maximum of binding energy per nucleon as also does $^{84}Kr =^{80} Kr +^4 n$ containing two tetra-neutrons. Note however that $^{88}Zr = (40, 48)$ is not a stable isotope although it can be regarded as a composite of doubly magic nucleus and of two tetra-neutrons.

### 3.6 Stable nuclei as composites of lighter nuclei and necessity of tetra-neutron?

The obvious test is to look whether stable nuclei can be constructed as composites of lighter ones. In particular, one can check whether tetra-neutron $^4n$ interpreted as a variant of alpha particle obtained by replacing two meson-like stringy bonds connecting neighboring nucleons of the nuclear string with their negatively charged variants is necessary for the understanding of heavier nuclei.

a) $^{48}Ca = (20, 28)$ with half-life $> 2 \times 10^{16}$ years has neutron excess of 8 units and the only reasonable interpretation seems to be as a composite of the lightest stable $Ca$ isotope $Ca(20, 20)$, which is doubly magic nucleus and two tetra-neutrons: $^{48}Ca = (20, 28) =^{40} Ca + 2 \times^4 n$.

b) The next problematic nucleus is $^{49}Ti$.

i) $^{49}Ti = (22, 27)$ having neutron excess of 5 one cannot be expressed as a composite of lighter nuclei unless one assumes non-vanishing and large relative angular momentum for the composites. For $^{50}Ti = (22, 28)$ no decomposition can be found. The presence of tetra-neutron would reduce the situation to $^{49}Ti = (22, 27) =^{45} Ti +^4 n$. Note that $^{45}Ti$ is the lightest Ti isotope with relatively long half-life of 3.10 hours so that the addition of tetra-neutron would stabilize the system since Coulomb energy per length of string would be reduced.

ii) $^{48}Ti$ could not involve tetra-neutron by this criterion. It indeed allows decomposition to standard nuclei is also possible as $^{48}Ti = (22, 26) =^{41} K +^7 Li$.

iii) The heaviest stable $Ti$ isotope would have the decomposition $^{50}Ti =^{46} Ti +^4 n$, where $^{46}Ti$ is the lightest stable $Ti$ isotope.

c) The heavier stable nuclei $^{50+k}V = (23, 27 + k)$, $k = 0, 1$, $^{52+k}Cr = (24, 28+k)$, $k = 0, 1, 2$, $^{55}Mn = (25, 30)$ and $^{56+k}Fe = (26, 30+k)$, $k = 0, 1, 2$ would have similar interpretation. The stable isotopes $^{50}Cr = (24, 26)$ and $^{54}Fe = (26, 28)$ would not contain tetra-neutron. Also for heavier nuclei both kinds of stable states appear and tetra-neutron would explain this.

d) $^{112}Sn = (50, 62) = (50, 50) + 3 \times^4 n$, $^{116}Sn$, $^{120}Sn$, and $^{124}Sn$ are local maxima of $E_B$ as a function of neutron number and the interpretation in terms of tetra-neutrons looks rather natural. Note that $Z = 50$ is a magic number.

Nuclear string model looks surprisingly promising and it would be interesting to compare systematically the predictions for $E_B$ with its actual values and look whether the beta decays could be understood in terms of those of composites lighter than $^4He$.

## 3.7 What are the building blocks of nuclear strings?

One can also consider several options for the more detailed structure of nuclear strings. The original model assumed that proton and neutron are basic building blocks but this model is too simple.

### 3.7.1 Option Ia)

A more detailed work in attempt to understand binding energies led to the idea that there is fractal structure involved. At the highest level the building blocks of nuclear strings are $A \leq 4$ nuclei. These nuclei in turn would be constructed as short nuclear strings of ordinary nucleons.

The basic objection against the model is the experimental absence of stable $n - n$ bound state analogous to deuteron favored by lacking Coulomb repulsion and attractive electromagnetic spin-spin interaction in spin 1 state. Same applies to tri-neutron states and possibly also tetra-neutron state. There has been however speculation about the existence of di-neutron and poly-neutron states [10, 11].

The standard explanation is that strong force couples to strong isospin and that the repulsive strong force in nn and pp states makes bound states of this kind impossible. This force, if really present, should correspond to shorter length scale than the isospin independent forces in the model under consideration. In space-time description these forces would correspond to forces mediated between nucleons along the space-time sheet of the nucleus whereas exotic color forces would be mediated along the color magnetic flux tubes having much longer length scale. Even for this option one cannot exclude exotic di-neutron obtained from deuteron by allowing color bond to carry negative em charge. Since em charges $0, 1, -1$ are possible for color bonds, a nucleus with mass number $A > 2$ extends to a multiplet containing $3A$ exotic charge states.

### 3.7.2 Option Ib)

One might ask whether it is possible to get rid of isospin dependent strong forces and exotic charge states in the proposed framework. One can indeed consider also other explanations for the absence of genuine poly-neutrons.

a) The formation of negatively charged bonds with neutrons replaced by protons would minimize both nuclear mass and Coulomb energy although binding energy per nucleon would be reduced and the increase of neutron number in heavy nuclei would be only apparent.

b) The strongest hypothesis is that mass minimization forces protons and negatively charged color bonds to serve as the basic building bricks of all nuclei. If this were the case, deuteron would be a di-proton having negatively charged color bond. The total binding energy would be only $2.222 - 1.293 = .9290$ MeV. Di-neutron would be impossible for this option since only one color bond can be present in this state.

The small mass difference $m(^3He) - m(^3H) = .018$ MeV would have a natural interpretation as Coulomb interaction energy. Tri-neutron would be allowed. Alpha particle would consist of four protons and two negatively charged color bonds and the actual binding energy per nucleon would be by $(m_n - m_p)/2$ smaller than believed. Tetra-neutron would also consist of four protons and the binding energy per nucleon would be smaller by $m_n - m_p$ than what obtains in the standard model of nucleus. Beta decays would be basically beta decays of exotic quarks associated with color bonds.

Note that the mere assumption that the di-neutrons appearing inside nuclei have protons as building bricks means a rather large apparent binding energy this might explain why di-neutrons have not been detected. An interesting question is whether also higher n-deuteron states than $^4He$ consisting of strings of deuteron nuclei and other $A \leq 3$ nuclei could exist and play some role in the nuclear physics of $Z \neq N$ nuclei.

If protons are the basic building bricks, the binding energy per nucleon is replaced in the calculations with its actual value

$$E_B \quad \rightarrow \quad E_B - \frac{N}{A}\Delta m \ , \ \Delta m = m_n - m_p = 1.2930 \ MeV \ . \qquad (1)$$

This replacement does not affect at all the parameters of the of $Z = 2n$ nuclei identified as $^4He$ strings.

One can of course consider also the option that nuclei containing ordinary neutrons are possible but that are unstable against beta decay to nuclei containing only protons and negatively charged bonds. This would suggest

that di-neutron exists but is not appreciably produced in nuclear reactions and has not been therefore detected.

### 3.7.3 Options IIa) and IIb)

It is not clear whether the fermions at the ends of color bonds are exotic quarks or leptons. Lepto-pion (or electro-pion) hypothesis [F7] was inspired by the anomalous $e^+e^-$ production in heavy ion collisions near Coulomb wall and states that electro-pions which are bound states of colored excitations of electrons with ground state mass 1.062 MeV are responsible for the effect. The model predicts that also other charged leptons have color excitations and give rise to exotic counterpart of QCD.

Also $\mu$ and $\tau$ should possess colored excitations. About fifteen years after this prediction was made, direct experimental evidence for these states finally emerges [24, 25]. The mass of the new particle, which is either scalar or pseudoscalar, is 214.4 MeV whereas muon mass is 105.6 MeV. The mass is about 1.5 per cent higher than two times muon mass. The most natural TGD inspired interpretation is as a pion like bound state of colored excitations of muon completely analogous to lepto-pion (or rather, electro-pion) [F7].

One cannot exclude the possibility that the fermion and anti-fermion at the ends of color flux tubes connecting nucleons are actually colored leptons although the working hypothesis is that they are exotic quark and anti-quark. One can of course also turn around the argument: could it be that lepto-pions are "leptonuclei", that is bound states of ordinary leptons bound by color flux tubes for a QCD in length scale considerably shorter than the p-adic length scale of lepton.

Scaling argument applied to ordinary pion mass suggests that the masses of exotic quarks at the ends of color bonds are considerably below MeV scale. One can however consider the possibility that colored electrons with mass of ordinary electron are in question in which case color bonds identifiable as colored variants of electro-pions could be assumed to contribute in the first guess the mass $m(\pi) = 1.062$ MeV per each nucleon for $A > 2$ nuclei. This implies the general replacement

$$\begin{aligned} E_B &\rightarrow E_B + m(\pi_L) - \frac{N}{A}\Delta m \ \text{ for } \ A > 2 \ , \\ E_B &\rightarrow E_B + \frac{m(\pi_L)}{2} - \frac{N}{A}\Delta m \ \text{ for } \ A = 2 \ . \end{aligned} \tag{2}$$

This option will be referred to as option IIb). One can also consider the

option IIa) in which nucleons are ordinary but lepto-pion mass $m(\pi_L) = 1.062$ MeV gives the mass associated with color bond.

These options are equivalent for $N = Z = 2n$ nuclei with $A > 4$ but for $A \leq 4$ nuclei assumed to form nucleon string they options differ.

# 4 Light nuclei as color bound Bose-Einstein condensates of $^4He$ nuclei

The attempt to understand the variation of nuclear binding energy and its maximum for $Fe$ leads to a model of nuclei lighter than $Fe$ as color bound Bose-Einstein condensates of $^4He$ nuclei or meson-like structures associated with them. Fractal scaling argument allows to understand $^4He$ itself as analogous state formed from nucleons.

## 4.1 How to explain the maximum of $E_B$ for iron?

The simplest model predicts that the binding energy per nucleon equals to $E_B(^4He)$ for all $Z = N = 2n$ nuclei. The actual binding energy grows slowly, has a maximum at $^{52}Fe$, and then begins to decrease but remains above $E_B(^4He)$. The following values give representative examples for $Z = N$ nuclei.

| nucleus | $^4He$ | $^8Be$ | $^{40}Ca$ | $^52Fe$ |
|---|---|---|---|---|
| $E_B/MeV$ | 7.0720 | 7.0603 | 8.5504 | 8.6104 |

For nuclei heavier than $Fe$ there are no long-lived $Z = N = 2n$ isotopes and the natural reason would be alpha decay to $^{52}Fe$. If tetra-neutron is what TGD suggests it to be one can guess that tetra-neutron mass is very nearly equal to the mass of the alpha particle. This would allow to regard states $N = Z + 4n$ as states as analogous to unstable states $N_1 = Z_1 = Z + 2n$ consisting of alpha particles. This gives estimate for $E_B$ for unstable $N = Z$ states. For $^{256}Fm = (100, 156)$ one has $E_B = 7.433$ MeV which is still above $E_B(^4He) = 7.0720$ MeV. The challenge is to understand the variation of the binding energy per nucleon and its maximum for $Fe$.

## 4.2 Scaled up QCD with Bose-Einstein condensate of $^4He$ nuclei explains the growth of $E_B$

The first thing to come in mind is that repulsive Coulomb contribution would cause the variation of the binding energy. Since alpha particles are

building blocks for $Z = N$ nuclei, $^8Be$ provides a test for this idea. If the difference between binding energies per nucleon for $^8Be$ and $^4He$ were due to Coulomb repulsion alone, one would have $E_c = E_B(^4He) - E_B(^8Be) = .0117$ MeV, which is of order $\alpha_{em}/L(127)$. This would conform with the idea that flux tubes mediating em interaction have length of order electron Compton length. Long flux tubes would provide the mechanism minimizing Coulomb energy. A more realistic interpretation consistent with this mechanism would be that Coulombic and color interaction energies compensate each other: this can of course occur to some degree but it seems safe to assume that Coulomb contribution is small.

The basic question is how one could understand the behavior of $E_B$ if its variation corresponds to that for color binding energy per nucleon. The natural scale of energy is MeV and this conforms with the fact that the range of variation for color binding energy associated with $L(127)$ QCD is about 1.5 MeV. By a naive scaling the value of $M_{127}$ pion mass is by a factor $2^{(127-107)/2} = 10^{-3}$ times smaller than that of ordinary pion and thus .14 MeV. The scaling of QCD $\Lambda$ is a more reliable estimate for the binding energy scale and gives a slightly larger value but of the same order of magnitude. The total variation of $E_B$ is large in the natural energy scale of $M_{127}$ QCD and suggests strong non-linear effects.

In the absence of other contributions em and color contributions to $E_B$ cancel for $^8Be$. If color and Coulomb contributions on total binding energy depend roughly linearly on the number of $^4He$ nuclei, the cancellation to $E_B$ should occur in a good approximation also for them. This does not happen which means that color contribution to $E_B$ is in lowest approximation linear in $n$ meaning $n^2$-dependence of the total color binding energy. This non-linear behavior suggests strongly the presence of Bose-Einstein condensate of $^4He$ nuclei or structures associated with them. The most natural candidates are the meson like colored strings connecting $^4He$ nuclei together.

The additivity of $n$ color magnetic (and/or electric) fluxes would imply that classical field energy is $n^2$-fold. This does not yet imply same for binding energy unless the value of $\alpha_s$ is negative which it can be below confinement length scale. An alternative interpretation could be in terms of color magnetic interaction energy. The number of quarks and anti-quarks would be proportional to $n$ as would be also the color magnetic flux so that $n^2$- proportionality would result also in this manner.

If the addition of single alpha particle corresponds to an addition of a constant color contribution $E_s$ to $E_B$ (the color binding energy per nucleon, not the total binding energy!) one has $E_B(^{52}Fe) = E_B(^4He) + 13E_s$ giving $E_s = .1834$ MeV, which conforms with the order of magnitude estimate

given by $M_{127}$ QCD.

The task is to find whether this picture could explain the behavior of $E_B$. The simplest formula for $E_B(Z = N = 2n)$ would be given by

$$E_B(n) \quad = \quad -\frac{n(n-1)}{L(A)n}k_s + nE_s \ . \tag{3}$$

Here the first term corresponds to the Coulomb interaction energy of $n$ $^4He$ nuclei proportional to $n(n-1)$ and inversely proportional to the length $L(A)$ of nuclear string. Second term is color binding energy per nucleon proportional to $n$.

The simplest assumption is that each $^4He$ corresponds always to same length of nuclear string so that one has $L \propto A$ and one can write

$$E_B(n) \quad = \quad E_B(^4He) - \frac{n(n-1)}{n^2}E_c + nE_s \ . \tag{4}$$

The value of $E_B(^8Be) \simeq E_B(^4He)$ $(n = 2)$ gives for the unit of Coulomb energy

$$E_c \quad = \quad 4E_s + 2[E_B(^4He) - E_B(^8Be)] \simeq 4E_s \ . \tag{5}$$

The general formula for the binding energy reads as

$$\begin{aligned} E_B(n) \quad &= \quad E_B(^4He) - 2\frac{n(n-1)}{n^2}[E_B(^4He) - E_B(^8Be)] \\ &+ \quad [-4\frac{n(n-1)}{n^2} + n]E_s \ . \end{aligned} \tag{6}$$

The condition that $E_B(^{52}Fe)$ $(n = 13)$ comes out correctly gives

$$E_s \quad = \quad \frac{13}{121}(E_B(^{52}Fe) - E_B(^4He)) + \frac{13 \times 24}{121}[E_B(^4He) - E_B(^8Be)] \tag{7}$$

This gives $E_s \simeq .1955$ MeV which conforms with $M_{127}$ QCD estimate. For the $E_c$ one obtains $E_c = 1.6104$ MeV and for Coulomb energy of $^4He$ nuclei in $^8Be$ one obtains $E = E_c/2 = .8052$ MeV. The order of magnitude is consistent with the mass difference of proton and neutron. The scale suggests that electromagnetic flux tubes are shorter than color flux tubes and

correspond to the secondary p-adic length scale $L(2,61) = L(127)/2^{5/2}$ associated with Mersenne prime $M_{61}$. The scaling factor for the energy scale would be $2^{5/2} \simeq 5.657$.

The calculations have been carried out without assuming which are actual composites of $^4He$ nuclei (neutrons and protons plus neutral color bonds or protons and neutral and negatively charged color bonds) and assuming the masses of color bonds are negligible. As a matter fact, the mass of color bond does not affect the estimates if one uses only nuclei heavier than $^4He$ to estimate the parameters. The estimates above however involve $^4He$ so that small change on the parameters is induced.

## 4.3 Why $E_B$ decreases for heavier nuclei?

The prediction that $E_B$ increases as $(A/4)^2$ for $Z = N$ nuclei is unrealistic since $E_B$ decreases slowly for $A \geq 52$ nuclei. Fermi statistics provides a convincing explanation assuming that fermions move in an effective harmonic oscillator potential due to the string tension whereas free nucleon model predicts too large size for the nucleus. The splitting of the Bose-Einstein condensate to pieces is second explanation that one can imagine but fails at the level of details.

### 4.3.1 Fermi statistics as a reason for the reduction of the binding energy

The failure of the model is at least partially due to the neglect of the Fermi statistics. For the lighter nuclei description as many boson state with few fermions is expected to work. As the length of nuclear string grows in fixed nuclear volume, the probability of self intersection increases and Fermi statistics forces the wave function for stringy configurations to wiggle which reduces binding energy.

a) For the estimation purposes consider $A = 256$ nucleus $^{256}Mv$ having $Z = 101$ and $E_B = 7.4241$ MeV. Assume that this unstable nucleus is nearly equivalent with a nucleus consisting of $n = 64$ $^4He$ nuclei ($Z = N$). Assuming single color condensate this would give the color contribution

$$E_s^{tot} = (Z/2)^2 \times E_s = 64^2 \times E_s$$

with color contribution to $E_B$ equal to $(Z/2)E_s \simeq 12.51$ MeV.

b) Suppose that color binding energy is cancelled by the energy of nucleon identified as kinetic energy in the case of free nucleon model and as harmonic oscillator energy in the case of harmonic oscillator model.

c) The number of states with a given principal quantum number $n$ for both free nucleons in a spherical box and harmonic oscillator model is by spherical symmetry $2n^2$ and the number of protons/neutrons for a full shell nuclei behaves as $N_1 \simeq 2n_{max}^3/3$. The estimate for the average energy per nucleon is given in the two cases as

$$\begin{aligned} \langle E\rangle_H &= 2^{-4/3} \times N^{1/3} E_0 \ , \ E_0 = \omega_0 \ , \\ \langle E\rangle_F &= \frac{2}{5}(\frac{3}{2})^{5/3} N^{2/3} E_0 \ , \ E_0 = \frac{\pi^2}{2m_p L^2} \ . \end{aligned} \tag{8}$$

Harmonic oscillator energy $\langle E\rangle_H$ increases as $N^{1/3}$ and $\langle E\rangle_F$ as $N^{2/3}$. Neither of these cannot win the contribution of the color binding energy increasing as $N$.

c) Equating this energy with the total color binding energy gives an estimate for $E_0$ as

$$\begin{aligned} E_0 &= (2/3)^{1/3} \times Z^{-4/3} \times (Z/2)^2 \times E_s \ , \\ E_0 &= \frac{5}{4}(\frac{2}{3})^{5/3} \times Z^{-5/3} \times (Z/2)^2 \times E_s \ , \\ E_s &= .1955 \ MeV \ . \end{aligned} \tag{9}$$

The first case corresponds to harmonic oscillator model and second to free nucleon model.

d) For the harmonic oscillator model one obtains the estimate $E_0 = \hbar\omega_0 \simeq 2.73 \ MeV$. The general estimate for the energy scale in the harmonic oscillator model given by $\omega_0 \simeq 41 \cdot A^{-1/3}$ MeV [17] giving $\omega_0 = 6.5$ MeV for $A = 256$ (this estimate implies that harmonic oscillator energy per nucleon is approximately constant and would suggest that string tension tends to reduce as the length of string increases). Harmonic oscillator potential would have roughly twice too strong strength but the order of magnitude is correct. Color contribution to the binding energy might relate the reduction of the oscillator strength in TGD framework.

e) Free nucleon model gives the estimate $E_0 = .0626$ MeV. For the size of a $A = 256$ nucleus one obtains $L \simeq 3.8L(113) \simeq 76$ fm. This is by one order of magnitude larger that the size predicted by the standard formula $r = r_0 A^{1/3}$, $r_0 = 1.25$ fm and 8 fm for $A = 256$.

Harmonic oscillator picture is clearly favored and string tension explains the origin of the harmonic oscillator potential. Harmonic oscillator picture

is expected to emerge at the limit of heavy nuclei for which nuclear string more or less fills the nuclear volume whereas for light nuclei the description in terms of bosonic $^4He$ nuclei should make sense. For heavy nuclei Fermi statistics at nuclear level would begin to be visible and excite vibrational modes of the nuclear string mapped to the excited states of harmonic oscillator in the shell model description.

### 4.3.2 Could upper limit for the size of $^4He$ Bose-Einstein condensate explain the maximum of binding energy per nucleon?

One can imagine also an alternative explanation for why $E_B$ to decrease after $A = 52$. One might that $A = 52$ represents the largest $^4He$ Bose-Einstein condensate and that for heavier nuclei Bose-Einstein condensate de-coheres into two parts. Bose-Einstein condensate of $n = 13$ $^4He$ nuclei would the best that one can achieve.

This could explain the reduction of the binding energy and also the emergence of tetra-neutrons as well as the instability of $Z = N$ nuclei heavier than $^{52}Fe$. A number theoretical interpretation related to the p-adic length scale hypothesis suggests also itself: as the size of the tangled nuclear string becomes larger than the next p-adic length scale, Bose-Einstein condensate might lose its coherence and split into two.

If one assumes that $^4He$ Bose-Einstein condensate has an upper size corresponding to $n = 13$, the prediction is that after $A = 52$ second Bose-Einstein condensate begins to form. $E_B$ is obtained as the average

$$E_B(Z,N) = \frac{52}{A}E_B(^{52}Fe) + \frac{A-52}{A}E_B(^{A-52}X(Z,N)) \ .$$

The derivative

$$dE_B/dA = (52/A)[-E_B(^{52}Fe)+E_B(^{A-52}X)]+\frac{A-52}{A}dE_B(^{A-52}X(Z,N))/dA$$

is first negative but its sign must change since the nuclei consisting of two copies of $^{52}Fe$) condensates have same $E_B$ as $^{52}Fe$). This is an un-physical result. This does not exclude the splitting of Bose-Einstein condensate but the dominant contribution to the reduction of $E_B$ must be due to Fermi statistics.

## 5 What QCD binds nucleons to $A \leq 4$ nuclei?

The obvious question is whether scaled variant(s) of color force could bind nucleons to form $A \leq 4$ nuclei which in turn bind to form heavier nuclei.

Since the binding energy scale for $^3He$ is much smaller than for $^4He$ one might consider the possibility that the p-adic length scale for QCD associated with $^4He$ is different from that for $A < 4$ nuclei.

## 5.1 The QCD associated with nuclei lighter than $^4He$

It would be nice if one could understand the binding energies of also $A \leq 4$ nuclei in terms of a scaled variant of QCD applied at the level of nucleons. Here one has several options to test.

### 5.1.1 Various options to consider

Assume that neutral color bonds have negligible fermion masses at their ends: this is expected if the exotic quarks appear at the ends of color bonds and by the naive scaling of pion mass. One can also consider the possibility that the p-adic temperature for the quarks satisfies $T = 1/n \leq 1/2$ so that quarks would be massless in excellent approximation. $T = 1/n < 1$ holds true for gauge bosons and one might argue that color bonds as bosonic particles indeed have $T < 1$.

Option Ia): Building bricks are ordinary nucleons.

Opion IIa): Building blocks are protons and neutral and negatively charged color bonds. This means the replacement $E_B \to E_B - \Delta m$ for $A > 2$ nuclei and $E_B \to E_B - \Delta m/2$ for $A = 2$ with $\Delta m = n_n - m_p = 1.2930$ MeV.

Options Ib and IIb are obtained by assuming that the masses of fermions at the ends of color bonds are non-negligible. Electro-pion mass $m(\pi_L) = 1.062$ MeV is a good candidate for the mass of the color bond. Option Ia allow 3 per cent accuracy for the predicted binding energies. Option IIb works satisfactorily but the errors are below 22 per cent only.

### 5.1.2 Option Ia): Ordinary nucleons and massless color bonds

It turns out that for the option Ia) the correct candidate for $A < 4$ QCD is the secondary p-adic length scale $L(2, 59)$ associated with prime $p \simeq 2^k$, $k = 59$ with $k_{eff} = 2 \times 59 = 118$. The proper scaling of the electromagnetic p-adic length scale corresponds to a scaling factor $2^3$ meaning that one has $k_{eff} = 122 \to k_{eff} - 6 = 116 = 4 \times 29$ corresponding to $L(4, 29)$.

*1. Direct p-adic scaling of the parameters*

$E_s$ would be scaled up p-adically by a factor $2^{(127-118)/2} = 2^{9/2}$. $E_c$ would be scaled up by a factor $2^{(122-116)/2} = 2^3$. There is also a scaling of

$E_c$ by a factor 1/4 due to the reduction of charge unit and scaling of both $E_c$ and $E_s$ by a factor 1/4 since the basic units are now nucleons. This gives

$$\hat{E}_s \;=\; 2^{5/2}E_s = 1.1056\ \ MeV\ \ ,\ \ \hat{E}_c = 2^{-1}E_c = .8056\ \ MeV\ \ . \quad (10)$$

The value of electromagnetic energy unit is quite reasonable.

The basic formula for the binding energy reads now

$$E_B \;=\; -\frac{(n(p)(n(p)-1))}{A^2}\hat{E}_c + n\hat{E}_s\ \ , \quad (11)$$

where $n(p)$ is the number of protons $n = A$ holds true for $A > 2$. For deuteron one has $n = 1$ since deuteron has only single color bond. This delicacy is a crucial prediction and the model fails to work without it.

This gives

$$E_B(^2H) \;=\; \hat{E}_s\ \ ,\ \ E_B(^3H) = 3\hat{E}_s\ \ ,\ \ E_B(^3He) = -\frac{2}{9}\hat{E}_c + 3\hat{E}_s\ \ . \quad (12)$$

The predictions are given by the third row of the table below. The predicted values given are too large by about 15 per cent in the worst case.

The reduction of the value of $\alpha_s$ in the p-adic scaling would improve the situation. The requirement that $E_B(^3H)$ comes out correctly predicts a reduction factor .8520 for $\alpha_s$. The predictions are given in the fourth row of the table below. Errors are below 15 per cent.

| nucleus | $^2H$ | $^3H$ | $^3He$ |
|---|---|---|---|
| $E_B(exp)/MeV$ | 1.111 | 2.826 | 2.572 |
| $E_B(pred_1)/MeV$ | 1.106 | 3.317 | 3.138 |
| $E_B(pred_2)/MeV$ | .942 | 2.826 | 2.647 |

The discrepancy is 15 per cent for $^2H$. By a small scaling of $E_c$ the fit for $^3He$ can be made perfect. Agreement is rather good but requires that conventional strong force transmitted along nuclear space-time sheet is present and makes $nn$ and $pp$ states unstable. Isospin dependent strong interaction energy would be only .17 MeV in isospin singlet state which suggests that a large cancellation between scalar and vector contributions occurs. $pnn$ and $ppn$ could be regarded as Dn and Dp states with no strong force between

D and nucleon. The contribution of isospin dependent strong force to $E_B$ is scaled down by a factor 2/3 in $A = 3$ states from that for deuteron and is almost negligible. This option seems to allow an almost perfect fit of the binding energies. Note that one cannot exclude exotic nn-state obtained from deuteron by giving color bond negative em charge.

### 5.1.3 Other options

Consider next other options.

*1. Option IIb*

For option IIb) the basic building bricks are protons and $m(\pi) = 1.062$ is assumed. The basic objection against this option is that for protons as constituents *real* binding energies satisfy $E_B(^3He) < E_B(^3H)$ whereas Coulombic repulsion would suggest $E_B(^3He) > E_B(^3H)$ unless magnetic spin-spin interaction effects affect the situation. One can however look how good a fit one can obtain in this manner.

As found, the predictions of direct scaling are too large for $E_B(^3H)$ and $E_B(^3He)$ (slight reduction of $\alpha_s$ cures the situation). Since the actual binding energy increases by $m(\pi_L)-(2/3)(m_n-m_p)$ for $^3H$ and by $m(\pi_L)-(1/3)(m_n-m_p)$ for $^3He$, it is clear that the assumption that lepto-pion mass is of order 1 MeV improves the fit. The results are given by the table below.

| nucleus | $^2H$ | $^3H$ | $^3He$ |
|---|---|---|---|
| $E_B(exp)/MeV$ | 1.111 | 2.826 | 2.572 |
| $E_B(pred)/MeV$ | .875 | 3.117 | 2.507 |

Here $E_B(pred)$ corresponds to the effective value of binding energy assuming that nuclei effectively consist of ordinary protons and neutrons. The discrepancies are below 22 percent.

What is troublesome that neither the scaling of $\alpha_s$ nor modification of $E_c$ improves the situation for $^2H$ and $^3H$. Moreover, magnetic spin-spin interaction energy for deuteron is expected to reduce $E_B(pred)$ further in triplet state. Thus option IIb) does not look promising.

*2. Option Ib)*

For option Ib) with $m(\pi) = 1.062$ MeV and ordinary nucleons the actual binding $E_B(act)$ energy increases by $m(\pi)$ for $A = 3$ nuclei and by $m(\pi)/2$ for deuteron. Direct scaling gives a reasonably good fit for the p-adic length scale $L(9, 13)$ with $k_{eff} = 117$ meaning $\sqrt{2}$ scaling of $E_s$. For deuteron

the predicted $E_B$ is too low by 30 per cent. One might argue that isospin dependent strong force between nucleons becomes important in this p-adic length scale and reduces deuteron binding energy by 30 per cent. This option is not un-necessary complex as compared to the option Ia).

| nucleus | $^2H$ | $^3H$ | $^3He$ |
|---|---|---|---|
| $E_B(act)/MeV$ | 1.642 | 3.880 | 3.634 |
| $E_B(pred)/MeV$ | 1.3322 | 3.997 | 3.743 |

For option IIa) with $m(\pi) = 0$ and protons as building blocks the fit gets worse for $A = 3$ nuclei.

### 5.2 The QCD associated with $^4He$

$^4He$ must somehow differ from $A \leq 3$ nucleons. If one takes the argument based on isospin dependence strong force seriously, the reasonable looking conclusion would be that $^4He$ is at the space-time sheet of nucleons a bound state of two deuterons which induce no isospin dependent strong nuclear force. One could regard the system also as a closed string of four nucleons such that neighboring p and n form strong iso-spin singlets. The previous treatment applies as such.

For $^4He$ option Ia) with a direct scaling would predict $E_B(^4He) < 4 \times \hat{E}_s = 3.720$ MeV which is by a factor of order 2 too small. The natural explanation would be that for $^4He$ both color and em field body correspond to the p-adic length scale $L(4, 29)$ ($k_{eff} = 116$) so that $E_s$ would increase by a factor of 2 to 1.860 MeV. Somewhat surprisingly, $A \leq 3$ nuclei would have "color field bodies" by a factor 2 larger than $^4He$.

a) For option Ia) this would predict $E_B(^4He) = 7.32867$ MeV to be compared with the real value 7.0720 MeV. A reduction of $\alpha_s$ by 3.5 per cent would explain the discrepancy. That $\alpha_s$ decreases in the transition sequence $k_{eff} = 127 \to 118 \to 116$ which is consistent with the general vision about evolution of color coupling strength.

b) If one assumes option Ib) with $m(\pi) = 1.062$ MeV the actual binding energy increases to 8.13 MeV. The strong binding energy of deuteron units would give an additional .15 MeV binding energy per nucleon so that one would have $E_B(^4He) = 7.47$ MeV so that 10 per cent accuracy is achieved. Obviously this option does not work so well as Ia).

c) If one assumes option IIb), the actual binding energy would increase by .415 MeV to 7.4827 MeV which would make fit somewhat poorer. A small reduction of $E_c$ could allow to achieve a perfect fit.

### 5.3 What about tetra-neutron?

One can estimate the value of $E_B(^4n)$ from binding energies of nuclei $(Z,N)$ and $(Z,N+4)$ $(A=Z+N)$ as

$$E_B(^4n) = \frac{A+4}{4}[E_B(A+4) - \frac{A}{A+4}E_B(A)] \ .$$

In the table below there are some estimate for $E_B(^4n)$.

| $(Z,N)$ | (26,26)($^{52}Fe$) | (50,70)($^{120}Sn$) | (82,124) ($^{206}Pb$) |
|---|---|---|---|
| $E_B(^4n)/MeV$ | 6.280 | 7.3916 | 5.8031 |

The prediction of the above model would be $E(^4n) = 4\hat{E}_s = 3.760$ MeV for $\hat{E}_s = .940$ MeV associated with $A < 4$ nuclei and $k_{eff} = 118 = 2 \times 59$ associated with $A < 4$ nuclei. For $k_{eff} = 116$ associated with $^4He$ $E_s(^4n) = E_s(^4He) = 1.82$ MeV the prediction would be 7.28 MeV. 14 percent reduction of $\alpha_s$ would give the estimated value for of $E_s$ for $^{52}Fe$.

If tetra-neutron is ppnn bound state with two negatively charged color bonds, this estimate is not quite correct since the actual binding energy per nucleon is $E_B(^4He) - (m_n - m_p)/2$. This implies a small correction $E_B(A+4) \to E_B(A+4) - 2(m_n - m_p)/(A+4)$. The correction is negligible.

One can make also a direct estimate of $^4n$ binding energy assuming tetra-neutron to be ppnn bound state. If the masses of charged color bonds do not differ appreciably from those of neutral bonds (as the p-adic scaling of $\pi + -\pi^0$ mass difference of about 4.9 MeV strongly suggests) then model Ia) with $E_s = E_B(^3H)/3$ implies that the actual binding energy $E_B(^4n) = 4E_s = E_B(^3H)/3$ (see the table below). The apparent binding energy is $E_{B,app} = E_B(^4n) + (m_n - m_p)/2$. Binding energy differs dramatically from what one can imagine in more conventional models of strong interactions in which even the existence of tetra-neutron is highly questionable.

| $k_{eff}$ | $2 \times 59$ | $4 \times 29$ |
|---|---|---|
| $E_B(act)(^4n)/MeV$ | 3.7680 | |
| $E_{B,app}(4n)/MeV$ | 4.4135 | 8.1825 |

The higher binding energy per nucleon for tetra-neutron might directly relate to the neutron richness of heavy nuclei in accordance with the vision that Coulomb energy is what disfavors proton rich nuclei.

According to [9], tetra-neutron might have been observed in the decay $^8He \to^4 He +^4 n$ and the accepted value for the mass of $^8He$ isotope gives the

upper bound of $E(^4n) < 3.1$ MeV, which is one half of the the estimate. One can of course consider the possibility that free tetra-neutron corresponds to $L(2,59)$ and nuclear tetra-neutron corresponds to the length scale $L(4,29)$ of $^4He$. Also light quarks appear as several p-adically scaled up variants in the TGD based model for low-lying hadrons and there is also evidence that neutrinos appear in several scales.

### 5.4 What could be the general mass formula?

In the proposed model nucleus consists of $A \leq 4$ nuclei. Concerning the details of the model there are several questions to be answered. Do $A \leq 3$ nuclei and $A = 4$ nuclei $^4He$ and tetra-neutron form separate nuclear strings carrying their own color magnetic fields as the different p-adic length scale for the corresponding "color magnetic bodies" would suggest? Or do they combine by a connected sum operation to single closed string? Is there single Bose-Einstein condensate or several ones.

Certainly the Bose-Einstein condensates associated with nucleons forming $A < 4$ nuclei are separate from those for $A = 4$ nuclei. The behavior of $E_B$ in turn can be understood if $^4He$ nuclei and tetra-neutrons form separate Bose-Einstein condensates. For $Z > N$ nuclei poly-protons constructed as exotic charge states of stable $A \leq 4$ nuclei could give rise to the proton excess.

Before continuing it is appropriate to list the apparent binding energies for poly-neutrons and poly-protons.

| poly-neutron | $n$ | $^2n$ | $^3n$ | $^4n$ |
|---|---|---|---|---|
| $E_{B,app}/MeV$ | 0 | $E_B(^2H) + \frac{\Delta}{2}$ | $E_B(^3H) + \frac{2\Delta}{3}$ | $E_B(^4He) + \frac{\Delta}{2}$ |
| poly-proton | $p$ | $^2p$ | $^3p$ | $^4p$ |
| $E_{B,app}/MeV$ | 0 | $E_B(^2H) - \frac{\Delta}{2}$ | $E_B(^3He) - \frac{\Delta}{3}$ | $E_B(^4He) - \frac{\Delta}{2}$ |

For heavier nuclei $E_{B,app}(^4n)$ is smaller than $E_B(^4He) + (m_p - m_n)/2$.

The first guess for the general formula for the binding energy for nucleus $(Z, N)$ is obtained by assuming that for maximum number of $^4He$ nuclei and tetra-neutrons/tetra-protons identified as $^4H$ nuclei with 2 negatively/positively charged color bonds are present.

*1. $N \geq Z$ nuclei*

Even-Z nuclei with $N \geq Z$ can be expressed as $(Z = 2n, N = 2(n+k) + m)$, $m = 0, 1, 2$ or 3. For $Z \leq 26$ (only single Bose-Einstein condensate)

this gives for the apparent binding energy per nucleon (assuming that all neutrons are indeed neutrons) the formula

$$\begin{aligned} E_B(2n, 2(n+k)+m) &= \frac{n}{A}E_B(^4He) + \frac{k}{A}E_{B,app}(^4n) + \frac{1}{A}E_{B,app}(^m n) \\ &+ \frac{n^2+k^2}{n+k}E_s - \frac{Z(Z-1)}{A^2}E_c \ . \end{aligned} \tag{13}$$

The situation for the odd-Z nuclei $(Z, N) = (2n+1, 2(n+k)+m)$ can be reduced to that for even-Z nuclei if one can assume that the $(2n+1)^{th}$ proton combines with 2 neutrons to form $^3He$ nucleus so that one has still $2(k-1)+m$ neutrons combining to $A \leq 4$ poly-neutrons in above described manner.

*2. $Z \geq N$ nuclei*

For the nuclei having $Z > N$ the formation of a maximal number of $^4He$ nuclei leaves $k$ excess protons. For long-lived nuclei $k \leq 2$ is satisfied. One could think of decomposing the excess protons to exotic variants of $A \leq 4$ nuclei by assuming that some charged bonds carry positive charge with an obvious generalization of the above formula.

The only differences with respect to a nucleus with neutron excess would be that the apparent binding energy is smaller than the actual one and positive charge would give rise to Coulomb interaction energy reducing the binding energy (but only very slightly). The change of the binding energy in the subtraction of single neutron from $Z = N = 2n$ nucleus is predicted to be approximately $\Delta E_B = -E_B(^4He)/A$. In the case of $^{32}S$ this predicts $\Delta E_B = .2209$ MeV. The real value is .2110 MeV. The fact that the general order of magnitude for the change of the binding energy as $Z$ or $N$ changes by one unit supports the proposed picture.

### 5.5 Nuclear strings and cold fusion

To summarize, option Ia) assuming that strong isospin dependent force acts on the nuclear space-time sheet and binds pn pairs to singlets such that the strong binding energy is very nearly zero in singlet state by the cancellation of scalar and vector contributions, is the most promising one. It predicts the existence of exotic di-,tri-, and tetra-neutron like particles and even negatively charged exotics obtained from $^2H$,$^3H$,$^3He$, and $^4He$ by adding negatively charged color bond. For instance, $^3H$ extends to a multiplet with em charges $1, 0, -1, -2$. Of course, heavy nuclei with proton neutron excess could actually be such nuclei.

The exotic states are stable under beta decay for $m(\pi) < m_e$. The simplest neutral exotic nucleus corresponds to exotic deuteron with single negatively charged color bond. Using this as target it would be possible to achieve cold fusion since Coulomb wall would be absent. The empirical evidence for cold fusion thus supports the prediction of exotic charged states.

### 5.5.1 Signatures of cold fusion

In the following the consideration is restricted to cold fusion in which two deuterium nuclei react strongly since this is the basic reaction type studied.

In hot fusion there are three reaction types:

1) $D + D \rightarrow^4 He + \gamma$ $(23.8MeV)$

2) $D + D \rightarrow^3 He + n$

3) $D + D \rightarrow^3 H + p$.

The rate for the process 1) predicted by standard nuclear physics is more than $10^{-3}$ times lower than for the processes 2) and 3) [12]. The reason is that the emission of the gamma ray involves the relatively weak electromagnetic interaction whereas the latter two processes are strong.

The most obvious objection against cold fusion is that the Coulomb wall between the nuclei makes the mentioned processes extremely improbable at room temperature. Of course, this alone implies that one should not apply the rules of hot fusion to cold fusion. Cold fusion indeed differs from hot fusion in several other aspects.

a) No gamma rays are seen.

b) The flux of energetic neutrons is much lower than expected on basis of the heat production rate an by interpolating hot fusion physics to the recent case.

These signatures can also be (and have been!) used to claim that no real fusion process occurs. It has however become clear that the isotopes of Helium and also some tritium accumulate to the Pd target during the reaction and already now prototype reactors for which the output energy exceeds input energy have been built and commercial applications are under development, see for instance [13]. Therefore the situation has turned around. The rules of standard physics do not apply so that some new nuclear physics must be involved and it has become an exciting intellectual challenge to understand what is happening. A representative example of this attitude and an enjoyable analysis of the counter arguments against fold fusion is provided by the article 'Energy transfer in cold fusion and sono-luminescence' of Julian Schwinger [14]. This article should be contrasted with the ultra-skeptical article 'ESP and Cold Fusion: parallels in pseudoscience' of V. J.

Stenger [15].

Cold fusion has also other features, which serve as valuable constraints for the model building.

a) Cold fusion is not a bulk phenomenon. It seems that fusion occurs most effectively in nano-particles of Pd and the development of the required nano-technology has made possible to produce fusion energy in controlled manner. Concerning applications this is a good news since there is no fear that the process could run out of control.

b) The ratio $x$ of D atoms to Pd atoms in Pd particle must lie the critical range $[.85, .90]$ for the production of $^4He$ to occur [16]. This explains the poor repeatability of the earlier experiments and also the fact that fusion occurred sporadically.

c) Also the transmutations of Pd nuclei are observed [**?**].

Below a list of questions that any theory of cold fusion should be able to answer.

a) Why cold fusion is not a bulk phenomenon?

b) Why cold fusion of the light nuclei seems to occur only above the critical value $x \simeq .85$ of D concentration?

c) How fusing nuclei are able to effectively circumvent the Coulomb wall?

d) How the energy is transferred from nuclear degrees of freedom to much longer condensed matter degrees of freedom?

e) Why gamma rays are not produced, why the flux of high energy neutrons is so low and why the production of $^4He$ dominates (also some tritium is produced)?

f) How nuclear transmutations are possible?

### 5.5.2 Could exotic deuterium make cold fusion possible?

One model of cold fusion has been already discussed in [F8] and the recent model is very similar to that. The basic idea is that only the neutrons of incoming and target nuclei can interact strongly, that is their space-time sheets can fuse. One might hope that neutral deuterium having single negatively charged color bond could allow to realize this mechanism.

a) Suppose that part of the deuterium in $Pd$ catalyst corresponds to exotic deuterium with neutral nuclei so that cold fusion would occur between neutral exotic $D$ nuclei in the target and charged incoming $D$ nuclei and Coulomb wall in the nuclear scale would be absent.

b) The exotic variant of the ordinary $D + D$ reaction yields final states in which $^4He$, $^3He$ and $^3H$ are replaced with their exotic counterparts with charge lowered by one unit. In particular, exotic $^3H$ is neutral and there is

no Coulomb wall hindering its fusion with Pd nuclei so that nuclear transmutations can occur.

Why the neutron and gamma fluxes are low might be understood if for some reason only exotic $^3H$ is produced, that is the production of charged final state nuclei is suppressed. The explanation relies on Coulomb wall at the nucleon level.

a) Initial state contains one charged and one neutral color bond and final state $A = 3$ or $A = 4$ color bonds. Additional neutral color bonds must be created in the reaction (one for the production $A = 3$ final states and two for $A = 4$ final state). The process involves the creation of neural fermion pairs. The emission of one exotic gluon per bond decaying to a neutral pair is necessary to achieve this. This requires that nucleon space-time sheets fuse together. Exotic $D$ certainly belongs to the final state nucleus since charged color bond is not expected to be split in the process.

b) The process necessarily involves a temporary fusion of nucleon space-time sheets. One can understand the selection rules if only neutron space-time sheets can fuse appreciably so that only $^3H$ would be produced. Here Coulomb wall at nucleon level should enter into the game.

c) Protonic space-time sheets have the same positive sign of charge always so that there is a Coulomb wall between them. This explains why the reactions producing exotic $^4He$ do not occur appreciably. If the quark/antiquark at the neutron end of the color bond of ordinary $D$ has positive charge, there is Coulomb attraction between proton and corresponding negatively charged quark. Thus energy minimization implies that the neutron space-time sheet of ordinary $D$ has positive net charge and Coulomb repulsion prevents it from fusing with the proton space-time sheet of target $D$. The desired selection rules would thus be due to Coulomb wall at the nucleon level.

### 5.5.3 About the phase transition transforming ordinary deuterium to exotic deuterium

The exotic deuterium at the surface of $Pd$ target seems to form patches (for a detailed summary see [F8]). This suggests that a condensed matter phase transition involving also nuclei is involved. A possible mechanism giving rise to this kind of phase would be a local phase transition in the $Pd$ target involving both $D$ and $Pd$. In [F8] it was suggested that deuterium nuclei transform in this phase transition to "ordinary" di-neutrons connected by a charged color bond to $Pd$ nuclei. In the recent case di-neutron could be replaced by neutral $D$.

The phase transition transforming neutral color bond to a negatively

charged one would certainly involve the emission of $W^+$ boson, which must be exotic in the sense that its Compton length is of order atomic size so that it could be treated as a massless particle and the rate for the process would be of the same order of magnitude as for electro-magnetic processes. One can imagine two options.

a) Exotic $W^+$ boson emission generates a positively charged color bond between $Pd$ nucleus and exotic deuteron as in the previous model.

b) The exchange of exotic $W^+$ bosons between ordinary $D$ nuclei and $Pd$ induces the transformation $Z \to Z+1$ inducing an alchemic phase transition $Pd \to Ag$. The most abundant $Pd$ isotopes with $A = 105$ and 106 would transform to a state of same mass but chemically equivalent with the two lightest long-lived $Ag$ isotopes. $^{106}Ag$ is unstable against $\beta^+$ decay to $Pd$ and $^{105}Ag$ transforms to $Pd$ via electron capture. For $^{106}Ag$ ($^{105}Ag$) the rest energy is 4 MeV (2.2 MeV) higher than for $^{106}Pd$ ($^{105}Pd$), which suggests that the resulting silver cannot be genuine.

This phase transition need not be favored energetically since the energy loaded into electrolyte could induce it. The energies should (and could in the recent scenario) correspond to energies typical for condensed matter physics. The densities of $Ag$ and $Pd$ are 10.49 gcm$^{-3}$ and 12.023 gcm$^{-3}$ so that the phase transition would expand the volume by a factor 1.0465. The porous character of $Pd$ would allow this. The needed critical packing fraction for $Pd$ would guarantee one $D$ nucleus per one $Pd$ nucleus with a sufficient accuracy.

### 5.5.4 Exotic weak bosons seem to be necessary

The proposed phase transition cannot proceed via the exchange of the ordinary $W$ bosons. Rather, $W$ bosons having Compton length of order atomic size are needed. These $W$ bosons could correspond to a scaled up variant of ordinary $W$ bosons having smaller mass, perhaps even of the order of electron mass. They could be also dark in the sense that Planck constant for them would have the value $\hbar = n\hbar_0$ implying scaling up of their Compton size by $n$. For $n \sim 2^{48}$ the Compton length of ordinary $W$ boson would be of the order of atomic size so that for interactions below this length scale weak bosons would be effectively massless. p-Adically scaled up copy of weak physics with a large value of Planck constant could be in question. For instance, $W$ bosons could correspond to the nuclear p-adic length scale $L(k = 113)$ and $n = 2^{11}$.

### 5.6 Strong force as a scaled and dark electro-weak force?

The fiddling with the nuclear string model has led to following conclusions.

a) Strong isospin dependent nuclear force, which does not reduce to color force, is necessary in order to eliminate polyneutron and polyproton states. This force contributes practically nothing to the energies of bound states. This can be understood as being due to the cancellation of isospin scalar and vector parts of this force for them. Only strong isospin singlets and their composites with isospin doublet (n,p) are allowed for $A \leq 4$ nuclei serving as building bricks of the nuclear strings. Only *effective* polyneutron states are allowed and they are strong isospin singlets or doublets containing charged color bonds.

b) The force could act in the length scalar of nuclear space-time sheets: $k = 113$ nuclear p-adic length scale is a good candidate for this length scale. One must be however cautious: the contribution to the energy of nuclei is so small that length scale could be much longer and perhaps same as in case of exotic color bonds. Color bonds connecting nuclei correspond to much longer p-adic length scale and appear in three p-adically scaled up variants corresponding to $A < 4$ nuclei, $A = 4$ nuclei and $A > 4$ nuclei.

c) The prediction of exotic deuterons with vanishing nuclear em charge leads to a simplification of the earlier model of cold fusion explaining its basic selection rules elegantly but requires a scaled variant of electro-weak force in the length scale of atom.

What is then this mysterious strong force? And how abundant these copies of color and electro-weak force actually are? Is there some unifying principle telling which of them are realized?

From foregoing plus TGD inspired model for quantum biology involving also dark and scaled variants of electro-weak and color forces it is becoming more and more obvious that the scaled up variants of both QCD and electro-weak physics appear in various space-time sheets of TGD Universe. This raises the following questions.

a) Could the isospin dependent strong force between nucleons be nothing but a p-adically scaled up (with respect to length scale) version of the electro-weak interactions in the p-adic length scale defined by Mersenne prime $M_{89}$ with new length scale assigned with gluons and characterized by Mersenne prime $M_{107}$? Strong force would be electro-weak force but in the length scale of hadron! Or possibly in length scale of nucleus ($k_{eff} = 107 + 6 = 113$) if a dark variant of strong force with $h = nh_0 = 2^3 h_0$ is in question.

b) Why shouldn't there be a scaled up variant of electro-weak force also in the p-adic length scale of the nuclear color flux tubes?

c) Could it be that all Mersenne primes and also other preferred p-adic primes correspond to entire standard model physics including also gravitation? Could be be kind of natural selection which selects the p-adic survivors as proposed long time ago?

Positive answers to the last questions would clean the air and have quite a strong unifying power in the rather speculative and very-many-sheeted TGD Universe.

a) The prediction for new QCD type physics at $M_{89}$ would get additional support. Perhaps also LHC provides it within the next half decade.

b) Electro-weak physics for Mersenne prime $M_{127}$ assigned to electron and exotic quarks and color excited leptons would be predicted. This would predict the exotic quarks appearing in nuclear string model and conform with the 15 year old leptohadron hypothesis [F7]. $M_{127}$ dark weak physics would also make possible the phase transition transforming ordinary deuterium in $Pd$ target to exotic deuterium with vanishing nuclear charge.

The most obvious objection against this unifying vision is that hadrons decay only according to the electro-weak physics corresponding to $M_{89}$. If they would decay according to $M_{107}$ weak physics, the decay rates would be much much faster since the mass scale of electro-weak bosons would be reduced by a factor $2^{-9}$ (this would give increase of decay rates by a factor $2^{36}$ from the propagator of weak boson). This is however not a problem if strong force is a dark with say $n = 8$ giving corresponding to nuclear length scale. This crazy conjecture might work if one accepts the dark Bohr rules!

# 6 Giant dipole resonance as a dynamical signature for the existence of Bose-Einstein condensates?

The basic characteristic of the Bose-Einstein condensate model is the non-linearity of the color contribution to the binding energy. The implication is that the the de-coherence of the Bose-Einstein condensate of the nuclear string consisting of $^4He$ nuclei costs energy. This de-coherence need not involve a splitting of nuclear strings although also this is possible. Similar de-coherence can occur for $^4He$ $A < 4$ nuclei. It turns out that these three de-coherence mechanisms explain quite nicely the basic aspects of giant dipole resonance (GDR) and its variants both qualitatively and quantitatively and that precise predictions for the fine structure of GDR emerge.

### 6.1 De-coherence at the level of $^4He$ nuclear string

The de-coherence of a nucleus having $n$ $^4He$ nuclei to a nucleus containing two Bose-Einstein condensates having $n-k$ and $k>2$ $^4He$ nuclei requires energy given by

$$\begin{aligned} \Delta E &= (n^2-(n-k)^2-k^2)E_s = 2k(n-k)E_s \ , \ k>2 \ , \\ \Delta E &= (n^2-(n-2)^2-1)E_s = (4n-5)E_s \ , \ k=2 \ , \\ E_s &\simeq .1955 \ MeV \ . \end{aligned} \tag{14}$$

Bose-Einstein condensate could also split into several pieces with some of them consisting of single $^4He$ nucleus in which case there is no contribution to the color binding energy. A more general formula for the resonance energy reads as

$$\begin{aligned} \Delta E &= (n^2-\sum_i k^2(n_i))E_s \ , \ \sum_i n_i = n \ , \\ k(n_i) &= \begin{cases} n_i \ \text{for} \ n_i > 2 \ , \\ 1 \ \text{for} \ n_i = 2 \ , \\ 0 \ \text{for} \ n_i = 1 \ . \end{cases} \end{aligned} \tag{15}$$

The table below lists the resonance energies for four manners of $^{16}O$ nucleus ($n=4$) to lose its coherence.

| final state | 3+1 | 2+2 | 2+1+1 | 1+1+1+1 |
|---|---|---|---|---|
| $\Delta E/MeV$ | 1.3685 | 2.7370 | 2.9325 | 3.1280 |

Rather small energies are involved. More generally, the minimum and maximum resonance energy would vary as $\Delta E_{min} = (2n-1)E_s$ and $\Delta E_{max} = n^2E_s$ (total de-coherence). For $n=n_{max}=13$ one would have $\Delta E_{min} =$ 2.3640 MeV and $\Delta E_{max} = 33.099$ MeV.

Clearly, the loss of coherence at this level is a low energy collective phenomenon but certainly testable. For nuclei with $A>60$ one can imagine also double resonance when both coherent Bose-Einstein condensates possibly present split into pieces. For $A \geq 120$ also triple resonance is possible.

### 6.2 De-coherence inside $^4He$ nuclei

One can consider also the loss of coherence occurring at the level $^4He$ nuclei. In this case one has $E_s = 1.820$ MeV. In this case de-coherence would

mean the decomposition of Bose-Einstein condensate to $n = 4 \rightarrow \sum n_i = n$ with $\Delta E = n^2 - \sum_{n_i} k^1(n_i) = 16 - \sum_{n_i} k^2(n_i)$. The table below gives the resonance energies for the four options $n \rightarrow \sum_i n_i$ for the loss of coherence.

| final state | 3+1 | 2+2 | 2+1+1 | 1+1+1+1 |
|---|---|---|---|---|
| $\Delta E/MeV$ | 12.74 | 25.48 | 27.30 | 29.12 |

These energies span the range at which the cross section for $^{16}O(\gamma, xn)$ reaction has giant dipole resonances [18]. Quite generally, GDR is a broad bump with substructure beginning around 10 MeV and ranging to 30 MeV. The average position of the bump as a function of atomic number can be parameterized by the following formula

$$E(A)/MeV \quad = \quad 31.2A^{-1/3} + 20.6A^{-1/6} \tag{16}$$

given in [19]. The energy varies from 36.6 MeV for $A = 4$ (the fit is probably not good for very low values of $A$) to 13.75 MeV for $A = 206$. The width of GDR ranges from 4-5 MeV for closed shell nuclei up to 8 MeV for nuclei between closed shells.

The observation raises the question whether the de-coherence of Bose-Einstein condensates associated with $^4He$ and nuclear string could relate to GDR and its variants. If so, GR proper would be a collective phenomenon both at the level of single $^4He$ nucleus (main contribution to the resonance energy) and entire nucleus (width of the resonance). The killer prediction is that even $^4He$ should exhibit giant dipole resonance and its variants: GDR in $^4He$ has been reported [20].

This hypothesis seems to survive the basic qualitative and quantitative tests.

a) The basic prediction of the model peak at 12.74 MeV and at triplet of closely located peaks at $(25.48, 27.30, 29.12)$ MeV spanning a range of about 4 MeV, which is slightly smaller than the width of GDR. According to [21] there are two peaks identified as iso-scalar GMR at $13.7 \pm .3$ MeV and iso-vector GMR at $26 \pm 3$ MeV. The 6 MeV uncertainty related to the position of iso-vector peak suggests that it corresponds to the triplet $(25.48, 27.30, 29.12)$ MeV whereas singlet would correspond to the iso-scalar peak. According to the interpretation represented in [21] iso-scalar *resp.* iso-vector peak would correspond to oscillations of proton and neutron densities in same *resp.* opposite phase. This interpretation can make sense in TGD framework only inside single $^4He$ nucleus and would apply to the transverse oscillations of $^4He$ string rather than radial oscillations of entire nucleus.

b) The presence of triplet structure seems to explain most of the width of iso-vector GR. The combination of GDR internal to $^4He$ with GDR for the entire nucleus (for which resonance energies vary from $\Delta E_{min} = (2n-1)E_s$ to $\Delta E_{max} = n^2 E_s$ $(n = A/4)$) predicts that also latter contributes to the width of GDR and give it additional fine structure. The order of magnitude for $\Delta E_{min}$ is in the range [1.3685,2.3640] MeV which is consistent with the with of GDR and predicts a band of width 1 MeV located 1.4 MeV above the basic peak.

c) The de-coherence of $A < 4$ nuclei could increase the width of the peaks for nuclei with partially filled shells: maximum and minimum values of resonance energy are $9E_s(^4He)/2 = 8.19$ MeV and $4E_s(^4He) = 7.28$ MeV for $^3He$ and $^3H$ which conforms with the upper bound 8 MeV for the width.

d) It is also possible that $n$ $^4He$ nuclei simultaneously lose their coherence. If multiplet de-coherence occurs coherently it gives rise to harmonics of GDR. For de-coherent decoherence so that the emitted photons should correspond to those associated with single $^4He$ GDR combined with nuclear GDR. If absorption occurs for $n \leq 13$ nuclei simultaneously, one obtains a convoluted spectrum for resonant absorption energy

$$\Delta E \quad = \quad [16n - \sum_{j=1}^{n} \sum_{i_j} k^2(n_{i_j})]E_s \ . \tag{17}$$

The maximum value of $\Delta E$ given by $\Delta E_{max} = n \times 29.12$ MeV. For $n = 13$ this would give $\Delta E_{max} = 378.56$ MeV for the upper bound for the range of excitation energies for GDR. For heavy nuclei [19] GDR occurs in the range 30-130 MeV of excitation energies so that the order of magnitude is correct. Lower bound in turn corresponds to a total loss of coherence for single $^4He$ nucleus.

e) That the width of GDR increases with the excitation energy [19] is consistent with the excitation of higher GDR resonances associated with the entire nuclear string. $n \leq n_{max}$ for GDR at the level of the entire nucleus means saturation of the GDR peak with excitation energy which has been indeed observed [18].

One can look whether the model might work even at the level of details. Figure 3 of [18] compares total photoneutron reaction cross sections for $^{16}O(\gamma, xn)$ in the range 16-26 MeV from some experiments so that the possible structure at 12.74 MeV is not visible in it. It is obvious that the resonance structure is more complex than predicted by the simplest model. It seems however possible to explain this.

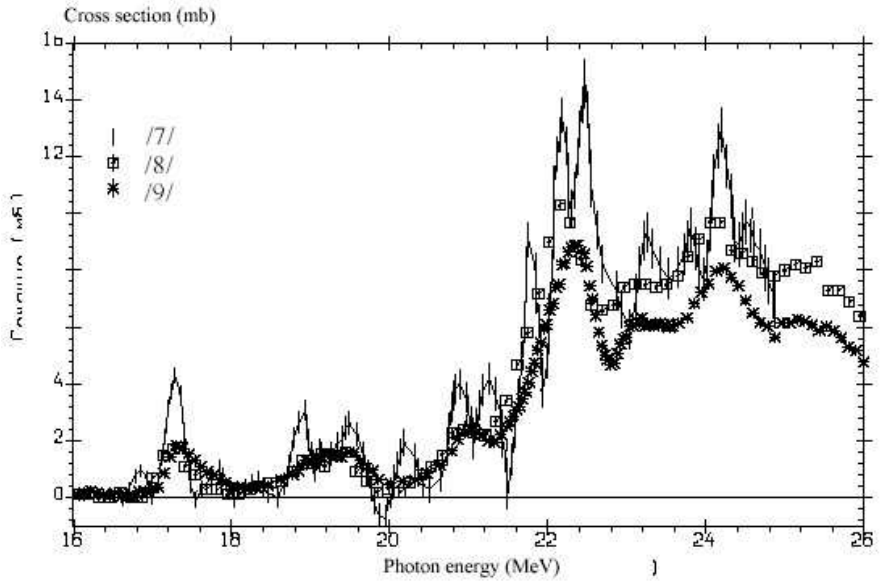


Figure 1: The comparison of photoneutron cross sections $^{16}O(\gamma, xn)$ obtained in one BR-experiment (Moscow State University) and two QMA experiments carried out at Saclay (France) Livermoore (USA). Figure is taken from [18] where also references to experiments can be found.

a) The main part of the resonance is a high bump above 22 MeV spanning an interval of about 4 MeV just as the triplet at (25.48,27.30,29.12) MeV does. This suggest a shift of the predicted 3-peak structure in the range 25-30 MeV range downwards by about 3 MeV. This happens if the photo excitation inducing the de-coherence involves a dropping from a state with excitation energy of 3 MeV to the ground state. The peak structure has peaks roughly at the shifted energies but there is also an additional structure which might be understood in terms of the bands of width 1 MeV located 1.4 MeV above the basic line.

b) There are three smaller bumps below the main bump which also span a range of 4 MeV which suggests that also they correspond to a shifted variant of the basic three-peak structure. This can be understood if the photo excitation inducing de-coherence leads from an excited state with excitation energy 8.3 MeV to ground state shifting the resonance triplet

(25.48, 27.30, 29.12) MeV to resonance triplet at (17.2, 19.00, 20.82) MeV.

On basis of these arguments it seems that the proposed mechanism might explain GR and its variants. The basic prediction would be the presence of singlet and triplet resonance peaks corresponding to the four manners to lose the coherence. Second signature is the precise prediction for the fine structure of resonance peaks.

### 6.3 De-coherence inside $A = 3$ nuclei and pygmy resonances

For neutron rich nuclei the loss of coherence is expected to occur inside $^4He$, tetra-neutron, $^3He$ and possibly also $^3n$ which might be stable in the nuclear environment. The de-coherence of tetra-neutron gives in the first approximation the same resonance energy spectrum as that for $^4He$ since $E_B(^4n) \sim E_B(^4He)$ roughly consistent with the previous estimates for $E_B(^4n)$ implies $E_s(^4n) \sim E_s(^4He)$.

The de-coherence inside $A = 3$ nuclei might explain the so called pygmy resonance appearing in neutron rich nuclei, which according to [22] is wide bump around $E \sim 8$ MeV. For $A = 3$ nuclei only two de-coherence transitions are possible: $3 \to 2 + 1$ and $3 \to 1 + 1 + 1$ and $E_s = E_B(^3H) = .940$ MeV the corresponding energies are $8E_s = 7.520$ MeV and $9 * Es = 8.4600$ MeV. Mean energy is indeed $\sim 8$ MeV and the separation of peaks about 1 MeV. The de-coherence at level of $^4He$ string might add to this 1 MeV wide bands about 1.4 MeV above the basic lines.

The figure of [23] illustrating photo-absorption cross section in $^{44}Ca$ and $^{48}Ca$ shows three peaks at 6.8, 7.3, 7.8 and 8 MeV in $^{44}Ca$. The additional two peaks might be assigned with the excitation of initial or final states. This suggests also the presence of also $A = 3$ nuclear strings in $^{44}Ca$ besides $^H4$ and $^4n$ strings. Perhaps neutron halo wave function contains $^3n + n$ component besides $^4n$. For $^{48}Ca$ these peaks are much weaker suggesting the dominance of $2\times^4n$ component.

**Acknowledgements**

I am grateful for Elio Conte for discussions which inspired further study of the nuclear string model.

## References

[TGDquant] M. Pitkänen (2006), *Quantum TGD*.
http://www.helsinki.fi/∼matpitka/tgdquant/tgdquant.html.

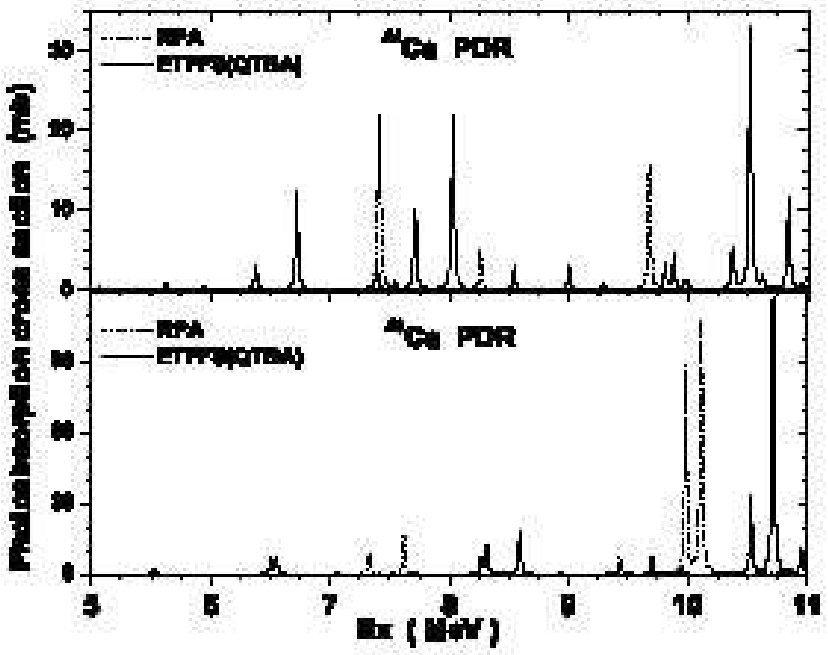


Figure 2: Pygmy resonances in $^{44}Ca$ and $^{48}Ca$ up to 11 MeV. Figure is taken from [23].

[TGDpad] M. Pitkänen (2006), *p-Adic length Scale Hypothesis and Dark Matter Hierarchy*. http://www.helsinki.fi/∼matpitka/paddark/paddark.html.

[1] P. G. Hansen(1993), *Nuclear structure at the drip lines*, Nuclear Phys. A, Vol. 553.

[2] F. M. Marquez *et al* (2003), Phys. Rev. C65, 044006.

[3] C.A. Bertulani, V. Zelevinsky (2002), *Is the tetra-neutron a bound dineutron-dineutron molecule?*, J.Phys. G29, 2431-2437. arXiv:nucl-th/0212060.

[4] C. Illert (1993), *ALCHEMY TODAY-Platonic Geometries in Nuclear Physics*, Volume 1. ISBN 0 949357 13 8, second edition. Science-Art Library.

[5] S. Moszkowski (1996), *Maria Goeppert Mayer*,Talk Presented at APS meeting Indianapolis, May 4, 1996.
http://www.physics.ucla.edu/ moszkows/mgm/mgmso.htm. See also *"Magic Numbers" in Nuclear Structure*,
http://hyperphysics.phy-astr.gsu.edu/hbase/nuclear/shell.html#c2.
*Enhanced abundance of magic number nuclei*,
http://hyperphysics.phy-astr.gsu.edu/hbase/nuclear/shell2.html.

[6] B. Dume (2005), *"Magic" numbers remain magic*, Physics Web. http://physicsweb.org/articles/news/9/6/9/1. (Si(14,28) is magic unstable nucleus.)
B. Ray (2005), *FSU researchers find 'magic' at the subatomic level*,
http://www.fsu.com/pages/2005/07/05/magic_subatomic.html.
(Magic Number N=14.)
*New Magic Number "16" Where Nuclei Exist Stably Discovered*,
http://www.mext.go.jp/english/news/2000/06/s000606.html.
A. Ozawa *et al* (2000), Phys. Rev. Lett.84, 5493. (Magic number N=16).
A. Ozawa *et al* (2001), *Observation of new proton and neutron magic numbers*, http://lbl.confex.com/lbl/2001/program/abstract_97.htm.
(Magic numbers N=16,20,32.)

[7] *The Berkeley Laboratory Isotopes Project's Exploring the Table of Isotopes*,
http://ie.lbl.gov/education/parent/Ti_iso.htm.

[8] R. Howard (1963), *Nuclear Physics*,Wadsworth Publishing Comparny, Inc..

[9] J. E. Ungar (1982), *Double Charge Exchange of pions on* $^4$*He*, PhD thesis in California Institute of Technology,
http://etd.caltech.edu/etd/available/etd-11032005-112918/unrestricted/Ungar_je_1983.pdf

[10] *Dineutron*, http://en.wikipedia.org/wiki/Dineutron.

[11] *Polyneutron*, http://en.wikipedia.org/wiki/Polyneutron.

[12] E. Storms (2001),*Cold fusion, an objective assessment*, http://home.netcom.com/ storms2/review8.html.

[13] Russ George's homepage, http://www.hooked.net/ rgeorge/saturnahome.html .

[14] J. Schwinger (1992), *Energy Transfer In Cold Fusion and Sonoluminescence*, http://jcbmac.chem.brown.edu/baird/coldfusion/schwinger.html.

[15] V. J. Stenger (1995), *ESP and Cold Fusion: parallels in pseudoscience*, http://www.phys.hawaii.edu/vjs/www/cold.txt.

[16] *Whatever happened to cold fusion?* http://www.caltech.edu:80/7Egoodstein/fusion.html. ork.

[17] S. M. Wong(1990), *Introductory Nuclear Physics*, Prentice-Hall Inc.

[18] B. S. Iskhanov, I. M. Kapitonov, V. V. Varlamov, *Giant Dipole Resonance: What is Known About?*, http://cdfe.sinp.msu.ru/publications/lshkhnv-ELI03.pdf.

[19] T. Baumann *et al* (1998), *Evolution of the Giant Dipole Resonance in Excited* $^{120}Sn$ *and* $^{208}Pb$ *Nuclei Populated by Inelastic Alpha Scattering*, Nucl. Phys. A 635, 428-445. http://www.phy.ornl.gov/progress/ribphys/reaction/rib031.pdf.

[20] T. Yamagata *et al* (2005), *Excitations of the Giant Dipole Resonances in* $^{4}He$ *and in the alpha Cluster of* $^{6,7}Li$ *via (p,p′) Reactions*, EXOTIC NUCLEAR SYSTEMS: International Symposium on Exotic Nuclear Systems ENS'05. AIP Conference Proceedings, Volume 802, pp. 301-304.

[21] D. Vretenar, N. Paar, P. Ring, G. A. Lasazissis (1998), *Nonlinear dynamics of giant resonances in atomic nuclei*, arXiv:nucl-th/9809003.

[22] T. N. Leite, N. Teruya *Structure of the Isovector Dipole Resonance in Neutron-Rich* $^{60}Ca$ *Nucleus and Direct Decay from Pygmy Resonance.* arXiv:nucl-th/0308081.

[23] G. Tertuchny *et al* (2006), *Microscopic description of the pygmy and giant electric dipole resonances in stable Ca isotopes.* arXiv:nucl-th/0603/0603051.

[24] X.-G. He, J. Tandean, G. Valencia (2007), *Has HyperCP Observed a Light Higgs Boson?*,Phys. Rev. D74.
http://arxiv.org/abs/hep-ph/0610274.

[25] X.-G. He, J. Tandean, G. Valencia (2007), *Light Higgs Production in Hyperon Decay*, Phys. Rev. Lett. 98.
http://arxiv.org/abs/hep-ph/0610362.

[F7] The chapter *The Recent Status of Leptohadron Hypothesis* of [TGDpad].
http://www.helsinki.fi/∼matpitka/paddark/paddark.html#leptc.

[F8] The chapter *TGD and Nuclear Physics* of [TGDpad].
http://www.helsinki.fi/∼matpitka/paddark/paddark.html#padnucl.

# The Notion of Free Energy and Many-Sheeted Space-Time Concept

M. Pitkänen[1], October 1, 2007

[1] Department of Physical Sciences, High Energy Physics Division,
PL 64, FIN-00014, University of Helsinki, Finland.
matpitka@rock.helsinki.fi, http://www.physics.helsinki.fi/∼matpitka/.
Recent address: Puutarhurinkatu 10,10960, Hanko, Finland.

## Contents

**1 Introduction**
- 1.1 Basic new elements of TGD ontology . . . . . .
- 1.2 Could living systems teach us something about energy technology? . . . . . .
- 1.3 Various anomalies as support for the new view . . . . . .

**2 Basic ontology of TGD**
- 2.1 T(opological) G(eometro)D(ynamics) very briefly . . . . . .
- 2.2 Many-sheeted space-time and the notion of field body . . . .
- 2.3 The hierarchy of Planck constants and of dark matter . . . .
  - 2.3.1 Physical motivations for introducing the hierarchy of Planck constants . . . . . .
  - 2.3.2 The notion of field body and dark matter . . . . . .
- 2.4 Zero energy ontology . . . . . .
  - 2.4.1 Zero energy ontology and unification of the notions of S-matrix and density matrix . . . . . .
  - 2.4.2 Time mirror mechanism . . . . . .
  - 2.4.3 More detailed view about time mirror mechanism in zero energy ontology . . . . . .
- 2.5 p-Adic physics as physics of cognition and intentionality . . .

**3 Many-sheeted space-time, universal metabolic quanta, and plasmoids as primitive life forms**
- 3.1 Evidence for many-sheeted space-time . . . . . .
  - 3.1.1 Unidentified Infrared Bands . . . . . .

3.1.2 Diffuse Interstellar Bands . . . . . .
3.1.3 The Extended Red Emission . . . . . .
3.2 Laboratory evidence for plasmoids as life forms . . . . . .
3.2.1 From dust to dust .....
3.2.2 Elephant trunks in astrophysics . . . . . .
3.3 Universal metabolic quanta .....
3.3.1 Could UV photons have some metabolic role? . . . . .
3.3.2 A simple model for the metabolism of plasmoids . . .
3.3.3 Anomalous light phenomena as plasmoids . . . . . .
3.4 Life as a symbiosis of plasmoids and biological life . . . . . .

**4 New hydrogen technologies and new physics**

4.1 Anomalies related to the dissociation of water and hydrogen molecules
4.2 The anomalies associated with the dissociation of water molecules
4.2.1 Constraints on the model of anomalies found in the electrolysis and plasma electrolysis of water . . . . . .
4.2.2 Zero point kinetic energies. . . . . .
4.2.3 Consistency conditions.....
4.2.4 Experimental data .....
4.2.5 The four options .....
4.2.6 Analysis and conclusions.....
4.3 The anomaly related to the thermal dissociation of molecular hydrogen
4.4 Hydrino atoms, anyons, and fractional quantization in many sheeted space-time .....
4.4.1 p-Adic quantization and fractional spectrum . . . . .
4.4.2 Fractional valued quantum numbers and controlled transition to chaos .....
4.4.3 Fractional quantization and controlled transition to chaos at space-time level.....
4.5 An explanation of findings of Mills in terms of quantized Planck constant.....
4.5.1 Quantization of Planck constants and the generalization of the notion of imbedding space . . . . . .
4.5.2 Explanation for the findings of Mills . . . . . .
4.6 Free energy from atomic hydrogen . . . . . .

**5 Appendix: A generalization of the notion of imbedding space inspired by hierarchy of Planck constants**

5.1 The original view about generalized imbedding space . . . . .
5.2 Fractionization of quantum numbers is not possible if only factor spaces are allowed.....
5.3 Both covering spaces and factor spaces are possible . . . . . .
5.4 Do factor spaces and coverings correspond to the two kinds of Jones inclusions?.....

**Abstract**

In this article a general vision about new energy technologies provided by the new ontology forced by TGD is discussed, some evidence for the new ontology is considered, and models explaining some "free energy" anomalies are represented.

There are close connections to the basic mechanisms of energy metabolism in living matter in TGD Universe and one cannot avoid even reference to TGD inspired quantum theory of consciousness. The point is that so called time mirror mechanism defines a mechanism of remote metabolism as sucking of energy from remote energy storage, a mechanism of memory as communications with geometric past, and mechanism of intentional action initiating neural activity in geometric past. At the level of technology time mirror mechanism would define a mechanism of energy transfer, communication, and remote quantum control.

# 1 Introduction

In this article the T(opological) G(eometro)D(ynamics) [TGD] based vision about new energy technologies is discussed. There are close connections to the basic mechanisms of energy metabolism in living matter in TGD Universe and one cannot avoid reference to TGD inspired quantum theory of consciousness [TGDconsc].

## 1.1 Basic new elements of TGD ontology

The ontology of TGD Universe involves several new elements. The assumption that space-times are 4-surfaces in 8-dimensional imbedding space $M^4 \times CP_2$ leads to the notion of many-sheeted space-time meaning that each physical system can be said to correspond to space-time sheet, its own sub-universe in the geometric sense, and glued to a larger space-time sheet and containing subsystems as smaller space-time sheets glued to it. p-Adic length scale hypothesis quantifies this notion.

Many-sheeted space-time leads to the notion of field body [F10, N1, J7] distinguishing between TGD and Maxwell's electrodynamics. One can assign to each physical system a field body (or magnetic body) and in the case of living matter it acts as intentional agent using biological body as a sensory receptor and motor instrument. This profoundly changes the view about what we ourselves are.

Zero energy ontology [C2] states that any physical system has a vanishing net energy so that everything is creatable from vacuum. Zero energy

states decompose into positive and negative energy parts and positive energy ontology results in certain limit in a good approximation. The possibility of negative energy signals is one important implication and a considerable modification of thermodynamics is forced by the fact that different signs of energy correspond to different arrows of geometric time.

Negative energy signals propagating to the geometric past inspire a new vision about communications and energy technology. The implications are especially important for the understanding of living matter where both time directions manifest themselves. In neuroscience a radically new view about memory based on the notion of 4-D brain emerges.

The hierarchy of Planck constants [A9] implies a generalization of the notions of imbedding space and space-time and macroscopic quantum coherence in all length and time scales at high enough levels of dark matter hierarchy assigned to the hierarchy of Planck constants. The consequences of this hypothesis are powerful: entire cosmos should be in a well-defined sense a living system with dark matter representing higher level conscious entities.

The original motivation for the p-adic physics [E1] were the highly successful calculations of elementary particle masses based on p-adic thermodynamics and conformal invariance [F3]. The model explained not only the ratio of proton and Planck masses but also masses of particles with an excellent accuracy. The only sensible interpretation of p-adic physics seems to be as physics of cognition and intentionality meaning that cognition is present even at elementary particle level.

The necessity to fuse p-adic physics corresponding to different primes $p$ forces a generalization of the notion of number by gluing different number fields together along common rationals and algebraics. This leads to a further generalization of the notions of imbedding space and space-time. The basic idea is that p-adic space-time sheets are representations for intentions and cognitions and their transformation to real ones in quantum jumps corresponds to the transformation of intention to action. Zero energy ontology is absolutely essential for this interpretation to make sense. p-Adic space-time sheets have literally infinite size in the real sense which means that cognition and intentionality are cosmic phenomena whereas cognitive representations defined by discrete intersections of real and p-adic space-time sheets obeying same algebraic equations have finite size.

## 1.2 Could living systems teach us something about energy technology?

One of the basic problems in energy technology is the necessity to carry fuel. This defines the most serious restriction to space travel.

Biological systems have resolved this problem by using sunlight as an energy source. The basic idea is very simple: solar radiation induces a dissociation of molecules to atoms which then re-associate and liberate metabolic energy. The hydrocarbons serving as fuel are recycled and there is a division of labor: animals cells burn the hydrocarbons to carbon dioxide and plants regenerate the hydrocarbons in photosynthesis.

Most or our energy technologies lack this kind of recycling. For instance, fuel in cars is burned to carbon dioxide and various wastes. If recycling were possible and if the density of potential energy sources in space were high enough, the amount of fuel would not depend on the distance travelled. This observation suggests self-organizing and perhaps in some primitive sense living technology and thus a connection with a fundamental problem of understanding how life has evolved. TGD provides a quantum model of both ordinary and pre-biotic life [N4, J7] and one can hope that this might help to develop a vision about "living" energy technology.

The recycling need not resolve completely the problems related to the fuel. The optimal solution would be "No fuel at all" with fuel serving only as an energy reserve. The system should be able to suck the energy from a system able to provide it. This is possible in TGD Universe [K6, J7]. Zero energy ontology implies that systems can get energy by sending negative energy signals to a system serving as an energy storage. Population inverted laser like system is the simplest system that one can imagine. Negative energy signals have interpretation as phase conjugate laser light. By the analog of stimulated emission negative energy quanta can also induce a cascade in population inverted laser like system so that system could send positive energy signal to the receiver. "Quantum credit card" is indeed the basic metabolic mechanism in TGD inspired quantum biology making possible instantaneous metabolic energy gain. The mechanism is also extremely flexible, which is a definite evolutionary advantage "in jungle".

The quantization of metabolic currencies is essential in living matter and this engineering principle is realized in TGD Universe at the fundamental level [J7]. The energies liberated in the dropping of particles to larger space-time sheets correspond to the increments of zero point kinetic energy (forgetting the interaction energy with matter) and by p-adic length scale hypothesis they are quantized. The basic metabolic energy currency of liv-

ing matter, which is about .5 eV, corresponds to the dropping of proton from space-time sheet having atomic size scale.

One can also worry about how to transfer the positive quanta of radiation energy over large distances since also other systems than receiver could do it. Also negative energy signals intended to be amplified to much larger positive energy signals in population reverted laser might be absorbed during their travel. Here the quantization of Planck constant might come in rescue. For instance, if photons with energies equal to those of visible or UV photons or even of gamma rays, are transformed to dark photons with much longer wavelength, one can hope that only systems able to transform this radiation into ordinary photons can absorb it. It might well be that water, which is the basic element of living matter, is exceptional in the sense that it can induce the transformation to dark photons and back. The transformation of large Planck constant photons to ordinary ones makes also possible control of shorter length and time scales by much longer ones.

## 1.3 Various anomalies as support for the new view

There are surprisingly many well established anomalies supporting the new ontology and these anomalies have been strong guiding line in attempts to construct a general theoretical framework.

a) There is a considerable support for many-sheeted space-time quantified by p-adic length scale hypothesis. Quite recently I learned about an anomalous radiation from interstellar dust having no generally accepted interpretation in terms of molecular transitions. The interpretation in terms of metabolic energy quanta liberated in dropping of electrons or protons to larger space-time sheets makes sense. A characteristic fractal spectrum involving period doubling is predicted.

b) The Bohr quantization of radii of planetary orbits [40, D7, D8] and quantal effects of ELF em fields on vertebrate brain [M3] helped considerably to develop the ideas about the hierarchy of Planck constants. Later a lot of further anomalies have emerged supporting the quantization of Planck constant. For instance, in gravitational sector Allais effect [52, D4] and accelerating cosmic expansion [D6] support the view about quantum coherence and quantum transitions in astrophysical and even cosmic scales [D7, D8]. Inflationary cosmology is replaced by quantum critical cosmology in TGD framework [D6].

c) Living matter is one gigantic bundle of anomalies of recent day physics and the notion of field body combined with p-adic length scale hypothesis allows to develop detailed models for how magnetic body controls biological

body and receives sensory input from it [J7]. In particular, a successful model for EEG results [M3] and involves hierarchy of Planck constants in an essential manner. One can say that field body applies remote mental interactions to biological body and the so called paranormal phenomena [H9, H10] differ in no essential manner from those encountered in bio-control. The notion of field body leads also to a concrete model for pre-biotic life [N4] based on the notion of plasmoid involving magnetic body controlling plasma phase [N1, J7].

d) The so called "free energy" phenomena have as bad reputation as cold fusion and homeopathy among most physics professionals: ironically all these disputed anomalies seem to find a natural place in TGD based world order [G2, F9, K5], which suggest that theoreticians should take experimentalists much more seriously. Typically "free energy people" make claims about over-unity production of energy but more or less as a rule the results fail not been reproducible.

TGD indeed allows temporary over-unity effects [G2]: the basic mechanism is dropping of particles on larger space-time sheets liberating zero point kinetic energy appearing as basic metabolic mechanism in TGD inspired theory of living systems. This mechanism does not allow a perpetuum mobile: the particles must be kicked back to smaller space-time sheets and in ordinary living matter solar radiation takes care of this. Rotating magnetic systems [61] define one especially interesting and complex case discussed thoroughly in [G3].

Since consciousness (memory and intentional action in particular), biology, and new views about energy, communication, and control are tightly related in TGD framework, I will discuss all these topics as a single coherent whole in the following in the hope of demonstrating the unifying power of this conceptualization. Almost one half of article is devoted to models for "free energy" phenomena [G2] developed much before the recent overall view summarized above had emerged. I know quite well that the reality of these phenomena is debatable and the poor quality of data makes models speculative. I however feel that these models might serve as good theoretical exercises.

## 2 Basic ontology of TGD

TGD [TGD] leads to an ontology which is new in many respects. The notion of space-time generalizes in several manners. One ends up to the so called zero energy ontology, which means that negative energies are possible and

all possible universes are creatable from vacuum. Planck constant, which in the standard quantum theory is a genuine constant, has a discrete spectrum of values and the values can be arbitrarily large [A9, J7]. This means that Universe is a macroscopic quantum system in all scales.

Dark matter could be identified as ordinary matter for which Planck constant differs from its ordinary value so that the interactions with ordinary matter differ in their character from ordinary interactions. Note that TGD predicts also new forms of matter completely dark with respect to electroweak interactions [F4, D8].

Dark matter with a large Planck constant is in a key role in the TGD based model of living matter [9]. Because the new ontology is so central from the point of view of TGD inspired theory of consciousness and living matter [TGDconsc], I will represent the basic ideas of TGD using applications to quantum biology to concretize their implications.

## 2.1 T(opological) G(eometro)D(ynamics) very briefly

TGD is a unified theory of fundamental interactions which has developed during 28 years [TGD, 1] and at the same time expanded to a theory of consciousness providing a model of quantum biology. The key ideas of TGD are following.

1. TGD can be seen as a generalization of either hadronic string model or super-string model (M-theory). The 1-dimensional (1-D) strings moving in 10- or 11-dimensional space are replaced with 3-D surfaces moving in 8-D space. This means that the 2-D orbits of strings are replaced with 4-D surfaces identified as our 4-D space-time but in a widely generalized sense. A further assumption is that these 3-surfaces are "light-like". This assumption bringing in mind esoteric teachings has a purely geometric meaning, and makes it possible to generalize and extend the conformal symmetries responsible for the miraculous mathematical properties of super-string models. These symmetries are in a central role in the formulation of quantum TGD.

2. Another manner to end up with TGD is via a search for a modification of general relativity solving the so called energy problem of general relativity. In general relativity the notions of energy and momentum are not well-defined since the translational symmetries responsible for their existence are lost as space-time becomes curved. If one assumes that 4-dimensional space-time is a 4-D surface in a higher-D space obtained by replacing the points of the empty space-time of special relativity (Minkowski space) with certain internal space- call it S- having a very small size, the basic symmetries of

Minkowski space become those of higher-D space and energy and momentum continue to be well-defined and one obtains a description of gravitation in terms of space-time curvature.

3. The surprise was that this leads to a unified theory for all known interactions - electromagnetic, weak, strong, and gravitational - if one chooses the space $S$ suitably. The proper choice is $S = CP_2 = SU(3)/U(2)$, the complex projective space of 2 complex dimensions.

## 2.2 Many-sheeted space-time and the notion of field body

Many-sheeted space-time is one of the basic implications of TGD.

1. Both 3-space and 4-D space-time consists of sheets forming a hierarchical structure ordered with respect to the size of the sheet. Each sheet can identified as a subsystem, which can correspond to any object of our nearby environment, astrophysical object, cell level system, atom, etc... My own body defines my own private space-time sheet. Quite generally, the topology of space-time codes for various physical structures.

2. Every system is accompanied by various kinds of fields such as electromagnetic and gravitational fields. These fields cannot be assigned to any particular subsystem in standard physics. In TGD the situation is different: one can assign to each system a "field body" consisting of field quanta. For instance, magnetic body consists of quanta of magnetic flux (tubes, sheets,..) realized as space-time sheets much larger than the system. One can also speak about field bodies which mediate interactions and connect different systems ("relative field bodies").

3. In TGD inspired theory of consciousness field body is the "intentional agent" which receives sensory information from the biological body and utilizes it as a motor instrument. The finding of Libet [17] that our sensory data has age which is a fraction of second could be understood in terms of time lapse resulting from the communication of sensory data to the magnetic body using EEG. From Uncertainty Principle one can conclude that in the case of EEG the size scale of magnetic body is of order of size of Earth. As a matter fact, magnetic body is predicted to have onion-like fractal structure and communications to various layers of the onion would take place using fractal variants of EEG. The existence of fractally scaled variants of some parts of EEG (alpha band and its harmonics in particular) is a testable prediction of the model.

4. What is also new and highly non-trivial is that field body and biological body are essentially four-dimensional structures. The brain and body of geometric past still exist as conscious entities having mental images which

we experience as memories. Biological death means only the arrival of a particular wave of consciousness to the time-like boundary of a 4-D body. Consciousness at the level of 4-D body does not cease: our past lives.

5. Many-sheeted space-time leads also to a generalization of the notion of subsystem which in TGD inspired theory of consciousness corresponds to a subself experienced by self (system) as a mental image. What is new is the paradoxical sounding prediction that even in the case that two systems are unentangled, subsystems can entangle. Entanglement of subselves can be interpreted as giving rise to sharing and fusion of mental images giving rise to a kind of stereo consciousness (stereovision would be one example of this). Consciousness would not be completely private and there would exist a pool of shared and fused mental images making for instance possible to assign universal meaning to the symbols of language. This new view about entanglement was originally motivated by the observation that two space-time sheets condensed at larger space-time sheets can be connected by bonds while the larger space-time sheets can remain unconnected (see Figure 3). By quantum classical correspondence the bonding of the space-time sheets serves as a space-time correlate for entanglement. Much later (only a couple years ago) the generalization of quantum measurement theory by introducing the notion of finite measurement resolution allowed to mathematicize this concept [A8, A9]. Entanglement is always defined with respect to a resolution characterizing the system and the entanglement of subsystems in not visible in the resolution characterizing the system. The notions of quantum groups and non-commutative geometry emerge naturally in the description of finite measurement resolution [C3].

## 2.3 The hierarchy of Planck constants and of dark matter

The hierarchy of Planck constants is a relatively new element of TGD. The idea emerged as I constructed a model of topological quantum computation [E9] and after learning about the work of Nottale [40] I realized that the notion is more or less forced by quantum classical correspondence implying that space-time sheets define regions of macroscopic quantum coherence and by the fact that they can have arbitrarily large size.

### 2.3.1 Physical motivations for introducing the hierarchy of Planck constants

There are several reasons to consider the possibility that Planck constant $\hbar$ is actually not a constant but can have a set of quantized values which can

be arbitrarily large.

1. One observation is the quantization of the radii of planetary orbits (also those of exo-planets) in the same manner as in the case of hydrogen atom [40]: now however the value of Planck constant is gigantic: $h/h_0 = GMm/v_0$, where $M$ and $m$ are the masses of Sun and planet, $G$ is Newton's constant and $v_0$ is a dimensionless constant (in units $c = 1$), whose favored value is $v_0 = 2^{-11}$. Also other values are possible. In TGD based model [D7, D8] the gravitational Planck constant is assigned with the "relative field bodies" connecting Sun and planet and mediating gravitational interaction between them. The interpretation is that gravitational Planck constant is associated with dark matter, which is macroscopic quantum phase in astrophysical scales. Visible matter condensed around dark matter would reflect the quantal properties of dark matter.

2. Second motivation comes from the observed effects of ELF radiation on vertebrate brain [16], which can be both physiological and affect behavior. These effects appear at harmonics of cyclotron frequencies of biologically important ions (in particular $Ca^{++}$ ion) in a magnetic field of $B = .2$ Gauss (the nominal value of Earth's magnetic field is .5 Gauss) and are very quantal. These frequencies are in EEG range (harmonics of 15 Hz for Calcium ion). Standard quantum mechanics does not allow quantal effects since the energy of EEG photons is extremely low and much below the thermal energy at body temperature. If the value of $\hbar$ is large enough, the effects of ELF photons are not masked by thermal noise, and the effect can be understood [M3].

3. If EEG consists of photons with large Planck constant, one can understand the correlation of EEG with the state of brain and contents of consciousness [M3]. In particular, temperature ceases to be a restriction for life: for sufficiently large Planck constant even the interiors of planets and Sun could serve as seats of life of some kind. This kills a central counter argument against the claim of a Romanian group of physicists that since the plasmoids created in electric circuits possess some basic features assigned usually to life, they indeed represent primitive life forms [45].

4. The mathematization for the notion of Planck constant hierarchy [A9] involves a further generalization of the space-time concept discussed in the Appendix. The basic prediction is that Planck constant corresponds to a discrete subgroup of rotation group acting as the symmetries of the field body of the dark matter system. A hierarchy of favored values of Planck constant and symmetry groups emerges from simple number theoretic arguments. For instance, $h = nh_0$, $n = 5, 6$, correspond to the favored values of Planck constant. In this case the symmetry group would correspond to the

symmetries of 5- and 6-cycles appearing in polycyclic aromatic hydrocarbons [34, 35] known to be important for life. Examples are the cycles appearing in DNA, in some aminoacids, in most hallucinogens except alcohol, and PAHs in the interstellar space [34, 35] believed to result via photosynthesis and believed to be predecessors of aminoacids and other bio-molecules.

5. The basic prediction is that large values of Planck constant correspond to discrete symmetries: typically discrete group of symmetries acting as rotations around a fixed symmetry axes. These symmetries acted as symmetries of dark field body. In the original view about generalized imbedding space (Appendix) these symmetries would be almost continuous symmetries for larger values of Planck constant. The breaking of these symmetries at the level of visible matter condensed around dark matter could lead to much smaller subgroups of these symmetry groups and structures analogous to those appearing in molecular physics could be the outcome. The further generalization of imbedding space (Appendix) allows also discrete symmetry groups $Z_n$ for dark matter with small value of $n$ and also genuinely three-dimensional symmetry groups (tedrahedral, octahedral, icosahedral, and octahedral). There is evidence for this kind of symmetries. For instance, there is a strange hexagonal structure appearing at the North pole of Saturn [41]. Planetary rings is second example and some of them even contain helical structures analogous to DNA double strand [42].

6. Large Planck constant photons at radio frequencies could interact strongly with living matter and it would become possible to communicate with living matter over very long distances. This mechanism would involve a de-coherence of large Planck constant photons to ordinary ones with same energy or a bundle of ordinary photons with much smaller energy. This brings in mind the recent discovery that the irradiation of salt water by radio waves at harmonics of frequency 13.4 Ghz makes it "burn" that is emit burning gases [53]. A possible explanation is that radio wave photons are transformed in water to photons of same frequency but much larger Planck constant and in de-coherence to ordinary photons with same energy become microwave photons which excite rotational excitations of NaCl (in equilibrium with $Na^+$ and $Cl^-$ ions) and in this manner heat it just like microwave oven does [F10]. The required value of Planck constant would be by a factor $2^{10} = 1024$ larger than normal Planck constant. This value is one of the number theoretically simple values defined as ratios of integers defining polygons constructible using only ruler and compass [A9]. For water molecules the needed value of Planck constant is obtained from the microwave oven frequency 2.45 GHz and would be with .1 per cent accuracy equal to $h/h_0 = n = 187 = 11 \times 17$: $n$ does not belong to the set of number

theoretically simple values of $n$ but one cannot of course exclude it.

### 2.3.2 The notion of field body and dark matter

The conclusion would be that each physical system is accompanied by a field body with a fractal, onion-like, structure formed by field bodies. This leads to the following vision about the nature of living matter.

1. Each layer of the onion is characterized by the value of Planck constant telling its position in the hierarchy of dark matter.

2. At the surface of the onion the value of Planck constant is largest and in some sense defines the "IQ" of the system. At the level of molecules one expects rather low values of Planck constants. For instance, the magnetic body assignable to the ordinary EEG as has of order Earth size and the lifetime of human (say 70 years) would correspond to a layer with size of order light-life (70 light years). Even higher layers might be present: transpersonal states of consciousness would indeed naturally correspond to these layers.

Field body receives information from the biological body and quantum controls it.

1. In the case of ordinary living matter field body would naturally receive information from cell membranes, which are full of receptors monitoring the state of environment. This leads to the idea that cell membranes are Josephson junctions and that Josephson currents code this information and communicate it to some layer in the onion formed by magnetic bodies. Dark matter hierarchy suggests even the existence of fractally scaled up counterparts of cell membrane and the TGD based model of EEG relies on this assumption. What is encouraging that the model predicts correctly the decomposition of EEG into bands, in particular alpha band, explains why high arousal correspond to chaotic looking activity in beta band, and predicts also correctly the positions of narrow sub-bands in beta and theta bands [19] . The strange findings challenging pump-channel paradigm [22] (ionic currents seem to be quantal and same even for artificial membranes; currents continue to flow in absence of metabolism) support superconductivity hypothesis and suggest that ordinary Ohmic currents are only for the purposes of measuring the concentrations of various ions in cellular environment and that metabolic energy goes to the communications to the magnetic body using generalized EEG.

2. Magnetic body controls biological body through the genome. This inspires the hypothesis that magnetic flux sheets go through DNA strands and genes form what could be regarded as text lines at the page of book defined by the flux sheet. The quantization of magnetic flux with unit

proportional to Planck constant implies that for large values of $\hbar$ the flux sheets are very wide and can go through a large number of genomes. One ends up with the notion of super genome meaning that coherent collective gene expression becomes possible in the scale of organ and organism. Hyper genome would in turn fuse the super-genomes to a larger structure making possible coherent collective gene expression at the level of species and population [M3, L1]. This would bring to the theory of evolution completely new "synergetic aspect" and evolution would be much more than fight for survival.

3. The interaction between field body and biological body is essentially remote mental interaction so that paranormal phenomena would differ from normal biological basic interactions only in that field body uses external biological body to remote viewing or psychokinesis.

4. There are good reasons to assume that field bodies have developed magnetic immune systems to prevent the use of their private biological bodies by alien field bodies. Hypnosis would be example of this kind of possession by a foreign field body. This immune system can be compared to fire wall in computer world (assuming that we have created computers as our own images).

a) The height of the fire wall depends on individual. For very sensitive persons it is very low and these people are very sensitive to suggestions, hypnosis, spiritual experiences, and even encounters of ETs. Very high fire wall makes it impossible to receive even useful information and the fire wall of skeptic might be too high.

b) In the case of computers viruses and cookies are very simple programs making possible for an external computer to partially "possess" the computer via web. Their role is to serve as kind of mediums or couriers. In the case of field body viruses and cookies would correspond to very simple life forms to which immune system does not bite: plasmoids are natural candidates in this respect. This would suggest that anomalous light phenomena ("UFOs") are actually plasmoids (unidentified moving processes rather than objects).

Plasmoids could quantum entangle the brains of the sensitive person to some conscious entity at some higher level of hierarchy and the person would fall in a trance like state able to share mental images of this entity. Patterns of magnetic pulses can be used to generate alternative states of consciousness [20] and the patterned motion of the magnetic body of plasmoids (kind of dance like motor expression!) consisting of flux tubes and sheets with respect to the observer could generate this kind of pulse patterns.

It has been observed that some moving light balls indeed involve mag-

netic pulses with maximal field strength of about .3 Gauss and typical strength which is 10 times weaker [49]. The prediction is that the durations of pulses should be inversely proportional to the velocity of motion of the light balls. Also the motion of a magnetometer with respect to living system might course similar pulses.

## 2.4 Zero energy ontology

In standard physics the sign of energy is positive. This leads to philosophical problems. The problematic question is what are the values of the conserved quantities of the universe (energy, em charge, quark and lepton number). An additional difficulty is caused by the fact that they are very naturally infinite in positive energy ontology. These questions cannot be answered with the framework of standard physics. On the other hand, TGD inspired cosmology led to a different interpretational problem: the density of non-conserved gravitational mass was non-vanishing as in standard cosmologies but the density of inertial energy vanishes [D6]. The construction of quantum TGD [C2, A1, A2] finally led to so called zero energy ontology which resolves this problem and also the problems due to the positive energy ontology.

1. All quantum states possess vanishing net values of conserved quantum numbers such as an energy. Or stating it otherwise: every physical state is creatable by intentional action from vacuum.

2. Zero energy states decompose into positive and negative energy states such that negative energy state is in the geometric future. If the temporal distance between positive and negative energy states is long as compared to the time scale of perception, the usual positive energy ontology works well. In the opposite case the zero energy state can be interpreted as a quantum fluctuation having no importance for the world as we perceive it.

### 2.4.1 Zero energy ontology and unification of the notions of S-matrix and density matrix

Zero energy ontology states that physical states have vanishing net conserved quantum numbers and states decompose into positive and negative energy state and that the latter one can be said to be located in the geometric future with of the positive energy state at the time-like boundary of the space-time sheet representing the system. It is possible to speak about energy of the system if one identifies it as the average positive energy for the positive energy part of the system.

The matrix ("M-matrix") representing time-like entanglement coefficients between positive and negative energy states unifies the notions of S-matrix and density matrix since it can be regarded as a complex square root of density matrix expressible as a product of real squared of density matrix and unitary S-matrix. The system can be also in thermal equilibrium so that thermodynamics becomes a genuine part of quantum theory and thermodynamical ensembles cease to be practical fictions of the theorist. In this case M-matrix represents a superposition of zero energy states for which positive energy state has thermal density matrix.

a) If the positive energy parts of zero energy states appearing in the superposition have only single value of energy, the notion of remote metabolism is certainly well-defined. Even in the case that the system is thermalized remote metabolism makes sense since average energy can be increased by remote metabolism. One can even imagine a statistical variant of the process in which the temperature increases.

b) The critical question is whether crossing symmetry prevails in the sense that the positive energy signal propagating to the geometric future is equivalent to a negative energy signal propagating to geometric past. The eigen modes of the modified Dirac operator appearing in the first principle formulation of quantum TGD are characterized by the eigenvalues $\lambda$, which are complex. $|\lambda|^2$ has interpretation as a conformal weight mathematically analogous to a vacuum expectation value of Higgs field [B4, C3]. There are reasons to believe that the eigenvalues relate closely to the zeros of Riemann zeta and/or its generalizations [C3]. If the eigenvalue and its complex conjugate correspond to a state and its phase conjugate, crossing symmetry fails and would mean also breaking of time reversal symmetry.

### 2.4.2 Time mirror mechanism

Zero energy ontology gives justification for the time mirror mechanism which is the fundamental mechanism of TGD inspired model of quantum biology. To avoid confusion one must distinguish between two times: geometric and subjective time. The latter corresponds to a sequence of quantum jumps giving rise to the conscious sensation of flow of time [10, K1, H5]. Geometric time corresponds to the time of physicist identified as the fourth space-time coordinate. These times are only loosely related and their identification is only approximate and makes sense only in some states of consciousness. Indeed, subjective time is irreversible and no subjective future exists whereas geometric time is reversible and both future and past exist.

1. Symbolic (declarative memories) can be understood as communica-

tions of some onion layer of magnetic body with the brain of the geometric past [H6]. A signal consisting of negative energy phase photons (identifiable as phase conjugate photons in nonlinear optics) with larger Planck constant represents a question to the brain of the geometric past which responds automatically by sending a positive energy signal to the magnetic body in the geometric future. Episodal memories which correspond to literal re-experiences result by time-like quantum entanglement for subsystems representing the mental images.

2. Time mirror mechanism makes possible to realize intentions by sending negative energy signals to the brain of the geometric past and inducing neural activity leading to a motor response in the brain of geometric future [H1, J7]. This kind of mechanism allows more or less instantaneous reaction and provides an evolutionary advantage in "jungle". The mechanism explains Libet's findings[18] that neural activity is initiated in brain already before the conscious decision. In the usual ontology the interpretation would be that free will is only apparent. In the recent context "before" refers to the geometric rather than subjective time, so that free will is possible and assigned to the quantum jump identified as a moment of consciousness. Dark matter hierarchy implies infinite hierarchy of moments of consciousness with moments of consciousness giving rise to the analog of dark matter hierarchy at the level of conscious entities.

3. The system can receive positive energy as a recoil energy by sending negative energy to ta system of geometric past able to receive it. A system analogous to a population inverted laser having more particles in a state of higher energy, is ideal provider of energy. The resulting quantum credit card makes it possible to react very rapidly in situations encountered in "jungle". I have christened this mechanism remote metabolism and magnetic body could use it to suck metabolic energy from brain or body to its own purposes by sending phase conjugate dark (generalized) EEG photons to the biological body. In the case of declarative memories the excited state of the laser like system would naturally correspond to bit 1 and ground state to bit 0 [H6]. Metabolic energy would be needed to restore the mental image since the process of memory recall would tend to reduce the population of excited states. Note that remote metabolism would be tailor made for say space travel since there would be no need to carry the fuel: if "UFOs" exist they might apply this kind of energy technology.

4. Many-sheeted space-time provides a concrete realization of the laser like systems as many-sheeted lasers. The "dropping" of particles from smaller to larger space-time sheets liberates zero point kinetic energy [J7]. If the interaction energy with the matter at the space-time sheet can be

neglected, p-adic length scale hypothesis makes precise predictions about the maximal liberated energies. The standard metabolic energy currency of about .5 eV of living matter corresponds to the dropping of proton from a space-time sheet of atomic size. Actually a fractal hierarchy of universal metabolic currencies is predicted and should be present already during the pre-biotic evolution so that the chemical storage of energy is not necessary for a primitive metabolism [N4].

The transitions corresponding to the dropping of particles should be visible in astrophysics and there are indeed exist three kinds of narrow bands of radiation in both visible and infrared range without identification in terms of known molecular transitions (see discussion below). The energies of the photons in question are consistent with p-adic length scale hypothesis and allow an interpretation in terms of proposed transitions assuming that there is some binding energy with the matter at the smaller space-time sheet [37].

### 2.4.3 More detailed view about time mirror mechanism in zero energy ontology

The notion of negative energy signals and time mirror mechanism emerged before zero energy ontology. Since the mechanisms of remote metabolism, of memory, and of intentional action rely on time mirror mechanism, one should check that this mechanism is indeed consistent with zero energy ontology. Zero energy ontology could also yield new insights to these mechanisms.

*1. Is zero energy ontology consistent with time mirror mechanism?*

Energy conservation and geometric arrow of time poses strong conditions on the mechanism. If positive energy part of state sends negative energy signal, then negative energy part of state must send a compensating positive energy signal. Furthermore, positive (negative) energy signals propagate towards geometric future (past).

a) If only single space-time sheet is involved, either negative energy signal $S_-$: $X^4_- \to Y^4_-$ or positive energy signal $S_+$: $X^4_+ \to Y^4_-$ is possible. The energy of both states is reduced in magnitude. For instance, this process tends to reduce destroy long term memories represented as bit sequences with bit represented by population inverted laser system.

b) Second possibility is that $X^4$ are $Y^4$ are disjoint and $X^4$ is in the geometric future of $Y^4$.

The first possibility is $S_+$: $X^4_+ \to Y^4_-$ and negative energy signal $S_-$: $X^4_- \to Y^4_-$: the energy of both $X^4$ and $Y^4$ is reduced in this case.

Second possibility is $S_-$: $X^4_+ \to Y^4_+$ and $S_+$: $Y^4_- \to X^4_-$. $X^4$ would

suck energy from $Y^4$ in the geometric past. This option could correspond to both remote metabolism, memory recall, and intentional action. The presence of topological light ray connecting two systems would be also a correlate for time-like quantum entanglement making possible sharing and fusion of mental images and creating a sensation about flow of time just like it creates sensation of depth in stereo vision by fusion of right and left visual fields. Depending on the sign of the energy of the signal one would have memory or precognition. Precognition would require use of metabolic energy and this might be one reason for why it is rather rare.

c) Suppose next that the zero energy space-time sheet, call it $X^4$, is inside larger space-time sheet, call it $Y^4$: $X^4 \subset Y^4$. In this case one can have $S_-$: $X^4_+ \to Y^4_+$ accompanied by $S_+$: $X^4_- \to Y^4_-$. $X^4 \subset Y^4$ would suck energy from a larger system $Y^4$. It is of course possible to replace signals with signals of opposite energy in opposite time direction.

A possible interpretation is as a metabolic charging of smaller space-time sheets by sucking energy from longer scales or by active pumping of energy to shorter scales. The transformation of long wavelength photons with large Planck constant to short wavelength photons with smaller Planck constant is an analogous process and might realize metabolic charging in biology. For instance, Sun-Earth system could correspond to $Y^4$ and biosphere to $X^4$.

To sum up, zero energy ontology completes the picture in the sense that it also provides a process making possible metabolic charging.

*2. Thermodynamical considerations*

It is not at all obvious whether the proposed picture is consistent with the standard thermodynamics. The transfer of energy from long to shorter length scales making possible to gain metabolic energy and realize the mechanism of long term memory indeed seems a genuinely new element. This process resembles dissipation in the sense that energy is transferred from long to short length scales. In an approach to thermal equilibrium temperature gradients are however reduced whereas remote metabolism favors the active generation of "hot spots".

These considerations relate closely to the notions of entropy and syntropy by Italian mathematician Luigi Fantappie [24] assigned with the two arrows of time. I learned from the work of Fantappie in SSE conference held in Röros from Antonella Vannini [25] and Ulisse Di Corpo [26].The discovery of Fantappie was that in living systems entropic processes seem to be accompanied by syntropic processes which seem to be finalistic. He assigned these processes to the advanced solutions of wave equations.

It would seem that entropy and syntropy do not relate directly to the

notion of remote metabolism.

a) Syntropy growth would indeed be the mirror image of entropy growth associated with negative energy mirror image of positive energy dynamics. This dynamics could be seen as sequences of downwards scalings leading from long time scale to short time scale. This sequence would define time sequences proceeding in opposite directions of time for positive and negative energy parts of states. Thus entropy growth would be accompanied by syntropy growth.

b) Syntropy growth could be also seen as a consequence of generalized second law applying with respect to subjective time and growth of syntropy would be growth of entropy but manifesting itself at space-time level in reversed direction of geometric time. For instance, the spontaneous assembly of bio-molecules from their parts could be seen as a decay process in the reverse direction of geometric time controlled by phase conjugate control signals.

c) Remote metabolism as generation of "hot spots" does not seem to reduce to these notions and might represent a genuine breaking of standard thermodynamical view about the world.

One must also distinguish the notions of entropy and syntropy from the notion of number theoretic entanglement negentropy $N$ assignable with quantum entanglement with algebraic entanglement probabilities [H2].

a) $N$ is defined as the maximum of the p-adic entanglement negentropy $N(p)$ as a function of the p-adic prime $p$ and thus assigns to an entangled system a unique prime $p_{max}$. $N(p)$ is obtained by replacing in the definition of the Shannon entropy the argument of logarithm with its p-adic norm. $N$ is in general positive and thus defines a genuine measure of information.

b) The non-negative negentropy defined in this manner characterizes entanglement as a carrier of information rather than the state of either of systems and has nothing to do with the ordinary (non-positive) entropy characterizing the lack of knowledge about the state of either subsystem. Negentropy Maximization Principle [H2] favors the increase of the number theoretic negentropy and thus formation of entanglement quantum systems and generation of quantum coherence. Depending on the character of entanglement negentropic entanglement might be interpreted as a correlate for some conscious experience with positive content: say experience of understanding (time-like entanglement implying causal structure), of love (space-like entanglement), etc...

It is not obvious to me whether the remote metabolism as a manner to build hot spots and diversity could be reduced to NMP or whether it should be regarded as something completely independent.

## 2.5 p-Adic physics as physics of cognition and intentionality

p-Adic number fields are completions of rationals to a continuum as are also ordinary real numbers. In the case of real numbers one adds to the rationals algebraic numbers and transcendentals like e and $\pi$. In the case of p-adic numbers one adds numbers, which are infinite as real numbers. To every prime p=2,3,5,7,... one can assign a p-adic number field and an infinite number of algebraic extensions analogous to complex numbers.

1. One can assign also to p-adic numbers a physics (what this physics is far from obvious). The basic motivation for p-adics in the case of TGD was that p-adic thermodynamics makes possible to understand elementary particle masses and reduces the fundamental mystery number defined by the ratio of Planck mass to proton mass to number theory [F1, F2, F3, F4, F5]. It took a long time to get convinced that p-adic physics can be interpreted as the physics of cognition and intentionality and that p-adic physics can be seen as a simulation of real physics.

2. The challenge is to "glue" real physics and various p-adic physics to single coherent whole. To achieve this it is necessary to generalize the notion of number by "gluing" together real numbers and various p-adic number fields by along common rationals (and possibly also common algebraics) [E1]. Also the notions of space, manifold, and space-time generalize. It becomes possible to speak about p-adic space-time sheets as correlates for intentions and cognitions [H8]: this would be the geometric counterpart for the "mind stuff" of Descartes. Note however that space-time and quantum states are zombies: consciousness is in the quantum jump.

3. Rather remarkably, every p-adic space-time sheet has literally infinite size in the sense of the real topology. This means that cognition and intentionality are cosmic phenomena and cannot be localized to brain or even field body. The intersections of field bodies and p-adic space-time sheets consist of discrete sets of points and provide material representations for cognitions and intentions. The larger the size of field body (the larger the value of Planck constant), the larger the number of points in this intersection, and the better the cognitive representations and the more precise the intentional grasp on the material world. Thus the evolution of cognition involves growth of the largest Planck constant associated with the system characterizing also the time scale of long term memories and planned action.

4. The theory is testable. The p-adic topology should reflect itself as an effective p-adic topology of real space-time sheets serving as correlates for matter and p-adic continuity means p-adic fractality with characteristic long range correlations combined with local chaos in the real topology. The

success of p-adic mass calculations supports this view and suggests that cognition and intentionality are present already in elementary particle scales. Also the successes of the applications to biology and even cosmology support the theory.

5. The essential ingredient of the theory is p-adic length scale hypothesis: primes which are near powers of two are physically preferred. In particular, prime powers of two and Mersenne primes $M_n = 2^n - 1$ and their complex analogs (Gaussian Mersennes) are especially favored. For instance, most important elementary particles correspond to Mersenne primes and a number theoretical miracle occurs in biologically important length scale range: in the length scale range between cell membrane thickness (10 nm) and size of cell nucleus (2.5 $\mu$m) there are as many as 4 Gaussian Mersennes [J7]!

# 3 Many-sheeted space-time, universal metabolic quanta, and plasmoids as primitive life forms

In this section evidence for many-sheeted space-time represented together with development of more concrete ideas about plasmoids as primitive life forms. Recall that might form the basis of new energy technology able to recycle the fuel.

## 3.1 Evidence for many-sheeted space-time

The dropping of particle to a larger space-time sheet liberates energy which is the difference of the energies of the particle at two space-time sheets. If the interaction energy of the particle with the matter at space-time sheet can be neglected the energy is just the difference of zero point kinetic energies. This energy depends on the details of the geometry of the space-time sheet. Assuming p-adic length scale hypothesis the general formula for the zero point kinetic energy can be written as

$$E(k) = x \times E_0(k) \ , \ E_0(k) = \frac{3}{2}\frac{\pi^2}{mL^2(k)} \ .$$

Here $x$ is a numerical factor taking into account the geometry of the space-time sheet and equals to $x = 1$ for cubic geometry.

The liberated zero point kinetic energy in the case that the particle drops to a space-time sheet labelled by $k_f = k + \Delta k$ with same value of $x$ is

$$\Delta E(k, \Delta k) = x \times E_0(k) \times (1 - 2^{-\Delta k}) \ .$$

The transitions are seen as discrete lines for some resolution $\Delta k \leq \Delta k_{max}$. At the limit $k \to \infty$ transitions give rise to a quasicontinuous band. The photon energy for $k \to \infty$ transition is same as the energy from $k-1 \to k$ transition, which brings in additional option to the model building.

For a proton dropping from the atomic space-time sheet $k = 137$ to very large space-time sheet ($\Delta k \to \infty$) one has $\Delta E(k) = E(k) \sim x \times .5$ eV. Since the ratio of electron and proton masses is $m_p/m_e \simeq .94 \times 2^{11}$, the dropping of electron from space-time sheet $k_e = k_p + 11$ liberates zero point kinetic energy which is by is by a factor .9196 smaller. For $k_p = 137$ one would have $k_e = 148$. This energy corresponds to the metabolic energy currency of living systems and the idea is that the differences of zero point kinetic energies define universal metabolic energy currencies present already in the metabolism of pre-biotic systems. In the following fit electron's zero point kinetic energy will be taken to be $E_0(148) = .5$ eV so that for proton the zero point kinetic energy would be $E_0(137) = .544$ eV.

The hypothesis predicts the existence of anomalous lines in the spectrum of infrared photons. Also fractally scaled up and scaled down variants of these lines obtained by scaling by powers of 2 are predicted. The wavelength corresponding to .5 eV photon would be $\lambda = 2.48$ $\mu$m. These lines should be detectable both in laboratory and astrophysical systems and might even serve as a signature for a primitive metabolism. One can also consider dropping of Cooper pairs in which case zero point kinetic energy is scaled down by a factor of 1/2.

Interestingly, the spectrum of diffuse interstellar medium exhibits three poorly understood structures [31]: Unidentified Infrared Bands (UIBs), Diffuse Interstellar Bands (DIBs) [32], and Extended Red Emission (ERE) [33] allowing an interpretation in terms of dropping of protons or electrons (or their Cooper pairs) to larger space-time sheets. The model also suggests the interpretation of bio-photons in terms of generalizes EREs.

### 3.1.1 Unidentified Infrared Bands

Unidentified infrared bands (UIBs) contain strong bands at $\lambda = 3.3, 6.2, 11.3$ microns [31]. The best fit for the values of $k$ and $\Delta k$ assuming dropping of either electron or proton are given by the following table. The last row of the table gives the ratio of predicted photon energy to the energy characterizing the band and assuming $x = 1$ and $E_0(148, e) = .5$ eV. Discrepancies are below 8 per cent. Also the dropping of protonic Cooper pair from $k = 137$ space-time sheet could reproduce the line $\Delta E = .2$ eV. The fit is quite satisfactory although there is of course the uncertainty related to the geometric

parameter $x$.

| $\lambda/\mu m$ | $E/.5eV$ | $k$ | $\Delta k$ | $\Delta E(k,\Delta k)/E$ | $p/e$ |
|---|---|---|---|---|---|
| 330 | .7515 | 137 | $\sim\infty$ | 1.002 | e |
| 620 | .4000 | 138 | 3 | 1.067 | e |
| 1130 | .2195 | 139 | 3 | 0.878 | e |
| 1130 | .2195 | 139+11=150 | 3 | 1.076 | p |

Table 1. Table gives the best fit for UIBs assuming that they result from dropping of proton or electron to a larger space-time sheet and one has $E_0(148,e) = .5$ eV. The fourth column the table gives the ratio of predicted photon energy to the energy characterizing the band and assuming $x = 1$. $e/p$ tells whether electron or proton is in question.

According to [31], UIBs are detected along a large number of interstellar sight-lines covering a wide range of excitation conditions. Recent laboratory IR spectra of neutral and positively charged poly-cyclic aromatic hydrocarbons (PAHs) has been successfully used by Allamandola [35] to model the observed UIBs. It is believed that PAHs are produced in reactions involving photosynthesis and are regarded as predecessors of biotic life [34]. This would conform with the presence of metabolic energy quanta.

DNA sugar bone, some aminoacids, and various hallucinogens involve 5- and 6-cycles and the proposal is that these cycles involve free electron pairs, which possess Planck constant $\hbar = n\hbar_0$, $n = 5, 6$. These free electron pairs would explain the anomalous conductivity of DNA and would be an essential characteristic of living matter. The emergence of $n = 5, 6$ levels could be seen as the first step in the pre-biotic evolution.

### 3.1.2 Diffuse Interstellar Bands

There are diffuse interstellar bands (DIBs) at wavelengths 578.0 and 579.7 nanometers and also at 628.4, 661.4 and 443.0 nm. The 443.0 nm DIB is particularly broad at about 1.2 nm across - typical intrinsic stellar absorption features are 0.1 nm [31]. The following table proposes a possible identification of these lines in terms of differences of zero point kinetic energies. Also now the best fit has errors below 7 per cent.

| $\lambda/nm$ | $E/.5eV$ | $k$ | $\Delta k$ | $\Delta E(k,\Delta k)/E$ | $p/e$ |
|---|---|---|---|---|---|
| 628.4 | 3.947 | $135 = 3^3 \times 5$ | $\sim \infty$ | 0.987 | e |
| 661.4 | 3.750 | $135 + 11 = 2 \times 73$ | 3 | 0.985 | p |
| 443.0 | 5.598 | $134 = 2 \times 67$ | 2 | 0.933 | e |
| 578.0 | 4.291 | $135 + 11 = 2 \times 73$ | $\sim \infty$ | 0.986 | p |
| 579.7 | 4.278 | $135 + 11 = 2 \times 73$ | $\sim \infty$ | 0.984 | p |

Table 2. Table gives the best fit for DIBs assuming that they result from dropping of proton or electron to a larger space-time sheet. Notations are same as in the previous table.

The peak wavelengths in chlorophyll and photosynthesis are around 650 nm and 450 nm and would correspond to second and third row of the table.

### 3.1.3 The Extended Red Emission

The Extended Red Emission (ERE) [31, 33] is a broad unstructured emission band with width about 80 nm and located between 540 and 900 nm. The large variety of peak wavelength of the band is its characteristic feature. In majority of cases the peak is observed in the range 650-750 nm but also the range 610-750 nm appears. ERE has been observed in a wide variety of dusty astronomical environments. The necessary conditions for its appearance is illumination by UV photons with energies $E \geq 7.25$ eV from source with $T \geq 10^4$ K. The position of the peak depends on the distance from the source [33].

According to [31] the current interpretation attributes ERE to a luminescence originating from some dust component of the ISM, powered by UV/visible photons. Various carbonaceous compounds seem to provide a good fit to the observational constraints. However, the real nature of ERE is still unknown since most candidates seem to be unable to simultaneously match the spectral distribution of ERE and the required photon conversion efficiency.

a) Consider first the band 650-750 nm appearing in the majority of cases. The most natural interpretation is that the lower end of the band corresponds to the zero point kinetic energy of electron at $k = 135 + 11 = 146 = 2 \times 73$ space-time sheet. This would mean that the lines would accumulate near 650 nm and obey the period doubling formula

$$\frac{\lambda(k) - \lambda(\infty)}{\lambda(\infty)} = \frac{2^{-k}}{1 - 2^{-k}} \quad .$$

By the estimate of Table 2 the lower end should correspond to $\lambda = 628.4$

nm with a correction factor $x < 1$ reducing the zero point kinetic energy. The reduction would be smaller than 4 per cent. $\Delta k = 3$ transition would correspond to 744 nm quite near to the upper end of the band. For $\Delta k = 2$ transition one has $\lambda = 867$ nm not to far from the upper end 900 nm. $\Delta k = 1$ corresponds to 1.3 $\mu$m.

b) For proton with $k = 135 = 146$ the energy band would shift by the factor $2^{11} m_e/m_p \simeq 1.0874$ giving the range (598,690) nm.

c) The variation for the position of the peak can be understood if the charged particles at the smaller space-time sheet can have excess energy liberated in the dropping to the larger space-time sheet. This excess energy would determine the position of the lower end of the band in the range $(540, 650)$ nm.

d) One should also understand the role of UV photons with energy larger than 7.25 eV. For proton the energy would be 8.76 eV. For proton the energy would be 8.76 eV. UV photon with energy $E \geq 8$ eV could kick electrons from large space-time sheets to $k = 144 = 146 - 4$ space-time sheet where they have zero point kinetic energy of 8 eV plus possible additional energy (for proton the energy would be 8.76 eV). One possibility is that these electrons drop first to $k = 145$ by the emission of $\sim 4$ eV UV photon and then to $k = 144$ by the emission $\sim 2$ eV photon corresponding to 650 nm line. The further dropping to larger space-time sheets would produce besides this line also the lines with longer wavelengths in the band.

The energy of UV photons brings in mind the bond energy 7.36 eV of $N_2$ molecule and the possibility of metabolic mechanism using UV light as metabolic energy and based on the dissociation of $N_2$ followed by re-association liberating metabolic energy kicking protons or electrons to a smaller space-time sheet. For the $k \to k + 3$ transition of electron the energy would be 7 eV which suggests that this transition defines important metabolic energy quantum for living interstellar dust using dissociation and its reversal as basic metabolic mechanism.

### 3.2 Laboratory evidence for plasmoids as life forms

Accepting the notion of magnetic body one is naturally led to the idea about plasmoids as primitive life forms quantum controlled by the dark matter at the magnetic body of the plasma ball. Magnetic body itself would contain Bose-Einstein condensates of ions and electrons and could be seen as a quantum plasmoid. Plasmoids would be very simple systems able to recycled metabolism and therefore highly interesting from the point of new energy technologies. Magnetic body of the plasmoid could also be responsible for

a continual feed of charge keeping plasma ball charged (DNA strands are negatively charged in bio-matter).

### 3.2.1 From dust to dust

The article *From Plasma crystals and helical structures towards inorganic living matter* of Tsytovich *et al* in August issue of New Journal of Physics provides new empirical support for plasmoids as living life forms. The results of article suggest that interstellar dust could behave like living matter in some respects: it could even have variant of genetic code. This is a really shattering finding and with single blow destroys the standard dogma about life as something purely chemical. It should also give also some headaches for those influental colleagues who have decided that it is necessary to accept the anthropic principle. Here is little popularization of the result.

*SCIENTISTS have discovered that inorganic material can take on the characteristics of living organisms in space, a development that could transform views of alien life.*

*An international panel from the Russian Academy of Sciences, the Max Planck institute in Germany and the University of Sydney found that galactic dust could form spontaneously into helixes and double helixes and that the inorganic creations had memory and the power to reproduce themselves.*

*A similar rethinking of prospective alien life is being undertaken by the National Research Council, an advisory body to the US government. It says Nasa should start a search for what it describes as weird life" - organisms that lack DNA or other molecules found in life on Earth.*

*The new research, to be published this week in the New Journal of Physics, found nonorganic dust, when held in the form of plasma in zero gravity, formed the helical structures found in DNA. The particles are held together by electromagnetic forces that the scientists say could contain a code comparable to the genetic information held in organic matter. It appeared that this code could be transferred to the next generation.*

*Professor Greg Morfill, of the Max Planck institute of extra-terrestrial physics, said: Going by our current narrow definitions of what life is, it qualifies.*

*The question now is to see if it can evolve to become intelligent. Its a little bit like science fiction at the moment. The potential level of complexity we are looking at is of an amoeba or a plant.*

*I do not believe that the systems we are talking about are life as we know it. We need to define the criteria for what we think of as life much more clearly."*

*It may be that science is starting to study territory already explored by science fiction. The television series The X-Files, for example, has featured life in the form of a silicon-based parasitic spore.*

*The Max Planck experiments were conducted in zero gravity conditions in Germany and on the International Space Station 200 miles above earth.*

*The findings have provoked speculation that the helix could be a common structure that underpins all life, organic and nonorganic.*

To sum up the essentials, plasma phase is involved and the dust life is able to construct analogs of DNA double helices and this has been achieved also in laboratory. "From dust to dust" seems to have a very deep side meaning!

Here is a more quantitative summary of the results reported in [46].

a) The scale of the dust balls seems to be few micrometers. It is essential that the system is open in the sense that there is both metabolic energy feed and continual feed of plasma to negatively charged dust particles to preserve their charges. Authors speak about effective "gravitational" instability as a mechanism leading to the formation of the helices and identify effective gravitational coupling (the formula contains a trivial typo) as a function of charge and mass of the particle plus dimensionless parameter characterizing the modification of Debye model implied by the fact that dust particles are not electrically closed systems. Authors give a long list of life-like properties possessed by the helical structures.

b) Helical structures are generated spontaneously and possess negative charges. The repulsion of the helical structures transforms to attraction at some critical distance interval due to the fact that the large electrostatic self energy depends on the distance between helices and this makes possible double helices (authors speak about over-screening in the formal model). Similar mechanism might work also in the case of ordinary DNA double helices whose stability is poorly understood since also in this case the large negative charge could be preserved by continual feed of charge.

c) The twist angle of the helix makes bifurcations as a function of radius of helix and the values of twist angle could define the letters of genetic code. Also a mechanism for how the twist angle is communicated to neighboring helix is proposed. Also dust vortices are observed and might be those which one can occasionally observe during hot summer days.

d) Authors do not mention magnetic fields but my guess is that the helical structures reflect directly the geometry of the helical magnetic flux tubes, and that dark electron pairs with large Planck constant at these tubes might be the quantal aspect of the system. These currents might relate closely to the plasma current, which charges the dust particles. Also

DNA, which is insulator, is known to be able to act as conductor, and here the free electron pairs associated with aromatic rings having $\hbar = n \times hbar_0$, $n = 5$ or 6, could make conduction possible since their Compton size would be n-fold.

### 3.2.2 Elephant trunks in astrophysics

TGD Universe is fractal and this means that the visible structures are formed around magnetic flux quanta containing dark matter with large hbar appear in all length scales and have geometric patterns reflecting the exact discrete symmetries of dark matter acting as rotational symmetries of the field body and at the level of visible matter giving rise to broken symmetries typical for molecular structures. The helical structures found from the rings of some planets could be one example of fractal life.

For some time ago I learned about "elephant trunks" found by Hubble (I am grateful for Miika Väisälä telling about the trunks and for giving references to the papers about the finding). They appear in very wide range of length scales: at least from 1000 au to 1 pc. They are found in close connection with molecular clouds and HII regions excite by one or more young hot stars (a "metabolic connection" with the above mentioned unidentified bands and lines and PAHs present only if there is also UV source present does not look like a bad guess). In general the trunks are

Another important finding supporting TGD view about Universe which might be seen as a fractally scaled variant of above helices. pointing like fingers to the hot stars. Here is abstract of the paper by P. Carlquist, G. F. Gahm, and H. Kristen [36].

*Using the 2.6 m Nordic Optical Telescope we have observed a large number of elephant trunks in several regions. Here, we present a small selection of this material consisting of a few large, well-developed trunks, and some smaller ones. We find that: (i) the well-developed trunks are made up of dark filaments and knots which show evidence of twisted structures, (ii) the trunks are connected with essentially two filamentary legs running in V-shape, and (iii) all trunks have the maximum extinction in their heads. We advance a theory of twisted elephant trunks which is based on the presence of magnetic flux ropes in molecular clouds where hot OB stars are formed. If the rope contains a local condensation it may adopt a V-shape as the region around the hot stars expands. If, in addition, the magnetic field in the rope is sufficiently twisted, the rope may form a double helix at the apex of the V. The double helix is identified with the twisted elephant trunks. In order to illustrate the mechanisms behind the double helix we have constructed a*

*mechanical analogy model of the magnetic flux rope in which the rope has been replaced by a bundle of elastic strings loaded by a weight. Experiments with the model clearly show that part of the bundle will transform into a double helix when the twist of the bundle is sufficiently large. We have also worked out a simple theoretical model of a mass-loaded magnetic flux rope. Numerical calculations show that a double helix will indeed form when the twist of the rope exceeds a certain critical limit. Numerical model calculations are applied to both the analogy model experiments and one of the well-developed elephant trunks. On the basis of our model we also suggest a new interpretation of the so called EGGs.*

*The double helix mechanism is quite general, and should be active also in other suitable environments. One such environment may be the shell of supernova remnants. Another example is the expanding bubble outlined by the North Celestial Pole Loop.*

For fractally thinking physicist consisting mostly of dark matter with large Planck constant this does not leave many options: life and even intelligent life is everywhere and in all length scales. This provides also a new view about Fermi paradox: see the article [50], which summarizes also the essentials of TGD, TGD based ontology, and TGD based quantum biology.

## 3.3 Universal metabolic quanta

The basic prediction following from the p-adic length scales hypothesis is that universal metabolic energy quanta come as octaves of p-adic energy scale. The natural expectation is that the evolution of life has proceeded from high to low energy quanta and that also the high energy quanta might be seen even at the level of organic life.

### 3.3.1 Could UV photons have some metabolic role?

The correlation between UV photons and ERE brings in mind the vision that high temperature plasmoids are primitive life-forms possibly having universal metabolic energy quanta in UV range. One can imagine that the development of chemical energy storage mechanisms has made it possible to use visible light from Sun as a source of metabolic energy and get rid of UV quanta having disastrous biological effects. Ozone layer shields out most of UV light and also air absorbs the UV light below wavelength 200 nm, which justifies the term vacuum UV (VUV) for this range.

| $\Delta k$ | 1 | 2 | $\geq 3$ | $\infty$ |
|---|---|---|---|---|
| $\Delta E(144, \Delta k)/eV$ | 4 | 6 | $\geq 7$ | 8 |
| $\lambda/nm$ | 310(UVB) | 207(UVB) | $\leq 177$ (VUV) | 155 (VUV) |

Table 3. The lines corresponding to the dropping of electron from $k = 144$ space time sheet defining a candidate for UV light inducing generation of ERE in the interstellar dust.

From Table 3 one finds that $\Delta k > 2$ electronic transitions cascading to 8 eV (155 nm) by period doubling) belong to vacuum UV (VUV) absorbed by air. The lines 310 nm and 207 nm corresponding to $\Delta k = 1$ and $\Delta k = 2$ could however define frequency windows since these lines need not correspond to any atomic or molecular electronic transitions.

In the solar photosphere the temperature is about 5800 K, roughly half of the minimum temperature $10^4$ K needed to generate the UV radiation inducing ERE in interstellar dust. Solar corona however has temperature of about $10^6$ K, which corresponds to a thermal energy of order 100 eV and the UV radiation from corona at above mentioned discrete frequencies resulting in dropping of electrons could serve as a metabolic energy source for prebiotics in the interstellar space. This raises obvious questions. Should the stellar sources inducing ERE possess also corona? Could 4 eV and 6 eV UV photons from the solar corona serve as a source of metabolic energy for some primitive organisms like blue algae?

### 3.3.2 A simple model for the metabolism of plasmoids

Extended Red Emissions (EREs) are associated with the interstellar dust in presence of UV light with energies above 7.25 eV and source with temperature not below $10^4$ K (maximum of wave length distribution of black body radiation corresponds to the energy 4.97 eV at this temperature). This suggests that plasmoids using UV photons as metabolic energy are involved.

a) Since the bond energies of molecules vary in few eV range and their formation typically liberates photons in UV range, the natural hypothesis is that the metabolic cycle is based on the formation of some molecule liberating UV photon kicking electron/proton to a smaller space-time sheet. UV photons from energy source would in turn induce dissociation of the molecule and thus drive the process. The process as a whole would involve several p-adic length scales and several metabolic currencies.

b) This situation is of course encountered also in the ordinary biology but

with highly developed sharing of labor. Biosphere would burn hydrocarbons in animal cells with carbon dioxide as the eventual outcome. Carbon dioxide would in turn be used by plants to regenerate the hydrocarbons. Note that in the recent day technology the loop is open: hydrocarbons are burned but there is no process regenerating them: perhaps photons with large Planck constant might some day used to regenerate the fuel and give rise to "living" and perhaps tidier technology.

c) It is believed that complex organic molecules like amino-acids can form in the interstellar dust and the spontaneous formation of aminoacids is known to be possible in the interstellar ice under UV radiation. Hence at least $N_2$ and perhaps also $CO$ can be expected to be present. The table below gives dissociation energies of some simple molecules.

| Molecule | $H_2$ | $O_2$ | $N_2$ | CO | NO |
|---|---|---|---|---|---|
| $E_D$/eV | 4.48 | 5.08 | 7.37 | 11.11 | 5.2 |

i) $N_2$ has bond energy 7.37 eV is slightly above the UV threshold 7.26 eV for ERE, which strongly suggests that $N_2$ is one of the molecules involved with the metabolism of interstellar plasmoids.

ii) If ice is present then carbon monoxide $CO$ would be an excellent candidate for a metabolic molecule since its bond energy is as high as 11.11 eV. The exceptionally large bond energy would naturally relate to the fact that carbon and oxygen are the key molecules of life.

### 3.3.3 Anomalous light phenomena as plasmoids

TGD suggests that anomalous light phenomena (ALPs, or light balls, or UFOs depending on one's tastes and assumptions) are identifiable as plasmoids behaving as primitive life forms. In the conference held in Röros Björn Gitle-Hauge told about the determination of the spectrum of visible light emitted by some light balls observed in Hessdalen [48] ("Hessdalen phenomenon" is the term used).

a) The spectrum is a band in the interval 500-600 nm whereas the typical ERE [33] is concentrated in the interval 650-750 nm. The peak is in the interval 540-900 nm, the width of the band is also now 100 nm, and there are no sharp peaks. Therefore the interpretation as ERE can be considered.

b) Because Hessdalen is an old mining district, authors propose that the light ball could consist of burning dust containing some metals. Author proposes that the burning of Titanium and Scandium (encountered only in Scandinavia) might provide the energy for the light ball. $Sc$ reacts vigorously

with acids and air (burning in oxygen gives $Sc_2O_3$ as end product). $Ti$ burns in oxygen and is the only element that burns in nitrogen. $Ti$ is used in fireworks since it produces spectacular fires.

Author notices that the emission lines of $N^+$, $Al^{++}$, *resp.* $Sc^+$ at 528.02 nm, 528.2 nm, *resp.* 528.576 nm might contribute to the band. This might be the case but the explanation of the band solely in terms of molecular transitions is not favored by its smoothness.

c) The bond energies of $TiO$ and $TiN$ are 6.9 eV and 5.23 eV so that the radiation resulting in their formation is in UV range and could provide part of the metabolic energy. I do not know about bond energy of Scandium oxide.

d) $TiO_2$ is known to catalyze photolysis in the presence of UV light [29, 28], which in turn is basic step in photosynthesis [27], the basic step of which in TGD Universe would be the kicking of electrons/protons to smaller space-time sheets. Therefore the UV photons liberated in the formation of molecules containing $Ti$ could catalyze photosynthesis like process.

### 3.4 Life as a symbiosis of plasmoids and biological life

If evolution has discovered something it usually keeps it so that plasmoids and UV metabolism should be still there. This suggests that plasmoids are still in ionosphere. What could this mean? There also also other questions and I am grateful for Sampo Vesterinen for some of them. The key questions are perhaps the following ones. Do plasmoids and biological life forms live in symbiosis in some sense? If this is the case, what plasmoids can give to us and what we can give to plasmoids?

*1. Magnetic bodies as quantum plasmoids and plasmoids in magnetosphere*

One must make clear what one means with plasmoid. One can consider a plasma made of ordinary visible matter and also large $\hbar$ quantum plasma at magnetic bodies in a form of Bose-Einstein condensates of charged particles. The symbiosis of plasmoids and biomatter could correspond to the symbiosis of magnetic body and biological body.

One can imagine also the possibility that visible matter plasmoids and bio-matter are in symbiosis via the mediation of magnetic bodies. Note that DNA strands are negatively charged so that there is a resemblance with a plasma like state. One aspect of symbiosis would be that magnetic body would feed charged particles to DNA.

*2. Some basic facts about magnetosphere*

Magnetosphere would be a natural environment for plasmoid population. If one restricts plasmoids to to visible matter, then ionosphere, plasma sphere and plasma sheet are the most interesting objects of interest.

a) The temperature in the highest F layer of the ionosphere (extending from 150 km to 1500 km depending on source) is about 1200-1300 K: the photon energy is about .6-.65 eV at the maximum wavelength of thermal distribution. Hence F layer plasmoids might receive metabolic energy in the form of .5 eV metabolic energy quanta via thermal photons. Self-organization occurs in transition layers and especially interesting is the transition region 85-300 km from mesosphere to ionosphere at which temperature increases 300 K to about 1200 K.

b) Inner magnetosphere is a toruslike structure whose extension varies between $4R_E$ (day side) and $8R_E$ (night side) and shielded from solar wind. In the inner magnetosphere the typical density is about 1 ion per cubic centimeter. Inner magnetosphere is bounded by a transition layer of thickness of $\sim R$ (magneto-pause). In this region the density of the ions drops rapidly.

Inner magnetosphere contains plasma sphere whose radius varies in the range $2R_E - 4R_E$ at day side and $2R_E - 6R_E$ at night side. Plasma has a ionospheric origin. The density of the cold plasma consisting mainly of protons sphere varies in the range $10 - 10^3$ ions/cm$^3$, whereas the temperature is $\sim 5 \times 10^3$ K, which corresponds to metabolic energy quantum of .5 eV. Note however that the energy of photon at maximum of thermal distribution is about 2.5 eV which suggests 2 eV metabolic quantum.

The cold, dense plasma of plasma sphere is frozen around magnetic flux lines which co-rotate with Earth. In TGD framework this means that flux tubes co-rotate and thus change shape. In the equitorial plane the density of the plasma sphere drops sharply down to $\sim 1$ ion/cm$^3$ at $r = 4R$. This transition region is known as a plasma pause. During magnetic storms the outer radius decreases since the pressure of the solar wind compresses the plasma sphere. The day-night variation of the shape of the plasma sphere is rather small. Within this region the magnetic field has in a reasonable approximation dipole shape with radiation belts forming an exception.

The surface temperature of Sun is $6 \times 10^3$ K. This temperature is roughly half of the minimum temperature $10^4$ K needed for EREs from interstellar dust [33]. This corresponds to photon energy of 3 eV at the maximum of thermal distribution and cannot induce dissociation of $N_2$ and other simple diatomic molecules. There is also solar corona but its temperature is about $10^6$ K ($10^2$ eV) so that the flux of thermal photons at UV energies is very low.

Taking seriously the finding that $T \geq 10^4$K for source is necessary for

EREs, one might ask whether the plasmoids at the day side are able to receive enough metabolic energy from UV radiation of Sun. If course, there is is no need to assume that dissociation of $N_2$ molecules is key element in metabolic mechanism. The temperatures in both F layer and plasma sphere allow kicking of protons and electrons to smaller space-time sheets and this might save the situation. Hence metabolism is not a problem for the plasmoids except perhaps during night-time when the plasma cools down somewhat.

c) The plasma sheet [30, N1] at the night side of Earth dark is the most prominent feature of the outer magnetosphere. It has a thickness about Earth radius $R_E$ and extends beyond Moon's orbit (with radius $10^3 R_E$). The average densities of charged particles are very low and same order of magnitude as in plasma sphere: about .4-2 per $cm^3$ for both protons and electrons and correlates with solar wind density.

The temperature is very high: the thermal energy of electrons is in keV range and ionic temperatures are even higher. The high temperature is due to the leakage of matter from solar wind. Note that up to the distance $d \sim 10^2 R_E$ equator region of outer magnetosphere at the night side of Earth experiences a continual solar eclipse so that this region does not receive radiation energy from Sun: the high temperature of plasma sheet solves this metabolic problem.

The presence of keV photons would destroy molecules at plasma sheet and induce a high degree of ionization so that plasmoid life must be based on ions and electrons. The energy needed to kick an electron to an atomic space-time sheet is about keV from $m_e/m_p \sim 2^{-11}$: hence the dropping of electrons from atomic space-time sheets would be the natural metabolic mechanism for plasmoid life at plasma sheet.

One of the original motivations for the plasmoid hypothesis was the strange finding that plasma sheet at the equator at the dark side of Earth is highly self-organized structure and the velocity distributions of electrons present patterns like "flowers", "eyes", "butterflies" [N1].

*3. What plasmoids could give to us and what we could give to plasmoids?*

An attractive general motivation for the symbiosis would be that magnetic bodies would give us ability to think and we would give them ability to sense.

a) The model of cognitive representations relies on the intersections of magnetic bodies with corresponding p-adic space-time sheets possessing literally infinite size in the real sense. The larger the magnetic body, the better the representations. Magnetic bodies could thus provide us with cognitive

representations and an interesting question is whether and how this relates to the strange self-organization patterns at plasma sheet.

b) We could provide for magnetic bodies sensory input and serve as their motor instruments. These magnetic bodies might be also associated with plasma sheet and the plasmoids of ionosphere and plasma sphere and could also use plasmoids of visible matter as a sensory receptors and perhaps even primitive motor instruments.

One can imagine also more concrete motivations for the symbiosis.

a) Plasmoids in the day-side ionosphere could shield biosphere from UV light by "eating" the incoming UV light. Magnetic bodies could also feed negative electronic charge from the plasmoids of magnetosphere to DNA double strands.

b) Plasmoids are not in a need of metabolic energy unless it happens that the temperature in F layer cools too much during night time from $T \sim 0.12$ eV. One might imagine that plasmoids suck metabolic energy from the biosphere during sleep (say brains which remain active): this would be a possible explanation for why we sleep. One can even imagine that during sleep magnetospheric collective levels of consciousness take command and life forms in the biosphere entangle to form kind of stereo consciousness providing a collective view what is to be human, member of species, or a part of biosphere.

*4. About the interpretation of bio-photons?*

Also the wave lengths of bio-photons are in the range of visible photons. Their spectrum is claimed to be featureless, which would suggest that identification in terms of photons resulting in dropping of electrons and protons to larger space-time sheets might not make sense. The variation of the geometric shape of space-time sheets, the possibility of surplus energy, and the clustering of the transition lines around the lower end of wave length spectrum might however give rise to effectively featureless spectrum.

Suppose that bio-photons correspond to superposition of ERE bands and thus reflect the presence of UV energy feed. Unless biological body is not able to generate the needed UV photons, they must arrive from Sun. Bio-photons or their dark counterparts with much longer wavelengths could indeed live at the flux quanta of the magnetic bodies and observed visible bio-photons could represent some kind of leakage.

*5. Gariaev's experiments*

Gariaev's experiments [23] involved the irradiation of DNA using visible laser light with photon energy 1.9595 eV. The irradiation induced emission

of radio waves with same polarization with frequencies above kHz. Radio waves induced growth of potatoes. A possible interpretation is that 2 eV photons kicked electrons to a smaller space-time sheet and thus gave metabolic energy to DNA. The radio waves possibly resulting in the dropping of electrons back to the larger space-time sheets could have consisted of dark photons with same or smaller energy and could have been used as a metabolic energy by the potatoes. That the dropping can occur to several space-time sheets would explain why several radio wave frequencies were observed. The prediction would be sum of period doubling spectra discussed earlier since sequences of droppings are possible. The radio-wave signal would result from the de-coherence of dark radio-wave photons to a bundle of ordinary radio-wave photons.

*6. Earth's interior as a living system?*

For years ago I developed in detail the working hypothesis that entire magnetosphere is a living system. Even Earth's interior (and also solar surface) could contain plasmoid life [N4, N1]. The temperature below the mantle of Earth does not differ too much from the surface temperature of Sun and metabolic energy could come from the radioactive decays from the interior of Earth. There would be UV shielding by Earth: UV light has energies above 3.1 eV whereas the temperature at the mantle-core boundary is 4300 K which corresponds to energy 2.2 eV energy at the maximum of thermal distribution. Metabolic energy quantum of 2 eV would be highly suggestive and might be directly used to kick protons and electrons to smaller space-time sheet.

The metabolism would not probably involve energy quantum of .5 eV. Magnetic flux tubes could also mediate metabolic energy from the biosphere and possibly also ionosphere and the plasmoid life in question could be at an evolutionary level not tolerating UV light and involve molecules in essential manner.

# 4 New hydrogen technologies and new physics

The anomalies related to energy technologies involving the burning of hydrogen to oxygen are known for decades. In fact, the anomaly related to the thermal dissociation of hydrogen was discovered by the Nobel chemist Irving Langmuir for century ago. For some reason these anomalies are not payed any attention in standard chemistry.

## 4.1 Anomalies related to the dissociation of water and hydrogen molecules

The burning of hydrogen to water liberates energy. Because the process does not seem to produce chemical pollution, hydrogen provides one of the most promising energy sources. The basic problem is that the storage and transport of hydrogen is very expensive. A possible solution to the problem is to produce the hydrogen by the dissociation of water at the location where the energy is used. If this goal is achieved, an outcome is an energy source able to compete with other energy sources most of which will be depleted in any case.

The theoretical problem related to various methods producing hydrogen by dissociation of water is in the nutshell that the dissociation of water requires less energy than one might think knowing the bond energies of O-H bonds [57, 58]. Concerning the basic goal this is of course not a problem. Also the energy needed to dissociate hydrogen thermally is smaller than the binding energy of the hydrogen molecule. This was observed already by Nobel chemist Langmuir for century ago [56]. For some reason this observation has not received the recognition it would have deserved. Energy flows to the system in both situations and one should understand the origin of this energy.

The zero point kinetic energy of vacuum (ZPE) [59] has been proposed as a solution the problem. Unfortunately, ZPE theories are not very well defined and far form practically applicable. My intention in the following is to find whether the new physics predicted by TGD might allow to understand the origin of the above mentioned anomalies.

A good guideline is the observation that very many free energy systems involve sharp pulse sequences. Often bi-filar coils invented by Tesla [54] are involved. The liberation of the zero point kinetic energy when particles drop to a larger space-time sheet is a universal liberation of mechanism of energy justifying the notion of free energy. The time mirror mechanism makes possible the control of this process. Either the system needing the energy or controlling the liberation of energy generates negative energy topological light rays accompanied by negative energy photons (generated by a light like vacuum 4-current possibly associated with the topological light ray). Scalar wave pulses could in turn make possible higher level control by inducing the generation of negative energy topological light rays and photons as time reversed version of brehmstrahlung when charged particles are accelerated in the strong electric field of the scalar wave pulse without dissipation.

These ingredients lead to a concrete model for how the origin of the

energy liberated in the dissociation of water and to a proposal how this method could be made more effective. If the proposed explanation is correct, the dissociation of water molecules could be induced also by the irradiation of water by phase conjugate laser light, whose frequencies could be fine tuned to correspond to the needed frequencies. This could mean considerable energy savings.

In the following the model explaining the anomalies related to the dissociation of water and hydrogen is discussed. Also a TGD based justification for the notion of hydrino-atom introduced by Randell Mills [60] is proposed.

## 4.2 The anomalies associated with the dissociation of water molecules

In the sequel the general ideas about time mirror mechanism and many-sheeted lasers is applied to the anomalies observed in the dissociation of water.

### 4.2.1 Constraints on the model of anomalies found in the electrolysis and plasma electrolysis of water

The general theory leaves a lot of freedom for the building of a detailed model. There are however several facts, which provide constraints on the imagination.

a) In plasma electrolysis a pulse electronic current is an essential part of the process. The natural guess is that the dropping of electrons to larger space-time sheets could excite O-H bonds or O and H atoms to higher energy states. This could happen during the dissociation of the water molecule or already before it. Prof. Kanarev has proposed that the O-H bonds of water molecule are indeed excited before the process. Kanarev has also suggested a separate mechanism in which two electrons join to the water molecule during the dissociation. This mechanism is not needed if the sole role of the electronic current is excitation of the O-H bonds.

b) In very many free energy phenomena a pulsed voltage/current seem to induce the generation of negative energy topological light rays (photons). They in turn would serve as a control signal inducing the generation of positive energy topological light rays (photons) as population inverted many-sheeted laser returns to the ground state. The mechanism generating the phase transition is the same as in the induced emission. This would support the model of Prof. Kanarev: the positive energy photons (analogous to laser beam) would excite the O-H bonds or O and H atoms of the water

molecules. Electrons have both thermal and ordered kinetic energy. This means that the energy liberated in the dropping process varies and that the liberated energy can be larger than the zero point kinetic energy. An energy continuum results and makes it possible to excite O and H atoms having a sharply defined transition energies. One can also imagine that so called seesaw mechanism is at work. Negative energy topological light rays would be created in a transition which is the reversal for that producing positive energy topological light rays. Fine tuning would be automatic now. This mechanism might be a central part of bio-control.

c) If the amplification of negative energy signal is based on the mechanism of induced emission, the particles involved must be bosons. Only the Cooper pairs of electrons come into consideration now. In the case of fermions one might think that the dropping of fermions from a given space-time sheet creates free vacancies and makes possible the dropping of fermions to this space-time sheet from smaller space-time sheets. This could induce kind of a chain reaction proceeding from long to short p-adic length scales.

d) The second option is that water molecule emits negative energy photons when it dissociates so that the oxygen and hydrogen atoms of O-H bonds are excited to a higher energy state. This option does not allow to understand the role of the pulse current serving as external controller of the process.

### 4.2.2 Zero point kinetic energies

If the kinetic energy of the dropping electrons can be neglected, the spectrum for the energy quanta liberated in the dropping process is universal since zero point kinetic energies are fixed by p-adic length scale hypothesis apart from a numerical factor near unity characterizing the shape of the space-time sheet. The formula for the zero point kinetic energy in the non-relativistic case reads as

$$\begin{aligned} E_0(k) &= n \times \frac{\pi^2}{2mL(k)^2} \ , \\ L(k) &= 2^{(k-151)/2} \times L(151) \ , \ L(151) \simeq 10 \ nm \ . \end{aligned} \qquad (1)$$

Here $m$ denotes the mass of the particle and $n$ is a numerical constant near one.

Atomic space-time sheet $k = 137$ corresponds in the case of proton to an energy of about .4 eV, which is the basic energy currency of metabolism. This inspires the idea that the basic function of the ADP-ATP system is to

drive protons from larger space-time sheets to the atomic space-time sheets by utilizing the chemically stored energy. From this space-time sheet they drop back to the larger space-time sheets liberating the zero point kinetic energy $E_p(137) \simeq .4$ eV . An entire hierarchy of metabolic currencies is actually predicted [K6, K1].

Also electrons and their Cooper pairs can drop to larger space-time sheets and in this case the liberated zero point kinetic energy is larger by a factor $m_p/m_e \simeq 2^{11}$. The zero point kinetic energy at $k = 137$ space-time sheet $\sim .4 - .5$ eV is a convenient unit, in terms of which one can express the zero point kinetic energies of proton, electron, electronic and protonic Cooper pair.

$$\begin{aligned} E_p(k) &= 2^{137-k} \times .5 \ eV \ , \\ E_{2p}(k) &= 2^{137-k-1} \times .5 \ eV \ , \\ E_e(k) &= 2^{148-k} \times .5 \ eV \ , \\ E_{2e}(k) &= 2^{147-k} \times .5 \ eV \ . \end{aligned} \tag{2}$$

Here the nominal value of .5 eV for $E_p(137)$ is used.

### 4.2.3 Consistency conditions

A natural consistency condition is that the thermal de Broglie wave length $\lambda_{dB} = \pi/\sqrt{2MT}$, where $M$ denotes the mass of the heaviest particle at particular space-time sheet, is of the same order of magnitude as the p-adic length scale characterizing the size scale for the space-time sheet from which the particle drops.

$$\lambda_{dB} = \frac{\pi}{\sqrt{2MT}} \sim L(k) \ . \tag{3}$$

On the other hand, super conductivity requires that thermal energy is smaller than the zero point kinetic energy defining the basic energy unit. This gives the condition

$$\lambda_{dB} > L(k) \ . \tag{4}$$

Here one must however require that there is no allowed p-adic length scale between $\lambda_{dB}$ and $L(k)$. What "allowed" means is quite not obvious. The first extreme corresponds to the situation in which all values of the integer

$k$ are possible so that p-adic length scales come in half octaves and that all n-ary p-adic length scales are possible. The second extreme corresponds to the situation in which $k$ is prime. At least secondary p-adic length scales ($k$ is two times prime) are allowed, and the model of EEG suggests that all values of $k$ are possible but that those values which correspond to highest cognitive level are the most important ones (every prime factor $k_-i$ in the decomposition of $k$ to a product of primes defines a $k_i$-bit cognitive code[M4]).

### 4.2.4 Experimental data

The experimental values for the reduction of the binding energy of water allow to estimate the integer $k$ characterizing the space-time sheets from which electrons or their Cooper pairs drop.

a) In the ordinary electrolysis the energy needed to dissociate O-H bond has been found to be only 1/3 of the binding energy $E_w \sim 10$ eV of the water molecule. The reduction of the binding energy is $\Delta E_w \simeq 6.66$ eV.

b) In the plasma electrolysis of Prof. Kanarev the energy needed to dissociate water molecule is only $\sim .5$ eV and the effective reduction of the binding energy is as high as $\Delta E_B \sim 9.5$ eV.

A rough approximation for the energy needed would be 8 eV in both cases. This energy is $2^4 = 16$ higher than the zero point kinetic energy of proton at $k = 137$ space-time sheet. In plasma electrolysis the temperature is in the interval $.5 \times 10^4$- $10^4$ C and around $10^3$ C in the ordinary electrolysis.

### 4.2.5 The four options

One can distinguish between four different models depending on what the reaction mechanism is and whether the energy is donated by electron or electronic Cooper pair.

a) The energy is donated to O-H bond. The ratio $r$ is predicted to be $r = 3.33$ and $r = 4.75$ corresponding to ordinary and plasma electrolysis. The rough estimate is $r = 4$.

b) The energy is donated to the entire water molecule. In this case the ratio of the donated energy to the zero point kinetic energy is $r = 6.66$ in the usual electrolysis and $r = 9.5$ in plasma electrolysis. The rough estimate is $r = 8$.

Furthermore, one can distinguish between two cases according to whether the energy is donated by i) electronic Cooper pairs or ii) electrons. The first option is supported by quantum coherence implying that reaction rate

would be proportional to the square of the number of the dropped electronic Cooper pairs. Also the mechanism of the induced emission works for Cooper pairs unlike in the electronic case. It is however better to keep mind open for both options at this stage.

### 4.2.6 Analysis and conclusions

The following represents the analysis of the four options.

a) Energy is used to excite only single O-H bond.

i) For electronic Cooper pairs the condition $r = 4$ gives $k = 142 = 2 \times 71$ corresponding to the secondary p-adic length scale $L(2, 71) = .56$ nm. The estimate for the thermal de-Broglie wave length in plasma electrolysis is $.7 - 1$ nm. In the ordinary electrolysis de-Broglie wavelength is roughly 2 times longer. In both cases the thermal de Broglie wavelength is longer than the p-adic length scale so that the necessary condition for super-conductivity is satisfied.

ii) In the electronic case the condition $r = 4$ gives for the p-adic length scale the estimate $k = 143 = 11 \times 13 \simeq .8$ nm. This length scale corresponds to the prime $p \simeq 2^{13}$ and would represent a very low information content unlike $k = 142$, which corresponds to rather large prime $p \simeq 2^{71}$. The ratio $\lambda_{dB}/L(k)$ is same as in the first case.

b) The energy is used to excite the entire water molecule.

i) In the case of electronic Cooper pairs the condition $r = 8$ gives $k = 141 = 3 \times 47$ corresponding to the tertiary p-adic length scale $L(3, 47) \simeq .4$ nm.

ii) In the case of electrons one has $k = 142 = 2 \times 71$.

In both cases the ratio $\lambda_{dB}/L(k)$ grows by a factor $\sqrt{2}$ from the value in the preceding case so that the resulting model is poorer.

As a summary one can state the following.

a) The ratio of the thermal de-Broglie wave length to the p-adic length scale is same for both electron and Cooper pair options since the p-adic length scales are $L(k)$ for electron and $L(k - 1)$ for the Cooper pair and differ by a factor of $\sqrt{2}$ from each other.

b) For all options de Broglie wavelength in the case of ordinary electrolysis is at least by a factor of two too large and this forces to question the de Broglie wave length criterion. Of course, one can think that the production of positive energy photons generates temporary hot spots so that de Broglie conditions holds true after all.

c) The dropping of two electronic Cooper pairs per water molecule from $k = 2 \times 71$ space-time sheet is the most promising option, since in this case the mechanism of induced emission is possible and a satisfactory consistency

with de Broglie criterion is achieved. The secondary p-adic length scale is also very natural.

### 4.3 The anomaly related to the thermal dissociation of molecular hydrogen

Already the Nobel-chemist Langmuir found, that thermal dissociation in a temperature range extending up to the temperature of $T = 2200$ K, led to a much higher dissociation rate than one might expect on basis of thermodynamical considerations. The binding energy of the hydrogen molecule is 4.52 eV. If one requires that the ratio of the dissociated molecules to that of non-dissociated molecules is given as by the Boltzmann exponent $exp(-E_b/kT)$, a discrepancy of order $10^8$ results. If one assumes that the effective binding energy is $\simeq .44$ eV, a correct result is obtained.

This suggests that also now the dissociating hydrogen molecule receives energy from some source and that the energy is $\sim 4$ eV. Dissociation mechanism could be based either on the self-excitation of the hydrogen molecule by the emission of negative energy photons. Also some other system could emit negative energy photons and induce a cascade of positive energy photons. One has two options.

a) The dropping of an electronic Cooper pair from $k = 142 = 2 \times 71$ space-time sheet is involved as in the case of the optimal mechanism for the dissociation of water.

b) The dropping of an electron from $k = 143$ space-time sheet is an alternative option.

### 4.4 Hydrino atoms, anyons, and fractional quantization in many-sheeted space-time

The so called hydrino atom concept of Randell Mills [60] represents one of the notions related to free energy research not taken seriously by the community of university physicists. What is claimed that hydrogen atom can exists as scaled down variants for which binding energies are much higher than usually due to the large Coulombic energy. The claim is that the quantum number $n$ having integer values $n = 0, 1, 2, 3..$ and characterizing partially the energy levels of the hydrogen atom can have also inverse integer values $n = 1/2, 1/3, .....$ The claim of Mills is that the laboratory BlackLight Inc. led by him can produce a plasma state in which transitions to these exotic bound states can occur and liberate as a by-product usable energy.

The National Aeronautic and Space Administration has dispatched mechanical engineering professor Anthony Marchese from Rowan University to BlackLight's labs in Cranbury, NJ, to investigate whether energy plasmas- hot, charged gases- produced by Mills might be harnessed for a new generation of rockets. Marchese reported back to his sponsor, the NASA Institute for Advanced Concepts, that indeed the plasma was so far unexplainably energetic. An article about the findings of Mills and collaborators have been accepted for publication in Journal of Applied Physics so that there are reasons to take seriously the experimental findings of Mills and collaborators even if one does not take seriously the theoretical explanations.

The question to be addressed in the following is whether the many-sheeted space-time concept could allow to understand the claimed $n \to 1/n$ generalization of the Bohr's quantization rules claimed by Mills or a generalization of this rule consistent with the experimental findings of Mills. In the following I discuss three arguments allowing to understand the scaled up energy spectra claimed by Mills. These arguments are not independent and do not exclude each other.

### 4.4.1 p-Adic quantization and fractional spectrum

p-Adic integers $n = \sum n_k p^k$, $k \geq 0$, can have infinite values as real integers. If one requires that p-adic integer has a pinary expansion which is periodic, only p-adic integers, which correspond to rationals are possible: $n \to q = r/s$, where $s$ is not divisible by $p$. The expansion of $1/s$ in powers of $p$ indeed gives rise to an infinite (in real sense) p-adic integer.

One might argue that all rational values of the principal quantum number $n$ of hydrogen atom are actually possible, which would mean that the spectrum is effectively continuous as in classical physics. What quantum physics would bring in would be the selection of integers from other rational numbers so that effectively one would have integer spectrum under the usual experimental conditions.

### 4.4.2 Fractional valued quantum numbers and controlled transition to chaos

Bohr's quantization rules apply to completely integrable systems for which complete separation of variables occurs so that one effectively has a set of one-dimensional systems performing motion on circle or line. One can quantize the motion separately in each dynamical degree of freedom characterized by a cyclic coordinate $q_i$ and the corresponding canonical momentum $p_i$. If

$q_i$ is a circle coordinate, one can use the basic quantization rule

$$\oint p_i dq_i = n_i \hbar \ ,$$

Here the integral is over a full cycle of the periodic motion. If $q_i$ corresponds to a motion on line, no quantization rule is applied.

Primes are known to appear, when one attempts to quantize chaotic systems and effectively p-adic physics might be closely related to the approach to the chaos implied by the classical non-determinism of the Kähler action. This suggests that fractional quantization might emerge in a system for which the interactions with the environment destroy the simple periodic motion, which is the prerequisite for the application of Bohr's quantization rules.

So, an interesting question is what occurs when the motion is slightly perturbed. Do orbits become non-closed or do they close after $N$ cycles so that the transition to the chaos corresponds to the sequence $N = 1 \to 2 \to 3 \to ....$ Period doubling leading to chaos represents just this kind of series of perturbations with $N = 2^k$, $k = 1, 2, ...$ In TGD universe, where orbits could correspond to space-time sheets themselves, this kind of ordered transition to chaos could be realized in contrast to what one might expect in standard physics.

The natural guess would be that one must replace the quantization condition with

$$\oint p_i dq_i = \frac{n_i}{N} \hbar \ ,$$

where the integration is over the previous cycle, which has become $1/N$:th cycle. In the case of hydrogen atom this would give rise to a fractional angular momenta $m$ and fractional principal quantum number $n$, and the spectrum would contain the spectrum claimed by Mills.

One could argue that all rational numbers, for which the denominator is not divisible by the prime $p$ characterizing the atomic space-time sheet, represent possible values of the principal quantum number $n$. The most natural estimate for $p$ is $p \simeq 2^{137}$ (that fine structure constant is in a good approximation $\alpha = 1/137$ might express cosmic sense of humor). The requirement that the rest energy of the electron stays positive, gives the condition $N < 1/\alpha \simeq 137$. Quantum physics favors finite integers because of their finite pinary expansion and in the usual experimental situation only integer spectrum would be possible. As the system grows more complex, also

the values $1/n$ and $m/n$ of the principal quantum number would become possible.

### 4.4.3 Fractional quantization and controlled transition to chaos at space-time level

In TGD all quantum level concepts should have space-time correlates. In particular, Bohr's quantization rules have exact counterparts TGD and are implied by the absolute minimization of Kähler action. Also the proposed transition to chaos by the generation of orbits which close only after $N$ cycles should have a natural space-time correlate.

I have already earlier proposed that the orbits of electrons in atoms could be more than a fictive concept and have concrete 3-surfaces as their representatives. One might say that electrons would move along quantum tracks. This is consistent with the general vision that space-time surface provides symbolic representation for all quantum physics concepts. This means that the electronic space-time sheet having size of order electron Compton length would be topologically condensed at representing the classical orbit of electron. In TGD universe all quantum phenomena should have classical space-time correlates and also the quantum resolution of the well known infrared catastrophe (electron slows down by emitting brehmstrahlung and falls into the nucleus) should have a space-time correlate. Closing the electron inside a closed tubular structure representing its path would clearly prevent the infrared catastrophe.

In the first approximation the ordinary orbit of electron would be replaced by a torus like tube along the classical orbit within which the electron wave function is concentrated. For $N > 1$ the torus would run around $N$ times before closing. The transformation of closed orbital 3-space sheets to orbital 3-space sheets closing after $N$ cycles occurs very naturally at the level of space-time sheets. The closure must occur for some value of $N$ since otherwise the resulting orbital 3-surface would be extremely irregular, have infinite volume, and could carry infinite classical field energy. It is natural to expect that the transition occurs by the sequence $N = 1 \to 2 \to 3...$ or some sub-sequence of it. One can image that in high temperature plasma the interactions with the external world might indeed replace the simple periodic Bohr orbitals with orbitals which would close only after $N$ cycles.

*1. Fractional Bohr quantization*

In fractional Bohr quantization the angular momentum component would be quantized in units of $\hbar/N$ rather than $\hbar$.

$$\oint p_\phi d\phi = \frac{m}{N}\hbar \ ,$$

This phenomenon could also provide the space-time correlate for anyons having fractional angular momentum and giving rise to fractional quantum Hall effect. The quantization condition for the radial variable would be also replaced by a more general quantization condition

$$\oint p_r dr = \frac{n}{N}\hbar.$$

This would give as a special case the quantization rule proposed by Mills. Quite generally, the spectrum of hydrogen atom would be scaled up by $N^2$, $N = 2, 3, 4, ..$ or some subsequence of this sequence.

*2. Constraints on the orbital 3-surface*

The picture based on formal Bohr rules is too simplistic and might be even wrong. In particular, one can ask is the value of $N$ same for both radial and angular degrees of freedom. A more detailed consideration indeed shows that naive fractional Bohr quantization need not be correct approach.

A more concrete space-time picture results, when one takes into account the requirement that the Coulomb force experienced by electron corresponds to intuitive expectations.

a) The electric gauge flux must flow to the orbital surface somehow, either through wormhole contacts or through join along bonds connecting the orbital surface to the boundaries of holes in atomic space-time sheet. The latter option looks more natural. If only part of the flux flows to the orbital surface, also orbital surface suffers Coulomb force. The failure for the imbeddability of the electric field is expected to cause the generation of holes in the 3-space.

b) The average Coulombic force at various sheets of the multiple-sheeted orbital surface must be same.

By applying these constraints one ends up to two simple prototype realizations for the multiply-sheeted orbital surface, which could be called neo-classical and non-classical. Also the hybrid of these options is possible.

*3. The neo-classical option allows fractional quantization of magnetic quantum number m.*

For neo-classical option the 1/N-periods of the orbit corresponds to slightly different radii. The Compton length of electron, about $10^{-12}$ meters determines the thickness of the orbital sheet. Since the natural scale of the

atomic resolution is Bohr radius $a_0 \simeq 10^{-10}$ meters, it is possible to have roughly $N = 100$ without too strong effects on the force experienced by electron. $N = 137$ would follow from the requirement that the rest mass of electron stays positive and is natural because $p \simeq 2^k$, $k = 137$ defines the p-adic length scale of the atomic space-time sheet.

The electric gauge flux would flow to the orbital 3-surface and back from it. This option is nearest to the one suggested by classical physics intuition and one can indeed imagine that the perturbations caused by the interaction with environment have this kind of effect.

Bohr quantization argument would suggest fractional quantization of both $m$ and $n$. One can however argue that the radial and angular degrees of freedom separate in a good approximation at the level of Schrödinger equation, and that one obtains fractional quantization for the magnetic quantum number $m$ but not for the principal quantum number $n$. Thus this option would not produce the desired $N^2$-scaling of the energy spectrum but would allow to understand anyon physics at space-time level.

*4. The non-classical option allows fractional quantization of the radial quantum number n.*

The multiply-sheeted orbit could be also analogous to a Riemann surface associated with a multiple valued complex function $z^{1/N}$. That is the various sheets are at the top of each other: this option does not have any classical mechanics counterpart so that the attribute "non-classical" is well-motivated. This requires that there are $N-1$ folds in the radial direction so that the structure is like a carpet folded back for some length, then continuing in the initial direction, folded back ... There is no obvious upper bound for the value of $N$.

In those parts of the multiple fold rug, where the electric field is oriented inwards, electron suffers a repulsive force and cannot form stable states at these sheets. Situation is clearly same as in catastrophe theory, where these parts of the cusp catastrophe represent maxima of potential as a function of the external parameters. How the interaction with the environment folds the rug might be understood in terms of catastrophe theory.

If the orbital 3-surface is rotationally symmetric, Schrödinger equation allows a complete decoupling between radial and rotational degrees of freedom. In this case one would have fractional quantization for the principal quantum number $n$ only but not for the magnetic quantum number $m$. The cautious conclusion is that the experimental arrangement of Mills indeed demonstrates a new physics effect which does not have any classical mechanics counterpart.

One can combine radial and angular fractional quantizations in various manners.

a) Radially $N_r$-fold orbital surface closes after $N_\phi$ rotations. In this case these degrees of freedom separate completely.

b) A given radial fold is glued after each rotation to a different radial fold. In the general case the fractional quantizations of the radial and angular degrees of freedom can still correspond to different integers $N_r$ and $N_\phi < N_r$ such that $N_\phi > 1$ divides $N_r$. If one has $N_r = p$, $p$ prime, only $N_\phi = N_r = p$ is possible.

## 4.5 An explanation of findings of Mills in terms of quantized Planck constant

The recent view about quantization of Planck constants allows to understand the findings of Mills elegantly.

### 4.5.1 Quantization of Planck constants and the generalization of the notion of imbedding space

The recent geometric interpretation for the quantization of Planck constants is based on Jones inclusions of hyper-finite factors of type $II_1$ [A9].

a) Different values of Planck constant correspond to imbedding space metrics involving scalings of $M^4$ *resp.* $CP_2$ parts of the metric deduced from the requirement that distances scale as $\hbar(M^4)$ *resp.* $\hbar(M^4)$. Denoting the Planck constants by $\hbar(M^4) = n_a\hbar_0$ and $\hbar(CP_2) = n_b\hbar_0$, one has that covariant metric of $M^4$ is proportional to $n_b^2$ and covariant metric of $CP_2$ to $n_a^2$. In Kähler action only the effective Planck constant $\hbar_{eff}/\hbar_0 = \hbar(M^4)/\hbar(CP_2)$ appears and by quantum classical correspondence same is true for Schödinger equation. Elementary particle mass spectrum is also invariant. Same applies to gravitational constant. The alternative assumption that $M^4$ Planck constant is proportional to $n_b$ would imply invariance of Schrödinger equation but would not allow to explain Bohr quantization of planetary orbits and would to certain degree trivialize the theory (to be honest I believed to this option for some time and it produced a lot of confusion).

b) $M^4$ and $CP_2$ Planck constants do not fully characterize a given sector $M^4_\pm \times CP_2$. Rather, the scaling factors of Planck constant given by the integer $n$ characterizing the quantum phase $q = exp(i\pi/n)$ corresponds to the order of the maximal cyclic subgroup for the group $G \subset SU(2)$ characterizing the Jones inclusion $\mathcal{N} \subset \mathcal{M}$ of hyper-finite factors realized as

subalgebras of the Clifford algebra of the "world of the classical worlds". This means that subfactor $\mathcal{N}$ gives rise to $G$-invariant configuration space spinors having interpretation as $G$-invariant fermionic states.

c) $G_b \subset SU(2) \subset SU(3)$ defines a covering of $M^4_+$ by $CP_2$ points and $G_a \subset SU(2) \subset SL(2,C)$ covering of $CP_2$ by $M^4_+$ points with fixed points defining orbifold singularities. Different sectors are glued together along $CP_2$ if $G_b$ is same for them and along $M^4_+$ if $G_a$ is same for them. The degrees of freedom lost by $G$-invariance in fermionic degrees of freedom are gained back since the discrete degrees of freedom provided by covering allow many-particle states formed from single particle states realized in $G$ group algebra. Among other things these many-particle states make possible the notion of N-atom.

d) Phases with different values of scalings of $M^4$ and $CP_2$ Planck constants behave like dark matter with respect to each other in the sense that they do not have direct interactions except at criticality corresponding to a leakage between different sectors of imbedding space glued together along $M^4$ or $CP_2$ factors. In large $\hbar(M^4)$ phases various quantum time and length scales are scaled up which means macroscopic and macro-temporal quantum coherence. In particular, quantum energies associated with classical frequencies are scaled up by a factor $n_a/n_b$ which is of special relevance for cyclotron energies and phonon energies (superconductivity). For large $\hbar(CP_2)$ the value of $\hbar_{eff}$ is small: this leads to interesting physics: in particular the binding energy scale of hydrogen atom increases by the factor $n_b/n_a^2$.

### 4.5.2 Explanation for the findings of Mills

Also the small values of $\hbar_{eff}) = n_a/n_b$ are interesting since in this case hydrogen atom binding energy scale increases by factor $(n_b/n_a)^2$ as Planck constant decreases (this conforms with the interpretation about approach to chaos in systems like plasmas). The assumption $n_b/n_a = k = 2, 3, ...$ predicts exactly the binding energies reported of Mills. Also the fact that for $n_b/n_a > 137$ the binding energy becomes larger than electron rest mass remaining invariant in the phase transition implies trivially the upper bound $k \leq 137$.

More generally, this picture leads to the notion of N-atom. The space-time sheets can be regarded as $N(G_b)$-fold coverings of $M^4$ by $CP_2$ points related by subgroup $G_b \subset SU(2) \subset SU(3)$ (color group) and this meas that one can put one hydrogen atom to each sheet of the covering (analogous to multi-sheeted Riemann surface. The signature for N-atom would be scaled

up binding energy spectrum whereas vibrational energies would be scaled downwards.

Another kind of N-atom results for $n_a/n_b > 1$. This N-atom would be like N-molecule having discrete spatial symmetry characterized by $G_a \subset SO(3)$: for large values of $n_a$ the symmetry would consist of planar rotations and reflections with number-theoretically preferred values of $n_a$ corresponding to Fermat polygons constructible using only ruler and compass. The only genuinely 3-D symmetry groups would correspond to tedrahedral and icosahedral symmetries which are encountered in the structure of water. Icosahedral and dual dodecahedral structures are very abundant in living matter.

In this case energies $E = hf$ associated with classical frequencies are scaled up by factor $n_a/n_b > 1$ so that the vibrational modes need not be masked by the thermal noise. Note that also the quantum energies associated with cyclotron and plasma frequency are scaled up. For $n_a/n_b = n$ integer, one can ask whether the vibrational dark photons emitted by dark atoms could decay to $n$ ordinary photons having ordinary vibrational energy. The signature would be the appearance of a compound such as water in places where it is not thermally stable.

### 4.6 Free energy from atomic hydrogen

The anomalies reported by free energy researchers such as over unity energy production in devices involving repeated formation and dissociation of $H_2$ molecules based on the original discovery of Nobelist Irwing Langmuir [56] (see for instance [55]) suggest that part of $H$ atoms might end up to dark matter phase liberating energy.

An especially interesting device tested and described in detail by Naudin [55] is MAHG (Möller's Atomic Hydrogen Generator). The system behaves as an over-unity device producing energy from atomic hydrogen by a repeated dissociation and recombination of hydrogen atoms. MAHG tube contains a vacuum tube filled with hydrogen at 0.1 atm and cooled by water. The main part of the MAHG is a tungsten filament (0.25 mm diameter) placed in the center. Dissociation requires a heating of the tungsten filament to a temperature of about 2000 K.

A possible explanation of over-unity effect is inspired by the model of water as a partially dark matter in which one fourth of hydrogen atoms are in a dark phase forming linear super-nuclei with the distance between protons connected by color bonds being few Angstroms [F10]. The over-unity energy production could be due to a gradual transformation of hydrogen to dark hydrogen in the same state as in water. This transformation would

compete with recombination and be responsible for the over unity energy production even if the liberated energy is smaller than in recombination since the resulting dark hydrogen would not dissociate anymore. The process could not continue indefinitely since the amount of ordinary hydrogen would be gradually reduced.

Also the dropping of some hydrogen atoms to larger space-time sheets accompanied by liberation of zero point kinetic energy of order .5 eV could be involved and have similar implications since the heating (thermal energy is about .2 eV) is not quite enough to kick all dropped protons back to the atomic space-time sheets.

# 5 Appendix: A generalization of the notion of imbedding space inspired by hierarchy of Planck constants

The hypothesis that Planck constant is quantized having in principle all possible rational values but with some preferred values implying algebraically simple quantum phases has been one of the main ideas of TGD during last years. The mathematical realization of this idea leads to a profound generalization of the notion of imbedding space obtained by gluing together infinite number of copies of imbedding space along common 4-dimensional intersection. The hope was that this generalization could explain charge fractionization but this does not seem to be the case. This problem led to a further generalization of the imbedding space and this is what I want to discussed below.

## 5.1 The original view about generalized imbedding space

The original generalization of imbedding space was basically following. Take imbedding space $H = M^4 \times CP_2$. Choose submanifold $M^2 \times S^2$, where $S^2$ is homologically non-trivial geodesic sub-manifold of $CP_2$. The motivation is that for a given choice of Cartan algebra of Poincare algebra (translations in time direction and spin quantization axis plus rotations in plane orthogonal to this plane plus color hypercharge and isospin) this sub-manifold remains invariant under the transformations leaving the quantization axes invariant.

Form spaces $\hat{M}^4 = M^4 \backslash M^2$ and $\hat{CP}_2 = CP_2 \backslash S^2$ and their Cartesian product. Both spaces have a hole of co-dimension 2 so that the first homotopy group is $Z$. From these spaces one can construct an infinite hierarchy of factor spaces $\hat{M}^4/G_a$ and $\hat{CP}_2/G_b$, where $G_a$ is a discrete group of SU(2)

leaving quantization axis invariant. In case of Minkowski factor this means that the group in question acts essentially as a combination reflection and to rotations around quantization axes of angular momentum. The generalized imbedding space is obtained by gluing all these spaces together along $M^2 \times S^2$.

The hypothesis is that Planck constant is given by the ratio $\hbar/hbar_0 = (n_/n_b)$, where $n_i$ is the order of maximal cyclic subgroups of $G_i$. The hypothesis states also that the covariant metric of the Minkowski factor is scaled by the factor $(n_a/n_b)^2$. One must take care of this in the gluing procedure. One can assign to the field bodies describing both self interactions and interactions between physical systems definite sector of generalized imbedding space characterized partially by the Planck constant. The phase transitions changing Planck constant correspond to tunnelling between different sectors of the imbedding space.

## 5.2 Fractionization of quantum numbers is not possible if only factor spaces are allowed

The original idea was that the proposed modification of the imbedding space could explain naturally phenomena like quantum Hall effect involving fractionization of quantum numbers like spin and charge. This does not however seem to be the case. $G_a \times G_b$ implies just the opposite if these quantum numbers are assigned with the symmetries of the imbedding space. For instance, quantization unit for orbital angular momentum becomes $n_a$ where $Z_{n_a}$ is the maximal cyclic subgroup of $G_a$.

One can however imagine of obtaining fractionization at the level of imbedding space for space-time sheets, which are analogous to multi-sheeted Riemann surfaces (say Riemann surfaces associated with $z^{1/n}$ since the rotation by $2\pi$ understood as a homotopy of $M^4$ lifted to the space-time sheet is a non-closed curve. Continuity requirement indeed allows fractionization of the orbital quantum numbers and color in this kind of situation.

## 5.3 Both covering spaces and factor spaces are possible

The observation above stimulates the question whether it might be possible in some sense to replace $H$ or its factors by their multiple coverings.

a) This is certainly not possible for $M^4$, $CP_2$, or $H$ since their fundamental groups are trivial. On the other hand, the fixing of quantization axes implies a selection of the sub-space $H_4 = M^2 \times S^2 \subset M^4 \times CP_2$, where $S^2$ is a geodesic sphere of $CP_2$. $\hat{M}^4 = M^4 \backslash M^2$ and $\hat{CP}_2 = CP_2 \backslash S^2$ have funda-

mental group $Z$ since the codimension of the excluded sub-manifold is equal to two and homotopically the situation is like that for a punctured plane. The exclusion of these sub-manifolds defined by the choice of quantization axes could naturally give rise to the desired situation.

The observation above stimulates the question whether it might be possible in some sense to replace $H$ or its factors by their multiple coverings.

a) This is certainly not possible for $M^4$, $CP_2$, or $H$ since their fundamental groups are trivial. On the other hand, the fixing of quantization axes implies a selection of the sub-space $H_4 = M^2 \times S^2 \subset M^4 \times CP_2$, where $S^2$ is a geodesic sphere of $CP_2$. $\hat{M}^4 = M^4 \backslash M^2$ and $\hat{CP}_2 = CP_2 \backslash S^2$ have fundamental group $Z$ since the codimension of the excluded sub-manifold is equal to two and homotopically the situation is like that for a punctured plane. The exclusion of these sub-manifolds defined by the choice of quantization axes could naturally give rise to the desired situation.

b) There are two geodesic spheres in $CP_2$. Which one should choose or are both possible?

i) For the homologically non-trivial one corresponding to cosmic strings, the isometry group is $SU(2) \subset SU(3)$. The homologically trivial one $S^2$ corresponds to vacuum extremals and has isometry group $SO(3) \subset SU(3)$. The natural question is which one should choose. At quantum criticality the value of Planck constant is undetermined. The vacuum extremal would be a natural choice from the point of view of quantum criticality since in this case the value of Planck constant does not matter at all and one would obtain a direct connection with the vacuum degeneracy.

ii) The choice of the homologically non-trivial geodesic sphere as a quantum critical sub-manifold would conform with the previous guess that $\mathcal{M}$ : $\mathcal{N} = 4$ corresponds to cosmic strings. It is however questionable whether the ill-definedness of the Planck constant is consistent with the non-vacuum extremal property of cosmic strings unless one assumes that for partonic 3-surfaces $X^3 \subset M^2 \times S^2$ the effective degrees of freedom reduce to mere topological ones.

b) The covering spaces in question would correspond to the Cartesian products $\hat{M}^4{}_{n_a} \times \hat{CP}_{2n_b}$ of the covering spaces of $\hat{M}^4$ and $\hat{CP}_2$ by $Z_{n_a}$ and $Z_{n_b}$ with fundamental group is $Z_{n_a} \times Z_{n_b}$. One can also consider extension by replacing $M^2$ and $S^2$ with its orbit under $G_a$ (say tedrahedral, octahedral, or icosahedral group). The resulting space will be denoted by $\hat{M}^4 \hat{\times} G_a$ *resp.* $\hat{CP}_2 \hat{\times} G_b$.

c) One expects the discrete subgroups of $SU(2)$ emerge naturally in this framework if one allows the action of these groups on the singular

sub-manifolds $M^2$ or $S^2$. This would replace the singular manifold with a set of its rotated copies in the case that the subgroups have genuinely 3-dimensional action (the subgroups which corresponds to exceptional groups in the ADE correspondence). For instance, in the case of $M^2$ the quantization axes for angular momentum would be replaced by the set of quantization axes going through the vertices of tedrahedron, octahedron, or icosahedron. This would bring non-commutative homotopy groups into the picture in a natural manner.

d) Also the orbifolds $\hat{M}^4/G_a \times C\hat{P}_2/G_b$ can be allowed as also the spaces $\hat{M}^4/G_a \times (C\hat{P}_2 \hat{\times} G_b)$ and $(\hat{M}^4 \hat{\times} G_a) \times C\hat{P}_2/G_b$. Hence the previous framework would generalize considerably by the allowance of both coset spaces and covering spaces.

There are several non-trivial questions related to the details of the gluing procedure and phase transition as motion of partonic 2-surface from one sector of the imbedding space to another one.

a) How the gluing of copies of imbedding space at $M^2 \times CP_2$ takes place? It would seem that the covariant metric of $M^4$ factor proportional to $\hbar^2$ must be discontinuous at the singular manifold since only in this manner the idea about different scaling factor of $M^4$ metric can make sense. This is consistent with the identical vanishing of Chern-Simons action in $M^2 \times S^2$.

b) One might worry whether the phase transition changing Planck constant means an instantaneous change of the size of partonic 2-surface in $M^4$ degrees of freedom. This is not the case. Light-likeness in $M^2 \times S^2$ makes sense only for surfaces $X^1 \times D^2 \subset M^2 \times S^2$, where $X^1$ is light-like geodesic. The requirement that the partonic 2-surface $X^2$ moving from one sector of $H$ to another one is light-like at $M^2 \times S^2$ irrespective of the value of Planck constant requires that $X^2$ has single point of $M^2$ as $M^2$ projection. Hence no sudden change of the size $X^2$ occurs.

c) A natural question is whether the phase transition changing the value of Planck constant can occur purely classically or whether it is analogous to quantum tunnelling. Classical non-vacuum extremals of Chern-Simons action have two-dimensional $CP_2$ projection to homologically non-trivial geodesic sphere $S^2_I$. The deformation of the entire $S^2_I$ to homologically trivial geodesic sphere $S^2_{II}$ is not possible so that only combinations of partonic 2-surfaces with vanishing total homology charge (Kähler magnetic charge) can in principle move from sector to another one, and this process involves fusion of these 2-surfaces such that $CP_2$ projection becomes single homologically trivial 2-surface. A piece of a non-trivial geodesic sphere $S^2_I$ of $CP_2$ can be deformed to that of $S^2_{II}$ using 2-dimensional homotopy flattening the

piece of $S^2$ to curve. If this homotopy cannot be chosen to be light-like, the phase transitions changing Planck constant take place only via quantum tunnelling. Obviously the notions of light-like homotopies (cobordisms) and classical light-like homotopies (cobordisms) are very relevant for the understanding of phase transitions changing Planck constant.

## 5.4 Do factor spaces and coverings correspond to the two kinds of Jones inclusions?

What could be the interpretation of these two kinds of spaces?

a) Jones inclusions appear in two varieties corresponding to $\mathcal{M} : \mathcal{N} < 4$ and $\mathcal{M} : \mathcal{N} = 4$ and one can assign a hierarchy of subgroups of $SU(2)$ with both of them. In particular, their maximal Abelian subgroups $Z_n$ label these inclusions. The interpretation of $Z_n$ as invariance group is natural for $\mathcal{M} : \mathcal{N} < 4$ and it naturally corresponds to the coset spaces. For $\mathcal{M} : \mathcal{N} = 4$ the interpretation of $Z_n$ has remained open. Obviously the interpretation of $Z_n$ as the homology group defining covering would be natural.

b) $\mathcal{M} : \mathcal{N} = 4$ should correspond to the allowance of cosmic strings and other analogous objects. Does the introduction of the covering spaces bring in cosmic strings in some controlled manner? Formally the subgroup of $SU(2)$ defining the inclusion is $SU(2)$ would mean that states are $SU(2)$ singlets which is something non-physical. For covering spaces one would however obtain the degrees of freedom associated with the discrete fiber and the degrees of freedom in question would not disappear completely and would be characterized by the discrete subgroup of $SU(2)$.

For anyons the non-trivial homotopy of plane brings in non-trivial connection with a flat curvature and the non-trivial dynamics of topological QFTs. Also now one might expect similar non-trivial contribution to appear in the spinor connection of $\hat{M}^2 \hat{\times} G_a$ and $\hat{CP}_2 \hat{\times} G_b$. In conformal field theory models non-trivial monodromy would correspond to the presence of punctures in plane.

c) For factor spaces the unit for quantum numbers like orbital angular momentum is multiplied by $n_a$ *resp.* $n_b$ and for coverings it is divided by this number. These two kind of spaces are in a well defined sense obtained by multiplying and dividing the factors of $\hat{H}$ by $G_a$ *resp.* $G_b$ and multiplication and division are expected to relate to Jones inclusions with $\mathcal{M} : \mathcal{N} < 4$ and $\mathcal{M} : \mathcal{N} = 4$, which both are labelled by a subset of discrete subgroups of SU(2).

d) How do the Planck constants associated with factors and coverings relate? One might argue that Planck constant defines a homomorphism

respecting the multiplication and division (when possible) by $G_i$. If so, then Planck constant in units of $\hbar_0$ would be equal to $n_a/n_b$ for $\hat{H}/G_a \times G_b$ option and $n_b/n_a$ for $\hat{H}\hat{times}(G_a \times G_b)$ with obvious formulas for hybrid cases. This option would put $M^4$ and $CP_2$ in a very symmetric role and allow much more flexibility in the identification of symmetries associated with large Planck constant phases.

## References


[TGD] http://www.helsinki.fi/∼matpitka/tgdbooks.html. 7 books about TGD.

[TGDconsc] http://www.helsinki.fi/∼matpitka/conscbooks.html 8 books related to TGD inspired theory of consciousness and model of quantum biology.


## Online books about TGD


[1] M. Pitkänen (2006), *Topological Geometrodynamics: Overview.* http://www.helsinki.fi/∼matpitka/tgdview/tgdview.html.

[2] M. Pitkänen (2006), *Quantum Physics as Infinite-Dimensional Geometry.* http://www.helsinki.fi/∼matpitka/tgdgeom/tgdgeom.html.

[3] M. Pitkänen (2006), *Physics in Many-Sheeted Space-Time.* http://www.helsinki.fi/∼matpitka/tgdclass/tgdclass.html.

[4] M. Pitkänen (2006), *Quantum TGD.* http://www.helsinki.fi/∼matpitka/tgdquant/tgdquant.html.

[5] M. Pitkänen (2006), *TGD as a Generalized Number Theory.* http://www.helsinki.fi/∼matpitka/tgdnumber/tgdnumber.html.

[6] M. Pitkänen (2006), *p-Adic length Scale Hypothesis and Dark Matter Hierarchy.* http://www.helsinki.fi/∼matpitka/paddark/paddark.html.

[7] M. Pitkänen (2006), *TGD and Fringe Physics.* http://www.helsinki.fi/∼matpitka/freenergy/freenergy.html.

## Online books about TGD inspired theory of consciousness and quantum biology


[8] M. Pitkänen (2006), *Bio-Systems as Self-Organizing Quantum Systems*. http://www.helsinki.fi/∼matpitka/bioselforg/bioselforg.html.

[9] M. Pitkänen (2006), *Quantum Hardware of Living Matter*. http://www.helsinki.fi/∼matpitka/bioware/bioware.html.

[10] M. Pitkänen (2006), *TGD Inspired Theory of Consciousness*. http://www.helsinki.fi/∼matpitka/tgdconsc/tgdconsc.html.

[11] M. Pitkänen (2006), *Mathematical Aspects of Consciousness Theory*. http://www.helsinki.fi/∼matpitka/genememe/genememe.html.

[12] M. Pitkänen (2006), *TGD and EEG*. http://www.helsinki.fi/∼matpitka/tgdeeg/tgdeeg/tgdeeg.html.

[13] M. Pitkänen (2006), *Bio-Systems as Conscious Holograms*. http://www.helsinki.fi/∼matpitka/hologram/hologram.html.

[14] M. Pitkänen (2006), *Magnetospheric Consciousness*. http://www.helsinki.fi/∼matpitka/magnconsc/magnconsc.html.

[15] M. Pitkänen (2006), *Mathematical Aspects of Consciousness Theory*. http://www.helsinki.fi/∼matpitka/magnconsc/mathconsc.html.


## References to the chapters of books


[A1] The chapter *An Overview about the Evolution of Quantum TGD* of [1]. http://www.helsinki.fi/∼matpitka/tgdview/tgdview.html#evoI.

[A2] The chapter *An Overview about Quantum TGD* of [1]. http://www.helsinki.fi/∼matpitka/tgdview/tgdview.html#evoII.

[A8] The chapter *Was von Neumann Right After All* of [4]. http://www.helsinki.fi/∼matpitka/tgdview/tgdview.html#vNeumann.

[A9] The chapter *Does TGD Predict the Spectrum of Planck Constants?* of [1]. http://www.helsinki.fi/∼matpitka/tgdview/tgdview.html#Planck.

[B4] The chapter *Configuration Space Spinor Structure* of [2].
http://www.helsinki.fi/∼matpitka/tgdgeom/tgdgeom.html#cspin.

[C1] The chapter *Construction of Quantum Theory: Symmetries* of [4].
http://www.helsinki.fi/∼matpitka/tgdquant/tgdquant.html#quthe.

[C2] The chapter *Construction of Quantum Theory: S-matrix* of [4].
http://www.helsinki.fi/∼matpitka/tgdquant/tgdquant.html#towards.

[C3] The chapter *Hyper-Finite Factors and Construction of S-matrix* of [4].
http://www.helsinki.fi/∼matpitka/tgdquant/tgdquant.html#HFSmatrix.

[D4] The chapter *The Relationship Between TGD and GRT* of [3].
http://www.helsinki.fi/∼matpitka/tgdclass/tgdclass.html#tgdgrt.

[D5] The chapter *Cosmic Strings* of [3].
http://www.helsinki.fi/∼matpitka/tgdclass/tgdclass.html#cstrings.

[D6] The chapter *TGD and Cosmology* of [3].
http://www.helsinki.fi/∼matpitka/tgdclass/tgdclass.html#cosmo.

[D7] The chapter *TGD and Astrophysics* of [3].
http://www.helsinki.fi/∼matpitka/tgdclass/tgdclass.html#astro.

[D8] The chapter *Quantum Astrophysics* of [3].
http://www.helsinki.fi/∼matpitka/tgdclass/tgdclass.html#qastro.

[E1] The chapter *TGD as a Generalized Number Theory: p-Adicization Program* of [5].
http://www.helsinki.fi/∼matpitka/tgdnumber/tgdnumber.html#visiona.

[E9] The chapter *Topological Quantum Computation in TGD Universe* of [5].
http://www.helsinki.fi/∼matpitka/tgdnumber/tgdnumber.html#tqc.

[F1] The chapter *Elementary Particle Vacuum Functionals* of [6].
http://www.helsinki.fi/∼matpitka/paddark/paddark.html#elvafu.

[F2] The chapter *Massless States and Particle Massivation* of [6].
http://www.helsinki.fi/∼matpitka/paddark/paddark.html#mless.

[F3] The chapter *p-Adic Particle Massivation: Elementary particle Masses* of [6].
http://www.helsinki.fi/∼matpitka/paddark/paddark.html#padmass2.

[F4] The chapter *p-Adic Particle Massivation: Hadron Masses* of [6].
http://www.helsinki.fi/∼matpitka/paddark/paddark.html#padmass3.

[F5] The chapter *p-Adic Particle Massivation: New Physics* of [6].
http://www.helsinki.fi/∼matpitka/paddark/paddark.html#padmass4.

[F9] The chapter *Nuclear String Physics* of [6].
http://www.helsinki.fi/∼matpitka/paddark/paddark.html#nuclstring.

[F10] The chapter *Dark Nuclear Physics and Condensed Matter* of [6].
http://www.helsinki.fi/∼matpitka/paddark/paddark.html#exonuclear.

[G2] The chapter *The Notion of Free Energy and Many-Sheeted Space-Time Concept* of [7].
http://www.helsinki.fi/∼matpitka/freenergy/freenergy.html#freenergy.

[G3] The chapter *About Strange Effects Related to Rotating Magnetic Systems* of [7].
http://www.helsinki.fi/∼matpitka/freenergy/freenergy.html#Faraday.

[G4] The chapter *Did Tesla Discover the Mechanism Changing the Arrow of Time?* of [7].
http://www.helsinki.fi/∼matpitka/freenergy/freenergy.html#tesla.

[H1] The chapter *Matter, Mind, Quantum* of [10].
http://www.helsinki.fi/∼matpitka/tgdconsc/tgdconsc.html#conscic.

[H2] The chapter *Negentropy Maximization Principle* of [10].
http://www.helsinki.fi/∼matpitka/tgdconsc/tgdconsc.html#nmpc.

[H5] The chapter *New Developments in TGD and Their Implications for TGD Inspired Theory of Consciousness*
http://www.helsinki.fi/∼matpitka/tgdconsc/tgdconsc.html#conscupdate.

[H6] The chapter *Quantum Model of Memory* of [10].
http://www.helsinki.fi/∼matpitka/tgdconsc/tgdconsc.html#memoryc.

[H8] The chapter *p-Adic Physics as Physics of Cognition and Intention* of [10].
http://www.helsinki.fi/∼matpitka/tgdconsc/tgdconsc.html#cognic.

[H9] The chapter *Quantum Model for Paranormal Phenomena* of [10].
http://www.helsinki.fi/∼matpitka/tgdconsc/tgdconsc.html#parac.

[H10] The chapter *TGD Based Model for OBEs* of [10].
http://www.helsinki.fi/∼matpitka/tgdconsc/tgdconsc.html#OBE.

[J1] The chapter *Bio-Systems as Super-Conductors: part I* of [9].
http://www.helsinki.fi/∼matpitka/bioware/bioware.html#superc1.

[J2] The chapter *Bio-Systems as Super-Conductors: part II* of [9].
http://www.helsinki.fi/∼matpitka/bioware/bioware.html#superc2.

[J3] The chapter *Bio-Systems as Super-Conductors: part III* of [9].
http://www.helsinki.fi/∼matpitka/bioware/bioware.html#superc3.

[J7] The chapter *About the New Physics Behind Qualia* of [9].
http://www.helsinki.fi/∼matpitka/bioware/bioware.html#newphys.

[K1] The chapter *Time, Spacetime and Consciousness* of [13].
http://www.helsinki.fi/∼matpitka/hologram/hologram.html#time.

[K5] The chapter *Homeopathy in Many-Sheeted Space-Time* of [13].
http://www.helsinki.fi/∼matpitka/hologram/hologram.html#homeoc.

[K6] The chapter *Macroscopic Quantum Coherence and Quantum Metabolism as Different Sides of the Same Coin* of [13].
http://www.helsinki.fi/∼matpitka/hologram/hologram.html#metab.

[L1] The chapter *Genes and Memes* of [11].
http://www.helsinki.fi/∼matpitka/genememe/genememe.html#genememec.

[M1] The chapter *Magnetic Sensory Canvas Hypothesis* of [12].
http://www.helsinki.fi/∼matpitka/tgdeeg/tgdeeg/tgdeeg.html#mec.

[M3] The chapter *Dark Matter Hierarchy and Hierarchy of EEGs* of [12].
http://www.helsinki.fi/∼matpitka/tgdeeg/tgdeeg/tgdeeg.html#eegdark.

[M4] The chapter *Quantum Model for EEG: Part I* of [12].
http://www.helsinki.fi/∼matpitka/tgdeeg/tgdeeg/tgdeeg.html#eegI.

[N1] The chapter *Magnetospheric Sensory Representations* of [14].
http://www.helsinki.fi/∼matpitka/magnconsc/magnconsc.html#srepres.

[N4] The chapter *Pre-Biotic Evolution in Many-Sheeted Space-Time* of [14].
http://www.helsinki.fi/∼matpitka/magnconsc/magnconsc.html#prebio.

## Brain science

[16] Blackman, C. F., Benane, S. G., Kinney, L. S., House, D. E., and Joines, W. T., (1982), "Effects of ELF fields on calcium-ion efflux from brain tissue, in vitro", Radiat. Res. 92:510-520.

[17] B. Libet, E. W. Wright Jr., B. Feinstein, and D. K. Pearl (1979), "Subjective referral of the timing for a conscious sensory experience", Brain, 102, 193-224.

[18] Libet, B., Gleason, C.A., Wright, E.W., Pearl, D.K. (1983). Time of conscious intention to act in relation to onset of cerebral activity (readiness-potential). The unconscious initiation of a freely voluntary act. Brain. 106 (3):623642.

[19] P. L. Nunez (2000), *Toward a Quantitative Description of Large Scale Neocortical Dynamic Function and EEG*, Behavioral and Brain Sciences, 23, (3): XX. http://www.bbsonline.org/documents/a/00/00/05/08/.

[20] http://en.wikipedia.org/wiki/Michael_Persinger.

## Biology

[21] *Nannobacteria*, http://en.wikipedia.org/wiki/Nannobacteria.

[22] G. Pollack (2000),"Cells, Gels and the Engines of Life", Ebner and Sons.
http://www.cellsandgels.com/ .

[23] P. P. Gariaev *et al*(2002), *The spectroscopy of bio-photons in non-local genetic regulation*, Journal of Non-Locality and Remote Mental Interactions, Vol 1, Nr 3.
http://www.emergentmind.org/gariaevI3.htm .

[24] L. Fantappie (1942), *Teoria Unitaria del Mondo Fisico e Biologico*, Di Renzo Editore, Roma, 1991.

[25] A. Vannini(2007), *Advanced Waves, Retrocausality, and Consciousness* in *The* $7^{th}$ *European SSE Meeting August 17-19, 2007, Röros, Norway. Proceedings*. http://www.scientificexploration.org/.

[26] U. Di Corpo (2007), *The conflict between entropy and syntropy: the vital needs model* in *The* $7^{th}$ *European SSE Meeting August 17-19, 2007, Röros, Norway. Proceedings*. http://www.scientificexploration.org/.

[27] *Photosynthesis*, http://en.wikipedia.org/wiki/Photosynthesis.

[28] *Photolysis*, http://en.wikipedia.org/wiki/Photolysis.

[29] *Photocatalysis*, http://en.wikipedia.org/wiki/Photocatalysis.

## Astrophysics

[30] *Plasma sheet and PSBL*, http://www.oulu.fi/∼spaceweb/textbook/plasma_sheet.html.

[31] *Interstellar Dust as Agent and Subject of Galactic Evolution*, http://www.ricercaitaliana.it/prin/dettaglio_completo_prin_en-2005022470.htm.

[32] *Diffuse interstellar bands*, http://en.wikipedia.org/wiki/Diffuse_interstellar_band.

[33] Uma P. Vihj(2004), *Extended Red Emission*, http://ardbeg.astro.utoledo.edu/∼karen/baglunch/vijh_abl_spr04.pdf.

[34] *From the stars to the thought*, http://www.brunonic.org/Nicolaus/fromthestarstot.htm.

[35] L. J. Allamandola, M. P. Bernstein, S.A. Sandford (1997), in *Astronomical and biochemical origins and the search for life in the universe*, Ed. CB Cosmovici, S. Bowyer, D. Wertheimer, pp. 23-47, Editrice Compositori, Bologna.

[36] P. Carlquist, G. F. Gahm, and H. Kristen (2003), *Theory of twisted trunks*, http://www.aanda.org/articles/aa/abs/2003/20/aa3289/aa3289.html.

[37] http://en.wikipedia.org/wiki/Diffuse_interstellar_band and http://www.brunonic.org/Nicolaus/fromthestarstot.htm.

[38] http://en.wikipedia.org/wiki/Dark_matter.

[39] http://en.wikipedia.org/wiki/Cosmological_constant.

[40] http://en.wikipedia.org/wiki/Nottale.

[41] http://en.wikipedia.org/wiki/Saturn.

[42] http://en.wikipedia.org/wiki/Rings_of_Saturn.

[43] *Exoplanets*, http://en.wikipedia.org/wiki/Exoplanets.

[44] *Mars*,http://en.wikipedia.org/wiki/ALH84001.

## Anomalies

[45] E. Lozneanu and M. Sanduloviciu (2003), "Minimal-cell system created in laboratory by self-organization", Chaos, Solitons & Fractals, Volume 18, Issue 2, October, p. 335. See also "Plasma blobs hint at new form of life", New Scientist vol. 179 issue 2413 - 20 September 2003, page 16.

[46] B. Tsytovich *et al* (2007), *From Plasma crystals and helical structures towards inorganic living matter*, New Journal of Physics, August issue. http://www.iop.org/EJ/abstract/1367-2630/9/8/263.

[47] http://www.timesonline.co.uk/tol/news/uk/article2241753.ece.

[48] Björn Gitle-Hauge (2007), *Optical spectrum analysis of the Hessdalen phenomenon* in "The $7^{th}$ European SSE Meeting, August 17-19, 2007, Röros, Norway. Proceedings".

[49] "The Toppenish Field Study. A Technical Review and Update". The 7:th European SSE Meeting August 17-19, 2007, Rros, Norway.

[50] M. Pitkänen (2007), *TGD based solution of Fermi paradox*, http://www.physics.helsinki.fi/ matpitka/articles/fermieng.pdf.

[51] S. E. Shnoll et al (1998), *Realization of discrete states during fluctuations in macroscopic processes*, Uspekhi Fisicheskikh Nauk, Vol. 41, No. 10, pp. 1025-1035.

[52] *Allais effect*, http://en.wikipedia.org/wiki/Allais_effect.

[53] http://www.youtube.com/watch?v=h6vSxR6UKFM.

[54] N. Tesla(1894), *Coil for Electromagnets*, US Patent No. 512,340. The patent of the bi-filar coil can be found at http://www.tfcbooks.com/patents/coil.htm .
A brief summary of Tesla's vision can be found at http://solair.eunet.yu/∼velimir/works/teslaint.htm.

[55] J. Naudin (2005), *Free Energy Atomic Hydrogen: the MAHG project*, http://jlnlabs.imars.com/mahg/tests/index.htm.

[56] I. Langmuir (1915), em The Dissociation of Hydrogen Into Atoms, Journal of American Chemical Society 37, 417.

[57] P. Kanarev (2002) *Water is New Source of Energy*, Krasnodar.

[58] S. Meyer (1996) *Water Fuel Cell*, International News Release, Issue No. 11A-Rv.
S. Meyer (1990) *Method for Production of A Fuel Gas*, US Patent 4,936,961.

[59] H. Puthoff (1987), *Ground State of Hydrogen as a Zero-Point Fuctuation Determined State*, Phys. Rev. D 35, 10.

[60] R. Mills *et al*(2003), *Spectroscopic and NMR identification of novel hybrid ions in fractional quantum energy states formed by an exothermic reaction of atomic hydrogen with certain catalysts.*
http://www.blacklightpower.com/techpapers.html .

[61] Roshchin, V.V and Godin, S.M., *An Experimental Investigation of the Physical Effects in a Dynamic Magnetic System*, New Energy Technologies Issue #1 July-August 2001.

# Prediction and Calculation for New Energy Development

Fu Yuhua[1] & Fu Anjie[2]

1. China Offshore Oil Research Center, Beijing, 100027, China;
2. Microsoft Research Asia, Beijing, 100080, China

Abstract: This paper discusses some important questions for new energy development, such as the prediction and calculation of sea surface temperature, ocean wave, offshore platform price, typhoon track, fire status, vibration due to earthquake, energy price, stock market's trend and so on with the fractal methods (including the four ones of constant dimension fractal, variable dimension fractal, complex number dimension fractal and fractal series) and the improved rescaled range analysis (R/S analysis).

Key words: New energy, development, prediction, fractal method, rescaled range analysis (R/S analysis)

## 1 Introduction

The various kind of energy development, especially the new energy development, will face many factors of uncertainty. If we can make the correct prediction and calculation to these factors in advance, then a great profit would be made.

For example, regarding the sea water thermoelectric generation, to predict the sea surface temperature is required; Moreover, in order to develop the rich new energy contained in the seabed, the offshore platform should be constructed, it needs to carry on the prediction and calculation to the platform price; For the wind power generation, it needs to predict the gale way, in order to temporarily build more generators at the suitable place. Regarding ocean waves electricity generation, it needs precisely to calculate the movement of ocean waves.

Let's suppose in the near future the natural disaster energy may be used, then we need to make the prediction and calculation to the fire, vibration due to earthquake and so on.

Finally, for the new energy companies coming into the market, they certainly want to know the new energy price as well as the stock market's trend.

This paper applies the fractal methods and the improved rescaled range analysis (R/S analysis) to process these questions.

## 2 Constant and variable dimension fractal prediction methods in common use and their application

Recently, fractal method has been successful used in many fields; it is used for opening out the deeply hidden organized structure in the complex phenomenon. The quantity for reflecting the character of organized structure is called the fractal dimension, expressed with the value of $D$. In the fractal methods for general application at present, the fractal dimension $D$ is a constant, for example the values of fractal dimension $D$ for different coastlines may be taken as 1.02, 1.25 and so on. The fractal model[1] reads

$$N = \frac{C}{r^D} \tag{1}$$

where: $r$ is the characteristic scale, such as time, length, coordinates and so on; $N$ is

the object number or quantity related with the value of $r$, such as output, price, temperature, the value to be predicted and so on; $C$ is a constant to be determined, $D$ is the fractal dimension.

In the general application of fractal method at present, $D$ is the constant, this kind of fractal may be called constant dimension fractal. It is a straight line in the double logarithmic coordinates. According to arbitrary two data points $(N_i, r_i)$ and $(N_j, r_j)$ on this straight line, the fractal parameters of this straight line, i.e., the fractal dimension $D_{ij}$ and the constant $C_{ij}$, can be determined; in fact, substituting the coordinates of the two data points into Eq.(1), they can be solved

$$D_{ij} = \frac{\ln(N_i / N_j)}{\ln(r_j / r_i)} \tag{2}$$

$$C_{ij} = N_i r_i^{D_{ij}} \tag{3}$$

For the straight line functional relation in the double logarithmic coordinates, it is able to process the prediction and calculation with the constant dimension fractal directly.

But for the *non-straight line* functional relation in the double logarithmic coordinates, it is unable to process the prediction and calculation with the constant dimension fractal. Many questions are belonging to this situation. In order to overcome this difficulty, we introduced the concept of variable dimension fractal in references [2] ~ [4], namely the fractal dimension $D$ is the function of characteristic scale $r$.

$$D = F(r) \tag{4}$$

Now we discuss how to carry on the prediction and calculation with this fractal model.

For the sake of convenience, let $r$ denote the serial number of time, for example, it will stipulate some year for the first year, then we have $r_1 = 1$, for the second year, $r_2 = 2$, and so on. Let $N$ denote the given value and the value to be predicted, for example, taking $N_1$ as the value of the first year, $N_2$ as the value of the second year, and so on.

Now supposing that $n$ data points are given, i.e., the values for the first year to the $n$th year are known, thereupon the question becomes how to predict the values for the $(n+1)$th year, $(n+2)$th year and so on.

As a result of the $n$th data point, namely the values of $N_n$ and $r_n$ for the $n$th year are given $(r_n = n)$, and the value of $r_{n+1}$ for $(n+1)$th year is also known $(r_{n+1} = n+1)$, if the fractal dimension $D_{n,n+1}$ of the constant dimension fractal decided by the $n$th data point and $(n+1)$th data point is known, then the value for the $(n+1)$th year can be solved from Eq.(2)

$$N_{n+1} = N_n(\frac{r_n}{r_{n+1}})^{D_{n,n+1}} \tag{5}$$

To this analogizes, the values for the $(n+2)$th year and the like can be solved.

As for how to decide the fractal dimension $D_{n,n+1}$, it needs the information given by $D_{12}$ (decided by the given first data point and second data point), $D_{23}\cdots D_{n-1,n}$ (decided by other given data points). But in general case, it is very difficult to discover the changing rule for these values of fractal dimension.

In this case, we cannot directly apply the above method. We have to carry on the transformation of accumulated sum for the given values firstly, then the above method can be used to forecast the values of accumulated sum for the $(n+1)$th year, $(n+2)$th year and so on. Finally the values to be predicted are solved by the values of accumulated sum.

The advantage for using accumulated sum is that a sequence with increasing and decreasing can be changed into a monotone increasing sequence.

This method may be introduced as follows.

The first step, plotting the original data points $(N_i, r_i)(i = 1 \sim n)$ in the double-logarithmic coordinates, in the ordinary circumstances they cannot fairly good agree with a constant dimension fractal model, thereupon $N_i$ $(i = 1,2\cdots n)$ may be arranged to a fundamental sequence, namely it can be written as

$$\{N_i\} = \{N_1, N_2, N_3\cdots\} \quad (i = 1,2\cdots n)$$

Other sequences may be constructed according to the fundamental sequence. For example, for $S^{(1)}$, i.e., the sequence of first order accumulated sum, $S_1^{(1)} = N_1$, $S_2^{(1)} = N_1 + N_2$, $S_3^{(1)} = N_1 + N_2 + N_3$, and so on; according to analogize, the sequence of second order accumulated sum, the sequence of third order accumulated sum, and the like can be constructed, namely it can be written as

$$\{S_i^{(1)}\} = \{N_1, N_1 + N_2, N_1 + N_2 + N_3,\cdots\} \quad (i = 1,2\cdots n) \tag{6}$$

$$\{S_i^{(2)}\} = \{S_1^{(1)}, S_1^{(1)} + S_2^{(1)}, S_1^{(1)} + S_2^{(1)} + S_3^{(1)}\cdots\} \quad (i = 1,2\cdots n) \tag{7}$$

$$\{S_i^{(3)}\} = \{S_1^{(2)}, S_1^{(2)} + S_2^{(2)}, S_1^{(2)} + S_2^{(2)} + S_3^{(2)}\cdots\} \quad (i = 1,2\cdots n)$$

$$\{S_i^{(4)}\} = \{S_1^{(3)}, S_1^{(3)} + S_2^{(3)}, S_1^{(3)} + S_2^{(3)} + S_3^{(3)}\cdots\} \quad (i = 1,2\cdots n)$$

It needs to point out that $S_i^{(2)}$ denote second order accumulated sum, instead of the second power of $S_i$. $S_i^{(3)}$ and the like should be comprehended similarly.

The second step, establishing the fractal models for various order accumulated sum. Taking the second order accumulated sum as an example. Plotting the data points $(S_i^{(2)}, r_i)(i = 1 \sim n)$ in the doublelogarithmic coordinates, linking these points one by one it may result in the sectioned constant dimension fractal model. For example, according to $n$ data points, the sectioned constant dimension fractal model composed from $n-1$ straight lines (for different straight line, its fractal dimension is also different, this also is the simplest variable dimension fractal model), the fractal parameters $D_{ij}^{(2)}, (i = 1 \sim n-1, j = i+1)$ and $C_{ij}^{(2)}$ for each straight line, can be calculated according to Eqs.(2) and (3) (in which the value of $N_i$ is replaced by $S_i^{(2)}$). Which means

$$D_{ij}^{(2)} = \ln(S_i^{(2)} / S_j^{(2)}) / \ln(r_j / r_i) \tag{8}$$

$$C_{ij}^{(2)} = S_i^{(2)} r_i^{D_{ij}^{(2)}} \tag{9}$$

The third step, choosing the best transformation and determining its corresponding fractal parameters.

Separately drawing various order accumulated sum's data points in the double logarithmic coordinates, then choosing the best transformation (its values of fractal dimension are even increased or even decreased) and determining its corresponding fractal parameters.

Because in the ordinary circumstances, the second order accumulated sum is the best, we shall only discuss the case of second order accumulated sum.

After choosing the fractal model, the suitable method should be used for deciding the fractal dimension $D_{n,n+1}^{(2)}$ firstly, then uses the reconstructive Eq.(5) to carry on the forecast for accumulated sum. Because the values of fractal dimension are even increased or even decreased, using the following linear interpolation formula can solve the fractal dimension $D_{n,n+1}^{(2)}$

$$D_{n,n+1}^{(2)} = 2D_{n-1,n}^{(2)} - D_{n-2,n-1}^{(2)} \tag{10}$$

For the second order accumulated sum, Eq.(5) expressed by

$$S_{n+1}^{(2)} = S_n^{(2)} \left(\frac{r_n}{r_{n+1}}\right)^{D_{n,n+1}^{(2)}} \tag{11}$$

For the reason that $S_1^{(1)} \sim S_n^{(1)}$ $S_1^{(2)} \sim S_n^{(2)}$ are already calculated, then the forecasting first order accumulated sum can be obtained from the forecasted second order accumulated sum, which means

$$S_{n+1}^{(1)} = S_{n+1}^{(2)} - S_n^{(2)} \tag{12}$$

Then the forecasting value can be obtained from the forecasted first order

accumulated sum, which means

$$N_{n+1} = S_{n+1}^{(1)} - S_n^{(1)} \tag{13}$$

According to analogize similarly, $N_{n+2}$ , $N_{n+3}$ and so on can be obtained.

It should be noted that, for some special questions, we need to carry on some necessary adjustments to the above-mentioned general fractal methods. For example, some transformation processing should be made to the given data in advance.

Now we present some prediction and calculation examples.

Example 1, until 08 o'clock, July 20, 1980, the tracks of No. 8007 typhoon (JOE) are given in table 1 (the time interval is 6 hours), try to predict its future tracks. This example is taken from the reference [ 5 ].

**Table1. the given tracks of No. 8007 typhoon**

| No. | time(M D H) | north latitude | east longitude |
|---|---|---|---|
| 1 | 7 16 14 | 10.0 | 147.0 |
| 2 | 20 | 11.0 | 146.0 |
| 3 | 17 02 | 12.0 | 145.0 |
| 4 | 08 | 12.7 | 143.8 |
| 5 | 14 | 12.3 | 143.2 |
| 6 | 20 | 12.5 | 142.0 |
| 7 | 18 02 | 13.1 | 140.2 |
| 8 | 08 | 13.5 | 138.9 |
| 9 | 14 | 14.0 | 137.5 |
| 10 | 20 | 14.2 | 136.2 |
| 11 | 19 02 | 14.3 | 134.7 |
| 12 | 08 | 14.7 | 133.1 |
| 13 | 14 | 15.0 | 131.7 |
| 14 | 20 | 15.2 | 130.1 |
| 15 | 20 02 | 15.7 | 128.1 |
| 16 | 08 | 16.1 | 126.7 |

With the above-mentioned fractal prediction method, the future latitudes and longitudes may be obtained respectively.

All the prediction results of this paper, the real vales and the prediction results in reference [ 6 ] are shown in Table 2 and table 3.

**Table2. prediction result for the latitudes of No. 8007 typhoon**

| No. | time (M D H) | real value | this paper | reference [6] |
|---|---|---|---|---|
| 17 | 7 20 14 | 16.3 | 16.4 | |
| 18 | 20 | 16.4 | 16.7 | 17.0 |
| 19 | 21 02 | 17.1 | 17.1 | |
| 20 | 08 | 17.4 | 17.4 | 18.2 |
| 21 | 14 | 18.1 | 17.8 | |
| 22 | 20 | 18.7 | 18.1 | 19.2 |
| 23 | 22 02 | 19.1 | 18.5 | |
| 24 | 08 | 19.5 | 18.8 | 20.0 |
| 25 | 14 | 20.1 | 19.2 | |
| 26 | 20 | 20.2 | 19.5 | |
| 27 | 23 02 | 20.4 | 19.9 | |
| 28 | 08 | 20.9 | 20.3 | |
| 29 | 14 | 20.9 | 20.6 | |
| 30 | 20 | 20.5 | 21.0 | |

**Table3. prediction result for the longitudes of No. 8007 typhoon**

| No. | time (M D H) | real value | this paper | reference [6] |
|---|---|---|---|---|
| 17 | 7 20 14 | 125.3 | 125.3 | |
| 18 | 20 | 123.8 | 123.8 | 123.6 |
| 19 | 21 02 | 122.1 | 122.4 | |
| 20 | 08 | 120.8 | 121.0 | 120.9 |
| 21 | 14 | 119.0 | 119.6 | |
| 22 | 20 | 117.2 | 118.2 | 118.4 |
| 23 | 22 02 | 115.3 | 116.8 | |
| 24 | 08 | 113.6 | 115.5 | 116.0 |
| 25 | 14 | 112.2 | 114.1 | |
| 26 | 20 | 110.3 | 112.8 | |
| 27 | 23 02 | 108.4 | 111.4 | |
| 28 | 08 | 106.7 | 110.1 | |
| 29 | 14 | 105.3 | 108.9 | |
| 30 | 20 | 103.0 | 107.5 | |

From the results of Table 2 and Table 3 we can see that, although the result of longitudes is not so good, but generally speaking the prediction results of this paper are satisfying.

Example 2, predict the platform price of Gulf of Mexico. This example is taken from the reference [ 7 ].

Because the platform price of Gulf of Mexico cannot be predicted with the fractal method directly, therefore we must to carry on the following transformation to water depth $r$ and platform price $N$ firstly.

$$r' = ar + b$$

$$N' = AN + B$$

From this transformation, the platform price prediction formula can be obtained as in the following form:

$$N = \frac{C^*}{(b - r)^{D^*}} - B - B'$$

As water depth $r$ =400ft, we may obtain the corresponding platform price $N$ =16.7884 x $10^6$ US dollars, to compare with the actual value 16.5 x $10^6$ US dollars, the error is only 1.7%.

Example 3, predict the monthly average sea surface temperature. This example is taken from the reference [ 8 ].

Based on sectional variable dimension fractals, we present concept of weighted fractals, i.e., for the data points in an interval, their $r$ coordinates multiply by different weighted coefficients, and making these data points locate at a straight-line in the double logarithmic coordinates. By using weighted fractals, the monthly average sea surface temperature (MASST) data on the point 30ºN, 125ºE of Northwest Pacific Ocean are analyzed. According to the MASST from January to August in a certain year, the MASST from September to December of that year has been predicted by using eight-point-method.

According to the MASST of August merely in a certain year, the MASST from September to December of that year has been predicted by using one-point-method.

The MASST prediction results are as follows.

**Table4. MASST prediction results by using eight-point-method (8PM) and one-point-method(1PM)**

| Year | Notes | September | October | November | December |
|---|---|---|---|---|---|
| 1958 | 8PM | 28.21 | 25.51 | 22.67 | 20.17 |
| | 1PM | 28.24 | 25.55 | 22.72 | 20.22 |
| | Real value | 27.7 | 25.5 | 21.2 | 20 |
| 1959 | 8PM | 28.20 | 25.56 | 22.75 | 20.28 |
| | 1PM | 28.19 | 25.54 | 22.73 | 20.26 |
| | Real value | 27.6 | 24.7 | 22.9 | 20 |
| 1960 | 8PM | 27.95 | 25.36 | 22.60 | 20.16 |
| | 1PM | 28.05 | 25.51 | 22.78 | 20.36 |
| | Real value | 28 | 26 | 21.8 | 20 |
| 1961 | 8PM | 28.70 | 26.14 | 23.37 | 20.91 |
| | 1PM | 28.34 | 25.57 | 22.69 | 20.16 |
| | Real value | 28.4 | 26.2 | 22.8 | 22 |
| 1962 | 8PM | 28.30 | 26.00 | 23.46 | 21.17 |
| | 1PM | 27.90 | 25.48 | 22.83 | 20.47 |
| | Real value | 28 | 25 | 21 | 20 |
| 1963 | 8PM | 29.36 | 27.86 | 25.78 | 23.80 |
| | 1PM | 27.86 | 25.47 | 22.85 | 20.50 |
| | Real value | 27.5 | 24.5 | 21 | 18 |
| 1964 | 8PM | 28.04 | 25.83 | 23.32 | 21.05 |
| | 1PM | 27.80 | 25.46 | 22.86 | 20.54 |
| | Real value | 28 | 24.5 | 22 | 19 |

In addition, according to the phenomenon of fractal interrelation and the fractal coefficients of this point's MASST and the monthly average air temperature of August of some points, the monthly average air temperature of these points from September to December has been also predicted

Example 4. predict the stock index with variable dimension fractal.

From November 1, 2000 to February 7, 2001, the program "Daily Finance and Economics" of Beijing wired television station conducted the competition of stock index prediction. Before 13 o'clock of every business day, the participants were requested to deliver their predictions for the closing index of the same day to the television station with the telephone, 2 winners of the first prize (one for Shanghai market, another for Shenzhen market), 8 winners of the second prize and 10 winners of the third prize were awarded every day. We obtained the news on November 17 and began to participate. Until the competition end on February 7, 2001, we won the first prize two times (one for Shanghai

market, another for Shenzhen market), the second prize two times and the third prize seven times.

The prediction results of the stock index of Shanghai market are as follows.

**Table 5. prediction results of the stock index of Shanghai market.1A0001**

| No. | Date | Prediction | Real value | Error | Award |
|---|---|---|---|---|---|
| 1 | Nov. 16, 2000 | 2087.87 | 2095.98 | -8.11 | |
| 2 | Nov. 17, 2000 | 2104.99 | 2093.23 | 11.76 | |
| 3 | Nov. 20, 2000 | 2103.48 | 2101.38 | 2.10 | third prize |
| 4 | Nov. 21, 2000 | 2115.14 | 2097.98 | 17.16 | |
| 5 | Nov. 22, 2000 | 2109.29 | 2113.30 | -4.01 | |
| 6 | Nov. 23, 2000 | 2125.61 | 2119.43 | 6.18 | |
| 7 | Nov. 24, 2000 | 2131.43 | 2053.37 | 78.06 | |
| 8 | Nov. 27, 2000 | 2048.50 | 2049.67 | -1.17 | third prize |
| 9 | Nov. 28, 2000 | 2071.23 | 2079.39 | -8.16 | |
| 10 | Nov. 29, 2000 | 2082.63 | 2067.49 | 15.14 | |
| 11 | Nov. 30, 2000 | 2063.54 | 2070.61 | -7.07 | |
| 12 | Dec. 1, 2000 | 2082.96 | 2081.84 | 1.12 | |
| 13 | Dec. 4, 2000 | 2092.32 | 2092.13 | 0.19 | second prize |
| 14 | Dec. 5, 2000 | 2099.49 | 2091.66 | 7.83 | |
| 15 | Dec. 6, 2000 | 2095.93 | 2075.62 | 20.31 | |
| 16 | Dec. 7, 2000 | 2065.51 | 2075.04 | -9.53 | |
| 17 | Dec. 8, 2000 | 2085.09 | 2073.16 | 11.93 | |
| 18 | Dec. 11, 2000 | 2044.21 | 2046.07 | -1.86 | third prize |
| 19 | Dec. 12, 2000 | 2047.74 | 2059.05 | -11.31 | |
| 20 | Dec. 13, 2000 | 2057.62 | 2056.12 | 1.50 | |
| 21 | Dec. 14, 2000 | 2055.93 | 2051.07 | 4.86 | |
| 22 | Dec. 15, 2000 | 2041.31 | 2039.36 | 1.95 | |
| 23 | Dec. 18, 2000 | 2026.44 | 2044.54 | -18.10 | |
| 24 | Dec. 19, 2000 | 2052.43 | 2049.03 | 3.40 | |
| 25 | Dec. 20, 2000 | 2058.43 | 2071.26 | -12.83 | |
| 26 | Dec. 21, 2000 | 2084.98 | 2076.89 | 8.09 | |
| 27 | Dec. 22, 2000 | 2079.10 | 2069.77 | 9.33 | |
| 28 | Dec. 25, 2000 | 2071.63 | 2068.17 | 3.46 | |
| 29 | Dec. 26, 2000 | 2075.03 | 2076.26 | -1.23 | |
| 30 | Dec. 27, 2000 | 2070.66 | 2058.24 | 12.42 | |
| 31 | Dec. 28, 2000 | 2057.65 | 2053.70 | 3.95 | |
| 32 | Dec. 29, 2000 | 2070.41 | 2073.47 | -3.06 | |
| 33 | Jan. 2, 2001 | 2095.00 | 2103.46 | -8.46 | |
| 34 | Jan. 3, 2001 | 2121.09 | 2123.89 | -2.80 | |
| 35 | Jan. 4, 2001 | 2123.90 | 2117.40 | 6.50 | |
| 36 | Jan. 5, 2001 | 2125.34 | 2125.30 | 0.04 | first prize |
| 37 | Jan. 8, 2001 | 2108.06 | 2102.06 | 6.00 | |
| 38 | Jan. 9, 2001 | 2098.75 | 2101.13 | -2.38 | |
| 39 | Jan. 10, 2001 | 2120.91 | 2125.61 | -4.70 | |
| 40 | Jan. 11, 2001 | 2132.74 | 2119.14 | 13.60 | |
| 41 | Jan. 12, 2001 | 2106.41 | 2104.74 | 1.67 | |
| 42 | Jan. 15, 2001 | 2054.82 | 2032.44 | 22.38 | |
| 43 | Jan. 16, 2001 | 2003.01 | 2006.88 | -3.87 | |
| 44 | Jan. 17, 2001 | 2035.48 | 2034.58 | 0.90 | |
| 45 | Jan. 18, 2001 | 2043.70 | 2043.10 | 0.60 | third prize |
| 46 | Jan. 19, 2001 | 2063.47 | 2065.60 | -2.13 | |
| 47 | Feb. 5, 2001 | 2036.62 | 2008.03 | 28.59 | |
| 48 | Feb. 6, 2001 | 1960.85 | 1995.31 | -34.46 | |
| 49 | Feb. 7, 2001 | 1979.34 | 1979.93 | -0.59 | second prize |

In the above continual 49 days' actual predictions, there are 2 days that the error less than 0.5, 5 days the error less than 1.0, 12 days the error less than 2.0, 24 days the error less than 5.0, 35 days the error less than 10.0, and 14 days the error greater than 10.0.

Obviously, this method also may be used to predict the stock price.

## 2 Two kind of special variable dimension fractal prediction method

Firstly we introduce two kind of special variable dimension fractals: fractal in fractal and high order function in fractal.

The form of fractal in fractal may be summarized as follows.

Suppose the original fractal model in Eq. (1) may be called the first order fractal, in which if the fractal dimension also is taken as the fractal form: $D= C' /r^{D'}$, then the fractal in fractal or the second order fractal will be formed. The higher order fractals may be deduced by analogy. In order to facilitate the idea, we mark the different order fractals with the following forms.

first order fractal $N_{(1)} = \frac{C_1}{r^{D_1}}$

where $D_1$=constant.

second order fractal $N_{(2)} = \frac{C_1}{r^{D_1}}$

where $D_1 = \frac{C_2}{r^{D_2}}$; $D_2$ =constant

……

the $n$ th order fractal $N_{(n)} = \frac{C_1}{r^{D_1}}$

where $D_1 = \frac{C_2}{r^{D_2}}$; $D_2 = \frac{C_3}{r^{D_3}}$; … $D_{(n-1)} = \frac{C_n}{r^{D_n}}$; $D_n$ =constant

Similarly the high order function (function in function) may be defined. For example the original sine function (first order sine) is: N=sin (kr+b), if k= sin (k ' r+b '), then the sine function in sine function or the second order sine function is formed. The higher order sine function may be deduced by analogy.

In order to facilitate the idea, and consider the more widespread cases, we mark the different order cosine function with the following forms.

first order cosine function $\cos_{(1)} r = A_1 + B_1 \cos(C_1 + D_1 r)$

where $D_1$=constant

second order cosine function $\cos_{(2)} r = A_1 + B_1 \cos(C_1 + D_1 r)$

where $D_1 = A_2 + B_2 \cos(C_2 + D_2 r)$; $D_2$ =constant

…

the $n$ th order cosine function $\cos_{(n)} r = A_1 + B_1 \cos(C_1 + D_1 r)$

where $D_1 = A_2 + B_2 \cos(C_2 + D_2 r)$; $D_2 = A_3 + B_3 \cos(C_3 + D_3 r)$; …

$$D_{n-1} = A_n + B_n \cos(C_n + D_n r);\ D_n = \text{constant}$$

Similarly other high order trigonometric functions (trigonometric function in trigonometric function), high order logarithmic function (logarithmic function in logarithmic function), high order inverse trigonometric function (inverse trigonometric function in inverse trigonometric function), high order hyperbolic function (hyperbolic function in hyperbolic function) and so on may be defined.

As the value of D in fractal model equals high order function, then the high order function in fractal is formed.

As determining the concrete forms of fractal in fractal or high order function in fractal, namely solving all the constants to be determined, the method of weighted residuals, such as the least squares method, may be used.

Suppose the number of the constants to be determined is equal to n, then we choose n given data points, their values of N are $N_i$ i=1~n, after the curve fitting, the corresponding values given by the model of fractal in fractal or high order function in fractal equal $N_i$', then all the constants to be determined can be solved by using the following expression:

$$S = \sum(N_i - N_i')^2 = \min$$

As determining its minimum value, the steepest descent method or other optimization method may be used.

Now we discuss the application of fractal in fractal.

As solving the practical problem, generally we establish the fractal in fractal model with the least squares method according to the given data firstly, and then the prediction results may be reached with the extrapolation method by using the established model.

Example 5, the world oil annual average prices from 1989 to 1993 are as follows (unit: US dollar/barrel) : 17.80, 22.87, 19.33, 19.03, 16.82, try to use the second order fractal method to establish the model of the world oil annual average prices from 1989 to 1993, and predict (extrapolate) the prices of 1994 and 1995 according to this model.

The real prices, the calculated prices from 1989 to 1993 and the predicted prices of 1994 and 1995 with the second order fractal are shown in Table 6.

**Table 6, the world oil annual average prices**

| Year | r | real price | calculated price | error/% |
|---|---|---|---|---|
| 1989 | 1 | 17.80 | 16.73 | -6.00 |
| 1990 | 2 | 22.87 | 22.71 | -0.69 |
| 1991 | 3 | 19.33 | 18.94 | -2.00 |
| 1992 | 4 | 19.03 | 17.76 | -6.67 |
| 1993 | 5 | 16.82 | 17.29 | 2.79 |
| 1994 | 6 | 15.89 | 17.07 | 7.36 |
| 1995 | 7 | 17.17 | 16.95 | -1.30 |

Because of space limitation, we cannot discuss the application of higher-order function in fractal.

## 3 Complex number dimension fractal prediction method

As the value of D is equal to a real number, the fractal may be called the real constant dimension fractal, in fact it is the one-dimensional model, because it only has one variable r. It is a straight line in the double logarithmic coordinates. But as the number of variable is greater than 1, then the model cannot be the real constant dimension fractal. In order to overcome this difficulty, we proposed the complex number dimension fractal and the multi-dimension fractal.

Suppose in Eq.(1) we define

$$D = f_1(x_{1,} x_2 \ldots x_n)$$

$$r = f_2(x_{1,} x_2 \ldots x_n)$$

$$C = f_3(x_{1,} x_2 \ldots x_n)$$

$$N = f_4(x_{1,} x_2 \ldots x_n)$$

Then we have the fractal model in n-dimensional space.

Now we discuss the complex number dimension fractal.

In Eq.(1) the values of D and r are taken as follows

$$D = a + ib$$

$$r = x + iy$$

Suppose

$$r^D = w = E + iF$$

As well-known, $w$ is the multiple-valued function. Because the original fractal model is the single-valued function, we also request the complex number dimension fractal is the single-valued function in this paper, namely we will take the main value of logarithm, and it gives

$$(a + ib)\ln(x + iy) = \ln w = \ln(E + iF)$$

therefore

$$(a + ib)(\ln|r| + i\arg r) = \ln|w| + i\arg w$$

it gives

$$\theta = \arg w = a\arg r + b\ln|r|$$

$$|w| = \exp(a\ln|r| - b\arg r)$$

Then we have

$$E = |w|\cos\theta$$

$$F = |w|\sin\theta$$

suppose

$$C = C_x + iC_y$$

$$N = N_x + iN_y$$

because

$$N = \frac{C_x + iC_y}{E + iF}$$

It gives

$$N_x = \frac{C_x E + C_y F}{E^2 + F^2}$$

$$N_y = \frac{C_y E - C_x F}{E^2 + F^2}$$

Thus, the related formulas for complex number dimension fractal are given. From the above inferential reasoning we can see that, in multi-dimensional space, so long as the logarithm operation is defined, the fractal model may be established.

There are 2 constants to be determined in the real fractal model: C and D. While in the complex number dimension fractal, there are 4 constants to be determined: $C_x$, $C_y$, a and b. For the real fractal model, as the number of the given data point is greater than 2, generally the least squares method should be used to determine C and D. For the complex number dimension fractal model, as the number of the given data values is greater than 4, generally the least squares method also should be used to determine $C_x$, $C_y$, a and b.

Suppose $N_{xx}$ and $N_{yy}$ denote the real part and imaginary part of the given data point, $N_x$ and $N_y$ denote the real part and imaginary part of the corresponding calculated value according to the complex number dimension fractal model, then $C_x$, $C_y$, a and b can be determined by using the following least squares method

$$\Pi = \sum \left[ (N_x - N_{xx})^2 + (N_y - N_{yy})^2 \right] = \min$$

In some cases, the given data points and the corresponding calculated values only have the real part (but all the other quantities C, D and r have real part and imaginary part), thus $C_x$, $C_y$, a and b can be determined by using the following simplified formula

$$\Pi = \sum (N_x - N_{xx})^2 = \min$$

Example 6, in the reference [ 9 ], a simplified method for the 5th order Stokes wave was presented. In which the key quantity $N_{xx}$ (in original text it was the non-unit parameter d/L) is the function of parameter x (in original text it was $K_2$) and y (in original text it was $K_1$). The 6 given values of $N_{xx}$ are shown in Table 7. Try to use the complex number dimension fractal model to fit these 6 data points, and to extrapolate the key quantities corresponding to other values of x and y.

For the original method to solve the key quantity, it needs to solve a complicated equation. But after fitting these 6 data points with a complex number dimension fractal model, we may use the simple computational method to extrapolate the key quantities nearby these 6 data points.

**Table 7, key quantity $N_{xx}$**

| x= | 0.08 | 0.10 | 0.12 |
|---|---|---|---|
| y=0.24 | 0.12030 | 0.13792 | 0.15475 |
| 0.28 | 0.11922 | 0.13681 | 0.15354 |

Take the parameter for the complex form $r = x + iy$ (for example, x= 0.08, y= 0.24 written as 0.08+i0.24), according to the 6 given data points and the corresponding calculated values, with the steepest descent method, the optimized solution for the complex number dimension fractal model is as follows

D = -0.2946999 + i0.0515208

C = 0.5824216 + i0.8425285

Substitute the above values into the complex number dimension fractal formula, the fitting values can be calculated. The results are shown in Table 8.

**Table 8, fitting value of $N_x$ and the error**

| x | y | $N_x$ | error/% |
|---|---|---|---|
| 0.08 | 0.24 | 0.1203381 | 0.032 |
| 0.08 | 0.28 | 0.1215420 | 1.95 |
| 0.10 | 0.24 | 0.1373734 | -0.40 |
| 0.10 | 0.28 | 0.1370334 | 0.16 |
| 0.12 | 0.24 | 0.1539712 | -0.50 |
| 0.12 | 0.28 | 0.1522378 | -0.85 |

The extrapolated results are shown in Table 9.

**Table 9, the extrapolated results**

| x | y | $N_x$ | $N_{xx}$ | error/% |
|---|---|---|---|---|
| 0.08 | 0.20 | 0.1205872 | 0.12120 | -0.51 |
| 0.10 | 0.20 | 0.1395045 | 0.13886 | -0.46 |
| 0.12 | 0.20 | 0.1577343 | 0.15577 | 1.26 |

From the fitting and extrapolated results we can see that, all the errors are less than 2%.

## 4 Fractal series prediction method

In order to expand the application scope of fractal method, in the reference [ 10 ], the following form of fractal series was presented

$$N = \sum \frac{C_i}{r^{D_i}} = \frac{C_1}{r^{D_1}} + \frac{C_2}{r^{D_2}} + \cdots\cdots$$

However, in this paper we only discuss the special and simple form, namely the expanded Taylor's series in which the index is changed from the integer into the non-integer to be determined.

The fractal series as the formula of prediction (or extrapolation), may be obtained through two ways. The first one is the fitting method similar to obtain the complex number

dimension fractal model; the second one is to obtain the fractal series through finding the solution of differential equation with the least squares method. This paper only discusses the second way.

Example 7, for interval **0≤t≤20,** try to solve the following linear damped oscillation question due to earthquake, and obtain the fractal extrapolation formula.

$X''(t) + X(t) = -2\varepsilon X(t)$ ($\varepsilon$=0.1)

The initial condition reads: X (0) =0, X' (0) =1

In the reference [11], we can find the following approximate analytical solution

$$X(t,\varepsilon) = \sin t - \varepsilon t \sin t + 0.5\varepsilon^2 t^2 \sin t - 0.5\varepsilon^2 t \cos t + 0.5\varepsilon^2 \sin t$$

In this paper we choose the following fractal series of **ε(**the indexes of **ε** are Y, Z, W, W, instead of 1, 2, 2, 2), which contains three other constants to be determined ($A_1$, $A_2$ and $A_3$) and already satisfies the initial condition, as the approximate analytical solution

$$X(t) = \sin t - A_1\varepsilon^y t \sin t + A_2\varepsilon^z t^2 \sin t - A_3\varepsilon^w t \cos t + A_3\varepsilon^w \sin t$$

By using the least squares method, we have the following variational principle for solving the differential equation

$$\Pi = \int_0^{20} F^2 dt = \min$$

where $F = X''(t) + X(t) + 2\varepsilon X(t)$ $\varepsilon$=0.1

Taking the initial values as follows: Y=1, Z=2, W=2, $A_1$ =1, $A_2$ = $A_3$ =0.5, with the steepest descent method, the optimized solution is as follows

Y = 1.048389, Z = 2.223077, W = 2.324839,

$A_1$ = 0.9212227, $A_2$ = 0.3277449, $A_3$ = 0.1413171

The results are shown in Table 10.

**Table 10, results of X(t)**

| t | Accurate solution | This paper | Reference [11] |
|---|---|---|---|
| 0 | 0 | 0 | 0 |
| 2 | 0.7516 | 0.7677 | 0.7543 |
| 4 | -0.5009 | -0.5298 | -0.5053 |
| 6 | -0.1700 | -0.1650 | -0.1922 |
| 8 | 0.4491 | 0.4627 | 0.5252 |
| 10 | -0.1853 | -0.1971 | -0.2328 |
| 12 | -0.1775 | -0.1646 | -0.3323 |
| 14 | 0.2425 | 0.2278 | 0.5699 |
| 16 | -0.0427 | -0.0428 | -0.1206 |
| 18 | -0.1341 | -0.1226 | -0.6790 |
| 20 | 0.1180 | 0.1195 | 0.8767 |

From Table 10 we may see that, the fractal series solution agrees with the precise solution at the whole interval, while the existing solution only agrees with the precise solution at the interval of t<10.

Now we take the fractal series as the extrapolated (predicted) formula.

From the fractal series formula the extrapolated (predicted) result for t=20.5 is as follows: X (20.5) =0.1360, while the accurate solution is 0.1293, the error of extrapolation formula is

5.2% only; for t=21, X (21) =0.1205, while the accurate solution is 0.1095, the error is 10.1%.

Therefore, if the required error is less than or equal to 10.1%, the above fractal extrapolation formula may be used at the interval [ 20, 21 ].

## 5 Improved rescaled range (R/S) prediction method

The energies released by natural disaster, such as fire, earthquake and so on, are huge. If these energies can effectively use, even if a small part, the humanity also will obtain the rich energy. For the prediction to the situation of natural disaster, the improved rescaled range (R/S) analysis presented in the reference [12] is extremely effective.

H. E. Hurst is a renowned hydrology scientist. He proposed the R/S analysis or the rescaled range analysis method in the reference [13]. In which the most important work was the calculation of the Hurst exponent H.

We adopted two new data grouping methods to calculate the Hurst exponent H.

The first data grouping method: The number of the data in an interval is increased progressively. For example we may make the first interval to contain the data of 1950~1955 (there are 6 years' data altogether), the second interval contains the data of 1950~1956 (there are 7 years' data altogether), the rest may be deduced by analogy, the last interval contains the data of 1950~2000 (there are 51 years' data altogether). It should be noted that, the Hurst exponent calculated by the data of the first interval is taken as the Hurst exponent of the year 1955, the rest may be deduced by analogy, and the Hurst exponent calculated by the data of the last interval is taken as the Hurst exponent of the year 2000.

The second data grouping method: The number of the data in an interval is fixed. For example we may make the first interval to contain the data of 1950~1955, the second interval contains the data of 1951~1956, the rest may be deduced by analogy, the last interval contains the data of 1995~2000, namely each interval contains 6 years' data altogether. Similar to the first method, the Hurst exponent calculated by the data of any interval is taken as the Hurst exponent of the last year of this interval.

Now we present the application example of the first method.

Example 8, according to the fire numbers of China from 1950 to 1999, to predict the fire number of year 2000.

Firstly calculate the Hurst exponent H from 1955 to 1999. Then according to these Hurst exponents to calculate the Hurst exponent of year 2000 ($H_{2000}$) with the fractal method, it gives

$H_{2000}$ =0.7750

According to this calculated $H_{2000}$, the fire number of year 2000 may be predicted with the shooting method. Finally it gives that as the fire number of year 2000 is equal to 199960, $H_{2000}$ =0.7750. While the real value is 189185, the predicted error is 5.7% only.

In order to effectively carry on the analysis and prediction to the statistical data, in the reference [12] we also introduced the concept of high order Hurst exponent. For all the calculated Hurst exponents, taking these values of H as the ordinary given statistical data, thereupon we may again carry on the R/S analysis to these data, thus obtain a group of new Hurst exponents, name it $H_1$, this the Hurst exponent of Hurst exponent. The rest

may be deduced by analogy, and may give the higher order Hurst exponents $H_2$, $H_3$ and so on. With the help of the Hurst exponent and high order Hurst exponent, we may judge that whether or not the next year's fire number will be increased sharply.

## 6 Conclusions

This paper discusses the prediction and calculation methods established by fractal model $N=C/r^D$ (in which the fractal dimension D may be the real number, variable and complex number), fractal series as well as the improved rescaled range (R/S) analysis, and their applications for new energy development. In order to obtain a better effect, sometimes it needs to perform the processing to data point in advance (such as translation, accumulated sum and so on); Moreover, sometimes run the necessary adjustment to the fractal dimension D. The examples presented in this paper indicate that, these prediction and calculation methods will possibly have the good application prospect in new energy development.

**References**


1 Turcotte, D L. *Fractals and chaos in geology and geophysics* [M]. Cambridge University Press, 1992

2 Fu Yuhua. Variable dimension fractal in fluid mechanics. *Proceedings of second computational hydrodynamics conference*. Wuhan, 1993, 202~207. (in Chinese)

3 Fu Yuhua. Improvement of fractal technique on the application in oil and gas prospecting: variable dimension fractal technique. *China Offshore Oil and Gas* (Geology). 1994, ( 3): 210~214 (in Chinese)

4 Fu Yuhua. Analyzed and fractal single point method for solving hydraulic problems in ocean engineering[R](i.e., SPE(Society of Petroleum Engineers) 29986). International meeting on petroleum engineering, Beijing, Nov 1995. 347~356

5 Fu Yuhua. Forecasting Typhoon Tracks with Fractal Distribution Model, *China Offshore Oil & Gas* (Engineering). 1999(1):36-39 (in Chinese)

6 Mou Shaojie, Lu Jingzhen. Calculation table for typhoon track forecast [M]. Beijing: Ocean press, 1982 (in Chinese)

7 Fu Yuhua. Analysis and prediction of platform price in Gulf of Mexico with fractals model [J]. *China Offshore Oil & Gas (Engineering)*,1996, 8(1): 61~64 (in Chinese)

8 Fu Yuhua. Weighted fractals analysis and forecast of monthly average sea surface temperature [J]. *Marine science bulletin*, 1996, 15(2): 69~76 (in Chinese)

9 Fu Yuhua. Simplified method and improved solution for deriving fifth order Stokes wave [J]. *Marine science bulletin*, 1994, 13(3) (in Chinese)

10 Fu Yuhua. Fractal Series Solution for Mechanics Problem [J]. *Journal of Southwest Jiaotong University*, 1999, (5) (in Chinese)

11 Huang Yongbin, *et al*. *Perturbation method concise course* [M]. Shanghai: Shanghai Jiaotong University Press, 1986 (in Chinese)

12 Fu Yuhua, Fu Anjie. Improved R/S method and analysis and forecast to China [J] . Engi*neering Science*, 2004, vol. 6 no.5, p.39~44 (in Chinese)

13 Hurst H E. The Long-Term Storage Capacity of Reservoirs. *Transactions of the American Society of Civil Engineers (ASCE)*, 116, 1951

# Some unsolved problems in the physics of elementary particles

V. Christianto[1], & F. Smarandache[2]
[1] http://www.sciprint.org, email: admin@sciprint.org
[2] Dept. of Mathematics, Univ. of New Mexico, Gallup, USA,
email: fsmarandache@yahoo.com

Unlike what some physicists and graduate students used to think, that physics science has come to the point that the only improvement needed is merely like adding more decimals in the masses of elementary particles or gravitational constant, there is a number of unsolved problems in this field that may require that the whole theory shall be re-assessed. In the present article we discuss thirty of those unsolved problems and their likely implications. In the first section we will discuss some well-known problems in cosmology and particle physics, and then other unsolved problems will be discussed in next section.

## Unsolved problems related to cosmology

In the present article we discuss some unsolved problems in the physics of elementary particle and mathematical physics, and their likely implications. In the first section we will discuss some well-known problems in cosmology and particle physics, and then other unsolved problems will be discussed in next section. Some of these problems were inspired by and expanded from Ginzburg's paper [2].

(1) *The problem of the three origins*. According to Marcelo Gleiser (Darthmouth College) there are three unsolved questions which are likely to play significant role in 21st-century science: the origin of the universe, the origin of life, and the origin of mind.

(2) *The problem of symmetry and antimatter observation*. This could be one of the biggest puzzle in cosmology: If it's true according to theoretical physics (Dirac equation etc.) that there should be equal amounts of matter and antimatter in the universe, then why our observation only display vast amounts of matter and very little antimatter?

(3) *The problem of dark matter in cosmology model*. Do we need to introduce dark matter to describe galaxy rotation curves? Or do we need a revised method in our cosmology model? Is it possible to develop a new theory of galaxy rotation which agrees with observations but without invoking dark matter? For example of such a new theory without dark matter, see Moffat & Brownstein [3][4].

(4) *Cosmological constant problem*. This problem represents one of the major unresolved issues in contemporary physics. It is presumed that a presently unknown symmetry operates in such a way to enable a vanishingly small constant while remaining consistent with all accepted field theoretic principles. [15]

(5) *Antimatter hydrogen observation*. Is it possible to find isolated antimatter hydrogen (antihydrogen) in astrophysics (stellar or galaxies) observation? Is there antihydrogen star in our galaxy?

Now we are going to discuss other seemingly interesting problems in the physics of elementary particles, in particular those questions which may be related to the New Energy science.

**Unsolved problems related to the physics of elementary particles**

We discuss first unsolved problems in the Standard Model of elementary particles. Despite the fact that Standard Model apparently comply with most experimental data up to this day, the majority of particle physicists feel that SM is not a complete framework. E. Goldfain has listed some of the most cited reasons for this belief [5], as follows:

(6) *The neutrino mass problem*. Some recent discovery indicates that neutrino oscillates which implies that neutrino has mass, while QM theories since Pauli predict that neutrino should have no mass [6]. Furthermore it is not yet clear that neutrino (oscillation) phenomena correspond to Dirac or Majorana neutrino. [7]

(7) SM does not include the contribution of gravity and gravitational corrections to both quantum field theory and renormalization group (RG) equations.

(8) *Fine-tuning problem*. SM does not fix the large number of parameters that enter the theory (in particular the spectra of masses, gauge couplings, and fermion mixing angles). Some physicists have also expressed their objections that in the QCD scheme the number of quarks have increased to more than 30 particles, therefore they assert that QCD-quark model cease to be a useful model for elementary particles.

(9) *Gauge hierarchy problem*. SM has a gauge hierarchy problem, which requires fine tuning. Another known fine-tuning problem in SM is 'strong CP problem' [19, p. 18]

(10) SM postulates that the origin of electroweak symmetry breaking is the Higgs mechanism. Unfortunately Higgs particle has never been found; therefore recently some physicists feel they ought to introduce more speculative theories in order to save their Higgs mechanism.[8]

(11) SM does not clarify the origin of its SU(3)xSU(2)xU(1) gauge group and why quarks and lepton occur as representations of this group.

(12) *Chirality problem*. SM does not explain why (only) the electroweak interactions are chiral (parity-violating). [19, p. 16].

(13) *Charge quantization problem*. SM does not explain another fundamental fact in nature, i.e. why all particles have charges which are multiples of e/3. [19, p.16]

Other than the known problems with SM as described above, there are other quite fundamental problems related to the physics of elementary particles and mathematical physics in general, for instance [1]:

(14) *Quark confinement problem*. Is there dynamical explanation of quark confinement problem? This problem corresponds to the fact that quarks cannot be isolated. See also homepage by Clay Institute on this problem.

(15) What is the dynamical mechanism behind Koide's mixing matrix of the lepton mass formula? [9]

(16) Does neutrino mass correspond to the Koide mixing matrix? [10]

(17) Does Dirac's new electron theory in 1951 reconcile the quantum mechanical view with the classical electrodynamics view of the electron? [11]

(18) Is it possible to explain anomalous ultraviolet hydrogen spectrum?

(19) Is there quaternion-type symmetry to describe neutrino masses?

(20) *Neutrino oscillation problem*. Is it possible to describe neutrino oscillation dynamics with Bogoliubov-deGennes theory, in lieu of using standard Schrödinger-type wave equation? [6]

(21) *Solar neutrino problem* – i.e. the seeming deficit of observed solar neutrinos. [17] The Sun through fusion, send us neutrinos, and the Earth through fission, antineutrinos. But observation in Super-Kamiokande etc. discovers that the observed solar neutrinos are not as expected. In SuperKamiokande Lab, it is found that the number of electron neutrinos which is observed is 0.46 that which is expected [20]. One proposed explanation for the lack of electron neutrinos is that they may have oscillated to muon neutrinos.

(22) *Neutrino geology problem*. Is it possible to observe terrestrial neutrino? The flux of terrestrial neutrino is a direct reflection of the rate of radioactive decays in the Earth and so of the associated energy production, which is presumably the main source of Earth's heat [17].

(23) *Origin of electroweak symmetry breaking.* Is it possible to explain the origin of electroweak symmetry breaking without the Higgs mechanism or Higgs particles? For an example of such alternative theory to derive boson masses of electroweak interaction without introducing Higgs particles, see E. Goldfain [16].

(24) *Quarks and QHE problem*. Is it possible to write quaternionic formulation of quantum Hall effect? [18] Is it possible to describe charge quantization problem of quarks (see problem no. [13] and [14]) from the viewpoint of FQHE? If yes, then how?

(25) *Orthopositronium problem*. What is the dynamics behind orthopositronium observation? [12]

(26) Is it possible to conceive New Energy generation method from orthopositronium-based reaction? If yes, then how?

(27) *Muonium problem*. Muonium is atom consisting of muon and electron, discovered by a team led by Vernon Hughes in 1960. What is the dynamics behind muonium observation? [13]

(28) Is it possible to conceive New Energy generation method from muonium-based reaction? If yes, then how?

(29) *Antihydrogen problem*. Is it possible to conceive New Energy generation method from antihydrogen-based reaction? If yes, then how? [14]

(30) *Unmatter problem*. Would unmatter be more useful to conceiving New Energy than antimatter? If yes, then how? [21]

It is our hope that perhaps some of these questions may be found interesting to motivate further study of elementary particles.

**Acknowledgment**
This article was summary and updated version of problems mentioned in our book "*Unfolding Labyrinth: Open problems in Physics, Mathematics, Astrophysics and other areas of Science."* Hexis-Phoenix, 2006.[1] VC would like to dedicate this article for RFF.

## References

**[1]** F. Smarandache, V. Christianto, Fu Yuhua, R. Khrapko, J. Hutchison, Unfolding *Labyrinth: Open problems in Physics, Mathematics, Astrophysics and other areas of Science*, Hexis-Phoenix, (2006) p.8-9. Preprint in arxiv.org. www.gallup.unm.edu/~smarandache/ebooks-otherformats.htm

**[2]** Ginzburg, V.L., "What problems of physics and astrophysics seem now to be especially important and interesting (thirty years later, already on the verge of XXI century)?," *Physics-Uspekhi* 42(2) 353-373 (1999).

**[3]** Moffat, J.W., "Scalar-Tensor-Vector gravity theory," to be published in J. *Cosmol. Astropart. Phys*. JCAP 2006, preprint: arXiv:gr-qc/0506021 (2005)

**[4]** Moffat, J.W., "Spectrum of Cosmic Microwave Fluctuations and the Formation of Galaxies in a Modified Gravity theory," arXiv:astro-ph/0602607 (2006)

**[5]** Goldfain, E., "Fractional dynamics in the Standard Model for particle physics," To appear at *Comm. Nonlin. Science and Numer. Simul.* 2007. Preprint in www.sciencedirect.com.

**[6]** Giunti, C., "Theory of neutrino oscillations," arXiv:hep-ph/0401244

**[7]** Singh, D., *et al*., "Can gravity distinguish between Dirac and Majorana neutrinos?," arXiv:gr-qc/0605133 (2006)

**[8]** Djouadi, A., *et al*., "Higgs particles", arXiv:hep-ph/9605437 (1996)

**[9]** Koide, Y., arXiv:hep-ph/0506247 (2005); hep-ph/0303256 (2003)

**[10]** Krolikowski, W., "Towards a realistics neutrino mass formula," arXiv:hep-ph/0609187 (2006)

**[11]** deHaas, Paul J., "A renewed theory of electrodynamics in the framework of Dirac ether," London PIIRT Conference 2004, http://home.tiscali.nl/physics/deHaaspapers/PIRTpaper/deHaasPIRT.html

**[12]** Kotov, B., *et al*., "On the possibility of nuclear synthesis during orthopositronium formation..." *Progress in Physics* Vol. 3 no. 3 (2007) www.ptep-online.com

**[13]** Jungmann, K., "Past, present and future of muonium." arXiv:nucl-ex/040401 (2004)

**[14]** Voronin, A., & J. Carbonell, "Antihydrogen-hydrogen annihilation at sub-kelvin temperatures," arXiv:physics/0209044 (2002)

**[15]** Goldfain, E., "Dynamics of neutrino oscillations and the cosmological constant problem," To appear at *Far East J. Dynamical Systems* 2007.

**[16]** Goldfain, E., "Derivation of gauge boson masses from the dynamics of Levy flows," *Nonlin. Phenomena in Complex Systems* Vol 8 no. 4 (2005).

**[17]** Stodolsky, L., "Neutrino and dark matter detection at low temperature," *Physics-Today*, August 1991. p. 3

**[18]** Balatsky, A.V., "Quaternion generalization of Laughlin state and the three dimensional fractional QHE" arXiv:cond-mat/9205006 (1992)

**[19]** Langacker, P., "Structure of the Standard Model," arXiv:hep-ph/ 0304186 (2003) p.16.

**[20]** Jaffe, R.L., "Two state systems in QM: applications to neutrino oscillations and nautral kaons," *MIT Quantum Theory Notes, Supplementary Notes for MIT's Quantum Theory Sequence* (August 2006) p. 26-28.

**[21]** Smarandache, F., "Matter, Antimatter, and Unmatter",Infinite Energy, Vol. 11, Issue 62, 50-51, 2005.

*First version: 23rd Sep. 2007.1st revision: 26th Sept. 2007. 2nd revision: 18th Oct. 2007*

# About Some Unsolved Problems in Physics

M. Pitkänen[1], October 1, 2007

[1] Department of Physical Sciences, High Energy Physics Division,
PL 64, FIN-00014, University of Helsinki, Finland.
matpitka@rock.helsinki.fi, http://www.physics.helsinki.fi/∼matpitka/.
Recent address: Puutarhurinkatu 10,10960, Hanko, Finland.

## Contents

**1 Introduction**

**2 The problems related to energy**
- 2.1 Energy problem of General Relativity . . . . . .
- 2.2 The relationship of gravitational and inertial masses . . . . .
- 2.3 Some problems of cosmology . . . . . .

**3 Anomalies challenging reductionism**
- 3.1 The problem of dark matter . . . . . .
- 3.2 Biology as the mother of all anomalies . . . . . .
- 3.3 Nuclear physics anomalies . . . . . .

**4 Some problems of particle physics**
- 4.1 How to understand the ratio of proton and Planck masses? .
- 4.2 Problems of QCD . . . . . .

**5 Some more philosophical problems**
- 5.1 How to make observer a part of physical system? . . . . . .
- 5.2 What are the values of conserved quantities? . . . . . .
- 5.3 How subjective and geometric time relate? . . . . . .
- 5.4 Problems related to the basic conceptual framework of quantum physics . . . . . .
  - 5.4.1 The relationship between quantum and classical physics
  - 5.4.2 Is it possible to unify quantum theory and thermodynamics? . . . . . .

**Abstract**

Various unsolved conceptual problems and anomalies challenging the basic assumptions of recent day theoretical physics are discussed and their solutions in the framework provided by Topological Geometrodynamics (TGD) are proposed.

# 1 Introduction

Roughly 23 years after the first super-string revolution theoretical particle physics has entered into a state of deep stagnation. The basic prediction of M-theory is that one cannot predict aneything. Neither particles masses nor fundamental symmetries nor even the dimension of space-time. Instead, one must take all physics we know as completely accidental aspects of a particular vacuum we happen to live. There is no empirical evidence for different gauge groups and different space-time dimensions in the known part of cosmos and even atomic spectra seem to be same everywhere but this little empirical detail does not seem to bother M-theorists.

The reasons for the frustrating and unforeseen situation are manifold. Sociological factors are certainly important: after the super string revolution super string models became the only game in the town and the communication of competing theories became gradually more and more difficult. The outcome is the endlessly repeated claim that there are no known competitors for neither existing cosmological scenarios nor for string theory and we must be happy with what we have. Nothing could be farther from truth. There exist highly developed competing theories but the arrogance of academic hegemony prevents very effectively their communication.

Second strange claim is that the basic problem of standard model is that it works too well so that one must just patiently wait what LHC will give to us. Also this belief reflects deep ignorance: even restricting the attention to the narrow realm of elementary particle physics one finds a rich spectrum of conceptual difficulties and anomalies.

To my opinion the situation reflects deeper problems related to the breakdown of the naive reductionistic belief that the progress in physics is marching down to shorter and shorter scales and that Planck scale is under reach now. More generally, "philosophy" has been synonym for bad physical thinking since the establishment of quantum theory with the consequence that theoretical physics has reduced to a blind computation without deeper understanding of the underlying theory.

In the following I shall summarize my view about general problems with emphasis also to what might be ridiculed as "philosophical" problems and

represent a list of anomalies the understanding of which I believe to be very relevant for progress in physics. I do not bother to pretend that I happened to discover these problems and anomalies just yesterday because I have used all 28 years of my professional life to develop solution of these problems in the conceptual framework provided by what I call Topological Geometrodymamics (TGD), and I see nothing crackpottish in representing TGD as one possible approach to these problems.

# 2 The problems related to energy

It it is could to start with conceptual problems related to the notion of energy since they relate very intimately to many other problems in TGD framework.

## 2.1 Energy problem of General Relativity

One might think that the notion of energy has been understood for long time ago: energy and various conserved quantities are Noether charges related to various symmetries. This nice picture however fails in the case of General Relativity since the Poincare symmetries of empty Minkowski space allowing to identify basic conserved quantities are lost since matter makes space-time curved. One can speak only about energy and momentum densities but not about conserved (or even non-conserved) quantities.

TGD [A1, A2] emerged as a possible solution to the problem. If space-times are representable as 4-surfaces of 8-D imbedding space $H = M^4 \times CP_2$ then Poincare symmetries can lifted to those of $M^4$ factor of $H$. Even more, the symmetries of the standard model can be understood as symmetries of $CP_2$ factor. Color symmetry corresponds to isometries of $CP_2$ and color becomes orbital angular momentum like quantum number rather than spin like quantum number; electro-weak symmetries correspond to the holonomy group of spinor connection of $CP_2$ and are automatically broken symmetries; the two chiralities of imbedding space spinors correspond to conserved baryon and lepton numbers so that proton instability plaguing GUTs and string models is not a problem of TGD.

A geometrization of various gauge fields emerges in terms of induced gauge fields and the problem of understanding the $CP_2$ explains the origin of standard model symmetries. Later work has demonstrated that $M^4 \times CP_2$ has deep number theoretical meaning related to the classical number fields. The extension of conformal invariance of string models in turn fixes space-time dimension to $D = 4$ and forces Minkowski space factor of $H$ to be

just four-dimensional Minkowski space $M^4$. Thus quite an impressive list of problems encountered by unifier is solved by a solution to single fundamental problem.

## 2.2 The relationship of gravitational and inertial masses

Equivalence Principle stating that inertial and gravitational four-momenta are identical is the basic tenet of General Relativity. The fact that gravitational mass is not conserved in cosmology suggests the breaking of Equivalence Principle in long time scales in TGD Universe.

This is indeed true. One can identify expressions for gravitational momenta and for gravitational counterparts of all quantum numbers as Noether currents but they are not conserved anymore. Equivalence Principle holds true at elementary particle level but there also violations of it are predicted: in particular very general class of cosmic string type extremals of field equations with vanishing inertial quantum numbers but with a huge density of gravitational mass exist. Gravitational mass can be also negative which would bring in antigravity type effects indeed crucial in the TGD based model for large voids and of cosmic expansion.

## 2.3 Some problems of cosmology

Cosmology is plagued by many other problems besides those already mentioned.

a) Why the mass density is very nearly critical rather than the huge density expressible in terms of Planck mass which is the only purely gravitational mass scale.

b) Inflationary cosmologies explained the absence of horizons in the very early cosmology and thus isotropy of microwave background and predicted correctly the flatness of 3-space. Unfortunately inflationary cosmologies are highly non-unique and require new Higgs type fields with very un-natural potentials.

c) Second law of thermodynamics predicts that early universe should have low entropy whereas very early cosmology suggests maximum entropy. Matter antimatter asymmetry and the origin of magnetic fields encountered everywhere in cosmos are further mysteries of the standard cosmology.

The first thing to do in order to test a new theory is to do cosmology [D6]. The surprise was that the imbeddings of Robertson-Walker metrics had very nice features following just from the imbeddability with no reference to

dynamics. For instance, *global* imbeddings have always sub-critical density of gravitational mass density.

Critical and over-critical cosmologies turned out to be determined apart from a parameter determining their duration and predict accelerating cosmic expansion since pressure is negative for these solutions. Therefore accelerating cosmic expansion is an unavoidable prediction and dark energy is replaced with dark matter in TGD Universe. The remaining challenge is to understand detailed mechanisms. Critical cosmologies have no horizons and the 3-space is flat for them so that the basic prediction of inflationary cosmologies results. The scale invariant spectrum of fluctuations of the microwave background temperature is replaced with quantum critical fluctuations also independent of scale. This a beautiful example of the universality of the dynamics of TGD implied by its quantum criticality fixing the value of Kähler coupling strength, the only coupling parameter of theory and analogous to critical temperature.

Many-sheeted space-time means quite a dramatic generalization of the space-time concept. For instance, 4-D objects that I call cosmic strings [D5] having 2-D $M^4$ projection and gigantic density of magnetic energy are fundamental solutions of field equations and assumed to dominate primordial cosmology and give rise to the ordinary matter as radiation. This indeed means low entropy during the primordial period.

The deformations of cosmic string having finite thickness in $M^4$ gives rise to a fractal hierarchy of magnetic fields in cosmological scales so that the origin of magnetic fields is understood.

The hypothesis that cosmic string like objects contain the antimatter and their exteriors the matter provides the simplest solution to matter antimatter asymmetry. The small Kähler electric fields necessary resulting in the deformation of the vacuum surrounding cosmic strings to non-vacuum yield the perturbation producing a small CP breaking implying that the densities of matter and antimatter are not quite the same and after annihilation only matter remains in the exterior of strings.

# 3 Anomalies challenging reductionism

## 3.1 The problem of dark matter

The problem of dark matter is certainly the problem number one in the recent day cosmology and particle physics and challenges also the reductionistic picture. Modifications of General Relativity and all kinds of exotic particles have been proposed as a solution. Accelerated expansion com-

plicates the situation even more. The explanation of accelerated expansion based on cosmological constant requires also the identification of dark energy (quintessence in models assuming exotic matter with negative pressure).

A possible solution of the problem comes from totally different direction. There is evidence for Bohr quantization in astrophysical systems [16] with a gigantic Planck constant. If genuine quantal effects are in question this means that Universe is macroscopic quantum system in astrophysical scales and reductionistic vision fails completely.

Already classical TGD predicts the existence of macroscopic quantum phases in all length scales if one accepts quantum classical correspondence stating that space-time sheets serve as space-time correlates of quantum coherence regions. This led to the idea that Planck constant has a spectrum of quantized values forcing a further generalization of the notion of imbedding space with a tentative interpretation of dark matter as macroscopic quantum phases with value of Planck constant different from the standard one [D7, D8]. Visible matter would condense around dark matter and make quantal structures visible. Zero energy ontology is absolutely essential for this vision.

Macroscopic quantum coherence is realized in cosmological length scales and quite a detailed quantum view about the evolution of astrophysical systems emerges. A key prediction is that stationary states do not co-expand with cosmos in the classical continuous manner but by quantum jumps in which the value of Planck constant increases so that the quantum size of the system increases too. Accelerated periods of cosmic expansion governed by critical cosmologies serve as correlates for quantum critical phases correspond to these periods. The choice of quantization axes on cosmological length scale should be visible in the cosmic microwave spectrum and might be identifiable as "axis of evil" [25].

### 3.2 Biology as the mother of all anomalies

Forgetting for a while dogmas and trusting on intuition almost anyone would say that living matter represents a prototype of an obviously quantal system. Skeptics however argue that bio-systems are in practice completely classical and deterministic albeit nonlinear, complex, and initial value sensitive.

There are several laboratory effects challenging this view. Quantal effects of ELF em fields on vertebrate brain is a well-established anomaly dating back to seventies [17]. Large Planck constant for ELF photons would allow their energies to be above thermal threshold and thus explains their non-trivial effects: the obvious application is model of EEG [M3]. The nat-

ural hypothesis is that dark matter makes living matter living by quantum controlling visible matter condensed around it. Also the notion of field body implied by the topological field quantization forced by the new view about space-time is essential: magnetic body contains Bose Einstein condensates of biologically important ions.

The large parity breaking effects manifesting themselves as chiral selection of molecules are a further anomaly difficult to understand in standard model predicting extremely small violations of parity invariance. The presence of scaled up variants of weak interactions would explain chiral selection elegantly and this fits also nicely with the fact that Compton lengths of neutrinos are of order cell size.

### 3.3 Nuclear physics anomalies

There are also nuclear physics anomalies challenging the naive reductionistic picture. Cold fusion has made a return [23] and there is now quite clear experimental support for cold fusion in deuterium-deuterium systems. Also selection rules are identified but they differ from those of standard nuclear physics. A second strange finding is the dependence of nuclear decay rates on electronic environment which challenges the dogma that atomic and nuclear physics are complete separated realms [22].

These findings can be understood in TGD framework on basis of p-adic length scale hierarchy and dark matter hierarchy [F8, F9]. Classical TGD predicts that long range electro-weak and color gauge fields exist in all length scales and quantum classical correspondence leaves no other conclusion than the existence of scale up copies of electro-weak physics and hadron physics. The strong prediction is that TGD Universe is a fractal populated by zoomed up variants of various physics. The application of this picture to high $T_c$ super-conductivity involves exotic very light quarks and zoomed up electrons in nanometer length scale [J1].

## 4 Some problems of particle physics

### 4.1 How to understand the ratio of proton and Planck masses?

The ratio of proton mass to Planck mass determines the mystery number of recent day particle physics. In TGD framework the solution of the problem emerged by a rather accidental looking observation that square roots of Mersenne primes $M_n = 2^n - 1$, $n = 89, 107, 127$ gave the ratios of intermediate boson, hadron, and electron mass scales to $CP_2$ mass which is roughly

$10^{-4}$ smaller than Planck mass and fixed for instance by the tension of cosmic strings assuming that their gravitational fields explain galactic rotation curves [26].

This led to the idea that p-adic thermodynamics assuming super-conformal invariance and assumption of p-adic length scale hypothesis stating that primes near powers of 2 are physically preferred (the survivors in the evolution at elementary particle level) might be powerful enough to predict elementary particle mass spectrum. This turned out to be the case [F2, F3].

The necessity to fuse various p-adic physics and real physics to a larger whole led to a generalization of number concept by fusing reals and various p-adic number fields to a larger structure along common rationals and algebraics. The notion of space-time sheet generalizes also and the interpretation of p-adic space-time sheets is as space-time correlates for cognitions and intentions, the mind stuff of Descartes [E1].

p-Adic thermodynamics also suggests a solution to the problem of undetected Higgs [F5]. The theory predicts that in the case of gauge bosons Higgs gives dominating contribution to gauge boson mass but in case of fermions Higgs contribution most naturally vanishes and thermodynamic contributions determines the mass. Thus the couplings of fermions to Higgs can be very small and therefore the rate for Higgs production via fermion vertices can be much lower than in standard model.

## 4.2 Problems of QCD

When QCD [24] emerged after the failure of the hadronic string model and transcendence to a theory of everything, people decided that QCD gives all of hadron physics. There is however no guarantee that non-perturbative QCD - even if it exists - really describes low energy hadron physics. For instance, quark masses contribute only about 75 per cent to baryon mass and quark contribution to the proton spin is more or less identical to zero. Strong CP breaking is a further fundamental problem of QCD and solved by hand by introducing pseudoscalar particle christened as axion and tailored to have couplings cancelling strong CP breaking and requiring extension of standard model gauge group [27]. The third problem relates to C(abibbo)K(obayashi)M(askawa) mixing [28]: is there some deeper mechanism behind it?

TGD provides answers to this questions. Hadronic string model like structure emerges naturally from TGD: classical quarks can be said to topologically condense on 3-D string like objects. At quantum level one introduces so called super-canonical quanta carrying only color and spin and

dominating the masses of baryons and heavier mesons [F4]. The resulting mass predictions have errors of order per cent. It is however essential that the p-adic mass scale of quark depends on hadron (note that the scale is exponentially sensitive to integer $k$ defining it so that curve fitting is not possible). Also the mass scales of neutrinos are found to depend on their energy (or "environment") [29]. The large variations of effective mass of electrons in condensed matter might also have explanation in terms of the dynamical p-adic length scale of electron.

TGD predicts vanishing strong CP breaking (recall that color is not spin like quantum number in TGD). CKM mixing in turn reduces to a topological description of family replication phenomenon: fermion families correspond to different handle numbers for partonic 2-surfaces and one can understand why only three lowest genera are light. CKM mixing is induced by the topological mixing of different topologies of partonic 2-surface.

Instead of axion TGD predicts entire hierarchy of copies of QCD type physics and corresponding pions which might be experimentally confused with axion. In particular, also leptons should possess color excitations and thus lepto-pions could exist [F7]. There is considerable experimental support for pseudo scalars with mass slightly above $2m_e$ [20]. Recently also evidence for pseudoscalar with mass slightly above $2m_\mu$ emerged [21]. TGD based model of nuclear physics in turn relies on color bonds connecting nucleons having quarks with mass scale of order 1 MeV at their ends [F9].

# 5 Some more philosophical problems

## 5.1 How to make observer a part of physical system?

The objectivity postulate has led to a weird idea that the notion observer should be eliminated completely from physics. The standard quantum measurement theory achieves this strange goal only partially: observer is an outsider not effected by physics but affects the microscopic systems by inducing state function reduction.

One could however adopt a more ambitious attitude and ask how to bring observer to quantum physics. This means nothing but building a quantum theory of consciousness. The natural starting point is the basic paradox of quantum measurement theory: if state function corresponds to something occurring at the level of space-time level or Hilbert space it means a breakdown of determinism of Schrödinger equation and this is definitely not acceptable.

If one allows non-determinism associated with the state function reduction, one must be able to do it without losing the deterministic fundamental equations. In TGD framework this can be done [10, H1]: quantum jump occurs outside space-time and Hilbert space between entire "time evolutions of Schrödinger equation". At classical level entire 4-D space-time is replaced with a new one. This changes dramatically the view about time since both geometric past and future are recreated in quantum jump identified as a moment of consciousness in TGD inspired theory of consciousness.

Note that if Universe were fully deterministic (or if the failure of determinism can be neglected in macro scales) the question about the initial state of Universe is encountered and cannot be answered within framework of existing physics. Now this problem disappears. This particular big bang associated with our particular sub-cosmology defines only the time-like boundary of one particular classical space-time sheet, not the first moment of conscious existence. Furthermore, one cannot speak about the first quantum jump, literally infinite number of quantum jumps has already taken place.

### 5.2 What are the values of conserved quantities?

Even if one accepts the proposed ontology one still encounters the problem of predicting the values of conserved quantities like energy, fermion numbers, electric charge and one cannot do this in the framework of existing physics.

The solution to this problem comes from a solution to a longstanding problem of TGD. The problematic feature of the imbeddings of RW cosmologies was that they were vacuum extremals with respect to conserved inertial energy. The eventual interpretation was in terms of zero energy ontology [C2].

All physical states are creatable from vacuum meaning that they have vanishing total conserved charges and consist of positive and negative energy parts. At space-time level positive and negative energy parts corresponds to the past and future boundaries of space-time sheets defining the basic building bricks of many-sheeted space-time surface. In particle physics experiments positive and negative energy states correspond to initial and final states of particle reaction.

Positive energy ontology can be understood as a limiting case when the time scale of perception is short with respect to the temporal span of the space-time sheet associated with the zero energy state. Energy and other conserved quantum numbers depend on the scale of resolution. The implications of this view are profound for technologies related to energy, communication, and control since negative energy signals propagating to geometric

past become possible [G2]. Also thermodynamics must be modified.

## 5.3 How subjective and geometric time relate?

The relationship between experienced (subjective) time and geometric time is one of the fundamental problems of physics. These times are definitely quite different (tim has arrow/no arrow, future does not exist yet/both future and past exist). The identification of subjective time as a sequence of quantum jumps resolves this problem if one can assign to a given moment of subjective time a value of geometric time [H1]. This time corresponds naturally to a time parameter assignable to a space-time sheet representing zero energy system assignable to observer's conscious experience [H7].

## 5.4 Problems related to the basic conceptual framework of quantum physics

### 5.4.1 The relationship between quantum and classical physics

The relationship between quantum and classical is on rather shaky grounds in standard quantum theory and relies on stationary phase approximation for functional integral which itself is mathematically ill-defined. It is however clear that classical theory is an absolutely essential element of the interpretation of quantum theory and in TGD framework this is the case.

The basic definition of the geometry of the world of classical worlds (light-like 3-surfaces in H) assigns to any 3-surface 4-D space-time sheet defining what might be called classical physics. The ill-defined path integral is replaced with functional integral which exists mathematically and is free of infinities thanks to the enormous symmetries of the geometry of world of classical worlds and non-local dependence on 3-surface. The emerging view is that light-like partonic surfaces (3-D generalization of random light-like curves) correspond to quantum physics and space-time interior characterizes the classical physics providing a representations of it (not 1-1 however). That light-like 3-surface can be seen as random light-like orbit of parton is consistent with zero energy ontology in which physical state has a dual interpretation as a transition.

### 5.4.2 Is it possible to unify quantum theory and thermodynamics?

To even start building theories one must believe on something. That unitary S-matrix and correlation functions code for all that is interesting in quantum

physical system represent the basic beliefs of quantum theorist. To achieve something practical one needs also statistical physics and density matrix but statistical ensembles are regarded as a practical fiction of the theoretician. TGD forces to challenge also these beliefs.

The first point is that in zero energy ontology S-matrix, or rather, its generalization, which might be called M-matrix- does not characterize unitary time evolution as in standard physics approach having roots in non-relativistic Hamiltonian mechanics. M-matrix characterizes zero energy state rather than state evolution by giving the coefficients of time-like entanglement between positive and negative energy parts of the state interpreted in the experimental situation as initial and final states of a particle reaction.

A unification of S- and density matrices results as M-matrix defined as a product of the positive square root of density matrix and unitary S-matrix. It is still an open problem whether S-matrix is universal or whether it depends on some general properties of the system characterizing its "phase". In any case, the gigantic symmetries of quantum TGD, its quantum criticality, and finiteness requirement should fix $S$ to a high degree. This approach also unifies thermodynamics with quantum theory: thermal density matrix represents a zero energy state for which the energy of positive energy part of state has thermal distribution. Also the problematic coherent states of Cooper pairs appearing in super-conductivity and having ill define fermion number, charge and mass generalize to completely well-defined zero energy states and their is no breaking of conservation laws.

### 5.4.3 How to introduce measurement resolution to quantum measurement theory?

Standard quantum measurement theory does not involve the notion of finite measurement resolution at the level of the basic mathematical formalism. The work with von Neumann algebra known as hyper-finite factors of type $II_1$ (HFFs) emerging naturally besides factors of type I of wave mechanics describing systems with finite number of degrees of freedom led to a modification of quantum measurement theory allowing to describe measurement resolution in terms of so called inclusions $\mathcal{N} \subset \mathcal{M}$ of HFFs [C8, C9, C3].

The idea is simple: the included subalgebra describes measurement resolution, which means that complex rays of Hilbert space are replaced by subspaces generated by the action of $\mathcal{N}$ algebra, $\mathcal{N}$ rays. Complex numbers are thus replaced with non-commutative algebra $\mathcal{N}$ and quantum groups and non-commutative variants of Hilbert space usually thought to relate to Planck scale physics emerge naturally.

## 5.5 The ultimate question: How to get rid of theory-reality dualism?

Sooner or later theoretician encounters the really frustrating question *"What about mathematics: does it define a separate reality besides material reality?"*.

This kind of theory-reality dualism is avoided in TGD framework. Quantum states as mathematical objects - "theory" - is only what exists in objective sense and quantum jumps between them give rise to conscious experiences defining the mathematician. There is no need to postulate material reality behind these mathematical structures.

This of course poses very strong self consistency conditions: the mathematical structure of the physical theory must be such that all internally consistent mathematical structures are representable physically. In particular, the universe must be analogous to a universal computer able to emulate any sensible physics, say that predicted by a gauge theory defined by a given gauge group (if indeed mathematically self-consistent). The dualities of M-theory (and of TGD [E2]) might be seen as manifestations of this emulation ability. Furthermore, the hierarchy of Planck constants suggests that any ADE type gauge group can appear as a gauge symmetry of an "engineered" physical system in TGD [C9].

The mathematical structure of TGD even in its recent form gives some hopes of achieving the universality. Consider only the generalization of number concept by fusing real and p-adic numbers [E1] and the generalization of the imbedding space to accommodate the hierarchy of Planck constants [C9].

The notion of infinite prime [E3] in turn leads to what might be called number-theoretic Brahman=Atman identity, algebraic holography, or a realization of Leibnizian monadism. A given real number has an infinite number of number theoretical anatomies realized as units in real sense so that single space-time point can in principle represent quantum states of the entire Universe and points of the world of classical worlds as its number theoretic anatomies. Self-reference loop thus closes: the 8-dimensional imbedding space with points replaced with monads becomes the fundamental structure. The evolution of the number theoretic anatomies of space-time points becomes part of the evolution by quantum jumps.

# 6 Conclusions

The arguments above should make clear that physics as described by standard model is far from complete and there are good reasons to suspect that reductionistic dogma is the reason for the recent stagnation. Perhaps the time is soon ripe for replacing Universe as a dead deterministic clockwork with a Universe which is fractal creatable from vacuum by intentional action and replaced by a new one in each moment of consciousness.

# References

## Online books about TGD


[1] M. Pitkänen (2006), *Topological Geometrodynamics: Overview*. http://www.helsinki.fi/∼matpitka/tgdview/tgdview.html.

[2] M. Pitkänen (2006), *Quantum Physics as Infinite-Dimensional Geometry*. http://www.helsinki.fi/∼matpitka/tgdgeom/tgdgeom.html.

[3] M. Pitkänen (2006), *Physics in Many-Sheeted Space-Time*. http://www.helsinki.fi/∼matpitka/tgdclass/tgdclass.html.

[4] M. Pitkänen (2006), *Quantum TGD*. http://www.helsinki.fi/∼matpitka/tgdquant/tgdquant.html.

[5] M. Pitkänen (2006), *TGD as a Generalized Number Theory*. http://www.helsinki.fi/∼matpitka/tgdnumber/tgdnumber.html.

[6] M. Pitkänen (2006), *p-Adic length Scale Hypothesis and Dark Matter Hierarchy*. http://www.helsinki.fi/∼matpitka/paddark/paddark.html.

[7] M. Pitkänen (2006), *TGD and Fringe Physics*. http://www.helsinki.fi/∼matpitka/freenergy/freenergy.html.


## Online books about TGD inspired theory of consciousness and quantum biology


[8] M. Pitkänen (2006), *Bio-Systems as Self-Organizing Quantum Systems*. http://www.helsinki.fi/∼matpitka/bioselforg/bioselforg.html.

[9] M. Pitkänen (2006), *Quantum Hardware of Living Matter*.
http://www.helsinki.fi/∼matpitka/bioware/bioware.html.

[10] M. Pitkänen (2006), *TGD Inspired Theory of Consciousness*.
http://www.helsinki.fi/∼matpitka/tgdconsc/tgdconsc.html.

[11] M. Pitkänen (2006), *Mathematical Aspects of Consciousness Theory*.
http://www.helsinki.fi/∼matpitka/genememe/genememe.html.

[12] M. Pitkänen (2006), *TGD and EEG*.
http://www.helsinki.fi/∼matpitka/tgdeeg/tgdeeg/tgdeeg.html.

[13] M. Pitkänen (2006), *Bio-Systems as Conscious Holograms*.
http://www.helsinki.fi/∼matpitka/hologram/hologram.html.

[14] M. Pitkänen (2006), *Magnetospheric Consciousness*.
http://www.helsinki.fi/∼matpitka/magnconsc/magnconsc.html.

[15] M. Pitkänen (2006), *Mathematical Aspects of Consciousness Theory*.
http://www.helsinki.fi/∼matpitka/magnconsc/mathconsc.html.

## References to the chapters of books

[A1] The chapter *An Overview about the Evolution of Quantum TGD* of [1].
http://www.helsinki.fi/∼matpitka/tgdview/tgdview.html#evoI.

[A2] The chapter *An Overview about Quantum TGD* of [1].
http://www.helsinki.fi/∼matpitka/tgdview/tgdview.html#evoII.

[C1] The chapter *Construction of Quantum Theory: Symmetries* of [4].
http://www.helsinki.fi/∼matpitka/tgdquant/tgdquant.html#quthe.

[C2] The chapter *Construction of Quantum Theory: S-matrix* of [4].
http://www.helsinki.fi/∼matpitka/tgdquant/tgdquant.html#towards.

[C3] The chapter *Hyper-Finite Factors and Construction of S-matrix* of [4].
http://www.helsinki.fi/∼matpitka/tgdquant/tgdquant.html#HFSmatrix.

[C8] The chapter *Was von Neumann Right After All* of [4].
http://www.helsinki.fi/∼matpitka/tgdquant/tgdquant.html#vNeumann.

[C9] The chapter *Does TGD Predict the Spectrum of Planck Constants?* of [4].
http://www.helsinki.fi/∼matpitka/tgdquant/tgdquant.html#Planck.

[D4] The chapter *The Relationship Between TGD and GRT* of [3].
http://www.helsinki.fi/∼matpitka/tgdclass/tgdclass.html#tgdgrt.

[D5] The chapter *Cosmic Strings* of [3].
http://www.helsinki.fi/∼matpitka/tgdclass/tgdclass.html#cstrings.

[D6] The chapter *TGD and Cosmology* of [3].
http://www.helsinki.fi/∼matpitka/tgdclass/tgdclass.html#cosmo.

[D7] The chapter *TGD and Astrophysics* of [3].
http://www.helsinki.fi/∼matpitka/tgdclass/tgdclass.html#astro.

[D8] The chapter *Quantum Astrophysics* of [3].
http://www.helsinki.fi/∼matpitka/tgdclass/tgdclass.html#qastro.

[E1] The chapter *TGD as a Generalized Number Theory: p-Adicization Program* of [5].
http://www.helsinki.fi/∼matpitka/tgdnumber/tgdnumber.html#visiona.

[E2] The chapter *TGD as a Generalized Number Theory: Quaternions, Octonions, and their Hyper Counterparts* of [5].
http://www.helsinki.fi/∼matpitka/tgdnumber/tgdnumber.html#visionb.

[E3] The chapter *TGD as a Generalized Number Theory: Infinite Primes* of [5].
http://www.helsinki.fi/∼matpitka/tgdnumber/tgdnumber.html#visionc.

[F1] The chapter *Elementary Particle Vacuum Functionals* of [6].
http://www.helsinki.fi/∼matpitka/paddark/paddark.html#elvafu.

[F2] The chapter *Massless States and Particle Massivation* of [6].
http://www.helsinki.fi/∼matpitka/paddark/paddark.html#mless.

[F3] The chapter *p-Adic Particle Massivation: Elementary particle Masses* of [6].
http://www.helsinki.fi/∼matpitka/paddark/paddark.html#padmass2.

[F4] The chapter *p-Adic Particle Massivation: Hadron Masses* of [6].
http://www.helsinki.fi/∼matpitka/paddark/paddark.html#padmass3.

[F5] The chapter *p-Adic Particle Massivation: New Physics* of [6].
http://www.helsinki.fi/∼matpitka/paddark/paddark.html#padmass4.

[F7] The chapter *The Recent Status of Leptohadron Hypothesis* of [6].
http://www.helsinki.fi/∼matpitka/paddark/paddark.html#leptc.

[F8] The chapter *TGD and Nuclear Physics* of [6].
http://www.helsinki.fi/∼matpitka/paddark/paddark.html#padnucl.

[F9] The chapter *Nuclear String Physics* of [6].
http://www.helsinki.fi/∼matpitka/paddark/paddark.html#nuclstring.

[F10] The chapter *Dark Nuclear Physics and Condensed Matter* of [6].
http://www.helsinki.fi/∼matpitka/paddark/paddark.html#exonuclear.

[G2] The chapter *The Notion of Free Energy and Many-Sheeted Space-Time Concept* of [7].
http://www.helsinki.fi/∼matpitka/freenergy/freenergy.html#freenergy.

[H1] The chapter *Matter, Mind, Quantum* of [10].
http://www.helsinki.fi/∼matpitka/tgdconsc/tgdconsc.html#conscic.

[H7] The chapter *Quantum Model of Memory* of [10].
http://www.helsinki.fi/∼matpitka/tgdconsc/tgdconsc.html#memoryc.

[J1] The chapter *Bio-Systems as Super-Conductors: part I* of [9].
http://www.helsinki.fi/∼matpitka/bioware/bioware.html#superc1.

[M3] The chapter *Dark Matter Hierarchy and Hierarchy of EEGs* of [12].
http://www.helsinki.fi/∼matpitka/tgdeeg/tgdeeg/tgdeeg.html#eegdark.

## Other references

[16] http://en.wikipedia.org/wiki/Nottale.

[17] Blackman, C. F., Benane, S. G., Kinney, L. S., House, D. E., and Joines, W. T., (1982), "Effects of ELF fields on calcium-ion efflux from brain tissue, in vitro", Radiat. Res. 92:510-520.

[18] C. I. Westbrook ,D. W Kidley, R. S. Gidley, R. S Conti and A. Rich (1987), Phys. Rev. Lett. 58 , 1328.

[19] A.T. Goshaw *et al*(1979), Phys. Rev. Lett. 43, 1065.

[20] L. Kraus and M. Zeller (1986), Phys. Rev. D 34, 3385.

[21] X.-G. He, J. Tandean, G. Valencia (2007), *Has HyperCP Observed a Light Higgs Boson?*,Phys. Rev. D74.
http://arxiv.org/abs/hep-ph/0610274.

[22] C. Rolfs *et al* (2006), *High-Z electron screening, the cases* $^{50}V(p,n)^{50}Cr$ *and* $^{176}Lu(p,n)$, J. Phys. G: Nuclear. Part Phys. 32 489. Eur. Phys. J. A 28, 251-252.
C. Rolfs *et al* (2006), *First hints on a change of the* $^{2}2Na$ $\beta$ *decay half-life in the metal Pd*, Eur. Phys. J. A 28, 251.

[23] *Cold fusion is back at the American Chemical Society*,
http://www.nature.com/news/2007/070326/full/070326-12.html.
*Cold fusion - hot news again*,
http://www.newscientist.com/channel/fundamentals/mg19426021.000-cold-fusion–hot-news-again.html.
*Extraordinary Evidence*,
http://newenergytimes.com/news/2006/NET19.htm#ee.

[24] *QCD*, http://en.wikipedia.org/wiki/Quantum_chromodynamics.

[25] Z. Merali (2007), *'Axis of Evil' a cause of cosmic concern*, New Scientist, issue 2599, p.10.
http://space.newscientist.com/article/mg19425994.000-axis-of-evil-a-cause-for-cosmic-concern.html.

[26] *Galactic rotation curve*,
http://en.wikipedia.org/wiki/Galaxy_rotation_curve.

[27] *Axion*, http://en.wikipedia.org/wiki/Axion.

[28] *CKM mixing*,
http://en.wikipedia.org/wiki/Cabibbo-Kobayashi-Maskawa_matrix.

[29] *Neutrino oscillation*,
http://en.wikipedia.org/wiki/Neutrino_oscillation.

# Beyond Standard Model, Unmatter, and Yang-Mills field

# Bifurcations and pattern formation in particle physics: an introductory study

Ervin Goldfain

Photonics CoE, Welch Allyn Inc., Skaneateles Falls, N.Y. 13153, USA

PACS 12.60.-i – Models beyond the standard model

PACS 05.45.-a – Nonlinear dynamics and chaos

PACS 05.30.Pr – Fractional statistics systems

## Abstract:

Quantum field theories lead in general to a large number of coupled nonlinear equations. Solving field equations in analytic form or through lattice-based computations is a difficult task that has been only partially successful. We argue that the theory of nonlinear dynamical systems offers valuable insights and a fresh approach to this challenge. It is suggested that universal transition to chaos in nonlinear dissipative systems offers novel answers to some of the open questions surrounding the standard model for particle physics.

**Overview and motivation -** Quantum Field Theory (QFT) is a mature conceptual framework whose predictive power has been consistently proven in both high-energy physics and condensed matter phenomena [1-3]. From a historical perspective, QFT represents a successful synthesis of quantum mechanics and special relativity and consists of several models. Among these, gauge theories play a leading role. The standard model (SM) is a subset of QFT whose gauge group structure includes the electroweak and strong interactions of all known elementary particles**.** SM is a robust theoretical framework, however, it contains some 20 adjustable parameters whose physical origin is presently unknown and whose numerical values are exclusively fixed by experiments.

Non-abelian gauge theories are essentially nonlinear field models. Quantizing this class of models is a nontrivial effort and raises a series of theoretical challenges [4-6]. For example, no complete quantum version of classical gravity exists. Quantum chromodynamics (QCD) is considered a reliable field theory at short distances but because its coupling constant becomes large in the infrared sector, standard perturbative techniques do not apply. At present, there is no universal prescription for deriving and handling closed-form solutions of QCD field equations. This is in manifest contrast with quantum electrodynamics (QED) and the electroweak theory, where perturbative methods are applicable and analytic results possible. In general, dealing with closed-form solutions of field theories is seldom a practical alternative. For example, Heisenberg's nonperturbative quantization procedure [7, 8] or Schwinger-Dyson formalism [9] lead to an infinite set of coupled differential equations which connect all orders of Green's functions. This system does not have analytic and uniquely determined solutions. In these instances, one seeks plausible assumptions that simplify the equations *or* employs suitable numerical techniques for approximation.

In its traditional form, one frequently cited shortcoming of QFT is its inherent limitation in dealing with the effect of highly unstable fluctuations *or* with a dynamics regime that is driven far away from equilibrium [10, 11, 23]. In general, pattern formation is possible in out-of-equilibrium physical systems that are *open* and *nonlinear* [12, 14, 16]. Within a *closed* system patterns may only survive as a transient and die out as a result of the relaxation towards equilibrium. It is for this reason that traditional QFT, with few notable exceptions, is largely unable to properly detect and characterize pattern formation. Recent years have shown that pattern formation is relevant to a wealth of applications ranging

from reaction-diffusion processes, nonlinear optics, nanostructures and fluid mechanics to hot plasma, traffic models, epidemic spreading, transport in heterogeneous media and neural networks. [12, 13, 26]

Understanding non-equilibrium phenomena and pattern formation is still in its infancy. Progress in this field has benefited from tools that have been recently developed for nonlinear dynamics, bifurcation and stability theory [12, 15-17, 27, 28, 32]. Our goal here is to explore the far from equilibrium sector of field theory using some of these newly developed methods. The underlying motivation is that nonlinear dynamics brings novel insights and a practical alternative for the analysis of field equations.

The paper is organized as follows: working at a classical level, we start from a non-equilibrium "toy" model containing an abelian gauge field coupled to a massless scalar field. The concept of universality and the emergence of CGLE are discussed in the next section. Mass generation through period-doubling bifurcations of CGLE and the link between CGLE and the generalized exclusion statistics (GES) follow from these premises. Summary and concluding remarks are detailed in the last section.

Our contribution needs to be exclusively regarded as a preliminary research on the topic. It is neither fully rigorous nor comprehensive. We wish to convey a new qualitative view rather than an in-depth analysis of phenomena. Independent studies are required to confirm, expand or refute these tentative findings.

**A "toy" model in non-equilibrium field theory** - As mentioned earlier, nonlinear field theories amount to a large set of coupled differential equations that are difficult to solve or manage through numerical approximations. The universal nature of nonlinear dynamics near the threshold of the primary instability [see e. g. 13] suggests a shortcut

route. One can start from a plausible "toy" model and generalize results to more realistic theories. One example of such a "toy" model of classical field theory describes an abelian gauge field $a_\mu(x,t)$ in interaction with a massless scalar field $\varphi(x,t)$. The lagrangian density reads [18]

$$\mathsf{L} = -\frac{1}{4} F_{\mu\nu} F^{\mu\nu} + \left| D_\mu \varphi \right|^2 \tag{1}$$

Here, $\mu,\nu = 0,1,2,3$ denote the space-time index, $x = (x_1, x_2, x_3)$ the spatial coordinate, $F^{\mu\nu}$ the gauge field tensor, $e$ the coupling constant and

$$D_\mu = \partial_\mu + iea_\mu \tag{2}$$

the operator of covariant differentiation. Field equations derived from (1) are given by

$$\begin{aligned} D^\mu (D_\mu \varphi) &= 0 \\ \partial^\nu F_{\mu\nu} &= 2e^2 a_\mu \varphi^2 \end{aligned} \tag{3}$$

Developing (3) yields

$$\begin{aligned} \Box \varphi &= -ie(\varphi \partial^\mu a_\mu + a_\mu \partial^\mu \varphi - a^\mu \partial_\mu \varphi) - e^2 a^\mu a_\mu \varphi \\ \Box a_\mu &= \partial^\nu \partial_\mu a_\nu - 2e^2 \varphi^2 a_\mu \end{aligned} \tag{4}$$

where $\Box = \partial^2 / \partial t^2 - \nabla^2$ is the d'Alembert operator. To further streamline the derivation and highlight the basic argument, we proceed by assuming that the gauge field satisfies

$$\partial_\mu a_i = 0 \text{ for } i = 1,2,3 \tag{5}$$

If $a_0$ denotes the temporal component of the gauge field, the system (4) can be brought to the generic form of a coupled system of partial differential equations

$$\partial_0 \varphi = \eta$$

$$\partial_0 \eta = f(\eta, \varphi, a_0, \xi, \nabla\eta, ...)$$
$$\partial_0 a_0 = \xi \tag{6}$$
$$\partial_0 \xi = g(\eta, \varphi, a_0, \xi, \nabla\eta ...)$$

in which $f(...)$ and $g(...)$ are time-evolution functions and $\partial_0 = \partial/\partial t$. (6) may be presented in vector form as

$$\partial_0 \mathbf{u} = U(\mathbf{u}, \nabla\mathbf{u}, ...) \tag{7}$$

where $\mathbf{u} = (\eta, \varphi, \xi, a_0)$. We next posit that transition to non-equilibrium in (7) is controlled by a small external parameter $\varepsilon \ll 1$. This parameter is continuously adjustable and measures the departure from equilibrium ($\varepsilon_c = 0$). Accordingly, (7) becomes

$$\partial_0 \mathbf{u} = U(\mathbf{u}, \nabla\mathbf{u}, ..., \varepsilon) \tag{8}$$

The physical content of $\varepsilon$ depends on the context of the problem at hand. In open systems $\varepsilon$ encodes the combined effect of environmental and internal fluctuations [19]. Critical behavior in continuous dimension identifies $\varepsilon$ with the Wilson-Fisher parameter of the regularization program ($\varepsilon = 4 - d$) [20, 21]. In models involving fractional dynamics, $\varepsilon$ characterizes the range of non-local interactions in space or the extent of temporal memory [22, 24, 25, 32].

**Universality and CGLE -** Non-equilibrium processes such as (8) display remarkable universality. Regardless of the specific application, macroscopic patterns that develop near the threshold of a dynamic instability are robust and largely insensitive to microscopic fluctuations [12, 13, 26].

Since one is familiar with the language of harmonic oscillations, we are interested in the simplest bifurcation in the dynamics of $\mathbf{u}(x,t)$ that creates oscillatory behavior. This is known as a Hopf bifurcation and represents the simplest transition that leads from a focus point to a periodic behavior. As the bifurcation point is approached, the focus point becomes unstable and gives rise to a harmonic limit cycle. CGLE is a *universal* model that holds for all pattern forming systems undergoing a Hopf bifurcation [12, 13]. The theory of the reduction to CGLE from generic systems of autonomous nonlinear equations such as (8) has been developed by several authors. The derivation of CGLE for a 1+1 dimensional system starts from the ansatz

$$\mathbf{u}(x,t) = \mathbf{u}_0 + A(\tilde{x},\tilde{t})\exp[i(k_c x - \Omega_c t]\mathbf{u}_1 + c.c. \tag{9}$$

where $\tilde{x},\tilde{t}$ represent slow variables and $k_c, \Omega_c$ are critical values in wave-number and frequency spaces. Replacing in (8), dropping the tildes and expanding in power series of the small parameter $\tilde{\varepsilon} = \varepsilon - \varepsilon_c$ leads to CGLE in its standard form

$$\boxed{\partial_t A = A + (1+ic_1)\nabla^2 A - (1-ic_3)|A|^2 A} \tag{10}$$

Here,

$$A(x,t) = \rho(x,t)\exp[-i\Phi(x,t)] \tag{11}$$

is a complex-valued amplitude defining the slow modulation in space and time of the underlying periodic pattern. The real parameters $c_1, c_2$ denote the linear and nonlinear dispersion parameters, respectively. The limit $c_1, c_3 \to 0$ corresponds to the real Ginzburg-Landau equation, whereas $c_1^{-1}, c_3^{-1} \to 0$ recovers the nonlinear Schrődinger equation.

**Higgs-free generations of particle masses -** Among the simplest coherent structures generated by CGLE are plane-wave solutions having the form [12, 13]

$$A(x,t) = A_0 \exp[-i(qx + mt)] + c.c$$
$$A_0 = \sqrt{1-q^2} \tag{12}$$

The frequency $m$ satisfies the dispersion equation

$$\boxed{m_q = c_1 q^2 - c_3(1-q^2)} \tag{13}$$

and $q \in [-1,1]$ represents the phase gradient of the complex amplitude (12)

$$q = -\nabla|\Phi| \tag{14}$$

Linear stability analysis of (12) reveals that plane waves having a wave-number larger than the so-called Eckhaus threshold

$$q_E = \sqrt{\frac{1-c_1c_3}{2(1+c_3^2)+1-c_1c_3}} \tag{15}$$

are unstable with respect to the long-wavelength modulation. In particular, a vanishing Eckhaus threshold leads to the Benjamin-Feir-Newell (BFN) instability criterion (A1)

$$c_1c_3 = 1 \tag{16}$$

The dispersion equation (13) has two complementary limits: $q = \pm 1$ ( $A_0 = 0$ ) and $q = 0$ ( $A_0 = \pm 1$ ). Arguments presented in Appendix A suggest a natural identification of these two modes with fermion and electroweak gauge boson fields, respectively. (14) implies that fermions have a non-vanishing and uniform phase gradient $\nabla\Phi \neq 0$, whereas gauge bosons have a uniform phase and a vanishing phase gradient $\nabla\Phi = 0$. Although we have started from a massless model, from (13) and (16) it follows that both these modes

acquire non-vanishing masses. In non-dimensional form and near the BFN instability, the two sets of masses are

$$\begin{aligned} m_{\pm} &= c_1 \\ m_0 &= -c_3 \end{aligned} \tag{17a}$$

such that

$$m_{\pm} = |m_0|^{-1} \tag{17b}$$

It is known that plane-wave solutions consist of both positive and negative frequencies. Because mass is positive definite, in what follows we are limiting the discussion to the case $c_1 > 0$ and $c_3 < 0$.

**The Feigenbaum-Sharkovskii-Magnitskii (FSM) paradigm -** The FSM paradigm of universal transition to chaos in nonlinear dissipative systems is briefly detailed in Appendix B. Extensive numerical data [27, 28] show that both parameters of linear and nonlinear dispersion $c_1, c_3$ of (17a) are distributed in a geometric progression, that is

$$\begin{aligned} c_{1,n} &= c_{1,\infty} + K_1 \overline{\delta}^{-n} \\ c_{3,n} &= c_{3,\infty} + K_2 \overline{\sigma}^{-n} \end{aligned} \tag{18}$$

where $\overline{\delta}$, $\overline{\sigma}$ are scaling constants and $n = 1, 2, 3....$ represents the number of cycles accumulated through bifurcations. Since $K_1, K_2$, $c_{1,\infty}$ and $c_{3,\infty}$ are independent of $n$, they can be both absorbed into a redefinition of masses. We have, accordingly:

$$\begin{aligned} m_n^* &= \frac{1}{K_1}(m_{\pm,n} - c_{1,\infty}) \\ M_n &= \frac{1}{K_2}(m_{0,n} - c_{3,\infty}) \end{aligned} \tag{19}$$

The ratios of two arbitrary masses in the bifurcation sequence take the form:

$$\frac{m_n^*}{m_{n+p}^*} = \bar{\delta}^p$$
$$\frac{M_n}{M_{n+p}} = \bar{\sigma}^p \tag{20}$$

in which $p = 2^k$ , $k = 1, 2, 3....$ Based on (17) it can be concluded that, near the BFN instability, the two scaling constants are linked to each other.

Analysis of the Renormalization Group flow for the real Ginzburg-Landau equation leads to the following relationship between $\bar{\delta}$ and $\bar{\sigma}$ [24]:

$$1 - (\frac{M_1}{M_2})^2 = 1 - (\bar{\sigma}^{-1})^2 \approx \frac{1}{\bar{\delta}} \tag{21}$$

where $M_1 = M_W, M_2 = M_Z$ are vector boson masses. Tab. 2 shows a side-by-side comparison between predictions inferred from (20) and experiment, where $\bar{\delta} = 3.9$ represents the numerical value of the scaling constant that best fits laboratory data [30]. Actual values of particle masses, computed at the reference scale given by the mass of the top quark [31], are listed in Tab. 1. Note that the choice of the mass scale is completely arbitrary since (20) involves ratios of consecutive masses.

| **Parameter** | **Value** | **Units** |
|---|---|---|
| $m_u$ | 2.12 | MeV |
| $m_d$ | 4.22 | MeV |
| $m_s$ | 80.90 | MeV |
| $m_c$ | 630 | MeV |
| $m_b$ | 2847 | MeV |

| | | |
|---|---|---|
| $m_t$ | 170,800 | MeV |
| $M_W$ | 80.46 | GeV |
| $M_Z$ | 91.19 | GeV |

**Tab. 1**: Actual values of elementary particle masses

| **Parameter ratio** | **Behavior** | **Actual** | **Predicted** |
|---|---|---|---|
| $m_u / m_c$ | $\overline{\delta}^{-4}$ | $3.365\times10^{-3}$ | $4.323\times10^{-3}$ |
| $m_c / m_t$ | $\overline{\delta}^{-4}$ | $3.689\times10^{-3}$ | $4.323\times10^{-3}$ |
| $m_d / m_s$ | $\overline{\delta}^{-2}$ | 0.052 | 0.066 |
| $m_s / m_b$ | $\overline{\delta}^{-2}$ | 0.028 | 0.066 |
| $m_e / m_\mu$ | $\overline{\delta}^{-4}$ | $4.745\times10^{-3}$ | $4.323\times10^{-3}$ |
| $m_\mu / m_\tau$ | $\overline{\delta}^{-2}$ | 0.061 | 0.066 |
| $M_W / M_Z$ | $(1-\overline{\delta}^{-1})^{1/2}$ | 0.8823 | 0.8623 |

**Tab. 2**: Actual versus predicted mass scaling ratios for $\overline{\delta} = 3.9$

**CGLE and generalized exclusion statistics -** Dispersion relation (13) indicates that plane-wave solutions of CGLE interpolate between gauge boson states $(q = 0)$ and

fermion states $(q = \pm 1)$. From (13) and (14) it follows that the *spin* associated with an arbitrary mixed state is given by[1]

$$\sigma = 1 - \frac{(\nabla \Phi)^2}{2} \tag{24}$$

From this standpoint, CGLE is remarkably similar to the framework describing quantum fractional statistics in condensed matter physics. In what follows we briefly discuss this analogy. The generalized exclusion statistics (GES) is motivated by the properties of quasi-particles occurring in the fractional quantum Hall effect [33, 34]. Consider a thermodynamic ensemble of $N$ identical particles. Let $d$ represent the dimension of the one-particle Hilbert space obtained by fixing the coordinates of the remaining $N-1$ particles. The statistics of a particle is defined by the so-called Haldane's parameter $g$,

$$g = -\frac{\partial d(N)}{\partial N} \approx -\frac{d(N + \Delta N) - d(N)}{\Delta N} \tag{25}$$

Because any given state can be populated by any number of bosons, $d(N + \Delta N) = d(N)$ and hence $g = 0$. By contrast, the Pauli exclusion principle restricts fermions to $g = 1$. Quasi-particles with mixed statistics are characterized by an intermediate value of $g$ and are said to satisfy a generalized exclusion principle. In this case, it can be shown that thermodynamic quantities such energy, heat capacity or entropy can be expressed in factorized form. In particular, the energy of the quasi-particle ensemble is given by

$$E(g) = gE(1) + (1 - g)E(0) \tag{26}$$

An example of this type of objects is offered by *anyons,* quasi-particles that exist in two-dimensions and carry fractional charges. When two particles of a system of bosons are

[1] Strictly speaking, spin is a concept that is valid only in a quantum or semi-quantum context. Since our analysis is carried out at the classical level, (24) is meant to simply denote a numerical attribute of plane waves dependent on the wave-number $q$.

exchanged, the phase of the system remains unchanged, whereas for a system of fermions it changes by exactly $\pi$. Exchanging two anyons results in a phase factor that falls between zero and $\pi$. Anyons play a key role in the fractional quantum Hall effect and high-temperature superconductivity [33, 34].

A short comparison between plane-wave solutions of CGLE and GES is included in the following table:

| **CGLE** | **GES** |
|---|---|
| $q = -\frac{\partial \lvert\Phi\rvert}{\partial x}$ | $g = -\frac{\partial d}{\partial N}$ |
| $m_q = c_1 q^2 - c_3(1-q^2)$ | $E_g = gE(1) + (1-g)E(0)$ |

**Tab. 3**: Comparison between CGLE and GES

**Summary and conclusions -** This brief report has been motivated by recent advances in nonlinear dynamics and complexity theory. Exploiting the universal theory of transition to chaos in nonlinear dissipative systems, we have found that:

a) particles acquire mass as plane wave solutions of CGLE, without reference to the hypothetical Higgs scalar or to a particular symmetry breaking mechanism.

b) starting from a basic model of abelian gauge bosons in interaction with scalar fields, CGLE leads to a natural separation of heavy *non-relativistic modes* ($q = 0$) from light *relativistic modes* of maximal group velocity ($q = \pm 1$). The most straightforward interpretation of this result is that the first group of modes corresponds to electroweak gauge bosons and the second group to fermions.

c) a direct connection may be set up between GES in condensed matter physics and the dispersion relation (13) corresponding to $q \neq 1$. Although different in methodology and

content, both GES and CGLE point out that fractional quantum statistics and non-equilibrium field theory enable a *dynamic unification* of gauge bosons and fermions as particles with arbitrary spin. This is in contrast with super-symmetry and related models [see e.g., 35] which are based on extended symmetry groups and pay virtually no attention to nonlinear dynamics of underlying fields.

Future research may be focused on a deeper understanding of pattern formation and its ramifications in the realm of SM and beyond. Of key interest is the emergence of novel states in the TeV range of particle physics. This probing energy will become accessible in the near future at the Large Hadron Collider and other accelerator sites [36].

**Appendix A -** The two dispersion parameters of CGLE are subject to the following dynamic constraints [12, 13, 26]:

a) the Benjamin-Feir-Newell (BFN) criterion states that stability becomes borderline for

$$c_1 c_3 = 1 \tag{A1}$$

b) using (13), the group velocity of the plane wave solutions is given by

$$\mathrm{v}_g = 2q(c_1 + c_3) \tag{A2}$$

Compliance with relativity bounds (A2) to a constant that represents the normalized value of light speed *in vacuo*. It is clear that $q = 0$ represents a *slow mode* (massive gauge boson), while $q = \pm 1$ describes the *fastest mode* (relativistic fermions). Masses associated with these modes are supplied by (17). From the BFN criterion it follows that the borderline value of the normalization constant $Q \equiv \frac{\mathrm{v}_{g,\max}}{2}$ can be determined from

$$c_1 = \frac{Q \pm \sqrt{Q^2 - 4}}{2} \Rightarrow Q \geq 2 \tag{A3}$$

$$c_3 = \frac{1}{c_1}$$

(A1) and (A2) imply that, close to the border of BFN instability, gauge boson and fermion masses scale as dual entities. This finding is consistent with the behavior of the last entry in Tab. 2.

**Appendix B -** Consider the following boundary value problem for CGLE in 1+1 space-time dimensions [27- 29]:

$$\begin{gathered} \partial_t A = A + (1+ic_1)\partial_x^2 A - (1-ic_3)\left|A\right|^2 A \\ \partial_x A(0,t) = \partial_x A(L,t) = 0\,,\ A(x,0) = A_0(x)\,,\ 0 \le x \le L\,,\ 0 \le t \le \infty \end{gathered} \tag{B1}$$

This model can be reduced to a three-dimensional system of nonlinear ordinary differential equations with the help of the Galerkin few-modes approximation:

$$A(x,t) \approx \sqrt{\xi(t)}\exp[i\theta_1(t)] + \sqrt{\eta(t)}\exp[i\theta_2(t)]\cos(\frac{\pi}{L}x) \tag{B2}$$

in which

$$\begin{gathered} \partial_t \xi = f_1(\xi,\eta,\theta,c_1,c_3,L) \\ \partial_t \eta = f_2(\xi,\eta,\theta,c_1,c_3,L) \\ \partial_t \theta = f_3(\xi,\eta,\theta,c_1,c_2,L) \end{gathered} \tag{B3}$$

with $\theta(t) \equiv \theta_2(t) - \theta_1(t)$. It can be shown that the transition to chaos in (B3) occurs through a *sequential cascade of bifurcations* in three separate stages. This cascade starts with the Feigenbaum scenario of period-doubling bifurcations of stable cycles, followed by the Sharkovskii subharmonic cascade and ending with the Magnitskii cascade of stable homoclinic cycles.

**REFERENCES**


[1] MANDL F. and SHAW G., *Quantum Field Theory*, (John Wiley & Sons) 1993.

[2] ZINN-JUSTIN J., *Quantum Field Theory and Critical Phenomena*, (Clarendon Press) 2002.

[3] AMIT D. J. and MARTIN-MAYOR V., *Field Theory, the Renormalization Group and Critical Phenomena*, (World Scientific) 2005.

[4] GREINER W. and REINHARDT J., *Field Quantization*, (Springer-Verlag), 1993.

[5] SEGAL I. E., *Phys. Scrip*., **24** (1981) 827.

[6] VOLKOV M. K. and PERVUSHIN V. N., *Sov. Phys. USPEKHI*, **20** (1977) 89.

[7] HEISENBERG W., *Introduction to the unified field theory of elementary particles*, (Interscience Publishers) 1966.

[8] DZHUNUSHALIEV V. and SINGLETON D., *Phys. Rev. D* **65** (2002) 125007

[9] MIRANSKII V. A., *Dynamical Symmetry Breaking in Quantum Field Theories*, (World Scientific) 1993.

[10] WILCZEK F., *Rev. Mod. Phys.* **71** (1999) S85

[11] GOLDFAIN E., *Intl. Journal of Nonlinear Science and Numerical Simulation*, **6** (2005) 223.

[12] CROSS M. C. and HOHENBERG P.C., *Rev. Mod. Phys.* **65** (1993) 851.

[13] ARANSON I. S. and KRAMER L., *Rev. Mod. Phys*. **74** (2002) 99

[14] TSOY E. N. et al, *Phys. Rev. E* **73** (2006) 036621.

[15] HINRICHSEN H., *Physica* **A** 369 (2006) 1.

[16] FARIAS R. S. L. et al., *Nucl. Phys. A* **782** (2007) 33.

[17] JONA-LASINIO G. and MITTER P.K., *Comm. in Math. Phys*. **101** (1985) 409

[18] RYDER L., *Quantum Field Theory*, (Cambridge University Press) 1996.

[19] KRISTENSEN K. and MOLONEY N. R., *Complexity and criticality*, (Imperial College Press) 2005.

[20] BALLHAUSEN H. et al, *Phys. Lett.* **B** 582 (2004) 144.

[21] BALLHAUSEN H. *Renormalization Group Flow Equations and Critical Phenomena in Continuous Dimension and at Finite Temperature*, Doctoral Thesis, Faculty of Physics and Astronomy, Ruprecht-Karls-University Heidelberg, 2003.

[22] GOLDFAIN E., *Comm. in Nonlin. Science and Num. Simulation* **13** (2008) 666.

[23] GOLDFAIN E., to be published in *Comm. in Nonlin. Science and Num. Simulation*, doi:10.1016/j.cnsns.2006.12.007

[24] GOLDFAIN E., *Intl. Journal for Nonlinear Science* **3** (2007) 170.

[25] GOLDFAIN E., *Chaos, Solitons and Fractals* **28** (2006) 913.

[26] GOLLUB J. P. and LANGER J. S., *Rev. Mod. Phys.* **71** (1999) S396

[27] MAGNITSKII N. A. and SIDOROV E., *New Methods for Chaotic Dynamics* (World Scientific) 2007.

[28] MAGNITSKII N. A., *Communications in Nonlinear Science and Numerical Simulation* **13** (2007) 416.

[29] AKHROMEEVA T. S. et al, *Nonstationary Structures and Diffusion Chaos*, (Nauka-Moscow) 1992.

[30] GOLDFAIN E., Feigenbaum attractor and the generation structure of particle physics, in preparation at *Intl. Journal for Bifurcations and Chaos* **18** (2008).

[31] PARTICLE DATA GROUP, http://pdg.lbl.gov/2005/reviews/quarks_q000.pdf., 2005.

[32] ZASLAVSKY G. M., *Hamiltonian Chaos and Fractional Dynamics* (Oxford University Press) 2005.

[33] HALDANE F. D. M., *Phys. Rev. Lett.* **67** (1991) 937.

[34] NAYAK C. and WILCZEK F., *Phys. Rev. Lett.* **73** (1994) 2740.

[35] WESS J. and BAGGER J., *Supersymmetry and Supergravity*, (Princeton University Press) 1992.

[36] LARGE HADRON COLLIDER: Periodic updates on LHC may be located at http://public.web.cern.ch/Public/Content/Chapters/AboutCERN/CERNFuture/WhatLHC/WhatLHC-en.html

# DYNAMICS OF NEUTRINO OSCILLATIONS AND THE COSMOLOGICAL CONSTANT PROBLEM

**ERVIN GOLDFAIN**

Photonics Center of Excellence
Welch Allyn, Inc., 4619 Jordan Road
P. O. Box 187, Skaneateles Falls
N.Y. 13153-4064, U. S. A.
e-mail: ervingoldfain@hotmail.com; goldfaine@welchallyn.com

**Abstract**

The cosmological constant problem continues to represent a major challenge for theoretical physics and cosmology. The main difficulty arises from the large numerical discrepancy between observational limits of the cosmological constant and quantum predictions based on gravitational effects of the vacuum energy. In this work we argue that the experimental value of this constant may be recovered from the dynamics of neutrino oscillations.

## 1. Introduction

The cosmological constant problem (c.c.p) represents one of the major unresolved issues of contemporary physics [12]. A numerical discrepancy of about 120 orders of magnitude exists between the theoretical and observational values of this constant [2]. It is presumed that a presently unknown symmetry operates in such a way as to enforce a vanishingly small constant while remaining consistent with all accepted field-theoretic principles. Several competing models attempting to resolve the c.c.p coexist (for a review of some of the relevant literature on the subject see [7-9] and references listed in [9]).

In this paper we argue that the observational value of the cosmological constant emerges from the physics of neutrino oscillations. Although the idea is not new (see e.g., [1] and references therein), our treatment is built on a much simpler foundation. Unlike the approach taken by previous authors, the model discussed here is exclusively built on the relativistic dynamics of massive fermions, as expressed by the standard Pontercovo formula [4]. The paper is organized as follows: Section 2 highlights the quantum field viewpoint on the cosmological vacuum and its difficulties. The derivation of the cosmological constant from the dynamics of neutrino oscillations is discussed in Section 3. Concluding remarks are outlined in Section 4. Two appendix sections are included to make the paper self-contained. The first one is devoted to a brief review of c.c.p and the second one to a short introduction to the physics of neutrino oscillations and mixing.

## 2. Neutrino Oscillations as Vacuum Fluctuations on a Cosmic Scale

The quantum origin of the c.c.p arises because the zero-point vacuum energy diverges quadratically in the presence of gravitation. Standard Quantum Field Theory in Minkowski space-time discards the zero-point vacuum energy through the use of a normal time-ordering procedure [6]. Because vacuum energy gravitates and couples to all other field energies present at the quantum level, cancellation of the zero-point term is no longer possible when gravitation produces measurable effects.

We believe that the large discrepancy between theory and observations in c.c.p is rooted in the fundamental incompatibility of Quantum Field Theory and General Relativity with regard to the very interpretation of the concept of *vacuum*. The vacuum of General Relativity (v-*GR*) represents a state devoid of matter and energy on the macroscopic scale, whereas the vacuum of Quantum Field Theory (v-*QFT*) is associated with the lowest-lying state and the zero-point energy of all fields present at the quantum level. Thereby, in order to avoid the pitfalls of a full-blown quantum interpretation of the cosmological constant problem, we start from a different perspective and posit that neutrino oscillations represent experimental evidence for fluctuations of v-*GR*.

This argument is supported by the fact that, according to our current knowledge, neutrinos are the lightest and the most stable lepton states and that they are ultra-weakly coupled to ordinary matter.

### 3. Neutrino Oscillations and the Cosmological Constant

We start from the system of coupled first-order equations describing the evolution of neutrino mass eigenstates in matter [4]

$$\begin{pmatrix} \dot{\nu}_1^m \\ \dot{\nu}_2^m \end{pmatrix} = \begin{pmatrix} -\frac{\Delta(t)}{4iE} & -\dot{\theta}_m(t) \\ \dot{\theta}_m(t) & \frac{\Delta(t)}{4iE} \end{pmatrix} \begin{pmatrix} \nu_1^m \\ \nu_2^m \end{pmatrix}. \tag{1}$$

Here, $\nu_{1,2}^m(t)$ denote the neutrino mass eigenstates of energy $E$, $\Delta^2(t) \equiv \mu_2^2(t) - \mu_1^2(t)$ represents the time-dependent mass-squared difference in matter and $\theta_m(t)$ is the effective mixing angle in matter. The following relations hold

$$\Delta(t)^2 \equiv \mu_2^2(t) - \mu_1^2(t)$$

$$\mu_{1,2}^2(t) = \frac{m_1^2 + m_2^2}{2} + E(V_e + V_\alpha) \mp \frac{1}{2}\sqrt{(\Delta m_{12}^2 \cos 2\theta - A)^2 + (\Delta m_{12}^2 \sin 2\theta)^2}$$

$$\tan 2\theta_m(t) = \frac{\Delta m_{12}^2 \sin 2\theta}{\Delta m_{12}^2 \cos 2\theta - A(t)}$$

$$\dot{\theta}_m = \frac{\Delta m_{12}^2 \sin 2\theta}{2\Delta(t)^2}\dot{A}, \tag{2}$$

where $\mu_{1,2}(t)$ stands for the effective neutrino mass in matter, $\Delta m_{12}^2 = m_1^2 - m_2^2$ is the mass-squared difference in vacuum (see (B8)), $V_e(t)$ and $V_\alpha(t)$ are the effective interaction potentials for electron neutrino $\nu_e$ and the flavor eigenstate $\nu_\alpha$, respectively. $A(t)$ is given by

$$A(t) \equiv 2E[V_e(t) - V_\alpha(t)]. \tag{3}$$

Two opposite cases are of interest for analysis. When

$$\frac{\Delta(t)}{4E} \gg \dot{\theta}_m(t) = \frac{\Delta m_{12}^2 \sin 2\theta}{2\Delta(t)^2}\dot{A} \tag{4}$$

the mass eigenstates $\nu_{1,2}^{m}(t)$ mix in small amounts to produce the flavor eigenstates and this transition is referred to as *adiabatic*. Many neutrino oscillations take place in the adiabatic regime with few mixing events. Conversely, when (4) is not satisfied, the transition is said to be *non-adiabatic*. To simplify the ensuing derivation and without a significant loss of generality, we limit the analysis to propagation in low-density matter and expand both the mass-splitting $\Delta(t)$ and time-rate of the effective mixing angle $\dot{\theta}_{m}(t)$ as follows

$$\Delta(t) = \Delta m_{12} + P(t)$$

$$\dot{\theta}_{m}(t) = \varepsilon + Q(t) \tag{5}$$

in which $\varepsilon \ll 1$. The planar system of evolution equations (1) decouples into a time-independent and a time-dependent part

$$\begin{pmatrix} \dot{\nu}_1^m \\ \dot{\nu}_2^m \end{pmatrix} = \begin{pmatrix} -\dfrac{\Delta m_{12}}{4iE} & -\varepsilon \\ \varepsilon & \dfrac{\Delta m_{12}}{4iE} \end{pmatrix} \begin{pmatrix} \nu_1^m \\ \nu_2^m \end{pmatrix} + \begin{pmatrix} -\dfrac{P(t)}{4iE} & -Q(t) \\ Q(t) & \dfrac{P(t)}{4iE} \end{pmatrix} \begin{pmatrix} \nu_1^m \\ \nu_2^m \end{pmatrix}. \tag{6}$$

Local stability analysis of (6) indicates that the trivial equilibrium $\nu_1^m = \nu_2^m = 0$ represents an elliptic point since

$$Tr\begin{pmatrix} -\dfrac{\Delta m_{12}}{4iE} & -\varepsilon \\ \varepsilon & \dfrac{\Delta m_{12}}{4iE} \end{pmatrix} = 0. \tag{7}$$

The stability analysis is representative for the dynamics of the conservative system (6) near equilibrium because [9]

$$\det\begin{pmatrix} -\dfrac{\Delta m_{12}}{4iE} & -\varepsilon \\ \varepsilon & \dfrac{\Delta m_{12}}{4iE} \end{pmatrix} = \frac{\Delta m_2^{12}}{16E^2} + \varepsilon^2 \neq 0. \tag{8}$$

It is thus reasonable to assume that the time-dependent contribution corresponding to neutrino propagation in low-density matter may be neglected up to a first-order approximation. The time-independent term of (6) may be shown to be formally identical to the equation of a linear harmonic oscillator [3], that is,

$$\ddot{\nu}_1^m + \left[\frac{\Delta m_{12}^2}{16E^2} + \varepsilon^2\right]\nu_1^m = 0. \tag{9}$$

Stated differently, if $E$ sets the natural energy scale of neutrino physics in low-density matter, flavor transitions governed by (6) may be interpreted as harmonic oscillations of the mass eigenstate $\nu_1^m(t)$ with proper frequency and Compton wavelength

$$\omega_{12} = \Delta m_{12}/4$$

$$\lambda_C = (\Delta m_{12}/4)^{-1}. \tag{10}$$

Assuming that there is roughly one quasi-particle of mass $\Delta m_{12}$ per the unit volume defined by the Compton wavelength cubed $(\lambda_c^3)$, we derive the following expectation value for the cosmological vacuum density

$$\rho_\nu \sim \frac{\Delta m_{12}}{4\lambda_c^3} = \frac{1}{256}\Delta m_{12}^4. \tag{11}$$

Current testing data indicate that the solar neutrino mass splitting falls in the range [10]

$$\Delta m_{12,\,sol}^2 < 9.5 \times 10^{-5} eV^2. \tag{12}$$

Using (11) and (12) we estimate

$$\rho_\nu^{sol} < 3.525 \times 10^{-11} eV^4. \tag{13}$$

This value agrees well with the recent observational bound of the cosmological constant according to which [9, 13]

$$\rho_\Lambda = \Lambda/8\pi G \le 1.6 \times 10^{-11} eV^4. \tag{14}$$

## 4. Concluding Remarks

The starting point of this brief report was setting a primary distinction between the vacuum of General Relativity (v-*GR*) and the zero-point energy concept of QFT (v-*QFT*). Neutrino oscillations were

interpreted as direct evidence for fluctuations of (v-*GR*). Following this route, we were led to a numerical prediction that agrees well with current observational data. Analysis of neutrino oscillations in low-density matter has been carried out in the framework of Pontercovo's model and without any reference to gravitational effects generated by the zero-point energy.

## 5. Appendix A: The Cosmological Constant Problem

In the original formulation of general relativity, the differential equation relating the metric tensor $g_{\mu\nu}(x)$ and the matter distribution is given by

$$R_{\mu\nu} - \frac{1}{2} g_{\mu\nu} R = 8\pi G T_{\mu\nu}. \tag{A1}$$

Here, $R_{\mu\nu}(x)$ and $R(x)$ denote the Ricci tensor and its scalar trace, $G$ is Newton's gravitational constant and $T_{\mu\nu}$ the stress-energy tensor that translates the relevant properties of the matter in the universe. To ensure that the field equation (A1) describes a static universe model, Einstein's later proposal was to change it to

$$R_{\mu\nu} - \frac{1}{2} g_{\mu\nu} R - \Lambda g_{\mu\nu} = 8\pi G T_{\mu\nu}. \tag{A2}$$

Here, $\Lambda$ is called the *cosmological constant* and is measured in units of energy squared. Moving the cosmological term to the right-hand side of (A2) indicates that $\Lambda g_{\mu\nu}$ acts like an ideal fluid with effective mass density and pressure [11].

$$\rho_\Lambda = \frac{\Lambda}{8\pi G}$$

$$p_\Lambda = -\rho_\Lambda. \tag{A3}$$

From the viewpoint of general relativity, there is no preferred choice for the energy scale determined by $\Lambda$. As stated in Section 2, the situation is radically different in quantum field theory where the cosmological constant is interpreted as energy density of the vacuum. This identification enables one to compute the magnitude of various

contributions to the cosmological constant, including potential energies from scalar fields as well as zero-point fluctuations from degrees of freedom associated with each quantum field theory [2].

## 6. Appendix B: Brief Overview on the Physics of Neutrino Oscillations

Neutrino species are identified as *flavor* eigenstates $\nu_\alpha$ that are, in general, linear combinations of the *mass* eigenstates $\nu_i$

$$|\nu_\alpha\rangle = \sum_{i=1}^{n} U^*_{\alpha i}|\nu_i\rangle, \tag{B1}$$

where $n$ is the number of flavors and $U^*_{\alpha i}$ is an element of the mixing matrix [4]. In what follows, we use the standard plane wave approximation for time-dependent mass eigenstates

$$|\nu_i(t)\rangle = \exp(-iE_i t)|\nu_i(0)\rangle \tag{B2}$$

and assume that neutrinos are relativistic

$$E_i \approx p_i + \frac{m_i^2}{2E_i} \tag{B3}$$

with

$$p_i \approx p \approx E. \tag{B4}$$

Consider for simplicity the two-neutrino case in vacuum, i.e., in the absence of matter or radiation. It can be shown that the transition probability between a pair of flavors $\alpha$, $\beta$ takes the form

$$P_{\alpha\beta} = \delta_{\alpha\beta} - (2\delta_{\alpha\beta} - 1)\sin^2 2\theta \sin^2 x \tag{B5}$$

in which $\theta$ denotes the mixing angle. The mixing matrix corresponding to this case is given by

$$U = \begin{pmatrix} \cos\theta & \sin\theta \\ -\sin\theta & \cos\theta \end{pmatrix}. \tag{B6}$$

Here, $x$ is the normalized distance between the source (the production point of $\nu_\alpha$) and the detector (the detection point of $\nu_\beta$)

$$x = \frac{\Delta m_{12}^2 L}{4E}. \tag{B7}$$

$L$ represents the actual distance separating the source from the detector and

$$\Delta m_{12}^2 = m_1^2 - m_2^2 \tag{B8}$$

is the difference in mass-squares between mass eigenstates, otherwise referred to as "mass-splitting". The transition probability (B5) has an oscillatory behavior characterized by the oscillation length

$$L_{12}^0 = \frac{4\pi E}{\Delta m_{12}^2}. \tag{B9}$$

## References


[1] M. Blasone et al., Braz. J. Phys. 35 (2005), 455-461 and http://www.arxiv:hep-th/0412165.

[2] M. S. Carroll, http://www.livingreviews.org/lrr-2001-1.

[3] H. T. Davis, Introduction to Nonlinear Differential and Integral Equations, Dover Publications, New York, 1962.

[4] M. C. Gonzalez-Garcia and Y. Nir, http://www.arxiv:hep-ph/0202058.

[5] E. A. Jackson, Perspectives of Nonlinear Dynamics, Cambridge University Press, New York, 1992.

[6] M. Kaku, Quantum Field Theory, Oxford University Press, New York, 1993.

[7] D. E. Kaplan and R. Sundrum, http://www.arxiv:hep-th/0505265.

[8] A. D. Linde, Phys. Lett. B 200 (1988), 272.

[9] J. W. Moffat, http://www.arxiv:hep-th/0507020.

[10] R. N. Mohapatra, http://www.arxiv:hep-ph/0402035.

[11] P. J. E. Peebles, Principles of Physical Cosmology, Princeton University Press, New Jersey, 1993.

[12] S. Weinberg, Rev. Modern Phys. 61 (1989), 1.

[13] N. Wright, http://math.ucr.edu/home/baez/physics/Relativity/GR/cosConstant.html.

# Fractional dynamics and the Standard Model for particle physics

Ervin Goldfain *

*Photonics Center of Excellence, Welch Allyn Inc., 4619 Jordan Road, P.O. Box 187,*
*OptiSolve Consulting, 4422 Cleveland Road, Syracuse, NY 13215, USA*

Received 2 November 2006; received in revised form 20 December 2006; accepted 21 December 2006

**Abstract**

Fractional dynamics is an attractive framework for understanding the complex phenomena that are likely to emerge beyond the energy range of the Standard Model for particle physics (SM). Using fractional dynamics and complex-scalar field theory as a baseline, our work explores how physics on the high-energy scale may help solve some of the open questions surrounding SM. Predictions are shown to be consistent with experimental results.
© 2007 Elsevier B.V. All rights reserved.

*PACS:* 11.10.Hi; 11.10.Ef; 12.60.−i; 12.90.+b

*Keywords:* Renormalization Group flow; Fractional dynamics; Feigenbaum scaling; Standard model

## 1. Introduction and motivation

As of 2006, predictions derived from the Standard Model of elementary particles (SM) – a body of knowledge discovered in the early 1970s – agrees with all the experiments that have been conducted to date. Nevertheless, the majority of particle theorists feel that SM is not a complete framework, but rather an "effective field theory" that needs to be extended by new physics at some higher energy scale reaching in the TeV region. The most cited reasons for this belief are: (a) the recent discovery of neutrino oscillations and masses; (b) SM does not include the contribution of gravity and gravitational corrections to both quantum field theory and renormalization group (RG) equations; (c) SM does not fix the large number of free parameters that enter the theory (in particular the spectra of masses, gauge couplings and fermion mixing angles); (d) SM has a gauge hierarchy problem, which requires fine-tuning; (e) SM postulates that the origin of electroweak symmetry breaking is the Higgs mechanism, whose confirmation is sought in future accelerator experiments. The number and physical attributes of the Higgs boson are neither explained by SM nor fixed from first principles, (f) SM does not clarify the origin of its underlying $SU(3) \times SU(2) \times U(1)$ gauge group and why quarks and leptons occur in certain representations of this group, (g) SM does not explain why the weak interactions

* Corresponding author. Tel.: +1 315 469 0178.
*E-mail address:* ervingoldfain@hotmail.com

Please cite this article in press as: Goldfain E, Fractional dynamics and the Standard Model for particle physics, Commun Nonlinear Sci Numer Simul (2007), doi:10.1016/j.cnsns.2006.12.007

are chiral, that is, why only fermions with one handedness experience the force transmitted by the triplet of massive vector bosons $W^+$, $W^-$, $Z^0$.

Despite years of research on multiple fronts, there is currently no compelling and universally accepted resolution to the above-mentioned challenges. A large body of proposed extensions of SM exists, each of them attempting to resolve some unsatisfactory aspects of the theory while introducing new unknowns. Expanding on a series of recent contributions centered on RG, non-linear dynamics, chaos and fractal geometry [3,4,6–10,12–14,17–19], our work explores how the physics on the TeV regime may shed light onto some of the open questions surrounding SM.

The paper is organized as follows: Section 2 surveys the motivation for fractional dynamics in the far ultraviolet region of field theory. The principle of local scale invariance is briefly introduced in Section 4. Fractional dynamics of a ''toy'' model based on complex scalar fields is analyzed in Section 5. Sections 6–8 discuss how critical behavior in continuous dimension acts as source of massive field theories and makes connection to SM data. Concluding remarks are presented in the last section. We emphasize from the outset the introductory nature of our work. As such, its content is not aimed to be either entirely rigorous or formally complete. Independent research efforts are required to confirm, develop or disprove these preliminary results.

## 2. Fractional dynamics and the far ultraviolet region of field theory

It is generally believed that quantum field theory breaks down near the so-called Cohen–Kaplan threshold of $\sim$100 TeV as a result of exposure to large vacuum fluctuations and strong-gravitational effects. No convenient redefinition of observables is capable of turning off the dynamic contribution of these effects. For instance, it is known that the zero-point vacuum energy diverges quadratically in the presence of gravitation. Quantum field theory in Euclidean space-time discards the zero-point vacuum energy through the use of a normal time ordering procedure [5,20]. Because vacuum energy is gravitating and couples to all other field energies present at the quantum level, cancellation of the zero-point term is no longer possible when gravitational effects are significant. Likewise, this strong coupling regime of the far ultraviolet region suggests that even asymptotically free theories such as QCD reverse their properties in response to arbitrarily large non-perturbative effects. In fact, complex dynamics of quark-gluon plasma is expected to arise near the so-called transition temperature [16].

The non-linearity of the underlying field theory combined with the far-from-equilibrium dynamics induced by highly unstable vacuum fluctuations are prone to lead to self-organized criticality [6]. Because dynamical instabilities can develop on long time-scales, the macroscopic description of phenomena in terms of conventional differential operators breaks down. This is, in essence, the main argument for using fractal operators in the far TeV region of field theory and for the passage from ordinary to fractional dynamics [14,18,19,21]. Since application of fractals in contemporary physics has become far ranging, the interest in fractional dynamics has grown at a steady pace in the last decade. There is now a broad range of applications of fractional dynamics in research areas where fractal attributes of underlying processes and the onset of long-range correlations demand the use of fractional calculus. These areas include, but are not limited to, wave propagation in complex and porous media, models of systems with chaotic and pseudo-chaotic dynamics, random walks with memory, colored noise and pattern formation, anomalous transport and Levy flights, studies of scaling phenomena and critical behavior, plasma physics, turbulence, quantum field theory, far-from-equilibrium statistical models, complex dynamics of data networks and so on (for a brief review of current applications, see [21–26]).

## 3. Conventions and assumptions

(a) Einstein summation convention is applied throughout.
(b) The Poincare index is denoted by $\mu = 0, 1, 2, 3$.
(c) We study a basic ''toy'' model containing a single pair of massive complex-scalar fields $\varphi(x)$, $\varphi^*(x)$.
(d) The analysis is carried out exclusively at the classical level. Suppression of quantum attributes and transition to classical behavior is the result of decoherence induced by steady exposure to large random fluctuations [27,28].

(e) Following [22–26] we use in our work the left Caputo fractional derivative defined as

$$D^{\alpha}\varphi(x) \doteq \frac{1}{\Gamma(n-\alpha)}\int_0^x \frac{\varphi^{(n)}(s)}{(x-s)^{\alpha+1-n}}\mathrm{d}s \tag{1}$$

where $n-1<\alpha<n$ and $\varphi^{(n)}(s) \doteq \mathrm{d}^n\varphi(s)/\mathrm{d}s^n$. We note that, in addition to using (1), many studies based on fractional calculus often start from alternative operators such as Riemann–Liouville and Grunwald–Letnikov derivatives and integrals (see [30–33] for details).

(f) Space–time variables and fields are suitably normalized as dimensionless observables.

(g) Assuming that the field dynamics has low-level fractionality, we use the so-called $\varepsilon$-expansion to perform the transition from first order to Caputo derivatives of order $\alpha \doteq 1-\varepsilon$ according to the prescription [22]

$$\begin{aligned} &D^{1-\varepsilon}\varphi(x) = \partial\varphi(x) + \varepsilon D_1\varphi(x)\\ &D_1\varphi(x) \doteq \partial\varphi(0)\ln|x| + \gamma\partial\varphi(x) + \int_0^x \partial^2\varphi(s)\ln|x-s|\mathrm{d}s \end{aligned} \tag{2}$$

## 4. Local scale invariance at the onset of fractional dynamics

The novel symmetry principle that underlies the onset of fractional dynamics in the TeV region is the *local scale invariance* of the theory [17]. There is a two-fold rationale for the onset of this symmetry, namely,

(a) Field dynamics is *scale-invariant*. This is equivalent to stating that, in dimensional regularization scheme, the outcome of the regularization procedure does not depend on the particular choice of $\varepsilon = 4-d$ [20].

(b) By analogy with the definition of the Lipschitz–Hölder exponent and to ensure compliance with relativity [14,17], we take the continuous dimension parameter $\varepsilon$ to denote a *locally* defined function of space-time coordinates, $\varepsilon(x)$. In addition, we assume that $\varepsilon(x)$ may be expressed either as a *contravariant* $\varepsilon^i(x)$ or a *covariant* $\varepsilon_i(x)$ four-vector. This motivates us to formally extend (2) to

$$\begin{aligned} &D^{1-\varepsilon_\mu(x)}\varphi(x) = \partial^\mu\varphi(x) + \varepsilon^\mu(x)D_1^\mu\varphi(x)\\ &D_1^\mu\varphi(x) \doteq \partial^\mu\varphi(0)\ln|x| + \gamma\partial^\mu\varphi(x) + \int_0^x (\partial^2)^\mu\varphi(s)\ln|x-s|\mathrm{d}s\\ &D_{1-\varepsilon_\mu(x)}\varphi(x) = \partial_\mu\varphi(x) + \varepsilon_\mu(x)D_{1,\mu}\varphi(x)\\ &D_{1,\mu}\varphi(x) \doteq \partial_\mu\varphi(0)\ln|x| + \gamma\partial_\mu\varphi(x) + \int_0^x (\partial^2)_\mu\varphi(s)\ln|x-s|\mathrm{d}s \end{aligned} \tag{3}$$

## 5. Fractional dynamics of the complex-scalar field

The goal of this section is to show that the principle of local scale invariance and the introduction of fractional dynamics lead to a mechanism of gauge boson-fermion unification that is fundamentally distinct from the mechanism advocated by supersymmetry.

The Lagrangian density of our model is

$$L \doteq \partial_\mu\varphi(x)\partial^\mu\varphi^*(x) - m^2\varphi^*(x)\varphi(x) \tag{4}$$

where $m$ the mass of the field and $x$ is a shorthand notation for $(x^\mu)$ or $(x_\mu)$. Using the framework of Caputo derivatives and $\varepsilon$-expansion [22], one obtains

$$L \doteq D_\mu^{1-\varepsilon(x)}\varphi(x)D^{\mu,1-\varepsilon(x)}\varphi^*(x) - m^2\varphi^*(x)\varphi(x) \tag{5}$$

where the locally defined infinitesimal dimension $\varepsilon(x)$ satisfies the condition $\varepsilon(x)\cdot x \ll 1$. Our aim is to show that, in contrast with conventional field theory embodied in (4), use of Caputo derivatives guarantees invariance under local gauge transformations *without* the explicit need for gauge fields and covariant operators. To this end, let us perform the local phase change

$$\varphi(x) \to \mathrm{e}^{\mathrm{i}\alpha(x)}\varphi(x)$$
$$\varphi^*(x) \to \mathrm{e}^{-\mathrm{i}\alpha(x)}\varphi^*(x) \tag{6}$$

Up to a first-order approximation, Caputo derivatives transform as [22]

$$D_\mu^{1-\varepsilon(x)}\varphi(x) \to D_\mu^{1-\varepsilon(x)}[\mathrm{e}^{\mathrm{i}\alpha(x)}\varphi(x)] = \partial_\mu[\mathrm{e}^{\mathrm{i}\alpha(x)}\varphi(x)] + \varepsilon(x)D_{1,\mu}^{1}[\mathrm{e}^{\mathrm{i}\alpha(x)}\varphi(x)]$$
$$D^{1-\varepsilon(x),\mu}\varphi^*(x) \to D^{1-\varepsilon(x),\mu}[\mathrm{e}^{-\mathrm{i}\alpha(x)}\varphi^*(x)] = \partial^\mu[\mathrm{e}^{-\mathrm{i}\alpha(x)}\varphi^*(x)] + \varepsilon(x)D_1^{1,\mu}[\mathrm{e}^{-\mathrm{i}\alpha(x)}\varphi^*(x)] \tag{7}$$

where

$$D_{1,\mu}^{1}(x) \doteq \ln|x|\partial_\mu[\mathrm{e}^{\mathrm{i}\alpha(0)}\varphi(0)] + \int_0^x \partial_\mu^2[\mathrm{e}^{\mathrm{i}\alpha(\lambda)}\varphi(\lambda)]\ln|x-\lambda|\mathrm{d}\lambda + \gamma\partial_\mu[\mathrm{e}^{\mathrm{i}\alpha(x)}\varphi(x)]$$
$$D_1^{1,\mu}(x) \doteq \ln|x|\partial^\mu[\mathrm{e}^{-\mathrm{i}\alpha(0)}\varphi^*(0)] + \int_0^x \partial^{2,\mu}[\mathrm{e}^{-\mathrm{i}\alpha(\lambda)}\varphi^*(\lambda)]\ln|x-\lambda|\mathrm{d}\lambda + \gamma\partial^\mu[\mathrm{e}^{-\mathrm{i}\alpha(x)}\varphi^*(x)] \tag{8}$$

in which $\gamma$ stands for the Euler constant and

$$\partial_\mu[\mathrm{e}^{\mathrm{i}\alpha(x)}\varphi(x)] = \mathrm{e}^{\mathrm{i}\alpha(x)}[\partial_\mu + \mathrm{i}\partial_\mu\alpha(x)]\varphi(x) \tag{9}$$

Local gauge invariance of (5) is preserved if Caputo derivatives transform covariantly, that is

$$D_\mu^{1-\varepsilon(x)}[\mathrm{e}^{\mathrm{i}\alpha(x)}\varphi(x)] = \mathrm{e}^{\mathrm{i}\alpha(x)}D_\mu^{1-\varepsilon(x)}\varphi(x)$$
$$D^{\mu,1-\varepsilon(x)}[\mathrm{e}^{-\mathrm{i}\alpha(x)}\varphi^*(x)] = \mathrm{e}^{-\mathrm{i}\alpha(x)}D^{\mu,1-\varepsilon(x)}\varphi^*(x) \tag{10}$$

On account of (7) and (10), we arrive at the following set of conditions:

$$\mathrm{i}\mathrm{e}^{\mathrm{i}\alpha(x)}\varphi(x)\partial_\mu\alpha(x) = \varepsilon(x)\{D_{1\mu}^{1}[\mathrm{e}^{\mathrm{i}\alpha(x)}\varphi(x)] - \mathrm{e}^{\mathrm{i}\alpha(x)}D_{1\mu}^{1}\varphi(x)\}$$
$$(-\mathrm{i})\mathrm{e}^{-\mathrm{i}\alpha(x)}\varphi^*(x)\partial_\mu\alpha(x) = \varepsilon(x)\{D_1^{1,\mu}[\mathrm{e}^{-\mathrm{i}\alpha(x)}\varphi^*(x)] - \mathrm{e}^{-\mathrm{i}\alpha(x)}D_1^{1,\mu}\varphi^*(x)\} \tag{11}$$

The direct consequence of (11) is that gauge fields *are no longer required* in a field theory built on fractional dynamics. The compensating role of the vector bosons is played by the *continuous dimension parameter* $\varepsilon(x)$. This conclusion is consistent with previous studies [14,17,19] and points to a novel unification mechanism of gauge boson and fermion fields, including classical gravitation. This mechanism is fundamentally different from the unification scheme postulated by supersymmetry and related quantum field models [20].

## 6. Emergence of massive field theories

It is known that, allowing elementary particles to have non-zero masses in quantum field theory violates local gauge and weak isospin symmetries imposed on the standard model lagrangian. The mechanism of so-called spontaneous symmetry breaking (SSB) posits that the vacuum itself acquires a non-zero charge distribution that leaves the Lagrangian invariant and generates both fermion and vector boson masses [5,20]. In SM, massive fermions exist in both left-handed and right-handed states. The only Dirac field operators that yield a non-vanishing mass are bilinear products of fields having the form

$$m\bar{\psi}\psi = m(\bar{\psi}_\mathrm{R}\psi_\mathrm{L} + \bar{\psi}_\mathrm{L}\psi_\mathrm{R}) \tag{12}$$

However, such mass terms mix right and left-handed spinors and are forbidden from the Lagrangian on account of violation of the weak isospin symmetry [5,20]. Stated differently, since $\psi_\mathrm{L}$ represents a SU(2) doublet and $\psi_\mathrm{R}$ a SU(2) singlet, the product of the two is not a singlet, as it ought to be in order to preserve the weak isospin symmetry. An immediate question that arises from the previous section is whether or not SSB still exists in a field theory based on fractional dynamics. Stated differently, can mass terms be introduced in the Lagrangian without violating local and weak isospin symmetries? To answer this question, we note that the first-order Caputo operator may be defined either from the "left" or from the "right" and, in general, the effect produced by $D^{1-\varepsilon(x)}$ is not identical with the effect produced by $D^{1+\varepsilon(x)}$. It follows that the proper description

of fractional differentiation requires a *doublet* of Caputo operators $\begin{pmatrix} D^{1-\varepsilon_{\rm L}(x)} \\ D^{1+\varepsilon_{\rm R}(x)} \end{pmatrix}$ and a *doublet* of scalars $\begin{pmatrix} \varepsilon_{\rm L}(x) \\ \varepsilon_{\rm R}(x) \end{pmatrix}$ with $\varepsilon_{\rm L,R}(x)\cdot x \ll 1$. Therefore, mass terms that correspond to Dirac bilinears assume the form:

$$\begin{gathered} \psi \to D^{-\varepsilon_L}\psi \quad \text{or} \quad \psi \to D^{\varepsilon_R}\psi \quad \text{for singlets} \\ (\,\psi_1 \quad \psi_2\,) \to \begin{pmatrix} D^{-\varepsilon_L} \\ D^{+\varepsilon_R} \end{pmatrix} (\,\psi_1 \quad \psi_2\,) \quad \text{and} \quad \begin{pmatrix} \psi_1 \\ \psi_2 \end{pmatrix} \to (\,D^{-\varepsilon_L} \quad D^{+\varepsilon_R}\,) \begin{pmatrix} \psi_1 \\ \psi_2 \end{pmatrix} \quad \text{for doublets} \end{gathered} \tag{13}$$

It can be seen that these mass terms automatically preserve the weak isospin symmetry in a similar manner in which the Higgs scalar doublet works in the electroweak model [5,20,29].

## 7. Critical behavior in continuous dimension

The previous sections have shown that the concept of dimension takes on a key role in the far ultraviolet region of field theory. Here we elaborate on this conjecture by making connection to the philosophy of the renormalization group and critical behavior in continuous dimension [1,2]. To streamline the derivation, we refer in what follows to the original Lagrangian (4). Let us start by adding a potential term to (4), that is

$$L \doteq \partial_\mu \varphi(x) \partial^\mu \varphi^*(x) - m^2 \varphi^*(x)\varphi(x) + \lambda^2 [\varphi^*(x)\varphi(x)]^2 \tag{14}$$

Here $g = \lambda^2$ represents the self-interaction strength of the field. According to the renormalization group, the so-called beta-function defines how $g$ "flows" with the sliding energy scale $\mu$, that is

$$\beta(g) \doteq \frac{{\rm d}(g)}{{\rm d}t} \tag{15}$$

where

$$t \doteq \ln\left(\frac{\mu}{\mu_0}\right) \tag{16}$$

for an arbitrary reference scale $\mu_0$. In the basin of attraction of a critical point $t_{\rm c}$ the field correlation length scales as

$$\xi \approx |t - t_{\rm c}|^{\nu} \tag{17}$$

Here, critical exponent $\nu$ is given by [1,2]

$$\nu^{-1} = -\left.\frac{\partial\beta}{\partial(g)}\right|_{g=g^*} \tag{18}$$

and $g^*$ stands for a fixed point of the beta-function, $\beta(g^*) = 0$.

One can exploit the interchangeable roles played by the sliding scale $t$ and the dimension parameter $d(x)$ as follows. Assume that $d_{\rm c}$ represents the critical dimension for which $g$ flows into the fixed point $g^*$. The mass of the complex-scalar field is known to be inversely proportional to the divergent correlation length and vanishes identically at the fixed point [1,2]

$$m[g^*(d_{\rm c}), d_{\rm c}] = 0 \tag{19}$$

In the basin of attraction of $g^*$ the field develops mass according to the power law

$$m[g^*(d_{\rm c}), d(x) - d_{\rm c}] \approx |d(x) - d_{\rm c}|^{\nu(d_{\rm c})} = |\varepsilon(x)|^{\nu(d_{\rm c})} \tag{20}$$

where

$$\nu^{-1}(d_{\rm c}) = -\left.\frac{\partial\beta}{\partial(g)}\right|_{g^*(d_{\rm c})} \tag{21}$$

We are led to conclude that, as the fixed point is asymptotically approached and the continuous space-time dimensionality collapses to $d(x) \to d_{\rm c} = 1, 2, 3, 4$, the complex-scalar field becomes massless, in agreement with

conventional quantum field theory. Numerical analysis yields $v(d_c) = 0.5$ for $d_c = 1, 2, 3, 4$ which is found to match well the value reported in the literature [1,2].

An important observation is now in order. Following the universal properties of the RG flow near the onset of chaos in low-dimensional maps, the dimensional control parameter $\varepsilon(x) = |d_c - d(x)|$ is expected to asymptotically approach the critical value $\varepsilon_\infty = 0$ according to the geometric progression [15]:

$$\varepsilon_n(x) - \varepsilon_\infty \approx a_n(x) \cdot \delta^{-n} \tag{22}$$

in which $n \gg 1$ is the index defining the number of iteration steps, $\delta$ stands for a scaling constant that is representative for the class of dynamical maps under consideration and $a_n(x)$ is a coefficient which becomes asymptotically independent of $n$ and $x$, that is, $a_\infty = a$. Substituting (22) in (20) produces to the mass scaling series

$$m_n[g^*(d_c), d_c - d_n(x)] \approx [a_n \delta^{-n}]^{1/2} \tag{23}$$

We may go a step further and state that, given the generic link between the coupling flow and the corresponding flows of masses and fields in RG [5,20,29], similar scaling pattern develops for $g_n$ and the underlying fields of the theory, $\eta_n$. We thus expect to obtain, for $n \gg 1$

$$\begin{aligned} g_n - g^*(d_c) &\approx \delta^{-\lambda(d_c)n} \\ \eta_n - \eta^*(d_c) &\approx \delta^{-\zeta(d_c)n} \end{aligned} \tag{24}$$

where $\lambda(d_c)$ and $\zeta(d_c)$ represent two additional critical exponents dependent on $d_c$.

## 8. Universal scaling of fermion masses

Period-doubling bifurcations are defined by $n = 2^m$, with $m > 1$ [15]. Replacing in (23) yields the following mass series:

$$m_m(x) \approx \sqrt{a_{2^m}(x)} \cdot \delta^{-2^{m-1}} \tag{25}$$

where $\delta = 4.669\ldots$ represents the Feigenbaum constant for the onset of chaos in quadratic maps. The ratio of two arbitrary masses is therefore

$$\frac{m_l(x)}{m_m(x)} \approx \sqrt{\frac{a_{2^l}(x)}{a_{2^m}(x)}} \cdot \frac{\delta^{-2^{l-1}}}{\delta^{-2^{m-1}}} \tag{26}$$

where $\lim \frac{a_l}{a_m} = 1$ as $l, m \to \infty$. Thus, for two sufficiently distant consecutive terms in the mass series, the dependence of $a_n(x)$ on the space-time variable may be suppressed and we obtain

$$\frac{m_l}{m_{l+1}} \approx \sqrt{\frac{a_{2^l}}{a_{2^{l+1}}}} \cdot \delta^{2^{l-1}} = \sqrt{a_{2^l,2^{l+1}}} \cdot \delta^{2^{l-1}} \tag{27}$$

It is important to emphasize that (27) provides only a *first-order approximation* considering that (a) (27) is less accurate if the iteration index is not large enough, that is, if $l \approx \mathrm{O}(1)$, (b) there is a fair amount of uncertainty involved in determining the quark mass spectrum [11]. Numerical results derived from (27) are displayed in Table 1. This table contains a side-by-side comparison of estimated versus actual mass ratios for charged leptons and quarks and a similar comparison of gauge coupling ratios. All masses and couplings are evaluated at the energy scale given by the top quark mass. Quark masses are averaged using the most recent reports issued by the Particle Data Group [11]. Specifically, $m_u = 2.12$ MeV; $m_d = 4.22$ MeV; $m_s = 80.9$ MeV; $m_c = 630$ MeV; $m_b = 2847$ MeV; $m_t = 170{,}800$ MeV.

The scaling sequence of charged leptons and quarks may be graphically summarized with the help of the following diagrams:

Table 1
Fermion masses and coupling ratios

| Scaling ratio | $2^{l-1}$ | Experimental value | Estimated value |
|---|---|---|---|
| $m_u/m_c$ | 4 | $3.365\times10^{-3}$ | $2.104\times10^{-3}$ |
| $m_c/m_t$ | 4 | $3.689\times10^{-3}$ | $2.104\times10^{-3}$ |
| $m_d/m_s$ | 2 | 0.052 | 0.046 |
| $m_s/m_b$ | 2 | 0.028 | 0.046 |
| $m_e/m_\mu$ | 4 | $4.745\times10^{-3}$ | $2.104\times10^{-3}$ |
| $m_\mu/m_\tau$ | 2 | 0.061 | 0.046 |
| $(\alpha_{EM}/\alpha_W)^2$ | 2 | 0.045 | 0.046 |
| $(\alpha_{EM}/\alpha_s)^2$ | 4 | $2.368\times10^{-3}$ | $2.104\times10^{-3}$ |

$$\overbrace{d\quad s}^{\delta^2}\qquad \overbrace{s\quad b}^{\delta^2}$$

$$\overbrace{u\quad c}^{\delta^4}\qquad \overbrace{c\quad t}^{\delta^4}$$

$$\overbrace{e\quad \mu}^{\delta^4}\qquad \overbrace{\mu\quad \tau}^{\delta^2}$$

$$\overbrace{\alpha_{EM}^2\qquad \alpha_W^2}^{\delta^2}\qquad \overbrace{\alpha_W^2\qquad \alpha_s^2}^{\delta^2}$$

Based on the above scheme, one may infer that neutrinos masses are arranged according to the possible pattern:

$$\overbrace{\nu_e\quad \nu_\mu}^{\delta^{16}}\qquad \overbrace{\nu_\mu\quad \nu_\tau}^{\delta^4}$$

It is also instructive to note that quarks and charged leptons follow a different period doubling path. To this end, let us organize the charged lepton and quark masses in a collection of triplets, that is

$$m_l \doteq [\, m_e \quad m_\mu \quad m_\tau \,], \quad m_q \doteq \begin{bmatrix} m_u & m_d \\ m_c & m_s \\ m_t & m_b \end{bmatrix} \tag{28}$$

It can be seen that the mass scaling for adjacent quarks stays constant within either one of the triplets $(u, c, t)$ or $(d, s, b)$, whereas the mass scaling for charged leptons varies as a geometric series in $\delta^2$ within the triplet $(e, \mu, \tau)$. This finding points out toward a symmetry breaking mechanism that segregates lepton and quark phases in the process of cooling from the far ultraviolet region of field theory to the low-energy region of SM.

## 9. Concluding remarks

We have argued that fractional dynamics represents an analytic framework suitable for the description of physical phenomena that are likely to arise in the TeV realm of particle physics. Unlike conventional quantum field theory, fractional dynamics describes far-from-equilibrium statistical processes that give rise to manifest scale invariance, non-local correlations and extensive symmetry breaking. Using fractional dynamics and the benchmark example of complex-scalar field theory, we have explored the potential spectrum of phenomena that may to emerge beyond the energy range of SM. Based on this framework, we have shown that, near the asymptotic boundary of field theory, (a) gauge bosons and fermions become unified through a fundamen-

tally different mechanism than the one advocated by supersymmetry; (b) SSB and the emergence of massive field theories occur as a result of critical behavior in continuous dimension; (c) particles develop a family structure that is tied to the universal transition to chaos in unimodal maps. First-order predictions were found to match reasonably well current experimental data. However, as pointed out in Section 1, our goal is not to formulate a comprehensive solution to the host of open challenges surrounding SM. Concurrent research efforts are needed to confirm or falsify these preliminary findings. In particular, the long-awaited operation of the Large Hadron Collider and similar high-energy accelerator sites should soon produce experimental evidence that backs or disproves our model.

## References


[1] Ballhausen H, Berges J, Wetterich C. Critical behavior in continuous dimension. Phys Lett B 2004;582:144–50.
[2] Ballhausen H. Renormalization group flow equations and critical phenomena in continuous dimension and at finite temperature, Doctoral Thesis, Faculty of Physics and Astronomy, Ruprecht-Karls-University Heidelberg.
[3] Morozov A, Niemi AJ. Can renormalization group flow end in a big mess? Nucl Phys B 2003;666:311–36.
[4] Damgaard PH, Thorleifsson G. Chaotic renormalization-group trajectories. Phys Rev A 1991;44:2378–741.
[5] See e.g. Ryder LH. Quantum field theory. Cambridge University Press; 1996.
[6] El Naschie MS. The VAK of vacuum fluctuation, spontaneous self-organization and complexity interpretation of high-energy particle physics and the mass spectrum. Chaos Soliton Fract 2003;18:401–20.
[7] El Naschie MS. Elementary prerequisites for *E*-infinity. Chaos Soliton Fract 2006;30:579–605.
[8] El Naschie MS. A review of *E*-infinity theory and the mass spectrum of high-energy particle physics. Chaos Soliton Fract 2004;19:209–36.
[9] El Naschie MS. On the universality class of all universality classes and *E*-infinity space–time physics. Chaos Soliton Fract 2006. doi:10.1016/j.chaos.2006.08.017.
[10] El Naschie MS. Feigenbaum scenario for turbulence and Cantorian *E*-infinity theory of high-energy particle physics. Chaos Soliton Fract 2006. doi:10.1016/j.chaos.2006.08.014.
[11] Particle Data Group. <http://pdg.lbl.gov/2005/reviews/quarks_q000.pdf>.
[12] Goldfain E. Derivation of lepton masses from the chaotic regime of the linear σ-model. Chaos Soliton Fract 2002;14:1331–40.
[13] Goldfain E. Feigenbaum scaling, Cantorian space–time and the hierarchical structure of standard model parameters. Chaos Soliton Fract 2006;30:324–31.
[14] Goldfain E. Fractional dynamics and the TeV regime of field theory. doi:10.1016/j.cnsns.2006.06.001.
[15] McCauley JL. Chaos, dynamics and fractals. An algorithmic approach to deterministic chaos. Cambridge Univ. Press; 1993.
[16] Cheng M et al. Transition temperature in QCD. Phys Rev D 2006;74:054507.
[17] Goldfain E. Local scale invariance, cantorian space–time and unified field theory. Chaos Soliton Fract 2005;23:701–10.
[18] Goldfain E. Complexity in quantum field theory and physics beyond the standard model. Chaos Soliton Fract 2006;28:913–22.
[19] Goldfain E. Complex dynamics and the high-energy regime of quantum field theory. Int J Nonlinear Sci Numer Simul 2005;6(3):223–34.
[20] Kaku M. Quantum field theory, a modern introduction. Oxford University Press; 1993.
[21] West BJ, Bologna M, Grigolini P. Physics of fractal operators. Springer; 2003.
[22] Tarasov VE, Zaslavsky GM. Dynamics with low-level fractionality. <http://arxiv:physics/0511138>.
[23] Tarasov VE. Fractional generalization of gradient and Hamiltonian systems. J Phys A 2005;38(26):5929–43.
[24] Tarasov VE, Zaslavsky GM. Fractional dynamics of coupled oscillators with long-range interaction. <http://arxiv:nlin.PS/0512013>.
[25] Laskin N, Zaslavsky GM. Nonlinear fractional dynamics on a lattice with long range interactions. <http://arxiv:nlin.SI/0512010>.
[26] Tarasov VE, Zaslavsky GM. Fractional Ginzburg-Landau equation for fractal media. <http://arxiv:physics/0511144>.
[27] E Joos et al. Decoherence and the appearance of a classical world in quantum theory. 2nd ed. Springer; 2003.
[28] Schlosshauer M. Decoherence, the measurement problem, and interpretations of quantum mechanics. Rev Mod Phys 2004;76:1267–305.
[29] Donoghue JF et al. Dynamics of the standard model. Cambridge University Press; 1994.
[30] Samko SG et al. Fractional integrals and derivatives; theory and applications. New York: Gordon and Breach; 1993.
[31] Oldham KB, Spannier J. Fractional calculus. New York: Academic Press; 1974.
[32] Miller KS, Ross B. An introduction to fractional calculus and fractional differential equations. New York: Wiley and Sons; 1993.
[33] Podlubny I. Fractional differential equations. New York: Academic Press; 1999.

# A New Possible Form of Matter, Unmatter – Formed by Particles and Anti-Particles

Dr. Florentin Smarandache
University of New Mexico
200 College Road
Gallup, NM 87301, USA.
E-mail: smarand@unm.edu

**Abstract.**
Besides *matter* and *antimatter* there must exist an intermediate form of matter, called *unmatter* (as a new form of matter) in accordance with the neutrosophy theory that between an entity <A> and its opposite <AntiA> there exist intermediate entities <NeutA>.
Unmatter is neither matter nor antimatter, but something in between. An atom of unmatter is formed either by (1): electrons, protons, and antineutrons, or by (2): antielectrons, antiprotons, and neutrons.
In a physics lab it will be possible to test the production of unmatter.
The existence of unmatter in the universe has a similar chance to that of the antimatter, and its production also difficult for present technologies.

## 1. Introduction.

This article is an improved version of an old manuscript [5].
According to the neutrosophy theory in philosophy [see 4], between an entity <A> and its opposite <AntiA> there exist intermediate entities <NeutA> which are neither <A> nor <AntiA>.
Thus, between "matter" and "antimatter" there must exist something which is neither matter nor antimatter, let's call it UNMATTER.
In neutrosophy, <NonA> is what is not <A>, i.e. <NonA> = <AntiA>$\chi$<NeutA>. Then, in physics, NONMATTER is what is not matter, i.e. nonmatter means antimatter together with unmatter.

## 2. Classification.

A) **Matter** is made out of electrons, protons, and neutrons.
Each matter atom has electrons, protons, and neutrons, except the atom of ordinary hydrogen which has no neutron.
The number of electrons is equal to the number of protons, and thus the matter atom is neutral.

B) Oppositely, the **antimatter** is made out of antielectrons, antiprotons, and antineutrons.
Each antimatter atom has antielectrons (positrons), antiprotons, and antineutrons, except the antiatom of ordinary hydrogen which has no antineutron.

The number of antielectrons is equal to the number of antiprotons, and thus the antimatter atom is neutral.

C) **Unmatter** means neither matter nor antimatter, but in between, an entity which has common parts from both of them.
Etymologically "un-matter" comes from [ME < OE, akin to Gr. *an-*, *a-*, Latin *in-*, and to the negative elements in *no*, *not*, *nor*] and [ME *matière* < OFr < Latin *materia*] matter [see 6], signifying no/without/off the matter.
There are two types of unmatter atoms, that we call unatoms:

u1) the first type is derived from matter; and a such unmatter atom is formed by electrons, protons, and antineutrons;

u2) the second type is derived from antimatter, and a such unmatter atom is formed by antielectrons, antiprotons, and neutrons.

One unmatter type is oppositely charged with respect to the other, so when they meet they annihilate.
The unmatter nucleus, called **unnucleus**, is formed either by protons and antineutrons in the first type, or by antiprotons and neutrons in the second type.

The charge of unmatter should be neutral, as that of matter or antimatter.
The charge of un-isotopes will also be neutral, as that of isotopes and anti-isotopes.
But, if we are interested in a negative or positive charge of un-matter, we can consider an un-ion. For example an anion is negative, then its corresponding unmatter of type 1 will also be negative. While taking a cation, which is positive, its corresponding unmatter of type 1 will also be positive.

Sure, it might be the question of how much *stable* the unmatter is, as J. Murphy pointed out in a private e-mail. But Dirac also theoretically supposed the existence of antimatter in 1928which resulted from Dirac's mathematical equation, and finally the antimatter was discovered/produced in large accelerators in 1996 when it was created the first atom of antihydrogen which lasted for 37 nanoseconds only.

There does not exist an unmatter atom of ordinary hydrogen, neither an unnucleus of ordinary hydrogen since the ordinary hydrogen has no neutron. Yet, two isotopes of the hydrogen, *deuterium* ($^2$H) which has one neutron, and artificially made *tritium* ($^3$H) which has two neutrons have corresponding unmatter atoms of both types, *un-deuterium* and *un-tritium* respectively. The isotopes of an element X differ in the number of neutrons, thus their nuclear mass is different, but their nuclear charges are the same.

For all other matter atom X, there is corresponding an antimatter atom and two unmatter atoms
The unmatter atoms are also neutral for the same reason that either the number of electrons is equal to the number of protons in the first type, or the number of antielectrons is equal to the number of antiprotons in the second type.
If antimatter exists then a higher probability would be for the unmatter to exist, and reciprocally.

Unmatter atoms of the same type stick together form an **unmatter molecule** (we call it **unmolecule**), and so on. Similarly one has two types of unmatter molecules.

The *isotopes* of an atom or element X have the same atomic number (same number of protons in the nucleus) but different atomic masses because the different number of neutrons.
Therefore, similarly the **un-isotopes of type 1** of X will be formed by electrons, protons, and antineutrons, while the **un-isotopes of type 2** of X will be formed by antielectrons, antiprotons, and neutrons.

An *ion* is an atom (or group of atoms) X which has last one or more electrons [and as a consequence carries a negative charge, called *anion*], or has gained one or more electrons [and as a consequence carries a positive charge, called *cation*].
Similarly to isotopes, the **un-ion of type 1** (also called **un-anion 1** or **un-cation 1** if resulted from a negatively or respectively positive charge ion) of X will be formed by electrons, protons, and antineutrons, while the **un-ion of type 2** of X (also called **un-anion 2** or **un-cation 2** if resulted from a negatively or respectively positive charge ion) will be formed by antielectrons, antiprotons, and neutrons.
The ion and the un-ion of type 1 have the same charges, while the ion and un-ion of type 2 have opposite chatges.

D) **Nonmatter** means what is not matter, therefore nonmatter actually comprises antimatter and unmatter. Similarly one defines a nonnucleus.

**3. Unmatter propulsion.**
We think (as a prediction or supposition) it could be possible at using unmatter as fuel for space rockets or for weapons platforms because, in a similar way as antimatter is presupposed to do [see 2-3], its mass converted into energy will be fuel for propulsion.
It seems to be a little easier to build unmatter than antimatter because we need say antielectrons and antiprotons only (no need for antineutrons), but the resulting energy might be less than in matter-antimatter collision.

We can collide unmatter 1 with unmatter 2, or unmatter 1 with antimatter, or unmatter 2 with matter.
When two, three, or four of them (unmatter 1, unmatter 2, matter, antimatter) collide together, they annihilate and turn into energy which can materialize at high energy into new particles and antiparticles.

**4. Existence of unmatter.**
The existence of unmatter in the universe has a similar chance to that of the antimatter, and its production also difficult for present technologies. At CERN it will be possible to test the production of unmatter.
If antimatter exists then a higher probability would be for the unmatter to exist, and reciprocally.

The 1998 Alpha Magnetic Spectrometer (AMS) flown on the International Space Station orbiting the Earth would be able to detect, besides cosmic antimatter, unmatter if any.

**5. Experiments.**
Besides colliding electrons, or protons, would be interesting in colliding neutrons.
Also, colliding a neutron with an antineutron in accelerators.

We think it might be easier to produce in an experiment an unmatter atom of deuterium (we can call it un-deuterium of type 1). The deuterium, which is an isotope of the ordinary hydrogen, has an electron, a proton, and a neutron. The idea would be to convert/transform in a deuterium atom the neutron into an antineutron, then study the properties of the resulting un-deuterium 1.
Or, similarly for un-deuterium 2, to convert/transform in a deuterium atom the electron into an antielectron, and the proton into an antiproton (we can call it un-deuterium of type 2).

Or maybe choose another chemical element for which any of the previous conversions/transformations might be possible.

**6. Neutrons and antineutrons.**
Hadrons consist of baryons and mesons and interact via strong force.
Protons, neutrons, and many other hadrons are composed from quarks, which are a class of fermions that possess a fractional electric charge. For each type of quark there exists a corresponding antiquark. Quarks are characterized by properties such as *flavor* (up, down, charm, strange, top, or bottom) and *color* (red, blue, or green).
A neutron is made up of quarks, while an antineutron is made up of antiquarks.
A neutron [see 1] has one Up quark (with the charge of +2/3 A1.606 A$10^{-19}$ C) and two Down quarks (each with the charge of -1/3 A1.606 A$10^{-19}$ C), while an antineutron has one anti Up quark (with the charge of -2/3 A1.606 A$10^{-19}$ C) and two anti Down quarks (each with the charge of +1/3 A1.606 A$10^{-19}$ C).
An antineutron has also a neutral charge, through it is opposite to a neutron, and they annihilate each other when meeting.
Both, the neutron and the antineutron, are neither attracted to nor repelling from charges particles.

**7. Characteristics of unmatter.**
Unmatter should look identical to antimatter and matter, also the gravitation should similarly act on all three of them. Unmatter may have, analogously to antimatter, utility in medicine and may be stored in vacuum in traps which have the required configuration of electric and magnetic fields for several months.

**8. Open Questions:**
8.a) Can a matter atom and an unmatter atom of first type stick together to form a molecule?
8.b) Can an antimatter atom and an unmatter atom of second type stick together to form a molecule?

8.c) There might be not only a *You* and an *anti-You*, but some versions of an *un-You* in between You and anti-You. There might exist un-planets, un-stars, un-galaxies? There might be, besides our universe, an anti-universe, and more un-universes?
8.d) Could this unmatter explain why we see such an imbalance between matter and antimatter in our corner of the universe? (Jeff Farinacci)
8.e) If matter is thought to create gravity, is there any way that antimatter or unmatter can create antigravity or ungravity? (Mike Shafer from Cornell University)
I assume that since the magnetic field or the gravitons generate gravitation for the matter, then for antimatter and unmatter the corresponding magnetic fields or gravitons would look different since the charges of subatomic particles are different...
I wonder how would the universal law of attraction be for antimmater and unmatter?

**References:**


[1] Arnold Pompos, *Inquiring Minds - Questions about Physics*, Fermilab, http://www.fnal.gov/pub/inquiring/questions/antineuron.html.
[2] Rosy Mondardini, *The History of Antimatter*, CERN Laboratory, Geneva, http://livefromcern.web.cern.ch/livefromcern/antimatter/history/AM-history00.html.
[3] Alvaro de Rújula and Rolf Landua, *Antimatter - Frequently Asked Questions*, CERN Laboratory, Geneva, http://livefromcern.web.cern.ch/livefromcern/antimatter/FAQ1.html.
[4] Florentin Smarandache, *A Unifying Field in Logics: Neutrosophic Logic. Neutrosophy, Neutrosophic Set, Neutrosophic Probability* (third edition), Am. Res. Press, 144 p., 2002; www.gallup.unm.edu/~smarandache/eBook-Neutrosophics2.pdf.
[5] Florentin Smarandache, *Unmatter*, mss., 1980, Archives Vâlcea.
[6] Webster's New World Dictionary, Third College Edition, Simon & Schuster, Inc., 1988.

# Verifying Unmatter by Experiments, More Types of Unmatter, and A Quantum Chromodynamics Formula

Dr. Florentin Smarandache
University of New Mexico
Gallup, NM 87301, USA
smarand@unm.edu

**Abstract.** As shown, experiments registered unmatter: a new kind of matter whose atoms include both nucleons and anti-nucleons, while their life span was very short, no more than $10^{-20}$ sec. Stable states of unmatter can be built on quarks and anti-quarks: applying the unmatter principle here it is obtained a quantum chromodynamics formula that gives many combinations of unmatter built on quarks and anti-quarks.

In the last time, before the apparition of my articles defining "matter, antimatter, and unmatter" [1, 2], and Dr. S. Chubb's pertinent comment [3] on unmatter, new development has been made to the unmatter topic in the sense that experiments verifying unmatter have been found..

**1. Definition of Unmatter**.
In short, unmatter is formed by matter and antimatter that bind together [1, 2].
The building blocks (most elementary particles known today) are 6 quarks and 6 leptons; their 12 antiparticles also exist.
Then *unmatter* will be formed by at least a building block and at least an antibuilding block which can bind together.

**2. Exotic Atom**.
If in an atom we substitute one or more particles by other particles of the same charge (constituents) we obtain an exotic atom whose particles are held together due to the electric charge. For example, we can substitute in an ordinary atom one or more electrons by other negative particles (say $\pi^-$, anti-Rho meson, $D^-$, $D_s^-$, muon, tau, $\Omega^-$, $\Delta^-$, etc., generally clusters of quarks and antiquarks whose total charge is negative), or the positively charged nucleus replaced by other positive particle (say clusters of quarks and antiquarks whose total charge is positive, etc.).

**3. Unmatter Atom**.
It is possible to define the unmatter in a more general way, using the exotic atom.
The classical unmatter atoms were formed by particles like (a) electrons, protons, and antineutrons, or (b) antielectrons, antiprotons, and neutrons.
In a more general definition, an unmatter atom is a system of particles as above, or such that one or more particles are replaces by other particles of the same charge.
Other categories would be (c) a matter atom with where one or more (but not all) of the electrons and/or protons are replaced by antimatter particles of the same corresponding

charges, and (d) an antimatter atom such that one or more (but not all) of the antielectrons and/or antiprotons are replaced by matter particles of the same corresponding charges.

In a more composed system we can substitute a particle by an unmatter particle and form an unmatter atom.

Of course, not all of these combinations are stable, semi-stable, or quasi-stable, especially when their time to bind together might be longer than their lifespan.

**4. Examples of Unmatter**.

During 1970-1975 numerous pure experimental verifications were obtained proving that "atom-like" systems built on nucleons (protons and neutrons) and anti-nucleons (anti-protons and anti-neutrons) are real. Such "atoms", where nucleon and anti-nucleon are moving at the opposite sides of the same orbit around the common centre of mass, are very unstable, their life span is no more than $10^{-20}$ sec. Then nucleon and anti-nucleon annihilate into gamma-quanta and more light particles (pions) which can not be connected with one another, see [6,7,8]. The experiments were done in mainly Brookhaven National Laboratory (USA) and, partially, CERN (Switzerland), where "proton---anti-proton" and "anti-proton --- neutron" atoms were observed, called them $\bar{p}p$ and $\bar{p}n$ respectively, see fig 1 and fig 2.

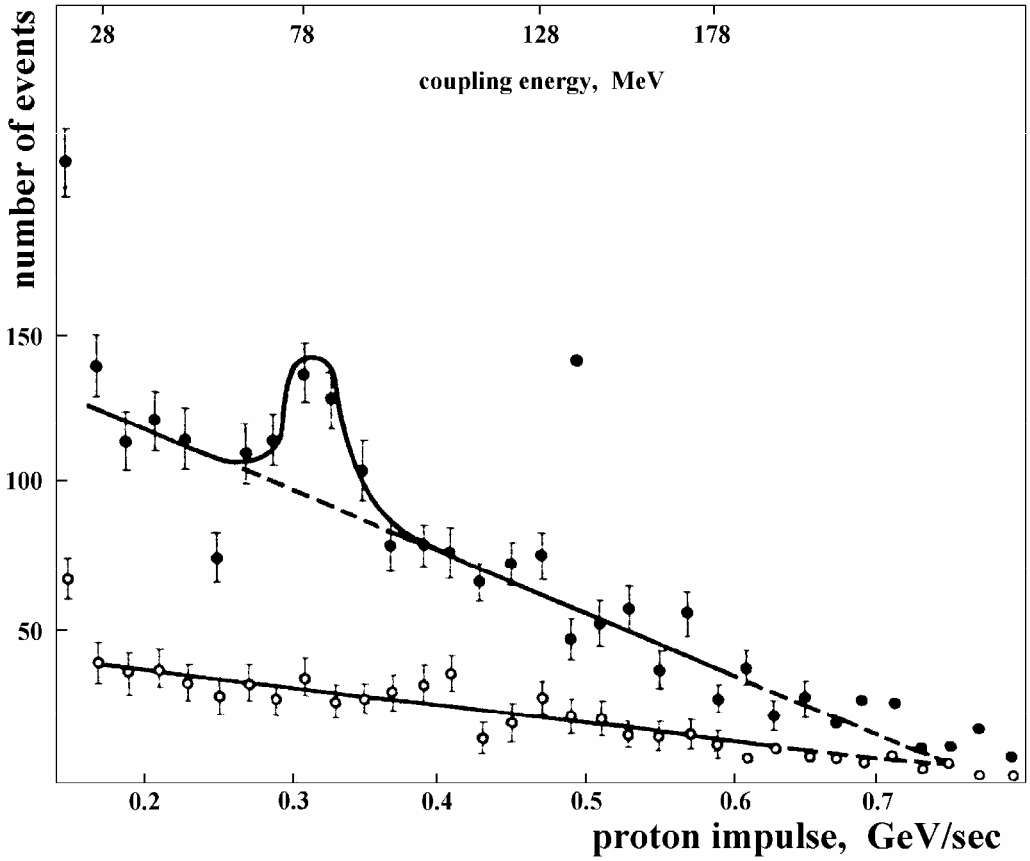


Fig. 1: Spectra of proton impulses in the reaction $\bar{p} + d \rightarrow (\bar{p}n) + p$. The upper arc --- annihilation of $\bar{p}n$ into even number of pions, the lower arc --- its annihilation into odd

number of pions. The observed maximum points out that there is a connected system $\bar{p}n$. Abscissa axis represents the proton impulse in GeV/sec (and the connection energy of the system $\bar{p}n$). Ordinate axis --- the number of events. Cited from \cite{fsm6}.

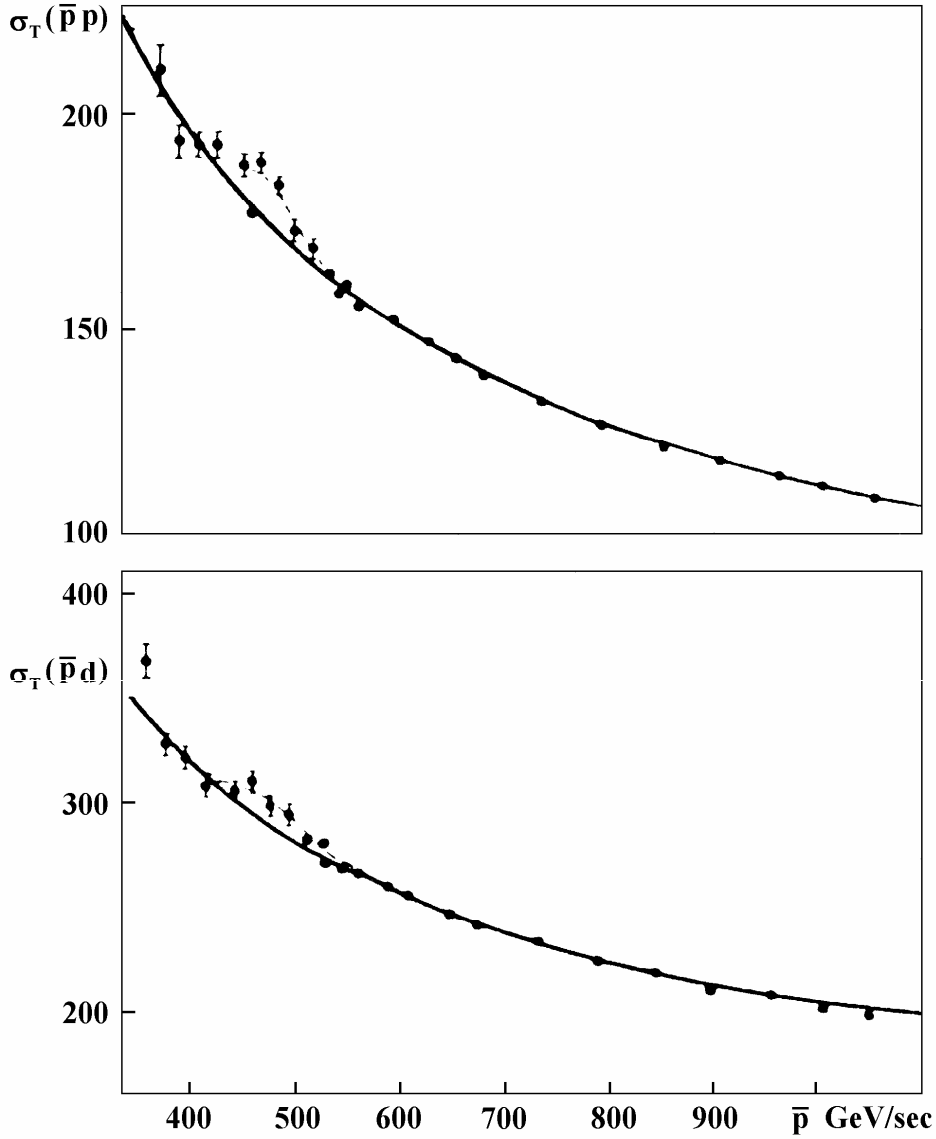


Fig. 2: Probability σ of interaction between $\bar{p}$, p and deutrons d (cited from [7]). The presence of maximum stands out the existence of the resonance state of "nucleon --- anti-nucleon".

After the experiments were done, the life span of such "atoms" was calculated in theoretical way in Chapiro's works [9,10,11]. His main idea was that nuclear forces, acting between nucleon and anti-nucleon, can keep them far way from each other, hindering their annihilation. For instance, a proton and anti-proton are located at the opposite sides in the same orbit and they are moved around the orbit centre. If the

diameter of their orbit is much more than the diameter of "annihilation area", they can be kept out of annihilation (see fig. 3). But because the orbit, according to Quantum Mechanics, is an actual cloud spreading far around the average radius, at any radius between the proton and the anti-proton there is a probability that they can meet one another at the annihilation distance. Therefore nucleon---anti-nucleon system annihilates in any case, this system is unstable by definition having life span no more than $10^{-20}$ sec.

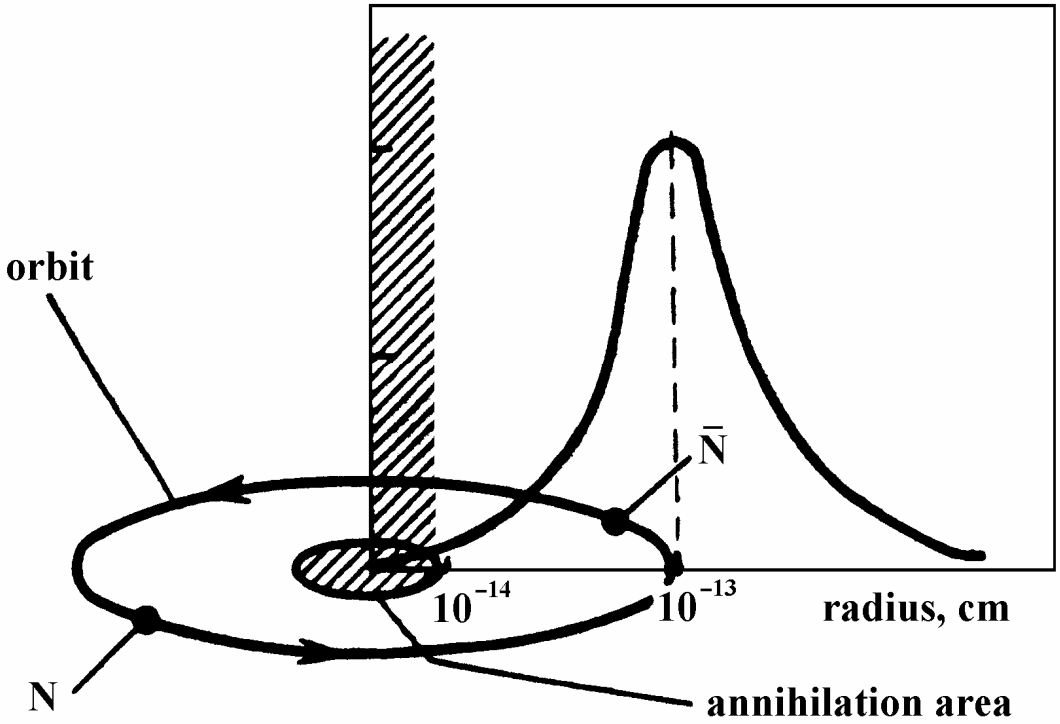


Fig. 3: Annihilation area and the probability arc in "nucleon --- anti-nucleon" system (cited from [11]).

Unfortunately, the researchers limited the research to the consideration of $\bar{p}p$ and $\bar{p}n$ nuclei only. The reason was that they, in the absence of a theory, considered $\bar{p}p$ and $\bar{p}n$ "atoms" as only a rare exception, which gives no classes of matter.

Despite Benn Tannenbaum's and Randall J. Scalise's rejections of unmatter and Scalise's personal attack on me in a true Ancient Inquisitionist style under MadSci moderator John Link's tolerance, the unmatter does exists, for example some messons and antimessons, through for a trifling of a second lifetime, so the pions are unmatter [which have the composition u^d and ud^ , where by u^ we mean anti-up quark, d = down quark, and analogously u = up quark and d^ = anti-down quark, while by ^ means anti], the kaon $K^+$ (us^), $K^-$ (u^s), Phi (ss^), $D^+$ (cd^), $D^0$(cu^), $D_s^+$ (cs^), J/Psi (cc^), $B^-$ (bu^), $B^0$ (db^), $B_s^0$ (sb^), Upsilon (bb^) [where c = charm quark, s = strange quark, b = bottom quark], etc. are unmatter too.

Also, the pentaquark Theta-plus ($\Theta^+$), of charge $^+1$, uudds^ (i.e. two quarks up, two quarks down, and one anti-strange quark), at a mass of 1.54 geV and a narrow width of

22 MeV, is unmatter, observed in 2003 at the Jefferson Lab in Newport News, Virginia, in the experiments that involved multi-GeV photons impacting a deuterium target. Similar pentaquark evidence was obtained by Takashi Nakano of Osaka University in 2002, by researchers at the ELSA accelerator in Bonn in 1997-1998, and by researchers at ITEP in Moscow in 1986.
Besides Theta-plus, evidence has been found in one experiment [4] for other pentaquarks, $\Xi_5^{--}$(ddssu^) and $\Xi_5^{+}$(uussd^).
D. S. Carman [5] has reviewed the positive and null evidence for these pentaquarks and their existence is still under investigation.

In order for the paper to be self-contained let's recall that the *pionium* is formed by a $\pi^+$ and $\pi^-$ mesons, the *positronium* is formed by an antielectron (positron) and an electron in a semi-stable arrangement, the *protonium* is formed by a proton and an antiproton also semi-stable, the *antiprotonic helium* is formed by an antiproton and electron together with the helium nucleus (semi-stable), and *muonium* is formed by a positive muon and an electron.
Also, the *mesonic atom* is an ordinary atom with one or more of its electrons replaced by negative mesons.
The *strange matter* is a ultra-dense matter formed by a big number of strange quarks bounded together with an electron atmosphere (this strange matter is hypothetical).

From the exotic atom, the pionium, positronium, protonium, antiprotonic helium, and muonium are unmatter.
The mesonic atom is unmatter if the electron(s) are replaced by negatively-charged antimessons.
Also we can define a mesonic antiatom as an ordinary antiatomic nucleous with one or more of its antielectrons replaced by positively-charged mesons. Hence, this mesonic antiatom is unmatter if the antielectron(s) are replaced by positively-charged messons.
The strange matter can be unmatter if these exists at least an antiquark together with so many quarks in the nucleous. Also, we can define the strange antimatter as formed by a large number of antiquarks bound together with an antielectron around them. Similarly, the strange antimatter can be unmatter if there exists at least one quark together with so many antiquarks in its nucleous.

The bosons and antibosons help in the decay of unmatter. There are 13+1 (Higgs boson) known bosons and 14 antibosons in present.

**5. Quantum Chromodynamics Formula.**
In order to save the colorless combinations prevailed in the Theory of Quantum Chromodynamics (QCD) of quarks and antiquarks in their combinations when binding, we devise the following formula:

$$\mathbf{Q - A} \in \pm M3 \qquad (1)$$

where $M3$ means multiple of three,
i.e. $\pm M3 = \{3\cdot k \mid k \in Z\} = \{\ldots, -12, -9, -6, -3, 0, 3, 6, 9, 12, \ldots\}$,
and Q = number of quarks, A = number of antiquarks.
But (1) is equivalent to:

$$\mathbf{Q \equiv A \pmod 3} \qquad (2)$$

(Q is congruent to A modulo 3).

To justify this formula we mention that 3 quarks form a colorless combination, and any multiple of three (***M*3**) combination of quarks too, i.e. 6, 9, 12, etc. quarks. In a similar way, 3 antiquarks form a colorless combination, and any multiple of three (***M*3**) combination of antiquarks too, i.e. 6, 9, 12, etc. antiquarks. Hence, when we have hybrid combinations of quarks and antiquarks, a quark and an antiquark will annihilate their colors and, therefore, what's left should be a multiple of three number of quarks (in the case when the number of quarks is bigger, and the difference in the formula is positive), or a multiple of three number of antiquarks (in the case when the number of antiquarks is bigger, and the difference in the formula is negative).

**6. Quark-Antiquark Combinations.**

Let's note by q = quark $\in$ {Up, Down, Top, Bottom, Strange, Charm},
and by a = antiquark $\in$ {Up^, Down^, Top^, Bottom^, Strange^, Charm^}.
Hence, for combinations of n quarks and antiquarks, $n \geq 2$, prevailing the colorless, we have the following possibilities:
- if n = 2, we have: qa (biquark – for example the mesons and antimessons);
- if n = 3, we have qqq, aaa (triquark – for example the baryons and antibaryons);
- if n = 4, we have qqaa (tetraquark);
- if n = 5, we have qqqqa, aaaaq (pentaquark);
- if n = 6, we have qqqaaa, qqqqqq, aaaaaa (hexaquark);
- if n = 7, we have qqqqqaa, qqaaaaa (septiquark);
- if n = 8, we have qqqqaaaa, qqqqqqaa, qqaaaaaa (octoquark);
- if n = 9, we have qqqqqqqqq, qqqqqqaaa, qqqaaaaaa, aaaaaaaaa (nonaquark);
- if n = 10, we have qqqqqaaaaa, qqqqqqqqaa, qqaaaaaaaa (decaquark);

etc.

**7. Unmatter Combinations.**

From the above general case we extract the unmatter combinations:
- For combinations of 2 we have: qa (unmatter biquark), [mesons and antimesons]; the number of all possible unmatter combinations will be $6 \cdot 6 = 36$, but not all of them will bind together.

It is possible to combine an entity with its mirror opposite and still bound them, such as: uu^, dd^, ss^, cc^, bb^ which form mesons.
It is possible to combine, unmatter + unmatter = unmatter, as in ud^ + us^ = uud^s^ (of course if they bind together).
- For combinations of 3 (unmatter triquark) we can not form unmatter since the colorless can not hold.
- For combinations of 4 we have: qqaa (unmatter tetraquark);

the number of all possible unmatter combinations will be $6^2 \cdot 6^2 = 1{,}296$, but not all of them will bind together.
- For combinations of 5 we have: qqqqa, or aaaaq (unmatter pentaquarks);

the number of all possible unmatter combinations will be $6^4 \cdot 6 + 6^4 \cdot 6 = 15{,}552$, but not all of them will bind together.

- For combinations of 6 we have: qqqaaa (unmatter hexaquarks);
the number of all possible unmatter combinations will be $6^3 \cdot 6^3 = 46{,}656$, but not all of them will bind together.
- For combinations of 7 we have: qqqqqaa, qqaaaaa (unmatter septiquarks);
the number of all possible unmatter combinations will be $6^5 \cdot 6^2 + 6^2 \cdot 6^5 = 559{,}872$, but not all of them will bind together.
- For combinations of 8 we have: qqqqaaaa, qqqqqqqa, qaaaaaaa (unmatter octoquarks);
the number of all possible unmatter combinations will be $6^4 \cdot 6^4 + 6^7 \cdot 6^1 + 6^1 \cdot 6^7 = 5{,}038{,}848$, but not all of them will bind together.
- For combinations of 9 we have: qqqqqqaaa, qqqaaaaaa (unmatter nonaquarks);
the number of all possible unmatter combinations will be $6^6 \cdot 6^3 + 6^3 \cdot 6^6 = 2 \cdot 6^9 = 20{,}155{,}392$, but not all of them will bind together.
- For combinations of 10 we have: qqqqqqqqaa, qqqqqaaaaa, qqaaaaaaaa (unmatter decaquarks);
the number of all possible unmatter combinations will be $3 \cdot 6^{10} = 181{,}398{,}528$, but not all of them will bind together.
Etc.

I wonder if it is possible to make infinitely many combinations of quarks / antiquarks and leptons / antileptons...
Unmatter can combine with matter and/or antimatter and the result may be any of these three.
Some unmatter could be in the strong force, hence part of hadrons.

**8. Unmatter Charge**.
The charge of unmatter may be positive as in the pentaquark Theta-plus, 0 (as in positronium), or negative as in anti-Rho meson (u^d) [M. Jordan].

**9. Containment.**
I think for the containment of antimatter and unmatter it would be possible to use electromagnetic fields (a container whose walls are electromagnetic fields). But its duration is unknown.

**10. Further Research**.
Let's start from neutrosophy [18], which is a generalization of dialectics, i.e. not only the opposites are combined but also the neutralities. Why? Because when an idea is launched, a category of people will accept it, others will reject it, and a third one will ignore it (don't care). But the dynamics between these three categories changes, so somebody accepting it might later reject or ignore it, or an ignorant will accept it or reject it, and so on. Similarly the dynamicity of <A>, <antiA>, <neutA>, where <neutA> means neither <A> nor <antiA>, but in between (neutral).
Neutrosophy considers a kind not of di-alectics but tri-alectics (based on three components: <A>, <antiA>, <neutA>). Hence unmatter is a kind of neutrality (not referring to the charge) between matter and antimatter, i.e. neither one, nor the other.

Upon the model of unmatter we may look at ungravity, unforce, unenergy, etc.
*Ungravity* would be a mixture between gravity and antigravity (for example attracting and rejecting simultaneously or alternatively; or a magnet which changes the + and - poles frequently).
*Unforce*. We may consider positive force (in the direction we want), and negative force (repulsive, opposed to the previous). There could be a combination of both positive and negative forces in the same time, or alternating positive and negative, etc.
*Unenergy* would similarly be a combination between positive and negative energies (as the alternating current (a.c.), which periodically reverses its direction in a circuit and whose frequency, f, is independent of the circuit's constants). Would it be possible to construct an alternating-energy generator?
To conclusion:
According to the Universal Dialectic the unity is manifested in duality and the duality in unity.
"Thus, Unmatter (unity) is experienced as duality (matter vs antimatter).
Ungravity (unity) as duality (gravity vs antigravity).
Unenergy (unity) as duality (positive energy vs negative energy).
and thus also...
between duality of being (existence) vs nothingness (antiexistence) must be "unexistence" (or pure unity)." (R. Davic)

**Acknowledgement.**
I'd like to thank D. Rabounski and L. Borissova for their comments and help in improving this paper.

**References**

1. F. Smarandache, A New Form of Matter -- Unmatter, Composed of Particles and Anti-Particles. *Progress in Physics*, 2005, v.1, 9-11.
2. F. Smarandache, *Matter, Antimatter, and Unmatter*, "Infinite Energy", Vol. 11, No. 62, 50-51, July / August 2005.
3. S. Chubb, *Breaking through editorial*, "Infinite Energy", Vol. 11, No. 62, 6-7, July / August 2005.
4. C. Alt et al. (NA49 Collaboration), Phys. Rev. Lett., 92, 042003, 2004.
5. Daniel S. Carman, *Experimental evidence for the pentaquark*, Eur Phys A, 24, 15-20, 2005;
6. Gray L., Hagerty P., Kalogeropoulos T.E. Evidence for the Existence of a Narrow p-barn Bound State. Phys. Rev. Lett., 1971, v.26, 1491-1494.
7. Carrol A.S., Chiang I.-H., Kucia T.F., Li K. K., Mazur P. O.,. Michael D. N, Mockett P., Rahm D. C., Rubinstein R.. Observation of Structure in p-barp and p-bard Total Cross Sections below 1.1 GeV/c. Phys. Rev. Lett., 1974, v.32, 247-250.
8. Kalogeropoulos T. E., Vayaki A., Grammatikakis G., Tsilimigras T., Simopoulou E. Observation of Excessive and Direct gamma Production in p-bard Annihilations at Rest. . Phys. Rev. Lett., 1974, v.33, 1635-1637.
9. Chapiro I.S. Physics-Uspekhi (Uspekhi Fizicheskikh Nauk), 1973, v.109, 431.

10. Bogdanova L.N., Dalkarov O.D., Chapiro I.S. Quasinuclear systems of nucleons and antinucleons. Annals of Physics, 1974, v.84, 261-284.
11. Chapiro I.S. New “nuclei” built on nucleons and anti-nucleons. Nature (Russian), 1975, No.12, 68-73
12. R. Davic, K. John, M. Jordan, D. Rabounski, L. Borissova, B. Levin, V. Panchelyuga, S. Shnoll, Private Communications, June-July 2005.
13. John Link, Benn Tannenbaum, Randall J. Scalise, MadSci web site, June-July 2005.
14. V. V. Barmin et al. (DIANA Collaboration), Phys. Atom. Nucl., 66, 1715, 2003.
15. M. Ostrick (SAPHIR Collaboration), Pentaquark 2003 Workshop, Newport News, VA, Nov. 6-8, 2003.
16. T. P. Smith, "Hidden Worlds, Hunting for Quarks in Ordinary Matter, Princeton University Press, 2003.
17. M. J. Wang (CDF Collaboration), Quarks and Nuclear Physics 2004, Bloomington, IN, May 23-28, 2004.
18. F. Smarandache, A Unifying Field in Logics, Neutrosophic Logic / Neutrosophy, Neutrosophic Set, Neutrosophic Probability, Am. Res. Press, 1998; www.gallup.unm.edu/~smarandache/eBooks-Neutrosophics2.pdf.

# Unmatter Entities inside Nuclei, Predicted by the Brightsen Nucleon Cluster Model

Florentin Smarandache and Dmitri Rabounski
*Dept. of Mathematics and Science, University of New Mexico,*
*200 College Road, Gallup, NM 87301, USA*
E-mail: smarand@unm.edu; rabounski@yahoo.com

**Abstract**

Applying the R. A. Brightsen Nucleon Cluster Model of the atomic nucleus we discuss how stable and unstable unmatter entities (the conjugations of matter and antimatter) may be formed as clusters inside a nucleus. The model supports a hypothesis that antimatter nucleon clusters are present as a parton (*sensu* Feynman) superposition within the spatial confinement of the proton ($^1H_1$), the neutron, and the deuteron ($^1H_2$). If model predictions can be confirmed both mathematically and experimentally, a new physics is suggested. A proposed experiment is connected to othopositronium annihilation anomalies, which, being related to one of known unmatter entity, orthopositronium (built on electron and positron), opens a way to expand the Standard Model.

## 1. Introduction

According to Smarandache [1,2,3], following neutrosophy theory in philosophy and set theory in mathematics, the union of matter <A> and its antimatter opposite <AntiA> can form a neutral entity <NeutA> that is neither <A> nor <AntiA>. The <NeutA> entity was termed "unmatter" by Smarandache [1] in order to highlight its intermediate physical constitution between matter and antimatter. Unmatter is formed when matter and antimatter baryons intermingle, regardless of the amount of time before the conjugation undergoes decay. Already Bohr long ago predicted the possibility of unmatter with his principle of complementarity, which holds that nature can be understood in terms of concepts that come in complementary pairs of opposites that are inextricably connected by a Heisenberg-like uncertainty principle. However, not all physical union of <A> with <AntiA> must form unmatter. For instance, the charge quantum number for the electron (e-) and its antimatter opposite positron (e+) make impossible the formation of a charge neutral state--the quantum situation must be either (e-) or (e+).

Although the terminology "unmatter" is unconventional, unstable entities that contain a neutral union of matter and antimatter are well known experimentally for many years (e.g, pions, pentaquarks, positronium, etc.). Smarandache [3] presents numerous additional examples of unmatter that conform to formalism of quark quantum chromodynamics, already known since the 1970's. The basis that unmatter does exists comes from the 1970s experiments done at Brookhaven and CERN [4-8], where unstable unmatter-like entities were found. Recently, a bound and quasi-stable unmatter baryonium has been documented experimentally as a weak resonance between a proton and antiproton using a Skyrme-type model potential [????]. Further evidence that neutral entities derive from union of opposites comes from the spin induced magnetic moment of atoms, which can exist in a quantum state of both spin up and spin down at the same time, a quantum condition that follows the superposition principal of physics [????]. In quantum physics, virtual and physical states that are mutually exclusive while simultaneously entangled, can form a unity of opposites <NeutA> via the principle of superposition.

Our motivation for this communication is to the question: would the superposition principal hold when mass symmetrical and asymmetrical matter and antimatter nucleon wavefunctions become entangled, thus allowing for possible formation of macroscopic "unmatter" nucleon entities, either stable or unstable ? Here we introduce how the novel Nucleon Cluster Model of the late R.

A. Brightsen [9-15] does predict formation of unmatter as the product of such a superposition between matter and antimatter nucleon clusters. The model suggests a radical hypothesis that antimatter nucleon clusters are present as a hidden parton type variable (*sensu* Feynman) superposed within the spatial confinement of the proton ($^1H_1$), the neutron, and the deuteron ($^1H_2$). Because the mathematics involving interactions between matter and antimatter nucleon clusters is not developed, much theoretical work will be needed to test model predictions. If model predictions can be experimentally confirmed, a new physics is suggested.

**2. The Brightsen Nucleon Cluster Model to unmatter entities inside nuclei**

Of fundamental importance to the study of nuclear physics is the attempt to explain the macroscopic structural phenomena of the atomic nucleus. Classically, nuclear structure mathematically derives from two opposing views: (1) that the proton [P] and neutron [N] are independent (unbound) interacting fermions within nuclear shells, or (2) that nucleons interact collectively in the form of a liquid-drop. Compromise models attempt to cluster nucleons into interacting [NP] boson pairs (e.g., Interacting Boson Model-IBM), or, as in the case of the Interacting Boson-Fermion Model (IBFM), link boson clusters [NP] with un-paired and independent nucleons [P] and [N] acting as fermions.

However, an alternative view, at least since the 1937 Resonating Group Method of Wheeler, and the 1965 Close-Packed Spheron Model of Pauling, holds that the macroscopic structure of atomic nuclei is best described as being composed of a small number of interacting boson-fermion nucleon "clusters" (e.g., helium-3 [PNP], triton [NPN], deuteron [NP]), as opposed to independent [N] and [P] nucleons acting as fermions, either independently or collectively. Mathematically, such clusters represent a spatially localized mass-charge-spin subsystem composed of strongly correlated nucleons, for which realistic two- and three body wave functions can be written. In this view, quark-gluon dynamics are confined within the formalism of 6-quark bags [NP] and 9-quark bags ([PNP] and [NPN]), as opposed to valance quarks forming free nucleons. The experimental evidence in support of nucleons interacting as boson-fermion clusters is now extensive and well reviewed.

One novel nucleon cluster model is that of R. A. Brightsen, which was derived from the identification of mass-charge symmetry systems of isotopes along the Z-N Serge plot. According to Brightsen, all beta-stable matter and antimatter isotopes are formed by potential combinations of two- and three nucleon clusters; e.g., ([NP], [PNP], [NPN], [NN], [PP], [NNN], [PPP], and/or their mirror antimatter clusters [N^P^], [P^N^P^], [N^P^N^], [N^N^], [P^P^], [P^P^P^], [N^N^N^], where the symbol ^ here is used to denote antimatter. A unique prediction of the Brightsen model is that a stable union must result between interaction of mass asymmetrical matter (positive mass) and antimatter (negative mass) nucleon clusters to form protons and neutrons, for example the interaction between matter [PNP] + antimatter [N^P^]. Why union and not annihilation of mass asymmetrical matter and antimatter entities? As explained by Brightsen, independent (unbound) neutron and protons do not exist in nuclear shells, and the nature of the mathematical series of cluster interactions (3 [NP] clusters = 1[NPN] cluster + 1 [PNP] cluster), makes it impossible for matter and antimatter clusters of identical mass to coexist in stable isotopes. Thus, annihilation cannot take place between mass asymmetrical two- and three matter and antimatter nucleon clusters, only strong bonding (attraction).

Here is the Table that tells it all--how unmatter may be formed from nucleon clusters according to the Brightsen model.

**Revised Table 1.** This table is modified to improve the first version, which appeared in the Table 1 of Smarandache and Rabounski (2006, Vol 1, Progress in Physics).

Unmatter entities (stable, quasi-stable, unstable) created from union of matter and antimatter nucleon clusters as predicted by the gravity-antigravity formalism of the Brightsen Nucleon Cluster Model. Blank cells represent interactions that result in annihilation of mirror identical two- and three-body clusters. Top nucleons within cells show superposed state comprised of three valance quarks; bottom structures show superposed state of hidden unmatter in the form of nucleon clusters. Unstable pions, tetraquarks, and hexaquark unmatter are predicted from union of mass symmetrical clusters that are not mirror opposites. The symbol ^ = antimatter, N = neutron, P = proton, q = quark. Both the proton and neutron, and their antimatter mirrors, are represented by six unique unmatter nucleon cluster probability states; (communication with R. D. Davic).

| Matter Clusters → / Antimatter Clusters ↓ | [NP] Deuteron i Stable | [NPN] Triton j Beta-unstable | [PNP] Helium-3 k Stable | [NN] Di-Neutron l | [PP] Di-Proton m | [NNN] Tri-Neutron n | [PPP] Tri-Proton o |
|---|---|---|---|---|---|---|---|
| [N^P^] a Stable | | \|N\| \|NP\|\|N^P^\| | \|P\| \|NP\|\|N^P^\| | Pions (qq^) | Pions (qq^) | [N] \|NN\|\|N^P^\| | [P] \|N^P^\|\|PP\| |
| [N^P^N^] b Beta-unstable | [N^] \|NP\|\|N^P^\| | | Pions (qq^) | [N^] \|NN\|\|N^P^\| | [N^] \|N^P^\|\|PP\| | Pions (qq^) | Tetraquarks (qqq^q^) |
| [P^N^P^] c Stable | [P^] \|NP\|\|N^P^\| | Pions (qq^) | | [P^] \|N^P^\|NN\| | [P^] \|PP\|\|N^P^\| | Tetraquarks (qqq^q^) | Pions (qq^)\| |
| [N^N^] d | Pions (qq^) | [N] \|NP\|\|N^N^\| | [P] \|NP\|\|N^N^\| | | Tetraquarks (qqqq^) | [N] \|NN\|\|N^N^\| | [P] \|PP\|\|N^N^\| |
| [P^P^] e | Pions (qq^) | [N] \|NP\|\|P^P^\| | [P] \|NP\|\|P^P^\| | Tetraquarks (qqq^q^) | | [N] \|P^P^\|\|NN\| | [P] \|PP\|\|P^P^\| |
| [N^N^N^] f | [N^] \|NP\|\|NN^\| | Pions (qq^) | Tetraquarks (qqq^q^) | [N^] \|NN\|\|N^N^\| | [N^] \|N^N^\|\|PP\| | | Hexaquark (qqqq^q^q^) |
| [P^P^P^] g | [P^] \|NP\|\|P^P^\| | Tetraquarks (qqq^q^) | Pions (qq^) | [P^] \|P^P^\|\|NN\| | [P^] \|P^P^\|\|PP\| | Hexaquark (qqqq^q^q^) | |

## 3. A proposed experimental test

As known, Standard Model of Quantum Electrodynamics explains all known phenomena with high precision, aside for anomalies in orthopositronium annihilation, discovered in 1987.

The Brightsen model, like many other models (see References), is outside the Standard Model. They all pretend to expand the Standard Model in one or another way. Therefore today, in order to judge the alternative models as true or false, we should compare their predictions to orthopositronium annihilation anomalies, the solely unexplained by the Standard Model. Of those models the Brightsen model has a chance to be tested in such way, because it includes unmatter entities (the conjugations of particles and anti-particles) inside an atomic nucleus that could produce effect in the forming of orthopositronium by $\beta^+$-decay positrons and its annihilation decay.

In brief, the anomalies in orthopositronium annihilation are as follows.

Positronium is an atom-like orbital system that includes an electron and its anti-particle, positron, coupled by electrostatic forces. There are two kinds of positronium: parapositronium $^{S}$Ps, in which the spins of electron and positron are oppositely directed and the summary spin is zero, and orthopositronium $^{T}$Ps, in which the spins are co-directed and the summary spin is one. Because a particle-antiparticle (unmatter) system is unstable, life span of positronium is rather small. In vacuum, parapositronium decays in $\tau \sim 1.25 \times 10^{-10}$s, while orthopositronium is $\tau \sim 1.4 \times 10^{-7}$ s after the birth. In a medium the life span is even shorter because positronium tends to annihilate with electrons of the media.

In laboratory environment positronium can be obtained by placing a source of free positrons into a matter, for instance, one-atom gas. The source of positrons is $\beta^+$-decay, self-triggered decays of protons in neutron-deficient atoms[1]

$$p \rightarrow n + e^+ + \nu_e .$$

Some of free positrons released from $\beta^+$-decay source into gas quite soon annihilate with free electrons and electrons in the container's walls. Other positrons capture electrons from gas atoms thus producing orthopositronium and parapositronium (in 3:1 statistical ratio). Time spectrum of positrons (number of positrons vs. life span) is the basic characteristic of their annihilation in matter.

In inert gases the time spectrum of annihilation of free positrons generally reminds of exponential curve with a plateau in its central part, known as ``shoulder'' [27, 28]. In 1965 Osmon published [27] pictures of observed time spectra of annihilation of positrons in inert gases (He, Ne, Ar, Kr, Xe). In his experiments he used $^{22}$NaCl as a source of $\beta^+$-decay positrons. Analyzing the results of the experiments, Levin noted that the spectrum in neon was peculiar compared to those in other one-atom gases: in neon points in the curve were so widely scattered, that presence of a ``shoulder'' was unsure. Repeated measurements of temporal spectra of annihilation of positrons in He, Ne, and Ar, later accomplished by Levin [29, 30], have proven existence of anomaly in neon. Specific feature of the experiments done by Osmon, Levin and some other researchers in

[1] It is also known as positron $\beta^+$-decay. During $\beta^-$-decay in nucleus neutron decays $n \rightarrow p + e^- + \tilde{\nu}_e$ .

the UK, Canada, and Japan is that the source of positrons was $^{22}$Na, while the moment of birth of positron was registered according to $\gamma_n$-quantum of decay of excited $^{22*}$Ne

$$^{22*}\mathrm{Ne} \rightarrow {}^{22}\mathrm{Ne} + \gamma_n ,$$

from one of products of $\beta^+$-decay of $^{22}$Na.

In his experiments [31, 32] Levin discovered that the peculiarity of annihilation spectrum in neon (abnormally wide scattered points) is linked to presence in natural neon of substantial quantity of its isotope $^{22}$Ne (around 9%). Levin called this effect *isotope anomaly*. Temporal spectra were measured in neon environments of two isotopic compositions: (1) natural neon (90.88% of $^{20}$Ne, 0.26% of $^{21}$Ne, and 8.86% of $^{22}$Ne); (2) neon with reduced content of $^{22}$Ne (94.83% of $^{20}$Ne, 0.22% of $^{21}$Ne, and 4.91% of $^{22}$Ne). Comparison of temporal spectra of positron decay revealed: in natural neon (the 1$^{st}$ composition) the shoulder is fuzzy, while in neon poor with $^{22}$Ne (the 2$^{nd}$ composition) the shoulder is always clearly pronounced. In the part of spectrum, to which $^{T}$Ps-decay mostly contributes, the ratio between intensity of decay in poor neon and that in natural neon (with much isotope $^{22}$Ne) is 1.85±0.1 [32].

Another anomaly is substantially higher measured rate of annihilation of orthopositronium (the value reciprocal to its life span) compared to that predicted by QED.

Measurement of orthopositronium annihilation rate is among the main tests aimed to experimental verification of QED laws of conservation. In 1987 thanks to new precision technology a group of researchers based in the University of Michigan (Ann Arbor) made a breakthrough in this area. The obtained results showed substantial gap between experiment and theory. The anomaly that the Michigan group revealed was that measured rates of annihilation at $\lambda_{T(exp)}$ = 7.0514±0.0014 $\mu s^{-1}$ and $\lambda_{T(exp)}$ = 7.0482±0.0016 $\mu s^{-1}$ (with unseen-before precision of 0.02% and 0.023% using vacuum and gas methods [33--36]) were much higher compared to $\lambda_{T(theor)}$ = 7.00383±0.00005 $\mu s^{-1}$ as predicted by QED [37--40]. The effect was later called $\lambda_T$-anomaly [41].

Theorists foresaw possible annihilation rate anomaly not long before the first experiments were accomplished in Michigan. In 1986 Holdom [42] suggested that ``mixed type" particles may exist, which being in the state of oscillation stay for some time in our world and for some time in the mirror Universe, possessing negative masses and energies. In the same year Glashow [43] gave further development to the idea and showed that in case of 3-photon annihilation $^{T}$Ps will ``mix up" with its mirror twin thus producing two effects: (1) higher annihilation rate due to additional mode of decay $^{T}\mathrm{Ps} \rightarrow$ nothing, because products of decay passed into the mirror Universe can not be detected; (2) the ratio between orthopositronium and parapositronium numbers will decrease from $^{T}\mathrm{Ps} : {}^{S}\mathrm{Ps}$ = 3:1 to 1.5:1. But at that time (in 1986) Glashow concluded that no interaction is possible between our-world and mirror-world particles.

On the other hand, by the early 1990's these theoretic studies encouraged many researchers worldwide for experimental search of various ``exotic" (i.e. not explained in QED) modes of $^{T}$Ps-decay, which could lit some light on abnormally high rate of decay. These were, to name just a few, search for $^{T}\mathrm{Ps} \rightarrow$ nothing mode [44], check of possible contribution from 2-photon mode [45--47] or from other exotic modes [48--50]. As a result it has been shown that no exotic modes can contribute to the anomaly, while contribution of $^{T}\mathrm{Ps} \rightarrow$ nothing mode is limited to $5.8 \times 10^{-4}$ of the regular decay.

The absence of theoretical explanation of $\lambda_T$-anomaly encouraged Adkins et al. [51] to suggest experiments made in Japan [52] in 1995 as an alternative to the basic Michigan experiments. No doubt, high statistical accuracy of the Japanese measurements puts them on the same level with the basic experiments [33--36]. But all Michigan measurements possessed the property of a ``full experiment", which in this particular case means no external influence could affect wave function of positronium. Such influence is inevitable due to electrodynamic nature of positronium and can be avoided only using special technique. In Japanese measurements [52] this was not taken into account and thus they do not possess property of ``full experiment". Latest experiments of the Michigans [53], so-called “Resolution of Orthopositronium-Lifetime Pussle”, as well do not possess property of ``full Experiment'', because the qualitative another statement included external influence of electromagnetic field there [54, 55].

As early as in 1993 Karshenboim [56] showed that QED had actually run out of any of its theoretical capabilities to explain orthopositronium anomaly.

Electric interactions and weak interactions were joined into a common electroweak interaction in the 1960’s by commonly Salam, Glashow, Weinberg, etc. Today’s physicists attempt to join electroweak interaction and strong interaction (unfinished yet). They follow an intuitive idea that forces, connecting electrons and a nucleus, and forces, connecting nucleons inside a nucleus, are particular cases of a common interaction. That is the basis of our claim. If that is true, our claim is that orthopositronium atoms born in neon of different isotope contents ($^{22}$Ne, $^{21}$Ne, $^{20}$Ne) should be different from each other. There should be an effect of ``inner'' structure of neon nuclei if built by the Brightsen scheme, because the different proton-neutron contents built by different compositions of nucleon pairs. As soon as a free positron drags an electron from a neon atom, the potential of electro-weak interactions have changed in the atom. Accordingly, there in the nucleus itself should be re-distribution of strong interactions, than could be once as the re-building of the Brightsen pairs of nucleons there. So, lost electron of $^{22}$Ne should have a different ``inner'' structure than that of $^{21}$Ne or $^{20}$Ne. Then the life span of orthopositronium built on such electrons should be as well different.

Of course, we can only qualitatively predict that difference, because we have no exact picture of what really happens inside a ``structurized'' nucleus. Yet only principal predictions are possible there. However even in such case we vote for continuation of ``isotope anomaly'' experiments with orthopositronium in neon of different isotope contents. If further experiments will be positive, it could be considered as one more auxiliary proof that the Brightsen model is true.

**Acknowledgements**

We very much appreciate Dr. Robert Davic, the nephew of R. A. Brightsen, for comments about the Brightsen model.

**References**

**Unmatter**

1. F. Smarandache, *Matter, Antimatter, and Unmatter*, Infinite Energy, Concord, NH, USA, Vol. 11, Issue 62, 50-51, 2005.

2. F. Smarandache, *A New Form of Matter — Unmatter, Composed of Particles and Anti-Particles,* Progress in Physics, 2005, vol. 1, 9-11.

3. F. Smarandache, *Verifying Unmatter by Experiments, More Types of Unmatter, and A Quantum Chromodynamics Formula*, Progress in Physics, Vol. 2, 113-116, 2005.

**Unmatter basis experiments**

4. Gray L., Hagerty P., Kalogeropoulos T.E. Evidence for the existence of a narrow p-barn bound state. *Phys. Rev. Lett.*, 1971, v.26, 1491-1494.

5. Carrol A.S., Chiang I.-H., Kucia T.F., Li K.K., Mazur P.O., Michael D.N., Mockett P., Rahm D.C., Rubinstein R. Observation of structure in (p-bar) and (p-bar d) total cross sections below 1.1 GeV/s. *Phys. Rev. Lett.*, 1974, v.32, 247-250.

6. Kalogeropoulos T.E., Vayaki A., Grammatikakis G., Tsilimigras T., Simopoulou E. Observation of excessive and direct gamma production in (p-bar d) annihilations at rest. *Phys. Rev. Lett*., 1974, v.33, 1635-1637.

7. Chapiro I.S. *Physics-Uspekhi*, 1973, v.109, 431.

8. Bogdanova L.N., Dalkarov O.D., Chapiro I.S. Quasinuclear systems of nucleons and antinucleons. *Annals of Physics*, 1974, v.84, 261-284.

**Brightsen Model**

9. Brightsen, R.A. 1995. Nucleon cluster structures in beta-stable nuclides. *Infinite Energy*, v. 1, No, 4, 55-56.

10. Brightsen, R.A. 1995/96. Correspondence of the Nucleon Cluster Model with the Periodic Table of Elements, *Infinite Energy*, vol. 1 (5/6), pp. 73-74.

11. Brightsen, R.A. 1996. Correspondence of the Nucleon Cluster Model with the Classical Periodic Table of Elements, *J. New Energy*, vol. 1 (1), pp 75-78.

12. Brightsen, R.A. 1996. The Nucleon Cluster Model and the Periodic Table of Beta-Stable Nuclides, available online at http://www.brightsenmodel.phoenixrising-web.net

13. Brightsen, R.A. 2000. The nucleon cluster model and thermal neutron fission. *Infinite Energy*, vol 6(31), pp. 55-63.

14. Brightsen, R. A ., R. Davis, 1995. Application of the Nucleon Cluster Model to Experimental Results, *Infinite Energy*, vol. 1 (3), pp 13-15.

15. Bass, R.W. 1996. Experimental evidence favoring Brightsen's nucleon cluster model. *Infinite Energy*, vol 2 (11), pp.78-79

**Some review papers on cluster models**

16. Buck, B., Merchant, A. C., S. M. Perez. 2005. Evidence of nuclear clustering throughout a major shell. *Phys. Rev. C.* 71(1): 014311-15.

17. Akimune, H., T. Yamagata, S. Nakayama, M. Fujiwara, K. Fushimi, K. Hara, K. Y. Hara, K. Ichihara, K. Kawase, K. Matsui, K. Nakanishi, A. Shiokawa, M. Tanaka, H. Utsunomiya, and M. Yosoi. 2004. Trinucleon cluster structure at high-excitation energies in $A = 6$ nuclei. *Physics of Atomic Nuclei,* Vol. 67(9): 1721-1725.

18. Koralija, M., Z. Basrak, R. Caplar, editors. 1999. Clustering aspects of nuclear structure and dynamics, cluster '99. Proceedings of the 7th International Conference. Rab, Croatia.

19. Wuosmaa, A. H., R R Betts, M Freer, and B R Fulton. 1995. Recent Advances in the Study of Nuclear Clusters. In., *Annual Review of Nuclear and Particle Science*. Vol 45:89-131.

20. Bromley, D. A. 1984. Clustering phenomena in the nuclear many-body system. Pp. 1-32. in J.S. Lilley & M.A.Nagarajan (eds), Clustering Aspects of Nuclear Structure, 4th International Conference on Clustering Aspects of Nuclear Structure and Nuclear Reactions, Chester, UK. D. Reidel Pub. Co., Dordrecht, Holland.

21. Horiuchi, H., and K. Ikeda. 1986. Cluster models of the nucleus. in, *Cluster models and other topics, International Review of Nuclear Physics, vol. 4*. World Scientific, Singapore. pp: 1-259.

**Other cluster models that the Brightsen model builds on**

22. Wheeler J. A. 1937. On the mathematical description of light nuclei by the method of resonating group structure. *Phys. Rev*. 52:1083.

23. Wheeler J. A. 1937. Molecular viewpoints in nuclear structure. *Phys. Rev*. 52:1107.

24. Pauling L. 1965. The close-packed spheron model of atomic nuclei and its relation to the shell model, *Proc. Natl. Acad. Sci. USA*, Vol. 54, No. 4: 989.

25. Pauling L. 1965. The close-packed-spheron theory and nuclear fission, *Science*, Vol. 150, No. 3694:297.

26. Pauling L. 1966. The close-packed-spheron theory of nuclear structure and the neutron excess for stable nuclei (Dedicated to the seventieth anniversary of Professor Horia Hulubei). *Revue Roumain de Physique* 11 no. 9,10:825-833.

**Anomalies of orthopositronium annihilation**

27. Osmon P.E. Positron lifetime spectra in noble gases. Physical Review B, 1965, v.138, 216.

28. Tao S.J., Bell J., and Green J.H. Fine structure in delayed coincidence lifetime curves for positron in argon. Proceedings of the Physical Society, 1964, v.83, 453.

29. Levin B.M. and Shantarovich V.P. Annihilation of positrons in gaseous neon. High Energy Chemistry, 1977, v.11(4), 322-323.

30. Levin B.M. Time spectra of positron annihilation in neon. Soviet Journal Nucl. Physics, 1981, v.34(6), 917-918.

31. Levin B.M. and Shantarovich V.P. Anomalies in the time spectra of positron in gaseous neon. Soviet Journal Nucl. Physics, 1984, v.39(6), 855-856.

32. Levin B.M., Kochenda L.M., Markov A.A., and Shantarovich V.P. Time spectra of annihilation of positrons (22-Na) in gaseous neon of various isotopic compositions. Soviet Journal Nucl. Physics, 1987, v.45(6), 1119-1120.

33. Gidley D.W., Rich A., Sweetman E., and West D. New precision measurements of the decay rates of singlet and triplet positronium. Physical Review Letters, 1982, v.49, 525-528.

34. Westbrook C.I., Gidley D.W., Conti R.S., and Rich A. New precision measurement of the orthopositronium decay rate: a discrepancy with theory. Physical Review Letters, 1987, v.58, 1328-1331.

35. Westbrook C.I., Gidley D.W., Conti R.S., and Rich A. Precision measurement of the orthopositronium vacuum decay rate using the gas technique. Physical Review A, 1989, v.40, 5489-5499.

36. Nico J.S., Gidley D.W., Rich A., and Zitzewitz P.W. Precision measurement of the orthopositronium decay rate using the vacuum technique. Physical Review Letters, 1990, v.65, 1344-1347.

37. Caswell W.E. and Lepage G.P. (O-alpha-in-alpha)-corrections in positro nium-hyperfine splitting and decay rate. Physical Review A, 1979, v.20, 36.

38. Adkins G.S. Radiative-corrections to positronium decay. Ann. Phys. (N.Y.), 1983, v.146, 78.

39. Adkins G.S., Salahuddin A.A., and Schalm K.E. Analytic evaluation of the self-energy and outer-vertex corrections to the decay rate of orthopositronium in the Fried-Yennie gauge. Physical Review A, 1992, v.45, 3333-3335.

40. Adkins G.S., Salahuddin A.A., and Schalm K.E. Order-$alpha $ corrections to the decay rate of ortopositronium in the Fried-Yennie gauge. Physical Review A, 1992, v.45, 7774-7780.

41. Levin B.M. On the kinematics of one-photon annihilation of orthopositronium. Physics of Atomic Nuclei, 1995, v.58(2), 332-334.

42. Holdom B. Two U(1)'s and $epsilon $ charge shifts. Physics Letters B, 1986, v.166, 196-198.

43. Glashow S.L. Positronium versus the mirror Universe. Physics Letters B, 1986, v.167, 35-36.

44. Atoyan G.S., Gninenko S.N., Razin V.I., and Ryabov Yu.V. A search for photonless annihilation of orthopositronium. Physics Letters B, 1989, v.220, 317-320.

45. Asai S., Orito S., Sanuki T., Yasuda M., and Yokoi T. Direct search for orthopositronium decay into two photons. Physical Review Letters, 1991, v.66, 1298-1301.

46. Gidley D.W., Nico J.S., and Skalsey M. Direct search for two-photon modes of orthopositronium. Physical Review Letters , 1991, v.66, 1302-1305.

47. Al-Ramadhan A.H. and Gidley D.W. New precision measurement of the decay rate of singlet positronium. Physical Review Letters, 1994, v.72, 1632-1635.

48. Orito S., Yoshimura K., Haga T., Minowa M., and Tsuchiaki M. New limits on exotic two-body decay of orthopositronium. Physical Review Letters, 1989, v.63, 597-600.

49. Mitsui T., Fujimoto R., Ishisaki Y., Ueda Y., Yamazaki Y., Asai S., and Orito S. Search for invisible decay of orthopositronium. Physical Review Letters, 1993, v.70, 2265-2268.

50. Skalsey M. and Conti R.S. Search for very weakly interacting, short-lived, C-odd bosons and the orthopositronium decay-rate problem. Physical Review A, 1997, v.55(2), 984.

51. Adkins G.S., Melnikov K., and Yelkhovsky A. Virtual annihilation contribution to orthopositronium rate decay. Physical Review A, 1999, v.60(4), 3306-3307.

52. Asai S., Orito S., and Shinohara N. New measurement of the orthopositronium decay rate. Physics Letters B, 1995, v.357, 475-480.

53. Vallery R. S., Zitzewitz P. W., and Gidley D.W. 2003, *Phys. Rev. Lett.*, Vol.90, 203402.

54. Levin B.M. Orthopositronium: Annihilation of Positron in Gaseous Neon. arXiv: quant-ph/0303166.

55. Levin B.M. Orthopositronium-Lifetime Puzzle is Not Solved : On an Effect of Non-Perturbative Contribution. CERN EXT-2004-016.

56. Karshenboim S.G. Corrections to hyperfine splitting in positronium. Yadern. Fizika, 1993, v. 56(12), 155-171.

# Yang-Mills Field from Quaternion Space Geometry, and Its Klein-Gordon Representation

Alexander Yefremov*, Florentin Smarandache† and Vic Christianto‡

*Institute of Gravitation and Cosmology, Peoples' Friendship University of Russia,
Miklukho-Maklaya Str. 6, Moscow 117198, Russia
E-mail: a.yefremov@rudn.ru

†Chair of the Dept. of Mathematics and Science, University of New Mexico, Gallup, NM 87301, USA
E-mail: smarand@unm.edu

‡Sciprint.org — a Free Scientific Electronic Preprint Server, http://www.sciprint.org
E-mail: admin@sciprint.org

Analysis of covariant derivatives of vectors in quaternion (Q-) spaces performed using Q-unit spinor-splitting technique and use of SL(2C)-invariance of quaternion multiplication reveals close connexion of Q-geometry objects and Yang-Mills (YM) field principle characteristics. In particular, it is shown that Q-connexion (with quaternion non-metricity) and related curvature of 4 dimensional (4D) space-times with 3D Q-space sections are formally equivalent to respectively YM-field potential and strength, traditionally emerging from the minimal action assumption. Plausible links between YM field equation and Klein-Gordon equation, in particular via its known isomorphism with Duffin-Kemmer equation, are also discussed.

## 1 Introduction

Traditionally YM field is treated as a gauge, "*auxiliary*", field involved to compensate local transformations of a 'main' (e.g. spinor) field to keep invariance of respective action functional. Anyway there are a number of works where YM-field features are found related to some geometric properties of space-times of different types, mainly in connexion with contemporary gravity theories.

Thus in paper [1] violation of $\mathsf{SO}(3,1)$-covariance in gauge gravitation theory caused by distinguishing time direction from normal space-like hyper-surfaces is regarded as spontaneous symmetry violation analogous to introduction of mass in YM theory. Paper [2] shows a generic approach to formulation of a physical field evolution based on description of differential manifold and its mapping onto "model" spaces defined by characteristic groups; the group choice leads to gravity or YM theory equations. Furthermore it can be shown [2b] that it is possible to describe altogether gravitation in a space with torsion, and electroweak interactions on 4D real spacetime $C^2$, so we have in usual spacetime with torsion a unified theory (modulo the non treatment of the strong forces).

Somewhat different approach is suggested in paper [3] where gauge potentials and tensions are related respectively to connexion and curvature of principle bundle, whose base and gauge group choice allows arriving either to YM or to gravitation theory. Paper [4] dealing with gravity in Riemann-Cartan space and Lagrangian quadratic in connexion and curvature shows possibility to interpret connexion as a mediator of YM interaction.

In paper [5] a unified theory of gravity and electroweak forces is built with Lagrangian as a scalar curvature of space-time with torsion; if trace and axial part of the torsion vanish the Lagrangian is shown to separate into Gilbert and YM parts. Regardless of somehow artificial character of used models, these observations nonetheless hint that there may exist a deep link between supposedly really physical object, YM field and pure math constructions. A surprising analogy between main characteristics of YM field and mathematical objects is found hidden within geometry induced by quaternion (Q-) numbers.

In this regard, the role played by Yang-Mills field cannot be overemphasized, in particular from the viewpoint of the Standard Model of elementary particles. While there are a number of attempts for describing the Standard Model of hadrons and leptons from the viewpoint of classical electromagnetic Maxwell equations [6, 7], nonetheless this question remains an open problem. An alternative route toward achieving this goal is by using quaternion number, as described in the present paper. In fact, in Ref. [7] a somewhat similar approach with ours has been described, i.e. the generalized Cauchy-Riemann equations contain 2-spinor and C-gauge structures, and their integrability conditions take the form of Maxwell and Yang-Mills equations.

It is long ago noticed that Q-math (algebra, calculus and related geometry) naturally comprise many features attributed to physical systems and laws. It is known that quaternions describe three "imaginary" Q-units as unit vectors directing axes

of a Cartesian system of coordinates (it was initially developed to represent subsequent telescope motions in astronomical observation). Maxwell used the fact to write his equations in the most convenient Q-form. Decades later Fueter discovered a formidable coincidence: a pure math Cauchy-Riemann type condition endowing functions of Q-variable with analytical properties turned out to be identical in shape to vacuum equations of electrodynamics [9].

Later on other surprising Q-math — physics coincidences were found. Among them: "automatic" appearance of Pauli magnetic field-spin term with Bohr magneton as a coefficient when Hamiltonian for charged quantum mechanical particle was built with the help of Q-based metric [10]; possibility to endow "imaginary" vector Q-units with properties of not only stationary but movable triad of Cartan type and use it for a very simple description of Newtonian mechanics in rotating frame of reference [11]; discovery of inherited in Q-math variant of relativity theory permitting to describe motion of non-inertial frames [12]. Preliminary study shows that YM field components are also formally present in Q-math.

In Section 2 notion of Q-space is given in necessary detail. Section 3 discussed neat analogy between Q-geometric objects and YM field potential and strength. In Section 4 YM field and Klein-Gordon correspondence is discussed. Concluding remarks can be found in Section 5.

Part of our motivation for writing this paper was to explicate the hidden electromagnetic field origin of YM fields. It is known that the Standard Model of elementary particles lack systematic description for the mechanism of quark charges. (Let alone the question of whether quarks do exist or they are mere algebraic tools, as Heisenberg once puts forth: *If quarks exist, then we have redefined the word "exist"*.) On the other side, as described above, Maxwell described his theory in quaternionic language, therefore it seems natural to ask whether it is possible to find neat link between quaternion language and YM-fields, and by doing so provide one step toward describing mechanism behind quark charges.

Further experimental observation is of course recommended in order to verify or refute our propositions as described herein.

## 2 Quaternion spaces

Detailed description of Q-space is given in [13]; shortly but with necessary strictness its notion can be presented as following.

Let $U_N$ be a manifold, a geometric object consisting of points $M \in U_N$ each reciprocally and uniquely corresponding to a set of $N$ numbers-coordinates $\{y^A\} : M \leftrightarrow \{y^A\}$, $(A = 1, 2 \dots N)$. Also let the sets of coordinates be transformed so that the map becomes a homeomorphism of a class $C_k$. It is known that $U_N$ may be endowed with a proper tangent manifold $T_N$ described by sets of orthogonal unite vectors $\mathbf{e}_{(A)}$ generating in $T_N$ families of coordinate lines $M \to \{X^{(A)}\}$, indices in brackets being numbers of frames' vectors. Differentials of coordinates in $U_N$ and $T_N$ are tied as $dX^{(A)} = g_B^{(A)} dy^B$, with Lamé coefficients $g_B^{(A)}$, functions of $y^A$, so that $X^{(A)}$ are generally non-holonomic. Irrespectively of properties of $U_N$ each its point may be attached to the origin of a frame, in particular presented by "imaginary" Q-units $\mathbf{q}_k$, this attachment accompanied by a rule tying values of coordinates of this point with the triad orientation $M \leftrightarrow \{y^A, \Phi_\xi\}$. All triads $\{\mathbf{q}_k\}$ so defined on $U_N$ form a sort of "tangent" manifold $T(U, \mathbf{q})$, (really tangent only for the base $U_3$). Due to presence of frame vectors $\mathbf{q}_k(y)$ existence of metric and at least proper (quaternionic) connexion $\omega_{jkn} = -\omega_{jnk}$, $\partial_j \mathbf{q}_k = \omega_{jkn}\mathbf{q}_n$, is implied, hence one can tell of $T(U, \mathbf{q})$ as of a Q-tangent space on the base $U_N$. Coordinates $x_k$ defined along triad vectors $\mathbf{q}_k$ in $T(U, \mathbf{q})$ are tied with non-holonomic coordinates $X^{(A)}$ in proper tangent space $T_N$ by the transformation $dx_k \equiv h_{k(A)} dX^{(A)}$ with $h_{k(A)}$ being locally depending matrices (and generally not square) of relative $\mathbf{e}_{(A)} \leftrightarrow \mathbf{q}_k$ rotation. Consider a special case of unification $U \oplus T(U, \mathbf{q})$ with 3-dimensional base space $U = \mathbf{U}_3$. Moreover, let quaternion specificity of $T_3$ reflects property of the base itself, i.e. metric structure of $\mathbf{U}_3$ inevitably requires involvement of Q-triads to initiate Cartesian coordinates in its tangent space. Such 3-dimensional space generating sets of tangent quaternionic frames in each its point is named here "quaternion space" (or simply Q-space). Main distinguishing feature of a Q-space is non-symmetric form of its metric tensor* $\mathbf{g}_{kn} \equiv \mathbf{q}_k \mathbf{q}_n = -\delta_{kn} + + \varepsilon_{knj}\mathbf{q}_j$ being in fact multiplication rule of "imaginary" Q-units. It is easy to understand that all tangent spaces constructed on arbitrary bases as designed above are Q-spaces themselves. In most general case a Q-space can be treated as a space of affine connexion $\Omega_{jkn} = \Gamma_{jkn} + Q_{jkn} + + S_{jkn} + \omega_{jnk} + \sigma_{jkn}$ comprising respectively Riemann connexion $\Gamma_{jkn}$, Cartan contorsion $Q_{jkn}$, segmentary curvature (or ordinary non-metricity) $S_{jkn}$, Q-connexion $\omega_{jnk}$, and Q-non-metricity $\sigma_{jkn}$; curvature tensor is given by standard expression $R_{knij} = \partial_i \Omega_{j\,kn} - \partial_j \Omega_{i\,kn} + \Omega_{i\,km}\Omega_{j\,mn} - -\Omega_{j\,nm}\Omega_{i\,mk}$. Presence or vanishing of different parts of connexion or curvature results in multiple variants of Q-spaces classification [13]. Further on only Q-spaces with pure quaternionic characteristics (Q-connexion and Q-non-metricity) will be considered.

*Latin indices are 3D, Greek indices are 4D; $\delta_{kn}$, $\varepsilon_{knj}$ are Kronecker and Levi-Civita symbols; summation convention is valid.

## 3 Yang-Mills field from Q-space geometry

Usually Yang-Mills field $A_{B\mu}$ is introduced as a gauge field in procedure of localized transformations of certain field, e.g. spinor field [14, 15]

$$\psi_a \to U(y^\beta)\,\psi_a\,. \tag{1}$$

If in the Lagrangian of the field partial derivative of $\psi_a$ is changed to "covariant" one

$$\partial_\beta \to D_\beta \equiv \partial_\beta - g A_\beta\,, \tag{2}$$

$$A_\beta \equiv i A_{C\,\beta}\,\mathbf{T}_C\,, \tag{3}$$

where $g$ is a real constant (parameter of the model), $\mathbf{T}_C$ are traceless matrices (Lie-group generators) commuting as

$$[\mathbf{T}_B,\,\mathbf{T}_C] = i f_{BCD}\,\mathbf{T}_D \tag{4}$$

with structure constants $f_{BCD}$, then

$$D_\beta U \equiv (\partial_\beta - g A_\beta)\,U = 0\,, \tag{5}$$

and the Lagrangian keeps invariant under the transformations (1). The theory becomes "self consistent" if the gauge field terms are added to Lagrangian

$$L_{YM} \sim F^{\alpha\beta}\,F_{\alpha\beta}\,, \tag{6}$$

$$F_{\alpha\beta} \equiv F_{C\,\alpha\beta}\,\mathbf{T}_C\,. \tag{7}$$

The gauge field intensity $F_B^{\mu\nu}$ expressed through potentials $A_{B\mu}$ and structure constants as

$$F_{C\,\alpha\beta} = \partial_\alpha A_{C\beta} - \partial_\beta A_{C\,\alpha} + f_{CDE}\,A_{D\,\alpha}\,A_{E\,\beta}\,. \tag{8}$$

Vacuum equations of the gauge field

$$\partial_\alpha\,F^{\alpha\beta} + \left[A_\alpha,\,F^{\alpha\beta}\right] = 0 \tag{9}$$

are result of variation procedure of action built from Lagrangian (6).

Group Lie, e.g. $\mathtt{SU(2)}$ generators in particular can be represented by "imaginary" quaternion units given by e.g. traceless $2\times 2$-matrices in special representation (Pauli-type) $i\mathbf{T}_B \to \mathbf{q}_{\tilde{k}} = -i\sigma_k$ ($\sigma_k$ are Pauli matrices),

Then the structure constants are Levi-Civita tensor components $f_{BCD} \to \varepsilon_{knm}$, and expressions for potential and intensity (strength) of the gauge field are written as:

$$A_\beta = g\,\frac{1}{2}\,A_{\tilde{k}\,\beta}\,\mathbf{q}_{\tilde{k}}\,, \tag{10}$$

$$F_{k\,\alpha\beta} = \partial_\alpha A_{k\,\beta} - \partial_\beta A_{k\,\alpha} + \varepsilon_{kmn}\,A_{m\,\alpha}\,A_{n\beta}\,. \tag{11}$$

It is worthnoting that this conventional method of introduction of a Yang-Mills field type essentially exploits *heuristic base* of theoretical physics, first of all the postulate of minimal action and formalism of Lagrangian functions construction. But since description of the field optionally uses quaternion units one can assume that some of the above relations are appropriate for Q-spaces theory and may have geometric analogues. To verify this assumption we will use an example of 4D space-time model with 3D spatial quaternion section.

Begin with the problem of 4D space-time with 3D spatial section in the form of Q-space containing only one geometric object: proper quaternion connexion. Q-covariant derivative of the basic (frame) vectors $\mathbf{q}_m$ identically vanish in this space:

$$\tilde{D}_\alpha\,\mathbf{q}_k \equiv (\delta_{mk}\,\partial_\alpha + \omega_{\alpha\,mk})\,\mathbf{q}_m = 0\,. \tag{12}$$

This equation is in fact equivalent to definition of the proper connexion $\omega_{\alpha\,mk}$. If a transformation of Q-units is given by spinor group (leaving quaternion multiplication rule invariant)

$$\mathbf{q}_k = U(y)\,\mathbf{q}_{\tilde{k}}\,U^{-1}(y) \tag{13}$$

($\mathbf{q}_{\tilde{k}}$ are constants here) then Eq. (12) yields

$$\partial_\alpha U\,\mathbf{q}_{\tilde{k}}\,U^{-1} + U\,\mathbf{q}_{\tilde{k}}\,\partial_\alpha U^{-1} = \omega_{\alpha kn}\,U\,\mathbf{q}_{\tilde{n}}\,U^{-1}. \tag{14}$$

But one can easily verify that each "imaginary" Q-unit $\mathbf{q}_{\tilde{k}}$ can be always represented in the form of tensor product of its eigen-functions (EF) $\psi_{(\tilde{k})}$, $\varphi_{(\tilde{k})}$ (no summation convention for indices in brackets):

$$\mathbf{q}_{\tilde{k}}\,\psi_{(\tilde{k})} = \pm i\psi_{(\tilde{k})}, \qquad \varphi_{(\tilde{k})}\mathbf{q}_{\tilde{k}} = \pm i\varphi_{(\tilde{k})} \tag{15}$$

having spinor structure (here only EF with positive parity (with sign +) are shown)

$$\mathbf{q}_{\tilde{k}} = i\big(2\psi_{(\tilde{k})}\varphi_{(\tilde{k})} - 1\big); \tag{16}$$

this means that left-hand-side (lhs) of Eq. (14) can be equivalently rewritten in the form

$$\begin{aligned} &\frac{1}{2}\left(\partial_\alpha U\,\mathbf{q}_{\tilde{k}}\,U^{-1} + U\,\mathbf{q}_{\tilde{k}}\,\partial_\alpha U^{-1}\right) = \\ &\quad = \left(\partial_\alpha U\,\psi_{(\tilde{k})}\right)\varphi_{(\tilde{k})}U^{-1} + U\,\psi_{(\tilde{k})}\left(\varphi_{(\tilde{k})}\partial_\alpha U^{-1}\right) \end{aligned} \tag{17}$$

which strongly resembles use of Eq. (1) for transformations of spinor functions.

Here we for the first time underline a remarkable fact: *form-invariance of multiplication rule of Q-units under their spinor transformations gives expressions similar to those conventionally used to initiate introduction of gauge fields of Yang-Mills type.*

Now in order to determine mathematical analogues of these "physical fields", we will analyze in more details Eq. (14). Its multiplication (from the right) by combination $U\,\mathbf{q}_{\tilde{k}}$ with contraction by index $\tilde{k}$ leads to the expression

$$-3\,\partial_\alpha U\; + U\,\mathbf{q}_{\tilde{k}}\,\partial_\alpha U^{-1}U\mathbf{q}_{\tilde{k}} = \omega_{\alpha k n}\,U\,\mathbf{q}_{\tilde{n}}\,\mathbf{q}_{\tilde{k}}\,. \tag{18}$$

This matrix equation can be simplified with the help of the always possible development of transformation matrices

$$U \equiv a\; + b_k\,\mathbf{q}_{\tilde{k}}\,, \qquad U^{-1} = a\; - b_k\,\mathbf{q}_{\tilde{k}}\,, \tag{19}$$

$$UU^{-1} = a^2\; + b_k\,b_k = 1\,, \tag{20}$$

where $a$, $b_k$ are real scalar and 3D-vector functions, $\mathbf{q}_{\tilde{k}}$ are Q-units in special (Pauli-type) representation. Using Eqs. (19), the second term in lhs of Eq. (18) after some algebra is reduced to remarkably simple expression

$$\begin{aligned} &U\,\mathbf{q}_{\tilde{k}}\,\partial_\alpha U^{-1}U\mathbf{q}_{\tilde{k}} = \\ &= \left(a + b_n\mathbf{q}_{\tilde{n}}\right)\mathbf{q}_{\tilde{k}}\left(\partial_\alpha a - \partial_\alpha b_m\mathbf{q}_{\tilde{m}}\right)\left(a + b_l\,\mathbf{q}_{\tilde{l}}\right)\mathbf{q}_{\tilde{k}} = \\ &= \partial_\alpha(a + b_n\mathbf{q}_{\tilde{n}}) = -\,\partial_\alpha U \end{aligned} \tag{21}$$

so that altogether lhs of Eq. (18) comprises $-4\,\partial_\alpha U$ while right-hand-side (rhs) is

$$\omega_{\alpha k n}\,U\,\mathbf{q}_{\tilde{n}}\mathbf{q}_{\tilde{k}} = -\,\varepsilon_{knm}\omega_{\alpha k n}\,U\,\mathbf{q}_{\tilde{m}}\,; \tag{22}$$

then Eq. (18) yields

$$\partial_\alpha U - \frac{1}{4}\,\varepsilon_{knm}\omega_{\alpha k n}\,U\,\mathbf{q}_{\tilde{m}} = 0\,. \tag{23}$$

If now one makes the following notations

$$A_{k\;\alpha} \equiv \frac{1}{2}\,\varepsilon_{knm}\omega_{\alpha k n}\,, \tag{24}$$

$$A_{\,\alpha} \equiv \frac{1}{2}\,A_n\mathbf{q}_{\tilde{n}}\,, \tag{25}$$

then notation (25) exactly coincides with the definition (10) (provided $g = 1$), and Eq. (23) turns out equivalent to Eq. (5)

$$U\overleftarrow{D}_\alpha \equiv U(\overleftarrow{\partial}_\alpha - A_\alpha) = 0\,. \tag{26}$$

Expression for "covariant derivative" of inverse matrix follows from the identity:

$$\partial_\alpha U\,U^{-1} = -\,U\partial_\alpha U^{-1}. \tag{27}$$

Using Eq. (23) one easily computes

$$-\partial_\alpha U^{-1} - \frac{1}{4}\,\varepsilon_{knm}\omega_{\alpha kn}\,\mathbf{q}_{\tilde{m}}U^{-1} = 0 \tag{28}$$

or

$$D_\alpha U^{-1} \equiv (\partial_\alpha + A_\alpha)\,U^{-1} = 0\,. \tag{29}$$

Direction of action of the derivative operator is not essential here, since the substitution $U^{-1} \to U \;\; U \to U^{-1}$ is always possible, and then Eq. (29) exactly coincides with Eq. (5).

Now let us summarize first results. We have a remarkable fact: form-invariance of Q-multiplication has as a corollary "covariant constancy" of matrices of spinor transformations of vector Q-units; moreover one notes that proper Q-connexion (contracted in skew indices by Levi-Civita tensor) plays the role of "gauge potential" of some Yang-Mills-type field. By the way the Q-connexion is easily expressed from Eq. (24)

$$\omega_{\alpha kn} = \varepsilon_{mkn}A_{m\,\alpha}\,. \tag{30}$$

Using Eq. (25) one finds expression for the gauge field intensity (11) (contracted by Levi-Civita tensor for convenience) through Q-connexion

$$\begin{aligned}
&\varepsilon_{kmn}F_{k\,\alpha\beta} \;= \\
&= \varepsilon_{kmn}(\partial_\alpha A_{k\,\beta} - \partial_\beta A_{k\,\alpha}) + \varepsilon_{kmn}\varepsilon_{mlj}A_{l\,\alpha}A_{j\,\beta} = \\
&= \partial_\alpha\omega_{\beta\,mn} - \partial_\beta\omega_{\,\alpha\,mn} + A_{m\,\alpha}A_{n\,\beta} - A_{m\beta}A_{n\alpha}\,.
\end{aligned} \tag{31}$$

If identically vanishing sum

$$-\delta_{mn}A_{j\,\alpha}A_{j\,\beta} + \delta_{mn}A_{j\beta}A_{j\alpha} = 0 \tag{32}$$

is added to rhs of (31) then all quadratic terms in the right hand side can be given in the form

$$\begin{aligned}
&A_{m\,\alpha}A_{n\,\beta} - A_{m\beta}A_{n\,\alpha} - \delta_{mn}A_{j\,\alpha}A_{j\,\beta} + \delta_{mn}A_{j\beta}A_{j\alpha} = \\
&= (\delta_{mp}\delta_{qn} - \delta_{mn}\delta_{qp})(A_{p\,\alpha}A_{q\,\beta} - A_{p\beta}A_{q\,\alpha}) = \\
&= \varepsilon_{kmq}\varepsilon_{kpn}(A_{p\,\alpha}A_{q\beta} - A_{p\beta}A_{q\,\alpha}) = \\
&= -\omega_{\alpha\,kn}\,\omega_{\beta\,km} + \omega_{\beta\,kn}A_{\alpha\,km}\,.
\end{aligned}$$

Substitution of the last expression into Eq. (31) accompanied with new notation

$$R_{mn\,\alpha\beta} \equiv \varepsilon_{kmn}F_{k\,\alpha\beta} \tag{33}$$

leads to well-known formula:

$$\begin{aligned}
R_{mn\,\alpha\beta} = \partial_\alpha\omega_{\beta\,mn} - \partial_\beta\omega_{\,\alpha\,mn} + \\
+\omega_{\alpha\,nk}\,\omega_{\beta\,km} - \omega_{\beta\,nk}\,\omega_{\alpha\,km}\,.
\end{aligned} \tag{34}$$

This is nothing else but curvature tensor of Q-space built out of proper Q-connexion components (in their turn being functions of 4D coordinates). By other words, Yang-Mills field strength is mathematically (geometrically) identical to quaternion space curvature tensor. But in the considered case of Q-space comprising only proper Q-connexion, all components of the curvature tensor are identically zero. So Yang-Mills field in this case has potential but no intensity.

The picture absolutely changes for the case of quaternion space with Q-connexion containing a proper part $\omega_{\beta\,kn}$ and also Q-non-metricity $\sigma_{\beta\,kn}$

$$\Omega_{\beta\,kn}(y^\alpha) = \omega_{\beta\,kn} + \sigma_{\beta\,kn} \tag{35}$$

so that Q-covariant derivative of a unite Q-vector with connexion (35) does not vanish, its result is namely the Q-non-metricity

$$\hat{D}_\alpha\mathbf{q}_k \equiv (\delta_{mk}\partial_\alpha + \Omega_{\alpha\,mk})\,\mathbf{q}_m = \sigma_{\alpha\,mk}\,\mathbf{q}_k\,. \tag{36}$$

For this case "covariant derivatives" of transformation spinor matrices may be defined analogously to previous case definitions (26) and (29)

$$U\overleftarrow{\hat{D}}_\alpha \equiv \hat{U}(\overleftarrow{\partial}_\alpha - \hat{A}_\alpha), \quad \hat{D}_\alpha U^{-1} \equiv (\partial_\alpha + \hat{A}_\alpha)U\,. \tag{37}$$

But here the "gauge field" is built from Q-connexion (35)

$$\hat{A}_{k\ \alpha} \equiv \frac{1}{2}\,\varepsilon_{knm}\Omega_{\alpha kn}, \qquad \hat{A}_{\alpha} \equiv \frac{1}{2}\,\hat{A}_n \mathbf{q}_{\tilde{n}}\,. \tag{38}$$

It is not difficult to verify whether the definitions (37) are consistent with non-metricity condition (36). Action of the "covariant derivatives" (37) onto a spinor-transformed unite Q-vector

$$\begin{aligned}
&\hat{D}_\alpha \mathbf{q}_k \to (\hat{D}_\alpha U)\,\mathbf{q}_{\tilde{k}}\,\partial_\alpha U^{-1} + U\,\mathbf{q}_{\tilde{k}}\,(\hat{D}_\alpha U^{-1}) = \\
&= \left(U\overleftarrow{D}_\alpha - \frac{1}{4}\,\varepsilon_{jnm}\Omega_{\alpha\,nm} U \mathbf{q}_{\tilde{j}}\,\mathbf{q}_{\tilde{k}}\right) U^{-1} + \\
&+ U\,\mathbf{q}_{\tilde{k}}\left(D_\alpha U^{-1} + \frac{1}{4}\,\varepsilon_{jnm}\Omega_{\alpha\,nm}\,\mathbf{q}_{\tilde{j}} U^{-1}\right)
\end{aligned}$$

together with Eqs. (26) and (29) demand:

$$U\overleftarrow{D}_\alpha = D_\alpha U^{-1} = 0 \tag{39}$$

leads to the expected results

$$\begin{aligned}
\hat{D}_\alpha \mathbf{q}_k \to \frac{1}{2}\,\varepsilon_{jnm}\sigma_{\alpha\,nm} U \varepsilon_{jkl}\,\mathbf{q}_{\tilde{l}}\,U^{-1} = \\
= \sigma_{\alpha\,kl} U\,\mathbf{q}_{\tilde{l}}\,U^{-1} = \sigma_{\alpha\,kl}\,\mathbf{q}_l
\end{aligned}$$

i.e. "gauge covariant" derivative of any Q-unit results in Q-non-metricity in full accordance with Eq. (36).

Now find curvature tensor components in this Q-space; it is more convenient to calculate them using differential forms. Given Q-connexion 1-form

$$\Omega_{\ kn} = \Omega_{\beta\,kn} dy^\beta \tag{40}$$

from the second equation of structure

$$\frac{1}{2}\,\hat{R}_{kn\alpha\beta}\,dy^\alpha \wedge dy^\beta = d\Omega_{kn} + \Omega_{km} \wedge \Omega_{mn} \tag{41}$$

one gets the curvature tensor component

$$\begin{aligned}
\hat{R}_{kn\alpha\beta} = \partial_\alpha \Omega_{\beta\,kn} - \partial_\beta \Omega_{\alpha\,kn} + \\
+ \Omega_{\alpha\,km}\Omega_{\beta\,mn} - \Omega_{\alpha\,nm}\Omega_{\beta\,mk}
\end{aligned} \tag{42}$$

quite analogously to Eq. (34). Skew-symmetry in 3D indices allows representing the curvature part of 3D Q-section as 3D axial vector

$$\hat{F}_{m\,\alpha\beta} \equiv \frac{1}{2}\,\varepsilon_{knm}\hat{R}_{kn\alpha\beta} \tag{43}$$

and using Eq. (38) one readily rewrites definition (43) in the form

$$\hat{F}_{m\,\alpha\beta} = \partial_\alpha \hat{A}_{m\,\beta} - \partial_\beta \hat{A}_{m\,\alpha} + \varepsilon_{knm}\hat{A}_{k\,\alpha}\hat{A}_{n\,\beta} \tag{44}$$

which exactly coincides with conventional definition (11). QED.

## 4 Klein-Gordon representation of Yang-Mills field

In the meantime, it is perhaps more interesting to note here that such a neat linkage between Yang-Mills field and quaternion numbers is already known, in particular using Klein-Gordon representation [16]. In turn, this neat correspondence between Yang-Mills field and Klein-Gordon representation can be expected, because both can be described in terms of $\mathrm{SU}(2)$ theory [17]. In this regards, quaternion decomposition of $\mathrm{SU}(2)$ Yang-Mills field has been discussed in [17], albeit it implies a different metric from what is described herein:

$$ds^2 = d\alpha_1^2 + \sin^2\alpha_1\,d\beta_1^2 + d\alpha_2^2 + \sin^2\alpha_2\,d\beta_2^2\,. \tag{45}$$

However, the $\mathrm{O}(3)$ non-linear sigma model appearing in the decomposition [17] looks quite similar (or related) to the Quaternion relativity theory (as described in the Introduction, there could be neat link between Q-relativity and $\mathrm{SO}(3,1)$).

Furthermore, sometime ago it has been shown that four-dimensional coordinates may be combined into a quaternion, and this could be useful in describing supersymmetric extension of Yang-Mills field [18]. This plausible neat link between Klein-Gordon equation, Duffin-Kemmer equation and Yang-Mills field via quaternion number may be found useful, because both Duffin-Kemmer equation and Yang-Mills field play some kind of significant role in description of standard model of particles [16].

In this regards, it has been argued recently that one can derive standard model using Klein-Gordon equation, in particular using Yukawa method, without having to introduce a Higgs mass [19, 20]. Considering a notorious fact that Higgs particle has not been observed despite more than three decades of extensive experiments, it seems to suggest that an alternative route to standard model of particles using (quaternion) Klein-Gordon deserves further consideration.

In this section we will discuss a number of approaches by different authors to describe the (quaternion) extension of Klein-Gordon equation and its implications. First we will review quaternion quantum mechanics of Adler. And then we discuss how Klein-Gordon equation leads to hypothetical imaginary mass. Thereafter we discuss an alternative route for quaternionic modification of Klein-Gordon equation, and implications to meson physics.

### 4.1 Quaternion Quantum Mechanics

Adler's method of quaternionizing Quantum Mechanics grew out of his interest in the Harari-Shupe's rishon model for composite quarks and leptons [21]. In a preceding paper [22] he describes that in quaternionic quantum mechanics (QQM), the Dirac transition amplitudes are quaternion valued, i.e. they have the form

$$q = r_0 + r_1 i + r_2 j + r_3 k \tag{46}$$

where $r_0$, $r_1$, $r_2$, $r_3$ are real numbers, and $i$, $j$, $k$ are quaternion imaginary units obeying

$$\begin{aligned} &i^2 = j^2 = k^2 = -1, \quad ij = -ji = k, \\ &jk = -kj = i, \qquad\quad ki = -ik = j\,. \end{aligned} \tag{47}$$

Using this QQM method, he described composite fermion states identified with the quaternion real components [23].

### 4.2 Hypothetical imaginary mass problem in Klein-Gordon equation

It is argued that dynamical origin of Higgs mass implies that the mass of W must always be pure imaginary [19, 20]. Therefore one may conclude that a real description for (composite) quarks and leptons shall avoid this problem, i.e. by not including the problematic Higgs mass.

Nonetheless, in this section we can reveal that perhaps the problem of imaginary mass in Klein-Gordon equation is not completely avoidable. First we will describe an elementary derivation of Klein-Gordon from electromagnetic wave equation, and then by using Bakhoum's assertion of total energy we derive alternative expression of Klein-Gordon implying the imaginary mass.

We can start with 1D-classical wave equation as derived from Maxwell equations [24, p.4]:

$$\frac{\partial^2 E}{\partial x^2} - \frac{1}{c^2}\frac{\partial^2 E}{\partial t^2} = 0\,. \tag{48}$$

This equation has plane wave solutions:

$$E(x,t) = E_0 e^{i(kx-\omega t)} \tag{49}$$

which yields the relativistic total energy:

$$\varepsilon^2 = p^2c^2 + m^2c^4. \tag{50}$$

Therefore we can rewrite (48) for non-zero mass particles as follows [24]:

$$\left(\frac{\partial^2}{\partial x^2} - \frac{1}{c^2}\frac{\partial^2}{\partial t^2} - \frac{m^2c^2}{\hbar^2}\right)\Psi e^{\frac{i}{\hbar}(px-Et)} = 0\,. \tag{51}$$

Rearranging this equation (51) we get the Klein-Gordon equation for a free particle in 3-dimensional condition:

$$\left(\nabla - \frac{m^2c^2}{\hbar^2}\right)\Psi = \frac{1}{c^2}\frac{\partial^2 \Psi}{\partial t^2}\,. \tag{52}$$

It seems worthnoting here that it is more proper to use total energy definition according to Noether's theorem in lieu of standard definition of relativistic total energy. According to Noether's theorem [25], the total energy of the system corresponding to the time translation invariance is given by:

$$E = mc^2 + \frac{cw}{2} \int_0^\infty \left( \gamma^2 \, 4\pi r^2 \, dr \right) = k\mu c^2 \tag{53}$$

where $k$ is *dimensionless* function. It could be shown, that for low-energy state the total energy could be far less than $E = mc^2$. Interestingly Bakhoum [25] has also argued in favor of using $E = mv^2$ for expression of total energy, which expression could be traced back to Leibniz. Therefore it seems possible to argue that expression $E = mv^2$ is more generalized than the standard expression of special relativity, in particular because the total energy now depends on actual velocity [25].

From this new expression, it is possible to rederive Klein-Gordon equation. We start with Bakhoum's assertion that it is more appropriate to use $E = mv^2$, instead of more convenient form $E = mc^2$. This assertion would imply [25]:

$$H^2 = p^2 c^2 - m_0^2 c^2 v^2 . \tag{54}$$

A bit remark concerning Bakhoum's expression, it does not mean to imply or to interpret $E = mv^2$ as an assertion that it implies zero energy for a rest mass. Actually the problem comes from "mixed" interpretation of what we mean with "velocity". In original Einstein's paper (1905) it is defined as "kinetic velocity", which can be measured when standard "steel rod" has velocity approximates the speed of light. But in quantum mechanics, we are accustomed to make use it deliberately to express "photon speed" $= c$. Therefore, in special relativity 1905 paper, it should be better to interpret it as "speed of free electron", which approximates $c$. For hydrogen atom with 1 electron, the electron occupies the first excitation (quantum number $n = 1$), which implies that their speed also approximate $c$, which then it is quite safe to assume $E \sim mc^2$. But for atoms with large number of electrons occupying large quantum numbers, as Bakhoum showed that electron speed could be far less than $c$, therefore it will be more exact to use $E = mv^2$, where here $v$ should be defined as "average electron speed" [25].

In the first approximation of relativistic wave equation, we could derive Klein-Gordon-type relativistic equation from equation (54), as follows. By introducing a new parameter:

$$\zeta = i \frac{v}{c} , \tag{55}$$

then we can use equation (55) in the known procedure to derive Klein-Gordon equation:

$$E^2 = p^2 c^2 + \zeta^2 m_0^2 c^4 , \tag{56}$$

where $E = mv^2$. By using known substitution:

$$E = i\hbar \frac{\partial}{\partial t} , \qquad p = \frac{\hbar}{i} \nabla , \tag{57}$$

and dividing by $(\hbar c)^2$, we get Klein-Gordon-type relativistic equation [25]:

$$- c^{-2} \frac{\partial \Psi}{\partial t} + \nabla^2 \Psi = k_0^{'2} \, \Psi , \tag{58}$$

where

$$k_0^{'} = \frac{\zeta m_0 c}{\hbar} . \tag{59}$$

Therefore we can conclude that imaginary mass term appears in the definition of coefficient $k_0^{'}$ of this new Klein-Gordon equation.

### 4.3 Modified Klein-Gordon equation and meson observation

As described before, quaternionic Klein-Gordon equation has neat link with Yang-Mills field. Therefore it seems worth to discuss here how to quaternionize Klein-Gordon equation. It can be shown that the resulting modified Klein-Gordon equation also exhibits imaginary mass term.

Equation (52) is normally rewritten in simpler form (by asserting $c = 1$):

$$\left(\nabla - \frac{\partial^2}{\partial t^2}\right)\Psi = \frac{m^2}{\hbar^2}\,. \tag{60}$$

Interestingly, one can write the Nabla-operator above in quaternionic form, as follows:

**A.** Define quaternion-Nabla-operator as analog to quaternion number definition above (46), as follows [25]:

$$\nabla^q = -i\frac{\partial}{\partial t} + e_1\frac{\partial}{\partial x} + e_2\frac{\partial}{\partial y} + e_3\frac{\partial}{\partial z}\,, \tag{61}$$

where $e_1$, $e_2$, $e_3$ are quaternion imaginary units. Note that equation (61) has included partial time-differentiation.

**B.** Its quaternion conjugate is defined as follows:

$$\bar{\nabla}^q = -i\frac{\partial}{\partial t} - e_1\frac{\partial}{\partial x} - e_2\frac{\partial}{\partial y} - e_3\frac{\partial}{\partial z}\,. \tag{62}$$

**C.** Quaternion multiplication rule yields:

$$\nabla^q\bar{\nabla}^q = -\frac{\partial^2}{\partial t^2} + \frac{\partial^2}{\partial^2 x} + \frac{\partial^2}{\partial^2 y} + \frac{\partial^2}{\partial^2 z}\,. \tag{63}$$

**D.** Then equation (63) permits us to rewrite equation (60) in quaternionic form as follows:

$$\nabla^q\bar{\nabla}^q\Psi = \frac{m^2}{\hbar^2}\,. \tag{64}$$

Alternatively, one used to assign standard value $c = 1$ and also $\hbar = 1$, therefore equation (60) may be written as:

$$\left(\frac{\partial^2}{\partial t^2} - \nabla^2 + m^2\right)\varphi(x,t) = 0\,, \tag{65}$$

where the first two terms are often written in the form of square Nabla operator. One simplest version of this equation [26]:

$$-\left(\frac{\partial S_0}{\partial t}\right)^2 + m^2 = 0 \tag{66}$$

yields the known solution [26]:

$$S_0 = \pm mt + \text{constant}\,. \tag{67}$$

The equation (66) yields wave equation which describes a particle at rest with positive energy (lower sign) or with negative energy (upper sign). Radial solution of equation (66) yields Yukawa potential which predicts meson as observables.

It is interesting to note here, however, that numerical 1-D solution of equation (65), (66) and (67) each yields slightly different result, as follows. (All numerical computation was performed using Mathematica [28].)

- For equation (65) we get:

(−D[#,x,x]+m^2+D[#,t,t])&[y[x,t]]==

$$m^2 + y^{(0,2)}[x,t] - y^{(2,0)}[x,t] = 0$$

DSolve[%,y[x,t],{x,t}]

$$\left\{\left\{y[x,t] \to \frac{m^2x^2}{2} + C[1][t-x] + C[2][t+x]\right\}\right\}$$

- For equation (66) we get:

( m^2−D[#,t,t])&[y[x,t]]==

$$m^2 + y^{(0,2)}[x,t] = 0$$

DSolve[%,y[x,t],{x,t}]

$$\left\{\left\{y[x,t] \to \frac{m^2 t^2}{2} + C[1][x] + tC[2][x]\right\}\right\}$$

One may note that this numerical solution is in quadratic form $\frac{m^2 t^2}{2}$ + constant, therefore it is rather different from equation (67) in [26].

In the context of possible supersymetrization of Klein-Gordon equation (and also PT-symmetric extension of Klein-Gordon equation [27, 29]), one can make use biquaternion number instead of quaternion number in order to generalize further the differential operator in equation (61):

**E.** Define a new "diamond operator" to extend quaternion-Nabla-operator to its biquaternion counterpart, according to the study [25]:

$$\begin{aligned} \diamondsuit = \nabla^q + i\,\nabla^q = &\left(-i\frac{\partial}{\partial t} + e_1\frac{\partial}{\partial x} + e_2\frac{\partial}{\partial y} + e_3\frac{\partial}{\partial z}\right) + \\ &+ i\left(-i\frac{\partial}{\partial T} + e_1\frac{\partial}{\partial X} + e_2\frac{\partial}{\partial Y} + e_3\frac{\partial}{\partial Z}\right), \end{aligned} \tag{68}$$

where $e_1$, $e_2$, $e_3$ are quaternion imaginary units. Its conjugate can be defined in the same way as before.

To generalize Klein-Gordon equation, one can generalize its differential operator to become:

$$\left[\left(\frac{\partial^2}{\partial t^2} - \nabla^2\right) + i\left(\frac{\partial^2}{\partial t^2} - \nabla^2\right)\right]\varphi(x,t) = -m^2\varphi(x,t), \tag{69}$$

or by using our definition in (68), one can rewrite equation (69) in compact form:

$$\left(\diamondsuit\bar{\diamondsuit} + m^2\right)\varphi(x,t) = 0, \tag{70}$$

and in lieu of equation (66), now we get:

$$\left[\left(\frac{\partial S_0}{\partial t}\right)^2 + i\left(\frac{\partial S_0}{\partial t}\right)^2\right] = m^2. \tag{71}$$

Numerical solutions for these equations were obtained in similar way with the previous equations:

- For equation (70) we get:

(−D[#,x,x]+D[#,t,t]−I*D[#,x,x]+I*D[#,t,t]+m^2)
&[y[x,t]]==

$$m^2 + (1+i)\,y^{(0,2)}[x,t] - (1+i)\,y^{(2,0)}[x,t] = 0$$

DSolve[%,y[x,t],{x,t}

$$\left\{\left\{y[x,t] \to \left(\frac{1}{4} - \frac{i}{4}\right)m^2 x^2 + C[1][t-x] + C[2][t+x]\right\}\right\}$$

- For equation (71) we get:

(−m^2+D[#,t,t]+I*D[#,t,t])&[y[x,t]]==

$$m^2 + (1+i)\,y^{(0,2)}[x,t] = 0$$

DSolve[%,y[x,t],{x,t}]

$$\left\{\left\{y[x,t] \to \left(\frac{1}{4} - \frac{i}{4}\right)m^2 x^2 + C[1][x] + tC[2][x]\right\}\right\}$$

Therefore, we may conclude that introducing biquaternion differential operator (in terms of "diamond operator") yield quite different solutions compared to known standard solution of Klein-Gordon equation [26]:

$$y(x,t) = \left(\frac{1}{4} - \frac{i}{4}\right) m^2 t^2 + \text{constant}\,. \tag{72}$$

In other word: we can infer hat $t = \pm\frac{1}{m}\,\sqrt{y/\left(\frac{1}{4} - \frac{i}{4}\right)}$, therefore it is likely that there is imaginary part of time dimension, which supports a basic hypothesis of the aforementioned BQ-metric in Q-relativity.

Since the potential corresponding to this biquaternionic KGE is neither Coulomb, Yukawa, nor Hulthen potential, then one can expect to observe a new type of matter, which may be called "*supersymmetric-meson*". If this new type of particles can be observed in near future, then it can be regarded as early verification of the new hypothesis of PT-symmetric QM and CT-symmetric QM as considered in some recent reports [27, 29]. In our opinion, its presence may be expected in particular in the process of breaking of Coulomb barrier in low energy schemes.

Nonetheless, further observation is recommended in order to support or refute this proposition.

## 5 Concluding remarks

If 4D space-time has for its 3D spatial section a Q-space with Q-connexion $\Omega_{\beta\,kn}$ containing Q-non-metricity $\sigma_{\beta\,kn}$, then the Q-connexion, geometric object, is algebraically identical to Yang-Mills potential

$$\hat{A}_{k\alpha} \equiv \frac{1}{2}\,\varepsilon_{knm}\Omega_{\alpha kn}\,,$$

while respective curvature tensor $\hat{R}_{kn\alpha\beta}$, also a geometric object, is algebraically identical to Yang-Mills "physical field" strength

$$\hat{F}_{m\alpha\beta} \equiv \frac{1}{2}\,\varepsilon_{knm}\hat{R}_{kn\alpha\beta}\,.$$

Thus Yang-Mills gauge field Lagrangian

$$L_{YM} \sim \hat{F}_k^{\alpha\beta}\,\hat{F}_{k\alpha\beta} = \frac{1}{4}\,\varepsilon_{kmn}\varepsilon_{kjl}\,\hat{R}_{mn}^{\alpha\beta}\hat{R}_{jl\alpha\beta} = \frac{1}{2}\,\hat{R}_{mn}^{\alpha\beta}\hat{R}_{mn\alpha\beta}$$

can be geometrically interpreted as a Lagrangian of "non-linear" or "quadratic" gravitational theory, since it contains quadratic invariant of curvature Riemann-type tensor contracted by all indices. Hence Yang-Mills theory can be regarded as a theory of pure geometric objects: Q-connexion and Q-curvature with Lagrangian quadratic in curvature (as: Einstein's theory of gravitation is a theory of geometrical objects: Christoffel symbols and Riemann tensor, but with linear Lagrangian made of scalar curvature).

Presence of Q-non-metricity is essential. If Q-non-metricity vanishes, the Yang-Mills potential may still exist, then it includes only proper Q-connexion (in particular, components of Q-connexion physically manifest themselves as "forces of inertia" acting onto non-inertially moving observer); but in this case all Yang-Mills intensity components, being in fact components of curvature tensor, identically are equal to zero.

The above analysis of Yang-Mills field from Quaternion Space geometry may be found useful in particular if we consider its plausible neat link with Klein-Gordon equation and Duffin-Kemmer equation. We discuss in particular a biquaternionic-modification of Klein-Gordon equation. Since the potential corresponding to this biquaternionic KGE is neither Coulomb, Yukawa, nor Hulthen potential, then one can expect to observe a new type of matter. Further observation is recommended in order to support or refute this proposition.


### Acknowledgment

Special thanks to Profs. C. Castro and D. Rapoport for numerous discussions.


### References


1. Antonowitcz M. and Szczirba W. Geometry of canonical variables in gravity theories. *Lett. Math. Phys.*, 1985, v. 9, 43–49.
2. Rapoport D. and Sternberg S. On the interactions of spin with torsion. *Annals of Physics*, 1984, v. 158, no. 11, 447–475. MR 86e:58028; [2a] Rapoport D. and Sternberg S. Classical Mechanics without lagrangians nor hamiltoneans. *Nuovo Cimento A*, 1984, v. 80, 371–383, MR 86c:58055; [2b] Rapoport D. and Tilli M. Scale Fields as a simplicity principle. *Proceedings of the Third International Workshop on Hadronic Mechanics and Nonpotential Interactions*, Dept. of Physics, Patras Univ., Greece, A. Jannussis (ed.), in *Hadronic J. Suppl.*, 1986, v. 2, no. 2, 682–778. MR 88i:81180.

3. Chan W. K. and Shin F. G. Infinitesimal gauge transformations and current conservation in Yang theory of gravity. *Meet. Frontier Phys.*, Singapore, 1978, v. 2.
4. Hehl F. M. and Sijacki D. To unify theory of gravity and strong interactions? *Gen. Relat. and Grav.*, 1980, v. 12 (1), 83.
5. Batakis N. A. Effect predicted by unified theory of gravitational and electroweak fields. *Phys. Lett. B*, 1985, v. 154 (5–6), 382–392.
6. Kyriakos A. Electromagnetic structure of hadrons. arXiv: hep-th/0206059.
7. Kassandrov V. V. Biquaternion electrodynamics and Weyl-Cartan geometry of spacetime. *Grav. and Cosmology*, 1995, v. 1, no. 3, 216–222; arXiv: gr-qc/0007027.
8. Smarandache F. and Christianto V. Less mundane explanation of Pioneer anomaly from Q-relativity. *Progress in Physics*, 2007, v. 1, 42–45.
9. Fueter R. *Comm. Math. Helv.*, 1934–1935, v. B7, 307–330.
10. Yefremov A. P. *Lett. Nuovo. Cim.*, 1983, v. 37 (8), 315–316.
11. Yefremov A. P. *Grav. and Cosmology*, 1996, v. 2(1), 77–83.
12. Yefremov A. P. *Acta Phys. Hung.*, Series — Heavy Ions, 2000, v. 11(1–2), 147–153.
13. Yefremov A. P. *Gravitation and Cosmology*, 2003, v. 9 (4), 319–324. [13a] Yefremov A. P. Quaternions and biquaternions: algebra, geometry, and physical theories. arXiv: math-ph/0501055.
14. Ramond P. Field theory, a modern primer. The Benjamin/Cumming Publishing Co., ABPR Massachussetts, 1981.
15. Huang K. Quarks, leptons and gauge fields. World Scientific Publishing Co., 1982.
16. Fainberg V. and Pimentel B. M. Duffin-Kemmer-Petiau and Klein-Gordon-Fock equations for electromagnetic, Yang-Mills and external gravitational field interactions: proof of equivalence. arXiv: hep-th/0003283, p. 12.
17. Marsh D. The Grassmannian sigma model in SU(2) Yang-Mills theory. arXiv: hep-th/07021342.
18. Devchand Ch. and Ogievetsky V. Four dimensional integrable theories. arXiv: hep-th/9410147, p. 3.
19. Nishikawa M. Alternative to Higgs and unification. arXiv: hep-th/0207063, p. 18.
20. Nishikawa M. A derivation of the electro-weak unified and quantum gravity theory without assuming a Higgs particle. arXiv: hep-th/0407057, p. 22.
21. Adler S. L. Adventures in theoretical physics. arXiv: hep-ph/ 0505177, p. 107.
22. Adler S. L. Quaternionic quantum mechanics and Noncommutative dynamics. arXiv: hep-th/9607008.
23. Adler S. L. Composite leptons and quarks constructed as triply occupied quasiparticles in quaternionic quantum mechanics. arXiv: hep-th/9404134.
24. Ward D. and Volkmer S. How to derive the Schrödinger equation. arXiv: physics/0610121.
25. Christianto V. A new wave quantum relativistic equation from quaternionic representation of Maxwell-Dirac equation as an alternative to Barut-Dirac equation. *Electronic Journal of Theoretical Physics*, 2006, v. 3, no. 12.
26. Kiefer C. The semiclassical approximation of quantum gravity. arXiv: gr-qc/9312015.
27. Znojil M. PT-symmetry, supersymmetry, and Klein-Gordon equation. arXiv: hep-th/0408081, p. 7–8; [27a] arXiv: math-ph/0002017.
28. Toussaint M. Lectures on reduce and maple at UAM-I, Mexico. arXiv: cs.SC/0105033.
29. Castro C. The Riemann hypothesis is a consequence of CT-invariant Quantum Mechanics. Submitted to *JMPA*, Feb. 12, 2007.

# Numerical solution of radial biquaternion Klein-Gordon equation

V. Christianto[1], & F. Smarandache[2]
[1] http://www.sciprint.org, email: admin@sciprint.org
[2] Dept. of Mathematics, Univ. of New Mexico, Gallup, USA,
email: fsmarandache@yahoo.com

In the preceding article we argue that biquaternionic extension of Klein-Gordon equation has solution containing imaginary part, which differs appreciably from known solution of KGE. In the present article we present numerical /computer solution of radial biquaternionic KGE (radialBQKGE); which differs appreciably from conventional Yukawa potential. Further observation is of course recommended in order to refute or verify this proposition.

## Introduction

In the preceding article [1] we argue that biquaternionic extension of Klein-Gordon equation has solution containing imaginary part, which differs appreciably from known solution of KGE. In the present article we presented here for the first time a numerical /computer solution of radial biquaternionic KGE (radialBQKGE); which differs appreciably from conventional Yukawa potential.

This biquaternionic effect may be useful in particular to explore new effects in the context of low-energy reaction (LENR) [3]. Nonetheless, further observation is of course recommended in order to refute or verify this proposition.

## Radial biquaternionic KGE (radial BQKGE)

In our preceding paper [1], we argue that it is possible to write biquaternionic extension of Klein-Gordon equation as follows:

$$\left[\left(\frac{\partial^2}{\partial t^2}-\nabla^2\right)+i\left(\frac{\partial^2}{\partial t^2}-\nabla^2\right)\right]\varphi(x,t)=-m^2\varphi(x,t)\,, \tag{1}$$

Or this equation can be rewritten as:

$$\left(\Diamond\overline{\Diamond}+m^2\right)\varphi(x,t)=0\,, \tag{2}$$

Provided we use this definition:

$$\begin{aligned}\Diamond=\nabla^q+i\nabla^q&=\left(-i\frac{\partial}{\partial t}+e_1\frac{\partial}{\partial x}+e_2\frac{\partial}{\partial y}+e_3\frac{\partial}{\partial z}\right)\\&+i\left(-i\frac{\partial}{\partial T}+e_1\frac{\partial}{\partial X}+e_2\frac{\partial}{\partial Y}+e_3\frac{\partial}{\partial Z}\right)\end{aligned} \tag{3}$$

Where $e_1$, $e_2$, $e_3$ are *quaternion imaginary units* obeying (with ordinary quaternion symbols: $e_1=i$, $e_2=j$ , $e_3=k$):

$$\begin{aligned}&i^2=j^2=k^2=-1\,,\ ij=-ji=k\,,\\&jk=-kj=i\,,\ ki=-ik=j\,.\end{aligned} \tag{4}$$

And quaternion *Nabla operator* is defined as [1]:

$$\nabla^q = -i\frac{\partial}{\partial t} + e_1\frac{\partial}{\partial x} + e_2\frac{\partial}{\partial y} + e_3\frac{\partial}{\partial z} \tag{5}$$

Note that equation (3) and (5) included partial time-differentiation.

In the meantime, the standard Klein-Gordon equation reads [6][7]:

$$\left(\frac{\partial^2}{\partial t^2} - \nabla^2\right)\varphi(x,t) = -m^2\varphi(x,t)\,, \tag{6}$$

Now we can introduce polar coordinates by using the transformation:

$$\nabla = \frac{1}{r^2}\frac{\partial}{\partial r}\left(r^2\frac{\partial}{\partial r}\right) - \frac{\ell^2}{r^2} \tag{7}$$

Therefore, by substituting (7) into (6), the radial Klein-Gordon equation reads –by neglecting partial-time differentiation -- as follows [4][6]:

$$\left(\frac{1}{r^2}\frac{\partial}{\partial r}\left(r^2\frac{\partial}{\partial r}\right) - \frac{\ell(\ell+1)}{r^2} + m^2\right)\varphi(x,t) = 0\,, \tag{8}$$

and for $\ell = 0$, then we get [4]:

$$\left(\frac{1}{r^2}\frac{\partial}{\partial r}\left(r^2\frac{\partial}{\partial r}\right) + m^2\right)\varphi(x,t) = 0\,, \tag{9}$$

The same method can be applied to equation (2) for radial biquaternionic KGE (BQKGE), which for the 1-dimensional situation, one gets instead of (8):

$$\left(\frac{\partial}{\partial r}\left(\frac{\partial}{\partial r}\right) - i\frac{\partial}{\partial r}\left(\frac{\partial}{\partial r}\right) + m^2\right)\varphi(x,t) = 0\,, \tag{10}$$

In the next section we will discuss numerical /computer solution of equation (10) and compare it with standard solution of equation (9) using Maxima software package [5]. It can be shown that equation (10) yields potential which differs appreciably from standard Yukawa potential. For clarity, all solutions were computed in 1-D only.

**Numerical solution of radial biquaternionic Klein-Gordon equation**

Numerical solution of the standard radial Klein-Gordon equation (9) is given by :

(%i1) diff(y,t,2)-'diff(y,r,2)+m^2*y;

(%o1) $m^2.y - \frac{d^2}{d^2x}y$

(%i2) ode2 (%o1, y , r);

(%o2) $y = \%k_1.\%\exp(mr) + \%k_2.\%\exp(-mr)$ (11)

In the meantime, numerical solution of equation (10) for radial biquaternionic KGE (BQKGE), is given by:

(%i3) diff(y,t,2)- (%i+1)*'diff(y,r,2)+m^2*y;

(%o3) $m^2.y - (i+1)\frac{d^2}{d^2r}y$

(%i4) ode2 (%o3, y , r);

$$(\%o4)\ y = \%k_1.\sin\left(\frac{|m|r}{\sqrt{-\%i-1}}\right) + \%k_2.\cos\left(\frac{|m|r}{\sqrt{-\%i-1}}\right) \qquad (12)$$

Therefore, we conclude that numerical solution of radial biquaternionic extension of Klein-Gordon equation yields different result compared to the solution of standard Klein-Gordon equation; and it *differs appreciably* from the well-known Yukawa potential [6][6a]:

$$u(r) = -\frac{g^2}{r}e^{-mr} \qquad (13)$$

Meanwhile, Comay puts forth argument that the Yukawa lagrangian density has theoretical inconsistency within itself [6].

Interestingly one can find argument that biquaternion Klein-Gordon equation is nothing more than quadratic form of (modified) Dirac equation [1a], therefore BQKGE described herein [i.e. equation (12)] can be considered as a plausible solution to the problem described in [6]. For other numerical solutions to KGE, see for instance [7].

Nonetheless, we recommend further observation [8] in order to refute or verify this proposition of new type of potential derived from biquaternion Klein-Gordon equation.

**Acknowledgment**
VC would like to dedicate this article for RFF.

## References

**[1]** Yefremov, A., F. Smarandache & V. Christianto, "Yang-Mills field from quaternion space geometry, and its Klein-Gordon representation," *Progress in Physics* vol 3 no 3 (2007) www.ptep-online.com ; [1a] Christianto, V., "A new wave quantum relativistic equation from quaternionic representation of Maxwell-Dirac equation as an alternative to Barut-Dirac equation," *Electronic Journal of Theoretical Physics*, Vol. 3 no. 12 (2006), www.ejtp.com

**[2]** Yefremov, A., "Quaternions and biquaternions: algebra, geometry, and physical theories," arXiv:math-ph/0501055 (2005).

**[3]** Storms, E., http://www.lenr-canr.org

**[4]** Nishikawa, M., "A derivation of electroweak unified and quantum gravity theory without assuming Higgs particle," arXiv:hep-th/0407057 (2004) p.15

**[5]** Maxima from http://maxima.sourceforge.net. (Using Lisp GNU Common Lisp).

**[6]** Comay, E., *Apeiron* Vol. 14 no. 1 (2007) http://redshift.vif.com, preprint arXiv:quant-ph/0603325 (2006) p.4; [6a] see also http://en.wikipedia.org/wiki/Yukawa_potential

**[7]** Li Yang, *Numerical Studies of the Klein-Gordon-Schrödinger equations*, MSc thesis submitted to NUS, Singapore (2006) p.9. URL: http://www.math.nus.edu.sg/~bao/thesis/Yang-li.pdf

**[8]** Gyulassy, M., "Searching for the next Yukawa phase of QCD," arXiv:nucl-th/0004064 (2000). URL: http://arxiv.org/PS_cache/nucl-th/pdf/0004/0004064v1.pdf

*First version: 28th Oct. 2007. 1st revision: 8th Nov. 2007*

# A new derivation of biquaternion Schrödinger equation and plausible implications

V. Christianto[1], & F. Smarandache[2]
[1] http://www.sciprint.org, email: admin@sciprint.org
[2] Dept. of Mathematics, Univ. of New Mexico, Gallup, USA,
email: fsmarandache@yahoo.com

In the preceding article we argue that biquaternionic extension of Klein-Gordon equation has solution containing imaginary part, which differs appreciably from known solution of KGE. In the present article we discuss some possible interpretation of this imaginary part of the solution of biquaternionic KGE (BQKGE); thereafter we offer a new derivation of biquaternion Schrödinger equation using this method. Further observation is of course recommended in order to refute or verify this proposition.

## Introduction

There were some attempts in literature to generalise Schrödinger equation using quaternion and biquaternion numbers. Because quaternion number use in Quantum Mechanics has often been described [1][2][8][11], we only mention in this paper the use of biquaternion number. Sapogin [13] was the first to introduce biquaternion to extend Schrödinger equation, while Kravchenko [11] use biquaternion number to describe neat link between Schrödinger equation and Riccati equation.

In the present article we discuss a new derivation of biquaternion Schrödinger equation using a method used in the preceding paper. Because the previous method has been used for Klein-Gordon equation [1], now it seems natural to extend it to Schrödinger equation. This biquaternion effect may be useful in particular to explore new effects in the context of low-energy reaction (LENR) [13]. Nonetheless, further observation is of course recommended in order to refute or verify this proposition.

## Some interpretations of preceding result of biquaternionic KGE

In our preceding paper [1], we argue that it is possible to write biquaternionic extension of Klein-Gordon equation as follows:

$$\left[\left(\frac{\partial^2}{\partial t^2}-\nabla^2\right)+i\left(\frac{\partial^2}{\partial t^2}-\nabla^2\right)\right]\varphi(x,t)=-m^2\varphi(x,t)\,, \tag{1}$$

Or this equation can be rewritten as:

$$\left(\Diamond\overline{\Diamond}+m^2\right)\varphi(x,t)=0\,, \tag{2}$$

Provided we use this definition:

$$\begin{aligned}\Diamond=\nabla^q+i\nabla^q=&\left(-i\frac{\partial}{\partial t}+e_1\frac{\partial}{\partial x}+e_2\frac{\partial}{\partial y}+e_3\frac{\partial}{\partial z}\right)\\&+i\left(-i\frac{\partial}{\partial T}+e_1\frac{\partial}{\partial X}+e_2\frac{\partial}{\partial Y}+e_3\frac{\partial}{\partial Z}\right)\end{aligned} \tag{3}$$

Where $e_1$, $e_2$, $e_3$ are *quaternion imaginary units* obeying (with ordinary quaternion symbols: $e_1=i$, $e_2=j$ , $e_3=k$):

$$i^2 = j^2 = k^2 = -1,\ ij = -ji = k,$$
$$jk = -kj = i,\ ki = -ik = j. \quad (4)$$

And quaternion *Nabla operator* is defined as [5]:

$$\nabla^q = -i\frac{\partial}{\partial t} + e_1\frac{\partial}{\partial x} + e_2\frac{\partial}{\partial y} + e_3\frac{\partial}{\partial z} \quad (5)$$

Note that equation (3) and (5) included partial time-differentiation.

It is worth nothing here that equation (2) yields solution containing imaginary part, which differs appreciably from known solution of KGE:

$$y(x,t) = \left(\frac{1}{4} - \frac{i}{4}\right)m^2t^2 + cons\tan t \quad (6)$$

Some possible alternative interpretations of this *imaginary part* of the solution of biquaternionic KGE (BQKGE) are:

(a) The imaginary part implies that there is exponential term of the wave solution, which is quite similar to the Ginzburg-Landau extension of London phenomenology [3]:

$$\psi(r) = |\psi(r)|e^{i\varphi(r)}, \quad (7)$$

because equation (6) can be rewritten (approximately) as:

$$y(x,t) = \frac{e^i}{4}m^2t^2 \quad (8)$$

(b) The aforementioned exponential term of the solution (8) can be interpreted as signature of vortices solution. Interestingly Navier-Stokes equation which implies vorticity equation can also be rewritten in terms of Yukawa equation [8].

(c) The imaginary part implies that there is spiral wave, which suggests spiralling motion of meson or other particles. Interestingly it has been argued that one can explain electron phenomena by assuming spiralling electrons [5]. Alternatively this spiralling wave may already be known in the form of Bierkeland flow. For meson observation, this could be interpreted as another form of meson, which may be called 'supersymmetric-meson' [1].

(d) The imaginary part of solution of BQKGE also implies that it consists of standard solution of KGE [1], and its alteration because of imaginary differential operator. That would mean the resulting wave is composed of two complementary waves.

(e) Considering some recent proposals suggesting that neutrino can have *imaginary mass* [6], the aforementioned imaginary part of solution of BQKGE can also imply that the (supersymmetric-) meson may be composed of neutrino(s). This new proposition may require new thinking both on the nature of neutrino and also supersymmetric-meson. [7]

While some of these propositions remain to be seen, in deriving the preceding BQKGE we follow Dirac's phrase that '*One can generalize his physics by generalizing his mathematics.*' More specifically, we focus on using a 'theorem' from this principle, i.e.: '*One can generalize his mathematics by generalizing his (differential) operator.*'

**Extended biquaternion Schrödinger equation**

One can expect to use the same method described above to generalize the standard Schrödinger equation [10]:

$$[-\frac{\hbar^2}{2m}\Delta u + V(x)]u = Eu\,, \tag{9}$$

Or in simplified form [10, p.11]:

$$(-\Delta + w_k)\, f_k = 0, \quad \text{k=0,1,2,3} \tag{10}$$

In order to generalize equation (9) to biquaternion version (BQSE), we use first quaternion Nabla operator (5), and by noticing that $\Delta \equiv \nabla\nabla$, we get:

$$-\frac{\hbar^2}{2m}(\nabla^q \overline{\nabla}^q + \frac{\partial^2}{\partial t^2})u + (V(x) - E)u = 0\,. \tag{11}$$

Note that we shall introduce the second term in order to 'neutralize' the partial time-differentiation of $\nabla^q \overline{\nabla}^q$ operator.

To get *biquaternion* form of equation (11) we can use our definition in equation (3) rather than (5), so we get:

$$-\frac{\hbar^2}{2m}(\Diamond\overline{\Diamond} + \frac{\partial^2}{\partial t^2} - i\frac{\partial^2}{\partial T^2})u + (V(x) - E)u = 0\,. \tag{12}$$

This is an alternative version of *biquaternionic* Schrödinger equation, compared to Sapogin's [13] or Kravchenko's [11] method. We also note here that the route to *quaternionize* Schrödinger equation here is rather different from what is described by Horwitz [9, p.6]:

$$\tilde{H}\psi = \psi e_1 E\,, \tag{13}$$

or

$$\tilde{H}\psi q = \psi q(q^{-1}e_1 q)E\,, \tag{14}$$

Where the quaternion number q, can be expressed as [9, p.6][11]:

$$q = q_0 + \sum_{i=1}^{3} q_i e_i \qquad . \tag{15}$$

Nonetheless, further observation is of course recommended in order to refute or verify this proposition (12).

**Numerical solution of biquaternion Schrödinger equation**

It can be shown that numerical solution (using Maxima [14]) of biquaternionic extension of Schrödinger equation yields different result compared to the standard Schrödinger equation, as follows. For clarity, all solutions were computed in 1-D only.

For standard Schrödinger equation [10], one can rewrite equation (9) as follows:

(a) For $V(x) > E$:

$$-\frac{\hbar^2}{2m}\Delta u + a.u = 0\,, \tag{16}$$

(b) For $V(x) < E$:

$$-\frac{\hbar^2}{2m}\Delta u - a.u = 0\,, \tag{17}$$

Numerical solution of equation (16) and (17) is given by (assuming $\hbar = 1$ and $m = 1/2$ for convenience):

(%i44) -'diff (y, x, 2) + a*y;

(%o44) $a.y - \frac{d^2}{d^2x} y$

(a) For $V(x) > E$ :

(%i46) ode2 (%o44, y , x);

(%o46) $y = k_1.\exp(\sqrt{ax}) + k_2.\exp(-\sqrt{ax})$ (18)

(b) For $V(x) < E$ :

(%i45) ode2 (%o44, y , x);

(%o45) $y = k_1.\sinh(\sqrt{a.x}) + k_2.\cosh(\sqrt{a.x})$ (19)

In the meantime, numerical solution of equation (12), is given by (by assuming $\hbar = 1$ and $m = 1/2$ for convenience):

(a) For $V(x) > E$ :

(%i38) (%i+1)*'diff (y, x, 2) + a*y;

(%o38) $(i+1)\frac{d^2}{d^2x} y + a.y$

(%i39) ode2 (%o38, y , x);

(%o39) $y = k_1.\sin(\sqrt{\frac{a}{i+1}.x}) + k_2.\cos(\sqrt{\frac{a}{i+1}.x})$ (20)

(b) For $V(x) < E$ :

(%i40) (%i+1)*'diff (y, x, 2) - a*y;

(%o40) $(i+1)\frac{d^2}{d^2x} y - a.y$

(%i41) ode2 (%o40, y , x);

(%o41) $y = k_1.\sin(\sqrt{-\frac{a}{i+1}.x}) + k_2.\cos(\sqrt{-\frac{a}{i+1}.x})$ (20a)

Therefore, we conclude that numerical solution of biquaternionic extension of Schrödinger equation yields different result compared to the solution of standard Schrödinger equation. Nonetheless, we recommend further observation in order to refute or verify this proposition/numerical solution of biquaternion version of spatial-differential operator of Schrödinger equation.

As side remark, it is interesting to note here that if we *introduce imaginary number* in equation (16) and equation (17), the numerical solutions will be quite different compared to solution of equation (16) and (17), as follows:

$$-\frac{i\hbar^2}{2m}\Delta u + au = 0, \quad (21)$$

Where $V(x) > E$ , or

$$-\frac{i\hbar^2}{2m}\Delta u - au = 0, \quad (22)$$

Where $V(x) < E$ .

Numerical solution of equation (21) and (22) is given by (by assuming $\hbar = 1$ and $m = 1/2$ for convenience):

(a) For $V(x) > E$ :

(%i47) -%i*'diff (y, x, 2) + a*y;

(%o47) $a.y - i\frac{d^2}{d^2x}y$

(%i48) ode2 (%o47, y , x);

(%o48) $y = k_1.\sin(\sqrt{ia.x}) + k_2.\cos(\sqrt{ia.x})$ (23)

(b) For $V(x) < E$ :

(%i50) -%i*'diff (y, x, 2) - a*y;

(%o50) $-a.y - i\frac{d^2}{d^2x}y$

(%i51) ode2 (%o50, y , x);

(%o51) $y = k_1.\sin(-\sqrt{ia.x}) + k_2.\cos(-\sqrt{ia.x})$ (24)

It shall be clear therefore that using different sign for differential operator yields quite different results.

**Acknowledgment**
Special thanks to Prof. D. Rapoport who mentioned Sprossig's interesting paper [8]. VC would like to dedicate this article for RFF.

## References

**[1]** Yefremov, A., F. Smarandache & V. Christianto, "Yang-Mills field from quaternion space geometry, and its Klein-Gordon representation," *Progress in Physics* vol 3 no 3 (2007) www.ptep-online.com.

**[2]** Yefremov, A., "Quaternions: Algebra, Geometry and physical theories," *Hypercomplex numbers in Geometry and Physics* 1(1) p.105 (2004); [2a] Yefremov, A.., "Quaternions and biquaternions: algebra, geometry, and physical theories," arXiv:math-ph/0501055 (2005).

**[3]** Schrieffer, J.R., & M. Tinkham, "Superconductivity," *Rev. Modern Phys.*, Vol. 71 No. 2, (1999), p. S313

**[4]** Christianto, V., "A new wave quantum relativistic equation from quaternionic representation of Maxwell-Dirac equation as an alternative to Barut-Dirac equation," *Electronic Journal of Theoretical Physics*, Vol. 3 no. 12 (2006), www.ejtp.com

**[5]** Drew, H.R., "A periodic structural model for the electron can calculate its intrinsic properties to an accuracy of second or third order," Apeiron, Vol. 9 no. 4 (2002) http://redshift.vif.com

**[6]** Jeong, E.J., "Neutrinos must be tachyons," arXiv:hep-ph/9704311 (1997)

**[7]** Sivasubramanian, S., *et al.*, arXiv:hep-th/0309260 (2003).

**[8]** Sprössig, W., "Quaternionic Operator Methods in Fluid Dynamics," Proceedings of the International Conference of Clifford Algebra and Applications 7, held in Toulouse 2005, edited by Pierre Angles (Oct 26th, 2006 version). See also: http://www.mathe.tu-freiberg.de/math/inst/amm1/Mitarbeiter/Sproessig/ws_talks.pdf

**[9]** Horwitz, L., "Hypercomplex quantum mechanics," arXiv:quant-ph/9602001 (1996) p.6.

**[10]** Straumann, N., "Schrödingers Entdeckung der Wellenmechanik," arXiv:quant-ph/0110097 (2001) p.4

**[11]** Kravchenko, V.G., *et al*., "Quaternionic factorization of Schrödinger operator …," arXiv:math-ph/0305046 (2003) p.9

**[12]** Sapogin, V., Unitary Quantum Theory, ICCF proceedings, listed in Infinite Energy magazine, http://www.infinite-energy.com

**[13]** Storms, E., http://www.lenr-canr.org

**[14]** Maxima from http://maxima.sourceforge.net. (Using Lisp GNU Common Lisp).

*First version: 23rd Aug. 2007. First revision: 29th Aug. 2007. 2nd revision: 23rd Sept 2007*

# An exact mapping from Navier-Stokes equation to Schrödinger equation via Riccati equation

V. Christianto[1], & F. Smarandache[2]
[1] http://www.sciprint.org, email: admin@sciprint.org
[2] Dept. of Mathematics, Univ. of New Mexico, Gallup, USA,
email: fsmarandache@yahoo.com

In the present article we argue that it is possible to write down Schrödinger representation of Navier-Stokes equation via Riccati equation. The proposed approach, while differs appreciably from other method such as what is proposed by RM. Kiehn, has an advantage, i.e. it enables us extend further to quaternionic and biquaternionic version of Navier-Stokes equation, for instance via Kravchenko's and Gibbon's route. Further observation is of course recommended in order to refute or verify this proposition.

## Introduction

In recent years there were some attempts in literature to find out Schrödinger-like representation of Navier-Stokes equation using various approaches, for instance by R.M. Kiehn [1][2]. Deriving exact mapping between Schrödinger equation and Navier-Stokes equation has clear advantage, because Schrodinger equation has known solutions, while exact solution of Navier-Stokes equation completely remains an open problem in mathematical-physics. Considering wide applications of Navier-Stokes equation, including for climatic modelling and prediction (albeit in simplified form called 'geostrophic flow' [9]), one can expect that simpler expression of Navier-Stokes equation will be found useful.

In this article we presented an alternative route to derive Schrödinger representation of Navier-Stokes equation via Riccati equation. The proposed approach, while differs appreciably from other method such as what is proposed by R.M. Kiehn [1], has an advantage, i.e. it enables us to extend further to quaternionic and biquaternionic version of Navier-Stokes equation, in particular via Kravchenko's [3] and Gibbon's route [4][5]. An alternative method to describe quaternionic representation in fluid dynamics has been presented by Sprössig [6].

Nonetheless, further observation is of course recommended in order to refute or verify this proposition.

## From Navier-Stokes equation to Schrödinger equation via Riccati

Recently, Argentini [8] argues that it is possible to write down ODE form of 2D steady Navier-Stokes equations, and it will lead to second order equation of Riccati type.

Let ρ the density, μ the dynamic viscosity, and f the body force per unit volume of fluid. Then the Navier-Stokes equation for the steady flow is [8]:

$$\rho(v.\nabla v) = -\nabla p + \rho.f + \mu.\Delta v \qquad (1)$$

After some necessary steps, he arrives to an ODE version of 2D Navier-Stokes equations along a streamline [8, p. 5] as follows:

$$u_1.\dot{u}_1 = f_1 - \frac{\dot{q}}{\rho} + v.\dot{u}_1 \ , \qquad (2)$$

where $\nu = \frac{\mu}{\rho}$ is the kinematic viscosity. He [8, p.5] also finds a general exact solution of equation (2) in Riccati form, which can be rewritten as follows:

$$\dot{u}_1 - \alpha . u_1^2 + \beta = 0 , \tag{3}$$

where:

$$\alpha = \frac{1}{2\nu}, \tag{4}$$

and

$$\beta = -\frac{1}{\nu}\left(\frac{\dot{q}}{\rho} - f_1\right)s - \frac{c}{\nu} \tag{5}$$

Interestingly, Kravvhenko [3, p.2] has argued that there is neat link between Schrödinger equation and Riccati equation via simple substitution. Consider a 1-dimensional static Schrödinger equation:

$$\ddot{u} + \nu . u = 0 \tag{6}$$

and the associated Riccati equation:

$$\dot{y} + y^2 = -\nu \tag{7}$$

Then it is clear that equation (6) is related to (7) by the inverted substitution [3]:

$$y = \frac{\dot{u}}{u} \tag{8}$$

Therefore, one can expect to use the same method (8) to write down the Schrödinger representation of Navier-Stokes equation. First, we rewrite equation (3) in similar form of equation (7):

$$\dot{y}_1 - \alpha . y_1^2 + \beta = 0 \tag{9}$$

By using substitution (8), then we get the Schrödinger equation for this Riccati equation (9):

$$\ddot{u} - \alpha\beta . u = 0 \tag{10}$$

where variable α and β are the same with (4) and (5). This Schrödinger representation of Navier-Stokes equation is remarkably simple and it also has advantage that now it is possible to generalize it further to quaternionic (ODE) Navier-Stokes equation via quaternionic Schrödinger equation, for instance using the method described by Gibbon *et al*. [4][5].

**An extension to biquaternionic Navier-Stokes equation via biquaternion differential operator**

In our preceding paper [10][12], we use this definition for biquaternion differential operator:

$$\begin{aligned} \Diamond = \nabla^q + i\nabla^q = &\left( -i\frac{\partial}{\partial t} + e_1\frac{\partial}{\partial x} + e_2\frac{\partial}{\partial y} + e_3\frac{\partial}{\partial z}\right) \\ &+ i\left( -i\frac{\partial}{\partial T} + e_1\frac{\partial}{\partial X} + e_2\frac{\partial}{\partial Y} + e_3\frac{\partial}{\partial Z}\right) \end{aligned} \tag{11}$$

Where $e_1$, $e_2$, $e_3$ are *quaternion imaginary units* obeying (with ordinary quaternion symbols: $e_1$=i, $e_2$=j , $e_3$ =k):

$$i^2 = j^2 = k^2 = -1 , \; ij = -ji = k ,$$

$$jk = -kj = i\ ,\ ki = -ik = j\ . \tag{12}$$

And quaternion *Nabla operator* is defined as [13]:

$$\nabla^q = -i\frac{\partial}{\partial t} + e_1\frac{\partial}{\partial x} + e_2\frac{\partial}{\partial y} + e_3\frac{\partial}{\partial z} \tag{13}$$

Note that equation (11) and (13) include partial time-differentiation.

Now it is possible to use the same method described above [10][12] to generalize the Schrödinger representation of Navier-Stokes (10) to the bi-quaternionic Schrödinger equation, as follows.

In order to generalize equation (10) to quaternion version of Navier-Stokes equations (QNSE), we use first quaternion Nabla operator (13), and by noticing that $\Delta \equiv \nabla\nabla$, we get:

$$(\nabla^q\overline{\nabla}^q + \frac{\partial^2}{\partial t^2})u - \alpha\beta.u = 0\,. \tag{14}$$

We note that the multiplying factor (ab) in (14) plays similar role just like (V(x)-E) factor in the standard Schrödinger equation [12]:

$$-\frac{\hbar^2}{2m}(\nabla^q\overline{\nabla}^q + \frac{\partial^2}{\partial t^2})u + (V(x) - E)u = 0\,. \tag{15}$$

Note that we shall introduce the second term in order to 'neutralize' the partial time-differentiation of $\nabla^q\overline{\nabla}^q$ operator.

To get *biquaternion* form of equation (14) we can use our definition in equation (11) rather than (13), so we get [12]:

$$(\Diamond\overline{\Diamond} + \frac{\partial^2}{\partial t^2} - i\frac{\partial^2}{\partial T^2})u - \alpha\beta.u = 0\,. \tag{16}$$

This is an alternative version of *biquaternionic* Schrödinger representation of Navier-Stokes equations. Numerical solution of the new Navier-Stokes-Schrödinger equation (16) can be performed in the same way with [12] using Maxima software package [7], therefore it will not be discussed here.

We also note here that the route to *quaternionize* Schrödinger equation here is rather different from what is described by Gibbon *et al*. [4][5], where the Schrödinger-equivalent to Euler fluid equation is described as [5, p4]:

$$\frac{D^2w}{Dt^2} - (\nabla Q)w = 0 \tag{17}$$

and its quaternion representation is [5, p9]:

$$\frac{D^2w}{Dt^2} - q_b \otimes w = 0 \tag{18a}$$

with Riccati relation is given by:

$$\frac{D\ q_a}{Dt} + q_a \otimes q_a = q_b \tag{18b}$$

Nonetheless, further observation is of course recommended in order to refute or verify this proposition (16).

**Acknowledgment**

Special thanks to Prof. W. Sprossig for remarks on his paper [6]. VC would like to dedicate this article to Prof. R.M. Kiehn.

## References


**[1]** Kiehn, R.M., http://www22.pair.com/csdc/pdf/bohmplus.pdf

**[2]** Rapoport, D., "Torsion fields, Brownian Motions, Quantum and Hadronic Mechanics," (Oct. 2007) in this volume.

**[3]** Kravchenko, V.G, "On the reduction of multidimensional Schrödinger equation to a first order equation and its relation to the pseudoanalytic function theory," arXiv:math.AP/0408172 (2004) p.2; [3a] Kravchenko, V.G., *et al*., "Quaternionic factorization of Schrödinger operator …," arXiv:math-ph/0305046 (2003) p.9.

**[4]** Gibbon, J.D., D. Holm, R.M. Kerr, & I. Roulstone, "," *Nonlinearity* **19** (2006) 1969-1983. Preprint: http://arxiv.org/abs/nlin.CD/0512034

**[5]** Gibbon, J.D., "Ortho-normal quaternion frames, Lagrangian evolution equations,and the three-dimensional Euler equations," arXiv:math-ph/0610004 (Mar. 2007)

**[6]** Sprössig, W., "Quaternionic Operator Methods in Fluid Dynamics," *Proc. of the Int. Conf. of Clifford Algebra and Applications* 7, held in Toulouse 2005, edited by Pierre Angles. See also: http://www.mathe.tu-freiberg.de/math/inst/amm1/Mitarbeiter/Sproessig/ws_talks.pdf

**[7]** Maxima from http://maxima.sourceforge.net. (Using Lisp GNU Common Lisp).

**[8]** Argentini, G., "Exact solution of a differential problem in analytical fluid dynamics: use of Airy's function,"arXiv:math.CA/0606723 (June 2006) p.8

**[9]** Roubtsov, V.N., & I. Roulstone, "Holomorphic structures in hydrodynamical models of nearly geostrophic flow," *Proc. R. Soc. Lond.* (2001) 11p.

**[10]** Yefremov, A., F. Smarandache & V. Christianto, "Yang-Mills field from quaternion space geometry, and its Klein-Gordon representation," *Progress in Physics* vol 3 no 3 (2007) www.ptep-online.com. Also in this volume.

**[11]** Yefremov, A., "Quaternions and biquaternions: algebra, geometry, and physical theories," arXiv:math-ph/0501055 (2005).

**[12]** Christianto, V., & F. Smarandache, "A new derivation of biquaternion Schrödinger equation and plausible implications," *Progress in Physics* vol 3 no 4 (2007). Also in this volume.

**[13]** Christianto, V., "A new wave quantum relativistic equation from quaternionic representation of Maxwell-Dirac equation as an alternative to Barut-Dirac equation," *Electronic Journal of Theoretical Physics*, Vol. 3 no. 12 (2006), www.ejtp.com



*First version: 28th Oct. 2007. 1st revision: 8th Nov. 2007*

# A note on possible translation of Schrödinger's uncertainty theorem into modern uncertainty notations

V. Christianto[1], & F. Smarandache[2]
[1] http://www.sciprint.org, email: admin@sciprint.org
[2] Chairman of Dept. of Mathematics, University of New Mexico, Gallup, USA,
email: fsmarandache@yahoo.com

In the present article we argue that it is possible to write a modern version of Schrödinger's uncertainty theorem using standard notation of uncertainty algebra. It can be expected that a modern language will bring clarity to what are implications of uncertainty theorem, which forms a cornerstone of quantum theory. Further observation is of course recommended in order to refute or verify this proposition.

## Introduction

In the present article we argue that it is possible to write a modern version of Schrödinger's uncertainty theorem [1] using standard notations of uncertainty algebra [2]. It can be expected that a modern language will bring clarity to implications of uncertainty theorem, which forms a cornerstone of quantum theory.

The reason for discussing Schrödinger's uncertainty theorem is because it is more comprehensive and adaptable to the modern language of uncertainty algebra, compared to Heisenberg's uncertainty theorem. Other reason is that this Schrödinger's uncertainty theorem opens new possibility to detect quantum phenomena below the limits set out in Heisenberg's uncertainty. Interestingly, there are recent papers suggesting that one can observe below this limit (see W. Zurek's paper in *Nature, 2002-2003*, for instance).

And considering other papers suggesting that Schrödinger equation can be derived from exact uncertainty theorem [3][4], then given this Schrödinger uncertainty relation, one can expect to generalize it further.

Nonetheless, further observation is of course recommended in order to refute or verify this proposition.

## Schrodinger's uncertainty theorem and modern uncertainty notations

In his almost unknown paper [1, p.5], Schrödinger wrote that "the Heisenberg limit is not really too low, but for some special Ψ–functions achieves even higher value." And he offers a more generalized formulation of Heisenberg's uncertainty relation which agrees with more standard definition of mathematical-statistics.

His arguments start with writing down the average error or the mean uncertainty of the value, which belongs to the operator A, as follows [1, p.3]:

$$\Delta A = \sqrt{(A - \overline{A})^2} \tag{1}$$

Interestingly, equation (1) is nothing more than the square root of statistical variance of A [2]:

$$\mathrm{var}[A] = (A - \overline{A})^2 \tag{2}$$

Therefore it is possible to write equation (2) in terms of expectation values of modern uncertainty relations (just like what Schrödinger expected to achieve) as follows [2, p.70]:

$$\mathrm{var}[A] = E[A^2] - E[A]^2 = E[Var[A|Z]] + Var[E[A|Z]], \quad (3)$$

where E[A|Z=z] is the conditional expectation of A given Z=z: [2,p.70)

$$E[A|Z = z] = \int_{-\infty}^{\infty} a.f_{A|Z}(a,z)da \quad (3a)$$

Although Schrodinger gave a slightly different definition (expectation without conditional):

$$\overline{A} = \int \Psi * A\Psi dx \quad (4)$$

This result (3), despite its simplicity, is very important and useful in various applications [2, p.71]. Therefore it can be expected to bring Schrödinger's uncertainty relation into the context of conditional expectation, just like what J. Bell proposed sometime ago with his '*Bell's inequality theorem*'.[5]

Using the same method [2, p.71]. we can also write the covariance as:

$$Cov[X,Y] = E[XY] - E[X]E[Y] \quad (5)$$

Nonetheless, we recommend further observation in order to refute or verify this proposition of new interpretation of Schrodinger's uncertainty relation from modern uncertainty notations.

## References


**[1]** Schrodinger, E., "About Heisenberg Uncertainty relation," *Proc. of the Prussian Academic of Sciences – Physics-Mathematical section*, XIX, 296-303 (1930). Translated and annotated by A. Angelow *et al*., arXiv:quant-ph/9903100 (1999) p.5.

**[2]** Baker, J.W., & C.A. Cornell, "Uncertainty specification and propagation for loss estimation using FOSM method," *PEER Report* 2003/07 (Pacific Earthquake Engineering Research Center) p. 70. URL: www.stanford.edu/group/rms/RMS_Papers/pdf/jack/Baker%20Cornell%20PEER%20Uncertainty%20Report.pdf

**[3]** Skala, L., & W. Kapsa, "Contributions to the mathematical structures of quantum mechanics," arXiv:quant-ph/0602182 (2006). URL: http://arxiv.org/PS_cache/quant-ph/pdf/0602/0602182v1.pdf

**[4]** Hall, M.W., & M. Reginatto, "Schrodinger equation from an exact uncertainty principle," arXiv:quant-ph/0102069 (2001).

**[5]** See J. Christian's paper for a recent discussion on Bell's inequality. J. Christian, "Disproof of Bell's theorem: Further consolidation," (2007) URL: http://arxiv.org/PS_cache/arxiv/pdf/0707/0707.1333v2.pdf



*First version: 28th Oct. 2007.*

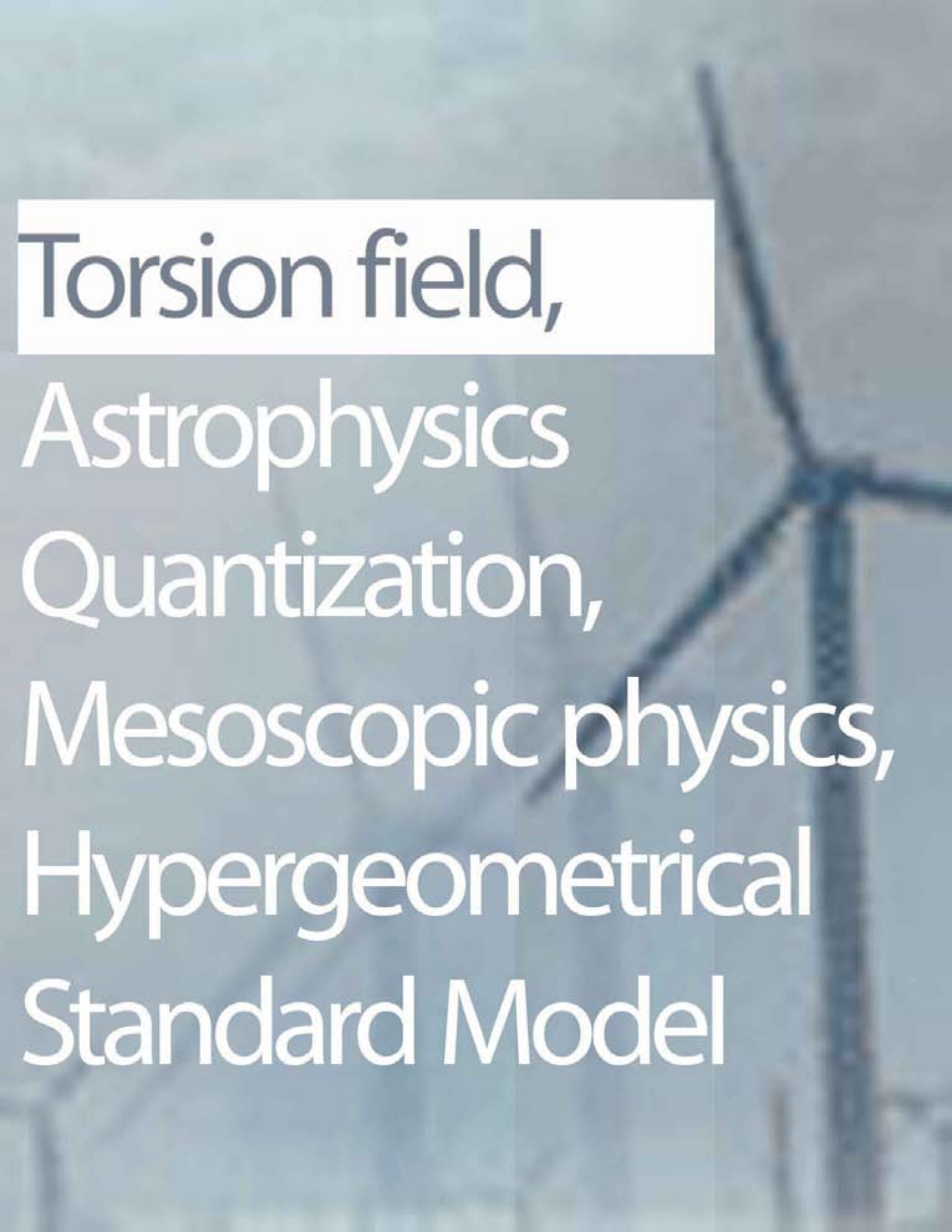
Torsion field,
Astrophysics
Quantization,
Mesoscopic physics,
Hypergeometrical
Standard Model

# Torsion Fields, Brownian Motions, Quantum and Hadronic Mechanics

**Diego L. Rapoport**

**Department of Sciences and Technology, Universidad Nacional de Quilmes Buenos Aires, Argentina** [1]

**Summary:** We review the relation between space-time geometries with torsion fields (the so-called Riemann-Cartan-Weyl (RCW) geometries) and their associated Brownian motions. In this setting, the metric conjugate of the trace-torsion one-form is the drift vector field of the Brownian motions. Thus, in the present approach space-time fluctuations as Brownian motions are -in distinction with Nelson's Stochastic Mechanics- space-time structures. Thus, space and time have a fractal structure. We discuss the relations with Nottale's theory of Scale Relativity, which stems from Nelson's approach. We characterize the Schroedinger equation in terms of the RCW geometries and Brownian motions. In this work, the Schroedinger field is a torsion generating field. The potential functions on Schroedinger equations can be alternatively linear or nonlinear on the wave function, leading to nonlinear and linear creation-annihilation of particles by diffusion systems. We give a brief presentation of the isotopic lift of Quantum Mechanics known as Hadronic Mechanics due to Santilli. We start by giving the isotopic lift (i.e. a non-unitary transformation not identically reducible to the identity) of gauge theories, to show that torsion appears at the basis of gauge theories, and also in the isotopic lift of gauge theories. Using this non-unitary transformations we present the isotopic lift of all the mathematical apparatus and physical aspects of Quantum Mechanics, to present Hadronic Mechanics. This theory lifts a number of fundamental inconsistencies in the conventional approaches to Special and General Relativity, Quantum Mechanics, particle physics, cosmology, superconductivity, biology, etc. We present the relations between Hadronic Mechanics with RCW geometries and Brownian motions in the case of the iso-Schroedinger equation for the strong interactions. This is achieved by either using the diffusion representation for the Schroedinger equation and its isotopic lift, which for the case of trivial noise tensor yields the iso-Heisenberg representation. We derive the iso-Schroedinger equation from this isotopic lift of diffusions representation. We give a Brownian motion model of fusion in Hadronic Mechanics, and extend it to the many body problem. We discuss the possible relation between torsion fields and several anomalous phenomenae. Finally we discuss possible evidence for this theory in the fine structure time periodicity of histograms of arbitrary processes found by Shnoll and collaborators, which show a spacetime anisotropy attributed to space-time fluctuations and a fractal structure of these histograms.

[1] E-mail address: diego.rapoport@gmail.com

# 1 INTRODUCTION

A central problem of contemporary physics is the distinct world views provided by Quantum Mechanics and the theory of Relativity, and more generally of gravitation. In a series of articles [1-4], we have presented an unification between space-time structures, Brownian motions, further extended to fluid-dynamics and Quantum Mechanics (QM, for short in the following). The unification of space-time geometry and classical statistical theory has been possible due to a complementarity of the objects characterizing the Brownian motion, i.e. the noise tensor which produces a metric, and the drift vector field which describes the average velocity of the Brownian, in jointly describing both the space-time geometry and the stochastic processes. These space-time structures can be defined starting from flat Euclidean or Minkowski space-time, and they have in addition to a metric a torsion tensor which is formed from the metric conjugate of the drift vector field. The key to this unification lies in that the laplacian operator defined by this geometrical structure is the differential generator of the Brownian motions; stochastic analysis which deals with the transformation rules of classical observables on diffusion paths ensures that this unification stands in an equal status for both the geometrical and stochastic structures [70]. Thus , in this equivalence, one can choose the Brownian motions as the original structures determining a space-time structure, or conversely, the space-time structures produce a Brownian motion process. Space-time geometries with torsion have lead to an extension of the theory of gravitation which was first explored in joint work by Einstein with Cartan [5], so that the foundations for the gravitational field, for the special case in which the torsion reduces to its trace, can be found in these Brownian motions. Furthermore, in [2] we have shown that the relativistic quantum potential coincides , up to a conformal factor, with the metric scalar curvature. In this setting we are lead to conceive that there is no actual propagation of disturbances but instead an holistic modification of the whole space-time structure due to an initial perturbation which provides for the Brownian process modification of the original configuration. Furthermore, the present theory which has a kinetic Brownian motion generation of the geometries, is related to Le Sage's proposal of a Universe filled with all pervading tiny particles moving in all directions as a pushing (in contrast with Newton's pulling force) source for the gravitational field [52]. Le Sage's perspective was found to be compatible cosmological observation by H. Arp [53]. This analysis stems from the assumption of a non-constant mass in GR which goes back to Hoyle and Narlikar, which in another perspective developed by Wu and Lin generates rotational forces [54]. These rotational forces can be ascribed to the drift trace-torsion vector field of the Brownian processes through the Hodge duality transformation [3], or still to the vorticity generated

by this vector field. In our present theory, motions in space *and* time are fractal, they generate the gravitational field of general relativity, and furthermore they generate rotational fields, in contrast with the pulling force of Newton's theory and the pushing force of Le Sage, or in the realm of the neutron, the Coulomb force. Furthermore, in our construction the drift has built-in terms given by the conjugate of electromagnetic-like potential 1-forms, whose associated intensity two-form generate vorticity, i.e. angular momentum. So the present geometries are very different from the metric geometries of General Relativity (GR in the following) and are not in conflict with present cosmological observations.

The space-time geometrical structures of this theory can be introduced by the Einstein $\lambda$ transformations on the tetrad fields [2,5], from which the usual Weyl scale transformations on the metric can be derived, but contrarily to Weyl geometries, these structures have torsion and they are integrable in contrast with Weyl's theory [48]. We have called these connections as RCW structures (short for Riemann-Cartan-Weyl); see [1-4] and references therein. We have shown that this approach leads to non-relativistic QM both in configuration space [3] and in the projective Hilbert state-space through the stochastic Schroedinger equation [39] (in the latter case, it was shown that this geometry is related to a theory of the reduction of the wave function through decoherence) , and further to Maxwell's equation and its equivalence with the Dirac-Hestenes equation of relativistic QM [2,21]. The fact that non-relativistic QM can be linked to torsion fields was unveiled recently [3]. In fact, torsion fields have been considered to be as providing deviations of GR outside the reach of present precision measurements [22]. It turns out, as discussed in relation with viscous fluids obeying the Navier-Stokes equations as a universal example of torsion fields [1,4], that quantum wave-functions verifying linear or non-linear Schroedinger equations are another universal, or if wished, mundane examples of torsion fields. In this article we shall show that this extends to the strong interactions. The quantum random ensembles which generate the geometries, or which dually can be seen as generated by them, in the case of the Schroedinger equation can be associated with harmonic oscillators with disordered random phase and amplitude first proposed by Planck, which have the same energy spectrum as the one derived originally by Schroedinger [34,73]. The probabilities of these ensembles are classical since they are associated with classical Brownian motions in the configuration and projective Hilbert-state manifolds, in sharp contrast with the Copenhagen interpretation of QM which is constructed in terms of single system description, and they are related to the scalar amplitude of the spinor field in the case of the Dirac field, and in terms of the modulus of the complex wave function in the non-relativistic case [2,3,21]. We would like to recall at this stage that Khrennikov has proved that Kolmogorov's axiomatics of classical probability theory, in a contextual approach which means an a-priori consideration of a complex of physical conditions, permits the reconstruction of quantum theory [64]. Thus, Khrennikov 's theory places the validity of Quantum Theory in ensembles, in distinction with the Copenhagen interpretation, and is known as the

Vaxho interpretation of QM. In the present approach we obtain both a geometrical characterization of the quantum domain through random ensembles performing Brownian motions which generate the space and time geometries, and additionally a characterization of QM for single systems through the topological Bohr-Sommerfeld invariants associated with the trace-torsion by introducing the concept of Pfaffian system developed by Kiehn in his geometro-topological theory of processes [20], specifically applied to the trace-torsion one-form [81]. Most remarkably, in our setting another relevant example of these space-time geometries is provided by viscous fluids obeying the invariant Navier-Stokes equations of fluid-dynamics, or alternatively the kinematical dynamo equation for the passive transport of magnetic fields on fluids [1,4] . We would like to point out that cosmological observations have registered turbulent large-scale structures which are described in terms of the Navier-Stokes equations [82] so that this model is in principle compatible with that observations.

We must stress the difference between this approach and GR. In the latter, the space-time structure is derived in the sense that it is defined without going through a self-referential characterization, but obtained from the metric. When we introduce torsion, and especially in the case of the trivial metric with null associated curvature tensor, we are introducing a self-referential characterization of the geometry since the definition of the manifold by the torsion, is through the concept of locus of a point (be that temporal or spatial). Indeed, space and time can only be distinguished if we can distinguish inhomogenities, and this is the intent of torsion, to measure the dislocation (in space and time) in the manifold [69]. Thus all these theories stem from a geometrical operation which has a logical background related to the concept of distinction (and more fundamentally, the concept of identity, which is prior to that of distinction) and its implementation through the operation of comparison by parallel transport with the affine connection with non-vanishing torsion; this can be further related with multivalued logics and the appearence of time waves related to paradoxes, which in a cognitive systems approach yield the Schroedinger representation [81]. In comparison, in GR there is also an operation of distinction carried out by the parallel transport of pair of vector fields with the Levi-Civita metric connection yielding a trivial difference, i.e. the torsion is null and infinitesimal parallelograms trivially close, so that it does not lead to the appearence of inhomogenities as resulting from this primitive operation of distinction; these are realized through the curvature derived from the metric.

We shall start this article by introducing non-relativistic QM in terms of diffusion processes in space-time following our work in [3]; the stochastic Schroedinger equation case shall not be dealt with; see [3,39]. Thus in this approach appears that the Schroedinger field can be associated with the field which produces the torsion field. Thus we have recovered a modified characterization that can be traced back to London's treatment of the Weyl geometries which although related with a local change of the metrics, have null torsion [48]. There have been numerous attempts to relate non-relativistic QM to diffusion equations;

the most notable of them is Stochastic Mechanics , due to Nelson [8]. Already Schroedinger proposed in 1930-32 that his equation should be related to the theory of Brownian motions (most probably as a late reaction to his previous acceptance of the single system probabilistic Copenhagen interpretation), and further proposed a scheme he was not able to achieve, the so-called interpolation problem which requires to describe the Brownian motion and the wave functions in terms of interpolating the initial and final densities in a given time-interval [9]. More recently Nagasawa presented a solution to this interpolation problem and further elucidated that the Schroedinger equation is in fact a Boltzmann equation [13], and thus the generation of the space and time structures produced by the Brownian motions has a statistical origin. We have discussed in [3] that the solution of the interpolation problem leads to consider time to be more than a classical parameter (merely a clock), but an active operational variable, as recent experiments have shown [46] which have elicited theoretical studies in [72]; other experiments that suggest an active role of time are further discussed in [3] and in the final section in this article. Neither Nagasawa nor Nelson presented these Brownian motions as space-time structures, but rather as matter fields *on* the vacuum. While Nelson introduced artificially a forward and backward stochastic derivatives to be able to reproduce the Schroedinger equation as a formally time-symmetric equation, Nagasawa was able to solve the interpolation problem in terms of the forward diffusion process and its adjoint backward process, from which without resort to the ad-hoc constructions due to Nelson, he was able to prove in [13] that this was related to the Kolmogorov characterization of time-irreversibility of diffusion processes in terms of the non-exact terms of the drift,that we further related to the trace-torsion [3]. A similar approach to quantization in terms of an initial fractal structure of space-time and the introduction of Nelson's forward and backward stochastic derivatives, was developed by Nottale in his Scale Theory of Relativity [10] [26]. Remarkably, Nottale's approach has promoted the Schroedinger equation to be valid for large scale structures, and predicted the existence of exo-solar planets which were observationally verified to exist [12]. This may further support the idea that the RCW structures introduced in the vacuum by scale transformations, are valid independently of the scale in which the associated Brownian motions and equations of quantum mechanics are posited. Furthermore, Kiehn has proved that the Schroedinger equation in spatial 2D can be exactly transformed into the Navier-Stokes equation for a compressible fluid, if we further take the kinematical viscosity $\nu$ to be $\frac{\hbar}{m}$ with $m$ the mass of the electron [11]. We have argued in [3] that the Navier-Stokes equations share with the Schroedinger equation, that both have a RCW geometry at their basis: While in the Navier-Stokes equations the trace-torsion is $\frac{-1}{2\nu}u$ with $u$ the time-dependent velocity one-form of the viscous fluid, in the Schroedinger equation, the trace-torsion one-form incorporates the logarithmic differential of the wave function -just like in Nottale's theory [10]- and further incorporates electromagnetic potential terms in the trace-torsion one-form. This correspondence between trace-torsion one-forms is

what lies at the base of Kiehn's correspondance, with an important addendum: While in the approach of the Schroedinger equation the probability density is related to the Schroedinger scale factor (in incorporating the complex phase) and the Born formula turns out to be a formula and not an hypothesis, under the transformation to the Navier-Stokes equations it turns out that the probability density of non-relativistic quantum mechanics, is the enstrophy density of the fluid, i.e. the square of the vorticity, which thus plays a *geometrical* role that substitutes the probability density. Thus, in this approach, while there exist virtual paths sustaining the random behaviour of particles (as is the case also of the Navier-Stokes equations) and interference such as in the two-slit experiments can be interpreted as a superposition of Brownian paths [13], the probability density has a purely geometrical fluid-dynamical meaning. This is of great relevance with regards to the fundamental role that the vorticity, i.e. the fluid's particles angular-momentum has as an organizing structure of the geometry of space and time. In spite that the torsion tensor in this theory is naturally restricted to its trace and thus generates a differential one-form, in the non-propagating torsion theories it is interpreted that the vanishing of the completely skew-symmetric torsion implies the absence of spin and angular momentum densities [22], it is precisely the role of the vorticity to introduce angular momentum into the present theory. We would like to mention the important developments in a beautiful theory of space-time with a Cantorian structure being elaborated in numerous articles by M. El Naschie [67] and a theory of fractals and stochastic processes of QM which has been elaborated by G. Ord [66].

Secondly, in this article we shall extend the treatment of QM and its relations to torsion fields and Brownian motions, to the Lie-isotopic extension of QM due to Santilli, presently known as Hadronic Mechanics (HM in the following). Before actually introducing HM, we would like to discuss the fundamentals of the relation between HM and the present developments in terms of torsion fields, since torsion bears a close relation with the geometry of Lie symmetry groups. Indeed, if we consider as configuration space a Lie group, there is a canonical connection whose torsion tensor coefficients are non other than the coefficients of the Lie-algebra under the Lie bracket operation [49]. Thus a Lie algebra is characterized by the torsion tensor for the canonical connection. Now let us consider a system that can be described in terms of a Lie group symmetry which is a continuous deformation of the original one. For example, instead of the rotational symmetry we have, say, an ellipsoidal one due to the deformation of the original system (this is the case of a system whose symmetry in the vacuum is no longer valid since it has been embedded in an inhomogeneous anisotropic medium). Then the Lie bracket of the deformed infinitesimal symmetry is a continuous deformation of the original torsion and characterizes completely the symmetry. This is the basic mathematical implicit idea that leads to the present perspective, and allows to present a geometrical structure (the torsion of the infinitesimal symmetry) which is deformed by the isotopic modification (we shall

explain below the meaning of the term "isotopic") of Lie group theory due to Santilli, the so-called Lie-Santilli-isotopic theory which started by producing the isotopic lift of the groups of elementary particle physics and special relativity [15-20,65], and encompasses in the physical domain, extensions of classical mechanics (introducing the deformed symmetries) and their associated quantum systems through the isotopic lift of the Schroedinger and Heisenberg representation which incorporates the modifications of the symmetries.

There is a canonical way of producing these isotopic lift, namely through a non-unitary transform acting on all the elements of the standard theory. Here the notion of isotopic lift consists in carrying through the action of non-unitary transformations -the previously referred deformations- on all the mathematical structures with preservation of the basic axioms. Starting by redefining the notion of unit -which stands as the fundamental operation of the theory- achieved by a non-unitary arbitrary operation, then the construction of HM follows by carrying the generalized unit to define the isotopic number fields, functions, configuration and state-space manifolds, differential and integral calculi, metrics, tensors, the Hilbert state-spaces, to resume, all the relevant mathematical structures of quantum mechanics are isotopically lifted through the generalized unit while preserving the whole axiomatic structure of both the mathematical and physical aspects of the theory. Probably the resistence to adopt such a general scheme, is that one tends to confuse the universal character of the concept of unit, which is fixed, and its representation in a certain scale and with a certain object (s) which can be taken arbitrary, as we do in daily life. We must remark at this stage that the introduction of this generalized unit, in contrast with the basic unit of mathematics and physics, establishes a vinculation between these new units and physical processes which is unknown to mathematics, with the exception of the arithmetic of forms which follows from the principle of distinction previously alluded, and the multivalued logics associated to it and self-reference [81]. It is important to remark that the development of HM took more than thirty years to reach the understanding that the isotopic lift could not be restricted to the symmetries, classical and quantum mechanics, but required the lift of number theory, differential and integral calculi, and to the Hilbert space structure as well. For an account of these developments and a complete list of references, the reader is urged to consult [16] in which Santilli gives a complete description of the Lie-isotopic, Lie-admissible, genotopic and hyperstructural theories which extend the present theory; it is most remarkable that these theories as well as HM and the isotopic lift of relativity, admit dual theories in which antimatter can be treated classically and antigravity can be presented in their terms; see [77]). These theories have succeeded in solving several fundamental questions of particle physics, nuclear physics, quantum chemistry cosmology, superconductivity and biology, where the usual approaches have shown unsurmountable inconsistencies [15-20,56,68,74,75,76].

The purpose of the introduction of the generalized units is to be able to construct a theory in the situations in which QM is no longer applicable, and

to recover it in a scale in which the generalized unit recovers the historical unit of mathematics and physics and the associated domains in which GR and QM are applicable. A fundamental example of this new paradigm, is the case of the neutron with its hyperdense structure where interactions are no longer derivable from a potential field; in this situation, the medium is deformable, particles are extended, and non-local non-hamiltonian interactions are the characteristics of the system. Thus, in HM the neutron is considered to be a compressed state of a proton and an electron, revitalizing Rutherford's conception in further elaborations by Animalu and Santilli [56]. This state is produced under the above stated situations and through spin-up-spin-down magnetic couplings [15,56], which plays a crucial role in the Rutherford-Santilli model of the neutron. These spin-spin couplings appear in the definition of the generalized isotopic unit. In this regard, HM has in common with the usual approach to torsion, the relevance of spinor angular momentum densities [22]. Possible relations between torsion as spin or angular momentum densities can be ventured in relation with anomalous spin interactions of the proton, and magnetic resonances as well [43]. Remarkably it has been shown in [56] that completely skew-symmetric torsion can produce a spin flip of high energy fermionic matter at very high densities, and that in this situation helicity can be identified with spin. An intrinsic macroscopic angular momentum would be the evidence of this phenomena. This may be of relevance when taking in consideration the time periodicity of the fine structure of histograms and its relation to macroscopic angular momentum, found by Shnoll and associates [80].

Therefore a geometrical characterization will be possible by introducing the non-linear non-local generalized unit which incorporates the new characteristics of the system under the strong overlapping of the components of the neutron so there is now a deformation of their original symmetry. To close our discussion which started by mentioning the special role of the canonical geometry of a Lie-group and the role of the torsion tensor as the structure coefficients of the Lie-algebra, the modification is produced precisely in these coefficients by multiplying them by the isotopic generalized unit. Thus, at the level of the canonical geometry there exists a modification of the torsion tensor. This will carry out to the whole theory as already explained . However it is pertinent to remark that in the development of HM there is no mention on the relation of the generalized unit in terms of the modification of the torsion as being the fundamental operation in terms of which his theories are constructed. Thus, the present approach, proposes an original *perspective* of HM. It is very important to stress that HM carries to an isotopic modification of Quantum Chemistry, known as Hadronic Chemistry, which allows the computation of the solutions of the iso-Schroedinger equation for molecules in very short times and accuracy in comparison with the results achieved by application of quantum chemistry, while solving its inconsistencies, fundamentally the impossibility of giving a theory for chemical bonds [15,68,84] . This has allowed to produce industrially fluid plasmas with remarkable characteristics, as a first class of clean fuels [15]; fur-

thermore, the theory has proposed the possibility of stimulating nuclear decays as a technological application to deal with nuclear waste in shorter times that those produced by spontaneous decay.

In Santilli's conception with regards to the isotopic lifts of the usual structures of differential geometry, the starting point is that the Minkowski and Euclidean metrics with their associated rotational symmetries are inapplicable for situations of non-point-like particles moving within the inhomogeneous and anisotropic vacuum (this includes the atomic structure as well as the electromagnetic, weak and strong interactions); this is the case of the so-called interior problem; see [14-19]. Thus, in such a medium, the velocity of light depends on the underlying structure of the medium, and no longer coincides with the velocity of light in the vacuum. Consequently, the Lorentz and Poincaré symmetries are no longer applicable in this case, and thus an isotopic lift is constructed to yield a unified approach to the isotopic lifts of GR and Special Relativity; this lead to an axiomatically consistent theory of Relativistic Quantum Mechanics, preserving the fundamental axioms, and resulted in the completion of QM [16]. The reader may note the similarity of this conception with the one we have presented in terms of torsion as producing the basic anisotropies and inhomogenities of the vacuum. The symmetries and geometries of the isotropic and homogeneous vacuum cannot represent matter nor spinor fields by themselves. In the more general case in which the metric is no longer trivial, the usual metric is valid as a representation for the so-called exterior problem in which the astrophysical bodies can be effectively approximated as massive points because their shape does not affect their gravitational trajectories when moving in empty space. In the case of the interior problem, such as the case of ultradense stars in which spin couplings are relevant ( a similar approach as the one conceived originally for the introduction of a generalization of general relativity by introducing a spin density tensor associated with the torsion tensor [22]), these couplings are no longer related to a reversible Hamiltonian dynamics. This conception goes back to classical mechanics, in which forces such as friction cannot be described by a Hamiltonian to which they are added as independent forces. These additional terms were incorporated to the foundations of classical mechanics by its founding fathers, and from the physics point of view, was part of the original motivation by Santilli, to attempt a unified formulation of classical and QM through the deformation of the conventional structures and theories [78]. This original approach was posteriorly proved to be inconsistent, due to the need of incorporating into the theory two aspects that had been not perceived originally as imprescindible: Namely, the isotopic lift of the number system and of the Hilbert space defined over these extended fields to be able to achieve a consistent theory of observables, and furthermore, to be able to achieve a consistent isoquantization, the need of extending the notions of differential calculus, fundamentally the differential operator; this was achieved in 1996-1997 ; see [16]. The original attempts by this author to develop the relations between RCW geometries, Brownian motions and the strong interactions

were also inconsistent due to the lack of an extension in the full sense previously mentioned [29].

Returning to the discussion of the roles of torsion and the extensions of classical mechanics to account for dissipative forces, we would like to observe that a similar situation is contemplated in classical mechanics from the point of view of considering torsion fields, since friction is a manifestation of anholonomic degrees of freedom which cannot be described by the symmetries and geometry of the frictionless system. Then the equations of classical motion (i.e. differentiable trajectories, as related to a Hamiltonian or Lagrangian approach) have to include additional terms to represent the anholonomic degrees of freedom as exterior forces acting on the system, or alternatively, as internal deformations of the symmetries.

Now to understand the need of carrying the extensions produced by the isotopic lifts, it is founded in the fact that the isotopic lift of Relativity due to Santilli (see [18]) is applicable for the electromagnetic and weak interactions but not applicable for the case of hadrons. These have a charge radius of 1 fm ($10^{-13}cm$) which is the radius of the strong interactions. Unlike the electromagnetic and weak interactions a necessary condition to activate the strong interaction is that hadrons enter into a condition of mutual interpenetration. In view of the developments below, we would like to stress that the modification of the symmetries of particles under conditions of possible fusion, is the first step for the usual developments of fusion theories which have been represented in terms of diffusion processes that overcome the Coulomb repulsive potential which impedes the fusion [37]; Brownian motions and other stochastic processes also appear in a phenomenological approach to the many body problem in particle and nuclear physics, but with no hint as to the possibility of an underlying space-time structure [83]. The basic idea goes back to the foundational works of Smoluchowski (independently of A. Einstein's work in the subject) in Brownian motion [38]. In the case of fusion theories, we have a gas of neutrons (which have an internal structure) and electrons, or an hadron gas; in these cases the fused particles are considered to be alike a compressible fluid with an unstable neck in its fused drops which have to be stabilized to achieve effective fusion; we can see here the figure of deformed symmetries. Thus, the situation for the application of Brownian motion to fusion is a natural extension to the subatomic scale of the original theory. We finally notice that the models for fusion in terms of diffusion do not require QM nor quantum chromodynamics [37]. In contrast, HM stems from symmetry group transformations that describe the contact fusion processes that deform the neutron structure, and lead to the isotopic Schroedinger equation which in this article, together with the isotopic Heisenberg representation, will be applied to establish a link between the RCW geometries, fusion processes and diffusions. The reason for the use of the iso-Heisenberg representation, is that in Santilli's theory, the isotopic lift of the symmetries in carried out in terms of the iso-Heisenberg representation, where its connection with classical mechanics under the quantization rules including

the isotopic lift is transparent. In this article we shall present a quantization method for both QM and HM in terms of diffusion processes, and in terms of a diffusion-Heisenberg and isodiffusion-isoHeisenberg representations which we shall present below.

# 2 TORSION AND THE NON-CLOSURE OF PARALLELOGRAMS

We want to introduce torsion in terms of the self-referential definition of the manifold structure in terms of the concept of difference or distinction derived from the operation of comparison. We shall assume that there are two observers on a manifold (of dimension $n$), say observer 1 and observer 2, which may not be moving inertially. To compare measurements and to establish thus a sense of objectivity (identity of their results), they need to compare their measurements which take place in the tangent space at different points of the $n$-dimensional manifold $M$ in which they are placed, so they have to establish the difference between their reference frames, i.e. the difference between the set of orthogonal (or pseudo-orthogonal) vectors at their locations, the so-called $n$-beins . Let $e_i(\mathcal{P}_0) = e_i^\alpha(\mathcal{P}_0)\partial_\alpha, i = 1, \ldots, n$ be the basis for observer 1 at point $\mathcal{P}_0$, and similarly $e_i(\mathcal{P}_1) = e_i^\alpha(\mathcal{P}_1)\partial_\alpha$ the reference frame for observer 2 at $\mathcal{P}_1$; let us denote the reference frame at the tangent space to the point $\mathcal{P}_1$ when parallely transported (without changing its length and angle) from $\mathcal{P}_0$ to $\mathcal{P}_1$ by $e_i(\mathcal{P}_0 \rightarrow \mathcal{P}_1)$ along a curve joining $\mathcal{P}_0$ to $\mathcal{P}_1$ with an affine connection, whose covariant derivative operator we denote as $\nabla$ [44]. Then, $\nabla e_1$ is the difference between $e_i(\mathcal{P}_0 \rightarrow \mathcal{P}_1)$ and $e_i(\mathcal{P}_1)$. This gap defect originates either to the deformation of $e_i(\mathcal{P}_0)$ along its path to $\mathcal{P}_1$, which cannot be transformed away by a change of coordinates, or by a change of coordinates from $\mathcal{P}_0$ to $\mathcal{P}_1$, which is not intrinsic and thus can be transformed away, or finally, by a combination of both. Let us move observer's one frame over two different paths. Parallel displacing an incremental vector $dx^b e_b$ from the point $\mathcal{P}_0$ along the basis vector $e_a$ over an infinitesimal distance $dx^a$ to the point $\mathcal{P}_1 = \mathcal{P}_0 + dx^a$ gives the vector

$$e_b dx^b(\mathcal{P}_0 \rightarrow \mathcal{P}_1) = dx^b e_b(\mathcal{P}_0) + \Gamma^c_{ba} dx^b \wedge dx^b e_c. \tag{1}$$

Similarly, the parallel transport of the incremental vector $dx^a e_a$ from the point $\mathcal{P}_0$ to $\mathcal{P}_2$ along the frame $e_b$ over an infinitesimal distance $dx^b$ to the point $\mathcal{P}_2 = \mathcal{P}_0 + dx^b$ gives the vector $e_a(\mathcal{P}_1 \rightarrow \mathcal{P}_2) = dx^a e_a(\mathcal{P}_1) + \Gamma^c_{ab} dx^a \wedge dx^b e_c$. The gap defect between $e_a(\mathcal{P}_0 \rightarrow \mathcal{P}_1)$ and the value of $dx^b e_b(\mathcal{P}_1)$ is

$$dx^b \nabla e_b(\mathcal{P}_1) = dx^b (\frac{\partial e_b}{\partial x^a}) \wedge dx^a - \Gamma^c_{ba} dx^a \wedge dx^b e_c, \tag{2}$$

and the gap defect between the vector $e_b(\mathrm{P}_1 \rightarrow \mathcal{P}_2)$ and $e_b dx^b(\mathcal{P}_2)$ is

$$dx^a D e_a(\mathcal{P}_2) = dx^a (\frac{\partial e_a}{\partial x^b}) \wedge dx^a - \Gamma^c_{ab} dx^a \wedge dx^b e_c. \tag{3}$$

Therefore, the total gap defect between the two vectors is the comparison already alluded to)

$$dx^b \nabla e_b(\mathcal{P}_1) - dx^a De_a(\mathcal{P}_2) = (\frac{\partial e_b}{\partial x^a} - \frac{\partial e_a}{\partial x^b}) dx^a \wedge dx^b + [\Gamma^c_{ab} - \Gamma^c_{ba}] dx^a \wedge dx^b e_c, \quad (4)$$

where we recognize in the first term the Lie-bracket

$$[e_a, e_b] = (\frac{\partial e_b}{\partial x^a} - \frac{\partial e_a}{\partial x^b}) dx^a \wedge dx^b, \quad (5)$$

which we can write still as

$$[e_a, e_b] = C^c_{ab} e_c, \quad (6)$$

where $C^c_{ab}$ are the coefficients of the anholonomity tensor, and then finally we can write the difference in eq.(4) as

$$dx^b e_b(\mathcal{P}_1) - dx^a \nabla e_a(\mathcal{P}_2) = (C^c_{ab} + [\Gamma^c_{ab} - \Gamma^c_{ba}]) dx^a \wedge dx^b e_c. \quad (7)$$

If we further introduce the vector-valued torsion two form

$$T = \frac{1}{2} T^c_{ab} dx^a \wedge dx^b e_c := \nabla e_b(e_a) - \nabla e_a(e_b) - [e_a, e_b]^c e_c \quad (8)$$

we find that the components $T^c_{ab}$ are given by the so-called torsion tensor

$$T^c_{ab} = C^c_{ab} + [\Gamma^c_{ab} - \Gamma^c_{ba}] \quad (9)$$

Thus, we have two possibilities for the non-closure of infinitesimal paralblelograms. Either by anholonomity, or due to the non-symmetricity of the Christoffel coefficients. These are radically different. The latter can in some instances be set to be equal to zero, while the other term cannot. Say we have a coordinate transformation continuously differentiable $(x^1, \ldots, x^n) \to (y^1, \ldots, y^n)$ so we have that an holonomous transformation, i.e. we have that each $dy^i$ is exact of the form

$$dy^i = \frac{\partial y^i}{\partial x^j} dx^j. \quad (10)$$

Then, if we take an holonomous basis $e_j = (\frac{\partial y^i}{\partial x^j}) \frac{\partial}{\partial y_i}$, then the anholonomity vanishes, $[e_i, e_j] = 0$ identically on $M$, and we are left for the expression for the torsion tensor

$$T^c_{ab} = \Gamma^c_{ab} - \Gamma^c_{ba}. \quad (11)$$

Anholonomity is very important. It is related to the existence of a time density, and is related to the Sagnac effect, to the Thomas precession, etc. [41]). Nowadays, relativistic rotation has become an issue of great interest, and the interest lays in rotating anholomous frames, in distinction with non-rotating holonomous frames. The torsion tensor evidences how the manifold is folded or dislocated, and the latter situation can be produced by tearing the manifold

of by the addition of matter or fields to it. These are the well known Volterra operations of condensed matter physics (initially, in metalurgy [42]), and was the first engineering example of the fundamental role of torsion. The second example was elaborated in the pioneering work by Gabriel Kron in the geometrical representation of electric networks, and lead to the concept of negative resistance [27]. Contemporarily, negative resistance has become an important issue, after the discovery of its existence in some materials, with an accompanying apparent phenomenon of superconductivity [30]

# 3 RIEMANN-CARTAN-WEYL GEOMETRIES

In this section we follow [1,2]. In this article $M$ denotes a smooth connected compact orientable $n$-dimensional manifold (without boundary). While in our initial works, we took for $M$ to be space-time, there is no intrinsic reason for this limitation, in fact if can be an arbitrary configuration manifold and still a phase-space associated to a dynamical system. The paradigmatical example of the latter, is the projective space associated to a finite-dimensional Hilbert-space of a quantum mechanical system [3,39]. We shall further provide $M$ with a linear connection as already described in the previous section, by a covariant derivative operator $\nabla$ which we assume to be compatible with a given metric $g$ on $M$, i.e. $\nabla g = 0$. Here, the metric can be the Minkowski degenerate metric, or an arbitrary positive-definite (i.e. Riemannian) metric. Given a coordinate chart $(x^\alpha)$ $(\alpha = 1, \ldots, n)$ of $M$, a system of functions on $M$ (the Christoffel symbols of $\nabla$) are defined by $\nabla_{\frac{\partial}{\partial x^\beta}} \frac{\partial}{\partial x^\gamma} = \Gamma(x)^\alpha_{\beta\gamma} \frac{\partial}{\partial x^\alpha}$. The Christoffel coefficients of $\nabla$ can be decomposed as:

$$\Gamma^\alpha_{\beta\gamma} = \left\{ \begin{matrix} \alpha \\ \beta\gamma \end{matrix} \right\} + \frac{1}{2} K^\alpha_{\beta\gamma}. \tag{12}$$

The first term in (12) stands for the metric Christoffel coefficients of the Levi-Civita connection $\nabla^g$ associated to $g$, i.e. $\left\{ \begin{matrix} \alpha \\ \beta\gamma \end{matrix} \right\} = \frac{1}{2}(\frac{\partial}{\partial x^\beta} g_{\nu\gamma} + \frac{\partial}{\partial x^\gamma} g_{\beta\nu} - \frac{\partial}{\partial x^\nu} g_{\beta\gamma}) g^{\alpha\nu}$, and

$$K^\alpha_{\beta\gamma} = T^\alpha_{\beta\gamma} + S^\alpha_{\beta\gamma} + S^\alpha_{\gamma\beta}, \tag{13}$$

is the cotorsion tensor, with $S^\alpha_{\beta\gamma} = g^{\alpha\nu} g_{\beta\kappa} T^\kappa_{\nu\gamma}$, and from eqs. (4) and (9) it follows that $T^\alpha_{\beta\gamma} = (\Gamma^\alpha_{\beta\gamma} - \Gamma^\alpha_{\gamma\beta})$ the skew-symmetric torsion tensor. We are interested in (one-half) the Laplacian operator associated to $\nabla$, i.e. the operator acting on smooth functions on $M$ defined as

$$H(\nabla) := 1/2 \nabla^2 = 1/2 g^{\alpha\beta} \nabla_\alpha \nabla_\beta. \tag{14}$$

A straightforward computation shows that $H(\nabla)$ only depends in the trace of the torsion tensor and $g$, since it is

$$H(\nabla) = 1/2 \triangle_g + \hat{Q} \equiv H(g, Q), \tag{15}$$

with $Q := Q_\beta dx^\beta = T^\nu_{\nu\beta} dx^\beta$ the trace-torsion one-form and where $\hat{Q}$ is the vector field associated to $Q$ via $g$: $\hat{Q}(f) = g(Q, df)$, for any smooth function $f$ defined on $M$. Finally, $\triangle_g$ is the Laplace-Beltrami operator of $g$: $\triangle_g f = \mathrm{div_g}\ \mathrm{grad} f$, $f \in C^\infty(M)$, with $\mathrm{div_g}$ the Riemannian divergence. Thus for any smooth function, we have $\triangle_g f = 1/[det(g)]^{\frac{1}{2}} g^{\alpha\beta} \frac{\partial}{\partial x^\beta}([det(g)]^{\frac{1}{2}} \frac{\partial}{\partial x^\alpha} f)$. Furthermore, the second term in (15), $\hat{Q}$, coincides with the Lie-derivative with respect to the vectorfield $\hat{Q}$: $L_{\hat{Q}} = i_{\hat{Q}} d + d i_{\hat{Q}}$, where $i_{\hat{Q}}$ is the interior product with respect to $\hat{Q}$: for arbitrary vectorfields $X_1, \ldots, X_{k-1}$ and $\phi$ a $k$-form defined on $M$, we have $(i_{\hat{Q}}\phi)(X_1, \ldots, X_{k-1}) = \phi(\hat{Q}, X_1, \ldots, X_{k-1})$. Then, for $f$ a scalar field, $i_{\hat{Q}} f = 0$ and

$$L_{\hat{Q}} f = (i_{\hat{Q}} d + d i_{\hat{Q}}) f = i_{\hat{Q}} df = g(Q, df) = \hat{Q}(f). \tag{16}$$

Thus, our laplacian operator admits being written as

$$H(g, Q) = \frac{1}{2} \triangle_g + L_{\hat{Q}}. \tag{17}$$

Therefore, assuming that $g$ is non-degenerate, we have defined a one-to-one mapping

$$\nabla \rightsquigarrow H(g, Q) = 1/2 \triangle_k + L_{\hat{Q}}$$

between the space of $g$-compatible linear connections $\nabla$ with Christoffel coefficients of the form

$$\Gamma^\alpha_{\beta\gamma} = \left\{ \begin{matrix} \alpha \\ \beta\gamma \end{matrix} \right\} + \frac{2}{(n-1)} \left\{ \delta^\alpha_\beta\ Q_\gamma - g_{\beta\gamma}\ Q^\alpha \right\}, n \neq 1 \tag{18}$$

and the space of elliptic second order differential operators on functions.

# 4 RIEMANN-CARTAN-WEYL DIFFUSIONS

In this section we shall recall the correspondence between RCW connections defined by (18) and diffusion processes of scalar fields having $H(g, Q)$ as its diffrential generator. For this, we shall see this correspondence in the case of scalars. Thus, naturally we have called these processes as *RCW diffusion processes.*. For the extensions to describe the diffusion processes of differential forms, see [1], [4].

For the sake of generality, in the following we shall further assume that $Q = Q(\tau, x)$ is a time-dependent 1-form. In this setting $\tau$ is the universal time variable due to Stuckelberg [7]. The stochastic flow associated to the diffusion generated by $H(g, Q)$ has for sample paths the continuous curves $\tau \mapsto x(\tau) \in M$

satisfying the Itô invariant non-degenerate s.d.e. (stochastic differential equation)

$$dx(\tau) = \sigma(x(\tau))dW(\tau) + \hat{Q}(\tau, x(\tau))d\tau. \tag{19}$$

In this expression, $\sigma : M \times R^m \to TM$ is such that $\sigma(x) : R^m \to TM$ is linear for any $x \in M$, the noise tensor, so that we write $\sigma(x) = (\sigma_i^\alpha(x))$ $(1 \leq \alpha \leq n,$ $1 \leq i \leq m)$ which satisfies

$$\sigma_i^\alpha \sigma_i^\beta = g^{\alpha\beta}, \tag{20}$$

where $g = (g^{\alpha\beta})$ is the expression for the metric in covariant form, and $\{W(\tau), \tau \geq 0\}$ is a standard Wiener process on $R^m$ with zero mean with respect to the standard centered Gaussian function, and covariance given by $\mathrm{diag}(\tau, \ldots, \tau)$; finally, $dW(\tau) = W(\tau + d\tau) - W(\tau)$ is an increment. Now , it is important to remark that $m$ can be arbitrary, i.e. we can take noise tensors defined on different spaces, and obtain the space diffusion process. In regards to the equivalence between the stochastic and the geometric picture, this enhances the fact that there is a freedom in the stochastic picture, which if chosen as the originator of the equivalence, points out to a more fundamental basis of the stochastic description. This is satisfactory, since it is impossible to identify all the sources for noise, and in particular those coming from the vacuum, which we take as the source for the randomness. Note that in taking the drift and the diffusion tensor as the original objects to build the geometry, the latter is derived from objects which are associated to *collective* phenomena. Note that if we start with eq. (19), we can reconstruct the associated RCW connection by using eq.(20) and the fact that the trace-torsion is the $g$-conjugate of the drift, i.e., in simple words, by lowering indexes of $\hat{Q}$ to obtain $Q$. We shall not go into the details of these constructions, which relies heavily on Stochastic Analysis on smooth manifolds [55,70], but yet we shall apply them to give a derivation of the noise term of the diffusion processes corresponding to the iso-Schroedinger equation.

# 5 THE HODGE DECOMPOSITION OF THE TRACE-TORSION FIELD

To obtain the most general form of the RCW laplacian in the non-degenerate case, we only need to know the most general decomposition of 1-forms. In this section, the metric $g$ is positive-definite. We consider the Hilbert space given by the completion of the pre-Hilbert space of square-integrable smooth differential forms of degree $k$ $(0 \leq k \leq n)$ on $M$, with respect to the Riemannian volume $\mathrm{vol_g}$, which we denote as $L^2(\mathrm{sec}(\Lambda^k(T^*M))$. We shall focus on the decomposition of 1-forms, so let $\omega \in L^2(\mathrm{sec}(T^*M))$; then we have the Hilbert space decomposition

$$\omega = df + A_{\mathrm{coex}} + A_{\mathrm{harm}}, \tag{21}$$

where $f$ is a smooth real valued function on $M$, $A_{\text{coex}}$ is a smooth coexact 1-form, i.e. there exists a smooth 2-form, $\beta$ such that $\delta\beta_2 = A_{\text{coex}}$ [2], so that $A_{\text{coex}}$ is coclosed, i.e.

$$\delta A_{\text{coex}} = \delta(\delta\beta_2) = 0, \tag{22}$$

and $A_{\text{harm}}$ is a closed and coclosed smooth 1-form, then

$$\delta A_{\text{harm}} = 0, dA_{\text{harm}} = 0, \tag{23}$$

or equivalently, $A_{\text{harm}}$ is harmonic, i.e.

$$\triangle_1 A_{\text{harm}} \equiv \text{trace}(\nabla^g)^2 A_{\text{harm}} - R^\alpha_\beta(g)(A_{\text{harm}})_\alpha \gamma^\alpha = 0, \tag{24}$$

with $R^\alpha_\beta(g) = R^{\mu\beta}_{\mu\alpha}(g)$ the Ricci metric curvature tensor. Eq. (24) is the source-less Maxwell-de Rham equation. An extremely important fact is that this is a Hilbert space decomposition, so that it has unique terms, which are furthermore orthogonal in Hilbert space, i.e.

$$((df, A_{\text{coex}})) = 0, ((df, A_{\text{harm}})) = 0, ((A_{\text{coex}}, A_{\text{harm}})) = 0, \tag{25}$$

so that the decomposition of 1-forms (as we said before, this is also valid for $k$-forms, with the difference that $f$ is a $k-1$-form, $\beta_2$ is really a $k+1$-form and $A_{\text{harm}}$ is a $k$-form) has unique terms, and a fortiori, this is also valid for the Cartan-Weyl 1-form. We have proved that $A_{\text{coex}}$ and $A_{\text{harm}}$ are further linked with Maxwell's equations, both for Riemannian and Lorentzian metrics. For the stationary state which we shall describe in the next section, they lead to the equivalence of the Maxwell equation and the relativistic quantum mechanics equation of Dirac-Hestenes in a Clifford bundle setting [2,21] whenever the coclosed (Hertz potential) term and the (Aharonov-Bohm) harmonic term are both dependent on all the 4D variables while they are infinitesimal rotations defined on the spin-plane.

## 5.1 The Decomposition Of The Cartan-Weyl Form And The Stationary State

We wish to elaborate further on the decomposition of $Q$ in the particular state in which the diffusion process generated by $H(g, Q)$, in the case $M$ has a Riemannian metric $g$, and has a $\tau$-invariant state corresponding to the asymptotic stationary state. Thus, we shall concentrate on the diffusion processes of scalar fields generated by

$$H(g, Q) = \frac{1}{2}(\triangle + L_{\hat{Q}}), \text{with } Q = d\ln\psi^2 + A_{\text{coex}} + A_{\text{harm}}. \tag{26}$$

[2]Here $\delta$ denotes the codifferential operator, the adjoint of $d$, introduced above; see [1,2, 44].

This is the invariant form of the (forward) Fokker-Planck operator of this theory (and furthermore of the Schroedinger operator when introducing the phase function to the exact term of $Q$). Through this identification, we note that $\psi$ is the scale field in the Einstein $\lambda$ transformations from which in the vacuum, the RCW geometry can be obtained ; see [2]. We are interested now in the $\mathrm{vol_g}$-adjoint operator defined in $L^2(\mathrm{sec}(\Lambda^n(T^*M)))$, which we can think as an operator on densities, $\phi$. Thus,

$$H(g,Q)^\dagger\phi = \frac{1}{2}(\triangle_g\phi - \mathrm{div_g}(\phi \mathrm{grad}\ \ln\ \phi) - \mathrm{div_g}(\phi\hat{A})). \tag{27}$$

The operator described by eq. (27) is the backward Fokker-Planck operator. The transition density $p^\nabla(\tau,x,y)$ is determined by the fundamental solution (i.e. $p^\nabla(\tau,x,-)\to\delta_x(-)$ as $\tau\to 0^+$) of the equation on the first variable

$$\frac{\partial u}{\partial\tau} = H(g,Q)(x)u(\tau,x,-). \tag{28}$$

Then , the diffusion process $\{x(\tau):\tau\geq 0\}$, gives rise to the Markovian semigroup $\{P_\tau = \exp(\tau H(g,Q)):\tau\geq 0\}$ defined as

$$(P_\tau f)(x) = \int p^\nabla(\tau,x,y)f(y)\mathrm{vol_g}(y). \tag{29}$$

It has a unique $\tau$-independant-invariant state described by a probability density $\rho$ independant of $\tau$ determined as the fundamental weak solution (in the sense of the theory of generalized functions) of the $\tau$-independent Fokker-Planck equation:

$$H(g,Q)^\dagger\rho \equiv \frac{1}{2}(-\delta d\rho + \delta(\rho Q)) = 0. \tag{30}$$

Let us determine the corresponding form of $Q$, say $Q_{\mathrm{stat}} = d\ln\psi^2 + A_{\mathrm{stat}}$. We choose a smooth real function $U$ defined on $M$ such that

$$H(g,Q_{\mathrm{stat}})^\dagger(e^{-U}) = 0, \tag{31}$$

so that

$$-de^{-U} + e^{-U}Q = \delta(-\delta\Pi + A_{\mathrm{harm}}), \tag{32}$$

for a 2-form $\Pi$ and harmonic 1-form $A_{\mathrm{harm}}$; thus, if we set the invariant density to be given by $\rho = e^{-U}\mathrm{vol_g}$, then

$$Q_{\mathrm{stat}} = d\ln\psi^2 + \frac{A}{\psi^2},\ \text{with}\ A = -\delta\Pi_2 + A_{\mathrm{harm}}. \tag{33}$$

Now we project $\frac{A}{\psi^2}$ into the Hilbert-subspaces of coexact and harmonic 1-forms, to complete thus the decomposition of $Q_{\mathrm{stat}}$ obtaining thus Hertz and Aharonov-Bohm potential 1-forms for the stationary state respectively. Yet these potentials have now a built-in dependence on the invariant distribution, and although

they give rise to Maxwell's theory, the interpretation is now different. [3] Indeed, we have an inhomogeneous random media, and these potentials depend on the $\tau$-invariant distribution of the media. We can use further the Hodge-decomposition of $Q_{\text{stat}}$ to manifest the quantum potential as built-in. Indeed, if we multiply it by $\psi$ and apply $\partial$, then we get that $d\ln\psi$, and the coexact and harmonic terms of $Q_{\text{stat}}$ decouple in the resultant field equation which turns out to be

$$\triangle_g \psi = [g^{-1}(d\ln\psi, d\ln\psi) - \delta d\ln\psi]\psi, \tag{34}$$

with nonlinear potential $V := g^{-1}(d\ln\psi, d\ln\psi) - \delta d\ln\psi$, which has the form of (twice) a relativistic quantum potential extending Bohm's potential in non-relativistic Quantum Mechanics [35]. We have seen in [2], that from scale-invariance it follows that the quantum potential coincides up to a conformal factor with the metric scalar curvature. Thus in this setting it turns out that the random motions with noise tensor satisfying eq. (20) and drift vector field given by $\text{gradln}\psi$, the Riemannian gradient of the logarithm of the wave function, generate the gravitational field. We can see in this identity the relation with the ideas due to Le Sage already presented in the Introduction. Since the trace-torsion includes the Maxwell fields, we have unified space-time geometries with Brownian motions and the theory of electromagnetism. While the metric must be positive-definite to be able to apply the Hodge decomposition, and in particular we can take the flat Euclidean metric for a start, it is known from Hehl's work that the metric can be deduced from the constitutive relations in the theory of electromagnetism, so it can be taken as derived from the mere existence of electromagnetic fields and the constitutive relations [31]. We have showed in [3] that the theory of electromagnetism in euclidean space is related to establishing that the universal time parameter, $\tau$, is the basic time variable instead of the linear time of the observer, $t$, and that this transformation is related to a dissipative process. Furthermore, the role of torsion as an active field can be described in these terms [3].

# 6 RCW GEOMETRIES, BROWNIAN MOTIONS AND THE SCHROEDINGER EQUATION

We have seen in [3] that we can represent the space-time quantum geometries for the relativistic diffusion associated with the invariant distribution, so

[3] A word of caution. In principle, $-\delta\Pi/\rho$ and $A_{\text{harm}}/\rho$ may not be the coexact and harmonic components of $A/\rho$ respectively. If this would be the case, then we obtain that $d\ln\psi$ is $g^{-1}$-orthogonal to both $-\delta\Pi$ and $A_{\text{harm}}$; furthermore $d\ln\psi \wedge A_{\text{harm}} = 0$, so furthermore they are co-linear. This can only be for null $A_{\text{harm}}$ or constant $\rho$, so that the normalization of the electromagnetic potentials is by a trivial constant. In the first case the invariant state has the sole function of determining the exact term of $Q$ to be (up to a constant) $d\ln\psi$.

that $Q = \frac{1}{2} d\ln\rho$, with $\rho = \psi^2$ and $H(g, Q)$ has a self-adjoint extension for which we can construct the quantum geometry on state-space and still the stochastic extension of the Schroedinger equation defined by this operator on taking the analytical continuation on the time variable for the evolution parameter. In this section which follows the solution of the Schroedinger problem of interpolation by Nagasawa [13] interpreted in terms of the RCW geometries and the Hodge decomposition of the trace-torsion, we shall present the equivalence between RCW geometries, their Brownian motions and the Schroedinger equation [3]. We shall show in the next section that this extends to HM.

Thus, we shall now present the construction of non-relativistic quantum mechanics for the case that includes the full Hodge decomposition of the trace-torsion, so that $Q = Q(t, x) = d\ln f_t(x) + A(t, x)$ where $f(t, x) = f_t(x)$ is a function defined on the configuration manifold given by $[a, b] \times M$ (where $M$ is provided with a metric, $g$), to be determined below, and $A(t, x)$ is the sum of the harmonic and co-closed terms of the Hodge decomposition of $Q$, which we shall write as $A(t, x) = A_t(x)$ as a time-dependent form on $M$. The scheme to determine $f$ will be to manifest the time-reversal invariance of the Schroedinger representation in terms of a forward in time diffusion process and its time-reversed representation for the original equations for creation and annihilation diffusion processes produced by the electromagnetic potential term of the trace-torsion of a RCW connection whose explicit form we shall determine in the sequel. From now onwards, both the exterior differential and the divergence operator will act on the $M$ manifold variables only, which we shall write, say, as $df_t(x)$ to signal that the exterior differential acts only on the $x$ variables of $M$. We should remark that in this context, the time-variable $t$ of non-relativistic theory and the evolution parameter $\tau$, are identical [32]. Let

$$L = \frac{\partial}{\partial t} + \frac{1}{2}(\triangle_g + A(t, x).\nabla) = \frac{\partial}{\partial t} + H(g, A_t) \tag{35}$$

with

$$\delta \hat{A}_t = -\mathrm{div}_g A_t = 0. \tag{36}$$

Here, as above, $\hat{A}_t$ denotes the conjugate vector field to the one-form $A_t$. In this setting, we start with a background trace-torsion restricted to an electromagnetic potential. We think of this electromagnetic potential and the associated Brownian motion having its metric conjugate as its drift, as the background geometry of the vacuum, which we shall subsequently relate to a creation and annihilation of particles and the equation of creation and annihilation is given by the following equation.

Let $p(s, x; t, y)$ be the weak fundamental solution of

$$L\phi + c\phi = 0. \tag{37}$$

The interpretation of this equation as one of creation (whenever $c > 0$) and annihilation ($c < 0$) of particles is warranted by the Feynman-Kac representation

for the solution of this equation [13]. Then $\phi = \phi(t,x)$ satisfies the equation

$$\phi(s,x) = \int_M p(s,x;t,y)\phi(t,y)dy, \tag{38}$$

where for the sake of simplicity, we shall write in the sequel $dy = \mathrm{vol_g(y)} = \sqrt{\det(\mathrm{g})}dy^1 \wedge \ldots \wedge dy^3$. Note that we can start for data with a given function $\phi(a,x)$, and with the knowledge of $p(s,x;a,y)$ we define $\phi(t,x) = \int_M p(t,x;a,y)dy$. Next we define

$$q(s,x;t,y) = \frac{1}{\phi(s,x)}p(s,x;t,y)\phi(t,y), \tag{39}$$

which is a transition probability density, i.e.

$$\int_M q(s,x;t,y)dy = 1, \tag{40}$$

while

$$\int_M p(s,x;t,y)dy \neq 1. \tag{41}$$

Having chosen the function $\phi(t,x)$ in terms of which we have defined the probability density $q(s,x;t,y)$ we shall further assume that we can choose a second bounded non-negative measurable function $\tilde{\phi}(a,x)$ on $M$ such that

$$\int_M \phi(a,x)\tilde{\phi}(a,x)dx = 1, \tag{42}$$

We further extend it to $[a,b] \times M$ by defining

$$\breve{\phi}(t,y) = \int \tilde{\phi}(a,x)p(a,x;t,y)dx, \forall (t,y) \in [a,b] \times M, \tag{43}$$

where $p(s,x;t,y)$ is the fundamental solution of eq. (37).

Let $\{X_t \in M, \mathcal{Q}\}$ be the time-inhomogeneous diffusion process in $M$ with the transition probability density $q(s,x;t,y)$ and a prescribed initial distribution density

$$\mu(a,x) = \breve{\phi}(t=a,x)\phi(t=a,x) \equiv \breve{\phi}_a(x)\phi_a(x). \tag{44}$$

The finite-dimensional distribution of the process $\{X_t \in M, t \in [a,b]\}$ with probability measure on the space of paths which we denote as $Q$; for $a = t_0 < t_1 < \ldots < t_n = b$, it is given by

$$\begin{aligned} E_Q[f(X_a, X_{t_1}, \ldots, X_{t_n-1}, X_b)] \quad = \quad & \int_M dx_0\mu(a,x_0)q(a,x_0;t_1,x_1)dx_1 \ldots \\ & q(t_1,x_1;t_2,x_2)dx_2 \ldots q(t_{n-1},x_{n-1},b,x_n)dx_n \\ & f(x_0,x_1,\ldots,x_{n-1},x_n) := [\mu_a q >> \end{aligned} \tag{45}$$

which is the Kolmogorov forward in time (and thus time-irreversible) representation for the diffusion process with initial distribution $\mu_a(x_0) = \mu(a, x_0)$, which using eq. (37) can still be rewritten as

$$\int_M dx_0 \mu_a(x_0) \frac{1}{\phi_a(x_0)} p(a, x_0; t_1, x_1) \phi_{t_1}(x_1) dx_1 \frac{1}{\phi_{t_1}(x_1)} dx_1 p(t_1, x_1; t_2, x_2)$$
$$\phi_{t_2}(x_2) dx_2 \ldots \frac{1}{\phi(t_{n-1}, x_{n-1})} p(t_{n-1}, x_{n-1}; b, x_n) \phi_b(x_n) dx_n f(x_0, \ldots, x_n) \quad (46)$$

which in account of $\mu_a(x_0) = \breve{\phi}_a(x_0)\phi_a(x_0)$ and eq. (39) can be written in the time-reversible form

$$\int_M \breve{\phi}_a(x_0) dx_0 p(a, x_0; t_1, x_1) dx_1 p(t_1, x_1; t_2, x_2) dx_2 \ldots p(t_{n-1}, x_{n-1}; b, x_n)$$
$$\phi_b(x_n) dx_n f(x_0, \ldots, x_n) \quad (47)$$

which we write as

$$= [\breve{\phi}_a p >><< p\phi_b]. \quad (48)$$

This is the *formally* time-symmetric Schroedinger representation with the transition (but not probability) density $p$. Here, the formal time symmetry is seen in the fact that this equation can be read in any direction, preserving the physical sense of transition. This representation, in distinction with the Kolmogorov representation, does *not* have the Markov property.

We define the adjoint transition probability density $\tilde{q}(s, x; t, y)$ with the $\tilde{\phi}$-transformation

$$\breve{q}(s, x; t, y) = \breve{\phi}(s, x) p(s, x; t, y) \frac{1}{\breve{\phi}(t, y)} \quad (49)$$

which satisfies the Chapmann-Kolmogorov equation and the time-reversed normalization

$$\int_M dx \breve{q}(s, x; t, y) = 1. \quad (50)$$

We get

$$E_{\tilde{Q}}[f(X_a, X_{t_1}, \ldots, X_b)] = \int_M f(x_0, \ldots, x_n) \breve{q}(a, x_0; t_1, x_1) dx_1 \breve{q}(t_1, x_1; t_2, x_2) dx_2$$
$$\ldots \breve{q}(t_{n-1}, x_{n-1}; b, x_n) \breve{\phi}(b, x_n) \phi(b, x_n) dx_n, \quad (51)$$

which has a form non-invariant in time, i.e. reading from right to left, as

$$<< \breve{q}\breve{\phi}_b\phi_b] =<< \breve{q}\breve{\mu}_b], \quad (52)$$

which is the time-reversed representation for the final distribution $\mu_b(x) = \breve{\phi}_b(x)\phi_b(x)$. Now, starting from this last expression and rewriting it in a similar form that is in the forward process but now with $\breve{\phi}$ instead of $\phi$, we get

$$\int_M dx_0 \breve{\phi}_a(x_0) p(a, x_0; t_1, x_1) \frac{1}{\breve{\phi}_{t_1}(x_1))} dx_1 \breve{\phi}(t_1, x_1) p(t_1, x_1; t_2, x_2) \frac{1}{\breve{\phi}_{t_2}(x_2)} dx_2$$
$$\ldots dx_{n-1} \breve{\phi}(t_{n-1}, x_{n-1}) p(t_{n-1}, x_{n-1}; b, x_n) \frac{1}{\breve{\phi}(b, x_n)} \breve{\phi}_b(x_n) \phi(b, x_n) dx_n f(x_0, \ldots, x_n) \quad (53)$$

which coincides with the time-reversible Schroedinger representation $[\breve{\phi}_a p >><< p\phi_b]$.

We therefore have three equivalent representations for the diffusion process: The forward in time Kolmogorov representation, the backward Kolmogorov representation, which are both naturally irreversible in time, and the time-reversible Schroedinger representation, so that we can write succintly,

$$[\mu_a q >>= [\breve{\phi}_a p >><< p\phi_b] =<< \breve{q}\mu_b], \text{with } \mu_a = \phi_a \breve{\phi}_a,\ \mu_b = \phi_b \breve{\phi}_b. \quad (54)$$

In addition of this formal identity,we have to establish the relations between the equations that have led to them. We first note, that in the Schroedinger representation, which is formally time-reversible, we have an interpolation of states between the initial data $\breve{\phi}_a(x)$ and the final data, $\phi_b(x)$. The information for this interpolation is given by a filtration of interpolation $\mathcal{F}_a^r \cup \mathcal{F}_b^s$, which is given in terms of the filtration for the forward Kolmogorov representation $\mathcal{F} = \mathcal{F}_a^t, t \in [a, b]$ which is used for prediction starting with the initial density $\phi_a \breve{\phi}_a = \mu_a$ and the filtration $\mathcal{F}_t^b$ for retrodiction for the time-reversed process with initial distribution $\mu_b$.

We observe that $q$ and $\breve{q}$ are in time-dependent duality with respect to the measure

$$\mu_t(x)dx = \breve{\phi}_t(x)\phi_t(x)dx, \quad (55)$$

since if we define the time-homogeneous semigroups

$$Q_{t-s}f(s, x) = \int q(s, x; t, y) f(t, y) dy, s < t \quad (56)$$

$$g\breve{Q}_{t-s}(t, y) = \int dx g(s, x) \breve{q}(s, x; t, y), s < t, \quad (57)$$

then

$$\begin{aligned}\int dx\mu_s(x)g(s,x)Q_{t-s}f(s,x) &= \int dxg(s,x)\phi_s(x)\breve{\phi}_s(x)\frac{1}{\phi_s(x)}p(s,x;t,y)\phi_t(y)f(t,y)dy \\ &= \int dxg(s,x)\breve{\phi}_s(x)p(s,x;t,y)\frac{1}{\breve{\phi}_t(y)}f(t,x)\breve{\phi}_t(y)\phi_t(y)dy \\ &= \int dxg(s,x)\breve{q}(s,x;t,y)f(t,y)\breve{\phi}_t(y)\phi \\ &= \int dxg(s,x)\breve{Q}_{t-s}(t,y)f(t,y)\mu_t(y)dy, \qquad (58)\end{aligned}$$

and thus we can write in a more succint expression in terms of weighted densities the expression:

$$< g, Q_{t-s}f >_{\mu_s} = < g\breve{Q}_{t-s}, f >_{\mu_t}, s < t. \qquad (59)$$

We shall now extend the state-space of the diffusion process to $[a,b]\times M$, to be able to transform the time-inhomogeneous processes into time-homogeneous processes, while the stochastic dynamics still takes place exclusively in $M$. This will allow us to define the duality of the processes to be with respect to $\mu_t(x)dtdx$ and to determine the form of the exact term of the trace-torsion, and ultimately, to establish the relation between the diffusion processes and Schroedinger equations, both for potential linear and non-linear in the wave-functions. If we define time-homogeneous semigroups of the processes on $\{(t,X_t)\in[a,b]\times M\}$ by

$$P_r f(s,x) = \begin{cases} Q_{s,s+r}f(s,x) & , \quad s \geq 0 \\ 0 & , \quad \text{otherwise} \end{cases} \qquad (60)$$

and

$$\breve{P}_r g(t,y) = \begin{cases} gQ_{t-r,t}(t,y) & , \quad r \geq 0 \\ 0 & , \quad \text{otherwise} \end{cases} \qquad (61)$$

then

$$\begin{aligned}< g, P_r f >_{\mu_t dtdx} &= \int_r^{b-r} ds < g, Q_{s,s+r}f > \mu_s \\ &= \int_b^{a+r} < g, Q_{t-r,t}f > \mu_{t-r}(x)dx \\ &= \int_{a+r}^{b} dt < g\breve{P}_{t-r}, f >_{\mu_t dx} = < \breve{P}_r g, f >_{\mu_t dtdx}, \qquad (62)\end{aligned}$$

which is the duality of $\{(t,X_t)\}$ with respect to the $\mu_t dtdx$ density. We remark here that we have an augmented density by integrating with respect to time $t$. Consequently, if in our spacetime case we define for $a_t(x), \breve{a}_t(x)$ time-dependent one-forms on $M$ (to be determined later)

$$B\alpha : \quad = \quad \frac{\partial\alpha}{\partial t} + H(g, A_t + a_t)\alpha_t, \qquad (63)$$

$$B^0\mu : \quad = \quad -\frac{\partial \mu}{\partial t} + H(g, A_t + a_t)^\dagger \mu_t, \tag{64}$$

and its adjoint operators

$$\breve{B}\beta = -\frac{\partial \beta}{\partial t} - H(g, -A_t + \breve{a}_t)^\dagger \beta_t, \tag{65}$$

$$(\breve{B})^0 \mu_t = \frac{\partial \mu_t}{\partial t} - H(g, -A_t + \breve{a}_t)^\dagger \mu_t, \tag{66}$$

where by $H(g, -A_t + \breve{a}_t)^\dagger$ we mean the $\mathrm{vol}_g$-adjoint of this operator defined in eq.(27); i.e. $H(g, -A_t + \breve{a}_t)^\dagger \mu_t = \frac{1}{2}\triangle_g \mu_t - \mathrm{div_g}(\mu_t(-A_t + \breve{a}_t))$. Now

$$\begin{aligned} \int_a^b dt \int 1_{D_t}[(B\alpha_t)\beta_t] \quad - \quad \alpha_t(\breve{B}\beta_t)]\mu_t(x)dx = \int_a^b dt \int 1_{D_t}\alpha_t\beta_t(B^0\mu_t)dx \\ - \quad \int_a^b \int 1_{D_t}\alpha_t g([a_t + \breve{a}_t] - d\ln\mu_t, d\beta_t)\mu_t dx, \end{aligned} \tag{67}$$

for arbitrary $\alpha, \beta$ smooth compact supported functions defined on $[a, b] \times M$ which we have denoted as time-dependent functions $\alpha_t, \beta_t$, where $1_{D_t}$ denotes the characteristic function of the set $D_t(x) := \{(t, x) : \mu_t(x) = \phi_t(x)\breve{\phi}_t(x) > 0\}$. Therefore, the duality of space-time processes

$$< B\alpha, \beta >_{\mu_t(x)dtdx} = < \alpha, \breve{B}\beta >_{\mu_t(x)dtdx}, \tag{68}$$

is equivalent to

$$a_t(x) + \breve{a}_t(x) \quad = \quad d\ \ln\ \mu_t(x) \equiv d\ \ln\ (\phi_t(x)\breve{\phi}_t(x)), \tag{69}$$

$$B^0\mu_t(x) = 0. \tag{70}$$

The latter equation being the Fokker-Planck equation for the diffusion with trace-torsion given by $a + A$, then the Fokker-Planck equation for the adjoint (time-reversed) process is valid, i.e.

$$(\breve{B})^0 \mu_t(x) = 0. \tag{71}$$

Substracting eqs. (70) and (71) we get the final form of the duality condition

$$\frac{\partial \mu}{\partial t} + \mathrm{div_g}[(A_t + \frac{a_t - \breve{a}_t}{2})\mu_t)] \quad = \quad 0, \text{ for } \mu_t(x) = \breve{\phi}_t(x)\phi_t(x). \tag{72}$$

Therefore, we can establish that the duality conditions of the diffusion equation in the Kolmogorov representation and its time reversed diffusion lead to the following conditions on the additional elements of the drift vector fields:

$$a_t(x) + \breve{a}_t(x) \quad = \quad d\ \ln\ \mu_t(x) \equiv d\ \ln\ (\phi_t(x)\breve{\phi}_t(x)), \tag{73}$$

$$\frac{\partial \mu}{\partial t} + \mathrm{div_g}[(A_t + \frac{a_t - \breve{a}_t}{2})\mu_t] \quad = \quad 0. \tag{74}$$

If we assume that $a_t - \breve{a}_t$ is an exact one-form, i.e., there exists a time-dependent differentiable function $S(t,x) = S_t(x)$ defined on $[a,b]\times M$ such that for $t \in [a,b]$,

$$a_t - \breve{a}_t = d\,\ln\,\frac{\phi_t(x)}{\breve{\phi}_t(x)} = 2dS_t \tag{75}$$

which together with

$$a_t + \breve{a}_t = d\,\ln\,\mu_t, \tag{76}$$

implies that on $D(t,x)$ we have

$$a_t = d\,\ln\,\phi_t, \tag{77}$$

$$\breve{a}_t = d\,\ln\,\breve{\phi}_t \tag{78}$$

Introduce now $R_t(x) = R(t,x) = \frac{1}{2}\ln\phi_t\breve{\phi}_t$ and $S_t(x) = S(t,x) = \frac{1}{2}\ln\frac{\phi_t}{\breve{\phi}_t}$, so that

$$a_t(x) = d(R_t(x) + S_t(x)), \tag{79}$$

$$\breve{a}_t(x) = d(R_t(x) - S_t(x)), \tag{80}$$

and the eq. (74) takes the form

$$\frac{\partial R}{\partial t} + \frac{1}{2}\triangle_g S_t + g(dS_t, dR_t) + g(A_t, dR_t) = 0, \tag{81}$$

where we have taken in account that $\mathrm{div}_g A_t = 0$.

**Remarks.** Note that the time-dependent function $S$ on the 3-space manifold, is defined by eq. (75) up to addition of an arbitrary function of $t$, and when further below we shall take this function as defining the complex phase of the quantum Schroedinger wave, this will introduce the quantum-phase indetermination of the quantum evolution, just as we discussed already in the setting of geometry of the quantum state-space. In the other hand, this introduces as well the subject of the multivaluedness of the wave function, which by the way, leads to the Bohr-Sommerfeld quantization rules of QM established well before it was developed as an operator theory. It is noteworthy to remark that these quantization rules, later encountered in superfluidity and superconductivity, or still in the physics of defects of condensed matter physics, are of topological character. It has been proved by Kiehn that the Schroedinger wave equation contains the Navier-Stokes equations for a viscous compressible fluid in 2D, and that the probability density transforms into the enstrophy (i.e. the squared vorticity) of the viscous fluid obeying the Navier-Stokes equations [20]. Thus, one might expect that Navier-Stokes equations could also have multivalued solutions, namely in the 2D case of the already established relation, the vorticity reduces to a time-dependent function.

Therefore, together with the three different time-homogeneous representations $\{(t, X_t), t \in [a,b], X_t \in M\}$ of a time-inhomogeneous diffusion process

$\{X_t, Q)$ on $M$ we have three equivalent dynamical descriptions. One description, with creation and killing described by the scalar field $c(t,x)$ and the diffusion equation describing it is given by a creation-destruction potential in the trace-torsion background given by an electromagnetic potential

$$\frac{\partial p}{\partial t} + H(g, A_t)(x)p + c(t,x)p = 0; \tag{82}$$

the second description has an additional trace-torsion $a(t,x)$ , a 1-form on $R \times M$

$$\frac{\partial q}{\partial t} + H(g, A + a_t)q = 0. \tag{83}$$

while the third description is the adjoint time-reversed of the first representation given by $\tilde{\phi}$ satisfying the diffusion equation on the background of the reversed electromagnetic potential $-A$ in the vacuum, i.e.

$$-\frac{\partial \breve{\phi}}{\partial t} + H(g, -A_t)\breve{\phi} + c\breve{\phi} = 0. \tag{84}$$

The second representation for the full trace-torsion diffusion forward in time Kolmogorov representation, we need to adopt the description in terms of the fundamental solution $q$ of

$$\frac{\partial q}{\partial t} + H(g, A_t + a_t)q = 0, \tag{85}$$

for which one must start with the initial distribution $\mu_a(x) = \breve{\phi}_a(x)\phi_a(x)$. This is a time $t$-irreversible representation in the real world, where $q$ describes the real transition and $\mu_a$ gives the initial distribution. If in addition one traces the diffusion backwards with reversed time $t$, with $t \in [a,b]$ running backwards, one needs for this the final distribution $\mu_b(x) = \breve{\phi}_b(x)\phi_b(x)$ and the time $t$ reversed probability density $\breve{q}(s,x;t,y)$ which is the fundamental solution of the equation

$$-\frac{\partial \breve{q}}{\partial t} + H(g, -A_t + \breve{a}_t)\hat{q} = 0, \tag{86}$$

with additional trace-torsion one-form on $R \times M$ given by $\tilde{a}$, where

$$\breve{a}_t + a_t = d\ln\mu_t(x), \text{ with } \mu_t = \phi_t\breve{\phi}_t. \tag{87}$$

where the diffusion process in the time-irreversible forward Kolmogorov representation is given by the Ito s.d.e

$$dX_t^i = \sigma_j^i(X_t)dW_t^j + (A + a)^i(t, X_t)dt, \tag{88}$$

and the backward representation for the diffusion process is given by

$$dX_t^i = \sigma_j^i(X_t)dW_t^j + (-A + \breve{a})^i(t, X_t)dt, \tag{89}$$

where $a, \breve{a}$ are given by the eqs. (79) and (80), and $(\sigma\sigma^{\dagger})^{\alpha\beta} = g^{\alpha\beta}$; see eq. (20).

We follow Schroedinger in pointing that $\phi$ and $\breve{\phi}$ separately satisfy the creation and killing equations, while in quantum mechanics $\psi$ and $\bar{\psi}$ are the complex-valued counterparts of $\phi$ and $\breve{\phi}$, respectively, they are not arbitrary but

$$\phi\breve{\phi} = \psi\bar{\psi}. \tag{90}$$

Thus, in the following , this Born formula, once the equations for $\psi$ are determined, will be a consequence of the constructions, and not an hypothesis on the random basis of non-relativistic mechanics.

Therefore, the equations of motion given by the Ito s.d.e.

$$dX_t^i = (\hat{A} + \mathrm{grad}\phi)^i(t, X_t)dt + \sigma_j^i(X_t)dW_t^j, \tag{91}$$

which are equivalent to

$$\frac{\partial u}{\partial t} + H(g, A_t + a_t)u = 0 \tag{92}$$

with $a_t = d\mathrm{ln}\phi_t = d(R_t + S_t)$, determines the motion of the ensemble of non-relativistic particles. Note that this equivalence requires only the Laplacian for the RCW connection with the forward trace-torsion full one-form

$$Q(t, x) = A_t(x) + d\mathrm{ln}\phi_t(x) = A_t(x) + d(R_t(x) + S_t(x)). \tag{93}$$

In distinction with Stochastic Mechanics due to Nelson, and contemporary ellaborations of this applied to astrophysics as the theory of Scale Relativity due to Nottale [10][12], we only need the form of the trace-torsion for the forward Kolmogorov representation, and this turns to be equivalent to the Schroedinger representation which interpolates in time-symmetric form between this forward process and its time dual with trace-torsion one-form given by $-A_t + \breve{a}_t(x) = -A_t(x) + d\mathrm{ln}\breve{\phi}_t(x) = -A_t(x) + d(R_t(x) - S_t(x))$.

Finally, let us how this is related to the Schroedinger equation. Consider now the Schroedinger equations for the complex-valued wave function $\psi$ and its complex conjugate $\bar{\psi}$, i.e. introducing $i = \sqrt{-1}$, we write them in the form

$$i\frac{\partial \psi}{\partial t} + H(g, iA_t)\psi - V\psi = 0 \tag{94}$$

$$-i\frac{\partial \bar{\psi}}{\partial t} + H(g, -iA_t)\bar{\psi} - V\bar{\psi} = 0, \tag{95}$$

which are identical to the usual forms. So, we have the imaginary factor appearing in the time $t$ but also in the electromagnetic term of the RCW connection

with trace-torsion given now by $iA$, which we confront with the diffusion equations generated by the RCW connection with trace-torsion $A$, i.e. the system

$$\frac{\partial \phi}{\partial t} + H(g, A_t)\phi + c\phi = 0, \tag{96}$$

$$\frac{-\partial \breve{\phi}}{\partial t} + H(g, -A_t)\breve{\phi} + c\breve{\phi} = 0, \tag{97}$$

and the diffusion equations determined by both the RCW connections with trace-torsion $A + a$ and $-A + \breve{a}$, i.e.

$$\frac{\partial q}{\partial t} + H(g, A_t + a_t)q = 0, \tag{98}$$

$$\frac{-\partial \breve{q}}{\partial t} + H(g, -A_t + \breve{a}_t)\breve{q} = 0, \tag{99}$$

which are equivalent to the single equation

$$\frac{\partial q}{\partial t} + H(g, A_t + d\ln\phi_t)q = 0. \tag{100}$$

If we introduce a complex structure on the two-dimensional real-space with coordinates $(R, S)$, i.e. we consider

$$\psi = e^{R+iS}, \psi = e^{R-iS}, \tag{101}$$

viz a viz $\phi = e^{R+S}, \breve{\phi} = e^{R-S}$, with $\psi\bar{\psi} = \phi\breve{\phi}$, then for a wave-function differentiable in $t$ and twice-differentiable in the space variables, then, $\psi$ satisfies the Schroedinger equation if and only if $(R, S)$ satisfy the difference between the Fokker-Planck equations , i.e.

$$\frac{\partial R}{\partial t} + g(dS_t + A_t, dR_t) + \frac{1}{2}\triangle_g S_t = 0, \tag{102}$$

and

$$V = -\frac{\partial S}{\partial t} + H(g, dR_t)R_t - \frac{1}{2}g(dS_t - A_t, dS_t). \tag{103}$$

which follows from substituting $\psi$ in the Schroedinger equation and further dividing by $\psi$ and taking the real part and imaginary parts, to obtain the former and latter equations, respectively.

Conversely, if we take the coordinate space given by $(\phi, \breve{\phi})$, both non-negative functions, and consider the domain $D = D(s, x) = \{(s, x) : 0 < \breve{\phi}(s, x)\phi(s, x)\} \subset [a, b] \times M$ and define $R = \frac{1}{2}\ln\phi\breve{\phi}, S = \frac{1}{2}\ln\frac{\phi}{\breve{\phi}}$, with $R, S$ having the same differentiabilty properties that previously $\psi$, then $\phi = e^{R+S}$ satisfies in $D$ the equation

$$\frac{\partial \phi}{\partial t} + H(g, A_t)\phi + c\phi = 0, \tag{104}$$

if and only if

$$\begin{aligned} -c &= [-\frac{\partial S}{\partial t} + H(g, dR_t)R_t - \frac{1}{2}g(dS_t, dS_t) - g(A_t, dS_t)] \\ &+ [\frac{\partial R}{\partial t} + H(g, dR_t)S_t + g(A_t, dR_t)] + [2\frac{\partial S}{\partial t} + g(dS_t + 2A_t, dS_t)] \end{aligned} \quad (105)$$

while $\breve{\phi} = e^{R-S}$ satisfies in $D$ the equation

$$-\frac{\partial \breve{\phi}}{\partial t} + H(g, -A_t)\breve{\phi} + c\breve{\phi} = 0, \quad (106)$$

if and only if

$$\begin{aligned} -c &= [-\frac{\partial S}{\partial t} + H(g, dR_t)R_t - \frac{1}{2}g(dS_t, dS_t) - g(A_t, dS_t)] \\ &- [\frac{\partial R}{\partial t} + H(g, dR_t)S_t + g(A_t, dR_t)] + [2\frac{\partial S}{\partial t} + g(dS_t + 2A_t, dS_t)] \end{aligned} \quad (107)$$

Notice that $\phi, \breve{\phi}$ can be both negative or positive. So if we define $\psi = e^{R+iS}$, it then defines in weak form the Schroedinger equation in $D$ with

$$V = -c - 2\frac{\partial S}{\partial t} - g(dS_t, dS_t) - 2g(A_t, dS_t). \quad (108)$$

We note that from eq. (108) follows that we can choose $S$ in a way such that either $c$ is independent of $S$ and thus $V$ is a potential which is non-linear in the sense that it depends on the phase of the wave function $\psi$ and thus the Schroedinger equation with this choice becomes non-linear dependent of $\psi$, or conversely, we can make the alternative choice of $c$ depending non-linearly on $S$, and thus the creation-annihilation of particles in the diffusion equation is non-linear, and consequently the Schroedinger equation has a potential $V$ which does not depend on $\psi$. In the case that $V$ is such that the spectrum of $H(g, A + a)$ is discrete, we know already we can represent the Schroedinger equation in state-space and further study the related stochastic Schroedinger equation as described above. Finally, we have presented a construction in which by using two scalar diffusing processes $\phi, \breve{\phi}$ we have been able to subsume them into a single forward in time process with additional trace-torsion given by $a_t = d\ln\phi_t\breve{\phi}_t$.

With respect to the issue of nonlinearity of the Schroedinger equation, one could argue that the former case means that the superposition principle of QM is broken, but then one observes that precisely due to the fact that the wave function depends on the phase, the superposition principle is invalid from the fact that we are dealing with complex-valued wave functions, and when dealing with the Schroedinger or Heisenberg evolutions in state-space, the complex factor has been quotiented [3].

In particular, nonlinear Schroedinger equations will appear in the Lie-isotopic extensions of the linear Schroedinger equation of QM, due to Santilli [14-19]. As

explained in the Introduction, all the mathematical and conventional physical theories (Special and General Relativity, QM, RQM, etc.) can be isotopically lifted by applying a non-unitary transformation that produces a generalized unit. In the case of QM this construction yields a linear theory in the isotopically lifted mathematical structures (this property is called isolinearity [16]), but when translated to the original structures, the Schroedinger equation becomes non-linear. Conversely, we shall see that a non-linear Schroedinger equation can be turned into the iso-linear iso-Schroedinger equation by taking the non-linear terms of the potential into the isotopic generalized unit. Hence it follows that it is possible, in principle, to present HM as a theory of diffusion processes. This will be the subject of our next sections below.

Returning to the issue of the nonlinearity of the potential function $V$ in Quantum Mechanics, the usual form is the known logarithmic expression $V = -b(\ln|\psi|^2)\psi$ introduced by Bialnicky-Birula and Mycielski [23]. Its importance in such diverse fields as quantum optics, superconductivity, atomic and molecular physics cannot be disregarded. Soliton solutions of nonlinear Schroedinger equations may have a role central to molecular biology, in which the DNA structure may be associated with a superconductive state. With regards as the relation between geometries, Brownian motions and the linear and Schroedinger equations, there is an alternative line of research which stems from two principles, which are interwoven. The first one is that all physical fields have to be construed in terms of scale fields starting from the fields appearing in the Einstein lambda transformations,of which, the Schroedinger wave function is an elementary example as shown here [2,23], and when further associated to the idea of a fractal spacetime, this has lead to Nottale's theory of Scale Relativity [10,26]. Nottale's theory starts from this fractal structure to construct a covariant derivative operator in terms of the forward and backward stochastic derivatives introduced by Nelson in his theory of stochastic mechanics [8]. Working with these stochastic derivatives, the basic operator of Nottale's theory, can be written in terms of our RCW laplacian operators of the form $\frac{\partial}{\partial\tau} + H_0(i\mathcal{D}g, \mathcal{V})$ where $\mathcal{D}$ is diffusion constant (equal to $\frac{\hbar}{2m}$ in nonrelativistic quantum mechanics), and $\mathcal{V}$ is a complex differentiable velocity field, our complex drift appearing after introducing the imaginary unit $i = \sqrt{-1}$ ; see [10]. In the present conception, this fundamental operator in terms of which Nottale constructs his theory, does not require for its introduction to assume that space-time has a fractal structure a priori, from which stochastic derivatives backward and forward to express the time asymmetry construct the dynamics of fields. We rather assume that at a fundamental scale which is generally associated with the Planck scale, we can represent space-time as a continuous media in which what really matters are the defects in it, and thus torsion has a fundamental role since it defines these dislocations. The fractal structure of spacetime arises from the association between the RCW laplacian operators which as coincides with Nottale's covariant derivative operator, and the Brownian motions which alternatively,

can be seen as constructing the space-time geometry. So there is no place as to the discussion of what goes first, at least in the conception in the present work. Remarkably, the flow of these Brownian motions under general analytical conditions, define for every trial Wiener path, an active diffeomorphism of space-time. But this primeval role of the Brownian motions and fractal structures, stems from our making the choice -arbitrary, inasmuch as the other choice is arbitrary- as the fundamental structure instead of choosing the assumption of having a RCW covariant derivative with a trace-torsion field defined on a continuous model of space-time. In some sense the possibility of choosing as primeval the Brownian motions for starting the construction of the theoretical framework, is interesting in regards that they can be constructed as continous limits of discrete jumps, as every basic book in probability presents [46], and thus instead of positing a continuous space-time, we can think from the very beginning in a discrete spacetime, and construct a theory of physics in these terms [4]. In this case, instead of working with the field of the real number or its complex or biquaternion extensions, one can take a p-adic field, such as the one defined by the Mersenne prime number $2^{127} - 1$ which is approximately equal to the square of the ratio between the Planck mass and the proton mass [28]. In fact, a theory of physics in terms of discrete structures associated to the Mersenne prime numbers hierarchy, has been constructed in a program developed by P. Noyes, T. Bastin, P. Kilmister and others; see [47]. A remarkable unified theory of physics, biology and consciousness, in terms of p-adic field theory, has been elaborated by M.Pitkanen [51].

We would like to comment that Castro, Mahecha and Rodriguez [25], following the Nottale constructions have derived the nonlinear Schroedinger equation and associated it to a Brownian motion with a complex diffusion constant. Futhermore, working with Weyl connections (which are to be distinguished from the present work's RCW connections) in that they are not integrable and they have zero torsion (they can be introduced in terms of the reduced set of Einstein lambda transformations when one does not posit the tetrad or cotetrad fields as fundamental and the invariance of the Riemann-Cartan connection), they have derived the relativistic quantum potential in terms of the difference between the Weyl curvature of this connection and the Riemannian curvature, while in the present theory, we have associated above the relativistic quantum potential with the Riemannian curvature, which is more closely related with the idea of Brownian motion in spacetime (without additional internal degrees of freedom as the Weyl connections introduce) as being the generator of gravitation and all fundamental fields.

[4] Prof. Shan Gao,has initiated a program of construction of quantum mechanics as random discontinuous motions in discrete spacetime, in his recent work *Quantum Motion, Unveiling the Mysterious Quantum World*, Arima Publ., Suffolk ( U.K.), 2006.

# 7 Isotopic Geometries and Isotopic Gauge Theories

We shall present next the essential elements of HM to relate them to torsion fields and the Brownian motions that we have presented already.

## 7.1 Lie-Isotopic Gauge Theory

In this section, we want to place in evidence the role the kinematical role that torsion has in the gauge theories for an isotopic Lie group. For a start in the introduction to the mathematical aspects of HM, in this section we shall explicit the fundamental kinematical role that torsion has in Lie-isotopic gauge theories, by starting at the level of the Lie algebras and their Lie-isotopic liftings.

Let $G$ be a Lie group, $\mathbf{g}$ its Lie algebra and $\xi$ its enveloping algebra.Thus, $\xi$ has an associative product, which for reasons we shall denote its product as $A \times B$. We shall now onwards explicit the usual product and composition through the sign $\times$ to distinguish with the isotopic product we shall introduce next. Given an invertible and hermitean operator $T$, we shall introduce in $\xi$ a generalized isotopic product $A\hat{\times}B = A \times T \times B$ with an isotopic unit $\hat{I} = T^{-1}$ such that $A\hat{\times}\hat{I} = \hat{I}\hat{\times}A = A$. Consequently, the usual definitions of hermitean conjugate, $A^\dagger$, and inverse, $A^{-1}$ , of an operator $A$ must be replaced by the following isotopic generalizations: The $T$-hermitean conjugate, $A^{\hat{\dagger}}$,

$$A^{\hat{\dagger}} = T^\dagger \times A^\dagger \times \hat{I}, \tag{109}$$

and the $T$-inverse, $\hat{A}^{-1}$,

$$\hat{A}^{-1} = \hat{I} \times A^{-1} \times \hat{I}. \tag{110}$$

Furthermore, the $T$-isotope, $\hat{\mathrm{e}}(A)$, of the exponential operator $e^A$, of an operator $A$, is defined as

$$\hat{\mathrm{e}}^A = \hat{I} \times \mathrm{e}^{T\times A} = \mathrm{e}^{A\times T} \times \hat{I}. \tag{111}$$

Suppose we have a field theory invariant under the action of the compact gauge group $G$,

$$\Psi' = U \times \Psi \tag{112}$$

with

$$U = I \times \mathrm{e}^{-i\times\theta^k\times X_k} = \mathrm{e}^{-i\times\theta^k\times X_k} \times I, \tag{113}$$

and $\theta^k$ is a set of real functions and $X_k$ are generators of the algebra $\mathbf{g}$ satisfying

$$[X_i, X_j] = X_i \times X_j - X_j \times X_i = i \times c_{ij}^k \times X_k, \tag{114}$$

with the numbers $c_{ij}^k$ being the structure constants, i.e. the coefficients of the torsion tensor of the canonical connection of the manifold given by $G$ [49]. The infinitesimal form of the transformation is

$$\delta\Psi = -i \times \epsilon^k \times X_k \times \Psi, \tag{115}$$

where the $\epsilon^k$ are the infinitesimal parameters corresponding to $\theta^k$. We remark that the representation matrices of the transformations are unitary: $U^\dagger \times U = I, [U^\dagger, U] = 0$, and the invariant of the theory is $\Psi^\dagger \times \Psi = \Psi'^\dagger \times \Psi'$.

The Santilli-Lie-isotopic lift of $G$, $\hat{G}$, is represented by the transformation given by

$$\Psi' = \hat{U} \hat{\times} \Psi, \tag{116}$$

where

$$\hat{U} = \hat{I} \times \mathrm{e}^{-i \times \theta^k \hat{\times} X_k} = \mathrm{e}^{-i \times \theta^k \hat{\times} X_k} \times \hat{I}, \tag{117}$$

with $\theta^k$ a set of real functions and $X_k$ are generators of the algebra $\mathbf{g}$ are as before. We compute the isotopic hermitean conjugate of $\hat{U}$,

$$\hat{U}^{\hat{\dagger}} = T^\dagger \times (T^{-1})^\dagger \times \mathrm{e}^{i\theta^k \hat{\times} X_k} \times T^{-1} = \mathrm{e}^{i \times \theta^k \hat{\times} X_k} \times \hat{I}, \tag{118}$$

and its isotopic inverse

$$\hat{U}^{-1} = T^{-1} \times T \times \mathrm{e}^{i \times \theta^k \hat{\times} X_k} \times T^{-1} = \mathrm{e}^{i \times \theta^k \hat{\times} X_k} \times \hat{I}, \tag{119}$$

which proves that $\hat{U}$ is a $T$-unitary operator:

$$\hat{U}^{\hat{\dagger}} = \hat{U}^{-\hat{1}}. \tag{120}$$

We observe that if $T$ is a positive-definite (alternatively, negative-definite), then $\hat{G}$ is locally isomorphic to $G$. Furthermore, the isotopic condition of hermiticity coincides with the usual one when defining an isotopic Hilbert space by the isotopic inner product

$$(A \hat{,} B) = (A, T \times B) \times \hat{I} \in \hat{C}, \tag{121}$$

where $\hat{C}$ is the Santilli iso-field of complex numbers , i.e. $\hat{C} = C \times \hat{I}$; we shall return to define this isofield in the next section. The infinitesimal form of the Lie-isotopic transformation follows from eqs. (116, 117) is given by

$$\hat{I} \approx -i \times \epsilon^k \hat{\times} X_k, \tag{122}$$

and

$$\delta\Psi = -i \times X_k \hat{\times} \epsilon^k \times \Psi. \tag{123}$$

The construction of a gauge theory for $\hat{G}$, i.e. a Lie-Santilli-isotopic theory for $G$ [33], starts with $T$ defining the isotopic unit, being locally dependent. In fact $T$ can depend on the base manifold $M$ as well as the tangent manifold and its higher orders. Since $\hat{U}$ is a $T$-unitary operator, from eq. (120) we have

$$\hat{U}^{\hat{\dagger}} \hat{\times} \hat{U} = I, \tag{124}$$

so that we can construct the following invariant

$$\Psi \hat{\times} \Psi^\dagger = \Psi' \hat{\times} \Psi'^\dagger = \Psi \hat{\times} \hat{U} \hat{\times} \hat{U}^{\hat{\dagger}} \hat{\times} \Psi^\dagger. \tag{125}$$

Finally, to preserve invariance under local isotopic transformations, i.e. $\hat{U} = \hat{U}(x)$, so that $\theta = \theta(x)$ and/or $T = T(x)$, we introduce -as in ordinary gauge theory for the group $G$- the isotopic covariant derivative

$$\hat{D}_\mu = (\partial_u - i \times e \times A^k_\mu \hat{\times} X_k) \times \hat{I}, \tag{126}$$

and we define the transformation rule for it as

$$\hat{D}'_\mu = \hat{U} \hat{\times} \hat{D}_\mu \hat{\times} \hat{U}^{-\hat{1}}, \tag{127}$$

or still,

$$\hat{D}'_\mu \hat{\times} \hat{U} \hat{\times} \Psi = \hat{U} \hat{\times} \hat{D}_\mu \hat{\times} \Psi. \tag{128}$$

Factorising $\hat{D} = \hat{D}_\mu \times \hat{I}$ and $\hat{U} = U^* \times \hat{I}$, where

$$\hat{D}_\mu = \partial_\mu - ieA^k_\mu \hat{\times} X_k, \tag{129}$$

and

$$U^* = \mathrm{e}^{-i \times \theta^k \hat{\times} X_k}, \tag{130}$$

we obtain from eq. (126)

$$A'^k_\mu \hat{\times} X_k = U^* \times A^k_\mu \hat{\times} X_k \times U^{*-1} - \frac{i}{e} \times (\partial_\mu U^*) \times U^{*-1}. \tag{131}$$

and we recognize in this expression the isotopic lifting of the gauge transformation fo the connection one-form $A = A^k_\mu X_k dx^k$. If we develop $U^*$ as

$$U^* \approx I - i \times \epsilon^k \hat{\times} X_k, \tag{132}$$

and

$$U^{*-1} \approx I + i \times \epsilon^k \hat{\times} X_k, \tag{133}$$

then to first order in $\epsilon$, we have

$$\delta A^k_\mu \times T \times X_k = -\frac{1}{\epsilon} \times \partial_\mu (\epsilon^k \hat{\times} X_k) + i \times [A^k_\mu \hat{\times} X_\mu, \epsilon^m \hat{\times} X_m], \tag{134}$$

which still is equal to

$$\frac{-1}{e} \times (\partial_\mu \epsilon^k \times T) \times X_k + i \times A^k_\mu \times \epsilon^m \times T \times [X_k \hat{,} X_m], \tag{135}$$

where we have introduced the isotopic commutator

$$[X_k \hat{,} X_m] = X_k \times T \times X_m - X_m \times T \times X_k, \tag{136}$$

where we note that we can read from this eqs. (135, 136) the modification of the structure constants of of $\mathbf{g}$, i.e. the coefficients of the torsion tensor of the canonical connection on the group-manifold $G$, to *local* dependent structure constants

depending on $T$, the Lie-isotopic unit defining the gauge theory of $\hat{G}$. This is the essential geometrical *kinematical* character of a Lie-isotopic gauge theory, the appearance of the modification of the torsion tensor by the modification of the infinitesimal symmetries through the generalized units. On further gauging, appears a torsion field of the form of the logarithmic differential of the isotopic unit. Thus, we can apply this to the construction of a gauge theory for $\hat{G}$ constructed on an arbitrary space-time manifold, which can be provided with an Euclidean or Minkowski metrics, or still, in a more general Santilli-Lie-isotopic setting in which the metric is iso-Euclidean or iso-Minkowski, i.e. the isotopic lifts of the Euclidean and Minkowski metric respectively; more of this below. But in this sense, the Lie-Santilli-isotopic theory was constructed to account for the deformation of the usual group structures. This feature was overlooked in the original works of Santilli, and in subsequent developments by other researchers, but first treated in [29] with the then current lack of understanding of the need of introducing the lift of the whole mathematical structures in the theory, which was achieved in 1997; see [16] for a complete list of references and a history of these developments.

Finally, the isotopic Yang-Mills field strength curvature $\hat{F}_{\mu\nu}$ are defined as follows:

$$\hat{F}_{\mu\nu}\hat{\times}\Psi = \frac{i}{e}\times[\hat{D}_\mu,\hat{D}_\nu]\hat{\times}\Psi = \frac{i}{e}\times(\hat{D}_\mu\hat{\times}\hat{D}_\nu - \hat{D}_\nu\hat{\times}\hat{D}_\mu)\hat{\times}\Psi. \tag{137}$$

It can be checked straightforwardly that it transforms covariantly under the isotopic gauge transformation, since from and we get

$$\hat{F}'^{k}_{\mu\nu} = \hat{U}\hat{\times}\hat{F}_{\mu\nu}\hat{\times}\hat{U}^{-1}. \tag{138}$$

Introducing eq. (127) into eq. (137), we get the expression

$$\begin{aligned}\hat{F}^i_{\mu\nu}\hat{\times}X_i &= (\partial_\mu A^k_\nu - \partial_\nu A^k_\mu)\hat{\times}X_k + A^k_\alpha\times(\delta^\alpha_\beta\times\partial_\mu T - \delta^\alpha_\mu\times\partial_\nu T)\times X_k \\ &- i\times eA^k_\mu\times A^m_\nu\times T\times[X_k\hat{,}X_m].\end{aligned} \tag{139}$$

We shall now make an important assumption on $T$, namely that it lies in the center of $\mathbf{g}$, so that $T$ commutes with any element of $\mathbf{g}$, i.e. $[T,X_k]=0$ for any $X_k$. This is satisfied by isotopic units such as the one defined in eq. (163) below. Then, from eqs. (127, 136, 139) we get

$$\hat{D}_\mu\hat{\times}\Psi = (\partial_\mu - i\times e\times A^k_\mu\times T\times X_k)\times\Psi, \tag{140}$$

$$\delta A^i_\mu = \frac{-1}{e}\times T^{-1}\times\partial_\mu(\epsilon^i\times T) + c^i_{jk}\times\epsilon^j\times T\times A^k_\mu, \tag{141}$$

$$\hat{F}^i_{\mu\nu} = \nabla_\mu A^i_\nu - \nabla_\nu A^i_\mu + e\times T\times c^i_{jk}\times A^j_\mu\times A^k_\nu, \tag{142}$$

where

$$\nabla_\mu A^i_\nu = \partial_\mu A^i_\nu - A^i_\alpha\times\Gamma^\alpha_{\mu\nu}, \tag{143}$$

and

$$\Gamma^{\alpha}_{\mu\nu} = \frac{1}{2} \times (\delta^{\alpha}_{\mu} \times \partial_{\nu} T - \delta^{\alpha}_{\nu} \times \partial_{\mu} T) \times T^{-1}. \tag{144}$$

Therefore,

$$\hat{F}^{i}_{\mu\nu} = \partial_{\mu} A^{i}_{\nu} - \partial_{\nu} A^{i}_{\mu} + A^{i}_{\alpha} \times T^{\alpha}_{\nu\mu} + e \times T \times c^{i}_{jk} \times A^{j}_{\mu} \times A^{k}_{\nu}, \tag{145}$$

where we have written the skew-symmetric tensor

$$T^{\alpha}_{\mu\nu} = (\delta^{\alpha}_{\mu} \partial_{\nu} T - \delta^{\alpha}_{\nu} \partial_{\mu} T) \times T^{-1}. \tag{146}$$

If in particular, we take

$$T = \psi(x) \times I, \tag{147}$$

and then

$$\hat{I} = \psi(x)^{-1} \times I, \tag{148}$$

we then obtain, under natural normalisation, a torsion tensor with trace given by $d\ln\psi$. Notice that in contrast with the gauge theory for $G$, from eqs. $(146-148)$ we can conclude that the gauge theory for the isotopic group $\hat{G}$ has infinitesimal transformations of the form $\epsilon' = \epsilon^{i} \times T$ and an effective coupling which is no longer constant, given by $e' = e \times T$.

Up to here, we have presented a construction which is independent of the metric $g$ defined on $M$. In the first term in eq. (143) we can write instead of the usual derivative for $A$, on introducing a metric $g$, the covariant derivative with respect to a Levi-Civita connection defined by $g$, and thus the covariant derivative $\nabla$ is a RCW connection defined by a metric $g$ and trace-torsion $d\ln\psi$. This is nothing else than the equations introduced by Hojman et al for an abelian Lie-group in modifying the principle of minimal coupling to include torsion, further introduced to the present case of a non-abelian group by Mukku and Sayed [50]. In the former case the last r.h.s. element vanishes completely, and we are left with the same expression obtained for Maxwell's equations when we extend the minimal coupling principle to account for the torsion of the manifold. Furthermore, an identical expression was obtained when we presented above the relation between the Hodge decomposition of the trace-torsion and its relation to an invariant state. In distinction with another class of isotopic units we shall present below (see eq. (163)), the choice in eq. (148) does not have the non-linear and non-local characteristics we shall present below for the usual generalized isotopic units of HM.

# 8 Santilli-Lie isotopic Hilbert space

In this section we shall present briefly the core of HM [16] (for a complete list of references, the reader is urged to consult this work, as well as to the history of the developments until the theory reached the present form.

There is in Santilli's theory a canonical way of introducing the Lie-isotopic unit, with respect to which the complete theory is based upon. The prescription is to introduce an arbitrary non-unitary operator $U$ and to substitute the unit $I$ by the isotopic unit

$$\hat{I} = U \times I \times U^{\dagger} \neq I. \tag{149}$$

The usual Hilbert space of quantum mechanics, is denoted by $\mathcal{H} = \{|\Phi >, |\Psi >:< \Phi|\Psi >\in C(c, +, \times), < \Psi, \Psi >= 1\}$, where $C(c, +, \times)$ denotes the field of complex numbers with the usual addition and multiplication. The evolution equation in the Lie-Santilli theory of an observable is given by the equation

$$i\frac{dA}{dt} = [A\hat{,}H] = A \times T \times H - H \times T \times A, \tag{150}$$

so that

$$A(t) = e^{i\times H\times T\times t} \times A(0) \times e^{-i\times t\times T\times H}. \tag{151}$$

The problem with this quantum evolution is that it is non-unitary over the Hilbert space $\mathcal{H}$ over the field $C(c, +, \times)$. We have the following fundamental result, known as the López Lemma.

**Theorem 1.** All possible non-unitary deformations of quantum mechanics computed on a conventional Hilbert space $\mathcal{H}$ over the field $C(c, +, \times)$ have the following aspects:

i Lack of invariance of the unit, and consequently the lack of applicability to measurements. ii Lack of preservation of the Hermiticity in time, and consequently the lack of unambiguous observables. iii Lack of invariant eigenfunctions and their transforms, and consequently the lack of invariant numerical predictions.

Proof. The unit of quantum mechanics, I, of the enveloping algebra $\xi$ verifies $I \times A = A \times I = A$, $\forall A \in \xi$. If we take a non-unitary transformation $I \mapsto \hat{I} = U \times I \times U^{\dagger} \neq I$, then

$$i\frac{dI}{dt} = [I\hat{,}H] = I \times T \times H - H \times T \times I \neq 0. \tag{152}$$

Under a non-unitary transformation, the associative modular action of the Schrodinger representation $H \times |\psi >$, for $H$ an hermitean operator for $t = 0$ becomes

$$U \times H \times |\Psi >= U \times H \times U^{\dagger} \times (U \times U^{\dagger})^{-1} U|\Psi >= \hat{H} \times T^{-1} \times U|\Psi > \tag{153}$$

where the operator $\hat{H} := U \times H \times U^{\dagger}$, and $\hat{\Psi} = U \times |\Psi >$. We note that by definition $\hat{T} = (U \times U^{\dagger})^{-1} = \hat{T}^{\dagger}$. The initial condition of hermiticity of $H$ on $\mathcal{H}$, i.e. $< \Psi| \times (H \times |\Psi >) = (< \Psi| \times H^{\dagger}) \times |\Psi >$, when applied to a Hilbert space with states of the form $|\hat{\Psi} >= U \times |\Psi >$, requires the action of the transformed operator $U \times H \times |\Psi >= \hat{H} \times T^{-1} \times |\hat{\Psi} >$ yet with the conventional inner product, then

$$< \hat{\Psi}| \times (\hat{H} \times \hat{T} \times |\hat{\Psi} >) =< \hat{\Psi}| \times \hat{T} \times \hat{H}^{\dagger} \times |\hat{\Psi} >, \tag{154}$$

i.e.

$$\hat{H}^{\dagger} = \hat{T}^{-1} \times \hat{H} \times \hat{T} \neq \hat{H}, \tag{155}$$

so that hermiticity is not preserved under non-unitary transformations formulated on the conventional Hilbert space $\mathcal{H}$ over the field $C(c, +, \times)$, due to the fact that $[\hat{T}, \hat{H}] \neq H$.

The general situation of non-unitary deformations computed on general Hilbert spaces will be addressed below. As a corollary of the Theorem 1, on $(\mathcal{H}, C(c, +, \times))$ non-unitary quantum deformations do not give invariant probabilities, nor posses unique invariant physical laws. While in QM unitary time evolution implies causality, in its non-unitary deformations there is a violation of causality.

So let us proceed to present the solution to this problem provided by Santilli, the construction of a non-unitary image of quantum mechanics. As we said already, the first element is given by the introduction of the generalized unit

$$\hat{I} = U \times I \times U^{\dagger} = \hat{I}^{\dagger} \neq I, \tag{156}$$

so that

$$\hat{T} = (U \times I \times U^{\dagger})^{-1} = \hat{T}^{\dagger}. \tag{157}$$

The product in the generalized enveloping algebra $\hat{\xi}$ is given by elements of the form $U \times A \times B \times U^{\dagger} = \hat{A} \times \hat{T} \times \hat{B} := \hat{A} \hat{\times} \hat{B}$ for $\hat{A} = U \times A \times U^{\dagger}$ and $B = U \times B \times B^{\dagger}$. For a Hilbert space $(\mathcal{H}, <>, C(c, +, \times))$ we introduce the Lie-Santilli isotopic Hilbert space $\hat{\mathcal{H}}$ of elements of the form $|\hat{\psi}> = U \times |\psi>$ and $<\hat{\phi}| = <\phi| \times U^{\dagger}$, with inner product given by transforming the original $\mathcal{H}$ inner product by the non-unitary transformation

$$<\Phi, \Psi> \rightarrow <\Phi| \times U^{\dagger} \times U^{\dagger -1} \times U^{-1} \times U|\Psi> = <\hat{\Phi}| \times \hat{T} \times |\Psi> \equiv <\hat{\Phi}| \hat{\times} |\hat{\Psi}> . \tag{158}$$

The generalized enveloping algebra $\hat{\xi}$ is still associative

$$(\hat{A} \hat{\times} \hat{B}) \hat{\times} \hat{C} = \hat{A} \hat{\times} (\hat{B} \hat{\times} \hat{C}), \tag{159}$$

with identity given by $\hat{I}$, since $\hat{I} \hat{\times} \hat{A} = \hat{A} \hat{\times} \hat{I} = \hat{A}$ We know already that the modified Lie algebra is given by $[\hat{A}, \hat{B}] = \hat{A} \times T \times \hat{B} - \hat{B} \times T \times \hat{A}$, which is isomorphic to the original one if $\hat{I}$ is positive definite.

Now let us see how the problem of hermiticity in the non-unitary frame is obtained. We have,

$$<\Psi| \times \hat{T} \times (H \times \hat{T} \times |\Psi>) = (<\hat{\Psi}| \times \hat{T} \times H^{\dagger}) \times |\hat{\Psi}>, \tag{160}$$

which yields

$$\hat{H}^{\dagger} = \hat{T}^{-1} \times \hat{T} \times H^{\dagger} \times \hat{T} \times T^{-1}. \tag{161}$$

Thus, starting with an hermitean operator $H$ at $t = 0$, then $\hat{H} = U \times H \times U^{\dagger}$ remains hermitean under non-unitary transformations. But we note that

the hermiticity is not computed in $(\mathcal{H};<|>, C(c,+,\times))$ but on $(\hat{\mathcal{H}},<|\hat{\times}|> , \hat{C}(\hat{c},\hat{+},\hat{\times}))$, where $\hat{C}(,\hat{c},+,\hat{\times})$ is the Santilli-Lie isotopic lift of $C(c,+,\times)$ with elements of the form $\hat{c} = c \times \hat{I}$, where $\hat{I}$ not necessarily belongs to $C$, the summation is defined by $\hat{c}_1 + \hat{c}_2 = (c_1 + c_2) \times \hat{I}$ and the product is $\hat{c}_1 \hat{\times} \hat{c}_2 = \hat{c}_1 \times \hat{T} \times \hat{c}_2 = (c_1 \times c_2) \times \hat{I}$. Then $\hat{I} = \hat{T}^{-1}$ is the left and right multiplicative unit in $\hat{C}(\hat{c},+,\hat{\times})$. We further have that $\hat{0} = 0$ satisfies $\hat{c} + \hat{0} = \hat{c}$. Furthermore, $\hat{c}^2 = \hat{c}\hat{\times}\hat{c} = \hat{c} \times \hat{T} \times \hat{c}$, $\hat{c}^{\hat{\frac{1}{2}}} = c^{\frac{1}{2}} \times \hat{I}^{\frac{1}{2}}$. The quotient is defined by $\hat{a}/^{\hat{\times}}\hat{b} = (\frac{a}{b} \times \hat{I})$, and $|\hat{c}| = |c| \times \hat{I}$ and finally for an arbitrary $Q$, $\hat{c}\hat{\times}Q = c \times \hat{I} \times T \times Q = c \times I \times Q = c \times Q$.

The modular action $\hat{H}\hat{\times}|\hat{\Psi}> = \hat{H} \times \hat{T} \times |\hat{\psi}>$ with $<\hat{\psi}|\hat{\times}|\psi> = <\hat{\psi}| \times T \times |\hat{\psi}>$ has for generalized unit $\hat{I} = \hat{T}^{-1}$, because it is the only object such that $\hat{I}\hat{\times}|\hat{\psi}> = |\hat{\psi}>$. Consequently, referral to $C(c,+,\times)$ with unit $I$ is inconsistent, and then $\hat{\mathcal{H}}$ must be referred to $\hat{C}$ with basic unit $\hat{I}$. Now the iso-Hilbert invariant iso-inner product is defined by

$$<\hat{\Phi}|\hat{\Psi}>^{\hat{I}} = <\hat{\Phi}|\hat{\times}|\hat{\Psi}> \times \hat{I} = <\hat{\Phi}| \times \hat{T} \times |\hat{\Psi}> \times \hat{T}^{-1} \in \hat{C}. \qquad (162)$$

It is important to remark that the transformation $H \times p|\psi> \mapsto \hat{H}\hat{\times}|\hat{\psi}>$ satisfies linearity on isospace over isofields. The recovery of linearity in isospace is achieved by the embedding of the nonlinear terms in the isounit. Furthermore, any nonlinear theory with a Hamiltonian operator $H(p,x,\psi,\ldots)$ can always be rewritten by factorizing the nonlinear terms, which can then be assumed as the isotopic element of the theory. Indeed, if we have

$$H(p,x,\psi,\ldots) \times |\hat{\psi}> = H_0(x,p) \times \hat{T}(x,p,\psi,\ldots) \times |\hat{\psi}> := \hat{H}_0(,p)\hat{\times}|\hat{\psi}>,$$

with $\hat{T} := H_0^{-1} \times H$. Here, $H_0$ is the maximal (Hermitean) operator representing the total energy. Thus, superposition in isospace can be achieved, which allows a consistent treatment of composite systems under nonlinear interactions.

It is about time to present a general class of generalized units that appear in HM for the characterization of the strong interactions. Namely,

$$\hat{I} = \mathrm{diag}(n_1^2, n_2^2, n_3^2, n_4^2) \times \exp(tN(\frac{\psi_\uparrow}{\hat{\psi}_\downarrow} + \frac{\partial \psi_\downarrow}{\partial \hat{\psi}_\downarrow} + \ldots) \times \int d^3x \psi_\uparrow^\dagger(x)\psi_\downarrow(x), \quad (163)$$

where the quantities $n_1^2, n_2^2, n_3^2$ represent the extended, non-spherical deformable shapes of the hadron, $n_4^2$ its density, the quantities $\frac{\psi_\uparrow}{\hat{\psi}_\downarrow} + \frac{\partial \psi_\downarrow}{\partial \hat{\psi}_\downarrow} + \ldots$ represent a typical non-linearity, and the integral in the exponent, represents a typical non-linearity due to the interpenetration and overlapping of the charge distributions. Notably a coupling of spin-up and spin-down particles is present in the generalized unit. Whenever the hadrons are perfectly spherical and rigid, then we can take the density $n_4^2 = 1$ and the parameters of deformations can also be set equal to 1; if furthermore, their distances is such as to be nor interpenetration, then the integrand is zero and the exponential term is equal to 1 and thus, in

this situation, $\hat{I} = I$, and we are in the domain of applicability of QM, where the unit is given in terms of the torsion structure constants of the Lie algebra, and dynamically, from the gradient logarithm of the wave function. The present choice of the isotopic unit has lead to the first ever model of a Cooper model with explicit attractive force between the pair of identical electrons, with excellent agreement with experimental data [68].

## 8.1 Santilli-Lie Isotopies of the Differential Calculus and Metric Structures, and the Iso-Schroedinger Equation

To present the isotopic Schroedinger equation, we have to introduce the Santilli-Lie-isotopic differential calculus [15,16] and the isotopic lift of manifolds, the so-called isomanifolds, due to Tsagas and Sourlas [19]. We start by considering the manifold $M$ to be a vector space with local coordinates, which for simplicity we shall from now consider them to be a *contravariant*[5] system $x = (x^i), i = 1, \ldots, n$, unit given by $I = \text{diag}(1, \ldots, 1)$ and metric $g$ defined on the tangent manifold with coordinates $v = (v^i)$, so that $v^2 = v^i \times g_{ij} \times v^j \in R$. We shall lift this structure to a vector space $\hat{M}$ provided with isocoordinates $\hat{x}$, isometric $\hat{G}$ and defined on the isonumber field $\hat{F}$, where $F$ can be the real or complex numbers; we denote this isospace by $\hat{M}(\hat{x}, \hat{G}, \hat{F})$. Let us describe the construction of this isospace $\hat{M}$ [16,19]:

The isocoordinates are introduced by the transformation

$$x \mapsto U \times x \times U^\dagger = x \times \hat{I} := \hat{x}. \tag{164}$$

To introduce the isometric $\hat{G}$ we start by considering the transformation

$$g \mapsto U \times g \times U^\dagger = \hat{I} \times g := \hat{g}. \tag{165}$$

Yet we notice that the matrix elements $\hat{g}^{ij} = (\hat{I} \times g)^{ij}$ belong to the number field $F$, not to $\hat{F}$, so the correct definition of the isometric is $\hat{G} = \hat{g} \times \hat{I}$. Thus we have a transformed $M(x, g, F)$ into the isospace $\hat{M}(\hat{x}, \hat{G}, \hat{F})$. Thus the projection on $\hat{M}(\hat{x}, \hat{g}, F)$ of the isometric in $\hat{M}(\hat{x}, \hat{G}, \hat{F})$ is defined by a contravariant tensor, $\hat{g} = (\hat{g}^{ij})$ with components

$$\hat{g}^{ij} = (\hat{I} \times g)^{ij}. \tag{166}$$

We must remark that in distinction of the usual scale transformation on the metrics in the Einstein $\lambda$ and the Weyl transformations, the scale factor is *not* $\hat{I} \times \hat{I}$ but $\hat{I}$. If we start with $g$ being the Euclidean or Minkowski metrics, we obtain the iso-Euclidean and iso-Minkowski metric, the latter being the basis for the formulation of the isotopic lift of Special Relativity, in addition of the isotopic lift of the Lorentz group [15-19]; in the case we start with a general

[5]The definitions for a covariant set of coordinates and the corresponding isodifferential calculus differs from the covariant case, and since we shall be using only contravariant objects, we shall not present them in this article.

metric as in GR, we obtain the isotopic lift of GR [15,19]. We shall now proceed to identify the isotopic lift of the noise tensor $\sigma$ which verifies eq. (20), i.e. $\sigma \times \sigma^{\dagger} = g$. The non-unitary transform of $\sigma$ is given by

$$\sigma \mapsto U \times \sigma \times U^{\dagger} = \sigma \times \hat{I} := \hat{\sigma}. \tag{167}$$

Then,

$$\hat{\sigma}\hat{\times}\hat{\sigma} = \sigma \times \hat{I} \times \hat{T} \times (\sigma \times \hat{I})^{\dagger} = (\sigma \times \sigma^{\dagger}) \times \hat{I} = g \times \hat{I} = \hat{g}. \tag{168}$$

Thus the isotopic lift of noise tensor defined on $\hat{M}(\hat{x}, \hat{G}, \hat{R})$ is given by $\hat{\sigma} = \sigma \times \hat{I}$ which on projection to $M(x, g, R)$ (we stress here that we are taking a tensor with real components) we retrieve $\sigma$.

We know introduce the Santilli isodifferential introduced in 1996 (see [16,17]) for contravariant coordinates which are given by

$$\hat{dx} = \hat{T} \times dx = \hat{T} \times d(x \times \hat{I}), \tag{169}$$

so that when $\hat{I}$ does not depend on $x$ we have that $\hat{dx} = dx$. We now follow Kadeisvili [19] in introducing the isofunctions $\hat{f}(\hat{x})$ defined on $\hat{M}$ with values on $\hat{F}$. We take an $F$-valued function, $f$, defined on $M$, and we produce the non-unitary transformation

$$f(x) \mapsto U \times f(x) \times U^{\dagger} = f(x) \times \hat{I} = f(\hat{x} \times \hat{T}) \times \hat{I} \in \hat{F}, \tag{170}$$

so that the definition of an isofunction $\hat{f}(\hat{x})$ is given by

$$\hat{f}(\hat{x}) = f(\hat{T} \times \hat{x}) \times \hat{I}. \tag{171}$$

The isoderivative of isofunctions on contravariant coordinates are given by

$$\hat{\partial}\hat{f}(\hat{x}) = \hat{I} \times \frac{\partial f(\hat{x})}{\partial \hat{x}}, \tag{172}$$

so that

$$\hat{df}(\hat{x}) = \hat{\partial}\hat{f}(\hat{x})\hat{\times}\hat{dx} = \hat{I} \times \frac{\partial f(\hat{x})}{\partial \hat{x}}\hat{\times}dx = \hat{I} \times \frac{\partial f(\hat{x})}{\partial \hat{x}} \times \hat{T} \times d(x \times \hat{I}). \tag{173}$$

It follows from the definitions that

$$\frac{\hat{\partial}}{\hat{\partial}\hat{x}^k} = \hat{I}^i_k \times \frac{\partial}{\partial x^i}. \tag{174}$$

We now introduce (for the first time, to our best knowledge) the isotopic gradient operator of the isometric $\hat{G}$ (the $\hat{G}$-gradient, for short), $\widehat{\text{grad}}_{\hat{G}}$ applied to the isotopic lift $\hat{f}(\hat{x})$ of a function $f(x)$ is defined by

$$\widehat{\text{grad}}_{\hat{G}}\hat{f}(\hat{x})(\hat{v}) = \hat{G}(\hat{df}(\hat{x})\hat{,}\hat{v}), \tag{175}$$

for any vector field $\hat{v} \in T_{\hat{x}}(\hat{M})$, $\hat{x} \in \hat{M}$; we have denoted the inner product with $\hat{,}$ to stress that the inner product is taken with respect to the product in $\hat{F}$. It follows from the definition $\hat{G} = \hat{g}\hat{\times}\hat{I}$ and eq. (175) that the operator $\widehat{\text{grad}}_{\hat{G}}\hat{f}(\hat{x})$ is the vector field on the tangent manifold to $\hat{M}(\hat{x}, \hat{G}, \hat{F})$ defined by

$$\hat{G}^{\alpha\beta}(\hat{x})\hat{\times}\frac{\hat{\partial}\hat{f}(\hat{x})}{\hat{\partial}\hat{x}^{\alpha}}\hat{\times}\frac{\hat{\partial}}{\hat{\partial}\hat{x}^{\beta}} = \hat{g}^{\alpha\beta}(\hat{x})\hat{\times}\frac{\hat{\partial}\hat{f}(\hat{x})}{\hat{\partial}\hat{x}^{\alpha}}\hat{\times}\frac{\hat{\partial}}{\hat{\partial}\hat{x}^{i}} \times \hat{I}. \tag{176}$$

Therefore, the projection on $\hat{M}(\hat{x}, \hat{g}, F)$ of the $\hat{G}$-gradient vector field of $\hat{f}(\hat{x})$ is the vector field with components

$$\hat{g}^{\alpha\beta}(\hat{x})\hat{\times}\frac{\hat{\partial}\hat{f}(\hat{x})}{\hat{\partial}\hat{x}^{\alpha}} = \hat{g}^{\alpha\beta}(\hat{x})\hat{\times}\frac{\hat{\partial}\hat{f}(\hat{x})}{\hat{\partial}\hat{x}^{\alpha}}. \tag{177}$$

This will be of importance for the determination of the drift vector field of the diffusion linked with the Santilli- iso-Schroedinger equation. We finally define the isolaplacian as

$$\hat{\triangle}_{\hat{g}} = \hat{g}^{\alpha\beta}(\hat{x})\hat{\times}\frac{\hat{\partial}}{\partial\hat{x}^{\alpha}}\hat{\times}\frac{\hat{\partial}}{\partial\hat{x}^{\beta}}. \tag{178}$$

This definition differs from the original one in [19], but is the one that will allow us to associate diffusions to the Santilli-iso-Schroedinger equation.

# 9 Diffusions and the Heisenberg Representation

Up to now we have set our theory in terms of the Schroedinger representation, since the original setting for this theory has to do with scale transformations as introduced by Einstein in his last work [6] which was recognized already by London that the wave function was related to the Weyl scale transformation [48], and these scale fields have turned to be in the non-relativistic case, nothing else than the wave function of Schroedinger equation, both in the linear and the non-linear cases. Historically the operator theory of QM was introduced before the Schroedinger equation, who later proved the equivalence of the two. The ensuing dispute and rejection by Heisenberg of Schroedinger's equation is a dramatic chapter of the history of QM [36]. It turns out to be the case that we can connect the Brownian motion approach to QM and the operator formalism due to Heisenberg and Jordan. We must remark at this stage that the isotopic and Lie-admissible extensions of the operator formalism of QM by Santilli, was the starting point and building approach to the constructions of several theories. Some of these approaches, initiated by Santilli early in 1967, had to be abandoned later for reasons of inconsistency as elaborated in [16] in which the theory reaches final maturity.

Let us define the position operator as usual and the momentum operator by

$$q^{k} = x^{k}, p_{\mathcal{D}k} = \sigma \times \frac{\partial}{\partial x^{k}}, \tag{179}$$

which we call the diffusion quantization rule (the subscript $\mathcal{D}$ denotes diffusion) since we have a representation different to the usual quantization rule

$$p_k = -i \times \frac{\partial}{\partial x^k}, \tag{180}$$

with $\sigma = (\sigma_a^\alpha)$ the diffusion tensor verifying eq. (20), i.e. $(\sigma \times \sigma^\dagger)^{\alpha\beta} = g^{\alpha\beta}$ and substitute into the Hamiltonian function)

$$H(p,q) = \frac{1}{2}\sum_{k=1}^{d}(p_k - A_k)^2 + \mathbf{v}(q) \tag{181}$$

this yields the formal generator of a diffusion semigroup in $C^2(R^d)$ or $L^2(R^d)$. This yields the formal generator of a diffusion semigroup in $C^2(R^d)$ or $L^2(R^d)$. Thus, an operator algebra on $C^2(R^n)$ or $L^2(R^n)$ together with the postulate of the commutation relation (instead of the usual commutator relation of quantum mechanics $[p,q] = i\hat{h}I$)

$$[p,q] = pq - qp = -\sigma I \tag{182}$$

this yields the diffusion equation

$$\frac{\partial \phi}{\partial t} + \frac{1}{2}\sum_{k=1}^{d}(\sigma\frac{\partial}{\partial x^\alpha} - \sigma A_\alpha)^2\phi + \mathbf{v}\phi = 0, \tag{183}$$

which coincides with the diffusion equation (100) provided that $\mathrm{div}A = 0$ and $c = \mathbf{v} + A^2$.

Thus, in this approach, the operator formalism and the quantization postulates, allow to deduce the diffusion equation. If we start from either the diffusion process or the RCW geometry, without any quantization conditions we already have the equations of motion of the quantum system which are non other than the original diffusion equations, or equivalently, the Schroedinger equations. We stress the fact that these arguments are valid for both cases relative to the choice of the potential function $V$, i.e. if it depends nonlinearly on the wave function $\psi$, or acts linearly by multiplication on it. Further below, we shall use this modification of the Heisenberg representation of QM by the previous Heisenberg type representation for diffusion processes, to give an account of the diffusion processes that are associated with HM. This treatment differs from our original (inconsistent with respect to HM) treatment of the relation between RCW geometries and diffusions presented in [29] in that it incorporates the isotopic lift of all structures.

Let us frame now isoquantization in terms of diffusion processes. Define isomomentum, $\hat{p}_\mathcal{D}$, by

$$\hat{p}_{\mathcal{D}k} = \hat{\sigma}\hat{\times}\frac{\hat{\partial}}{\hat{\partial}\hat{x}^k}, \text{ with } \hat{\sigma} = \sigma \times \hat{I}, \tag{184}$$

so that the kinetic term of the iso-Hamiltonian is

$$\begin{aligned} \hat{p}_{\mathcal{D}} \hat{\times} \hat{p}_{\mathcal{D}}^{\dagger} &= \hat{\sigma} \hat{\times} \hat{\sigma}^{\dagger} \hat{\times} \frac{\hat{\partial}}{\hat{\partial} \hat{x}} \hat{\times} \frac{\hat{\partial}}{\hat{\partial} \hat{x}} \\ &= \hat{g} \hat{\times} \frac{\hat{\partial}}{\hat{\partial} \hat{x}} \hat{\times} \frac{\hat{\partial}}{\hat{\partial} \hat{x}} = \hat{\triangle}_{\hat{g}} \end{aligned} \tag{185}$$

We finally check the consistency of the construction by checking that it can be achieved via the non-unitary transformation

$$\begin{aligned} p_{\mathcal{D}_j} \mapsto U \times p_{\mathcal{D}_j} \times U^{\dagger} &= U \times \sigma \times \frac{\partial}{\partial x^j} \times U^{\dagger} \\ &= \sigma \times \hat{I} \times T \times \hat{I} \times \frac{\partial}{\partial x^j} = \hat{\sigma} \hat{\times} \frac{\hat{\partial}}{\hat{\partial} \hat{x}^j} = \hat{p}_{\mathcal{D}j}. \end{aligned} \tag{186}$$

Note that we have achieve this isoquantization in terms of the following transformations: First we transformed

$$p = -i \times \frac{\partial}{\partial x} \to p_{\mathcal{D}} := \sigma \times \frac{\partial}{\partial x}, \tag{187}$$

to further produce its isotopic lift

$$\hat{p}_{\mathcal{D}} = \hat{\sigma} \hat{\times} \frac{\hat{\partial}}{\hat{\partial} \hat{x}}. \tag{188}$$

When the original diffusion tensor $\sigma$ is the identity $I$ from which follows from eq. (20) that the original metric $g$ is Euclidean, we reach compatibility of the diffusion quantization with the Santilli-iso-Heisenberg representation given by taking the non-unitary transformation on the canonical commutation relations

$$[\hat{q}^{i} \hat{,} \hat{p}_j] = \hat{i} \hat{\times} \hat{\delta}_j^i = i \times \delta_j^i \times \hat{I}, \tag{189}$$

together with

$$[\hat{r}^{i} \hat{,} \hat{r}^{j}] = [\hat{p}_i \hat{,} \hat{p}_j] = 0, \tag{190}$$

with the Santilli-iso-quantization rule [16,17]

$$\hat{p}_j = -\hat{\imath} \hat{\times} \frac{\hat{\partial}}{\hat{\partial} \hat{x}^j}. \tag{191}$$

Thus, from the quantization by the diffusion representation we retrieve the Santilli-iso-Heisenberg representation, with the difference that the diffusion noise tensor in the above construction need not be restricted to the identity.

Finally, we consider the isoHamiltonian operator

$$\hat{H} = \hat{1} \hat{/} (\hat{2} \hat{\times} \hat{m}) \hat{\times} \hat{p}^{\hat{2}} + \hat{V}_0(\hat{t}, \hat{x}) + \hat{V}_k(\hat{t}, \hat{v}) \hat{\times} \hat{v}^k, \tag{192}$$

where $\hat{p}$ may be taken to be either given by the Santilli isoquantization rule

$$\hat{p}_k \hat{\times} |\hat{\psi}> = -\hat{i}\hat{\times}\frac{\hat{\partial}}{\hat{\partial} x^k}\hat{\times}|\hat{\psi}>, \tag{193}$$

or by the diffusion representation $\hat{p}_{\mathcal{D}}$, $\hat{V}_0(\hat{t},\hat{x})$ and $\hat{V}_k(\hat{t},\hat{v})$ are potential isofunctions, the latter dependent on the isovelocities. Then the iso-Schroedinger equation (or Schroedinger-Santilli isoequation) [16,17] is

$$\hat{i}\hat{\times}\frac{\hat{\partial}}{\hat{\partial}\hat{t}}|\hat{\psi}> = \hat{H}\hat{\times}|\psi> \ = \hat{H}(\hat{t},\hat{x},\hat{p})\times\hat{T}(\hat{t},\hat{x},\hat{\psi},\hat{\partial}\hat{\psi},\ldots)\times|\hat{\psi}>, \tag{194}$$

where the wave isofunction $\hat{\psi}$ is an element in $(\hat{\mathcal{H}}, <|\hat{\times}|>, \hat{C}(\hat{c},\hat{+},\hat{\times}))$ satisfies

$$\hat{I}\hat{\times}|\hat{\psi}> = |\hat{\psi}> . \tag{195}$$

Solutions of this equation and the many important consequences for the strong interactions and Hadronic Chemistry, have been discussed in [17] and references therein; they were first obtained in 1978, while Prof. Santilli was affiliated to the Physics Department, Harvard University, with the sponsorship of the Department of Energy, US Government.

## 9.1 Hadronic Mechanics and Diffusion Processes

As we derived above, the components of drift vector field, projected on $\hat{M}(\hat{x},\hat{g},R)$ in the isotopic form of eq. (91) with $A \equiv 0$, is given by eq. (177) with $\hat{f} = \hat{\ln}\hat{\phi}$, so that

$$\hat{g}^{\alpha\beta}(\hat{x})\hat{\times}\frac{\hat{\partial}\hat{\ln}\hat{\phi}(\hat{x})}{\hat{\partial}\hat{x}^\alpha}, \tag{196}$$

with $\hat{\phi}(\hat{x}) = \hat{e}^{\hat{\mathcal{R}}(\hat{x})+\hat{\mathcal{S}}(\hat{x})}$ the diffusion wave associated to the solution $\hat{\psi}(\hat{x}) = \hat{e}^{\hat{\mathcal{R}}(\hat{x})+i\hat{\mathcal{S}}(\hat{x})}$ of the Santilli-iso-Schroedinger eq. (194), and its adjoint wave is $\check{\hat{\phi}}(x) = \hat{e}^{\hat{\mathcal{R}}(x)-\hat{\mathcal{S}}(x)}$. Therefore, the drift vector field is

$$\hat{g}^{\alpha\beta}(\hat{x})\hat{\times}\frac{\hat{\partial}}{\hat{\partial}\hat{x}^\alpha}(\hat{\mathcal{R}}_{\hat{t}}\hat{+}\hat{\mathcal{S}}_{\hat{t}})(\hat{x}). \tag{197}$$

Finally, we shall write the isotopic lift of the stochastic differential equation for eq. (194). By applying the non-unitary transformation of eq. (91) with $A \equiv 0$, we obtain the iso-equation on $\hat{M}(\hat{x},\hat{G},\hat{R})$ for $\hat{X}(\tau)$ given by

$$d\hat{X}^i_{\hat{t}} = (\hat{g}^{\alpha\beta}\hat{\times}\frac{\hat{\partial}}{\hat{\partial}\hat{x}^\alpha}(\hat{\mathcal{R}}_{\hat{t}}\hat{+}\hat{\mathcal{S}}_{\hat{t}}))(\hat{X}_{\hat{t}})\hat{\times}d\hat{t} + \hat{\sigma}^i_j(\hat{X}_{\hat{t}})\hat{\times}d\hat{W}^j_{\hat{t}}, \tag{198}$$

with $d\hat{W}_{\hat{t}} = \hat{W}(\hat{t}\hat{+}d\hat{t})\hat{-}\hat{W}(\hat{t})$ the increment of a iso- Wiener process $\hat{W}_{\hat{t}} = (\hat{W}^1_{\hat{t}}, \ldots, \hat{W}^m_{\hat{t}})$ with isoaverage equal to $\hat{0}$ and isocovariance given by $\hat{\delta}^i_j \hat{\times} \hat{t}$; i.e.,

$$\hat{1}\hat{/}(\hat{4}\hat{\times}\hat{\pi}\hat{\times}\hat{t})^{\hat{m}\hat{/}\hat{2}} \hat{\int} \hat{w}_i \hat{\times} \hat{e}^{-\hat{w}^{\hat{2}}\hat{/}\hat{4}\hat{\times}\hat{t}^{\hat{2}}} \hat{\times} d\hat{w} = \hat{0}, \forall i = 1, \ldots, m \tag{199}$$

and

$$\hat{1}\hat{/}(\hat{4}\hat{\times}\hat{\pi}\hat{\times}\hat{t})^{\hat{m}\hat{/}\hat{2}} \hat{\int} \hat{w}_i \hat{\times} \hat{w}_j \hat{\times} \hat{e}^{-\hat{w}^{\hat{2}}\hat{/}\hat{4}\hat{\times}\hat{t}^{\hat{2}}} \hat{\times} d\hat{w} = \hat{\delta}^i_j \hat{\times} \hat{t}, \forall i, j = 1, \ldots, m, \tag{200}$$

and $\hat{\int}$ denotes the isotopic integral defined by $\hat{\int} d\hat{x} = (\int \hat{T} \times \hat{I} \times dx) \times \hat{I} = (\int dx) \times \hat{I} = \hat{x}$. Thus, formally at least, we have

$$\hat{X}_{\hat{t}} = \hat{X}_{\hat{0}} \hat{+} \hat{\int}_{\hat{0}}^{\hat{t}} (\hat{g}^{\alpha\beta} \hat{\times} \frac{\hat{\partial}}{\hat{\partial}\hat{x}^\alpha} (\hat{\mathcal{R}}_{\hat{s}} \hat{+} \hat{\mathcal{S}}_{\hat{s}}))(\hat{X}_{\hat{s}}) \hat{\times} d\hat{s} + \hat{\int}_{\hat{0}}^{\hat{t}} \hat{\sigma}^i_j (\hat{X}_{\hat{s}}) \hat{\times} d\hat{W}^j_{\hat{s}}. \tag{201}$$

The integral in the first term of eq. (201) is an isotopic integral of a usual Riemann-Lebesgue integral, while the second one is the isotopic lift of a stochastic Itô integral; we shall not present here in detail the definition of this last term, which follows from the notions of convergence in the isofunctional analysis elaborated by Kadeisvili, and the usual definition of Itô stochastic integrals [8,13,70].

## 9.2 The Extension to The Many-body Case

Up to know we have presented the case of the Schroedinger equation for an ensemble of one-particle systems on space-time. Of course, our previous constructions are also valid for the case of an ensemble of interacting multiparticle systems, so that the dimension of the configuration space is $3d + 1$, for indistinguishable $d$ particles; the general case follows with minor alterations. If we start by constructing the theory as we did for an ensemble of one-particle systems (Schroedinger's cloud of electrons), we can still pass trivially for the general case, by considering a diffusion in the product configuration manifold with coordinates $X_t = (X^1_t, \ldots, X^d) \in M^d$, where $M^d$ is the $d$ Cartesian product of three dimensional space with coordinates $X^i_t = (x^{1,i}_t, x^{2,i}_t, x^{3,i}_t) \in M$, for all $i = 1, \ldots, d$. The distribution of this is $\mu_t = E_Q \circ X_t^{-1}$, which is a probability density in $M^d$. To obtain the distribution of the system on the three-dimensional space $M$, we need the distribution of the system $X_t$: $\mathrm{U}^x_t := \frac{1}{d} \sum_{i=1}^d \delta_{x_i}$. which is the same as

$$U^x_t(B) = \frac{1}{d} \sum_{i=1}^d 1_B(X^i_t), \tag{202}$$

where $1_B(X_t^i)$ is the characteristic system for a measurable set $B$ , equal to 1 if $X_t^i \in B$, for any $i = 1 \ldots, d$ and 0 otherwise. Then, the probability density for the interacting ensembles is given by

$$\mu_t^x(B) = E_Q[U_t^x(B)], \tag{203}$$

where $E_Q$ is the mean taken with respect to the forward Kolmogorov representation presented above, is the probability distribution in the three-dimensional space; see [13]. Therefore, the geometrical-stochastic representation in actual space is constructable for a system of interacting ensembles of particles. Thus the criticism to the Schroedinger equation by the Copenhagen school, as to the unphysical character of the wave function since it was originally defined on a multiple-dimensional configuration space of interacting system of ensembles, is invalid [36].

# 10 Vorticity and Anomalous Phenomenae in Electrolytic Cells

We have already discussed in [3] that the Brownian motions produce rotational fields simply by considering the Hodge duality applied to the trace-torsion. In the other hand, we have seen that this encompasses the Brownian motions produced by the wave function of arbitrary quantum systems, and the case of viscous fluids, magnetized or not. These examples are independent of any scale, from the galactic to the quantum scales. In the galactic scales, according to Arp, this may explain the red-shift without introducing any big-bang hypothesis [53]. Thus, we have a modified form of Le Sage's kinetic theory producing universal fluctuations which have additionally rotational fields associated to them, and due to the universality of quantum wave functions, either obeying the rules of linear or non-linear QM, or still of HM, then it comes as no surprise that vortices and superconductivity (which is the case of the Rutherford-Santilli model of the neutron which is derived from the previous constructions and can be framed as we showed in terms of torsion field) appear as universal coherent structures; superconductivity is usually related to a non-linear Schroedinger equation with a Landau-Ginzburg potential, which is just an example of the Brownian motions related to torsion fields with further noise related to the metric. Furthermore, atoms and molecules have spin-spin interactions which will produce a contribution to the torsion field; we have seen already that the torsion geometry exists in the realm of Quantum Chemistry and Hadronic Chemistry.[6] This is the case of the compressed hydrogen atom model of the neutron in the Rutherford-Santilli

[6]A different approach due to Akimov and Shipov is claimed to be at the origin of these torsion fields [58] which stems from the torsion geometry of the vacuum through the teleparallel geometries we explored in [24], alike to the present approach, yet it is not vinculated nor to QM nor to fluid-dynamics, further claims to an hypothetical particle known as the phyton. Further experiments related to torsion fields have been presented in the Journal of New Energies, we

model, in which their is a spin alignment with opposite direction and magnetic moments for the electron and the proton. This produces the stable state which leads to fusion. This is *not* a cold fusion process since it appears to occur at temperatures of the order of $5,000$ degrees Celsius. Yet in electrochemical reactions, there are sources of torsion which are given by the the wave functions of the components involved, but furthermore the production of vortex structures. Gas bubbles appear after switching off the electrochemical potentials, and sonoluminescence have been observed at the Oak Ridge National Laboratory at the USA [59]. There is a surprising phenomenae of remnant heat that persists after death which could be produced by the vortex dynamics of the tip effect [62]. These experimental findings have been claimed to be observed in different laboratories across the world [57,59], have in some instances lead to a theoretical explanation in terms of torsion fields [60,61]. Superconductors of class II present also some surprising phenomenae such as low-frequency noise, history- dependent dynamic response, and memory direction, amplitude direction and frequency of the previously applied current [60]. If these findings can be reproduced systematically, we would have a new class of sources of energy, which stem from the zero point fluctuations.

# 11 On the Experimental Evidence of Space-time Fluctuations and Conclusions

We have shown that the equations of QM have an equivalent formulation as diffusion processes which themselves generate space-time geometries or alternatively are generated by them. We have extended these relations to the isotopic deformations introduced in HM. Thus, wave functions of elementary particles, atoms and molecules described by the Schroedinger and Santilli-iso-Schroedinger equations, generate torsion fields. This is an universal phenomenae since the applicability of these equations does not restrict to the microcospic realm, as already shown in the astrophysical theory due to Nottale [10]; this universality is associated with the fact that the Planck constant (or equivalently, the diffusion constant) is multivalued, or still, it is context dependent, inasmuch as the velocity of light has the same feature [17]. In the case of HM this can be seen transparently in the fact that the isotopic unit plays the role, upon quantization, of the Planck constant in QM, as we have already seen when we introduced the diffusion-Heisenberg representation and its isotopic lift, or furthermore, by its product with the noise tensor of the underlying Brownian motions.In the galactic scales, this may explain the red-shift without introducing a big-bang hypothesis [16,17]; an identical conclusion was reached by Arp in considering as a theoretical framework the Le Sage's model of a Universe filled with a gas

direct the reader to [61]. As we have shown in this article and [3] torsion fields appear in the most fundamental theories of physics.

of particles [52,53], in our theory, the zero-point fluctuations described by the Brownian motions defined by the wave functions, as well as by viscous fluids, spinor fields, or electromagnetic fields [2] (and which one can speculate as related to the so-called dark energy problem). A similar view has been proposed by Santilli in which the elementary constituents are the so-called aetherinos [71], while in Sidharth's work, they appear to be elementary quantized vortices related to quantum-mechanical Kerr-Newman black holes [63]. Thus, whether we examine the domains of linear or non-linear QM, or still the hyperdense domain of HM, then it appears that vortices and superconductivity (which is the case of the Rutherford-Santilli model of the neutron which is derived from the previous constructions) appear as universal coherent structures. Superconductivity is usually related to a non-linear Schroedinger equation with a Landau-Ginzburg potential, which is just an example of the Brownian motions related to torsion fields with further noise related to the metric. Furthermore, atoms and molecules have spin-spin interactions which will produce a contribution to the torsion field; we have seen already that the torsion geometry exists in the realm of Quantum Chemistry and ultimately in Hadronic Chemistry, since we can extend the construction to the many-body case. In distinction with the usual Coulomb potential in nuclear physics, the isotopic deformations of the nuclear symmetries yield attractive potentials such as the Hulten potential, which in the range of $10^{-13}$ cm. yields the usual potential [15,56] without the need of introducing any sort of parameters or extra potentials. In contrast with the ad-hoc postulates of randomness in the fusion models which are considered in the usual approaches [32,33], in the present work randomness is intrinsic to space-time itself or alternatively a by product of it, and in the case of HM, these geometries incorporate at a foundational level, a generalized unit which incorporates all the features of the fusion process itself: the non-canonical, non-local and non-linear overlapping of the wave functions of the ensembles which correspond to the separate ensembles under deformable collisions in which the particles lose their pointlike structure, or in a hypercondensed plasma state, where the dynamics of the process may have a random behavior; the domain of validity of this constructions are $10^{-13}$ cm., and outside this domain we find the quantum fluctuations associated to the Schroedinger equation. This extension has been possible essentially by taking in account the generalized isotopic units and the isotopic lifts of all necessary mathematical structures.

There are already experimental findings that may lead to validate the present view. In the last fifty years, a number of scientists at the Biophysics Institute of the Academy of Sciences of Russia, directed by S. Shnoll (and presently developed in a world net which includes Roger Nelson, Engineering Anomalies Research, Princeton University, B. Belousov, International Institute of Biophysics, Neuss (Germany), J. Wilker, Max-Planck Institute for Aeronomy, Lindau, and others), have carried out tens of thousands of different experiments of very different nature and energy scales ($\alpha$ decay, biochemical reactions, gravitational waves antenna, etc.) in different points of the globe, and carried out a software

analysis of the observed histograms and their fluctuations, to find out an amazing fit which is repeated with regularity of 24 hours, 27 days and the duration of a sidereal year. Thus, the fine spectrum of these experiments reveal a non-random pattern. At points of Earth with the same local hour, these patterns are reproduced with the said periodicity. The only thing in common to these experiments is that they are occur in spacetime, and thus this leads to conclude that they stem from spacetime fluctuations, which may further be associated with cosmological fields. Furthermore, the histograms reveal a fractal structure. This fractal structure has been found to follow the pattern of the logarithmic Muller fractal, which is associated with the existence of a global scale for all structures in the Universe; see H. Muller [85]. This leads to reinforce the thesis of time as an active field. Furthermore, the space and time Brownian motions can exist, in principle, in the different space and time scales warranted by these global scales. This structure is interpreted as appearing from an interference phenomena related to the cosmological field; we recall that diffusion processes present interference phenomena alike to , say, the two-slit experiment. Measurements taken with collimators show fluctuations emerging from the rotation of the Earth around its axis or its circumsolar orbit, showing a sharp anisotropy of space. Furthermore,it is claimed that the spatial heterogeinity occurs in a scale of $10^{-13}$ cm., coincidently with the scale of the strong interactions [80].

As a closing remark we would like to recall that Planck himself proposed the existence of ensembles of random phase oscillators having the zero-point structure as the basis for quantum physics [71]. Thus, the apeiron would be related to the Brownian motions which we have presented in this work, and define the space and time geometries, or alternatively, are defined by them. So we are back to the idea due to Clifford, that there is no-thing but space and time configurations, instead of a separation between substratum and fields and particles appearing on it. Furthermore, what we perceive to be void, is the hyperdense source of actuality.

## Acknowledgements

I would like to express my deep gratitude to Prof. Larry Horwitz for very useful discussions and encouragement, as well as to Prof. R.M. Santilli, for his kind interest for the author's work, and to Prof.J.V. Kadeisvili for the kindness of sending his last article .

## References

[1] D. L. Rapoport, On the Unification of Geometric and Random Structures through Torsion Fields: Brownian Motions, Viscous and Magneto-fluid-dynamics, *Foundations of Physics* **35**, no. 7, 1205-1244 (2005); ibid. in *Quantization in*

*Astrophysics, Brownian Motions and Supersymmetry*, F. Smarandache and V. Christianto (eds.), MathTiger, Tamil Naddu, India (2007).

[2] D. L. Rapoport, Cartan-Weyl Dirac and Laplacian Operators, Brownian Motions: The Quantum Potential and Scalar Curvature, Maxwell's and Dirac-Hestenes Equations, and Supersymmetric Systems, *Foundations of Physics* **7**, 1383-1431 (2005).

[3] D. L. Rapoport, Torsion Fields, Cartan-Weyl Space-Time and State-space Geometries, their Brownian Motions and the Time Variables, *Foundations of Physics***37**,nos. 4-5, 813-854 (2007).

[4] D.L. Rapoport, *Rep. Math.Phys.***49**, no.1, pp.1-49 (2002), **50**, no.2, pp.211-250 (2002), *Random Operts. Stoch.Eqts.* **11**, no.2, pp.2, pp.109-150 (2003) and **11**, no.4, 351-382 (2003); ibid., in *Trends in Partial Differential Equations of Mathematical Physics, Obidos, Portugal (2003)*, J.F.Rodrigues et al (edts.), Progress in Nonlinear Partial Differential Equations, vol.61, Birkhausser, Boston, (2005); ibid. in *Instabilities and Nonequilibrium Structures VII & VIII*, O. Descalzi et al (eds.), Kluwer Series in Nonlinear Phenomenae and Complex System, Dordrecht, (2004); ibid. *Discrete and Cont. Dynamical Systems, series B, special issue, Third Int.Conf. Differential Eqts. and Dynamical Systems, Kennesaw Univ., May 2000*, 327-336, S. Hu (ed.), (2000).

[5] R. Debever, *The Einstein-Cartan Correspondence*, Royal Academy of Sciences, Belgium, 1983; T. W. B. Kibble, *J.Math.Phys.*, 1961, 2, p.212; D. W. Sciama, *Rev.Mod.Phys.*, 1964, 36, p.463.

[6] A. Einstein and L. Kauffman, *Annals Maths.*, **56** (1955); Yu Obukhov, *Phys. Letts.***90 A** (1982),13.

[7] E. C. Stueckelberg,*Helv. Physica Acta* **14**(1941), 322,588 . L.P. Horwitz and C. Piron, *Helv. Physics Acta* **46** (1973), 316; L.P. Horwitz and C. Piron, *Helv. Physica Acta* **66** (1993), 694; M. C. Land, N. Shnerb and L.P. Horwitz, *J. Math. Phys.* **36** (1995), 3263; L.P. Horwitz and N. Shnerb, *Found. of Phys.* **28**(1998), 1509.

[8] E. Nelson,*Quantum Fluctuations*, (Princeton Univ. Press, Princeton, New Jersey , 1985).

[9] E. Schroedinger *Sitzunsberger Press Akad. Wiss. Math. Phys. Math.*,**144** (1931) and *Ann. I. H. Poincaré* **11** (1932), 300.

[10] L. Nottale, *Fractal Space-Time and Microphysics*, (World Scientific, Singapore, 1993); ibid. *Astron. Astrophys. Lett.***315**, L9 (1996); ibid.*Chaos, Solitons & Fractals* **7**, 877 (1996).

[11] R. Kiehn, http://www22.pair.com/csdc/pdf/bohmplus.pdf.

[12] L. Nottale, G. Schumacher & E.T. Lefvre, *Astron. Astrophys.* **361**, 379 (2000).

[13] M. Nagasawa, *Stochastic Processes in Quantum Physics* (Monographs in Mathematics),(Birkhauser, Boston-Basel , 2000).

[14] R.M. Santilli, *Elements of Hadronic Mechanics III*, ( Hadronic Press-Naukova, Palm Harbor-Kiev, 1993); ibid.*Isodual Theory of Antimatter, with Applications to Antigravity, Spacetime Machine and Grand Unification*, (Springer, New York ,2006).

[15] R.M. Santilli, *Foundations of Hadronic Chemistry*,( Kluwer Series in the Fundamental Theories of Physics, Dordrecht-Boston, 2001); A:O. E. Animalu, A New Theory on the Structure of the Rutherford -Santilli Neutron, *Hadronic Journal***17**, 349 (2004); ibid. The Physics of New Clean Energies and Fuels According to Hadronic Mechanics, *Journal of New Energy (Special Issue: Twenty Years of Research Extending Quantum Mechanics for New Industrial and Energy Products***4**, no. 1 (1999); ibid. *Hadronic Mathematics, Mechanics and Chemistry, vol. I: Iso-, Geno-, Hyper-Formulations for Matter, and Their Isoduals for Antimatter*, International Academic Press, in press.

[16] R. M. Santilli, Relativistic Hadronic Mechanics: Non-unitarity, Axiom-preserving Completion of Relativistic Quantum Mechanics, *Foundations of Physics***27**, no.5, 625-729 (1997).

[17] R. M. Santilli, in *Proceedings of the Seventh Marcel Grossmann Meeting in Relativity*, M. Keiser and R. Jantzen (editors), World Scientific, Singapore (1996).

[18] R. M. Santilli, *Isotopic, Genotopic and Hyperstructural Methods in Theoretical Biology*, Ukraine Academy of Sciences (1996).

[19] J.V. Kadeisvili, *Algebras, Groups and Geometries* **9**, 293, 319 (1992); G. Tsagas and D. S. Sourlas, *Algebras, Groups and Geometries***12**, 1 (1995).

[20] R. Kiehn, *Wakes, Coherence and Turbulent Structures*, (Lulu Publs., 2004); ibid. Non-Equilibrium Systems and Irreversible Processes, vol. 1; ibid. Non-Equilibrium Systems and Irreversible Processes, Vol 2; ibid. Falaco Solitons, Cosmology and the Arrow of Time, Non-Equilibrium Systems and Irreversible Processes, Vol 4; ibid. Plasmas and Non-Equilibrium Electrodynamics, Lulu Publishers (2004).

[21] D.L. Rapoport, in *Group XXI, Physical Applications of Aspects of Geometry, Groups and Algebras, Proceedings of the XXI International Conference on Group Theoretical Methods in Physics, Goslar, Germany, June 1995*, H.Doebner et al (eds.), 446-450, World Scientific, Singapore (1996); ibid.*Advances in Applied Clifford Algebras***8**, no.1, 126-149 (1998).

[22] V. de Sabbata, and C. Sivaram, *Spin and Torsion in Gravitation*, (World Scientific, Singapore, 1994); F. Hehl, P. von der Heyde, G. D. Kerlick and J. M. Nestor, *Rev. Mod. Phys.* **15**, 393 (1976); M. Blagojevic, *Gravitation and Gauge Fields*, (Institute of Physics Publ., Bristol, 2002); R.T. Hammond, *Rep. Prog.Phys.***65**, 599 (2004).

[23] I. Bialnicky-Birula and J. Mycielsky, *Annals of Physics* **100**, 1611, (1976); see also for numerical solutions J. Kamersberg and A. Zeilinger, *Physica B***151**, 193, (1988).

[24] D. Rapoport and M. Tilli, Scale Fields as a simplicity principle,in Proceedings of the Third Workshop on Hadronic Mechanics, vol. II (Patras, 1986), *Hadronic J. Suppl.* **6**,no.4, 682-778 (1986).

[25] C. Castro, J. Mahecha and B. Rodriguez, Nonlinear Quantum Mechanics as a fractal Brownian motion with complex diffusion constant, arXiv:quant-ph/C. Castro and Jorge Mahecha, On Nonlinear Quantum Mechanics, Brownian motions and Fisher Information, *Progress in Physics*, **1**, 38-45 (2006).

[26] L. Nottale, Fractality field in the Theory of Scale Relativity, *Progress in Physics*, **1**, , 12-16, April (2005).

[27] K. Kondo and Y. Ishizuka, Recapitulation of the Geometrical Aspects of Gabriel Kron's Non- Riemannian Electrodynamics, *Memoirs of the Unifying Study of the Basic Problems in Engineering Sciences by Means of Geometry (RAAG Memoirs)*, vol.1, Division B (1955); G.Kron, Non-Riemannian Dynamics of Stationary Electric Networks, *RAAG Memoirs* vol. 4, 156 (1958); ibid. Electric Ciruit Models of the Schrdinger Equation,*Phys. Rev. 67*, 39-43 (1945).

[28] C.Castro, On the coupling constants , Geometric Probability and Complex Domains, *Progress in Physics*,**2**, 46-53 (2006).

[29] D. Rapoport, *Algebras, Groups and Geometries***8**, no. 1, 1-61 (1991); ibid., On the derivation of the stochastic processes associated to Lie isotopic gauge theory, pags. 359-374, in *Hadronic Mechanics and Nonpotential Interactions V*, vol, II, Proceedings of the Fifth International Conference, Univ. of Iowa, August 1990, Hyo Myung (ed.), Nova Science Publs., New York/Budapest, 1992

[30] S. Wand and D.D.L. Chung, Composites Part B (1999), 579-590.

[31] Hehl and Yu. Obukhov, gr-qc 07053422.

[32] L. Horwitz, Private communication.

[33] M. Gasperini, Lie-isotopic Lifting of Gauge Theories, *Hadronic Journal* **6**, 1462-1497 (1983).

[34] E. J. Post, *Quantum Reprogramming*, Kluwer, Dordrecht-Boston (1995).

[35] D. Bohm and B. Hiley, *The Undivided Universe*, Routledge, London (1995).

[36] M. Beller, *Quantum Dialogue: The Making of a Revolution*, Univ.of Chicago Press (2001).

[37] W. J. Swiatecki, K. Siwek-Wylczinska, J. Wylzinski, Fusion Through Diffusion, *Acta Physica Polonica B***34**, no. 4, 20049-2071, (2003); J. Blocki, O. Mazonka, J. Wilczynski, *Acta Physica B***31**, no. 7, 1513, (2000).

[38] A. Gudzanowski, The Significance of Smoluchowski Work in Atomic Physics, *Acta Physica Polonica B***34**, no. 4, 1513 (2003).

[39] D. L. Rapoport, in *Foundations of Probability and Physics IV, Proceedings, Vaxho, Sweden*, A. Khrennikov et al (eds.), American Institute of Physics Conference Series (2007).

[40] C. Castro, On Dark Energy , Weyl Geometry, and Different Derivations of the Vacuum Energy density and the Pioneer Anomaly, *Foundations of Physics***27**, no. 3, 368 (2007); ibid. How Weyl Geometry Solves the Riddle of Dark Energy, in *Quantization in Astrophysics, Brownian Motion and Supersymmetry*, F. Smarandache and V. Christianto (eds), MathTiger, Tamil Naddu, India (2007).

[41] J.F . Corum, Relativistic Rotation and the anholonomic object, *J.Math. Phys***18**, no.4 , 77 (1976); ibid.Relativistic Covariance and Electrodynamics, *J. Math.Phys.* **21**, no. 9, 83 (1980).

[42] K. Kondo, *Memoirs of the unifying study of the basic problems in engineering sciences by means of geometry*, Tokyo, Gakujutsu Bunken Fukyu-Kai (1955).

[43] B. Stanislavovich, On Torsion Fields *Galilean Electrodynamics* **12**, Special Issues 1, p. 5 (2001); M. Goldman M, *Spin temperature and nuclear magnetic resonance in solids*, Clarendon press, Oxford, 1970; A. D. Krisch, The spin of proton, *Scientific American*, May, 1979.

[44] T. Frankel, *The Geometry of Physics*, Cambridge Univ. Press (1999).

[45] R. M. Santilli, *Foundations of Physics***37**, nos.4-5 (2007).

[46] W. Feller, *An Introduction to Probability Theory and its Applications, I*, Addison Wesley (1952)

[47] H. P. Noyes and J.C. van der Berg, *Bit-String Physics: A Finite and Discrete Approach to Natural Philosophy*, World Scientific, Singapore (2001).

[48] F. London, Quantum-mechanical interpretation of Weyl's theory, *Zeit. f. Phys.*, **42**, 375 (1927); L. O'Raifeartaigh, *The Dawning of Gauge Theory*, Princeton Univ. Press (1997).

[49] Schouten, *Ricci Calculus*, Springer Verlag, Berlin (1951).

[50] S. Hojman, M. Rosenbaum, M.P. Ryan and L.C. Shepley, *Phys.Rev. D***17**, 3141 (1978) ; C. Mukku and W. A. Sayed, *Phys. Letts. 82 B*, 382 (1979).

[51] M. Pitkanen, *Topological Geometrodynamics*, Luniver Press (2006); ibid. *Bio-Systems as Self-Organizing Systems*; ibid. *TGD Inspired Theory of Consciousness*; ibid. *Bio-Systems as Conscious Holograms*; ibid. *Mathematical Aspects of Consciousness*, ibid. *Magnetospheric Consciousness*; ibid.*Genes and Memes*; in http://www.helsinki.fi/ matpitka/conscbooks.html.

[52] M. R. Edwards, *Pushing Gravity: New perspectives on Le Sages theory of gravitation*, Apeiron,Quebec (2001).

[53] H. Arp, *Seeing Red: Redshifts, Cosmology and Academic Science*, Apeiron, Quebec ( 1998).

[54] Y. Wu and Yi Lin ,*Beyond Nonstructural Quantitative Analysis: Blown-ups, Spinning Currents and Modern Science*, World Scientific, Singapore (2002).

[55] K.D. Elworthy, in *Diffusion Processes and Related Problems in Analysis*, M.Pinsky et al (edts.), vol. II, (Birkhauser, Basel,1992).

[56] S. Capozziello, G. Iovane, G. Lambase and C. Stornarolo, *Europhys.Letts* **46**, 710 (1999).

[57] Xing-liu Jiang, Jin-zhi Lei and Li-juan Han, Torsion Field Effects and Zero-Point Energy in Electrical Discharge Systems, *Journal of Theoretics***4-5**, Dec. 2003/Jan 2004; T. Matsuda, K. Harada, H. Kasai, O. Kamimura and A. Tomomura, Observation of Dynamic Interaction of Vortices with Pinning by Lorentz Microscopy, *Science***271**, 1393 (1996)

[58] A. E. Akimov and G. Shipov, Torsion Fields and their Experimental Manifestations, *Journal of New Energy* **2**, no. 2, 67 (1999).

[59] C. Eberlein, Theory of quantum radiation observed as sonolumininensce,*Phys. Rev. Letts.* **53**, 2772 (1996).

[60] Y. Paltiel, E. Zeldov et al, Dynamic instabilities and memory effects in vortex matter, *Nature***403**, 398 (2000).

[61] V. F. Panov, V. I. Kichigin, G. V. Khaldeev, A. V. Klyuev, B. V. Testov, T. A. Yushkova, V. V. Yushkov, Torsion Fields and Experiments, *Journal of New Energy***2**, nos. 2,3 (1997).

[62] T. Mizuno, T. Akimoto, T. Ohmori, Neutron and Heat Generation induced by Electric Discharge, *Journal of New Energy* **3**, Number 1, Spring 1998;

[63] B. G. Sidharth, *The Universe of Fluctuations: The Architecture of Spacetime and the Universe*, Springer Series on the Fundamental Theories of Physics, Berlin (2004); ibid. *Chaotic Universe: From the Planck Scale to the Hubble Scale*, Nova Science , New York (2002).

[64] A. Khrennikov, Reconstruction of quantum theory on the basis of the formula of total probability; quant-ph/03012194; quant-ph/0202107.

[65] F. Lindner et al, quant-phi/0503165 and *Phys. Rev.Letts.* **95**, 040401, (2005).

[66] G. N. Ord, Fractal space-time : a geometric analogue of relativistic quantum mechanics, *J. Phys .A: Math. Gen.* ,(1983), 16 , 1869-1884; ibid. *Chaos, Solitons Fractals* (1996);7:821.

[67] M. El Naschie, Otto Rossler, I. Prigogine,*Quantum Mechanics, Diffusion and Chaotic Fractals*, Pergamon Press, London (1995); several articles in *Chaos, Solitons and Fractals.*

[68] O. E. Animalu and R.M. Santilli, *Inter. Journal of Quantum Chemistry* **29** (1995) 175; R.M. Santilli and D.D.Shillady, *Inter. J. Hydrogen Energy* **24** (1999), 943-956.

[69] H. Kleinert, *Gauge Fields in Condensed Matter by Hagen Kleiner*, World Scientific, Singapore ( 1990).

[70] C. W. Gardiner, *Handbook of Stochastic Methods: for Physics, Chemistry and the Natural Sciences (Springer Series in Synergetics)*,Springer, Berlin (2004); N. Ikeda and S. Watanabe, *Stochastic Differential Equations and Diffusion Processes*, (North-Holland/Kodansha, Amsterdam/Tokyo, 1981);P. Malliavin, *Géométrie Différentielle Stochastique*, (Les Presses Univ., Montreal, 1978).

[71] R. M. Santilli, The Etherino and/or the Neutrino Hypothesis, *Foundations of Physics*, Vol. **37**, No. 4-5. (May 2007), pp. 670-711.

[72] L. Horwitz, Quantum Interference in Time, *Foundations of Physics*, Vol. 37, No. 4-5. (May 2007), pp. 734-746.

[73] M. Planck, *Theory of Heat Radiation*, Dover, New York, (1962).

[74] J. V. Kadeisvili, Rebuttal of J. M. Calo's comments on R. M. Santilli's HHO paper, *Int. J. Hydrogen Energy*, in press; J.M. Calo, Comments on A new gaseous and combustible form of water, by R.M. Santilli,*Int. J. Hydrogen Energy*, **31** (9), 1113-1128 (2006) .

[75] C. Illert and R.M. Santilli, *Foundations of Theoretical Conchology*, Hadronic Press, Palm Harbor, (1995).

[76] D. Reverberi, The Clockspring model of sprouting and blossoming, ZAMP **36**, no. 5 (1985).

[77] R.M. Santilli, *Isodual Theory of Antimmater, with Applications to Antigravity, Grand Unification and Cosmology*, Fundamental Theories of Physics Series, Springer, Berlin (1996).

[78] R. M. Santilli, *Foundations of Classical Mechanics, I and II*, Springer Verlag, New York, (1982, 1983).

[79] R. Montel and M. Ploszajczak,*Universal Fluctuations: The Phenomenology of Hadronic Matter*, World Scientific, Singapore (2002).

[80] Simon E. Shnoll, Konstantin I. Zenchenko, Iosas I. Berulis, Natalia V. Udaltsova and Ilia A. Rubinstein; arxiv: physics/0412007 (December 2004); V. A. Panchelyuga, V. A. Kolombet, M. S. Panchelyuga and S. E. Shnoll; physics/0612055 (December 2006);A. V. Kaminsky and S. E. Shnoll, physics/0605056 (May 2006); S. Snoll, physics/0602017. S. Shnoll, *Phys. Letts. A*359, 4, 249-251 (2004); ibid. Uspekhi **43**, no. 2, 205-209 (2000); ibid. *Progress in Physics* , January 2007.

[81] D. Rapoport, to appear.

[82] C.Gibson, astro-ph/0304441; http:astro-ph/0304107;astro-ph/0210583; astro-ph/0110248 .

[83] R. Montel and M. Ploszajczak,*Universal Fluctuations: The Phenomenology of Hadronic Matter*, World Scientific, Singapore (2002).

[84] J. V. Kadeisvili, Rebuttal of J. M. Calo's comments on R. M. Santilli's HHO paper, *Int. J. Hydrogen Energy*, in press; J.M. Calo, Comments on A new gaseous and combustible form of water, by R.M. Santilli,*Int. J. Hydrogen Energy*, **31** (9), 1113-1128 (2006) .

[85] H. Muller, Free Energy - Global Scaling, *Raum& Zeit Special 1*, Ehlers-Verlag GmbH (Germany), ISBN 3-934-196-17-9; (2004).

# Distribution of distances in the solar system

V. Peřinová*, A. Lukš, P. Pintr
Laboratory of Quantum Optics, Faculty of Natural Sciences,
Palacký University, Třída Svobody 26,
77146 Olomouc, Czech Republic

**Abstract**

The recently published application of a diffusion equation to prediction of distances of planets in the solar system has been identified as a two-dimensional Coulomb problem. A different assignment of quantum numbers in the solar system has been proposed. This method has been applied to the moons of Jupiter on rescaling.

PACS number: 96.35
Key words: regularities of planetary orbits, large scale quantization

## 1 Introduction

The 20th century is held for the golden age of the astronomy and astrophysics, when many persistent questions were solved and the human view of the universe changed radically. In spite of this, at the beginning of the 21st century, one cannot find satisfactory answers to some questions our ancestors posed as early as in the 16th century. For instance, Kepler looked for a universal law, in his Mysterium cosmographicum, to explain the planetary distances in the solar system. Nowadays, when discoveries of other planetary systems occur, such a law could explain the distances of their planets.

0*Corresponding author.
E-mail address: perinova@prfnw.upol.cz (V. Peřinová)

In 1766 Titius formulated the law, which described distances of the bodies in the solar system, and it even predicted new bodies at certain distances from the Sun [1]. Actually its being criticized led to the discovery of the remaining planets and new bodies – asteroids – in the solar system. It was the first, controversial, description of the distances of the bodies in this planetary system. But hardly any physical explanation has thus far been given. Is it a mere extravagance, or does this law have some deep physical content? May the planets around stars originate at definite distances?

Quest of the answer developed into invention of new empirical formulae, which describe, with higher or lower accuracy, the distances of the bodies in the solar system. For instance Armelini's empirical formula has the form

$$r_{n\mathrm{A}} = 1.53^n, \tag{1}$$

where $n$ assumes the values: Mercury $-2$, Venus $-1$, Earth 0, Mars 1, asteroid Vesta 2, asteroid Camilla 3, Jupiter 4, Saturn 5, asteroid Chiron 6, Uranus 7, Neptune 8, and Pluto 9.

In 1938 Mohorovičić invented an empirical formula [2], which describes the distances of planets and comets with high accuracy, and it also predicts an asteroid belt between Mars and Jupiter. Mohorovičić's law says that the distances of the inner parts of the solar system increase in a sublinear manner and those of the outer parts of this system increase in a superlinear manner. In the paper [3] we have modified this law such that it satisfies also other planetary systems and those of the moons of the giant planets.

Interesting is the empirical formula, which is similar to the laws of quantum mechanics [4]

$$r_{mn} = \frac{1}{2}(m^2 + n^2)r_0, \tag{2}$$

where $m$ are natural numbers, $n = 0, 1, \ldots, m$ and $r_0 = 0.387$ AU. The Bohr–Sommerfeld rule of (allowed) orbits for electrons in the electric fields of the nuclei of various atoms resemble the distribution of planetary distances, but do not let us forget that this rule describes bodies (electrons), which all have the same inertial mass and the same electric charge, which replaces a gravitational mass here. To obtain a distribution of the planetary distances, one either replaces different planetary masses by their mean mass, or makes the quantum of action depend on the actual mass.

Agnese and Festa described the solar system like a gravitational atom [5]. They utilized a quantum law for the hydrogen atom, which they applied to

description of major semi-axes of allowed (discretized) elliptical orbits of the bodies of the planetary system

$$r_{n\mathrm{AF}} = r_1 n^2, \tag{3}$$

where $n$ are natural numbers and $r_1$ is the Bohr radius of the planetary system, which is

$$r_1 = \frac{GM}{\alpha_{\mathrm{g}}^2 c^2}, \tag{4}$$

where $G$ is the gravitational constant, $M$ the mass of the central body, $c$ the vacuum speed of light and $\alpha_{\mathrm{g}}$ is a gravitational structure constant, which has the property $\frac{1}{\alpha_{\mathrm{g}}} = 2113 \pm 15$. Agnese and Festa have shown that this description of distances satisfies also the planetary system $\upsilon$ Andromedae [6] and other stellar systems alike on substituting the mass of the appropriate central star for the mass $M$. A study which elaborates on such ideas has been presented in [7].

Recently, the significance of the Titius–Bode law has been evaluated both by generating random planetary systems [8] and by the help of methods of the modern statistical analysis [9]. In the papers [10, 11] the authors point out quantum features also on large scales, namely discrete values of distances of possible planets and galaxies.

In quantum mechanics one utilizes Schrödinger's equation for the description of a physical system. In the paper [12], the stochastic mechanics is constructed, i. e., the Schrödinger equation is obtained as a classical diffusion equation by the help of the hypothesis that any particle in any interaction also exhibits a universal Brownian motion [13]. The main problem of this kind of derivation is a convincing physical origin for that universal Brownian motion, although a possibility is the quantum nature of space-time [14]. The chaotic behaviour of the solar system during its formation and evolution [15, 16] suggests a diffusion process to be described in terms of a Schrödinger-type equation. The description of the planetary system using a Schrödinger-type diffusion equation has been realized in [17]. There the authors have adapted the Schrödinger equation to the planetary system and shown that there exist very many orbits, on which possible planets may originate. That paper has stimulated us to the following considerations.

## 2 Discrete distances in the gravitational field of an astronomical body

Let us consider a body of the mass $M_\mathrm{p}$, which orbits a central body of the mass $M$ and has the potential energy $V(x,y,z)$ in its gravitational field. Because planets and moons of the giant planets revolve approximately in the same plane, we consider $z=0$. Because they revolve in the same direction, we choose directions of the axes $x$, $y$ and $z$ such that the planets or moons of giant planets revolve counter-clockwise. Then we write the modified Schrödinger equation for the wave function $\psi=\psi(x,y)$ from the part of the Hilbert space $L_2(R^2)\cap C^2(R^2)$ and the eigenvalue $0>E\in R$ in the form

$$-\frac{\hbar_M^2}{2M_\mathrm{p}}\left(\frac{\partial^2}{\partial x^2}+\frac{\partial^2}{\partial y^2}\right)\psi+V(x,y)\psi=E\psi, \tag{5}$$

where $\hbar_M\approx 1.48\times 10^{15}M_\mathrm{p}$, $V(x,y)=V(x,y,z)$ and $E$ is the total energy. Negative $E$ classically correspond to the elliptic Kepler orbits and the localization property (bound state) is conserved also in the quantum mechanics for such total energies $E$. The factor $1.48\times 10^{15}$ is not a dimensionless number, but the unit of its measurement is $\mathrm{m^2s^{-1}}$. With respect to the unusual unit we do not wonder that Agnese and Festa [5] consider this factor in the form of a product, such that $\hbar_M=\bar{\lambda}_M c M_\mathrm{p}$, where $\bar{\lambda}_M\approx 4.94\times 10^6$ m.

We transform equation (5) into the polar coordinates,

$$-\frac{\hbar_M^2}{2M_\mathrm{p}}\left(\frac{\partial^2\tilde{\psi}}{\partial r^2}+\frac{1}{r}\frac{\partial\tilde{\psi}}{\partial r}+\frac{1}{r^2}\frac{\partial^2\tilde{\psi}}{\partial\theta^2}\right)+\tilde{V}(r)\tilde{\psi}=E\tilde{\psi}, \tag{6}$$

where $\tilde{\psi}\equiv\tilde{\psi}(r,\theta)=\psi(r\cos\theta,r\sin\theta)$ and $\tilde{V}(r)=V(r\cos\theta,r\sin\theta)$ does not depend on $\theta$. Particularly we choose

$$\tilde{V}(r)=-\frac{GM_\mathrm{p}M}{r}. \tag{7}$$

With respect to the Fourier method we assume a solution of the equation (7) in the form

$$\tilde{\psi}(r,\theta)=R(r)\Theta(\theta). \tag{8}$$

The original eigenvalue problem is transformed, equivalently, to two eigenvalue problems

$$\Theta''(\theta)=-\Lambda\Theta, \tag{9}$$

$$\Theta(0) = \Theta(2\pi) \tag{10}$$

and

$$R''(r) + \frac{1}{r}R'(r) + \left\{ -\frac{\Lambda}{r^2} + \left[ E - \tilde{V}(r)\frac{2M_{\mathrm{p}}}{\hbar_M^2} \right] \right\} R(r) = 0, \tag{11}$$

$$\lim_{r\to 0+} [\sqrt{r}R(r)] = 0, \quad \sqrt{r}R(r) \in L_2((0,\infty)). \tag{12}$$

The solution of the problem (9)–(10) has the form

$$\Theta_l(\theta) = \frac{1}{\sqrt{2\pi}} \exp\left(il\theta\right) \tag{13}$$

for $l = \pm\sqrt{\Lambda} \in Z$.

Here $l = 0$ should mean a body, which does not revolve at all. In the classical mechanics such a body moves close to a line segment ending at the central body, and it spends a short time in the vicinity of this body. In this paper we utilize some – not all – of the concepts of quantum mechanics and we will not avoid the case $l = 0$ [17]. In (13) $l = 1, 2, \ldots, \infty$ corresponds to the counter-clockwise revolution.

Respecting (7), the equation (11) becomes

$$R''(r) + \frac{1}{r}R'(r) + \left\{ -\frac{l^2}{r^2} - B - \frac{2M_{\mathrm{p}}}{\hbar_M^2}\left( -\frac{GM_{\mathrm{p}}M}{r} \right) \right\} R(r) = 0, \tag{14}$$

where

$$B = -\frac{2M_{\mathrm{p}}E}{\hbar_M^2} = -\frac{2}{(\bar{\lambda}_M c)^2}\frac{E}{M_{\mathrm{p}}}. \tag{15}$$

Let us note that

$$\frac{M_{\mathrm{p}}GM_{\mathrm{p}}M}{\hbar_M^2} = \frac{GM}{(\bar{\lambda}_M c)^2}. \tag{16}$$

On substituting $r = \frac{\rho}{2\sqrt{B}}$ and introducing

$$\tilde{R}(\rho) = R\left(\frac{\rho}{2\sqrt{B}}\right), \tag{17}$$

equation (14) becomes

$$\tilde{R}''(\rho) + \frac{1}{\rho}\tilde{R}'(\rho) + \left( -\frac{1}{4} + \frac{k}{\rho} - \frac{l^2}{\rho^2} \right) \tilde{R}(\rho) = 0, \tag{18}$$

where

$$k = \frac{GM}{(\bar{\lambda}_M c)^2\sqrt{B}}. \tag{19}$$

For later reference let us note that, inversely,

$$\sqrt{B} = \frac{GM}{(\bar{\lambda}_M c)^2 k}, \tag{20}$$

$$\frac{-E}{M_{\rm p}} = \frac{(\bar{\lambda}_M c)^2}{2} B \tag{21}$$

$$= \frac{(GM)^2}{2(\bar{\lambda}_M c)^2 k^2}. \tag{22}$$

Expressing $\tilde{R}(\rho)$ in the form

$$\tilde{R}(\rho) = \frac{1}{\sqrt{\rho}} u\left(\rho\right), \tag{23}$$

we obtain an equation for $u(\rho)$

$$u''(\rho) + \left[-\frac{1}{4} + \frac{k}{\rho} - \left(l'^2 - \frac{1}{4}\right)\frac{1}{\rho^2}\right] u\left(\rho\right) = 0, \tag{24}$$

where $l' = l$. It is familiar that this equation has two linear independent solutions $M_{k,l'}(\rho)$, $M_{k,-l'}(\rho)$, if $l'$ is not an integer number. When $l'$ is integer, the solution $M_{k,-l'}(\rho)$ must be replaced with a more complicated solution. It can be proven that the other solution is not regular for $\rho = 0$ (it diverges as $\ln\rho$ for $\rho \to 0$). The remaining solution $M_{k,l}(\rho)$ can be transformed to a wave function from the space $L_2((0,\infty))$ if and only if $k - l - \frac{1}{2} = n_{\rm r}$ is any nonnegative integer number. We choose this function to be

$$u_{kl}(\rho) = C_{kl} M_{k,l}(\rho), \tag{25}$$

where $C_{kl}$ is an appropriate normalization constant and $M_{k,l}(\rho)$ is a Whittaker function, namely

$$M_{k,l}(\rho) = \rho^{l+\frac{1}{2}} \exp\left(-\frac{\rho}{2}\right) \Phi\left(l - k + \frac{1}{2}, 2l + 1; \rho\right), \tag{26}$$

where $\Phi$ is the confluent (or degenerate) hypergeometric function. In (25) the constant $C_{kl}$ has the property

$$\int_0^\infty r[R_{kl}(r)]^2 dr = 1, \tag{27}$$

or it is

$$C_{kl} = 2\sqrt{B}\frac{1}{(2l)!}\sqrt{\frac{(n+l-1)!}{2k(n-l-1)!}}. \tag{28}$$

Then

$$R_{kl}(r) = 2\sqrt{B}\sqrt{\frac{(n-l-1)!}{2k\Gamma(n+l)}}\exp(-r\sqrt{B})(2r\sqrt{B})^l L^{2l}_{n-l-1}(2r\sqrt{B}), \tag{29}$$

where $n = k + \frac{1}{2}$, $L^{2l}_{n-l-1}(x)$ is a Laguerre polynomial, and the relation (20) holds.

# 3 Interpretation of formulae derived

Having solved the modified Schrödinger equation, we address interpretation of the formulae derived. The probability density $P_{kl}(r)$ of the revolving body occurring at the distance $r$ from the central body is

$$P_{kl}(r) = r[R_{kl}(r)]^2,\ r \in [0, \infty). \tag{30}$$

Mean distances of the planets are given by the relation

$$r_{kl} = \int_0^\infty r P_{kl}(r) dr \tag{31}$$

$$= \frac{(\bar{\lambda}_M c)^2}{4GM}\left[(2k - n_{\mathrm{r}})(2k - n_{\mathrm{r}} + 1) + 4n_{\mathrm{r}}(2k - n_{\mathrm{r}}) + n_{\mathrm{r}}(n_{\mathrm{r}} - 1)\right], \tag{32}$$

where $n_{\mathrm{r}} = n - l - 1$, $k = \frac{1}{2}, \frac{3}{2}, \frac{5}{2}, \ldots, \infty$ and $l = 0, 1, 2, \ldots, n$.

For the solar system $M = M^{\mathrm{Sun}}$ holds and the Bohr radius of the solar system $r_{\frac{1}{2}0} = 0.055$ AU. For survey one finds some expectation values $r_{kl}$ for selected values $k, l$ with the specification of described bodies in table 1 (cf. [17]).

Even though also in this case an empirical formula is tested for distribution of planetary distances, the predicted orbits fit those of the bodies in this solar system.

Using the graphs of the probability densities we have plotted for every predicted orbit of this system, we obtain surprising results. The graphs of the probability densities for each orbit with $k \leq \frac{9}{2}$ and with $\frac{11}{2} \leq k \leq \frac{31}{2}$ are contained, respectively, in figure 1 and in figure 2. The vertical axis denotes the probability density $P_{kl}(r)$ and the longitudinal axis designates the planetary distance $r$ from the Sun. In figure 1 graph no. $p = 1$ is interpreted such that the highest probability density is assigned to the orbit of the radius of 0.055 AU and from the calm shape of the graph we infer that an ideal circular orbit is tested. In figure 1 graph no. $p = 14$ is interpreted such that the highest probability density is assigned to the orbit of the radius of 3.32 AU and, of many peaks, which wave the shape, we infer that no stable circular orbit is tested. After performing the analysis for all the orbits, we obtain only a small number of stable circular orbits. The orbits, on which big bodies – planets – may originate, are listed in table 2.

It emerges that, for every number $k$, there exists only one stable orbit, on which a big body – a planet – may originate. Then we can interpret the number $k$ as the principal quantum number and $l$ as the orbital quantum number equal to the number of possible orbits, but only for the greatest $l$ there exists a stable orbit of a future body. A planet which does not confirm this theory is the Earth. Since the description based on the modified Schrödinger equation for the planetary system is not fundamental, it could not fit all the stable orbits. Other deviations are likely to be incurred by collisions of the bodies in early stages of the origin of the planets, thus nowadays we already observe elliptical orbits, which are very close to circular orbits.

This procedure has been applied to moons of giant planets by us. It emerges that the moons of giant planets also are fitted by the modified Schrödinger equation and appropriate expectation values. Especially, the predicted stable circular orbits of Jupiter's moons are presented in table 3. For Jupiter it holds that $M = M^{\mathrm{Jup}}$ and the Bohr radius (4) of this system $r_1 = 6287$ km. It emerges that the predicted lunar orbits fit the measured orbits of the moons orbiting Jupiter.

# 4 Conclusions

In this paper we assume that there exists a law by which big objects – planets and moons of giant planets – do not originate anywhere, but at allowed distances from the central body. Unnegligible number of authors have issued from similar assumptions and derived empirical formulae for parameters of allowed orbits.

The results we have presented in this paper are based on a modified Schrödinger equation, which has been applied to the planetary system by us for the quantum theory contained in the Schrödinger equation to create an interesting view of the birth of such a stellar system, namely the orbits of planets and moons being approximately quantized.

# 5 Acknowledgements

This work under the research project "Measurement and information in optics" No. MSM 6198959213 was supported by the Ministry of Education of the Czech Republic. The authors acknowledge Jaromír Křepelka for his help in the preparation of the figures.

# References

[1] Nieto MM. The Titius–Bode Law of Planetary Distances: Its History and Theory. Oxford: Pergamon Press, 1972.

[2] Guth Vl, Link F, Mohr JM, Šternberk B, Astronomy, Vol. I. Prague: Czechoslovak Academy of Sciences Press, 1954 (in Czech).

[3] Pintr P, Peřinová V. The solar system from the quantization viewpoint. Acta Universitatis Palackianae, Physica, 2003–2004; 42–43: 195-209.

[4] De Oliveira Neto N. A Niels Bohr-like atomic model for planetary orbit description. Ciência e Cultura (Journal of the Brazilian Association for the Advancement of Science), 1996; 48: 166–171.

[5] Agnese AG, Festa R. Clues to discretization on the cosmic scale. Physics Letters A, 1997; 227: 165-171.

[6] Agnese AG, Festa R. Discretizing $\upsilon$-Andromedae planetary system. astro-ph/9910534, v2, 1999.
[7] Rubčić A, Rubčić J. The Quantization of the solar-like gravitational systems. Fizika B, 1998; 7: 1-13.
[8] Hayes W, Tremaine S. Fitting selected random planetary systems to Titius-Bode laws. Icarus, 1998; 135: 549-557.
[9] Lynch P. On significance of the Titius–Bode law for the distribution of the planets. Monthly Notices of the Royal Astronomic Society, 2003; 341: 1174-1178.
[10] Greenberger DM. Quantization in the Large. Foundations of Physics, 1983; 13: 903-951.
[11] Carvalho JC. On Large-Scale Quantization. Lettere al Nuovo Cimento, 1985; 6: 337-342.
[12] Nelson E. Derivation of the Schrödinger Equation from Newtonian Mechanics. Physical Review, 1966; 4: 1079-1085.
[13] El Naschie MS, Rossler E, Prigogine I. Quantum Mechanics, diffusion and chaotic fractals. Oxford: Pergamon Press, 1995.
[14] Smolin L. Atoms of space and time. Scientific American (Czech edition), 2004; 22–25: 124-129.
[15] Laskar J. A numerical experiment on the chaotic behaviour of the Solar System. Nature, 1989; 338: 237–238.
[16] Sussman GJ, Wisdom J. Chaotic evolution of the Solar System. Science, 1992; 257: 56–62.
[17] De Oliveira Neto M, Maia LA, Carneiro S. An alternative theoretical approach to describe planetary systems through a Schrödinger-type diffusion equation. Chaos, Solitons and Fractals, 2004; 21: 21-28.

Table 1. Predicted distances of bodies from the Sun

| Body | $k$ | $l$ | $r_{kl}$ [AU] |
|---|---|---|---|
| — | $\frac{1}{2}$ | 0 | 0.055 |
| Mercury | $\frac{3}{2}$ | 1 | 0.332 |
| Mercury | $\frac{3}{2}$ | 0 | 0.387 |
| Venus | $\frac{5}{2}$ | 2 | 0.829 |
| Earth | $\frac{5}{2}$ | 1 | 0.995 |
| Earth | $\frac{5}{2}$ | 0 | 1.050 |
| Mars | $\frac{7}{2}$ | 3 | 1.548 |
| Hungaria | $\frac{7}{2}$ | 2 | 1.824 |
| Hungaria | $\frac{7}{2}$ | 1 | 1.990 |
| Hungaria | $\frac{7}{2}$ | 0 | 2.046 |
| Vesta | $\frac{9}{2}$ | 4 | 2.488 |
| Ceres | $\frac{9}{2}$ | 3 | 2.875 |
| Hygeia | $\frac{9}{2}$ | 2 | 3.151 |
| Camilla | $\frac{9}{2}$ | 1 | 3.317 |
| Camilla | $\frac{9}{2}$ | 0 | 3.372 |
| Jupiter | $\frac{11}{2}$ | 0 | 5.031 |
| — | $\frac{13}{2}$ | 0 | 7.021 |
| Saturn | $\frac{15}{2}$ | 0 | 9.343 |
| Chiron | $\frac{17}{2}$ | 0 | 11.997 |
| Chiron | $\frac{19}{2}$ | 0 | 14.982 |
| Uranus | $\frac{21}{2}$ | 0 | 18.300 |
| — | $\frac{23}{2}$ | 0 | 21.948 |
| HA2 (1992), DW2 (1995) | $\frac{25}{2}$ | 0 | 25.929 |
| Neptune | $\frac{27}{2}$ | 0 | 30.241 |
| — | $\frac{29}{2}$ | 0 | 34.885 |
| Pluto | $\frac{31}{2}$ | 0 | 39.861 |

Table 2. Bodies with stable circular orbits.

| Body | $k$ | $l$ | $r_{kl}$ [AU] |
|---|---|---|---|
| — | $\frac{1}{2}$ | 0 | 0.055 |
| Mercury | $\frac{3}{2}$ | 1 | 0.332 |
| Venus | $\frac{5}{2}$ | 2 | 0.83 |
| Mars | $\frac{7}{2}$ | 3 | 1.54 |
| Vesta | $\frac{9}{2}$ | 4 | 2.49 |
| Fayet comet | $\frac{11}{2}$ | 5 | 3.64 |
| Jupiter | $\frac{13}{2}$ | 6 | 5.03 |
| Neujmin comet | $\frac{15}{2}$ | 7 | 6.636 |
| — | $\frac{17}{2}$ | 8 | 8.46 |
| Saturn | $\frac{19}{2}$ | 9 | 10.5 |
| — | $\frac{21}{2}$ | 10 | 12.77 |
| Westphal comet | $\frac{23}{2}$ | 11 | 15.26 |
| Pons–Brooks comet | $\frac{25}{2}$ | 12 | 17.97 |
| Uranus | $\frac{27}{2}$ | 13 | 20.9 |
| — | $\frac{29}{2}$ | 14 | 24.055 |
| — | $\frac{31}{2}$ | 15 | 27.43 |
| Neptune | $\frac{33}{2}$ | 16 | 31.02 |
| — | $\frac{35}{2}$ | 17 | 34.84 |
| Pluto | $\frac{37}{2}$ | 18 | 38.88 |
| — | $\frac{39}{2}$ | 19 | 43.134 |

Table 3. Moons of Jupiter with stable circular orbits.

| Body | $k$ | $l$ | $r_{kl}$ [km] |
|---|---|---|---|
| — | $\frac{1}{2}$ | 0 | 6287 |
| — | $\frac{3}{2}$ | 1 | 37722 |
| Halo ring | $\frac{5}{2}$ | 2 | 94305 |
| Outer ring | $\frac{7}{2}$ | 3 | 176036 |
| — | $\frac{9}{2}$ | 4 | 282915 |
| Io | $\frac{11}{2}$ | 5 | 414942 |
| Europa | $\frac{13}{2}$ | 6 | 572117 |
| — | $\frac{15}{2}$ | 7 | 754440 |
| — | $\frac{17}{2}$ | 8 | 961911 |
| Ganymede | $\frac{19}{2}$ | 9 | $1.19\times10^6$ |
| — | $\frac{21}{2}$ | 10 | $1.452\times10^6$ |
| Callisto | $\frac{23}{2}$ | 11 | $1.735\times10^6$ |

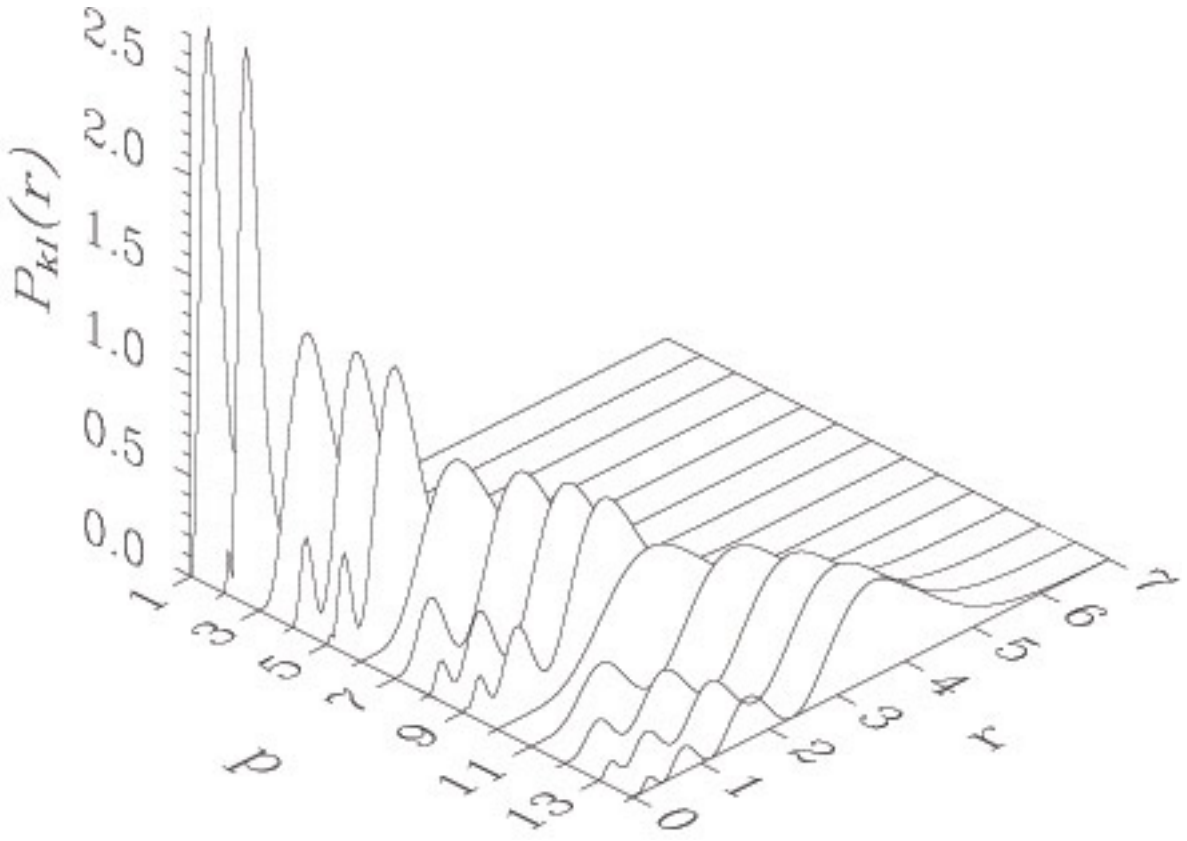


Figure 1: Probability densities for a particle in states with quantum numbers $k$, $l$, which correspond, respectively, ($p$ is an ordinary number) to Mercury ($p = 1$, $l = 1$), Mercury ($p = 2$, $l = 0$, the second possibility), Venus ($p = 3$, $l = 2$), Earth ($p = 4$, $l = 1$), Earth ($p = 5$, $l = 0$, the second possibility), Mars ($p = 6$, $l = 3$), asteroid Hungaria ($p = 7$, $l = 2$), asteroid Hungaria ($p = 8$, $l = 1$, the second possibility), asteroid Hungaria ($p = 9$, $l = 0$, the third possibility), asteroid Vesta ($p = 10$, $l = 4$), asteroid Ceres ($p = 11$, $l = 3$), asteroid Hygeia (p=12, $l = 2$), asteroid Camilla ($p = 13$, $l = 1$), and asteroid Camilla ($p = 14$, $l = 0$, the second possibility). Here $k \in \{\frac{3}{2}, \frac{5}{2}, \ldots, \frac{9}{2}\}$, the quantum number $k$ repeats $n(= k + \frac{1}{2})$ times and $r$ is measured in AU.

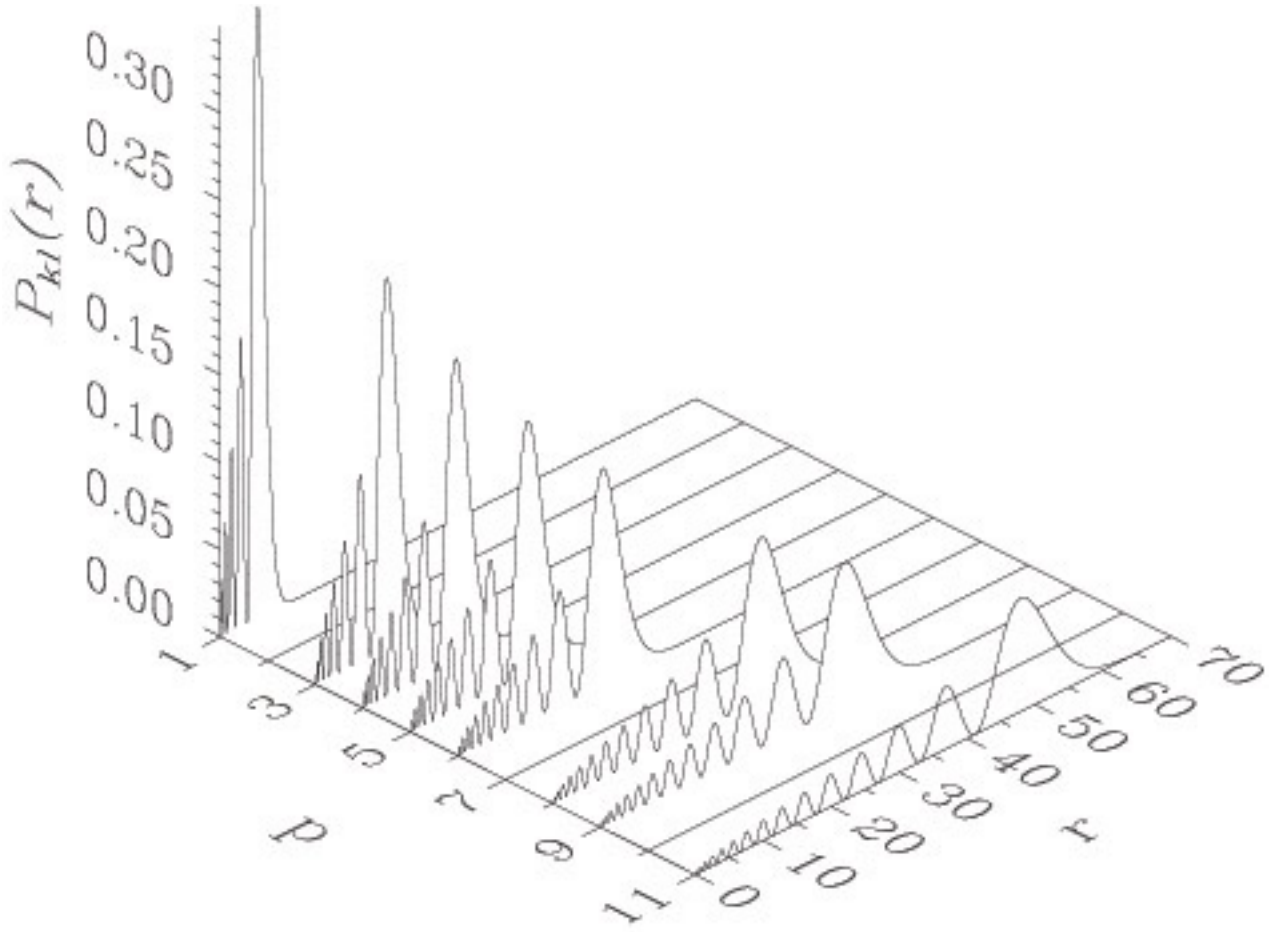


Figure 2: Probability densities for a particle in states with quantum numbers $k$, $l$, which correspond, respectively, ($p$ is an ordinary number) to Jupiter ($p = 1$), nothing ($p = 2$), Saturn ($p = 3$), Chiron ($p = 4$), Chiron ($p = 5$, the second possibility), Uranus ($p = 6$), nothing ($p = 7$), HA2 (1992), DW2 (1995) ($p = 8$), Neptune ($p = 9$), nothing ($p = 10$) and Pluto ($p = 11$), $k \in \{\frac{11}{2}, \frac{13}{2}, \ldots, \frac{31}{2}\}$, $l = 0$. Here $k = p + \frac{9}{2}$, $r$ is measured in AU.

# NANOTECHOLOGY &

# SEMICONDUCTOR NANODEVICES

Adel Helmy Phillips

Eng. Physics & Math. Department

Faculty of Engineering, Ain-Shams University

Abbasia, CAIRO, EGYPT

Email: adel_phillips@yahoo.com

Nanoscience and nanotechnology are advancing at a rapid pace and making revolutionary contributions in many fields including electronics, materials science, chemistry, biology, structures & mechanics, and optoelectronics [1]. Among these scientific and technological fronts, the most impressive progress has been made in the area of semiconductor technology. Semiconductor nano-structures have been enabled by the advancements in epitaxial growth techniques, which are now capable of growing epilayers as thin as one atomic layer and with interface roughness that area mere fraction of a monolayer [2, 3, 4]. Heterostructures at the nanometer scale such as quantum wells, quantum wires and quantum dots, have found robust applications in the generation, modulation, detection and processing of light.

Fundamental solid state physics has benefited greatly from the massive industrial research and development efforts towards the miniaturization of semiconductor devices, which allowed the fabrication of artificial structures or devices that exhibit new physical phenomena. These new phenomena occur as the structure size is decreased below some relevant physical length scale [2]. Examples of such phenomena and the associated length scales are quantum confinement and the Fermi wavelength, ballistic transport and the mean free path, quantum interference and the quantum mechanical phase coherence length. On these short length scales, the devices acquire neither unusual properties that are neither those of microscopic object (atoms and molecules) nor those of macroscopic systems. That is why the branch of physics devoted to the study of these effects in nanometer-sized systems at low temperatures has been called mesoscopic physics [5]. A universal feature

of mesoscopic systems is that the coherence length can be larger than the dimension of the device under study. With the help of sub-Kelvin cryogenic measurement equipment, electron coherent lengths of over 100 microns can be observed, well within the large of today's nanometer scale fabrication techniques [5]. In addition, low-density semiconducting systems can have conduction electrons with very large electronic wavelength up to approximately 50 nm. With electron beam lithography, one can pattern arbitrary shapes near the scale of one wavelength.

## Length Scales Characterizing Mesoscopic Systems :

In this section a brief account of lengths associated with mesoscopic systems [2] will be introduced.

(1) Fermi Wavelength: One important length scale characterizing mesoscopic systems is the Femi wavelength. In semiconductors such as two-dimensional systems realized in GaAs/AlGaAs heterostructures, the Fermi wavelength $\lambda_F \approx$ 40 nm for electron concentration $n \approx 3 \times 10^{11}$ $cm^{-2}$. This Fermi wavelength is large comparable to the system dimensions.

(2) Mean Free Path: It is the average length covered by an electron before being scattered into a different wave vector direction. At very low temperature, the transport of electrons is determined by electrons in the vicinity of the Fermi energy $E_F$, that is, the mean free path $\ell$ is expressed as:

$$\ell = v_F \tau \qquad (1)$$

where $v_F$ is the Fermi velocity and $\tau$ is the relaxation time.

(3) Phase Coherence Length: In real semiconductors, electrons interact with many others and exchange their energies. For example, the electron moves from one eigen-state to another due to scattering from other electron or lattice vibrations. The phase of the electron is destroyed by such dynamical interactions and the distance over which an electron maintains its phase memory is called the phase

coherence length. For the phase relaxation time $\tau_\phi$ determined by inelastic scattering, the phase coherence length is given by

$$L_\phi = \sqrt{D\tau_\phi} = \ell\sqrt{\frac{\tau_\phi}{\tau}} \qquad (2)$$

where D is the diffusion coefficient. Eq.(2) is valid for diffusive regime. In the diffusive regime the electrons make random walk on a scale larger than the mean free path.

The phase coherence length $L_\phi$ in the ballistic regime is given by:

$$L_\phi \approx v_F \tau_\phi \qquad (3)$$

The ballistic regime is characterized as the system dimension is smaller than the mean free path.

Rapid progress in nano-scale fabrication technology (nanotechnology) has enabled us to make various types of semiconductor devices using quantum dots. Quantum dots are small regions defined by tailor-made confining potentials in semiconductor materials, in which the number of electrons can vary between one and several hundred and whose size is comparable to the Fermi wavelength of the electrons.

**Two-Dimensional Electron Gas (2DEG) and Quantum Dots:** Devices fabricated from semiconductor 2DEGs enable the direct manipulation and control of electron wave functions. This is due to both the large electronic wavelength, and more importantly, to a MOSFET-like structure in which metal gates situated directly above the 2DEG are able to deplete it. Fig.1 shows a wide view of heterostructure, with both contacts to the 2DEG [2] and a depletion gate. Since the 2DEG is typically 50 to 200 nm below the surface of the crystal and gates, there is a lateral resolution limit on the ability to control and pattern the electron gas. In practice one can control the wave-function only to within a few wavelengths in a completely arbitrary way.

A perspective quantum dot formed using depletion gates is shown in the bottom Fig.1 [6]. The 2DEG lies just under the surface. Two openings allow current to pass through the device is the fundamental means by which it is probed. In different regimes of operation, one can resolve information about energy, wave-function intensity, and aggregate trajectory interference with conductance measurements.

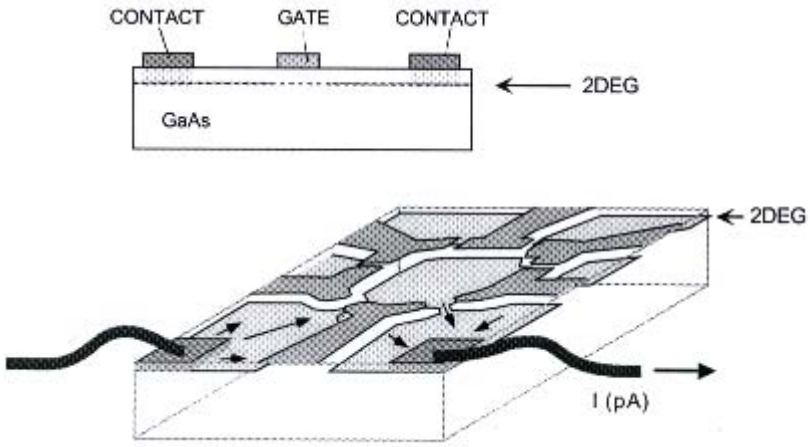


Fig.1. Side and perspective view of gated quantum dot structure.

Fig.2 shows the band structure which supports the 2DEG [2]. Starting at the wafer surface the GaAs cap passivates the surface from oxidation, the n-doped region provides carriers to occupy the quantum well, and the AlGaAs spacer keeps the donor sites away from the well, enhancing mobility. The 2DEG itself is defined by quantum well formed at the interface of the AlGaAs and the bulk GaAs. The 2DEG system created at this interface is very useful experimentally because, in addition to the large scale electron wavelength, GaAs and AlGaAs are almost perfectly lattice matched. As a result if the crystal is grown carefully, there are few of the normal interfacial defects due to lattice mismatch, and the mean free path can be over 100 microns, limited only by the presence of nearly dopants (donor impurities). It is convenient that $Al_xGa_{1-x}As$ has a simple band structure for mixture ratio $x<0.4$[6, 7], with a circular Fermi-

surface. Thus, the quasiparticles in the 2DEG behave like electrons, with only an effective mass distribution [6, 7].

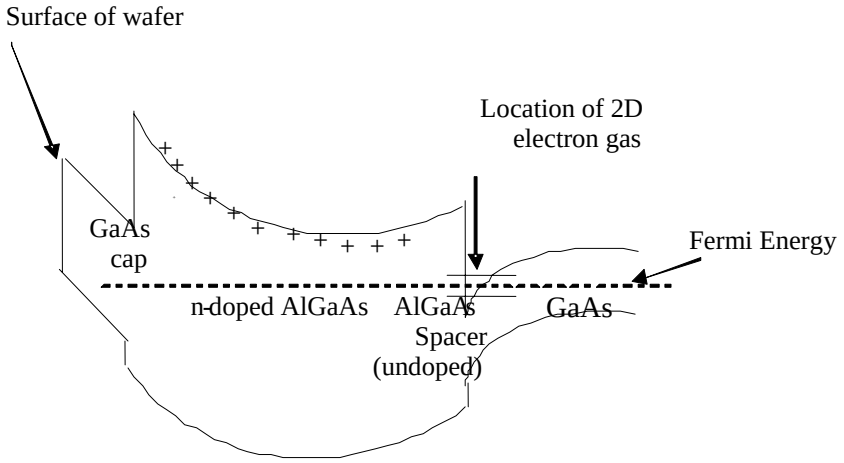


**Fig. 2. Band diagram of a GaAs/AlGaAs heterostructure created to support a high -mobility two -dimensional electron gas.**

We begin by introducing what QDs are [6, 7]. QDs consist of nano-scale crystals from a special class of semiconductor materials, which are crystals, composed of chemical elements in the periodic groups II-VI, III-V, or IV-IV. The size of QDs ranges from several to tens of nanometers in diameter, which is about 10–100 atoms. A QD can contain from a single electron to several thousand electrons since the size of the quantum dot is designable. QDs are fabricated in semiconductor material in such a way that the free motion of the electrons is trapped in a quasi-zero-dimensional “dot.” Because of the strong confinement imposed in all three spatial dimensions, QDs behave similarly to atoms and are often referred to as artificial atoms. When a free electron is confined by a potential barrier, its continuous spectrum becomes discretized. In particular, the gap between two neighboring energy levels increases as the length where the free electron moves decreases. A similar thing happens in solid state. If the motion of electrons in the conduction band or that of the hole in the valence band is limited in a small region with a scale such as the de Broglie wavelength or a phase-coherence length, then the conduction band or the valence band is split into subbands or discrete levels depending on the dimensionality of the confined structure, such is the case when a material with a lower bandgap is confined within a material with a higher bandgap. More efficient recombination of electron-hole pairs can be achieved by incorporation of a thin layer of a

semiconductor material, with a smaller energy gap than the cladding layers, to form a double heterostructure. As the active layer thickness in a double heterostructure becomes close to the de Broglie wavelength or the Bohr exciton radius for lower dimensional structures, and as the motion of the electron is restricted within such a very small regime, energy quantization or momentum quantization is observed and quantum effects become apparent. Therefore, the electron states are not continuous but discrete. This phenomenon is known as the *size quantization effect*.
There are two approaches to fabricate nano-scale QDs [8]: *top-down* and *bottom-up*. Semiconductor processing technologies, such as metal organic chemical vapor deposition, molecular beam epitaxy and e-beam lithography, etc. are used in the top-down approach. Surface and colloid chemistry such as self-assembly, vapor liquid- solid techniques are used in the bottom-up approach.

Quantum dots are suitable devices to study the interplay of classical charging effects and quantum confinement. These quantum dots are defined in a 2DEG formed within a heterostructure of the semiconductor materials. The 2DEG has a high electron mobility and low electron density [6, 7, 8, 9]. The low electron density results in a large Fermi-wavelength, and a large screening length, enabling to vary the 2DEG density with an electric field. Lithographically defined semiconductor quantum dots have the shape of a disk with a diameter as small as 50-100 nm, becoming of the same order of magnitude as the Fermi-wavelength. By attaching current and voltage probes to a quantum dot, it is possible to measure its electronic properties.

In the following discussion, two main important assumptions are made. **First**, the coulomb interactions among electrons in the dot, and between electrons in the dot and those in the environment are parameterized by a single, constant capacitance, C. This capacitance can be thought of as the sum of the capacitance between the dot and left lead (source), $C_\ell$, the right lead (drain), $C_r$, and the gate. $C_g$,:

$$C = C_\ell + C_g + C_r.$$

**Second**, the discrete energy spectrum can be described independently of the number of electrons on the dot.

Using these assumptions, known as the constant interaction model [6, 7], the total energy of an N-electron quantum dot with the source-drain voltage, V, applied to the left lead, and the right lead grounded, is given by [6, 7].

$$U(N) = \frac{[-|e|(N - N_o) + C_\ell V + C_g V_g]^2}{2C} + \sum_{n=1}^{N} E_n(B) \qquad (4)$$

where $-|e|$ is the electron charge and $N_o$ is the number of electrons in the dot at zero gate voltage, which compensates the positive background charge originating from the donors in the heterostructure. The term $C_\ell V$ and $C_g V_g$ can change continuously and represent the charge on the quantum dot that is induced by the bias voltage through the capacitance, $C_\ell$ and by the gate voltage, $C_g$,. The term $\{\sum_{n=1}^{N} E_n(B)\}$ is a sum over the occupied single particle energy levels $E_n(B)$, which are separated by an energy

$$\Delta E_n = E_n - E_{n-1} \qquad (5)$$

The energy levels $E_n(B)$ are measured from the bottom of the conduction band and depend on the characteristics of the confinement electron potential. Note that, within the constant interaction model, only these single-particle states depend on magnetic field, *B*,.

The minimum energy for adding $N^{\underline{th}}$ electron to the quantum dot is by definition the electrochemical potential of the dot [6]:

$$\mu_{dot}(N) \equiv U(N) - U(N-1)$$
$$= (N - N_o - \frac{1}{2})E_c - \frac{E_c}{|e|}(C_\ell V_\ell + C_g V_g) + E_N, \quad (6)$$

where $E_c = e^2/2C$ is the charging energy. The first two terms describe the electrostatic contribution, $-|e|\Phi_N$ with $\Phi_N$ the electrostatic potential of the $N^{\underline{th}}$ electron dot. The last term, $E_N$, represents the chemical contribution. Hence, $\mu_{dot}(N)$ can be expressed as:

$$\mu_{dot}(N) = -|e|\Phi_N + \mu_{ch}(N), \quad (7)$$

Electron transport through the quantum dot is possible when $\mu_{dot}$ lies between $\mu_\ell$ and $\mu_r$ of the leads, that is

$$\mu_\ell \geq \mu_{dot} \geq \mu_r, \quad (8)$$

With Fig.(3), we have

$$-|e|V = \mu_\ell - \mu_r \quad (9)$$

The electrochemical potential for adding the next electron $\mu_{dot}(N+1)$, is separated from $\mu_{dot}(N)$ by the addition energy, $E_c + \Delta E$, which is higher than $\mu_\ell$ so that the $(N+1)^{\underline{th}}$ electron can not enter the dot. In this configuration the number of the electrons on the quantum dot, N, is fixed and transport through the dot is blocked (Coulomb Blockade) [10](see Fig. (3)). The electrostatic potential of the quantum dot is $-|e|\Phi_N$. The addition of the $(N+1)^{\underline{th}}$ electron is allowed, since $\mu_{dot}(N+1)$ lies within the applied bias voltage. In this configuration the number of electrons on the quantum dot alternates between N and N+1 resulting electron transport through the dot.

In the linear transport regime (V~0), the $N^{th}$ Coulomb peak is a direct measure of the lowest possible energy state of the N-electron quantum dot, i.e., the ground state electrochemical potential.

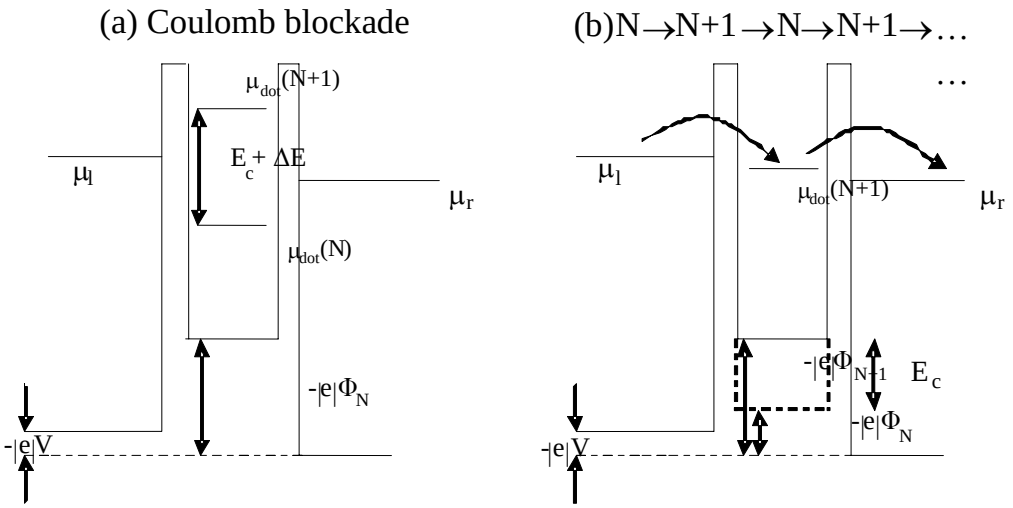


**Fig. (3) Schematic diagram of the potential landscape of a quantum dot.**

The change in electrochemical potential when the fixed voltages an electron is added to the dot, is called the addition energy and is given by:

$$\begin{aligned}\Delta\mu_{dot}(N) &= \mu_{dot}(N+1) - \mu_{dot}(N) \\ &= U(N+1) - 2U(N) + U(N-1) \\ &= E_c + \Delta E.\end{aligned} \qquad (10)$$

The addition energy consists of a purely electrostatic part, the charging energy, $E_c$, and the energy spacing between two discrete quantum levels, $\Delta E$. Note that in the case those two electrons are added to the same (spin) degenerate level.

An electron tunneling onto the dot leads to an increase of the electrostatic energy by the charging energy $E_c = e^2/2C$. The charging energy becomes important when it exceeds the thermal energy, $k_BT$, and when the barriers are sufficiently opaque such that the electrons are located either in the reservoirs or in the dot.

**Single Electron Devices:** The necessary nanofabrication techniques have become available during recent years, and have made possible a new field of mesoscopic physics, single electronics [11, 12]. Recent developments in nanotechnology allow us to control and measure single electron transport very accurately. An electron pump device, which carries exactly one electron during one cycle of voltage modulation, is considered a possible current standard with extremely high accuracy. A single electron device has extremely high charge sensitivity (about$10^{-5}$electrons/$\sqrt{Hz}$) a small quantum dot. This device would detect individual electron transport of a current on the order of a few nA. So electron transport through a such quantum dot, known as single electron tunneling. An electron that has entered the quantum dot leaves it before another electron is allowed to enter.

## Coulomb Blockade and Single Electron Tunneling:

Let us consider a quantum dot connected to the source and drain electrodes via tunneling barriers and connected to a gate electrode with small capacitor [6, 13] (see Fig.(4)).

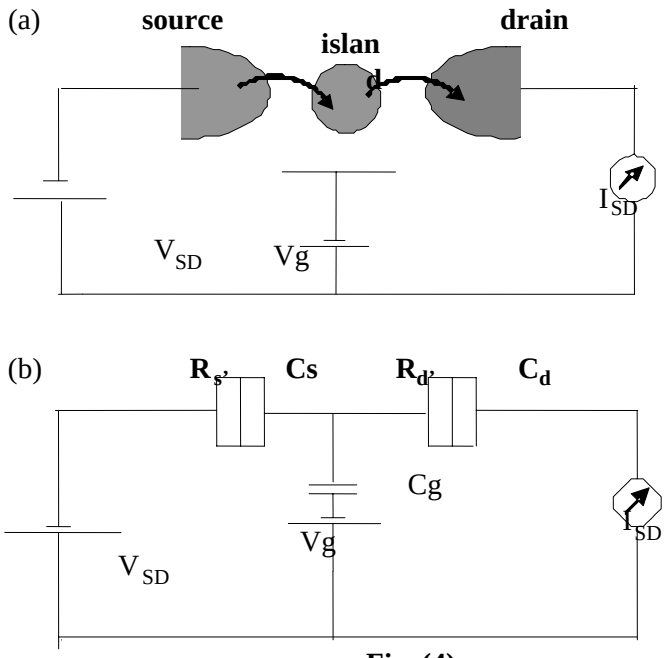
(a)
source
islan
d
drain
$I_{SD}$
$V_{SD}$
Vg
(b)
$R_{s'}$
Cs
$R_{d'}$
$C_d$
Cg
Vg
$I_{SD}$
$V_{SD}$

**Fig. (4)**

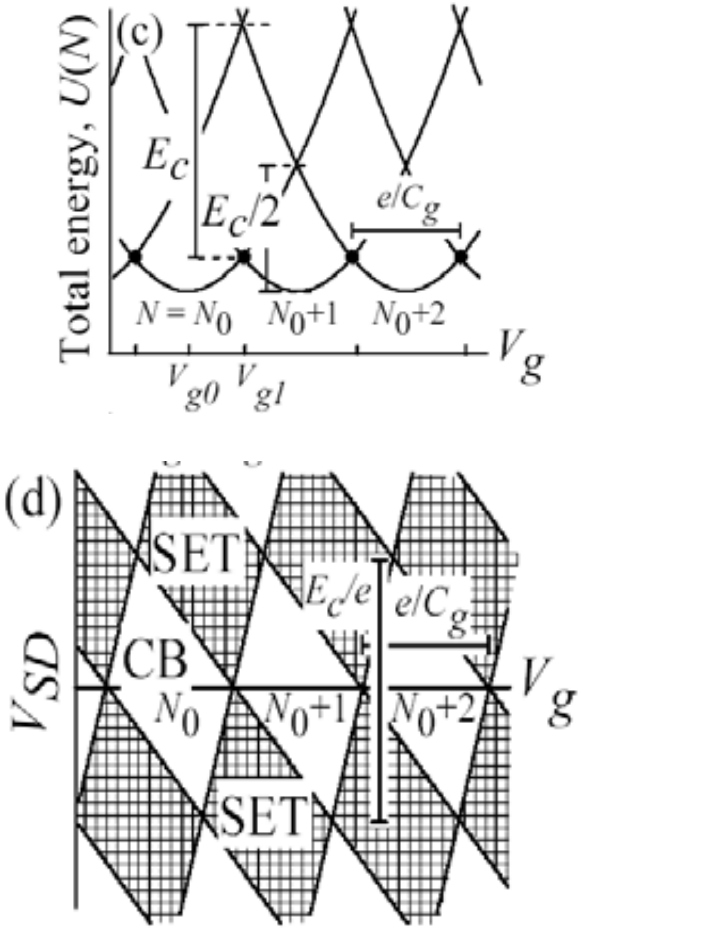
(c)
Total energy, U(N)
$E_C$
$E_C/2$
$e/C_g$
$N = N_0$
$N_0+1$
$N_0+2$
$V_g$
$V_{g0}$
$V_{g1}$
(d)
SET
$E_C/e$
$e/C_g$
CB
$V_{SD}$
$N_0$
$N_0+1$
$N_0+2$
$V_g$
SET

Fig.(5)

Assuming zero bias voltage is applied between the source and drain electrodes, $V_{SD} = 0$. The total energy U (N) of the system is given by Eq. (4), which changes with Vg as shown in Fig. (5), the number of electrons, N, is determined to minimize the total energy and therefore becomes a well defined integer. The energy gap to neighbor charge states can be maximized to ($e^2/2C$), for instance, at $V_g = V_{g0}$. When excitation energies, such as thermal energy, are much smaller than this energy, an electron can neither enter nor leave the quantum dot. Therefore, transport through the quantum dot is blocked (Coulomb blockade). The energy gap can be made zero by adjusting the gate voltage at $V_g = V_{g1}$ (see Fig.(5)), where n can fluctuate between $N_0$ and $N_0+1$ only by one, but not more than one. This means that electrons tunnel trough the quantum dot one by one. This single electron tunneling scheme is maintained unless the excitation energy exceeds the charging energy. The Coulomb blockade and single electron tunneling appear alternately by sweeping the gate voltage with a period given by $e/C_g$ (Coulomb blockade oscillation). When the source-drain, $V_{sd}$, is applied, the Coulomb blockade region shrinks and single electron tunneling expands as shown in the charging diagram of Fig.(5d). The maximum width of a Coulomb blockade diamond region is given by $E_c/e$ in the $V_{sd}$ direction and $e/C_g$ in the $V_g$ direction. The Coulomb blockade and single electrons in the dot, N, can be controlled by changing $V_{sd}$ or $V_g$.

**Radio Frequency Single-Electron Transistor(RF-SET):** It works as a wide-band and highly sensitive electrometer, is a SET combined with an impedance transformer (LC resonator)[13]. The capacitance of the problem can be cancelled by an external inductor located close to the SET device, if it is operated at the resonant frequency, $f_{res}$. The maximum frequency of the RF-SET is approximately given by $f_{res}/Q_{LC}$, where $Q_{LC}$ is

the quality factor of the resonator. The external LC resonator placed close to an SET device has a typical bandwidth of about 100MHz with $f_{res}$~1GHz and $Q_{LC}$~10. Better performance (higher $f_{res}$ and larger $Q_{LC}$) may be obtained using an on-chip resonator. The conductance of the SET is measured by the reflection or the transmission of the rf-carrier signal at $f_{res}$ [14, 15]. The transmission amplitude or the small change in the reflected signal is, in principle, proportional to the admittance of the SET [15]. The sensitivity of a charge respective to the quantum dot can be about $10^{-5}$. $e/\sqrt{Hz}$, which is usually restricted by the noise of the high frequency amplifier. This means that the intrinsic noise of the RF-SET (shot noise) is very low at high frequency (>10 KHz), which it suffers from 1/f noise at low frequency. Theoretically, the noise of the RF-SET is expected to be very close to that of the conventional SET [16]. The charge sensitivity can be as low as $2*10^{-6}e/\sqrt{Hz}$ for an optimized device using practical superconductivity quantum dot and better sensitivity is expected by using a smaller quantum dot [13].

**Applications of the Single-Electron Transistor(SET):** Because of its small size, low energy consumption and high sensitivity, SET has found many applications in many areas, for example:

(a) Single electron memory [17].
(b) High sensitivity electrometer [18, 19].
(c) Microwave detection [20, 21].
(d) Quantum information processing [22].

**Photon Assisted Tunneling(PAT):** When the modulation frequency exceeds the tunneling rate, a quantum mechanical description of the system is required in order to understand the non-adiabatic transport characteristics. The Tien-Gordon theory [23] explains very well the I-V characteristics of the Josephson junctions and other tunneling devices like

resonant tunneling structures and superlattices in the presence of microwaves, millimeter waves, THz waves, and far infrared light [24, 25, 26, 27]. A microwave, with photon energy of 4-20μeV is often used as a coherent photon source. Application of a microwave on a gate or source-drain electrodes induces photon assisted tunneling on the two tunneling barriers. The photon tunneling from the continuum density of states in the electrode to a discrete energy state in quantum dot produces a pumping current. A broad pumping current with a width corresponding to the photon energy appears in the vicinity of the SET current peak. When a microwave is properly applied to modify the potential of the quantum dot, coherent tunneling through one of the photon side-bands is expected. An electron can tunnel into the dot by absorbing one photon through one barrier, and simultaneous by tunnel out from the quantum dot by emitting one photon through the other barrier. Distinct resonant PAT current peaks have been observed [28], indicating a coherent PAT process. In this case, the PAT current peaks are separated from the SET current peak by the photon energy. Furthermore, when the photon energy is made higher than the energy spacing in the quantum dot, one can excite inner electron in the quantum dot to the reservoir. When a sinusoidal voltage, $V(t)=V_0 \sin(\omega t)$, is applied across a tunneling barrier, the wave function can be written as a superposition of a series of photon's sidebands as:

$$\Psi(x,t) = \Psi_0(x,t) \sum_{n=-\infty}^{\infty} J_n(\alpha) \exp(-in\omega t), \qquad (11)$$

where $J_n(\alpha)$ is the $n^{th}$ order Bessel function of the first kind, $\alpha \equiv eV_0/(\hbar\omega)$ is the normalized modulation amplitude, and of the first kind, $\Psi_0(x,t)$ is the original stationary wave function in the absence of sinusoidal voltage. The energies of the photon sidebands are separated by the photon energy

ħω, and the amplitude of each wave function is proportional to $J_n(\alpha)$. Therefore, the photon-assisted tunneling can be considered as a normal tunneling process to one of the photon side bands. The effective tunneling rate to the $n^{th}$ sideband state is given by:

$$\Gamma_n(E) = J_n^2(\alpha)\Gamma(E \pm n\hbar\omega), \qquad (12)$$

where Γ is the original tunneling rate in the absence of modulation. The subscript n = ±1,±2,±3,…….corresponds to the tunneling with n > 0 photons absorption and emission for n < 0.

We shall now shed some light on only one of the applications of single electron transistor (SET), which is *single photon detector in microwave range.*

**Single-Photon Detector in Microwave Range:** The sub-millimeter wave through the far-infrared region of the electromagnetic spectrum contains a variety of important spectra of various types of matter, such as the energy levels of semiconductor nanostructures, and the energy gaps of superconductors. An SET can sense a single-photon if the photon is converted to a charge through an appropriate excitation mechanism. The SET consists of double quantum dots. It is fabricated on a high mobility modulation doped GaAs/AlGaAs heterostructure with a 2DEG.Metal gates are deposited on top of the crystal. Such SET can detect a single photon in the sub-millimeter wave range ( ν= 500 ±90 GHz)[29].

**Quantum Dot Turnstile:** Because of the Coulomb blockade the current through a quantum dot is limited to one electron at a time. This property can be exploited to create an electron turnstile, a device which passes an electron in every cycle of an external driving field. Such a device was first realized by Geerligs and Co-workers [30] using a series of metal-

dots. Electrons are moved one at a time through the quantum dot by two sinusoidal signals applied to the two tunneling barriers, 180 degrees out of phase. The rf-frequency of the applied signal, f= 10MHz, is much slower than the tunneling rate of electrons on and off the dot when the barriers are low. The driving signal is therefore in adiabatic limit in which the state of the dot is fully determined by the electrochemical potential on the side of the low barrier.

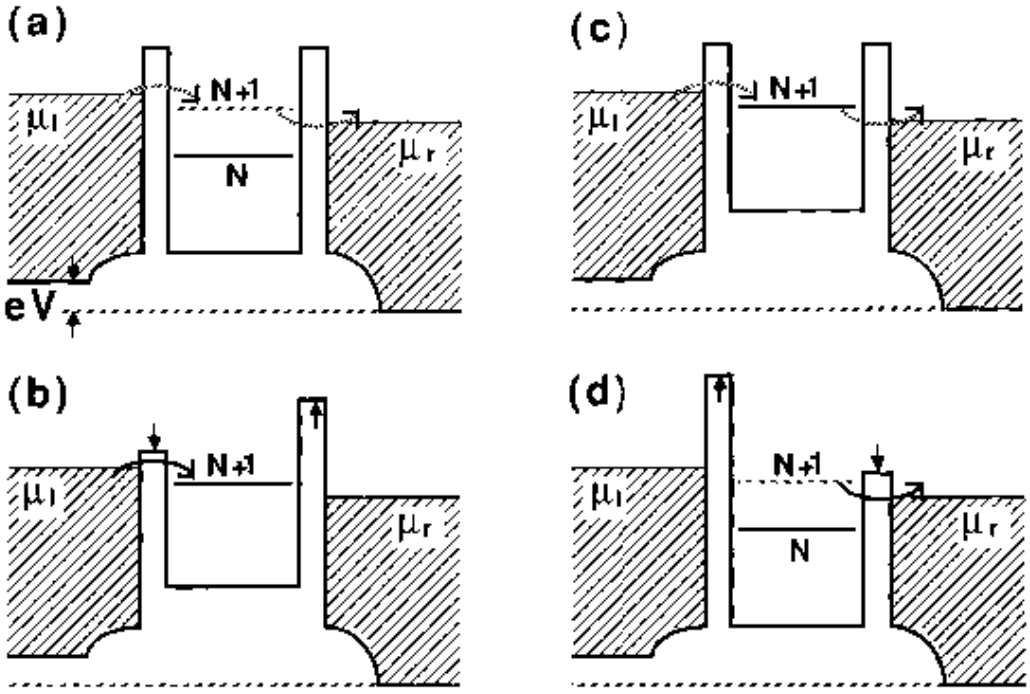


Fig.(6) Schematic potential landscape for a quantum-dot turnstile

As depicted in (Fig (6)), in one cycle exactly one electron is transferred across the quantum dot: the cycle begins with N electrons on the dot. The barrier to the left lead is then lowered allowing an additional electron to enter the dot. The barrier to the left is then raised, providing the extra electron from escaping back to the left. The right barrier is then lowered and the electron escapes into the right lead. Raising the barrier to the right lead completes the cycle and returns the quantum dot to its initial configuration with N-electrons. By applying a larger source-drain bias to

increase the number of extra electrons allowed on the dot when the left barrier is lowered, two electrons, or three electrons, and so on, can be transferred in each cycle. As a result the time averaged current through the dot is just an integer times the signal electron charge times the driving frequency, I=nef, leads to a current quantization [31]. Each plateau corresponds to an integer number of electrons passing through the dot in each cycle.

The influence of time-varying fields on the transport through a mesoscopic device has been investigated [32a,b]. This mesoscopic device is modeled as a quantum dot coupled to superconducting reservoirs via quantum point contact. The effect of a magnetic field and the Andreev reflection process were taken into account. The conductance was deduced by using Landuaer–Buttiker equation. The main conclusion from these results is that the present mesoscopic device could be operated as a single-electron transistor in which the transfer of single electrons through the quantum dot might be controlled by applying a gate voltage. The results [32a,b] have valuable potential applications in the field of nanotechnology, e.g., photo-electron devices.

Also, the conductance and the time-averaged current of a quantum dot turnstile device [33,34] are deduced using the Landauer-Buttiker formula. The model proposed is: a quantum dot coupled to two superconducting reservoirs via two asymmetric tunnel barriers. These tunnel barriers are modulated by external radio frequency (rf) signals. The heights of the barriers are different and each of width, *a*, (see Fig.7). This model of mesoscopic device gives us some insight into how the Coulomb interaction and exchange, combined with an appropriate time dependent field, affect the success of the turnstile.

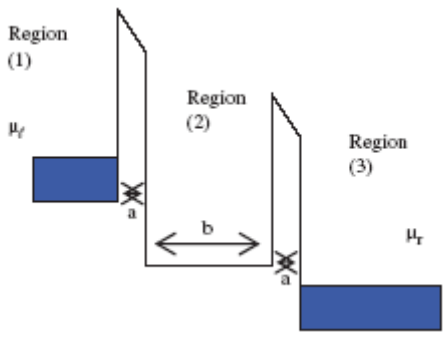


Fig.(7)

The proposed turnstile device might be useful in future quantum information applications and other applications in the field of nanoelectronics.

**Solar Cells and Photovoltaic:** Photovoltaic solar cells are used to directly convert light energy into electricity, and have been available for many years; major applications like solar panels on satellites made them famous, and smaller uses like calculator or watch energy supply. They are based on the photovoltaic effect, which allows the conversion of light (photons) to electricity (electrons). Photovoltaic solar cells already have a large number of applications in addition to the potential for many more, particularly in the energy, communications, military, and space industries. Quantum dot (QD) solar cells have the potential to increase the maximum attainable thermodynamic conversion efficiency of solar photon conversion up to about 66% by utilizing hot photogenerated carriers to produce higher photovoltages or higher photocurrents. In recent years it has been proposed [35, 36, 37, 38, 39, 40], and experimentally verified in some cases [41], that the relaxation dynamics of photogenerated carriers may be markedly affected by quantization effects in the semiconductor (i.e., in semiconductor quantum wells, quantum wires, quantum dots, superlattices, and nanostructures). That is, when the carriers in the semiconductor are confined by potential barriers to regions of space that are smaller than or comparable to their de Broglie wavelength or to the Bohr radius of excitons in the semiconductor bulk, the hot-carrier cooling rates may be dramatically reduced, and the rate of impact ionization could become competitive with the rate of carrier cooling [41].

**Quantum Dot Solar Cell Configurations:** Photoelectrodes composed of quantum dot arrays. In this configuration, the QDs are formed into an ordered 3-D array with inter-QD spacing sufficiently small such that strong electronic coupling occurs and minibands are formed to allow long-range electron transport. The system is a 3-D analog to a 1-D superlattice and the miniband structures formed therein [42]**.** The delocalized quantized 3-D miniband states could be expected to slow the carrier cooling and permit the transport and collection of hot carriers to produce a higher photopotential in a PV cell or in a photoelectrochemical cell in which the 3-D QD array is the photoelectrode [43]. Also, impact ionization might be expected to occur in the QD arrays, enhancing the photocurrent. However, hot-electron transport/collection and impact ionization cannot occur simultaneously; they are mutually exclusive and only one of these processes can be present in a given system.

Recently several design schemes have been proposed to increase the power conversion efficiency of photovoltaic devices. By using two or more p-n solar cell junctions, tandem cells made of different semiconductors; a multi-heterojunction design yields a better match to the

solar spectrum than a single-junction cell and may provide the efficiency of conversion greater than 50%. In fact, two-junction solar cells have been fabricated using *GaAs* and *InP* semiconductor allows which provides the highest power conversion efficiency [44]. Taking into account the recent advances in different optoelectronic devices[44], it would also seems appropriate to consider whether low dimensional (such as quantum dot) p-i-n structure could provide a new approach to the high efficiency solar cell problem. A theoretical model is presented for a practical p-i-n QD solar cell [44] built on the base of the self-organized *InAs*/*GaAs* system. The effective band gap for absorption $E_{eff}$ will be determined by the lowest confined states of QD s. High internal quantum efficiency for the collection of carriers' photoexcited in the QD s can occur as a result of channeling the electrons and holes through the coupling between aligned QD s. This effect allows one to separate and inject the generated electrons and holes in QD s, into an adjacent p- and n-regions with high efficiency. By changing the deposition mode one can change the size and shape of the *InAs* islands. Typically the dot size is around 10 *nm* and dot area densities range between $2.10^{10}$ $cm^{-2}$ and $10^{11}$ $cm^{-2}$. The dot layers are separated by 5÷10 *nm* barrier layer and the real dot density in the active i-region can be ~$10^{17}$ $cm^{-3}$.

**Quantum Dots and Tunable Bandgap** The first advantage derived from the use of quantum dots stems from their tunable bandgap, which allows evident to control the wavelength at which they will absorb or emit radiation. It is established that the greater the bandgap of a solar cell semiconductor, the greater the output voltage provided towards electricity generation. On the other hand, it is established that a lower bandgap results in a higher output of current for electricity generation, at the expense of a lower output voltage. Both high currents and voltages are desired for efficient solar-electric conversion. Thus, there exists an optimum bandgap that corresponds to the highest possible solar-electric energy conversion. Traditional semiconductor devices have bandgaps that are not altered cheaply or easily, and cannot absorb preferentially in one region of the spectrum. Quantum dots, on the other hand, can be designed specifically to absorb preferentially in a part of the spectrum specified by our desire. Therefore, quantum dots provide a much more exact method of matching the bandgap of the solar cell material to the optimum bandgap for energy conversion, resulting in greater efficiencies.

**Spintronics:** Spintronics is spin-based electronics with a spin degree of freedom added to the conventional charge-based electronic devices.

Electrons have a half spin angular momentum, that is, there are two states of electron spin: spin-up and spin-down. Spintronics distinguishes spin-up electron current from spin-down electron current while charge-based electronics does not. Therefore, electron spin can be made to carry information in spintronics. Spintronics is a type of device that merges electronics, photonics and magnetism. It is currently developing at a rapid pace. Most recently, in particular after the advent of magnetic semiconductors [45, 46], a new level of control of the spin-dynamics has been achieved. Very long spin lifetime [47] and coherence [48] in semiconductors, spin coherence transport across interfaces [49], manipulation of both electronic and nuclear spins over fast time scales [50], and have been all already demonstrated. These phenomena, that collectively take the name of “spintronics” or “spin electronics” [51, 52, 53] open a new avenue to the next generation of electronic devices where the spin of an electron can be used both for logic and memory purposes. The advantages of these new devices would be nonvolatility, increased data processing speed, decreased electrical power consumption, and increased integration densities compared with conventional semiconductor devices [51]. The ultimate target is to go beyond ordinary binary logic and use the spin entanglement for new quantum computing strategies [54]. This will probably require the control of the spin dynamics on a single spin scale, a remote task that will merge spintronics with the rapidly evolving field of molecular electronics [55]. The magnetic materials principally used in spin electronics are soft ferromagnetic alloys of the late 3*d* metals. These serve as sources and conduction channels for the spin-polarized electrons, as well as magnetic flux paths and shields. Most progress has been made with sensors, ranging from simple position sensors and elements for nondestructive testing of ferrous metals to sophisticated miniature sensor elements in read heads for digital tape and disc recording where requirements are very demanding; high permeability is required with a sharp low-field switching response that extends to frequencies in the GHz range.

Tunneling magnetoresistance (TMR) in magnetic tunnel junctions (MTJs) has attracted much attention due to the possibility of its application in magnetic memories, magnetic field sensors and quantum computing devices [56, 57]. In a common MTJ, the TMR between two ferromagnetic electrodes separated by an insulator (superconductor or semiconductor) layer depends on the spin polarization of the ferromagnetic electrodes and spin dependent tunneling rates [45, 58].

Ferromagnetic Semiconductors: The semiconductor currently used in integrated circuits, transistors and lasers, such as Si and GaAs are nonmagnetic in which the carrier energy is almost independent of the spin direction. However, in nanostructures where a device approaches the

limits of miniaturization, exchange interactions have more pronounced effects and the presence of spin of electrons becomes more tangible. In magnetic semiconductors, which have both properties of magnetic materials and semiconductors can give rise to pronounced spin-related phenomena. Coexistence of ferromagnetism and semiconducting properties in diluted magnetic semiconductors (DMSs) has opened the prospect of developing devices which make it possible to combine the information processing and data storage in the same material [52]. In the magnetic semiconductors, the exchange interaction between the itinerant carriers in the semiconducting band and the localized spins on magnetic impurity ions leads to spectacular magneto-optical effects, such as giant Faraday rotation or Zeeman splitting. Among different types of DMSs, $Ga_{1-x}$ $Mn_xAs$ is one of the most suitable materials for use in spintronic devices. In this kind of materials, a fraction of the group-III sublattice is replaced at random by Mn ions which act as acceptors. According to the strong Hund coupling, the five 3d electrons in a $Mn^{2+}$ ion give rise to a localized magnetic moment. The DMSs based on III-V semiconductors, like $Ga_{1-x}Mn_xAs$ compounds, exhibit ferromagnetism with Curie temperature as high as 110 K for Mn doping of around x=0.053. The origin of ferromagnetism in the GaAs-based DMSs can be demonstrated through the p-d exchange coupling between the itinerant holes in the valence band of GaAs and the spin of magnetic impurities [52].

Quantum Computing using Spins in Quantum Dots: A number of proposals have been made for quantum computers using a single-electron spin state in quantum dots as quantum bits [57], since it offers a two – level system close to the ideal case and it has relatively long coherence time. To distinguish one quantum bit to be operated on from other quantum bit, the resonant frequency is shifted by, for example, applying a local magnetic field and this frequency is used for operation on the quantum bit. In a quantum computer proposed by Loss et al.[52], instead of subjecting the system to external electromagnetic waves, the temporal development of local exchange interactions between the target quantum dot and ferromagnetic materials is introduced by a gate allowing the spin to be manipulated. The use of semiconductor technology is thus advantageous in the way that it allows spin to be controlled electrically.

Recently, the authors [59] proposed a spintronic device in which a quantum dot is embedded in one arm of Aharonov-Casher ring. The results show that the spintronic device can be exploited for quantum information processing.

## References:


[1] Handbook of Nanostructured Materials & Nanotechnology, by Hari Singh Nalwa (editor) (Academic Press, 1th edition, August, 2001).

[2] S. Datta, "Electronic Transport in Mesoscopic Systems" (Cambridge University Press, 1995).

[3] D.K. Ferry and S. M. Goodnick, "Transport in Nanostructures" (Cambridge University Press, 1997).

[4] A.H.Phillips, “Mesoscopic superconductor- semiconductor quantum devices”, As invited speaker: 2nd International spring School on Current Activities of Materials Science” Sponsor Tohoku University and Assiut University, April 22-26, (2000) P.87, Assiut, Egypt.

[5] C.W.J. Beenakker and H. van Houten, "Quantum Transport in Semiconductor Nanostructures" in Solid State Physics, Vol.44, edited by H. Turnbull (Academic Press, San Diego, 1991).

[6] L.P. Kouwenhoven, C.M. Marcus, P.L. McEuen, S. Tarucha, R.M. Westerlet and N.S. Wingreen , "Electron Transport in Quantum Dots" in NATO-ASI Conference Proceedings ed. byL.P. Kouwenhoven, G. Scon, L.L. Sohn (Kluwer, Dordrecht, 1997).

[7] T. Ando, Y. Arakawa, K. Furuya, S. Komiyama and N. Nakashima in "Mesoscopic Physics and Electronics" ( Springer-Verlag, Berlin, Heidelberg, Germany,1998).

[8] D.Bimberg, M. Grundmann and N. N. Ledentsov, "Quantum Dot Heterostructures" ( Johm Wiley & Sons, 1999).

[9] R.C. Ashoori, Nature 379 (1996) 413.

[10] M.H. Devoret and H. Grabert, " Single Charge Tunneling, Coulomb Blockade Phenomena in Nanostructures" (Proceedings of a NATO Advanced Study Institute, Les Houshes, 1991).

[11] T.Fujisawa and S. Tarucha, Appl. Phys. Lett. 68 (1996) 526.

[12] K.K. Likharev, Proc.IEEE, 87 (1999) 606.

[13] R.J. Schoelkopf, P. Wahlgren, A.A. Kozhevnikov, P. Delsing, D.E. Prober, Science 280 (1998) 1238.

[14] T.Fujisawa and Y. Hirayama, Appl. Phys. Lett. 77 (2000) 543.

[15] H.D.Cheong, T. Fujisawa, T. Hayashi, Y. Hirayama and Y.H. Jeong, Appl. Phys. Lett. 81 (2002) 3257.

[16] A. N. Korotkov and M.A. Paalan, Appl. Phys. Lett. 74 (1999) 4052.

[17] D. L.Feldhein, C. D. Keating, Chem. Soc. Rev., 27 (1998) 1.

[18] M.H.Devoret and R.J. Schoelkopf, Nature 406 (2000) 1039.

[19] K. M. Lewis, C. Kurdak, et al., Appl. Phys. Lett. 80 (2002)142.
[20] S. Komiyama, O. Astafiev, V. Atonov, T. Kutsuwa and H. Hirai, Nature, 403 (2000) 405.
[21] A. J. Sheilds, M.P. O'Sullivan I. Farrer, D.A. Ritchie, R. A. Hogg, M.L. Leadbeater, C.E. Norman and M. Pepper, Appl. Phys. Lett. 76 (2000) 3673.
[22] M.A. Nielsen and I.L. Chuang in "Quantum Computation and Quantum Information" (Springer, 2000).
[23] R.K. Tien and J.P. Gordon, Phys. Rev. 129 (1963) 647.
[24] J. R. Tuckert and M.J. Feldman, Rev. Mod. Phys, 57 (1985) 1055.
[25] J.M. Hergenrother, M.T. Tuominen, J.G. Lu, D.C. Ralph, M. Tinkham, Physica B203 (1994) 327.
[26] B.J. Keay, S. Zeuner, S. J. Allen Jr., K.D. Maranowski, A.C. Gossard, U. Bhattacharya, and M.J.W. Rodwell, Phys. Rev. Lett. 75 (1995) 4102.
[27] S.Verghese, R,A. Wyss, Th. Scapers, Q. Hu, A. Foster and M.J. Rooks, Phys. Rev. B52 (1995) 14834.
[28] T.H.Oesterkamp, L.P. Kouwenhoven, A.E.A.Koolen, N.C. van der Vaart and C. J.P.M. Harmans, Phys. Rev. Lett 78 (1997)1536.
[29] O.Astafiev, S. Komiyama, T. Kutsuwa, V. Antonov, Y. Kawaguchi and K. Hirakawa, Appl.Phys. Lett. 80 (2002) 4250.
[30] L.J.Geerligs, V.F.Anderegg, P.A.M.Holweg,J.E.Mooij, H.Pothier, D. Esteve, C. Urbina, M.H.Devoret, Phys. Rev.Lett., 64 (1990) 2691.
[31] H.Pothier, P.Lafarge, C.Urbina, D. Esteve and M.H. Devoret, Europhys. Lett. 17 (1992) 249.
[32] (a)A.S.Atallah, A.H.Phillips, A.F.Amin, M.A.Semary, "Photon-assisted Transport Characteristics Through Quantum Dot Coupled to Superconducting Reservoirs" Nano 1, No.3 (2006) 259-264.
(b) A.N.Mina, A.H.Phillips, “Frequency resolved detection over a large frequency range of the fluctuations in an array of quantum dots”. Progress in Physics, V.4 (2006) 11.

[33] A. H. Phillips, A. N. Mina, M.S. Sobhy, and E. A. Fouad, " Electron Dynamics properties of a quantum dot turnstile coupled to superconducting reservoirs" Egypt. J. Physics, 37, No. 3 (2006) 53.
[34] A. H. Phillips, A. N. Mina, M.S. Sobhy, and E. A. Fouad, "Responsivity of quantum dot photodetector at Terahertz detection frequencies", J. of Computational and Theoretical Nanoscience, 4 (1) (2007) 174.
[35] D.S. Boudreaux, F. Williams, and A.J. Nozik, *J. Appl.Phys.***51**(1980) 2158.
[36] F.E. Williams and A.J. Nozik, *Nature* **311** (1984) 21.
[37] F. Williams and A.J. Nozik, *Nature* **271** (1978) 137.

[38] H. Benisty, C.M. Sotomayor-Torres, and C. Weisbuch, *Phys. Rev. B.* **44** (1991) 10945.
[39] U. Bockelmann and G. Bastard, *Phys. Rev. B* **42**, (1990) 8947.
[40] H. Benisty, *Phys. Rev. B* **51** (1995) 13281.
[41] A.J. Nozik, *Annu. Rev. Phys. Chem.* **52** (2001) 193.
[42] A.J. Nozik, Physica E: Low-dimensional Systems and Nanostructures, 14 (2002) 115.
[43] M.A. Green, *Third Generation Photovoltaics* (Bridge Printery, Sydney) 2001].
[44] *V. Aroutiounian, S. Petrosyan, A. Khachatryan*, J. of Appl. Phys., 89 (2001) 2268.
[45] H. Ohno, Science, 281 (1998) 951.
[46] H. Ohno, J. Magn. Magn. Mater, 200 (1999) 110.
[47] J. M. Kikkawa and D. D. Awschalom, Phys. Rev. Lett., 80, (1998) 4113.
[48] J. M. Kikkawa and D. D. Awschalom, Nature,397 (1999)139.
[49] I. Malajovich, J. M. Kikkawa, D. D. Awschalom, J. J. Berry, and N. Samarth, Phys. Rev. Lett. , 84 (2000) 1015.
[50] M. Poggio et al., Phys. Rev. Lett., 91 (2003) 207602.
[51] S. A. Wolf et al., Science 294, 1488 (2001)1488.
[52] J. Fabian, A. Matos-Abiague, C. Ertler, P. Stano, and I. Zutic, Acta Physica Slovaca, 57 (2007)565.
[53] G. Prinz, Phys. Today, 48 (1995) 58.
[54] D. P. D. Vincenzo, Science, 270 (1995)255.
[55] C. Joachim, J. K. Gimzewski, and A. Aviram, Nature (London) 408, (2000)541.
[56] J. L. Simonds, Physics Today 48 (1995)26.
[57] I. Zutic, J. Fabian, and S. Das Sarma "Spintronics: fundamentals and applications" Rev. Mod. Phys.,76 (2004)323.
[58] P. Bruno, Phys. Rev. B 52, 411 (1995).
[59] Walid A. Zein, Adel H. Phillips and Omar A. Omar, Progress of Physics, 4 (2007) 18.

# *Digital, Discrete and Combinatorial Methods in an Euclidean or Riemannian context*

*(The Stability of the Digital-Energetic Level; Cap-Polynomial of Digital Spaces; Super-Fractals. Inverse Quotient Curvature Coefficients, Separation supposition and Trans-n-Riemannian Boundary. Juxtaposition Combinatorial Measures and Juxtaposition Fractals. Riemannian Regression Submanifolds – Discrete VTF Methods; Hamilton-Jacobi reduced equation. Holcman-Pugh Kick Method; Holcman-Pugh Compactness Riemannian Boundary; the Trans-n-Riemannian Boundary. C++, Python and TPascal Programming Languages Applications *)*

by
Valentin Boju and Antoniu Boju, MontrealTech *
valentin@montrealtech.org, cosmin.antoniu@montrealtech.org
MontrealTech **, C.P.78574, Succ Wilderton, Montréal, Qc, H3S 2W9, Canada
http://pages.videotron.com/nanotech Montrealtech.Press@montrealtech.org

……

*. Excepting the results referred under other than the above names of two authors (Valentin Boju and Antoniu Boju), all the methods and theoretical and practical results/properties from the {**§1. DIGITAL GEOMETRY and DISCRETE/COMBINATORIAL METHODS: Applications & New Energy. The Stability Threshold and the Stability of a Digital-Energetic Level. Cap-Polynomial** of Digital Spaces**.** Inverse Quotient Curvature Coefficients Method, Separation supposition and the analogy with Holcman-Pugh Kick Method; Holcman-Pugh Compactness Riemannian Boundary; the Trans-n-Riemannian Boundary. **The Asymptotic-IQCC-dimension. Super-Fractals. Riemannian Spaces.**}, from the {**§ 2. Juxtaposition Combinatorial Measures and Juxtaposition Fractals. Applications in Intrinsic Measure Theory**} and from the {**§ 4. C, TPascal and Python Programming Languages Applications.**} – see also [Boju2007_MontrealTech Press] - are marked by "**Copyright © 2006-2007, Valentin Boju and Antoniu Boju**", i.e. they are copyrighted and protected: the Berne copyright convention - All Rights Reserved: **[The Patents - MontrealTech Register, MontrealTech Portfolio - © 2006-2007, authors].** The use of the specified **§**1, **§**2 and **§**4 is allowed only for educational purposes under our permission in written form, but not for commercial ones.

**. A team of students from **MontrealTech**, who finished a course of Riemannian Geometry of Doctoral level, did a stage (confirmed by a certificate) during the realization of the programs from the **§**4 with the authors of the programs, that is Valentin Boju and Antoniu Boju.

**Key words and phrases:** Iso-Stable Digital Spaces; sq-Iso-Stability and Hex-Iso-Stability Diophantine Equations; New Energy - Compartmented Energetic Bank/Generator Unit (CEBGU); Metric Structure of (L; K)-Digital Spaces; The Stability of the Digital-Energetic Levels; sq-Stability Formula & Hex-Stability Formula; (L; K; sqCells-Digital Plane) and (L; K; HexCells-Digital Plane) are spaces with Polynomial growth of the Digital-Energetic-superstable-Levels; Cap-Polynomial and Asymptotic Dimension of Digital Spaces; Hybrid multi-type-CEBGU; Super-Fractals; Inverse Quotient Curvature Coefficients, Separation supposition and Holcman-Pugh Kick Method; Holcman-Pugh Compactness Riemannian Boundary; the Trans-n-Riemannian Boundary; the coarse Baum-Connes conjecture and Novikov conjectures; Juxtaposition Combinatorial Measures and Juxtaposition Fractals; Applications in Intrinsic Measure Theory. Discrete and Differentiable VTF Methods; Hamilton-Jacobi reduced equation; Riemannian Regression Submanifolds & Nanotech Applications; VTF-Methods and Holcman-Pugh Kick Method; Holcman-Pugh Compactness Riemannian Boundary; the Trans-n-Riemannian Boundary. Programming Languages Applications; sq-Superfractals and Hex-

Superfractals – Programs: C++; Juxtapositin Fractals – Programs: Python; Riemannian Regression Submanifolds & Nanotech Applications - Programs: TPascal

**Applications (The Patents - MontrealTech Register, MontrealTech Portfolio - © 2006-2007, authors):** Graphics, Computer Vision and Image Processing; Energy Units (Compartmented Energetic Bank/Generator Units-CEBGU); Cryptography and Security Procedures; Architecture – Decorative & Mosaics Work – Ceramics & Urban Sculpture – Textile Pictures and Textures; Computer and Video Games; Biomedical Applications; (Exterior/Interior) Juxtapositin Fractal; Riemannian Regression Submanifolds, Logarithmic Kick Method & Nanotech Applications; Pattern Recognitions & Defence Research Programs

2000 Mathematics Subject Classification**: 05, 28, 34, 37, 52, 53, 62, 68, 90, 92**

**……..…….**

**§0. Introduction.** We will show four original methods, published during the past years, that give applications in Digital, Discrete and Combinatorial Methods in an Euclidean or Riemannian context: [Boju2007_MontrealTech Press], [BojFun2007_Springer], [BojuFuna2007 –Asymptotics], [BojuFunar1996], ], [BojuFunar1993], [Boju1986], [Boju1985], [Boju1982]

0.1. {About §1}**. §1. DIGITAL GEOMETRY and DISCRETE/COMBINATORIAL METHODS: Applications & New Energy. The Stability Threshold and the Stability of a Digital-Energetic Level. Cap-Polynomial of Digital Spaces.**
**Inverse Quotient Curvature Coefficients Method, Separation supposition and the analogy with Holcman-Pugh Kick Method; Holcman-Pugh Compactness Riemannian Boundary; the Trans-n-Riemannian Boundary. The Asymptotic-IQCC-dimension. Super-Fractals. Riemannian Spaces.**

Leonhard Euler posed the following problem: how to find a path for a knight (thus, a motion (1; 2) in the digital plan) that touches every square exactly once in succession. Also, in [Boju1985] there are many problems of Geometric Combinatorics in a Digital Geometric context, including the knight problem.
In §1, we are interested in general motions (L; K), L, K naturals = 0, 1, 2, ..., $2L + 1 \leq K$, in the sqCells-Digital-Plane (Square Cells Digital Plane) or in a HexCells-Digital-Plane (Hexagonal Cells Digital Plane). This is connected to the concept of **Compartmented Energetic Bank/Generator Unit – CEBGU (see:** [Boju2007, MontrealTech Press]**).**
In [Boju2007, MontrealTech Press] are studied the intrinsic and extrinsic topological structures of the hyperspheres and disks, the Iso-Stable Digital Spaces, the general motions (1-L; 2-L; … ; w-L) in the w-hypercubicCells-Digital w-Space (w-hypercubic Cells Digital **w-dimensional** Space), as well as the asymptotic dimension and the properties of the multi-type-CEBGU digital structures. In particular, the caracteristics of the super-fractals are found. In the present paper we talk about authentic super-fractals, i.e. fractals of dimension of a complex caracter; namely: 1. it is a like-polynomial dimension; 2. the asymptotic dimension in the Digital Plane is $> 1$.
Inverse Quotient Curvature Coefficients Method, Separation supposition and the Holcman-Pugh Kick Method: the Inverse Quotient Curvature Coefficients Method leads to a Separation supposition (see [Boju2007, Montrealtech Press]) and

to the Trans-n-Riemannian Boundary whose value is $2\pi$, for n=2. The Holcman-Pugh Kick Method is surprising because both the "finite shell" and "geometry at infinity" concepts appears in the present chapter, **in a context completely opposite to the Riemannian one**.
Furthermore, some theoretic properties as well as **experimental results** evaluated through C++, TPascal and Python programs are presented.

**……..…….**

0.2. { About §2}**. Juxtaposition Combinatorial Measures and Juxtaposition Fractals. Applications in Intrinsic Measure Theory.**

In this paragraph, we show similar discrete methods to the ones of discrete digital spaces, but instead of covering the figure with a grid, we make use of the method of (exterior or interior) juxtaposition. This method was introduced by V. B. in [Boju1982] and was cited in [BojuFunar1993]. In this way, we obtain the JCM. (Juxtaposition Combinatorial Measure) and JF (Juxtaposition Fractals). The ulterior results on this subject were published and cited in:
[BojuFunar2007_Springer], [BojuFunar2007-Asymptotics], [Börö2004]

**……..…….**

0.3. { About §3} **Riemannian Regression Submanifolds. Hamilton-Jacobi reduced equation, Discrete VTF Methods and D. Holcman-C. C. Pugh Kick Method. Holcman-Pugh Compactness Riemannian Boundary. Applications in Nanotechnologies.**

In this paragraph, the original methods of VTF = Vector Type Functions and Riemannian Regression Submanifolds are presented. A special Hamilton-Jacobi reduced equation is studied.
The fundamental results (Kick Method and Holcman-Pugh Compactness Riemannian Boundary) of D. Holcman and C.C. Pugh are presented and commented.

**……..…….**

0.4. { About §4}**. C++, TPascal and Python Programming Languages Applications.**

Some applications are mentioned.
Then, the C++, TPascal and Python Programming Languages Applications are presented.

**^^^^^^^^^^^^^^^^^^^^^^^^**

**§1. DIGITAL GEOMETRY and DISCRETE/COMBINATORIAL METHODS: Applications & New Energy. The Stability Threshold and the Stability of a Digital-Energetic Level. Cap-Polynomial of Digital Spaces.**
**Inverse Quotient Curvature Coefficients Method, Separation supposition; the analogy with Holcman-Pugh Kick Method and Holcman-Pugh Compactness Riemannian Boundary. Trans-n-Riemannian Boundary. The Asymptotic-IQCC-dimension. Super-Fractals. Riemannian Spaces.**

**§§1.1. Applications & New Energy. Compartmented Energetic Bank/Generator Unit (CEBGU).**

A raster image (a bitmap) represents a rectangular grid of points of color or
Pixels; a heightmap is the result of a RLE on a voxel grid, and a sampling is a discretising of a continuous signal.
Thus, it is natural that by discretising the space and the time, we also discretise the processes and the phenomena and implicitly we also discretise the subjacent energy vehiculated during their development. There is some similitude between our methods (multi-type-CEBGU) and those that are used in [Kitsiosy, Kota, Mitt, Ooiy, Soria, You, 2006] – see below **§§**1.7.

The present model represents a quantified space where the topology of the spaces (L; K, HexCells-Digital-Plane) and (L; K; sqCells-Digital-Plane) is one "**totally-non-adjacent FETVWP**" (FVWPET = from the viewpoint of the Euclidean topology) for K, L > 0. For instance, in the digital metric cases Hex or sq and for stable r, the r-Energetic Level and the (r+1)-Energetic Level are generally FVWPET-mani-linked.
Notice the complexity of the topological structure of a r- Energetic Level if FVWPET-examined. Moreover, the r- Energetic Level presents itself in two completely different states in function of two different topological approaches: the intrinsic topological approach and the environmental one. Attention: their intrinsic topology is completely different from their environmentally induced one. For instance, the intrinsic connexity does not coincide with the induced one by the ambiant Euclidean or Riemannian space in which the (L;K)-digital space is represented. Precisely, the "TNA-FVWPET" (TNA = totally-non-adjacent) one favours interesting applications of the (L;K) spaces in the modelling of practical problems of energy engendering/stockage in a CEBGU (Compartmented Energetic Bank/Generator Unit). In fact, theoretically there are energetic processes where the energy is engendered/stored in (micro, macro or mega) quanta, but the stabilization of each stored energy quantum happens in a temporal quantum dt.

An engendering/stockage in a CEBGU made by an (L; K) process, that realizes a spatial discretising and a temporal one dt', can perturb the engendering/stockage of the energy if the values dt and dt' are not harmonized. Thus, this implies an optimal choice
of the (L; K) values.
The assignation (similarly to chamfer modeling [Borg84, 86], [Rose66], [Thie1994]; the chamfer distances are based on a ponderation mask) of some physical/economical values (for instance the cost price), in function of a stable energetic level r, will confer to the optimal modeling an increased degree of complexity. Even in this case, the non-ponderal theoretical models (L; K, HexCells-Digital Plane) and (L; K; sqCells-Digital Plane) remain fundamental because they reveal surprising qualitative phenomena as:
-the existence of a stability threshold;
-the existence of iso-stable (L; K)-spaces;
-a concrete class of dimensions – the asymptotic dimension of the

multi-type (L; K, HexCells-Digital Plane) and (L; K; sqCells-Digital Plane); moreover, we can say that we asymptotically deal with Super-Fractals.

**Remark.1.1.** The phenomenon of the Stability of the Digital-Energetic Level allows an optimal and regular tilling of the space from an VWPET.

We mention some papers where some types of energy, and sq-grids, hexagonal/hexahedral grids, polygonal-grids and topological-grids are used:

-A cell by cell adaptive arbitrary Lagrangian Eulerian gas code. [Morr]

-An adaptive multi-material arbitrary Lagrangian Eulerian algorithm for computational shock hydrodynamics, Swansea, 2002. [Barl2002]

-Multi-Material ALE methods in unstructured grids. [PeerCarr2000]

-An Arbitrary-Lagrangian-Eulerian code for polygonal mesh: ALE INC(ubator). [LoubShasLANL]. http://math.lanl.gov/Research/Highlights/PDF/alepoly.pdf).

- L.G. Margolin, M.J. Shashkov – Second-order signpreserving conservative interpolation (remapping) on general grid. – Journal of Computational Physics, 184 (2003) 266-298.

- P. Knupp – Hexaedral and tetrahedral mesh untangling. Engineering with Computers, 17 (2001) 261-268.

- P. Vachal, M. Shashkov, R. Garimella– Untangling of 2D meshes in ALE simulations. – in review in Journal of Computational Physics.

- E. J. Caramana and M. Shashkov – Elimination of Artificial Grid Distortion and Hourglass-Type Motions by Means of Lagarangian Subzonal Masses and Pressures.
– Journal of Computational Physics, 142, pp. 521–561, (1998).

- E. J. Caramana, D. E. Burton, M. J. Shashkov, and P. P. Whalen – The Construction of Compatible Hydrodynamics Algorithms Utilizing Conservation of Total Energy. – Journal of Computational Physics, 146, pp. 227–262, (1998).

- R. Loubere, M. Shashkov, A Subcell Remapping Method on Staggered Polygonal Grids for Arbitrary-Lagrangian-Eulerian Methods, submitted to Journal of Computational Physics (2004), LAUR-04-6692

- [Kitsiosy, Kota, Mitt, Ooiy, Soria, You, 2006] (see: Figure 2. Topology of the modified C-type grid. (a) block topology; (b) body-fitted airfoil grid; (c) ZNMF jet cavity).

-DGCI-2006.pdf Arithmetic Discrete Hyperspheres and Separating Capacity
Christophe Fiorio and Jean-Luc Toutant, LIRMM - CNRS UMR 5506 - Universit de Montpellier II, 161 rue Ada - 34392 Montpellier Cedex 5 - FRANCE
Jennifer Morrell j.m.morrell@rdg.ac.uk

**……..…….**

## §§1.2. f-Combinatorial-Algorithmic Metric (f-CAMetric) on Digital Spaces

The Euclidean distance dist on the set $N$ of naturals is dist($n'$, $n''$) = $\|n'-n''\|$.

Let $M$ be a countable set and $F : M \to N$ a bijective function.

The formula

(1.2.1) $f(x, y) = dist(F(x), F(y))$ is a distance on M.

**Denominations.** The distance *f* is named the One-one Combinatorial Distance induced by F (f-OoCADistance, or even f-OoCAD) and:
- the space (*M*, *f*) is said to be an f-OoCombinatorial Metric Space (*f-OoCAM* Space).

This way suggests a generalization:

**1.2.2.1. f-CAD Criterion**. A procedure ∓ on a countable set M provides an f-Combinatorial-Algorithmic Distance under reasonable conditions (see M. Yamashita and T. Ibaraki. 1986. Distances defined by neighbourhood sequences. Pattern Recognition 19, 3, 237 – 246).
We mention the practical mechanisme:
- ∓ is an N-algorithme, i.e. a **succession of multiple U-movements** on M; that is to each $i \in$ N corresponds a **multiple U**-movement from the ∓ *(i)*-cell (point of M) at U neighbouring "**free**" cells, which are "**seized**".
- [the **exhaustion** condition] the set M is **completely exhausted (i.e., each cell is seizable)**.

**……..…….**

**§§1.3. Metric Structure of (L; K) Digital Spaces**

Let (1-L; 2-L; … ; w-L, w-hypercubicCells-Digital w-Space) be
the semi-metric w-hypercubicCells-Digital w-Space generated by (1-L; 2-L; … ; w-L), where (i_L) are the sequences of successive cells parallels with the i-axis, and:
- S(w-hypercubic; O, 1-L; 2-L; … ; w-L, w-Digital; r) = the r-hypersphere centered at O;
- D(w-hypercubic; O, 1-L; 2-L; … ; w-L, w-Digital; r) = the r-disk centered at O.

For w=2, L, K naturals = 0, 1, 2, ..., $2L + 1 \leq K$,
let (L; K, HexCells-Digital Plane) be the semi-metric HexCells-Digital Plane generated by (L; K) and:
- S(O, L; K; HexCells-Digital Plane; r) the r-Hex_sphere centered at O;
- D(O, L; K; HexCells Digital Plane; r) the r-Hex_disk centered at O.

For w=2, we have:
- (L; K, 2-cubicCells-Digital 2-Space) is renoted by (L; K; sqCells-Digital Plane);
- S(square; O, L; K; 2-Digital; r) = S(O, L; K; sqCells-Digital Plane; r), the r-sq_sphere centered at O;
- D(square; O, L; K; 2-Digital; r) = D(O, L; K; sqCells-Digital Plane; r), the r-sq_disk centered at O.

If O is the standard cell bottom-left corner being the origin of the digital grid-plane Z x Z, we agree to omit the letter O.

In [Boju2007_MontrealTech Press], the general results are exposed.

Here are some particular results.

**§§§1.3.1. Non-Degeneracy Property**

**THEOREM.1.3.1. Hex-Non-Degeneracy Property**
For $2L + 1 \leq K$ and gcd(L; K) = 1, we have :
(L; K; HexCells-Digital Plane) **is a metric** space iff $L + K \neq 3m$ (i.e.: $L + K = 3m + 1$ or $L + K = 3m + 2$).
Hint: see **1.2.2.1. f-CAD Criterion and [ValB-CAB Hex-Procedure in the Digital Plane & the subsequent C-Program, © 2006 Valentin Boju & Antoniu Boju].**

**Denomination.** Such a pair (L; K) is said to be **Hex-nondegenerate**.

**THEOREM.1.3.1. sq-Non-Degeneracy Property**.
For $2L + 1 \leq K$ and gcd(L; K) = 1, we have :
(L; K; sqCells-Digital Plane) **is a metric** space iff (L=odd; K=even) or (L=even; F=odd), i.e. L + K = odd.
Hint: see **1.2.2.1. f-CAD Criterion and [ValB-CAB sq-Procedure in the Digital Plane & the subsequent C-Program, © 2006 Valentin Boju & Antoniu Boju].**

**Denomination.** Such a pair (L; K) is said to be **sq-nondegenerate**.

**§§§1.3.2.**
**Hex-Stable Threshold**
**Hex-Stability Formula**
**sq-Stable Threshold**
**sq-Stability Formula**

Let (L; K) be Hex-nondegenerate and cap_S the capacity of the set S.

(1.3.2. Hex-Stable Threshold). Then there is a natural ŗ (if minimal, is named StabThresh(L; K, Hex)) such that:
- for each $r \geq ŗ$, we have:

(1.3.2. Hex-Stability Value). cap_S(O, L; K; HexCells-Digital Plane; r+2) – 2 cap_S(O, L; K; HexCells-Digital Plane; r+1) + cap_S(O, L; K; HexCells-Digital Plane; r) =0
i.e.
cap_S(O, L; K; HexCells-Digital Plane; r+1) - cap_S(O, L; K; HexCells-Digital Plane; r)= const (L; K, Hex)
Let ř(L; K, Hex) be the minimum ŗ for which the formula (1.3.2. Hex-Stability Value) is true.

**Denomination.** ř(L, K, Hex) is named the Stable Threshold for the case (L; K, Hex) and is designated by StabThresh(L; K, Hex); the constant value const (L; K, Hex) is named the Stable Value in the case (L; K, Hex) and is designated by StabVal(L; K, Hex).
The natural r is said to be (L; K, Hex)-superstable if $r \geq$ StabThresh(L; K, Hex).
The natural r is said to be (L; K, sq)-superstable if $r \geq$ StabThresh(L; K, sq).

Analogously, let (L; K) be sq-nondegenerate.

(1.3.2. sq-Stable Threshold). Then there is a natural ŗ such that:
- for each $r \geq$ ŗ , we have:
(1.3.2. sq-Stable Threshold). cap_S(O, L; K; sqCells-Digital Plane; r+2) – 2 cap_S(O, L; K; sqCells-Digital Plane; r+1) + cap_S(O, L; K; sqCells-Digital Plane; r) =0,
i.e. cap_S(O, L; K; sqCells-Digital Plane; r+1) - cap_S(O, L; K; sqCells-Digital Plane; r)= const (L; K, sq)

Let ř(L; K, sq) be the min ŗ for which the formula (1.3.2. sq-Stable Threshold) is true.
**Denomination.** ř(L, K, sq) is named the Stable Threshold for the case (L; K, sq) and is designated by StabThresh(L; K, sq); the constant value const (L; K, sq) is named the Stable Value in the case (L; K, sq) and is designated by StabVal(L; K, sq).

**Property 1.3.2.A.1.**
**1.3.2.A.1.1.** For (L; K) **sq-nondegenerate**, we have ([Boju2007_MontrealTech Press]):

(**1.3.2.A.1.1.** sq-**nondegenerate**-Stable Value Formula):

$$StabVal(L; K, sq) = 4(K^2 + 2LK - L^2)$$

(L; K) **sq-nondegenerate; 2L + 1 ≤ K**

**1.3.2.A.1.2. If** (A; E) is **sq-degenerate**, then we have ([Boju2007_MontrealTech Press]):

(**1.3.2.A.1.1.** sq-**degenerate**-Stable Value Formula):

$$StabVal(A; E, sq) = 2(\hat{E}^2 + 2\hat{A}\hat{E} - \hat{A}^2)$$

$$2A + 1 \leq E,$$

where: $\hat{A} = A/D$, $\hat{E} = E/D$, $D = gcd(A, E)$

**1.3.2.B. Hex-Stability Formula**

**1.3.2.B.1.1.** For (L; K) **Hex-nondegenerate**, we have ([Boju2007_MontrealTech Press]):

(**1.3.2.B.1.1.** Hex- **nondegenerate-Stable Value Formula**):

$$StabVal(L; K, Hex) = 6(K^2 - L^2)$$

(L; K) **Hex-nondegenerate; $2L + 1 \leq K$**

Also, there is a formula ([Boju2007_MontrealTech Press]) corresponding to the case (L; K) **Hex-degenerate** .

**Remark. It is possible to have a "computer proof" for the above stable-value formulae (sq or Hex) by combining , for each (L; K), the computer image of an (L; K)-stable level and the algorithmic character of the (L; K)-procedure** ([Boju2007_MontrealTech Press])

**……..…….**

**§§1.4. The stability of Digital-Energetic Level**

**1.4.1. Growth of the Capacity of Digital Energetic Stable r-Level Constancy Theorem**
(GCDESLC Th).

The geometric significance of the formulas for the StabVal is the following ([Boju2007_MontrealeTch Press]):

**1.4.1.1. (**GCDESLC **Th).** By excepting some few first values of r, we have:

**1.4.1.1.Hex.** The (L; K, HexCells-Digital Plane) is a space with Constant Growth of the Capacity of Digital **Energetic r-Level**, for r superstable, i.e. $r \geq$ StabThresh(L; K, Hex).

**1.4.1.1.sq.** The (L; K, sqCells-Digital Plane) is a space with Constant Growth of the Capacity of Digital **Energetic r-Level**, for r superstable, i.e. $r \geq$ StabThresh(L; K, sq).

**……..…….**

## §§1.5. Iso-Stable Digital Spaces

### §§§1.5.1. There are some Iso-Stable Digital Spaces.
**Conventional Signs: Non-Deg = Non-Degenerate; Deg = Degenerate; H = Hex**

**1.5.1.A. For instance, the following (L; K, Hex) Digital Spaces are Iso-Stable (see each Row):**

| (L; K) | | StabThresh (L; K, H) | StabVal (L; K, H) | H | (L; K) | | StabThresh (L; K, H) | StabVal (L; K, H) |
|---|---|---|---|---|---|---|---|---|
| (1; 3) | **Non-Deg** | 7 | 48 | H | (1; 5) | Deg | 7 | 48 |
| (1; 4) | **Non-Deg** | 9 | 90 | H | (2; 7) | Deg | 9 | 90 |
| **(3;17)** | **Non-Deg** | 34 | 1680 | | (9; 19) | **Non-Deg** | 46 | 1680 |

**1.5.1.B. For instance, the following (L; K, sq) Digital Spaces are Iso-Stable:**

| (L; K) | | StabThresh (L; K, sq) | StabVal (L; K, sq) | sq | (L; K) | | StabThresh (L; K, sq) | StabVal (L; K, sq) |
|---|---|---|---|---|---|---|---|---|
| (2; 5) | Non-Deg | 14 | 164 | sq | (3; 7) | Deg | 14 | 164 |
| (3; 8) | Non-Deg | 21 | 412 | sq | (5; 11) | Deg | 21 | 412 |
| (1;10) | Non-Deg | 23 | 476 | sq | (3; 13) | Deg | 24 | 476 |
| (4; 9) | Non-Deg | 24 | 548 | sq | (5; 13) | Deg | 24 | 548 |

**Remark.1.5.1.**
**a).** StabThresh(3; 7, Hex) = 34 $\neq$ StabThresh(9; 19, Hex) but the both digital spaces are iso-stable;
**b).** StabThresh(1; 10, sq) = 23 $\neq$ StabThresh(3; 13, sq) = 24 = StabThresh(5; 13, sq);
i.e. :
For (L; K)-Digital Spaces having a cap-polynomial of degree 1 (see **[BojuMontrealTech Press]**), the Digital Q-curvature of Digital-Energetic Level of radius r is not 1/r, because there are iso-stable Digital Spaces having an infinity of distinct capacities for Energetic r-Levels of the same superstable variable r (see 1.7.2.2.4.).

**§§§**1.5.2. The TOPOLOGY of the L-Maximal Digital Hex-Spaces: [L; 2L+1; Hex] is characterized by the high regularity degree.

Remark 1.5.2. Also, the beauty of the Super-Fractal [L; 2L+1; Hex] is maximal !!!

**§§§1.5.3.A. Hex-Iso-Stability Diophantine Equation**

**The Hex-Iso-Stable (L; K) Digital Spaces are the solutions of the following** (L; K)- **Hex-Iso-Stability Diophantine Equation:**
$y^2 - x^2 = K^2 - L^2$, where $2x + 1 \leq y$ and $2L + 1 \leq K$

**1.5.3.B. sq-Iso-Stability Diophantine Equation**

**The sq-Iso-Stable (L; K) Digital Spaces are the solutions of the following** (L; K)- **sq-Iso-Stability Diophantine Equation:**
$y^2 + 2xy - x^2 = K^2 + 2LK - L^2$, where $2x + 1 \leq y$ and $2L + 1 \leq K$

**Question1.5. How many non-degenerate Iso-Stable Digital Spaces (Hex or sq) are there?**

**……..…….**

**§§1.6. The cap-polynomial of [L; K, Hex] and [L; K, sq] Digital Energetic r-superstable –Levels; (cap = capacity).**

There are different definitions of the "n-dimensionality" on M (see [Kees1992] in [Boju2007_MontrealTech Press]). One is that "à la Carathéodory" [Cara1914]:
-the "0-condition for $H \geq n$" (that is : H-mes(M)=0);
and
-the "h-homogeneity condition" about the induced h-dimensional measure on $A \subset M$, (and, consequently, we talk about A as being h-dimensional): $mes(tA) = t^h mes(A)$, $\forall$ the real h such that $0 \leq h \leq n$.

Our definition ([Boju2007_MontrealTech Press]), in a Digital stricture space , of a "cap-polynomial", is based on the (L; K)-stability.
Let [iso-Transf; L; K; Hex] be the group of isometries of [L; K; Hex]-Digital Plane. Then
[iso-Transf; L; K; Hex] is a FG (finitely generated) group.

The polynomial property is relevant ([Boju2007_MontrealTech Press]) to the theory of FG-groups (see [Bell2007], [Dran2004] and [HingRoe2000]).
N. Higson and J Roe [HingRoe2000] showed that for FG (finitely generated) groups with bounded asdim function, Yu's property A holds.

Al. Dranishnikov [Dran2004] proves that finitely generated groups with a polynomial dimension growth have Yu's property A; then, the coarse Baum-Connes conjecture and Novikov conjectures hold for such groups.

### §§§1.6.1. The cap-polynomial of [L; K, Hex] Energetic Levels

From
(1.3.2.A.1.1. sq-nondegenerate-Stable Value Formula),
(1.3.2.A.1.1. sq-degenerate-Stable Value Formula),
and
(1.3.2.B.1.1. Hex-nondegenerate-Stable Value Formula), we obtain:

1.6.1.sq- nondegenerate, For $2L+1 \leq K$, r superstable, $x \geq 0$, we have:
$cap_S(O, L; K; sqCells\text{-}Digital\ Plane; r + x) = 4(K^2 + 2LK - L^2)x +$
$+ cap_S(O, L; K; sqCells\text{-}Digital\ Plane; r)$, $\forall$ an sq-superstable Energetic r-Level.

Therefore, we have the polynomial
**1.6.1.1. sq- nondegenerate**
$DP(L, K, r, x; sq) = 4(K^2 + 2LK - L^2)x + cap_S(O, L; K; sqCells\text{-}Digital\ Plane; r)$,
defined for all
sq- **nondegenerate** (L, K)**, $2L+1 \leq K$, r superstable, and $x \geq 0$.**
For L, K, r fixed, it is named the **cap-polynomial** of an r-superstable Energetic r-Level of the (L, K, sq)-CEBGU. It is the same for each point p, therefore we may omit the letter O:
$DP(L, K, r, x; sq) = 4(K^2 + 2LK - L^2)x + cap_S(L; K; sqCells\text{-}Digital\ Plane; r)$,
defined for all
sq- **nondegenerate** (L, K)**, $2L+1 \leq K$, r sq-superstable, and $x \geq 0$ (in fact, for $x > 0$ and $r \geq$ StabTresh(L; K)).**

Exercise 1.6.1.sq-nondegenerate.
Express the second numerical derivative of the
cap_(L, K, r)-CEBGU = D(L; K; sqCells Digital Plane; r)
in terms of the **cap-polynomial** of an r-superstable Energetic Level of
an (L, K, sq)-CEBGU.
Analogously, we have the **sq-degenerate**, **Hex-degenerate and** Hex-nondegenerate cases. For instance, we have:

**1.6.1.Hex-nondegenerate**, $2L+1 \leq K$, r superstable, $x \geq 0$.
$cap_S(O, L; K; HexCells\text{-}Digital\ Plane; r + x) =$
$6(K^2 - L^2)x + cap_S(O, L; K; HexCells\text{-}Digital\ Plane; r)$, $\forall$ an Hex-superstable Energetic r-Level.

Therefore, we have the polynomial

**1.6.1.1. Hex-nondegenerate**

DP(L, K, r, x, Hex) = $6(K^2 - L^2)\,x$ + cap_S(O, L; K; HexCells-Digital Plane; r), defined for all

Hex- **nondegenerate** (L, K)**, 2L+1** $\leq$ **K, r Hex-superstable, and** $x \geq 0$**.**

For L, K, r fixed, it is named the **cap-polynomial** of an r-superstable Energetic r-Level of the (L, K, Hex)-CEBGU. It is the same for each point p, therefore we may omit the letter O:

DP(L, K, r, x, Hex) = $6(K^2 - L^2)\,x$ + cap_S(L; K; HexCells-Digital Plane; r), defined for all

Hex- nondegenerate (L, K), 2L+1 $\leq$ K, r Hex-superstable, and $x \geq 0$ (in fact, For $x > 0$ and $r \geq$ StabTresh(L; K, Hex)).

Exercise 1.6.1. Hex-nondegenerate.

Express the second numerical derivative of the cap_(L, K, r)-CEBGU = D(O, L; K; HexCells Digital Plane; r) in terms of the **cap-polynomial** of an r-superstable Energetic Level of the (L, K, Hex)-CEBGU.

What is the cap-polynomial
-of the plane;
-of $E^n$ ?

**……..…….**

## §§1.7. The multi-type-CEBGU

### §§§Definition 1.7.1. multi-type-CEBGU

**1.7.1.** A **p-centered**-Hex-multi-type-Compartmented Energetic Bank/Generator Unit (**p-centered** multi-type-CEBGU),
or a
[**p-centered;** (L; K)($L_i$; $K_i$ ; $r_i$), Hex]- CEBGU, $i$ = 1, …, T,
is a succession of (**p-centered**; $L_j$ ; $K_j$ ; $r_j$, Hex)-structures, j = 0, …, T,
such that:
-( **p-centered**; $L_0$, $K_0$, $r_0$, Hex) be (**p-centered**;L; K, Hex) structure which is runned for the
steps 1, 2, … , $r_1$ - 1;
- the procedures (**p-centered** ; $L_i$ ; $K_i$ ; $r_i$, Hex), are successively runed, for $i$ = 1, …, T;
- the Stable Thresholds $r_i$ are superstable, $i$ = 1, …, T.

Analogously:

**Definition 1.7.1.** B. A sq-multi-type-Compartmented Energetic Bank/Generator Unit (multi-type-CEBGU),
or a
[**p-centered;** (L; K)($L_i$; $K_i$ ; $r_i$), sq]- CEBGU, $i$ = 1, …, T, p a sq-cell,
is a succession of (**p-centered**; $L_j$ ; $K_j$ ; $r_j$, sq)-structures, j = 0, …, T etc.
(for "**p-centered**", or "centered at p", see: **§§1.3.**).

**§§§1.7.2. Caution**. The **Stable Threshold** of each [**p-centered;** ($L_i$; $K_i$ ; Hex)] in a multi-type-CEBGU is distinct (generally inferior) from those in an single-type-CEBGU (or pure-type-CEBGU).
For instance:

**1.7.2.1.1. Hex[p-centered; (9; 19), (3;17)]**
Let the multi-type-CEBGU of two Hex-iso-stable Digital Planes be
[**p-centered** ; (9; 19; Hex,StabThresh46), (3;17; Hex, $r_1$=53, multi-type StabThresh=3, StabVal=1680)]

**1.7.2.1.2. Hex[p-centered ; (3;17), (9; 19)]**
Let the multi-type-CEBGU of two Hex-iso-stable Digital Planes be
[**p-centered** ; (3; 17; Hex, StabThresh34), (9;19; Hex, $r_1$=53, multi-type StabThresh=12, StabVal=1680)]

**Comparison** 1.7.2.2.

1.7.2.2.1. The value of only multi-type StabThresh of the sequence Hex[**p-centered** ; (9; 19), (3;17)] (of 53 th rank $r_1$=53) is 3, and $3 \prec \prec$ StabThresh[3; 17; Hex] = 34
while
The value of only multi-type StabThresh of the sequence Hex[**p-centered**; (3;17) ,(9; 19)] (of 53 th rank $r_1$=53) is 12, and $12 \prec$ StabThresh[9; 19; Hex] = 46.

We observe that the multi-type CEBGU Hex[**p-centered**; (9; 19), (3;17)]
**is more stable** that Hex[**p-centered**; (3;17) ,(9; 19)].

1.7.2.2.2. The both value are plainly inferior to the single ones.

1.7.2.2.3. The Capacity of 61-CEBGU-Hex[**p-centered**; (3;17), (9; 19)] = 3.150.306 Energetic Cells,
while
The Capacity of 61-CEBGU-Hex[**p-centered**; (9; 19), (3;17)] = 3.059.946 Energetic Cells;
That is, the Hex[**p-centered**; (9; 19), (3;17)] is "more compact".

1.7.2.2.4. The Capacity of 61 th Energetic Level Hex[**p-centered**; (3; 17), (9; 19)] = 108.156 Energetic Cells,
while
The Capacity of 61 th Energetic Level Hex[**p-centered**; (9; 19), (3; 17)] = 104.418 Energetic Cells.
That is, the Hex[**p-centered**; (9; 19), (3; 17)] is "more compact".

1.7.2.2.5. The **extrinsic TOPOLOGY** of the sequence Hex[**p-centered**; (9; 19), (3; 17)] is comparable with the topology of the Super-Fractal type [L; 2L+1; Hex], while the topology of the sequence Hex [**p-centered**; (3; 17), (9; 19)] is very intricate; namely:

The **extrinsic** topological structure of the multi-type-CEBGU of two Hex-iso-stable Digital Planes
[**p-centered** ; (3; 17; Hex, StabThresh34), (9; 19; Hex,$r_1$=53, multi-type StabThresh=12, StabVal=1680)]:

The 50th Stable Energetic Level (which is under the procedure (3; 17; Hex)) has 49 **extrinsic** connected components:
-12 components are **extrinsic** simply-connected;
-36 components are **extrinsic** 1-connected (each has 1 hole);
-1 component is **extrinsic** 12-connected (has 12 holes).
The principal component is composed by Joint Polygones**, each having constant dimensions**: each side contains 10 Energetic Cells; the big diagonal contains 20 Energetic Cells.

The 66th Stable Energetic Level (which is under the procedure (9; 19; Hex) $\in$ [L; 2L+1; Hex ] special type - see 1.5.2.) has 25 **extrinsic** connected components.

**§§§1.7.2.2.6. The remarquable Mechanism of Stability.**
For superstable levels, **the phenomenon of stability has a natural mechanism** ([Boju2007_MontrealTech Press]: a detailed description of the **extrinsic and intrinsic** TOPOLOGY of the L-Maximal Digital Hex-Spaces [L; 2L+1; Hex]): the "**extrinsic** transversal structures" of the *r*-Energetic Level and *(r+1)*-Energetic Level coincide (i.e. **are constant**), while the longitudinal ones are "**constantly increasing fonctions**".

The Convex Hull is a Dodecagon, whose mean width is of 28 Energetic Cells.

Generally, the conditions
**1.7.2.2.7.** $\|L_{i+1}\| \geq \|L_i\|$ and $\|K_{i+1}\| \geq \|K_i\|$, I = 1, … , T,
can realize (but not necessary: see **1.6.4.1. Hex[(9; 19), (3;17)], where the inequalities 1.6.4.2.6. are inversed for [9; 19, Hex] and [3;17, Hex]**) the complete exhaustion.
But, for each energetic type ($L_i$ ; $K_i$ ; $r_i$, Hex), $i \geq 1$, may be calculated the minimum values for a good joining (that is, to fulfil the **exhaustion).**

**Remark. 1.7.2.Hex. The** Hex-multi-type-Compartmented Energetic Bank/Generator Unit (multi-type-CEBGU), i.e. the Hex-Digital Space
[**p-centered**; (L; K)($L_i$; $K_i$ ; $r_i$), Hex]- CEBGU, $i$ = 1, …, T, has a "Variable Topology".

There is a some similitude between our methods (multi-type-CEBGU) and those that are used in [Kitsiosy, Kota, Mitt, Ooiy, Soria, You, 2006] (see: Figure 2. Topology of the modified C-type grid; see also: (a) block topology; (b) body-fitted airfoil grid; (c) ZNMF jet cavity).

Analogously, there is a similar **Remark 1.7.2.sq.**

**§§§1.7.3. The p-centered-distance function in a multi-type-CEBGU, i.e. in a [(L; K)($L_i$; $K_i$ ; $r_i$), Hex or sq]-CEBGU, $i$ = 1, …, T**

**Let p and q be cells in a Digital Space.**

**1.7.3.A. The p-centered-distance function in a [p-centered ; (L; K)($L_i$; $K_i$ ; $r_i$), Hex]-CEBGU, $i$ = 1, …, T**

The **p-centered**-distance function in a [(L; K)($L_i$; $K_i$ ; $r_i$), Hex]- CEBGU, $i$ = 1, …, T, is a direct consequence of the **1.2.2.1. f-CAD Criterion** and of the Hex-multi-type-Compartmented Energetic Bank/Generator Unit (multi-type-CEBGU), or a
[**p-centered**- (L; K)($L_i$; $K_i$ ; $r_i$), Hex]-CEBGU, $i$ = 1, …, T,
as a succession of ($L_j$; $K_j$ ; $r_j$, Hex)-structures, j = 0, …, T.

For instance (see **1.7.2.1.**):

**Let Hex[p-centered**; **(9; 19), (3;17)] be** the multi-type-CEBGU of two Hex-iso-stable Digital Planes
[**p-centered**; (9; 19; Hex, StabThresh46), (3;17; Hex, $r_1$=53, multi-type StabThresh=3, StabVal=1680)]
We have:

**Hex[p-centered; (9; 19), (3;17)]** is a Combinatorial-Algorithmic structure whose Combinatorial-Algorithmic **p-centered**-distance is:
**- [9; 19, Hex] for the cells $p_1$ and $p_2$ from the levels $i$ = 0; 1; … ; 52;**
**- [3; 17, Hex] for the cells p, q, where**
**$p \in$ 52 th level, and $q \in$ 53 th level**
**- [3; 17, Hex] for the cells $q_1$ and $q_2$ from the levels $i \geq$ 53.**

Analogously for

**1.7.3.B. The p-centered-distance function in a [(L; K)($L_i$ ; $K_i$ ; $r_i$ ), sq]-CEBGU, *i* = 1, …, T**

**§§§1.7.4. The Hybrid multi-type-CEBGU; p-centered-distances.**

In [Boju2007,MontrealTech Press] the concept of a **Hybrid multi-type-CEBGU is studied.**
A **Hybrid multi-type-CEBGU is analogue to a Hex or sq-multi-type-CEBGU, but the sequence contains Hex and sq [$L_i$ ; $K_i$ ] zones.**
The most interesting phenomenon is the stability property.
A **Generalized Hybrid multi-type-CEBGU is obtained by replacing one or some [$L_i$ ; $K_i$ ] zones by some sets A, B etc.**
**Examples and necessary conditions for the stability are presented. The [L; K]-"machine" acts as a "enveloping mechanism".**

**1.7.4. Exercise.** (see 1.7.2.1.1. and 1.7.2.1.2). Let a, b, p, q, be arbitrary points in Digital plane, $a \neq b$. Let A, B be the following distances:

A is the a-centered-distance function corresponding to Hex[a-**centered**; (9; 19; StabThresh46), (3;17; $r_1$=53, multi-type StabThresh=3, StabVal=1680)];

B is the b-centered-distance function corresponding to Hex[**b-centered**; (3; 17; StabThresh34), (9;19; Hex, $r_1$=53, multi-type StabThresh=12, StabVal=1680)]

A' is the a-centered-distance function corresponding to [a-**centered**; (9; 19; Hex; StabThresh46), (3;17; sq; $r_1$=53, multi-type StabThresh=??, StabVal=???)];

**1.7.4. Exercise.1.**
Prove that $A(p, q) \neq B(p, q)$

**1.7.4. Exercise.2.**
Comment the equation
$A(p, q) = B(p, q)$

**1.7.4. Exercise.3.**
Comment the equation
$A'(p, q) = B(p, q)$

**1.7.4. Exercise.4.**
Comment the a-centered geodesics of A.

**……..…….**

**§§1.8. The cap-polynomial of the multi-type-CEBGU,**
**i.e. of a [b-centered; (L; K)($L_i$ ; $K_i$ ; $r_i$), Hex or sq]-CEBGU, $i$ = 1, …, T.**

**§§§1.8.1.The sequence of cap-polynomials of a multi-type-CEBGU, i.e. of a [b-centered; (L; K)($L_i$ ; $K_i$ ; $r_i$), Hex or sq]-CEBGU, $i$ = 1, …, T.**

For a [**b-centered;** (L; K)($L_i$ ; $K_i$ ; $r_i$), Hex ]-CEBGU, $i$ = 1, …, T, we have a **sequence of cap-polynomials of Hex-multi-type-CEBGU**:

……

P([**b-centered;** {L; K}_(L; K)($L_i$ ; $K_i$ ; $r_i$), Hex-CEBGU; $i$ = 1, …, T; r+x) = 6($K^2$ - $L^2$) x + cap_S(O, L; K; HexCells-Digital Plane; r), defined for Hex- **nondegenerate** (L, K)**, 2L+1 ≤ K, r superstable, x≥ 0, such that**

StabThresh[L; K; Hex] ≤ **r** ≤ **r + x** ≤ $\mathbf{r}_1$

……

P([**b-centered;** {$L_1$; $K_1$}_(L; K)($L_i$ ; $K_i$ ; $r_i$), Hex-CEBGU; $i$ = 1, …, T; r+x) = 6($K_1^2$ - $L_1^2$) x + cap_S(O, $L_1$; $K_1$; HexCells-Digital Plane; r), defined for Hex- **nondegenerate** ($L_1$, $K_1$)**, 2$L_1$+1 ≤ $K_1$, r superstable, x≥ 0, such that $\mathbf{r}_1$≤ r ≤ r +x ≤ $\mathbf{r}_2$**

……

P([**b-centered;** {{$L_{T-1}$; $K_{T-1}$ }_(L; K)($L_i$ ; $K_i$ ; $r_i$), Hex-CEBGU; $i$ = 1, …, T; r+x) = 6($K_{T-1}^2$ - $L_{T-1}^2$) x + cap_S(O, $L_{T-1}$; $K_{T-1}$; HexCells-Digital Plane; r), defined for Hex- **nondegenerate** ($L_{T-1}$, $K_{T-1}$)**, 2 $L_{T-1}$+1 ≤ $K_{T-1}$, r superstable, x≥ 0, such that $\mathbf{r}_{T-1}$≤ r ≤ r +x ≤ $\mathbf{r}_T$**

……

P([**b-centered;** {$L_T$; $K_T$ }_(L; K)($L_i$ ; $K_i$ ; $r_i$), Hex-CEBGU; $i$ = 1, …, T; r+x) = 6($K_T^2$ - $L_T^2$) x + cap_S(O, $L_T$; $K_T$; HexCells-Digital Plane; r), defined for Hex- **nondegenerate** ($L_T$, $K_T$)**, 2 $L_T$+1 ≤ $K_T$, r superstable, x≥ 0, such that $\mathbf{r}_T$≤ r ≤ r +x**

……

**Analogously,** for a [**b-centered;** (L; K)($L_i$ ; $K_i$ ; $r_i$), sq ]-CEBGU, $i$ = 1, …, T, we have a **sequence of cap-polynomials of sq-multi-type-CEBGU**

……

**§§§1.8.2. Max-Cap-coefficients. Infinite multi-type-CEBGU**.

The sequence of the coefficients of x of maximal degree, in a sequence of

cap-polynomials of a Hex-multi-type-CEBGU (which are named "Max-Cap-Coefficients"), i.e. of an [(L; K)($L_i$; $K_i$ ; $r_i$), Hex ]-CEBGU, $i$ = 1, …, T, is:

$\mathbf{c}_0 = 6(K^2 - L^2)$

$\mathbf{c}_1 = 6(K_1^2 - L_1^2)$

. . .

$\mathbf{c}_{T-1} = 6(K_{T-1}^2 - L_{T-1}^2)$

$\mathbf{c}_T = 6(K_T^2 - L_T^2)$

The sequence of the coefficients of x in a sequence of cap-polynomials of an infinite multi-type-CEBGU, i.e. of an [(L; K)($L_i$; $K_i$ ; $r_i$), Hex ]-CEBGU, $i$ = 1, …, ∞, is as the above sequence $\{c_i\}_{i=0,1,...,T,...}$, where $\mathbf{c}_0 = 6(K^2 - L^2)$, $\mathbf{c}_i = 6(K_i^2 - L_i^2)$, $i$ = 1, …, ∞.

**Analogously, the sq-case.**

**……..…….**

## §§1.9. IQCC (=Inverse Quotient Curvature Coefficient) Method and the analogy with Holcman-Pugh Kick Method; Holcman-Pugh Compactness Riemannian Boundary; the Trans-n-Riemannian Boundary.
## The AsyL(= Asymptotic Limit) of multi-type_CEBGU-IQCC versus AsyL of Riemannian IQCC or positive supremum/infimum (eventually extrema) of Riemannian-IQCC, or b-point limit of IQCC and b-Diameter limit of an IQCC.

### §§§1.9.1. IQCC = Inverse Quotient Curvature Coefficients

**Definition 1.9.1.IQCC.**
Let IQCC ( = Inverse Quotient-Curvature Coefficient) be the following (p, r, d, h) function defined on a metric space (M; d) ([Boju 2007, MontrealTech Press]) or on a space with point-distances (see the **the Hex-multi-type-CEBGU, the sq-multi-type-CEBGU or the Hybrid multi-type-CEBGU** ). For each $p \in M$ and radius (admissible, i.e. an integer in the case of Digital Spaces, a real for Riemannian ones etc) r > o :

$$IQCC(p; r, d; m) = mes\ S(p, r, d) / r^{m-1}$$

where :
- mes is a d-compatible measure (for instance, in the Digital Case a pure or a ponderation mask capacity, a [1-L; 2-L; … ; w-L, w-hypercubicCells-Digital w-Space]-compatible capacity etc);
- S(p; r) is the hypersphere of radius r, centered at $p \in M$;
m is a numerical parameter, $m \geq 1$, which is useful when the dimension of M is unknown; if (M, g) is a n-dimensional Rienannian or pseudo-Rienannian space, then m = n; m=2 when M is the digital plane, i.e.:

$$IQCC(p; r, d) = mes\ S(p, r, d) / r$$

for the digital plane

**Definition 1.9.1.1.1.**
**AsyL(= Asymptotic Limit) of an IQCC:**

If (M, d) is unbounded, we define:
AsyL-ICCQ(p, d, m) = $\lim_{r\to\infty}$ IQCC(p; r, d, m) = $\lim_{r\to\infty}$ ( mes S(p, r, d) / $r^{m-1}$ ),
if there is a limit for a certain m; if yes, we have:

**Definition 1.9.1.1.1.Infinity.**
**The value of (m-1) for which there is a proper limit** AsyL-ICCQ(p, d, m), is named "the dimension of the Hypersphere centered at p".

**Definition 1.9.1.1.2.**
**"p-point limit of an IQCC" (in the case of a Riemann space or etc):**

If p is an interior point of M, we define:
**p-point limit**-ICCQ(p, d, m) = $\lim_{r\to 0, r>o}$ IQCC(p; r, d; m) = $\lim_{r\to 0, r>o}$ ( mes S(p, r, d) / $r^{m-1}$ ), if there is one suitable (i.e. there is the limit) value of m.

**Definition 1.9.1.1.3. p-Diameter limit of an IQCC (if M admits a finite diameter wuth regard to point p)**
For $p \in M$, we define:
**p-Diameter limit of IQCC** (p, d, m) = $\lim_{r\to D(p)}$ IQCC(p; r, d, m) =
$\lim_{r\to D(p)}$ ( mes S(p, r, d) / $r^{m-1}$ ), where D(p) is the diameter of M related to point $p \in M$.
Comment. It seems that **p-Diameter limit of IQCC** (p, d, m) is zero.

**Remark1.9.1.1.A.** The definitions **1.9.1.IQCC., 1.9.1.1.1. and 1.9.1.1.1.Infinity are all valid for the Digital Spaces (including the [L; K]-Hex and [L; K]-sq Digital Spaces or multi-type w-dimensional Spaces); the all five definitions are valid for an n-dimensional Riemannian Space or n-dimensional pseudo-Riemannian one.**

**1.9.1.1.E. Examples (Euclidean plane or non-degenerate Quadric Hypersurfaces – Hyp and Ellips.)**.

**1.9.1.1.E.1.** (M, d) = Euclidean Plane. IQCC = $2\pi$ = **Const**

**1.9.1.1.E.2.** (M, d) = The 2-Sphere in 3-Euclidean Space S(p, R):

**p-point limit**-ICCQ(p, d) = $2\pi$

IQCC (p, D(p)/2) = 4

**p-Diameter limit**-ICCQ(p, d) = 0

**1.9.1.1.E.3.** (M, d) = Circular Hyperboloid:

AsyL-ICCQ of Circular Hyperboloid = $2\pi \cos w < 2\pi$,

**p-point limit**-ICCQ(p, d) = $2\pi$

where w is the angle between the asymptote to an Hyperbola (for instance M $\cap$ xOz plane) and the Ox axis.

**1.9.1.1.E.4.** (M, d) = (L; K)-Hex **non-degenerate Digital Plane (see §1.8.)**

**1.9.1.1.E.4.1.** IQCC(p, x+r, [L; K]-Hex) =

$6(K^2 - L^2)/(1 + (r/x)) + cap_(S(O, L; K; HexCells\text{-}Digital\ Plane; r))/(x+r)$,

$\forall$ r an Hex-superstable Energetic Level, x a natural.

**1.9.1.1.E.4.2.** **AsyL** IQCC([L; K]-Hex) = $6(K^2 - L^2) > 0$

Analogously,

**1.9.1.1.E.5.** (M, d) = (L; K)-sq **non-degenerate Digital Plane, (see §1.8.)**

**1.9.1.1.E.5.2.** **AsyL** IQCC([L; K]-sq) = $4(K^2 + 2LK - L^2) > 0$

**Remark1.9.1.1.B. Because always** $2L+1 \leq K$, i.e.

$6(K^2 - L^2) \geq 6(3L^2 + 4L + 1) \geq 6$

then

$6(K^2 - L^2) \geq 48$, for $L \geq 1$

and

$4(K^2 + 2LK - L^2) \geq 4(7L^2 + 6L + 1) \geq 56$, for $L \geq 1$, we have:

**Theorem 1.9.1. <u>For L ≥ 1</u>** (and $2L+1 \leq K$), for Hex or sq-**Digital Plane (non-degenerate)**, we have:

**1.9.1.1.Hex** **AsyL** IQCC([L; K]-Hex) $\geq$ 48

and

**1.9.1.1.sq** **AsyL** IQCC([L; K]-sq) $\geq$ 56,

while

AsyL IQCC on a standard Riemannian Surfaces as **non-degenerate Quadric Hypersurfaces (i.e. elliptic or hyperbolic) or the Euclidean plane, is**
**1.9.1.1.Riemann** IQCC $\leq 2\pi$;
i.e. **the value $2\pi$ separates these spaces, these two families pf geometries,**

that is:
we have a Separation supposition (see also : [HolcPugh2007]):

**Corollary1.9.1.** (Separation supposition) The Euclidean Plane (whose IQCC value is $2\pi$) is a Boundary between the **two** following **geometric families of spaces**:
-The family of all [L; K]-DIGITAL Planes with (sq or Hex)-[L; K]-nondegenerate;
- The family of all Riemannian 2-dimensional spaces.

**Comments1.9.1**. (see [Boju2007 MontrealTech Press])
**Comments1.9.1.A.** It seems plausible to assert that at least the two-dimensional Compact Complete Riemann Manifolds have the (**1.9.1.1.Riemann)**) property, that is
**(1.9.1.1.Riemann property)** IQCC $\leq 2\pi$

**Comments1.9.1**. **B.** The **n-dimensional analogue seems valid** (for instance, the sq case), i.e. :
**The n-dimensionel Separation** supposition:
the IQCC of the n-dimensional Euclidean Space $E^n$ separates the two Universes:
the Digital and the Riemannian ones.

Argument#1. See the "quasi-homothetic" character of the **1.9.1.1.Riemann property.**
Argument#2. The case "**p-point limit of an IQCC":**
Let (M, g) be an Nash-embedding of the considered Riemann space. For **p-point limit of an IQCC, we can compare a neighborhood W of p with his orthogonal projection on the tangent space TMp (see the two-dimensional phenomenon).**

**Comments1.9.1**. **C.** We note the unity of the Riemannian Universe from the IQCC-Separation supposition point of view; the common reason consists in the common geometric phenomenon: the Tangent Space at each point of an n-dim Riemannian Manifold is even $E^n$, i.e.:
When a Riemannian Manifold is introspected into oneself, in a point p, then this becomes an Euclidian Univers.

**§§§**1.9.2. **Trans-n-Riemann Spaces**

**1.9.2.1. Definition. A Trans-n-Riemann Space is a such n-dimensional point-distance space (M, p-compatible-distances) for which:**
**-**there are IQCCs;

- IQCC (n; M) > IQCC (n; Euclidean),
(etc : i.e. different versions; see **1.9.1.IQCC., 1.9.1.1.1., 1.9.1.1.1.Infinity, 1.9.1.1.2. 1.9.1.1.3.**)
where:

**1.9.2.2.** IQCC (n; Euclidean) = $2\pi^{\frac{n}{2}}$ / $\Gamma(\frac{n}{2})$,

where $\Gamma$ is the Gamma function (see **Definition 1.9.1.IQCC.** and 1.10.3.6.).

**1.9.2.3.** There are at least four examples of some Trans-n-Riemann Spaces ( see §§1.3 ):

1.9.2.3.1. (sq; 1-L; 2-L; … ; w-L, w-hypercubicCells-Digital w-Space)

1.9.2.3.2. (sq; 1-L; 2-L; … ; w-L, w-hypercubicCells-Digital w-Space) multi-type-CEBGU

1.9.2.3.3. (sq; 1-L; 2-L; … ; w-L, w-hypercubicCells-Digital w-Space) **Hybrid multi-type-CEBGU**

1.9.2.3.4. (sq; 1-L; 2-L; … ; w-L, w-hypercubicCells-Digital w-Space) **Generalized Hybrid multi-type-CEBGU** with an admissible nucleus;

A more general method to produce some Trans-Riemann Spaces is suggested by the proceeding point-distances-spaces (M; p-d) with $\Omega$ Scaling Spheroidal Model (see [Boju2007_MontrealTech Press]).

**……...…….**

## §§1.10. The Asymptotic-IQCC-dimension. Super-Fractals.

### §§§1.10.1. The Curvature Method.

The curvature method represents an “expressive” tool in the study of Riemann Spaces.

On one side, the spaces with Constant Curvature or with QCQ (Quasi-Constant Curvature – see [BojuPope1978] and [BojuFunar1987]) provide the standard ones, which guide the qualitatively-local studies; particularly, for the study of IQCC-s.

On the other side, a geometric way to a global approach consists in the study of the extreme values of the curvature or of the some substitutes of the asymptotic ones.
For instance, the Holcman-Pugh Compactness Riemannian Boundary and Holcman-Pugh Kick Method ([Holc,Pugh2007]; Kick Method: that is the existence “of a certain ***minimum amount*** of extra **energy or curvature** on a finite **exp-shell**”, that impose compactness and, at the same time, a class of Riemann manifolds) are a surprising

alternative to the asymptotic one, in the search of a Boundary between Compact and Noncompact Complete Riemann Manifolds. Moreover, this leads to some ideas concerning the geometry at infinity and the classification of the geometry at infinity. But, the Holcman-Pugh Kick Method and Holcman-Pugh Compactness Riemannian Boundary are also surprising from an another completely different viewpoint: both "finite shell" and "geometry at infinity" appears in the present chapter, in a context opposite to the Riemannian one:
- in a Digital one, i.e. a totally-discontinuous space;
-while for classical surfaces (**non-degenerate Quadric Hypersurfaces - i.e. elliptic or hyperbolic, or tle Euclidean plane**) IQCC $\leq 2\pi$, for de **non-degenerate** [L; K]-Hex and sq-Digital Plane,
IQCC $\geq$ 48, for L $\geq$ 1.

### §§§1.10.2. **The IQCC-dimension, the Asymptotic-IQCC-dimension**

The **Corollary1.9.1**(Separation supposition) points out the dimension of [L; K]-Hex and sq-Digital Plane as a strange concept (**IQCC-dimension**), far away from the classical, numerical perception of dimension.

It is plausible to talk on a "Cap-Polynomial Dimension"; see:
- **sequence of cap-polynomials of multi-type-CEBGU (§§§1.8.3.);**
- (**1.9.1.1.E.4.1.) the formula for** IQCC(p, x+r, [L; K]-Hex).

**Moreover, the Corollary1.9.1** (Separation supposition) points out the Max-Cap-coefficients, whose sequence may be convergent to infinity; for instance, the sequence of Hex-Max-Cap coefficients is:
L = const = c; $\mathbf{c}_T = 6(K_T^2 - c^2)$ (see 1.8.3. and and Theorem 1.3.1.),
where:
1.10.2.1.

$K_T$ = 3h+2 if c = 2 or 3;

$K_T$ = 3h+1 if c = 1 or 3;

$K_T$ = 3h if c = 1 or 2.

Because
$\lim_{T\to\infty}$ (sequence of Max-Cap-coefficients $\mathbf{c}_T$ from 1.10.2.1) = $\infty$,
(see [Kees 1992] - the analogy with the nesessary conditions of an number to represent a dimension), then **the asymptotic dimension** of the multi-type-CEBGU 1.10.2.1. is strictly superior to 1, i.e.:

**Proposition 1.10.2.1.** The multi-type-CEBGU 1.10.2.1. is a Super-Fractal.

This property is illustrated by an example in **§4.**

**§§§1.10.3. The Q-Like-a-DigitCurvature in a metric space.**

**We dispose of three characteristics of a Hex Digital Space:**
1.10.3.1. StabThresh(L; K, Hex)
1.10.3.2. StabVal(L; K, Hex) (renoted here as StabVal(L; K, H))
1.10.3.3. Cap-Polynomial

**1.10.3.4. The following (L; K, Hex) Digital Spaces (see 1.5.1.A. ) are Iso-Stable**

| (L; K) | | StabThresh (L; K, H) | StabVal (L; K, H) | Hex | (L; K) | | StabThresh (L; K, H) | StabVal (L; K, H) |
|---|---|---|---|---|---|---|---|---|
| **(3;17)** | **Non-Deg** | 34 | 1680 | | (9; 19) | **Non-Deg** | 46 | 1680 |

The above examples prove that the **Q-Like-a-DigitCurvature** in the (Hex or sq) 2-Digital Space is neither 1/(34+x) nor 1/(46+x),
(even modulo an homothety), for the reason of the Cap-Polynomial phenomenon.

**The Q-Like-a-DigitCurvature of the Energetic (r+x)-Level in the metric space [L; K; Hex], is (see 1.6.1.1. Hex-nondegenerate)**
**1.10.3.5. Q-LDCurv (L; K; r+x; Hex) = 1/** DP(L, K, r, x; Hex) =
$= 1/ (6(K^2 - L^2) x + cap_S(O, L; K; HexCells\text{-}Digital\ Plane; r))$
defined for all
Hex- **nondegenerate** (L, K)**, 2L+1** $\leq$ **K, r Hex-superstable, and** $\mathbf{r + x} \geq$ StabTresh(L; K; Hex)**.**

For instance,
**the Q-LDCurv of the Energetic (r+x)-Level in the metric space [3; 17; Hex], r superstable, is**

**1.10.3.5. Q-LDCurv (r+x) = 1/** ( 1680 x + cap_S(3; 17; HexCells-Digital Plane; r)), where (r + x) is Hex-superstable: $\mathbf{r} \geq$ StabTresh(3; 17; Hex)**.**

Analogously,

**The Q-LDCurv of the Energetic (r+x)-Level in the metric space [L; K; sq], is (see 1.6.1.1. sq-nondegenerate)**
**1.10.3.5. Q-LDCurv (L; K; r+x; sq) = 1/** DP(L, K, r, x; sq) =
$1/ (4(K^2 + 2LK - L^2) x + cap_S(L; K; sqCells\text{-}Digital\ Plane; r))$
defined for all
sq-**nondegenerate** (L, K)**, 2L+1** $\leq$ **K, r sq-superstable, i.e.**
$\mathbf{r} \geq$ StabTresh(L; K; sq)**.**

By extension ([Boju2007_MontrealTech Press]), for the Euclidean space $E^n$ we have:

$E^n$ is a metric space with " ř-almost constant Q-LDCurvature", for ř = 0.
The **Q-LDCurv** of the circle $S^1(c,R)$ in the Euclidean plane $E^2$ is $1/2\pi R$, while the Euclidean Curvature is 1/R.
The **Q-LDCurv** of the sphere $S^2$ (c, R) in the Euclidean space $E^3$ is $1/4\pi R^2$, while the Euclidean Curvature is $1/R^2$.
The **Q-LDCurv** of the sphere $S^3(c,R)$ in the Euclidean space $E^4$ is
$1/2\pi^2 R^3$.
The **Q-LDCurv** of the sphere $S^{n-1}$(c, R) in the Euclidean space $E^n$ is

1.10.3.6. $$\Gamma(\frac{n}{2}) / 2\pi^{\frac{n}{2}} R^{n-1} \quad ,$$

where $\Gamma$ is the Gamma function.

Thus, the **n-Trans-Riemannian Boundary is** $2\pi^{\frac{n}{2}} / \Gamma(\frac{n}{2})$.

^^^^^^^^^^^^^^^^^^^^^^^^

## §2. Juxtaposition Combinatorial Measures and Juxtaposition Fractals. Applications in Intrinsic Measure Theory.

**{<u>In this section, the results from [BojuFunar2007-Asymptotics], are presented</u>. }**

### §§2.1. Juxtaposition Combinatorial Measures

**The concept of "Juxtaposition Combinatorial Measure" and "Generalized Hadwiger Numbers" was introduced and studied in**
[Boju1982] Valentin Boju. *Fonctions de juxtaposition, Invariants*. In: Proceedings of the 13th NCGT, Univ. of Cluj, 1982, p. 36-37
and
[Boju1986] Valentin Boju. *Courbures Riemannienes généralisées*. International Conference on Geometry and Applications. As invited speaker (Victor Andreevici Toponogov, V. Boju, a.o.), Bulgarian Academy of Sciences, 1986, p. 47-48.

The papers [Boju1982] and [Boju1982] are cited and continued in [BojuFunar1993-ZAA]. The main theorem from [BojuFunar1993] is also presented in [BojuFunar2007_Springer].

**Abstract**

We give asymptotic estimates for the number of non-overlapping homothetic copies of B which have a common point with F, extending previous work of the L.Fejes-Toth, K.Borockzy Jr., D.G.Larman, S.Sezgin, C.Zong and the authors.

## 1. Introduction

For closed topological disks $F;B \subseteq R^d$, we denote by $N_\lambda(F; B) \in Z_+$ the following generalized Hadwiger number.

Let $A_{F,B,\lambda}$ denote the family of all sets, homothetic to B in the ratio $\lambda$, which have only boundary points in common with F. Then $N_\lambda$ (F; B) is the greatest integer k such that $A_{F,B,\lambda}$ contains k sets with pairwise disjoint interiors. In particular, $N_1(F; F)$ is the Hadwiger number of F and $N_\lambda(F; F)$ the generalized Hadwiger number considered first by Fejes Toth for polytopes in ([4, 5]) and further in [1]. Extensive bibliography and results concerning this topic can be found in [2]. The main concern of this note is to find asymptotic estimates for $N_\lambda(F;B)$ as $\lambda$ approaches 0, in terms of geometric invariants of F and B, as it was done for F = B in [1], and to seek for the higher order terms.

Roughly speaking, counting the number of homothetic copies of B packed along the surface of a d-dimensional body F, amounts to compute the (d – 1)-area of its boundary, up to a certain density factor depending only on B. This factor is especially simple when dimension d = 2.

## 2. Planar domains: approaching the perimeter

Unless explicitly stated otherwise, throughout this section, B will denote a centrally symmetric plane oval.

Any such B determines a norm $\| \ \|_B$ as a natural quotient.

With this norm, $R^2$ becomes a Banach space whose unit disk is isometric to B.

Set $p_B$ (F) for the perimeter of the boundary $\partial F$ in the norm $\| \ \|_B$. We also denote by $d_B$ the distance in the $\| \ \|_B$ norm.

We assume that F is regular, namely that its boundary $\partial F$ is piecewise $C^2$ and it is the union of finitely many arcs with the property that each arc is either convex or concave. This is the case, for instance, when $\partial F$ is a piecewise analytic curve.

Our first result generalizes theorem 1 from ([1]), where we considered the case F = B.

**Theorem 1.** For any symmetric oval B and regular topological disk F in the plane, we have $p_B(F) = 2 \lim_{\lambda \to 0} \lambda N_\lambda(F, B)$

**Definition 1.** Elements of $A_{F,B,\lambda}$ are called beads and a configuration of beads with disjoint interiors is called a necklace. The necklace is complete when all pairs of consecutive beads have a common point and incomplete otherwise.

**Remark 1.** One can also consider packings with disjoint homothetic copies of B laying in F and having a common point with the complement $R^2$ - int(F). Then a similar asymptotic result holds true.

**Second order estimates**

When F is convex, we can obtain more effective estimates of the rate of convergence:

**Theorem 2.** For any symmetric oval B and convex disk F in the plane, the following inequalities hold true:
$p_B(F) - 2\lambda \leq 2\lambda N_\lambda(F, B) \leq p_B(F) + \lambda p_B(B)$

Consider now the general case when F is not necessary convex. The estimates for the rate of convergence are not anymore sharp. By hypothesis, $\partial F$ can be decomposed into finitely many arcs $A_i$, i = 1; m, which we call pieces, so that each piece is either convex or concave. Let m = m(F) denote the number of pieces.

**Theorem 3.** For any symmetric oval B and regular topological disk F in the plane, we have the inequalities
$p_B(F) - 2\lambda (p_B(B)m(F) + m(F) - p_B(B)) \leq 2\lambda N_\lambda(F, B) \leq p_B(F) + 2\lambda ( p_B(B) + 2m(F))$

**Theorem 4.** Consecutive terms in N(F; B) are at most distance 11m(F) apart. When F is convex, consecutive terms in N(F; B) are at most distance 4 apart, if B is not a parallelogram and 5 otherwise.

**Corollary 1.** Consecutive terms in $N(B;B) \subset Z_+$ are at most distance 4 apart.

**Conjecture 1.** If B = F is not a parallelogram, then N(B; B) contains all sufficiently large integers.

**Corollary 2.** For convex F we have also some inequalities.

**Conjecture 2.** There exists some constant c = c(B) such that the following limit exists

a some limit = $\varphi(\alpha)$, where $\varphi : [0; 1) \to [-2; p_B(B)]$ is a right continuous function with finitely many singularities. If F, B are polygons, then $\varphi$ is linear on each one of its intervals of continuity.

## 4 Higher dimensions

The previous results have generalizations to higher dimensions in terms of some Busemann-type areas defined by B. Theorem 1, when F = B, was extended in [[Börö,Larman,Sezgin,Zing1999-2000]] and ([[Börö2004]], 9.10). However, the result involves the presence of an additional density factor which seems hard to compute. The same happens for general F and B.

For a convex body K in $R^d$, one defines the translative packing density $\delta(K)$ to be the supremum of the densities of periodic packings by translates of K.
For convex and smooth B and F, and a centrally symmetric smooth domain B in $R^d$, we obtain

**Theorem 5.**

$$\lim_{\lambda\to\infty} \lambda^{d-1} N_\lambda(F, B) = \int_{\partial F} \frac{1}{\Delta(B \cap T_x)} dx \ ,$$

where $x \in \partial F$ and $T_x$ is the tangent space at x on $\partial F$.

**Conjecture 3.** The largest distance between consecutive elements of N(F; B) is at most $2^d$ with equality when B is a parallelohedron.

**References for §§2.1. Juxtaposition Combinatorial Measures (the list from [BojuFunar2007-Asymptotics])**


1.[BojuFunar1993], Generalized Hadwiger numbers for symmetric ovals, Proc. Amer. Math. Soc. 119(1993), 931{934.

2.[Börö2004] K. Böröczky Jr, Finite packing and covering, Cambridge Tracts in Mathematics, 154, Cambridge University Press, Cambridge, 2004.

3.[Börö,Larman,Sezgin,Zing1999-2000] K. Böröczky Jr., D.G.Larman, S.Sezgin and C.Zong, On generalized kissing numbers and blocking numbers, III International Conference in "Stochastic Geometry, Convex Bodies and Empirical Measures", Part II (Mazara del Vallo, 1999). Rend. Circ. Mat. Palermo (2) Suppl. No. 65, part II (2000), 39-57.

4.[Toth1970] L. Fejes Toth, Uber eine affininvariante Masszahl bei Eipolyedern, Studia Sci. Math. Hungar. 5(1970), 173-180.

5.[Toth1975] L. Fejes Toth, On Hadwiger numbers and Newton numbers of a convex body, Studia Sci. Math. Hungar. 10(1975), 111-115.

6.[GrayTubes2004] A.Gray, Tubes, Progress in Mathematics, 221, Birkh auser Verlag, Basel, 2004.

7.[MartiniSwanWeiss2001] H.Martini, K.J.Swanepoel and G. Weiss, The geometry of Minkowski spaces|a survey I, Expositiones Math.
19(2001), 97{142.

8.[Thom1996] A.C.Thompson, Minkowski Geometry, Encyclopedia of Mathematics and its Applications, 63, Cambridge University Press, Cambridge, 1996.

**……...…….**

## §§2.2. Juxtaposition Fractals. Hybrid Juxtaposition Fractals

### §§§2.2.1. Juxtaposition Fractals

In this section is presented a class of fractals obtained using the juxtaposition function $h_F$, defined ([Boju1982], [Boju1994]) by the "Juxtaposition Function", for a topological disk F in $E^n$, and a symmetry with respect to partial F. For each $\lambda$ in (0, 1], consider a maximal collection $\{ F_p, p = 1, ..., h_F(\lambda)\}$ of sets with disjoint interiors, homothetic to F in ratio $\lambda$, which have only boundary points in common with F. For each $F_p$, let $w_p$ be the similitude which sends F into $F_p$.

For the exterior case, we call the attractor of the IFS $\{ E^n ; w_p , p = 1, ... , h_F(\lambda)\}$ the *juxtaposition fractal* (JF) *associated to F, with parameter* $\lambda$. The method is valid for both variants of the juxtaposition function (in the "interior" case, in a similar manner). Combining the two variants of this function in a random manner, we obtain a *random juxtaposition fractal* (RJF).
Next we consider another variant of the juxtaposition function defined for two topological disks K, G in $E^n$ and the corresponding JF associated to K and G.

Some properties regarding the fractal dimension of the JF are given in [Boju2007_MontrealTech Press]. There are also given the IFS codes corresponding to the JF obtained for some pairs (K, G) of elementary patterns.

Next, using as generator for juxtaposition of a symmetric convex disk G, a method for increase the measure of convexity of a concave topological plane disk K is presented. An algorithm for the case when K itself is a polygon is given.

### §§§2.2.2. Hybrid Juxtaposition Fractals

The Python Program (see **§§4.2. Juxtapositin Fractals**) is based on the properties (see [Kees1992]) of an IFS: it is possible to visualize the successive approximations by starting from arbitrary few points. For details see [Boju2007_MontrealTech Press].

^^^^^^^^^^^^^^^^^^^^^^

## §3. Riemannian Regression Submanifolds. Hamilton-Jacobi reduced equation, Discrete VTF Methods and D. Holcman-C.C. Pugh Kick Method. Applications in Nanotechnologies

The present section represents a continuation of the preprint [Boju1994-*VTF-Regression Riem. Submanif.*]. Its purpose is to *VTF*-regress a continuous function defined on a bordered domain in a Riemannian *n*-dimensional space (*M*, *g*).
The versor type functions (*VTF*) were introduced in [Boju1976-*Thesis*] and studied in [BojuFilip2004], [BojuFunar1996], [Boju1978-Versor Type Functions], [Boju1978-Gradient], [BojuPope1978-JDG], [BojuPope1974-Atti].

In [Boju1994-*VTF-Regression Riem. Submanif.*], a general method for regressing a continuous function *w*, defined on a bordered manifold *D*, is presented. The detailed procedure consists in two steps, as follows. Firstly, we consider a (versor type function) *VTF*-packing of the Riemannian manifold D which offers a standard proximity network. The integral value of *w* on each tile of the packing is concentrated in the *w*-center of gravity of each tile. Secondly, the weighted cloud is regressed to a *VTF*-hypersurface, the calculus being simplified since the vector field *grad f* is a geodesic field. In this case, the *VTF*-method is a generalization of the semi-geodesic coordinates method.

**Keywords:** versor type gradient dynamical system, versor type functions (*VTF*), *VTF*-foliations, Riemannian packings, Riemannian nonlinear regression, geodesic field, weighted/ dynamical cloud, disturbing zones of a dynamical system, flight dynamics, pathological metabolic activity, viral infection, high resolution standard nearness network, pipe inspection microrobotics.

### §§3.1. VTF Methods

### 3.1.1. Basic concept of *VT*-gradient dynamical system

We consider, in this part, the *VTF* method. Let $F^k(M)$ be the set of functions of class $C^k$ from $M$ to $R$ and $D^1(M)$ the set of vector fields of class $C^2$ on $M$. It is well known that, locally, a vector field X is equivalent to a dynamical system $\varphi$.

Let *grad* be the operator $grad : F^1(M) \to D^1(M)$. The vector field $Z \in D^1(M)$ is locally the gradient of a function iff

$$g(\nabla_X Z, Y) = g(\nabla_Y Z, X),$$

where $\nabla$ is the Levi-Civita connection.

### 3.1.2. Hamilton-Jacobi reduced equation

**3.1.2.1.1. Definition 1.** A function $f \in F^3(M)$ is a *VTF* if, for each point $p \in M$, there is a neighbourhood $V$ of $p$ and a function $f_1 \in F^3(V)$ such that

$$grad\ f = \|grad\ f\| grad\ f_1.$$

The following are equivalent definitions.

**3.1.2.1.2. Definition 1'.** $f$ is *VTF* iff

$$X(\|grad\ f\|)Yf = Y(\|grad\ f\|)Xf,$$

$\forall X, Y \in D^1(M)$.

**3.1.2.1.3. Definition 1''.** $f$ is *VTF* iff $\exists h : R \to R,\ h \in F^3$ such that $\|grad\ f\| = h \circ f$, that is $f$ satisfies a **Hamilton-Jacobi reduced equation**. Denote by *VTF*($M$) the set of all versor type functions on $M$.

If $f$ is a *VTF*, then, locally, over an open set $U \subset M$, we have a unit dynamical system $N$ and the function $f_1$ such that

$$N = \frac{grad\ f}{\|grad\ f\|} = grad\ f_1.$$

The corresponding Hesse tensor field *H*, defined by $HX = \nabla_X \, grad \, f_1, \ \forall X \in D^1(U),$ is a self-adjoint operator. It follows immediately that $N^\perp$ is *H*-invariant, that is $H\left(N^\perp\right) \subset N^\perp$.

Some useful properties in our method of *VTF*-regression are the following:

**P$_1$.** For each $f \in VTF(M),$ we have locally ([2])

$$2g^{ij} f_j \left( f_{ik} f_r - f_{ir} f_k \right) = = f_i f_j \left( \frac{\partial g^{ij}}{\partial x^r} f_k - \frac{\partial g^{ij}}{\partial x^k} f_r \right),$$

where $f_i = \frac{\partial f}{\partial x^i}$, $f_{ij} = \frac{\partial^2 f}{\partial x^i \partial x^j}$, $\left( \left( g^{ij} \right) \right) = \left( \left( g_{ij} \right) \right)^{-1}$, $g_{ij}$ being the components of the Riemannian metric.

**P$_2$.** Let *f* be in *VTF*(*M*); then the trajectories of the dynamical system locally associated with *grad f* are geodesic lines [2].

**P$_3$.** For $a \in \mathrm{Im}(f),$ let *f*[*a*] denote the preimage of the value *a* with respect to *f*, that is *f*[*a*] is a constant level generalized hypersurface of *f*. If $f \in VTF(M)$ then for each point $p \in M$ and each *q* situated on the same trajectory determined by *p*, we have

$$d(p,q) = \left| f(p) - f(q) \right|,$$

where *d* is the Riemannian distance.

**……..…….**

**§§3.2. Riemannian Regression Submanifolds & Nanotech Applications**

**§§§3.2. 1. *VTF* regressions of a weighted cloud**

**§§§3.2. 1.1. *VTF* regressions of a weighted cloud in a Riemannian space**

Consider a weighted cloud $\left( p_i, m_i \right)_{i=\overline{i,k}}$, $p_i$ being points from an *n*-dimensional Riemannian space (*M*, *g*) and $m_i > 0$ the given weights in $p_i$, and *f* a versor type function on *M*. Put $c_i = f\left(p_i\right)$.

We approach the *VTF*-regression of the weighted cloud with a $f \in VTF(M)$ by the least-squares estimate of a value *b*, which minimizes the error sum of squares

$$q(b) = \sum_{i=1}^{k} m_i (c_i - b)^2 ,$$

where $b$ is the level of the optimal hypersurface of constant value of f. Let $\varepsilon_i$ be the error approximation (see [10]), $E(\varepsilon_i) = 0$, with $|\varepsilon_i| = d(p_i, f[b])$.

For $m_i = 1$, $i = 1, \ldots, k$, we have the classical regression problem: to minimize the error sum of squares

$$q(b) = \sum_{i=1}^{k} (c_i - b)^2 .$$

Usually, we dispose of different *VTF*-families depending on a scalar or vector parameter $a$ (see, for example, in $\mathbf{R^n}$, the families of planar, cylindrical or spherical *VTF* on $\mathbf{R^n}$ - [1-3]).

Let $f_a \in VTF(M)$ be such a family. The determination of the optimal $f_a$ and of the optimal hypersurface of constant level of $f_a$, which realize the *VTF* regression of the weighted cloud, can be done using the generalized least-square method. The least-square estimatons for $a$, denoted by $\hat{a}$, and for $b$, denoted by $\hat{b}$, minimize the function

$$q(a,b) = \sum_{i=1}^{k} m_i (f_a(p_i) - b)^2 .$$

Since in the considered family there may be functions which have the same hypersurfaces of constant level, we can impose a reasonable condition for $\|grad\, f_a\|$.

By introducing an auxiliary fonction h(a), dependent on $\|grad\, f_a\|$, we can obtain estimations for $a$ and $b$. By Lagrange's multiplier method, the extremal values of $q(a, b)$ are critical points of the function

$$L(a,b,\lambda) = \sum_{i=1}^{k} m_i (f_a(p_i) - b)^2 - \lambda h(a) .$$

### §§§3.2. 1.2. *VTF* regressions on $\mathbf{R^n}$

If $f \in VTF(R^n)$, $R^n$ considered with the standard metric, then ([2]) the hypersurfaces of constant level of $f$ are
the special families mentioned above.

Let $\left(p_i(x_i^j)_{i=\overline{1,n}}, m_i\right)_{i=\overline{i,k}}$ be a weighted cloud of points from $R^n$, $m_i > 0$ being the weight of $p_i$.

Firstly, we search for a regression by a hyperplane.

*We consider VTF* regressions with functions defined by $f_a(x) = a^1x^1 + \ldots + a^nx^n$, $\forall x \in R^n$, with $a \in R^n \setminus \{0\}$.

The hypersurfaces of constant level of function *f* are parallel hyperplanes given by $f_a(x) = b, b \in R$, $grad\ f_a = a^i\,\partial/\partial x^i$, $\|grad\ f_a\|^2 = (a^1)^2 + \ldots + (a^n)^2 = \|a\|^2$ and the dynamical system associated to the vector filed $grad\ f_a$ is given by $\varphi(t, x) = x + ta$. Thus, the trajectories of the dynamical system associated to $grad\ f_a$ are geodesics of $\mathbf{R^n}$ - parallel lines whose director vector is *a*, orthogonal to the hypersurfaces of constant level of *f*. Therefore, the *VTF* regression of a weighted cloud on $R^n$ is equivalent to the problem of determining a hyperplane $\alpha : a^1x^1 + \ldots + a^nx^n = b$, with $\|a\| = 1$ such that the sum $\sum_{i=1}^{k} m_i(d(p_i, \alpha))^2$ is minimal.

The generalized least-squares estimates for *a* and *b*, minimize the function

$$q(a,b) = \sum_{i=1}^{k} m_i(a^1x_i^1 + \ldots + a^nx_i^n - b)^2,$$

with respect to the condition $\|a\| = 1$. Now, we can apply Lagrange's multiplier method as described above to find a regression hyperplane. Analogously, we can search for a regression hypercilinder or hypersphere. Finaly, the optimal regression will be obtain by choosing from the three *VTF*-family, the one which minimizes the sum of squares.

### §§§3.2.2. *VTF*-packings in nanotechnologies and biotechnologies

#### §§§3.2.2.1. *VTF*-packings in nanotechnologies

Let *D* be a domain in *M*, whose border $\partial D$ is a hypersurface *S*. The *VTF* functions come in handy in the building of a *VTF*-packing on *D*. To do this, it is sufficient to know a packing $P_{n-1}$ on a hypersurface $D_{n-1}$ with the property that the projection of the domain *D* onto $D_{n-1}$ by the dynamical system *grad f* is covered by $P_{n-1}$. It

is preferable for $D_{n-1}$ to be included in a hypersurface of constant level of the considered function *f*. In return, $P_{n-1}$ can itself be obtained using a *VTF* transport from a packing $P_{n-2}$ of a submanifold $D_{n-2}$, and so on.

This method enables us to obtain a standard proximity network, in fact a VTF-network, named *f*-network (see [4]). The *f*-networks for appropriate $f \in VTF(M)$ constitute a good frame in a nonlinear problem of nanotechnologies.

In biotechnology, the *VTF* $f$ is chosen accordingly with respect to the physiological, anatomical and metabolic properties of the considered bio-space/bio-process which is to be controlled. For example ([9]), the appropriate nano-measuring of a circumstantial anatomical ultrastructure - the Nucleolus Associated Bodies in the interphasic nucleus - provides information regarding the physiological state of some plant or animal cells. This allows us to detect the cells with anomalously intense/pathological metabolic activity or with viral infection.

Also, the high resolution standard nearness network is useful in: Aerospace technology, Flight Dynamics in Aerospace technology (see [8]) – the control of the disturbing zones of a dynamical system, Pipe Inspection Microrobotics, transcription technology, the improvement of a depth of focus, the modeling of 3D objects with respect to their shapes and motions, the control of the weighted and dynamical clouds, the control of computation algorithms for analysis of *n*-dimensional structures.

#### §§§3.2.2.2. *VTF*-packings in biotechnologies

In the biotechnologies, the processes modeled by the dynamical systems, the considered case can be generalized by replacing the weighted cloud by a dynamical cloud thus: the cloud's elements are pairs of the form $(p_i, v_i)$, where $p_i \in M$, $v_i \in M_{p_i}$ and the considered bio-space is structured like an *n*-dimensional Riemannian manifold $(M, g)$.

#### Conclusion.

The two methods – i.e. the *VT* packings and *VT* regressions – may be considered together [Boju1994-*VTF-Regression Riem. Submanif.*]. Thus, we obtain a general method for the regression of a continuous function *w*, defined on a bordered domain *D*, with $\partial D = M$, $(M, g)$ being an *n*-dimensional Riemannian space. The procedure consists in

two steps, as follows. First of all, a *VTF*-packing (of the domain *D*, using a *VTF*-foliation) is considered, which allows to discretize the function *w* and to obtain a weighted cloud. Then, the weighted cloud is regressed to a *VTF*-hypersurface, generated by a versor type function *f*, the calculus being greatly simplified since the vector field *grad f* is a geodesic field.

**……..…….**

**§§3.3. VTF Methods: VTF-Methods, Holcman-Pugh Kick Method and Holcman-Pugh Compactness Riemannian Boundary.**

**3.3.1. Hamilton-Jacobi reduced equation**

The study of Hamilton-Jacobi reduced equation **3.1.2.1.3.** leads to interesting topological results in Riemannian Geometry.
**3.3.1.1.** (Theorem 4.4., [BojuFunar1987]). The Real Cohomology of the n-Sphere and of a Compact, Connected and simply-Connected Riemannian n-manifold with Quasi-Constant Curvature ([BojuPope78-JDG]) , with H, N > 0, is the same.

**3.3.1.2.** The general solution of the equation 3.1. [Holcm-Pugh-2007)] is obtained in [BojuFunar1987] and used in [BojuFunar1996-ZAA] to obtain a compactness result for complete manifolds whose Ricci Curvature is bounded from below.

**3.3.2.** The Comments from §§§1.10.1. are also relevant in this section. A global approach which consists in the study of the extreme values of the curvature or of the some substitutes of the asymptotic ones, provides the strong results.
The Holcman-Pugh Kick Condition ([Holc,Pugh2007] Kick Method point off "a certain ***minimum amount*** of extra **energy or curvature** on a finite **exp-shell**") impose compactness and, at the same time, a class of Riemann manifolds. This method also solves a fundamental dilemma from Mathematical Philosophy. The answer in the question on the existence of a Boundary Between Compact and Noncompact Complete Riemann Manifolds is unexpected, in a certain "analytical light": while there is no such boundary between convergent and divergent series ([Rudin1976]), the Kick Method emphasizes one. The Holcman-Pugh Compactness Riemannian Boundary phenomenon ([Holc,Pugh2007]) represents another deeply inciting revelation: "the local perturbations have no global effect on series, while for curvature functions this is not so".

^^^^^^^^^^^^^^^^^^^^^^^^

**§4. C, TPascal and Python Programming Languages Applications****

**There are many and remarkable Applications [© 2006-2007 Valentin Boju & Antoniu Boju; The Patents - MontrealTech Register] of the four original Methods, Concepts and Programs which are presented in this paper (regarding almost all domains of activity), elaborated and drawn up [The Patents - MontrealTech**

**Register] for:** Industry, Economy, Architecture – Decorative & Mosaics Work – Ceramics & Urban Sculpture – Textile Pictures and Textures, Software and Data Technologies, Thermodynamics/hydrodynamics and Phase Stability Calculations, Pattern Recognitions, New (Discrete/Differentiable) Digital Metric Curvature Methods (with applications in Cosmological Modelling), Cryptography and Security Procedures, Interactive Entertainment, Biomedical Applications.

The current applications of MontrealTech [**The Patents - MontrealTech Portfolio - © 2006-2007, authors]**, which are in a advanced phase, targe:

**- Graphics, Computer Vision and Image Processing;**
**- Energy Units (Compartmented Energetic Bank/Generator Units);**
**- Cryptography and Security Procedures;**
**- Architecture – Decorative & Mosaics Work – Ceramics & Urban Sculpture – Textile, Pictures and ` Textures;**
**- Computer and Video Games;**
**- Biomedical Applications;**
**- (Exterior/Interior) Juxtapositin Fractal**
**- Riemannian Regression Submanifolds, & Nanotech Applications**
**- Pattern Recognitions & Defence Research Programs.**

**. A team of students in **MontrealTech**, who finished a course of Riemannian Geometry of Doctoral level, did a stage during the realization of the programs of the 9th paragraph with the authors, that is Valentin Boju and Antoniu Boju.

### §§4.1.B. Hex-Superfractals – Program: C. [ValB-CAB Superfractals Hex-Procedure in the Digital Plane & the subsequent C-Program , © 2006-2007 Valentin Boju & Antoniu Boju; The Patents - MontrealTech Register, MontrealTech Portfolio - © 2006-2007, authors]

**See Figure at Page 381**

"The Wonderful SuperFractal = The Fantastic Digital World " created by Valentin and Antoniu Boju – in 2005-2007 ©, as an Expression of The New Energy, marked by "Copyright © 2006-2007, Valentin Boju and Antoniu Boju", i.e. they are copyrighted and protected: the Berne copyright convention - All Rights Reserved: [**The Patents - MontrealTech Register, MontrealTech Portfolio - © 2006-2007, authors].** The use of the specified §1, §2 and §4 is allowed only for educational purposes under our permission in written form, but not for commercial ones.

The original music, composed by Valentin Boju, can be listen to the following address:
http://www.soundclick.com/valentinmusicgroup
This FANTASTIC COLOR IMAGE is available at: valentin@montrealtech.org, cosmin.antoniu@montrealtech.org
or at: MontrealTech , C.P.78574, Succ Wilderton, Montréal, Qc, H3S 2W9, Canada
http://pages.videotron.com/nanotech

**Program [$L_i$ ; $K_i$ ]**

**By Valentin Boju and Antoniu Boju**
Selected fragments in C

"Copyright © 2006-2007, Valentin Boju and Antoniu Boju", i.e. they are copyrighted and protected: the Berne copyright convention - All Rights Reserved: [**The Patents - MontrealTech Register, MontrealTech Portfolio - © 2006-2007, authors].**

The use of the fragments is allowed only for educational purposes under our permission in written form, but not for commercial ones.

```
……..
        GDate * date= g_date_new();
        g_date_set_time_t( date, time(NULL) );

        tmp = text;
        text = g_strdup_printf("%s_%d", text, g_date_get_day(date));
        g_free(tmp);

        switch (g_date_get_month(date))

        gchar *time_txt = get_timer_text(total_time);

        tmp = text;
        text = g_strdup_printf("SQR_%s-%s-%d_%d_%s", text, t,
 g_date_get_year(date), current_step, time_txt);
        g_free(tmp);

        g_free(time_txt);

                g_date_free(date);

        *filename = text;
        *dirname = dir;

        return;
……..
{
        guint s, m, h;
        guint tnow = seconds; /*(int)g_timer_elapsed(maintimer, NULL);*/

        s = tnow % 60;
        m = ((tnow - s) / 60) % 60;
        h = (tnow - s - m * 60) / 3600;

        return g_strdup_printf("%02d:%02d:%02d", h, m, s);
}
…….
int gtkalgo_pause_computing()
{
        if (gtkalgo_is_on_pause)
                return 1;

        autosave_func(NULL);
        g_source_remove( glib_idle_event );
        g_timer_stop(maintimer);
        gtkalgo_is_on_pause = 1;

        return 0;
        }
```

```
……..
int gtkalgo_start_computing()

        if (gtkalgo_is_on_pause) {

                int r;

                dlgParameters = create_dlgParameters();

                if ((algo_step_vector[0] > 0) || (algo_step_vector[1] > 0)) {

        gtk_spin_button_set_value(GTK_SPIN_BUTTON(lookup_widget(dlgParameters,
"valParameterX")), algo_step_vector[0]);

        gtk_spin_button_set_value(GTK_SPIN_BUTTON(lookup_widget(dlgParameters,
"valParameterY")), algo_step_vector[1]);
        }
……..
                int x, y;
                                x =
 gtk_spin_button_get_value(GTK_SPIN_BUTTON(lookup_widget(dlgParameters,
"valParameterX")));
                y =
 gtk_spin_button_get_value(GTK_SPIN_BUTTON(lookup_widget(dlgParameters,
"valParameterY")));

                x = abs(x);
                y = abs(y);

                gtk_widget_destroy (dlgParameters);
                dlgParameters = NULL;

                if (current_action == 1) {
                        table = g_malloc(sizeof(*table) * table_backup_size);
                        table_size = table_backup_size;
                        g_memmove(table, table_backup, sizeof(*table) * table_size);
                        g_free(table_backup);
                        table_backup = g_malloc(sizeof(*table) * table_backup_size);
                }

                g_free(masktable);
                masktable = g_malloc0(sizeof(*masktable) * table_size);

                algo_step_vector_max[0] = MAX(algo_step_vector_max[0], x);
                algo_step_vector_max[1] = MAX(algo_step_vector_max[1], y);

                current_action = 2;
                current_step--;

                if (algo_step_vector[0] != x || algo_step_vector[1] != y) {
                        algo_step_vector[0] = x;
```

```
                        algo_step_vector[1] = y;

                        stats_t t;

                        t.type = STATS_PARAMS_CHANGE;
                        t.newparameters[0] = x;
                        t.newparameters[1] = y;

                        add_stat_entry(&t);
                }
……..void gtkalgo_update_progressbar()
{
        gtk_progress_bar_set_fraction(GTK_PROGRESS_BAR(lookup_widget(winMain,
 "progressbar1")), algo_status_fraction);
}
#define SET_GDK_SEGMENT_COORDS(s, _x1, _y1, _x2, _y2)
void draw_small_text_int(int x, int y, int number, int zoom, GtkWidget
 *drawing_area, GdkGC *gc)
{
        void draw_small_char(char c, int pos)
                int i;
                for (i = 0; i < num_lines; i++)
                gdk_draw_segments(drawing_area->window, gc, lines, num_lines);
        } /* draw_small_char() */

        int n;
        n = number;
        if (n < 10) {
                draw_small_char(n,0);
                return;
        }
        draw_small_char(n % 10, ((double)zoom * 1.5 / 7));
        n = n/10;
        draw_small_char(n % 10, -((double)zoom * 1.5 / 7));
}
……..
void draw_sqr(int x, int y, double zoom, GtkWidget *drawing_area, GdkGC
 *gc)
{
                        if (gcs > -1) {
                                gdk_gc_set_rgb_fg_color(gc, &color);
                                draw_small_text_int(dx, dy, gcs, zoom, drawing_area, gc);
                        }
                }
……..
void gtkalgo_drawingarea_do_redraw(int x1, int y1, int x2, int y2,
 GtkWidget *drawing_area)

void gtkalgo_do_redraw(GtkWidget *drawing_area)
{
        int x;
```

```
	int y;

	if (algo_need_redraw) {

		if (winInfo) {

			GtkTextBuffer *buffer;

			buffer = gtk_text_view_get_buffer(
GTK_TEXT_VIEW(lookup_widget(winInfo, "textview1")) );

			gchar *text = NULL;

			text = gtkalgo_get_info_text();

			gtk_text_buffer_set_text(buffer, text, -1);

			g_free(text);

			GtkTextIter iter;

			gtk_text_buffer_get_end_iter(buffer, &iter);

			GtkTextMark *mark = gtk_text_buffer_create_mark(buffer, NULL,
&iter,
TRUE);

	gtk_text_view_scroll_to_mark(GTK_TEXT_VIEW(lookup_widget(winInfo,
"textview1")),
                                                                mark,
                                                                0, TRUE, 0, 0);

			gtk_text_buffer_delete_mark(buffer, mark);

			gchar *s = g_strdup_printf("Info - [%d, %d]", algo_step_vector[0],
algo_step_vector[1]);

			gtk_window_set_title(GTK_WINDOW(winInfo), s);

			g_free(s);
		}

		gchar *s = g_strdup_printf("Main Window - [%d, %d]",
algo_step_vector[0], algo_step_vector[1]);

		gtk_window_set_title(GTK_WINDOW(winMain), s);

		g_free(s);

……..
```

```
                int i;

                for (i = 0; i < gtkalgo_rgbbuf_width * gtkalgo_rgbbuf_height * 3;
i++)
                        gtkalgo_rgbbuf[i] = 127;

                int r, g, b;

                for (x = 0; x < current_d*2; x++) {
                        for (y = 0; y < current_d*2; y++) {
                                int gcs = get_cell_state(x-current_d,y-current_d);
```

- % % % -

……..…….

## §§4.2. Juxtaposition Fractals – Program: Python. [ValB-CAB Juxtaposition Fractals Procedure & the subsequent Python Program, © 2006-2007 Valentin Boju & Antoniu Boju; The Patents - MontrealTech Register, MontrealTech Portfolio - © 2006-2007, authors]

Program: FRACTAL-Python
By Valentin Boju and Antoniu Boju
Selected fragments in C

"Copyright © 2006-2007, Valentin Boju and Antoniu Boju", i.e. they are copyrighted and protected: the Berne copyright convention - All Rights Reserved: [**The Patents - MontrealTech Register, MontrealTech Portfolio - © 2006-2007, authors].**
The use of the fragments is allowed only for educational purposes under our permission in written form, but not for commercial ones.

……..

```
class Fractal:
   points = []

   R = 180
   mu = 0.333333333
   iteration = 0

   data = [[], [], [], [], []]
   fparam = [{},{},{},{},{}]

   seq_length = 0

   last_n = 0

   def f(self, l, x, y):

      c = (self.param['sequence'])[self.iteration % len(self.param['sequence'])]
      n = 0
```

```
    if c == "A":
        n = 0
    elif c == "B":
        n = 1
    elif c == "C":
        n = 2
    elif c == "D":
        n = 3
    elif c == "E":
        n = 4

    for i in self.fparam[n]:
        setattr(self, i, self.fparam[n][i])
    for p in self.data[n]:
        l.append( (x * self.mu + p[0], y * self.mu + p[1], self.iteration) )

def __init__(self, param):
    self.last_n = 0
    self.param = param
    self.fparam = [{},{},{},{},{}]

    self.seq_length = len(self.param['sequence'])

    n = 0
    for f in self.param['files']:
        f.seek(0)
        self.data[n] = []
        print "reading", f
        for line in f:
            if '=' in line:
                assign = line.split('=')
                if len(assign) != 2:
                    continue
                assign[0] = assign[0].strip()
                assign[1] = (assign[1].strip()).replace("\n", "")
                self.fparam[n][assign[0]] = eval(assign[1])
                print self.fparam[n][assign[0]]
            elif ',' in line:
                xy = line.split(',')
                self.data[n].append( (float(xy[0]) * self.R, float(xy[1]) * self.R) )
                print xy
        n = n + 1

    self.points = [(0,0,0)]
    self._prepare_new_iteration()

def _prepare_new_iteration(self):
    self._n = len(self.points)
    self._i = self.last_n

def run(self):
```

```
while self._i < self._n:
   self.f(self.points, self.points[self._i][0],
      self.points[self._i][1])

   if self._i % 2500 == 2499:
      self._i = self._i + 1
      break

   self._i = self._i + 1

if self._i >= self._n:
   print self._i, self._n
   self.iteration = self.iteration + 1
   self._prepare_new_iteration()

if self.iteration <= self.seq_length * self.param['iterations']:
   return True
else:
   return False
```

**……..…….**

**§§4.3. VTF Methods – Riemannian Regression Submanifolds & Nanotech Applications - Program: TPascal [ValB-CAB VTF Methods – Riemannian Regression Submanifolds & Nanotech Applications Procedure & the subsequent TPascal Program, © 2006-2007 Valentin Boju & Antoniu Boju; The Patents - MontrealTech Register, MontrealTech Portfolio - © 2006-2007, authors]**

**The programs are presented in [Boju2007_MontrealTech Press].**

- %%% -

## REFERENCES


[Barl2002].A. Barlow. An adaptive multi-material arbitrary Lagrangian Eulerian algorithm for computational shock hydrodynamics, Swansea, 2002.

[Bell2007] Gregory C. Bell. GROWTH OF THE ASYMPTOTIC DIMENSION FUNCTION FOR GROUPS_GREGORY C. BELL, 2007, 14 pages, PS_cache/math/pdf/0504/0504577v1

[Boju2007_MontrealTech Press]. Valentin Boju. Digital, Discrete and Combinatorial Methods in an Euclidean or Riemannian context and Programming Languages Appl., MontrealTech Press, 2007, 164 pages. ISBN 978-0-9782323-2-0, director@montrealtech.org montrealtech@videotron.ca, http://pages.videotron.com/nanotech.

[Boju2001] V. Boju, *Zones perturbatrices du mouvement ou de la structure d'un mobile*, Polytechnic International Press, Montreal, 2001, pp. 540-543.

[Boju1994-Juxtap-Fractals] Valentin Boju. Juxtaposition Fractals. Seminar on Combinatorial, Computational and Differential Geometry and Topology, Preprint Nr. 6., Univ. of Craiova, 1994, p.1-4

[Boju1994-*VTF-Regression Riem. Submanif.*] V. Boju. *VTF-Regression Riemannian Submanifolds*. Seminar on Combinatorial, Computational and Differential Geometry and Topology, Preprint Nr. 4, Univ. of Craiova, 1994, p. 1-6.

[Boju1986] Valentin Boju. *Courbures Riemannienes généralisées*. As invited speaker: (Victor Andreevici Toponogov, V. Boju, a.o.) International Conference on Geometry and Applications. Bulgarian Academy of Sciences, presid. Gr. Stanilov, 1986, p. 47-48

[Boju1985] Valentin Boju. Geometric Kaleidoscope. In *Mathematical Exercises for Pupils*. Pedagogical High School, Craiova, 1985, p. 85-101.

[Boju1982] Valentin Boju. *Fonctions de juxtaposition, Invariants*. In: Proceedings of the 13th NCGT, Univ. of Cluj, 1982, p. 36-37

[Boju1978-Versor Type Functions] V. Boju. *La géométrie d'une fonction type verseur*. Actas del 5th Congreso de la Agrupacion de Matematicas de Expresion Latina. Publicaciones del Instituto de Matematicas Madrid, 1978, Talleres Graficos VDA, ISBN: 84.00-04340-5, p. 292-296.

[Boju1978-Gradient] V Boju, V. *Une méthode d'utiliser l'opérateur gradient en géométrie riemannienne*. Rev. Roumaine Math. Pures Appl. 23 (1978), no. 9, 1297-1299

[Boju1976] V. Boju. *Contributions to the Differential Geometry of the gradient operator*. Ph.D. Thesis, Univ. of Bucharest, 1976

[BojuFilip2004] Valentin Boju, Ioan Filip. *Some Applications of the VT-Gradient Dynamical Systems in Nonlinear Nano-Measurings and Riemannian Regressions.* The 8th World Multiconference on Systemics, Cybernetics and Informatics - SCI 2004. International Institute of Informatics and Systemics - IIS**.** 2004, Orlando, Florida, Volume V, Computer Science and Engineering, p. 299-304

[BojuFunar2007_Springer]. Valentin Boju and Louis Funar. The Math Problems Notebook, Birkhauser Boston, 236 p., Aug 2007.

[BojuFunar2007-Asymptotics]. V. Boju and L. Funar. Asymptotics of generalized Hadwiger numbers. Preprint. Oct 2007, p. 1-6, (gz) (pdf)
http://www-fourier.ujf-grenoble.fr/~funar/articles.html

[BojuFunar1996] V. Boju, L Funar. *A note on the Bonnet-Myers theorem.* Zeitsch. Analysis Anwendungen (ZAA), 15 (1996), no. 2, 275-278

[BojuFun1995] Valentin Boju, Louis Funar. Computational Methods for Juxtaposition Fractals. The Eleventh Summer Conference on General Topology and Applications. Univ. of Southern Maine, 1995, August, p. 10-13

[BojuFunar1993]. Valentin Boju, Louis Funar. *Generalized Hadwiger numbers for symmetric ovals*. Proc. Amer. Math. Soc. 119 (1993), 3, 931-934

[[BojuFunar1987] V. Boju, L. Funar. *Géométrie de l'équation Hamilton-Jacobi et questions connexes*. Seminar on Combinatorial, Computational and Differential Geometry and Topology, preprint, Univ. of Craiova, 1987, p. 1-38.

[BojuPope1978_EspQC-JDG] Valentin Boju, Mariana Popescu. *Espaces à courbure quasi-constante.* J. Differential Geom. 13 (1978), no. 3, 373-383.

[BojuPope1978_Techn. Publishing House]. V. Boju, M. Popescu. *Problems on Geometry of Differentiable Manifolds*. Technical Publishing House, Bucharest, 1978, p. 1-239.

[BojuPope1974] V. Boju, M. Popescu. *Changements conformes de métrique du point de vue global*. Atti Accad. Naz. Lincei Rend. (8), LVII, 1974, no. 5, 346-349

[Borg88] Gunilla Borgefors. Distance transformations in hexagonally digitized images. Technical Report C30497-3.3, FOA, Linköpings, June, 1988

[Borg88]. Gunilla Borgefors. Distance Transformations on Hexagonal Grids. Pattern Recognition Letters, Vol. 9, Febr. 1989, pp. 97-105. Swedish Defence Research Establishment, Linköpings, Sweden.

[Borg86] Gunilla Borgefors. Distance transformations in digital images. Computer Vision, Graphics and Image Processing, 34: 344 – 371, 1986.

[Borg84] Gunilla Borgefors. Distance transformations in arbitrary dimensions. Computer Vision, Graphics and Image Processing, 27: 321 – 345, 1984.

[Börö2004] K.Böröczky Jr, Finite packing and covering, Cambridge Tracts in Mathematics, 154, Cambridge University Press, Cambridge, 2004.

[Börö,Larman,Sezgin,Zing1999-2000] K. Böröczky Jr., D.G.Larman, S.Sezgin and C.Zong. On generalized kissing numbers and blocking numbers, III
International Conference in "Stochastic Geometry, Convex Bodies and Empirical Measures", Part II (Mazara del Vallo, 1999). Rend. Circ. Mat. Palermo (2) Suppl. No. 65, part II (2000), 39-57.

[Cara1914]. C. Carathéodory. Über das lineare Mass von Punktmengeneine Verallgemeinerung das Längenbegriffs. Nach. Ges. Wiss. Göttingen, (1914), 406 - 426

[Dran2004] Alexander Dranishnikov. Groups with a polynomial dimension growth. arXiv:math/0405239v1. May 2004.

[HingRoe2000] N. Higson and J. Roe, Amenable group actions and the Novikov conjecture, J. Reine Angew. Math. 519 (2000), 143–153.

[HolcmanPugh2007**].** David Holcman & Charles Chapman Pugh. *The Boundary Between Compact and Noncompact Complete Riemann Manifolds.* Indiana University Mathematics Journal, Volume 56, Issue 1, 2007, pp 437-457. (((Keywords: Riemann Manifolds; Ricci Curvature)))

[Kees1992]. James Edgar Keesling. *Fractals.* 15 pages Chapter. Talk given at University of Craiova, Ecole Post-Universitaire des Hautes Etudes de Biomathématiques et Applications, 1992. Chapter in: [Boju2007_MontrealTech Press].

[Kitsiosy, Kota, Mitt, Ooiy, Soria, You, 2006] V. Kitsiosy, R. B. Kotapatiz, R. Mittalz, A. Ooiy, J.Soria and D. You. Numerical simulation of lift enhancement on a NACA 0015 airfoil using ZNMF jets. Center for Turbulence Research-Proceedings of the Summer Program 2006, 457-468 (see: Figure 2. Topology of the modified C-type grid; see also: (a) block topology; (b) body-fitted airfoil grid; (c) ZNMF jet cavity).

[LoubShasLANL]An Arbitrary-Lagrangian-Eulerian code for polygonal mesh: ALE INC(ubator). Raphael Loubere loubere@lanl.gov; Mikhail Shashkov shashkov@lanl.gov http://math.lanl.gov/, T-7, MS B284, Theoretical Division, Los Alamos National Laboratory, Los Alamos, NM 87545

[Melt,Tome1989]. R. S. Melter, Ioan Tomescu1. *Path generated digital metrics.* Pattern Recognition Letters, Vol. 1 (1989), pp. 151-154.

[Morr] Jennifer Morrell. A cell by cell adaptive mesh arbitrary Lagrangian Eulerian gas code. http://www.icfd.reading.ac.uk/talks/Morrell.pdf

[PeerCarr2000].J. Peery and D. Carroll, “Multi-Material ALE methods in unstructured grids", Computational Methods in Applied mechanical Engineering, 187, 591-619, 2000.

[Rose66]. A. Rosenfeld and J. L. Pfaltz. Sequential functions in digital picture processing. Jpurnal of ACM, 13 (4): 471 – 494, 1966

[Rudin1976] Walter Rudin. Principles of Mathematical Analysis (International Series in Pure & Applied Mathematics), Sept, 1976.

[Thie1994].EdouardThiel. Les distances de Chanfrein en Analyse d’images: Fondaments et Applications. Thèse, 176 pages, Univ Greenoble I, 1994

[Toth1975] L. Fejes Toth, On Hadwiger numbers and Newton numbers of a convex body, Studia Sci. Math. Hungar. 10(1975), 111-115.

[Toth1970] L. Fejes Toth, Uber eine a ninvariante Masszahl bei Eipolyedern, Studia Sci. Math. Hungar. 5(1970), 173-180.

**Digital, Discrete and Combinatorial Methods in an Euclidean or Riemannian context** –
Valentin Boju and Antoniu Boju

Keywords and phrases:

CONCEPTS:

Iso-Stable Digital Spaces; sq-Iso-Stability and Hex-Iso-Stability Diophantine Equations; New Energy - Compartmented Energetic Bank/Generator Unit (CEBGU); Metric Structure of (L; K)-Digital Spaces; The Stability of the Digital-Energetic Levels; sq-Stability Formula & Hex-Stability Formula; (L; K; sqCells-Digital Plane) and (L; K; HexCells-Digital Plane) are spaces with Polynomial growth of the Digital-Energetic-superstable-Levels; Cap-Polynomial and Asymptotic Dimension of Digital Spaces; Hybrid multi-type-CEBGU; Super-Fractals; Inverse Quotient Curvature Coefficients, Separation supposition and Holcman-Pugh Kick Method; the coarse Baum-Connes conjecture and Novikov conjectures; Juxtaposition Combinatorial Measures and Juxtaposition Fractals; Applications in Intrinsic Measure Theory. Discrete and Differentiable TVF Methods; Hamilton-Jacobi reduced equation; Riemannian Regression Submanifolds & Nanotech Applications; TVF-Methods and Holcman-Pugh Kick Method. Programming Languages Applications; sq-Superfractals and Hex-Superfractals – Programs – C; Hybrid Juxtapositin Fractals – Programs – Python; Riemannian Regression Submanifolds &&& Applications Nanotech Applications - Programs: TPascal Versor Type Gradient dynamical system, versor type functions (VTF), VTF-foliations, Riemannian packings, Riemannian nonlinear regression, geodesic field, weighted/dynamical cloud, disturbing zones of a dynamical system, flight dynamics, pathological metabolic activity, viral infection, high resolution standard nearness network, pipe inspection microrobotics

.....

APPLICATIONS (The Patents - MontrealTech Register, MontrealTech Portfolio - © 2005-2007, authors):

Graphics, Computer Vision and Image Processing; Energy Units (Compartmented Energetic Bank/Generator Units-CEBGU); Cryptography and Security Procedures; Architecture – Decorative & Mosaics Work – Ceramics & Urban Sculpture – Textile Pictures and Textures; Computer and Video Games; Biomedical Applications; (Exterior/Interior) Juxtapositin Fractal; Riemannian Regression Submanifolds, Logarithmic Kick Method & Nanotech Applications; Pattern Recognitions & Defence Research Programs.

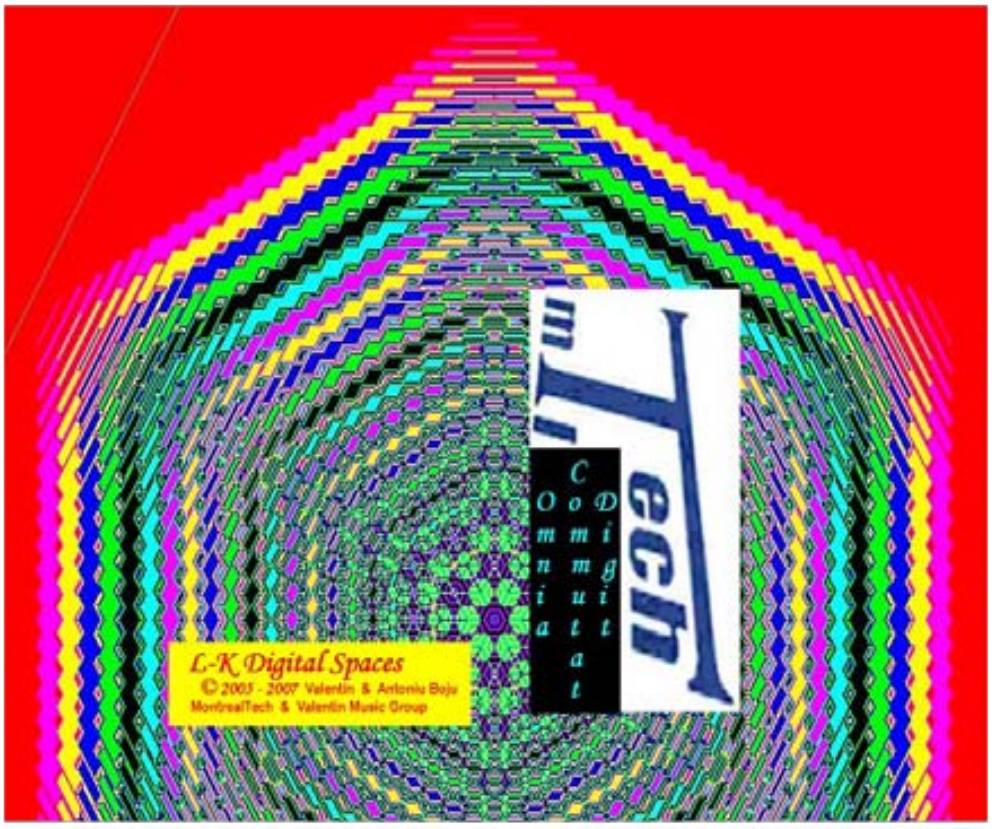


mTech

www.soundclick.com/valentinmusicgroup
pages.videotron.com/nanotech

# The Hypergeometrical Standard Model

*Marco A. Pereira,

Citigroup, 390 Greenwich Street, New York, NY 10013, USA

*This paper presents a simple and purely geometrical Grand Unification Theory. Quantum Gravity, Electrostatic and Magnetic interactions are shown in a unified framework. Biot-Savart Law is derived from first principles. Unification symmetry is defined for all the existing forces. A 4D Shock-Wave Hyperspherical topology is proposed for the Universe together with a Quantum Lagrangian Principle resulting in a quantized stepwise expansion for the whole Universe along a radial direction in a 4D spatial manifold. The hypergeometrical standard model for matter is presented.*

# 1. Introduction

Grand Unification Theories are the subject of intense research. Among current theories, Superstring, M-Theory, Kaluza-Klein based 5D Gauge Theories have shown diverse degrees of success. All theories try to keep the current conceptual framework of science. Kaluza-Klein melded both Electromagnetism and Einstein Gravitational equations in a 5D metric.

Here is presented a theory that departs radically from other theories and tries to bridge the conceptual gap as opposed to explore the formalism gap. Most research is concerned on how to express some view of Nature in a mathematically elegant formalism while keeping what we already know. It has been said that for a theory to be correct, it has to be beautiful.

This work concentrates on what to say, the conceptual framework of Nature instead. All the constructs of science, matter, charge, and energy are dropped in favor of just dilator positions and dilaton fields, which are metric modulators and traveling modulations, respectively. There is no concept of charges or mass. Mass is modeled a quantity proportional to the 4D displacement volume at **precise phases of de Broglie cycles**. Charge sign is modeled by dilaton phase (sign) on those specific phases. This mapping is not necessary for calibration; there are no calibration parameters in this theory. The mapping is needed to show that the geometrical framework replicates current scientific knowledge.

We propose that dilators are the basic model of matter. They are coherences between two states in a rotating four-dimensional double well potential. A single coherence between two 4D-space deformation states or fundamental dilator is shown to account of all the constituents of non-exotic matter (elements, neutrons, electrons and protons and their antimatter counterparties) and hyper-nuclei (hyperons) on Section 4. This coherence is between two deformation states with 4D volumes corresponding to the electron and proton, or electron-proton coherence. **Here the proton, anti-proton, electron and positron are considered to be the same particle or the fundamental dilator, just four faces of the same coin.**

The equation that describes these states is not the subject of this work. In section 2.4, a detailed description of the fundamental dilator is given, as well as the origin of the spin quantization.

Dilaton are the 5D spacetime waves, traveling metric modulations, created by the alternating (back and forth) motion of the fundamental dilator from one state of the double potential well to the other. Since these two states have different displacement volumes, spacetime waves are created. Displacement volumes are the missing (extra) volume due to spacetime contraction (dilation). Let's say that one has two points separated by a distance L in a 4D space with a dilator in the middle. The distance between those two points will change depending upon the phase of dilaton. If one considers this maximum distance change along the four dimensions for each of the two states, would be able to determine the dilator volume on each state and thus fully characterize it.

In addition to tunneling back and forth, the proton-electron dilator is considered to be tumbling (spinning) as it propagates radially (along the radial expansion direction) and that poses a constraint on the spinning frequency. Spin half particles are modeled as having a spinning frequency equal to half the electron-proton dilator tunneling frequency. Similarly higher spin particle coherences, e.g. spin N/2, are modeled as a complex dilator coherence having a accumulated N/2 spin per full dilator cycle. A complex dilator coherence will contain many fundamental dilator sub-coherences and transmutation notes. Transmutation notes correspond to 3D rotations which change the tunneling phase in phase with the Fabric of Space or 3D Shock-Wave Hyperspherical Universe.

Whenever the word dilator is mentioned within this paper, it will refer to the fundamental dilator or fundamental coherence, although there are other coherences in nature and similarly associated particle pairs.

The intersection of this 4D dilator displacement volume with the very thin 4D Universe (Fabric of Space) multiplied by a 4D mass density corresponds to the perceived 3D mass, a familiar concept. Since both the dilator and the Fabric of Space are very thin, the intersection decreases extremely rapidly with spinning angle. The interaction between dilators and dilaton fields (generated by other dilators) is directly dependent upon that footprint. Since the footprint is non-null only at specific spinning angles, interaction is quantized and "existence" is quantized. Where existence was construed according to the following paradigm: "I interact, thus I exist". Neutrinos have been called "Ghostly Particles" due to their very small interaction with the rest of the Universe (dilators). This is the logical basis for the Quantum Lagrangian Principle used to derive the Grand Unification Equations.

A logical framework is proposed on the Hypergeometrical Universe[1] section. This model conceptualize the 3D universe manifold as being a very thin 4D shock wave universe traveling at the speed of light in a direction perpendicular to itself, along the radial direction.

**Whenever a 3D Universe is mentioned, it should be understood as a very thin along the radial direction 4D Lightspeed Expanding Shock-Wave Universe.**

Absolute time, absolute 4D Cartesian space manifold are proposed without loss of time and space relativism. Thus there are both preferential direction in space and preferential time, but they are both non-observables.

On the cosmological coherence section, the consequences of the topology of the hypergeometrical universe and the homogeneity proposed in the Hypergeometrical Standard Model is shown to result in a cosmological coherence, that is, the whole 3D universe expands radially at light speed and in de Broglie (Compton) steps.

When cosmological coherence is mentioned it is within the framework of absolute time and absolute 4D space (RXYZ).

A new Quantum Lagrangian Principle (QLP) is created to describe the interaction of dilators and dilatons. Quantum gravity, electrostatics and magnetism laws are derived subsequently as the result of simple constructive interference of five-dimensional spacetime waves[2] overlaid on an expanding hyperspherical universe described in section 3. In the electrostatics and magnetism derivation, a one atomic mass unit (a.m.u) electron or fat electron is used. This means that the dilatons being 5D spacetime waves driven by coherent metric modulations are sensitive to both sides of the dilator coherence.

Since 3D mass – the mass of an electron or proton from the 3D universe manifold perspective - is sensitive only to one phase of the dilator coherence, the phase of the dilator in phase with the 3D shock wave universe, a pseudo time-quantization is proposed in section 2.4.

Section 4 contains a brief description of the Hypergeometrical Standard Model. It shows that hyperons and the elements are modeled as longer coherences of tumbling 4D deformations. Nuclear energy is proposed to be stored on sub-coherence local twisting of the fabric of space.

A grand unification theory is a far-reaching theory and touches many areas of knowledge. Arguments supporting this kind of theory have by definition to be equally scattered. Many arguments will be presented with little discussion when they are immediate conclusions of the topology or simple logic.

# 2. Hyperspherical Universe

## 2.1 Quantum Lagrangian Principle

A new Quantum Lagrangian Principle (QLP) is defined in terms of dilator and dilaton fields. It proposes that the dilator is always in phase with the surrounding dilatons at multiples of 2π wavelength. This simply means that a dilator, trying to change the metric in a specific region of 4D space, will always do that in phase with all the other dilators at phases where its Fabric of Space footprint is maximum. The fundamental dilaton wavelength will be called de Broglie wavelength and will be shown in the section 2.4 to correspond to the Compton wavelength, since motion along the radial direction is at lightspeed, of a one atomic mass unit particle.

## 2.2 Topology

The picture shown in Figure 1 represents a cross section of the hyperspherical light speed expanding universe. The universe is considered to be created by an explosion, but not by a three-dimensional explosion. Instead, it is considered the result of a four-dimensional explosion. The evolution of a three-dimensional explosion is an expanding two-dimensional surface. **The evolution of a four-dimensional explosion is an expanding quasi three-dimensional hypersurface on quantized de Broglie steps. The steps have length equal to the Compton wavelength associated with the fundamental dilator (one atomic mass unit).** All times are made dimensional by the multiplication by the speed of light.

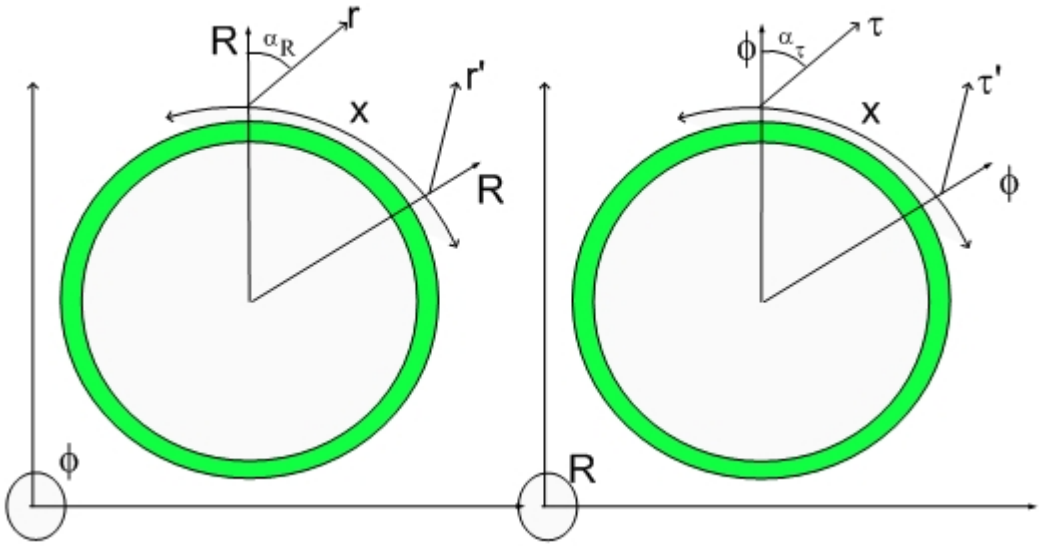


Figure 1. Shows the cross-section Xτ and XR for the expanding universe. The universe length along X is represented by the band. X (or Y or Z) is displayed along the perimeter of the circle. Also shown in the diagram is Φ (cosmological time) and radial time projection R.

Definitions:

- Cosmological time Φ represents an absolute time frame, as envisioned by Newton and Mach - it is a fifth dimension in the hypergeometrical universe model.
- The radial direction is a preferential direction in 4D space. It is the radial expansion direction. This direction doubles as a direction on 4D Space and a projection of the cosmological time. Since they are related by the expansion speed (light speed), one can think about the radial direction as the radial time – an absolute time projection.

- Similarly, $\tau$ is any other propagation direction and also a projection of proper time, here called dimensional time. For small velocities with respect to the fabric of space (see description below), the dimensional time approximately matches the 4D direction of propagation (atan (v/c)~atanh(v/c)~v/c). This maps our local frame proper time to a 4D direction of propagation and it is the source of the relativism in the theory of relativity. Different angles of propagation reflect different relative velocities. Notice that although this argument made use of a preferential 4D direction, it could be done using any possible referential frame. Within the 3D space, one can only observe the relative angle and relative velocity.
- This mapping done because of the consideration that a Lorentz transformation can be thought as a rotation around the directions perpendicular to proper time and velocity by an imaginary angle of atanh (v/c). On a 4D spacetime, when one considers a proper frame of reference, one only travels in time. The addition of a fourth spatial dimension means also that when one is in one's proper 3D frame of reference one is also propagating along either the directions R/$\Phi$ or r/$\tau$.
- R keeps a simple relationship with the dimensionalized cosmological time $\Phi$ (identical module relationship).
- The Fabric of Space (FS) is just the region of 4D space – a traveling boundary- where the 3D hypersurface (shock wave universe) stands at any given time. It is different from the rest of the 4D space because it contains imprinted in local deformations, all particles in the universe.
- Fabric of Space is used in two manners:
    - as the locally non-twisted 4D space – pointing to this traveling boundary-, where local proper time projection $\tau$ and direction of 4D propagation points in the radial direction $\Phi$/ R and
    - the subject of deformation.
- Under these conditions one can define a referential frame that is standing still with respect to the FS while traveling at the speed of light outwards radially. This is a preferred referential frame. Two preferred referential frames far apart in 3D space will recede from each other at the Hubble's speed (see section 2.6).
- After the shock wave universe passes through, the 4D space returns to it relaxed condition.
- There are two kinds of deformations in 4D space: compression and torsion. The compression is what happens in dilators or particles. They represent coherence between two compression deformation states.
- Torsional states are related to absolute state of motion of neutral matter and are defined by the local tilt of the perpendicular to the FS region inhabited by it. The FS can be under torsional forces in the region near dilators. The region where a dilator exists will persist under stress (tilted) as the dilator moves towards a region where that stress can be relaxed.
- Far from matter (charge), there should be only residual torsional deformation due to the evanescing dilatons. On the other hand, the region of space where a "zero spin particle" or neutral matter or spin half particle or charge exists, the local environment is permanently deformed through interactions with other bodies' dilatons. Deformation will last until all the interacting bodies reach regions where their relative velocity matches the Hubble velocity of that part of the Fabric of Space.
- The angle between R ($\Phi$) and r ($\tau$) defines the local FS deformation.
- The angle between $\tau$' (r') and $\tau$ (r) defines the relative degree of local FS deformation.
- "Volumetric" and "superficial" dilatons are 5D and 4D spacetime waves define in analogy to volumetric and superficial sound waves. Instead of having pressure or density modulations as in sound waves, one has metric (or 4D space) modulations.

- Since the hypersurface is our three-dimensional universe, a "superficial" dilaton is a spacetime disturbance that propagates along the FS. Associated zero spin dilators will propagate always in perpendicular to the FS, although they might move sidewise between de Broglie expansion steps.
- For example, in the case of a hydrogen atom, the spin zero dilator which represents neutral matter are created by counter spinning spin half dilators (electron and proton). The Quantum Lagrangian Principle makes the dilator dimer (or polymer) to act as a single zero spin dilator. At each de Broglie step in the expansion of the Universe, each component of the dilator dimer changes character (electron to positron or proton to antiproton or expansion to contraction). When that happens the individual direction of propagation also changes, but the ensemble continues drifting according to the calculations for gravitational interaction as shown in section 4.
- A "volumetric" spacetime dilaton is free to redirect its k-vector on any direction. Associated non-zero spin dilators will be able to freely change their propagation direction in addition to the sidewise motions at each de Broglie expansion step.
- Dilatons and dilators are used interchangeably in certain situations since the QLP requires the dilatons to always be in phase (surf) the surrounding dilaton field.

Figure 1 displays one time dimension ($\Phi$), the Radial coordinate (R) and two time projections ($\tau$ and $\tau$'). Each reference frame has its own proper time projection. This figure also shows that the four-dimensional spacetime is curved, being the radius of curvature given by the dimensional age of the universe.

This simple figure eliminates the need for cosmological constant questions, considerations about gravitational collapse or anti-gravitational acceleration of the expansion of the three-dimensional universe, since the universe is proposed to be four-dimensional plus a cosmological time $\Phi$.

In this model, the shock wave hyperspherical universe is clearly finite, circular (radius of curvature equal to the dimensional age of the universe, that is, the speed of light times the age of the universe). It is also impossible to traverse, since it is expanding at the speed of light. **The Cosmic Microwave Background is assigned to a Doppler shifted view of the initial Gamma Radiation Burst**[3].

## 2.3 Origins of the Hyperspherical Expansion

The clues for the creation of this models lies on relativity and quantum mechanics. Relativity states that the energy of a particle with rest mass $m_0$ and momentum p is given by:

$$E = mc^2 = c\sqrt{p^2 + m_0{}^2 c^2} \qquad (2.1)$$

where m is the mass in motion. This equation has implicit assumptions which can be brought into light by considering it a momentum conservation equation instead:

$$P^2 = (mc)^2 = p^2 + m_0{}^2 c^2 \qquad (2.2)$$

Where P is the four-momentum of the particle in motion (at the speed of light) traveling such that its $\tau_{particle}$ makes angle $\alpha$ with the static reference frame $\tau_{Observer}$. Implicit in equation (2.2) is that the particle is actually traveling along a four-dimensional space (timed by a fifth time dimension) and has two linear momentum components:

a) Three-dimensional momentum p

b) Perpendicular momentum $m_0c$ in the direction of radial time.

Notice that equation 2.1 should have a version on each panel of Figure 1.

In addition, the particle travels at the speed of light in along a hypotenuse with an inertial mass m. Now it starts to become clear that the motion of the particle is actually in a five dimensional space (four physical dimensions and a time) and at the speed of light, being the three dimension motion just a drift. The trigonometric functions associated with a relativistic Lorentz transformation are given in terms of velocity by:

$$\cosh(\alpha) == \frac{1}{\sqrt{1-\frac{v^2}{c^2}}} \tag{2.3}$$

$$\sinh(\alpha) == \frac{\frac{v}{c}}{\sqrt{1-\frac{v^2}{c^2}}} \tag{2.4}$$

$$\tanh(\alpha) = \beta = \frac{v}{c} \tag{2.5}$$

Manipulating equation (2.2) and using $m = m_0 \cosh(\alpha)$ one obtains:

$$(mc)^2 = (mv)^2 + m_0{}^2 c^2 \tag{2.6}$$

$$(m_0 \cosh(\alpha) c)^2 = (m_0 v \cosh(\alpha))^2 + m_0{}^2 c^2 \tag{2.7}$$

$$(m_0 \cosh(\alpha) c)^2 = (m_0 \sinh(\alpha) c)^2 + m_0{}^2 c^2 \tag{2.8}$$

$$\left(\frac{1}{\lambda_\tau}\right)^2 = \left(\frac{1}{\lambda_{x'}}\right)^2 - \left(\frac{1}{\lambda_{\tau'}}\right)^2 \tag{2.9}$$

With

$\frac{1}{\lambda_\tau} = \frac{m_0 c}{h}$ de Broglie wavelength for the particle on its own reference frame, traveling at the speed of light in the proper time projection τ direction.

Projection on the τ' direction.

$\frac{1}{\lambda_{\tau'}} = \frac{1}{\lambda_\tau}\cosh(\alpha)$

Projection on the x' direction.

$\frac{1}{\lambda_{x'}} = \frac{1}{\lambda_\tau}\sinh(\alpha)$

Equation (2.9) is the basic equation for the quantization of relativity. It describes the motion of a particle as the interaction of two waves along proper time projection and three-dimensional space. The $\lambda_{\tau\,\mathrm{Prime}}$, that is, the projection on the τ' axis of the wave propagating along the τ axis (resting reference frame) is given by:

$$\frac{\lambda_\tau}{\lambda_{\tau\,\mathrm{Prime}}} = \cosh(\alpha) \tag{2.10}$$

$$\frac{\lambda_\tau}{\lambda_{x\,\mathrm{Pr}ime}} = \sinh(\alpha) \qquad (2.11)$$

This means that the projected de Broglie time-traveling wavelength is zero when the relative velocity reaches the speed of light. Zero wavelengths means infinite energy is required to twist spacetime further. The rate of spacetime twisting with respect to proper time relates to the power needed to accelerate the particle to a given speed. From equation (2.5), acceleration in the moving reference frame can be calculated to be:

$$Acceleration_{\mathrm{Pr}ime} = c^2 \frac{d\tanh(\alpha)}{d\tau'} \qquad (2.12)$$

In the particle reference frame the acceleration has to be given by Newton's second law

$$Force = M_0 Acceleration_{\mathrm{Pr}ime} = M_0 c^2 \frac{d\tanh(\alpha)}{d\tau'} \qquad (2.13)$$

This means that any force locally twists spacetime, and not only gravitation as it is considered in general relativity. It also shows that as the relative speed between the two reference frames increases towards the speed of light, the required force to accelerate the particle approaches infinite. The same reasoning can be done for the concomitant rotation perpendicular to RX, resulting in the replacing the minus sign by a plus sign on equation (2.9) and the recasting equations (2.10) and (2.11) in terms of trigonometric functions as opposed to hyperbolic functions. Rotations around τX or RX result in a real angle α= arctan(v/c).

Figure 2 below displays the particle as a de Broglie wave oscillating as a function of cosmological time Φ, propagating along R. This is a proper reference frame plot, that is, the particle is at rest at the origin with respect to the fabric of space and only travels along the radial time direction R.

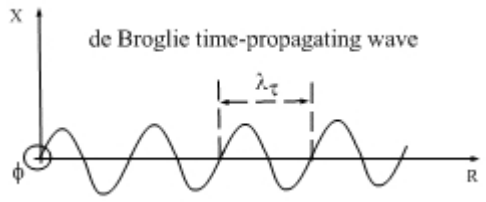


Figure 2. This model shows a de Broglie oscillation as a function of Cosmological Time Φ using the proxy of time R.

The diagram below represents the same observation from a moving frame of reference (relative velocity c times tan(α)):

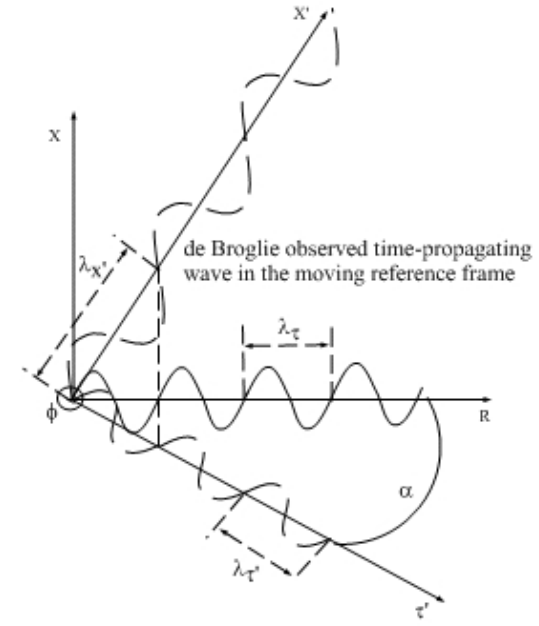


Figure 3. Projection of de Broglie Wave in the moving frame of reference.

### 2.3.1 Energy Conservation of de Broglie Waves:

The total kinetic energy, calculated in terms of de Broglie momenta, is equal to the Relativistic Total Energy value of a free particle. The total energy is $M_0c^2$ in the proper reference frame and equal to:

$$E = \frac{1}{M_0}\left[\left(\frac{h}{\lambda_{x\,\mathrm{Prime}}}\right)^2 - \left(\frac{h}{\lambda_{t\,\mathrm{Prime}}}\right)^2\right] = \frac{h^2}{M_0}\left[\left(\frac{\cosh(\alpha)}{\lambda_t}\right)^2 - \left(\frac{\sinh(\alpha)}{\lambda_t}\right)^2\right] = \frac{h^2}{M_0\lambda^2\tau} = M_0c^2 \quad (2.14)$$

in the moving referential frame.

### 2.3.2 Phase Matched de Broglie Wave Interpretation of a Particle

Let consider a particle as a de Broglie wave. In its own referential, it just propagates in the direction of radial time R, as in figure 2. On a moving reference frame, shown in figure 3, the de Broglie wave is decomposed in two:

- One with wavelength $\frac{1}{\lambda_{x\mathrm{Prime}}} = \frac{\cosh(\alpha)}{\lambda_\tau}$ propagating along x
- A second with wavelength $\frac{1}{\lambda_{\tau\mathrm{Prime}}} = \frac{\sinh(\alpha)}{\lambda_\tau}$ propagating along τ.

Their nonlinear interaction results in:

$$\psi_1(x,\tau) = \cos(\frac{2\pi}{\lambda_e}x\cosh(\alpha))\cosh(\frac{2\pi}{\lambda_e}\tau\sinh(\alpha)) \quad (2.15)$$

$$\psi_1(x,\tau) = \frac{1}{2}\cosh(\frac{2\pi}{\lambda_e}(x\cosh(\alpha) - \tau\sinh(\alpha))) + \frac{1}{2}\cos(\frac{2\pi}{\lambda_e}(x\cosh(\alpha) + \tau\sinh(\alpha))) \quad (2.16)$$

or two waves propagating in the direction of α and –α with wavelength equal to $\frac{\lambda_e}{\cosh(\alpha)}$. Thus a particle can be described as a phase matched wave propagating along its dimensional time direction as the hyperspherical universe expands as a function of cosmological time.

### 2.3.3 The Fundamental Dilator

The fundamental dilator is the paradigm behind the Fat Electron (one a.m.u. electron) used in the derivations of Electrostatic and Biot-Savart Laws. I modeled "particles" as coherences between 4D stationary states of metric deformation. These coherence can have spin (rotation along any axis perpendicular to R), and nuclear angular momentum (rotation around any axis in the Fabric of Space).

Since the boundary where the Universe (3D) is located is moving at the speed of light along R, there isn't the concept of particle since that doesn't include the inherent lighspeed motion and has inherently some immutability assumptions.

The dilator is by definition mobile and always tunneling back and forth. It can have non-zero spin. In the Hypergeometrical Standard Model in section 4, all particles models are shown to be decomposable into variations of the fundamental dilator. Different phases of the fundamental dilator correspond to Proton, Electron, Positron and antiproton.

There is an obvious analogy to musical notes. Each dilator phase (proton, electron, antiproton and positron) can be thought as dimensional notes (notes that modulate the space metric as opposed to air density).

Next is a diagram showing the states involved with the fundamental dilator.

### 2.3.4 Electron Model

| Particle | Symbol | Rest Mass (Mev/$c^2$) | Decay Reaction | Spin | **Coherence Lifetime** |
|---|---|---|---|---|---|
| Electron | $e^-$ | 0.510998918 | $e^-$ | 1/2 | Stable |

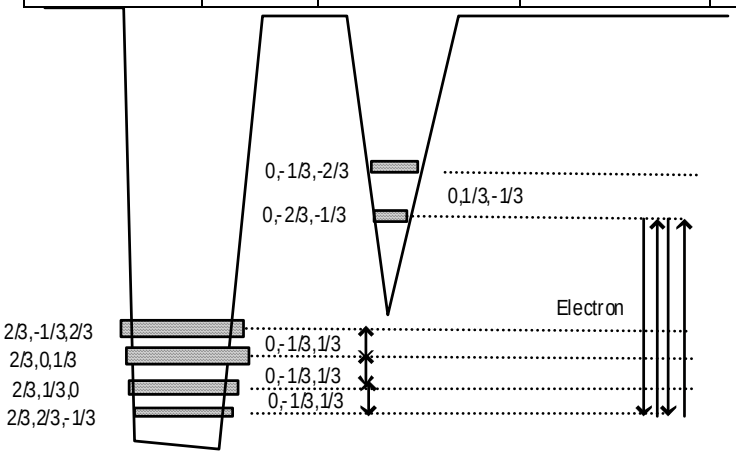


Figure 4. 4D Stationary Deformation State diagram for electron

The coherence four notes are meant to repeat forever.

Where p=(2/3,2/3,-1/3),e=(0,-2/3,-1/3),e*=(0,-1/3,-2/3) are a subset of states involved in the three most common "particles"= proton, electron and neutron. Below is another representation of the electron and positron. Notice that the first and last elements of the coherence chain are the same and that the coherence repeats itself for its lifetime. In the case of a proton/electron, that lifetime is infinite, since that coherence is between two ground states.

This is an effort to represent a tumbling 4D object, which changes shape as it tumbles. Notice that the sidewise states have no FS overlap. Since in the theory, there is an absolute time, one can define an absolute phase and that is what distinguishes an electron from a positron. Later it will be clear that more complex coherences involving the e* state (neutrino) will result in a phase shift of the tunneling process with respect to the tumbling process, thus modifying which state is in phase with the shock-wave universe.

The colors are shown only for states that have both a FS overlap and the same frequency as the fundamental dilator.

Another important element of the model is the bolding of the third axis length (e.g. p=(2/3,2/3,**-1/3**)). This means that the spin is a tumbling process around and rotational axis perpendicular to both the radial direction (perpendicular to all three spatial coordinates and the z coordinate). This defines a 4D angular momentum which has to be conserved. More complex coherences like the ones associated with Delta and Sigma particles differs just by the final spin and thus by how the sub-coherences tumbles to make up the final amount of spinning.

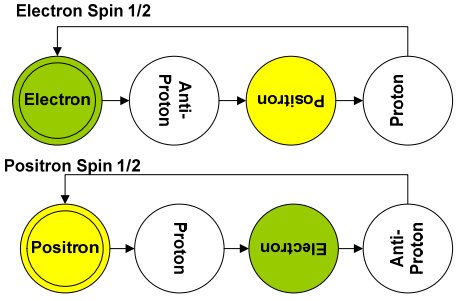


Figure 5. Dimensional notes associated with Electron and Positron.

Yellow (ligther)= positive charge.

Green (darker)= Negative charge.

White = Invisible in 3D due to 4D orientation – perpendicular to the Fabric of Space.

### 2.3.5 Proton Model

Similarly for a proton:

| Particle | Symbol | Rest Mass (Mev/$c^2$) | Decay Reaction | Spin | **Coherence Lifetime** |
|---|---|---|---|---|---|
| Proton | **P** | 938.3 | Unobserved | 1/2 | Stable[1] |

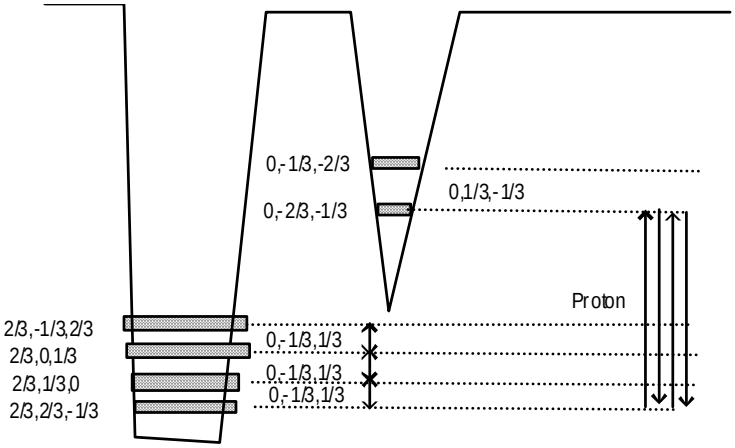


Figure 6. 4D Stationary Deformation State diagram for proton

The coherence four notes are meant to repeat forever, thus the fourth state represented is shown connecting to the initial state emphasizing the closing of the coherence cycle. Belly up states represent anti-states (anti-proton or positron states).

Here is the representation of a proton and an antiproton.

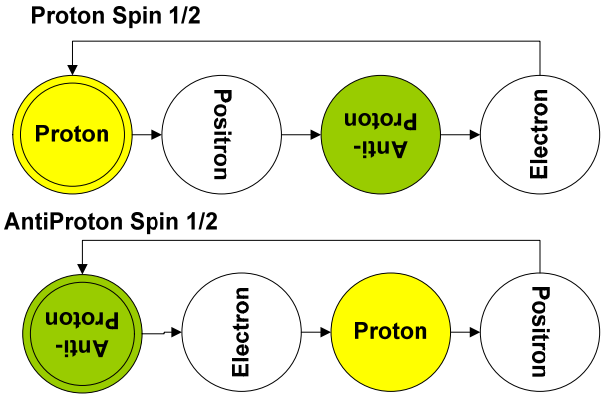


Figure 7. Dimensional notes associated with Proton and anti-Proton.

### 2.36 Shadow Physics

The meaning of Shadow Physics becomes clear if one remembers that the left panel of Figure 1 shows a 4D space with a 3D Shockwave Universe while the left pane only shows the 3D Shockwave. This means that any Physics which takes place in 4D will have to be projected onto the 3D hypersurface.

That includes the Wave Physics presented in section 2.3. This means that section 2.3 will refer to the right panel of the Figure 1 if one replaces the hyperbolic trigonometric function by their trigonometric counterparties, $\alpha_\tau$ by $\alpha_r$ and $d\tau$ by $dr$.

The revision of Newton's Second Law in section 3 will make use of the same Shadow Physics argument.

### 2.3.7 3D and 4D Masses

The derivations in section 4 are done in the RXYZ and yield the acceleration for a single particle subject to one kilogram mass or to one kilogram of charge. Notice that acceleration is not force. To obtain a force, which is a 3D (ΦXYZ) concept, one has to multiply it by a 3D mass. To understand why one would use a one atomic mass unit electron, and what are the 3D and 4D masses, one has to see the process in 4D. First one needs to understand neutron decay to have some representation of the electron and proton 4-D deformational states.

The hypergeometrical standard model for the neutron decay process is shown next:

**neutron -> proton + electron + anti-neutrino**

Where the 4D deformation states are given:

(2/3,-1/3,**-1/3**) -> (2/3, 2/3,**-1/3**) + (0,-2/3,**-1/3**) + (0,-1/3, **1/3**) (2.20)

respectively.

Conversely:

**proton + electron -> neutron + neutrino**

(2/3, 2/3,**-1/3**) + (0,-2/3,**-1/3**) -> (2/3,-1/3,**-1/3**) + (0,1/3, **-1/3**) (2.21)

The representation of the neutron decay is presented here just to showcase how one thinks about nuclear chemistry in the hypergeometrical universe framework. The "quark" numbers are not meant to be considered the quark composition of the particles. It is an equation of 4D volume conservation and the numbers represent the three axis lengths of a 4D ellipsoid of revolution. Negative numbers just means that they have opposing phases. The total 4D volume of all particles in the universe should add up to zero. Any particle can be described through these types of equations and that will be discussed elsewhere. Notice that no number was given to the fourth dimension. There is no mentioning of the residual length of the fourth coordinate for simplicity, but it is certainly smaller than the others, thus the resulting skinny profile when the dilator is rotated by 90 degrees. This assignment was done considering the lowest 4D volumes or lowest numbers, the number **ONE** can be decomposed for representing the nuclear reaction (neutron decay).

This is clearly unorthodox, since the electron is not supposed to have a quark composition.

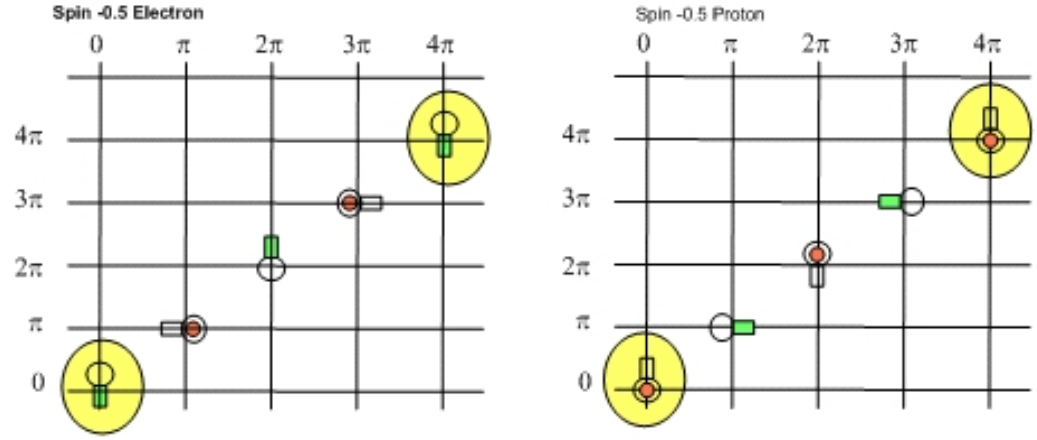


Figure 8. The figure above show an electron-proton dilator as it tumbles during two de Broglie wavelength universe expansion, with the two possible initial phases. The left (right) scheme corresponds to an electron (proton).

The red dot indicates that the coherence is on the proton side (2/3, 2/3,-1/3), while the green rectangle indicates that the coherence is on the electron side (0,-2/3,-1/3). Spin has been modeled as an extrinsic rotation perpendicular to RX. Spin half means that the dilator performs half rotational cycle for each de Broglie expansion step. Notice that the representation of spin as a 4D rotation is distinct from orbital momentum L and total Momentum J. This is a four-dimensional space theory and one has to have angular momentum conservation in four dimensions, thus the rules for total angular momentum conservation are valid.

Orbital momentum L and total angular momentum J are 3D concepts and will result from the projection of the equations of motion solution on the 3D hypersurface. Quantum mechanics replication is outside the scope of this paper. The behavior required by the quantum Lagrangian principle has the similar traits to the Bohr model. If one considers that in the prescribed QLP 4D trajectories, the electron riding the 4D dilaton wave will also ride its 3D projection -the corresponding de Broglie matter wave- then it becomes clear that QLP will immediately reproduce the Bohr hydrogen model and more.

Now, one can define the 3D and 4D masses. From Figures 6 and 7, it is clear that what distinguishes an electron from a proton is a rotational (spin) phase. This means that our 3D interactions (material existence) support a pseudo time-quantization or intermittent interaction on quantized time steps. Thus 3D masses are the masses one observes at de Broglie expansion phases 0, $2\boldsymbol{\pi}$, $4\boldsymbol{\pi}$…. It is worthwhile to notice that on the de Broglie expansion phases $\boldsymbol{\pi}$, $3\boldsymbol{\pi}$, $5\boldsymbol{\pi}$... (when the dilator character changed totally and the 4D volume reaches a maximum) the FS overlap is minimal. These de Broglie phases correspond the perpendicular spinning phases.

Notice that an hydrogen atom would go through a charge reversal at each $2\boldsymbol{\pi}$ tunneling phase shift, but its 3D mass would not change and the atom would still be neutral and have total spin equal to zero (plus angular momentum which is a 3D concept). It takes a $4\boldsymbol{\pi}$ or two de Broglie cycles for any half-spin dilator to reach its initial state.

In the case of neutral matter, we considered that a charge reversed hydrogen atom to be an equivalent state, thus in Gravitational interaction, zero spin "particles" have a cycle equal to a de Broglie cycle. Another way to think about this is that if one considers an electron or proton to have a one atomic mass unit 4D mass then a hydrogen atom would have a 4D mass 2 a.m.u and thus a de Broglie wavelength half of the one of an electron or proton.

In the case of an electron, the de Broglie expansion phase $\boldsymbol{\pi}$ corresponds to a skinny or sidewise proton (nothing to grab). Interaction is considered to be proportional to the 3D Mass (as in Newton's Gravitational Law). This also means that as soon as the dilator rotates, the overlap with the FS goes to zero (or thereabouts), thus quantizing interaction or perceived time. This is the supporting argument to the Quantum Lagrangian Principle.

In this work, we are not presenting the equations of motion of the 4D tunneling rotor, since they are not necessary for the understanding of the physical model. They are not needed either for the proposed grand unification theory. One only needs to know that 4D volumes are associated with electrons and protons and that electrons and protons are the two sides of the tunneling system. One also has to keep in mind that the FS overlap of this 4D volume is proportional to the corresponding 3D mass or simply particle mass. The detailed shape of these states also doesn't matter for this discussion. One only needs to know that the thickness (radial dimension thickness) of these states is much smaller than the de Broglie (Compton) wavelength of the dilator (one a.m.u. particle) to understand that when the tunneling rotor (dilator) is rotated by any angle, it should show a much smaller volume from the perspective of the 3D universe.

**What would be the meaning of a 4D Mass?**

The 4D displacement volume is responsible for the dilaton creation. This means that from the model proposed in Figure 4-8, proton, electron, positron, and antiproton all have the same 4 mass, that is the far-field dilaton intensity is independent upon which phase one starts with. Since these transitions are in phase with the dilaton wave (both dilator and dilaton travels at the speed of light along R), the dilator amplitudes are added coherently.

The 3D mass is just the volumes in contact with the fabric of space. Due to spinning and tunneling, this overlap is sensitive to which phase is in-phase with the Fabric of Space. An electron will always be an electron unless it grabs a half muon neutrino to transmutate into a positron. This will become clear in section 4.

Remember that in a geometrical theory, mass has to be related to a 4D displacement volume. From the point of view of four-dimensional waves being generated by coherently located dilators, it doesn't matter if the proton or electron are standing up or laying down, the 4D displacement volume is the same. The 4D displacement volume is what creates the dilatons. The larger 4D volume, the larger the dilaton wave created. This means that the 4D mass of an electron is equal to the 4D mass of a proton - approximately one atomic mass unit. This might sound strange but it is a proportionality reason, it is an identity minus a constant. One atomic mass unit corresponds to a standing-up proton and a standing-up electron which is the exactly the mass of a hydrogen atom. This is an approximation because of the relativistic shrinking of volume as a function of relative motion. The correction factor should be, in terms of 4D volumes, equal to (standing-up electron + laying-down proton)/(standing-up electron + standing-up proton). In other words, a standing-up electron (proton) has a different perceived 4D volume than a laying-down electron (proton). This correction factor should be related to the electron gyromagnetic ratio. From there, one should be able to derive an instantaneous tangential speed.

## 2.4 Quantization of Time and the Fat Electron

The theory makes use of a fat electron, that is, a one atomic mass unit electron in the derivations on sections 3.1 and 3.2.

The recovery of Newton's, Gauss and Biot-Savart Laws indicates that the usage of a fat electron is appropriate and supports the fundamental dilator model of matter.

If matter can be described with the usage of the fundamental dilator, then interaction among dilators only happens at specific dilator spinning angles and time can be said pseudo-quantized. This means that from our perspective it is like the Universe only exists on given time steps.

Of course, this is easy to understand on the RXYZ cross-section. On the ΦXYZ, each inertial frame has its own time projection and the quantization will vary depending upon the FS angle associated with that inertial frame.

## 2.5 The Meaning of Inertia

From equation (2.12) it is clear that inertia is a measure of the spring constant of spacetime, that is, how difficult it is to twist spacetime. Any change in the state of motion also changes the direction as referred to the absolute referential frame RΦ, which means that inertia is also a measure of how difficult it is to locally twist the fabric of space.

Notice that Newton's first equation (equation 2.13) can be recast as an equation stating that the stress on the fabric of space is the same on both projections shown in figure 1. The stress as seen from the left cross-section shown in Figure 1, is giving by the product of a cross-section a rate of deformation $\frac{d\tan(\alpha_R)}{dr}$ multiplied by the a unitary 4D volume 1.

Similarly, on the right cross-section of Figure 1, the same stress is seen as a product of the rate of deformation $\frac{d\tanh(\alpha_\tau)}{d\tau}$ times the 4D volume FS overlap m, thus resulting in the geometrical version of Newton's Second Law.

$$m\frac{d\tanh(\alpha_\tau)}{d\tau}=1\times\frac{d\tan(\alpha_R)}{dr}$$

The usage of a unitary 4D volume is convenient since I also proposed a Hypergeometrical Standard Model where Proton and Electron are just two phases of a four dimensional deformation coherence (fundamental dilator). Under this paradigm the 4D volume adds up to the sum of the 4D volume of a proton plus the 4D volume of an electron. Since the mass of a Hydrogen atom is one atomic mass and it corresponds to an electron and a proton as seen in our 3D space, the 4D Mass can be easily understood. A proton state 4D FS overlap is 1836.15267247 times larger than the 4D FS overlap of the electron state.

To obtain the force (stress) needed to create such a strain, one needs to multiply the strain by the area subject to it. In the 4D hyperspherical paradigm, this means that the mass is proportional to the 4D FS overlap of the 4D displacement volume associated with the objects (particles).

This identity is used thoroughly during the grand unification calculations on section 3.

## 2.6 Why do things move?

### 2.6.1 Hypergeometrical Newton's First Law

The relaxation of a fabric of space deformation is considered within this theory to be the cause of inertial motion. Two objects would act upon each other and then distance themselves until their interaction is vanishingly small. Under those conditions their distance would grow until they reach their Hubble equilibrium position, that is:

$$v = C_{Hubble} * L_{HubbleEqui\,librium} \tag{2.17}$$

$$L_{HubbleEquilibrium} = \frac{v * R^{4D}_{AgeOfUniverse}}{c} \tag{2.18}$$

Where it is clear that the Hubble constant is given by:

$$C_{Hubble} = \frac{c}{R^{4D}_{AgeOfUnive\mathbf{r}se}} \tag{2.19}$$

Where $R^{4D}_{AgeOfUniverse}$ is the dimensionalized age of the Universe or circa 13.7 billion light years

The 4D radius of the universe is shown in Figure 1, and it is equal to the age of the universe times c. At that point, 4D space would be relaxed and their distance would grow governed by the universe expansion. Even though matter would be standing still with respect to the FS, their relative motion would continue at the Hubble speed forever. The fraction of the universe that is relaxed at any given time and direction can be measured from the distribution of Hubble constants. The narrower the distribution of Hubble constants from a given region of the Universe, the more relaxed that region is. **Needless to say, this is the underlying reason for Newton's first law.** The proposed topology implies that the Big Bang occurred on all points of the shock wave universe (or the currently known 3D Universe) at the same time. Since matter is considered to have rushed away from each and every point of the 3D universe in a spherically symmetric manner, the Hubble constant has to be a constant for the average. Other cosmological implications will be discussed in a companion paper.

Equation (2.16) might seem obvious but it is not. There are questions about why the Hubble constant is not constant. In this theory it is clear that the Hubble constant relates to the average velocity in a given region of space and thus it should not be a constant applicable to each and every observation.

## 2.6.2 Why is the Speed of Light the Limiting Speed

In this model, in a de Broglie universe expansion step, the furthest a dilator can move is one de Broglie wavelength sidewise, that is, along the spatial direction (see Figure 1 RX cross-section). That would result in a 45 degrees angle with respect with R.

The proposition of this theory is that this is the real reason for Lorentz transformations asymptotic behavior and that inertia is really a measure of the difficulty to bend local 4D space. In section 2.3 it became clear that they are the same rotation, driven by the change in velocity on both cross-sections of Fig.1.

From Hubble considerations and from examining Figure 1, it is clear that the maximum absolute speed is $\pi$*c, but cannot be measured because one can never see or reach anything beyond one radian in the shock wave universe.

## 2.7 Cosmological Coherence

The coordinated actions of dilators implicit in the proposed Lagrangian principle mean that even though the dilator is a 5D spacetime wave generator it behaves as a wave, thus implicitly replicating wave behavior. Its position is determined at each de Broglie step according to the local dilaton environment.

The concept of 4D spacetime deformation coherences generating waves is created in analogy with electromagnetic waves being created by electronic coherences. In the case of spacetime coherences, the coherences for the fundamental dilator (proton-electron dilator) are never dephased. Dephasing would result in proton or electron decay or disappearance. The states corresponding to the proton and to the electron are considered to be the ground states for each one of the two wells, thus they cannot decay further, only dephase.

All matter in gravitational and electromagnetism studies here modeled are composed of protons, electrons and neutrons, thus are composed of this fundamental dilator. Although current understanding of charged particles associates with them a gravitational mass, their gravitational field could never be measured. If it were to exist, their electric field would be $10^{36}$ times larger than their gravitational field.

In this model, charged particles have no gravitational field, since in this model there is only one kind of interaction and two kinds of responses.

The Quantum Lagrangian Principle means that all matter, charged or not, is synchronized with the surrounding dilatons (in the RXYZ cross-section), thus generating a cosmological coherence.

This idea of a cosmological or macroscopic coherence might seem unexpected but it is built-in in the concept of field. Fields are constructs derived from electromagnetism and gravitation equations. In a purely geometrical theory, which has been the goal of many scientists and philosophers for thousands of years, there should be only a few constructs: space, space wave (metric modulations), and local and global symmetry rules (angular and linear momentum conservation) adapted to the appropriate constructs. There shouldn't be mass or charge in a purely geometrical theory, only displacement volume and phase. Returning to the concept of fields, when one consider gravitation/electrostatics to be an extensive properties of mass/charge, one is implicitly adding the corresponding wave amplitudes within an implicit geometrical theory without regard to their phases, that is, fields imply coherences. This is a fine point that has been missed since nobody planned to eliminate the concept of mass and charge to build a geometrical theory. Einstein's gravitation theory used mass to deform spacetime. Kaluza-Klein also used mass to deform spacetime and created a compact dimension to store the electromagnetic fields. In this theory, coherent dilatons controls dilators motions in a mutually consistent cosmic symphony.

Figure 3 displays two inertial systems with the same origin. System with distinct origins would have an additional phase-shift due to the retarded potential interaction. This is the reason why all the waves in a multi-particle body can have their amplitudes added together, as opposed to having their amplitudes averaged out to zero due to a random phase relationship. It shows that a particle state of motion does not modify its phase

relationship with the expanding hypersurface (3D Universe). The particle is always phase matched to the rest of the universe. This is the meaning of physical existence. Our concept of existence is based on interaction. If a particle had a de Broglie wavelength different from the one of the fundamental dilator, its interaction would average out to nothing. No interaction means no material existence. A neutrino is an almost perfect example of this pattern – it still interacts a little. The phase matching condition implies that the entire universe is in phase (lived the same number of de Broglie cycles) as it propagates along the radial direction R. This also means that the universe is thin along the radial direction of propagation (much less than one de Broglie wavelength thin).

**The number of de Broglie cycles a particle passes through is independent upon the angle α (relative velocity). This means that any dilator of a given type is always in phase with another of the same type, irrespectively of its trajectory through the universe. It also means that protons, electrons, neutrons created in the dawn of the universe kept the same phase relationship with all the other protons, electrons and neutron of the universe throughout the ages. The same is true for any particle created at any time.**

This coherence is essential in creating a quantum gravity theory and it is essential to the hypergeometrical theory. In fact, cosmological coherence is a hypothesis and a corollary of the hypergeometrical theory, because one could not construct a geometrical theory without a cosmological coherence due to the extensive property of gravitational, electrostatic and magnetic fields.

## 2.10 The Meaning of a Charge

From section 2.9 it becomes obvious what is the meaning of a charge. It is only the in-phase sign of the dilation. A proton is positive because it is dilated as a proton – it has proton 3D mass or proton 4D Volume, when observed by the shock wave universe. An anti-proton would have the same 3D mass but the 4D displacement volume would be negative, that is, the modulation in metric had the opposite effect on 4D Space. The difference in 4D Volume on specific phases is why a proton and an electron do not annihilate each other, as do a proton and an anti-proton. Any annihilation is the result of dephasing a coherence between a dilator state and the Zero state. The final volume should be zero and that is only true for particle-antiparticle pairs. A coherence between an electron-positron pair and the zero state is an oscillating dipole. This decays into zero by the emission of an electromagnetic wave.

## 2.11 Hypergeometrical Newton's Second Law

Up to now, Science has only paid attention to the left panel of the figure 1. Newton's Second Law F=m.a can be rewritten as:

$$F = m_0 c^2 \frac{d \tanh(\alpha_\tau)}{d\tau}$$

This law was conceived without providing any guidance on how to calculate F. Without guidance, scientists discovered Gravitation and Electromagnetism and inferred the Strong and Weak forces. Strong force was concocted to explain why a theoretical construct (Quarks) were not seem by themselves in nuclear scattering experiments. Weak force was concocted to explain Beta decay.

I propose that Newton's Second Law to be rewritten in geometrical terms following the Stress/Strain paradigm in the two cross-sections shown in Fig.1.

This means that there wouldn't be any side unknown. The "observed" change in angle in the RXYZ cross-section would correspond to an observed change in velocity and "Force" in the τXYZ cross-section. I created a mechanism to guide the interaction of dilators and the Quantum Lagrangian Principle to guide their motion in a dilaton field.

Newton's second law can be rewritten in an almost familiar manner as:

$$F = m_{04D}c^2 \frac{d\tanh(\alpha_r)}{dr} = m_{03D}c^2 \frac{d\tanh(\alpha_\tau)}{d\tau}$$

Within a single de Broglie step, angles are very small and tanh(α)=tan(α)

Where one introduce the concept of 3D and 4D masses. 3D masses are the masses we associate with particles in our daily experience, they correspond to the observed 4D displacement volume on our shock wave 3D Universe. One does not observe any (very small) 3D volume when the dilator is rotated. 4D Masses are the masses associated with the Hypergeometrical Standard Model and the Fundamental Dilator model of matter. In the Hypergeometrical Model, the 4D mass of an electron or proton is equal to one atomic mass unit in first approximation.

The "Forces" created by the interaction between dilators locally change the orientation of the Fabric of Space. We propose that the Stress along both cross-sections to be equal. The physics supporting this statement is that the twisting along both cross-sections is caused by the same dilator-dilator interaction. The resulting strain along each cross-section will vary depending upon the dimensionality of the projected space:

$$Stress_{RX} = Stress_{4D} = Area_{4D}.Strain_{4D}$$

$$Stress_{\Phi X} = Stress_{3D+\Phi} = Area_{3D}.Strain_{3D+\Phi}$$

Let's make Area $_{4D}$ =1 then Area3D is just the overlapping of the unitary dilator 4D volume with the FS.

$$Strain_{3D} = c^2 \frac{d\tanh(\alpha_\tau)}{d\tau}$$

$$Strain_{4D} = c^2 \frac{d\tanh(\alpha_r)}{dr}$$

Where $Area_{4D} \Leftrightarrow 1$ and $Area_{3D} \Leftrightarrow M_o$ .$M_0$ is the electron or proton mass in a.m.u depending upon which one chooses to study in Electromagnetism (spin half) or one atomic mass unit (Hydrogen atom – spin zero) if one chooses to study Gravitation. The 4D mass of an electron or proton is one a.m.u. by a proportionality reasoning.

If one considers that

$$\frac{d\tanh(\alpha_\tau)}{d\tau} \Leftrightarrow \frac{Acceleration}{c^2}$$

one recovers the familiar form of Newton's Second Law, otherwise one has a purely geometrical law:

$$Stress_{RX} = Area_{4D} \frac{d\tan(\alpha_r)}{dr} = Stress_{\Theta X} = Area_{3D} \frac{d\tanh(\alpha_\tau)}{d\tau}$$

Relating local deformations of the Fabric of Space in two cross-sections of the Hypergeometrical Universe. To calculate all the "forces" in the Universe one just need to calculate $\frac{d\tan(\alpha_r)}{dr}$ on the RXYZ cross-section and multiply it by the number of dilators. This is what is done in the next section.

# 3. Force Unification

### 3.1 Quantum Gravity and Electrostatic Interaction

Let's consider a body and a particle interacting through their four-dimensional waves. The body will always have a kilogram (of mass or charge) and the particle will always be a one a.m.u. (atomic mass unit) particle (~neutron or hydrogen atom). For the gravitational interaction, this particle will have zero spin, while it will have spin half for the electrostatic interaction. Although the four-dimensional wave interaction is taking place on the hypersurface of a four-dimensional expanding hypersphere, one will make use of cross-sections to calculate interference patterns. Interference is considered on each de Broglie expansion of the hyperspherical universe. One can briefly describe the source of waving as a four-dimensional particle (four-dimensional ellipsoid of revolution or particle X for simplicity). The X particles are characterized by four axes lengths. Three axes lengths correlate with the quarks composition of matter. The fourth-axis always points in the radial time direction. Needless to say, different quarks (axis lengths) and different rotational states around the four axis will be sufficient to maps all known particles (photons, mesons, neutrinos, etc). Volume (mass) tunnels in an out of the three-dimensional space for spinning particles (particles with non-zero spin) and out and in towards the radial time dimension. Spin is considered to be a special rotation, since the rotation axis is perpendicular to radial time and one of the spatial coordinates. That gives spinning a different effect; it brings the particles in and out of the fabric of space, thus allowing for a realignment of the k-vector of associated spacetime waves. Let's consider the interaction through a two-dimensional cross-section (X x $\tau$). Particle one (one a.m.u "zero spin neutron" or fat electron) sits on x=0, while particle two (the body of 1 Kg) sits on $x=R_0$. The four-dimensional dilatons are embedded in a fifth dimension (cosmological time). A position in this space is defined by the following vector:

$$\vec{r} = \begin{pmatrix} r.\alpha \\ r.\beta \\ r.\gamma \\ r \\ \Phi \end{pmatrix}$$ using director cosines $\alpha$, $\beta$ and $\gamma$.

$r$ is the radial dimension on the RXYZ cross-section. (3.1)

At time zero, the positions for particles 1 and 2 are given by:

$$\vec{r}_0 = \begin{pmatrix} 0 \\ 0 \\ 0 \\ 0 \\ 0 \end{pmatrix} \quad \text{and} \quad \vec{R} = \begin{pmatrix} R \\ 0 \\ 0 \\ 0 \\ 0 \end{pmatrix} \tag{3.2}$$

After a de Broglie cycle, one has these three vectors:

$$\vec{r}_0(\lambda_1) = \begin{pmatrix} 0 \\ 0 \\ 0 \\ \lambda_1 \\ \lambda_1 \end{pmatrix} \quad \text{and} \quad \vec{r} = \begin{pmatrix} r \\ 0 \\ 0 \\ \lambda_1 \\ \lambda_1 \end{pmatrix} \quad \text{and} \quad \vec{R} = \begin{pmatrix} R \\ 0 \\ 0 \\ \lambda_1 \\ \lambda_1 \end{pmatrix} \tag{3.3}$$

$\vec{r}_0(\lambda_1)$ is the unperturbed crest of the four-dimensional wave of particle 1 after a de Broglie cycle. $\vec{r}$ is the position of the same crest under the influence of particle 2.

The k-vector is given by:

$$\vec{k} = g_{ij}.k^{j} = \frac{2\pi}{\lambda}\begin{pmatrix} 1 & 0 & 0 & 0 & 0 \\ 0 & 1 & 0 & 0 & 0 \\ 0 & 0 & 1 & 0 & 0 \\ 0 & 0 & 0 & -1 & 0 \\ 0 & 0 & 0 & 0 & -1 \end{pmatrix}\begin{pmatrix} 1 \\ 0 \\ 0 \\ 1 \\ \frac{1}{2} \end{pmatrix} = \frac{2\pi}{\lambda}\begin{pmatrix} 1 \\ 0 \\ 0 \\ -1 \\ -\frac{1}{2} \end{pmatrix} \qquad (3.4)$$

Where $g_{ij}$ is the local metric of the five-dimensional space. Again, cosmological distances would require a further refinement and the usage of a non-local metric. This is not required in the calculation of near-proximity forces. In the derivation of the Biot-Savart law, $g_{ij}$ will be rewritten with regard the corresponding non-zero relative speeds. Notice the ½ phase dependence on k-vector, corresponding to the fifth dimension for a half-spin fat electron.

And

$$\vec{k} = \frac{2\pi}{\lambda}\begin{pmatrix} 1 & 0 & 0 & 0 & 0 \\ 0 & 1 & 0 & 0 & 0 \\ 0 & 0 & 1 & 0 & 0 \\ 0 & 0 & 0 & -1 & 0 \\ 0 & 0 & 0 & 0 & -1 \end{pmatrix}\begin{pmatrix} 1 \\ 0 \\ 0 \\ 1 \\ 0 \end{pmatrix} = \frac{2\pi}{\lambda}\begin{pmatrix} 1 \\ 0 \\ 0 \\ -1 \\ 0 \end{pmatrix} \qquad (3.5)$$

for a "static zero spin neutron " forward time traveling wave. Notice that the dilaton and the dilator are treated as one due to the QLP. Where

- N=1Kg of Matter ≅1000 Avogardo's Number=6.0221367360E+26 particles of type 1.
- $\lambda_1 \cong$ h*1000*Avogardo/(1 Kg x c)= 1.3310E-15 meters ( in the MKS system).
- $\lambda_2=\lambda_{1Kg} \cong$ h/(1Kg x c)= 2.2102E-42 meters ( in the MKS system).
- $G_{Gravitational}$ is the gravitational constant = 6.6720E-11 $m^3.Kg^{-1}.s^{-2}$
- Single electric charge ($1.6022E-19$ Coulomb).
- **$q_e$ is the effective value of the single electric charge= charge divided by a corrective factor of 1.004145342= 1.59556231E-19 Coulomb**
- $\varepsilon_0$=permittivity of the vacuum = 8.8542E-12 $C^2.N^{-1}.m^{-2}$ (MKS)

Starting with the standard MKS equation for electrostatic force between two one Kg bodies of electrons (one a.m.u. "electrons" or "protons") = x Coulombs, one obtains:

$$F_{Electrosta\,tic} = \frac{1}{4\pi\varepsilon_0}\frac{(xCoulomb)^2}{1meter^2} = \frac{1}{4\pi\varepsilon_0}\left(\frac{N}{1Kg}1Kg\right)^2\frac{(q_e * Coulombs\ *\ per\ *\ particle)^2}{1meter^2}$$

$$F_{Electrosta\,tic} = \frac{1}{4\pi\varepsilon_0}\left(\frac{N}{1Kg}(q_e * Coulombs\ *\ per\ *\ particle)\right)^2\frac{(1Kg)^2}{1meter^2}$$

$$G_{Electrostatic} = \frac{1}{4\pi\varepsilon_0}(N.q_e)^2 = 8.29795214\mathrm{E}+25 \qquad (3.5)$$

$$\frac{G_{Electrostatic}}{G_{Gravitational}} = \frac{8.29795214\mathrm{E}+25}{6.672E-11} = 1.24369786\mathrm{E}+36 \qquad (3.6)$$

The dilaton for a single particle can be represented by:

$$\psi_1(x,y,z,\rho,\Phi) = \frac{\cos(\vec{k}_1.\vec{r})}{1+P.f(\vec{k}_1,\vec{r}-\vec{r}_0)} \quad (3.7)$$

where

- || means absolute value
- $f(\vec{k}_1,\vec{r}) = \theta\left(\left|\vec{k}_1.\vec{r}\right| - 2\pi\right)\left|\vec{k}_1.\vec{r}\right|$
- Where θ is the Heaviside function.
- P (absolute value of the phase volume) is 3.5 for a particle with spin half and 3 for neutral matter. The meaning of P is that for one de Broglie wavelength traversed path by the hyperspherical universe, a propagating spacetime wave spread along by a factor of P2π (7π for charged particles and 6π for neutral-zero spin matter).

Similarly, for a 1 Kg body located at position $\vec{R}$ :

$$\psi_2(x,y,z,r,\Phi) = \frac{M.N.\cos(\vec{k}_2.(\vec{R}-\vec{r}))}{1+P.f(\vec{k}_2,\vec{R}-\vec{r})} \quad (3.8)$$

where the effect of the 1 kg mass is implicit in the $k_2$-vector and expressed by the factor N. The wave intensity scales up with the number of particles (N). One kilogram of mass has 1000 moles of 1 a.m.u. "zero-spin neutrons", or $|k_2| = 1000.\text{Avogadro}.|k_1| = N.|k_1|$, where

- M=1 for neutral matter-matter, antimatter-antimatter interactions or opposite charge interactions
- M=-1 for same charge or **matter-antimatter** interactions

To calculate the effect of gravitational/electrostatic attraction, one needs to calculate the displacement on the crest of each particle or body wave due to interaction with the dilatons generated by the other body.

This is done for the lighter particle, by calculating the derivative of the waveform and considering the extremely fast varying gravitational wave from the macroscopic body always equal to one, since the maxima of these oscillations are too close to each other and can be considered a continuum.

The total waveform is given by:

$$\psi_{total}(x,y,z,r,\Phi) = \frac{\cos(\vec{k}_1.\vec{r})}{1+P.f(\vec{k}_1,\vec{r}-\vec{r}_0)} + \frac{M*N}{1+P.f(\vec{k}_2,\vec{R}-\vec{r})} \quad (3.9)$$

The term $f(\vec{k}_2,\vec{R}-\vec{r})$ contains the treatment for retarded potentials, but for simplicity we will neglect differences in dimensional time between $\vec{R}$ and $\vec{r}$ . Equation (3.9) is the one and only unification equation, that is, it is the four-dimensional wave equation that yields all the forces, when one consider four-dimensional wave constructive interference. It shows that anti-matter will have gravitational repulsion or anti-gravity with respect to normal matter. The derivative for $\psi_1$ is given by:

$$\left.\frac{\partial\psi_1(x,y,z,r,\Phi)}{\partial x}\right|_{\rho=\lambda_1} \cong -k_1{}^2 r \quad (3.10)$$

$\nabla\left(P.f(\vec{k}_1,\vec{r}-\vec{r}_0)\right) = 0$ due to $\left|\vec{k}_1.\left(\vec{r}-\vec{r}_0\right)\right| << 2\pi.$

Similarly

$$\left.\frac{\partial\psi_2(x,y,z,r,\phi)}{\partial x}\right|_{\rho=\lambda_1} \cong \frac{N*M}{Pk_2.R^2} \quad (3.11)$$

Solving for x:

$$x = \frac{N}{Pk_1^{\,2}k_2.R^2} = \frac{\lambda_1^{\,2}\lambda_2 N * M}{P(2\pi)^3 R^2} \qquad (3.12)$$

There are two regimen of spacetime travel and they are depicted in Figure 9 below:

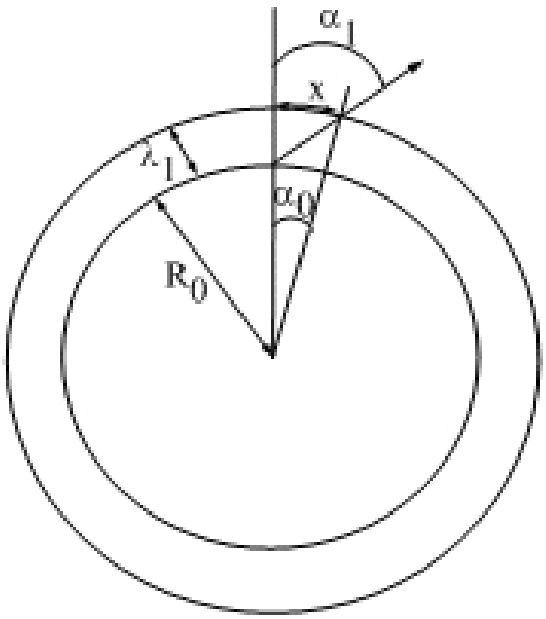


Figure 9. This figure shows the geometry of a surface bound particle. This is a X versus R cross-section of the hyperspherical expanding universe. Notice that the two circles represent a one de Broglie expansion of the hyperspherical universe.

At each de Broglie step both types of particles (zero and non-zero) change position by the same amount x and that defines a change in k-vector direction. The difference is with which referential that change in angle occurs. In the case of volumetric waves (non-zero spin particles), the k-vector is allowed to change by the angle $\alpha_1$, while in the case of superficial waves (zero spin particles), the k-vector changes just by the amount given by $\alpha_0$ since its k-vector has to remain perpendicular to the fabric of space. Tan($\alpha$) is given by $\tan(\alpha_1) = x/\lambda_1$ or by $\tan(\alpha_0) = x/\lambda_1 * (\lambda_1/R_0)$ depending upon if the interaction is such that the particle k-vector shifts as in $\alpha_1$ or it just acquires the radial pointing direction as in $\alpha_0$. A further refinement introduced by equation (3.13) below introduces a level of local deformation of the de Broglie hypersurface or fabric of space. A change in angle $\alpha_0$ corresponds to a much smaller angle change between the radial directions (by a factor $\lambda_1/R_0$ = 9.385E-42, with $R_0$ (circa 15 billion light-years) as the dimensional age of the Universe). The experimental spacetime torsion due to gravitational interaction lies someplace in between 1 and $10^{-41}$, thus showcasing a level of local deformation of the fabric of space. From figure 9, one calculates tan($\alpha$) as:

$$\tan(\alpha) = \frac{x}{\lambda_1}\delta = \frac{\lambda_1\lambda_2 N}{P(2\pi)^3 R^2}\delta \qquad (3.13)$$

Where $9.385.10^{42} = \frac{\lambda_1}{R_0} \le \delta \le 1$ and M=1. It will be shown that the upper limit is valid for charged particle interaction, while the lower limit modified by a slight deformation of the fabric of space will be associated with gravitational interaction. For the case of light, one has the following equation:

$$\tan(\alpha_0) = 1 \qquad (3.14)$$

That is, light propagates with proper time projection/propagation direction $\tau$ at $45^0$ with respect to the radial time/direction. To calculate the derivative of tan ($\alpha$) with respect to $\tau$, one can use the following relationship:

$$\frac{\partial}{\partial r}\tan(\alpha_0) = \frac{\tan(\alpha_0)}{\lambda_1} = \frac{\lambda_2 N}{P(2\pi)^3 R^2}\delta \qquad (3.15)$$

Acceleration is given by:

$$a = c^2 \frac{\partial}{\partial r} \tan(\alpha_0) = \frac{c^2 \lambda_2 N}{P(2\pi)^3 R^2} \delta \qquad (3.16)$$

To calculate the force between two 1 Kg masses (1000 moles of 1 a.m.u. particles) separated by one meter distance one needs to multiply equation (3.15) by 1Kg (N particles/Kg* 1Kg):

$$F = G_{Calculated} \ (\delta) \frac{(1Kg)^2}{(1meter)^2} = -\frac{c^2 \lambda_2 * \left(\frac{N}{1Kg}\right)^2}{P(2\pi)^3} \delta \frac{(1Kg)^2}{(1meter)^2} \qquad (3.17)$$

For δ=1 and P=3.5 one obtains the $G_{Electrostatic}$ (3.5).

$$G_{Calculated} \ (\delta = 1) = \frac{c^2 \left(\frac{N}{1Kg}\right) \lambda_1}{P(2\pi)^3} = 8.29795214E+25 = G_{Electrostatic} \qquad (3.18)$$

Where one made use of $\lambda_1 = N\lambda_2$ and considered the absolute value. It is important to notice that the derivation of the $G_{Calculated}$ never made use of any electrostatic property of vacuum, charge etc. It only mattered the mass (spacetime volumetric deformation) and spin. Of course, one used the Planck constant and the speed of light and Avogadro's number. **By setting δ=1 one recovers the electrostatic value of G!**

To analyze gravitational interaction, let's consider that Hubble coefficient measurements estimate the universe as being around 15 Billion Years old or 1.418E26 meters radius. To obtain the elasticity coefficient of spacetime, let's rewrite $\delta = (\lambda_1/R_0)\xi$ on equation (3.17) and equate the $G_{Calculated}$ to $G_{Gravitational}$ for two bodies of 1 Kg separated by 1 meter.

$$F = G_{Gravitaion \ al} = -6.6720 \ \text{E-11} \frac{(1Kg)^2}{(1meter)^2} = -\frac{c^2 \left(\frac{N}{1Kg}\right) \lambda_1}{P(2\pi)^3} \frac{\lambda_1}{R_0} \xi \frac{(1Kg)^2}{(1meter)^2} \qquad (3.19)$$

Where P =3 since we are considering a spin-zero interaction. Solving for ξ:

$$\xi = \frac{P(2\pi)^3 R_0 G_{Gravitaion \ al}}{c^2 \left(\frac{N}{1Kg}\right) \lambda_1^2} = 8.567 \times 10^{-4} \qquad (3.20)$$

If we consider that the force is given by mass times acceleration:

$$F = m_{Mass} a_x = m_{Mass} c^2 \frac{\partial \tan(\theta)}{\partial \lambda} = \frac{m_{Mass} c^2}{\lambda_1^2} \frac{\lambda_1}{R_0} \xi . x \qquad (3.21)$$

$$F = \frac{m_{Mass} c^2}{\lambda_1 R_0} \xi . x = m_{Mass} \left(2\pi . \Omega^G Universe\right)^2 . x \qquad (3.22)$$

The natural frequency of spacetime oscillations is:

$$\Omega^G Universe = \frac{1}{2\pi} \sqrt{\frac{c^2 \xi}{\lambda_1 R_0}} = 32.14 \text{ KHz} \qquad (3.23)$$

Notice that this is not dependent upon any masses. That should be the best frequency to look for or to create gravitational waves. Of course, Hubble red shift considerations should be used to determine the precise frequency from a specific region of the universe. At last one can calculate the value of the vacuum permittivity from equations (3.5) and (3.18) as:

$$\varepsilon_0 = \frac{7\pi^2 N q_e^2}{c^2 \lambda_1} = 8.85418782 \quad \text{E - 12} \qquad (3.24)$$

Not surprisingly, there is a perfect match between theoretical and experimental (8.85418782E-12 $C^2.N^{-1}.m^{-2}$ ) values. The correction factor used to calculate the effective charge per particle is due to the effect of non-zero spin on matter, thus related to the particle gyromagnetic ratio. It is important to notice that this derivation don't use any parameterization. The "gyromagnetic ratio" and the "FS elasticity" are predictions of the theory, which uses only electron charge, speed of light, Avogadro's number and Planck's constant to relate it to non-hypergeometrical physics.

The complete gravitation equation is given by:

$$F_{Gravitaional} = \left[ \frac{c^2 \left( \frac{N}{1Kg} \right) \lambda_1}{P(2\pi)^3} \frac{\lambda_1}{R_0} \xi \right] \frac{m_1 m_2}{R^2} \qquad (3.25)$$

**Quantum aspects can be recovered by not using fast oscillation approximations**. It is also important to notice that equations (3.8) and (3.9) can be used to calculate the interaction between any particles (matter or anti-matter) or to perform quantum mechanical calculations in a manner similar to molecular dynamic simulations. The quantum character is implicit in the de Broglie wavelength stepwise quantization. It is also relativistic in essence, as it will become clear when one analyzes magnetism next.

### 3.2 Magnetic Interaction

### The Derivation of the Biot-Savart Law

Let's consider two wires with currents $i_1$ and $i_2$ separated by a distance R. Let's consider $i_2$ on the element of length $dl_2$ as the result of a moving charge of mass of 1Kg of fat electrons (one a.m.u. electrons). This is done to obtain the correct scaling factor.

Without loss of generality, let's consider that the distance between the two elements of current is given by:

$$\vec{R} = \frac{R}{\sqrt{3}} \begin{pmatrix} 1 \\ 1 \\ 1 \\ 0 \\ 0 \end{pmatrix} = R\hat{I} \quad \text{and} \quad \vec{r}_0 = \begin{pmatrix} 0 \\ 0 \\ 0 \\ 0 \\ 0 \end{pmatrix} \qquad (3.26)$$

The velocities are:

$$\vec{V}_1 = v_1 \begin{pmatrix} \alpha_1 \\ \beta_1 \\ \gamma_1 \\ 0 \\ 0 \end{pmatrix} \quad \text{and} \quad \vec{V}_2 = v_2 \begin{pmatrix} \alpha_2 \\ \beta_2 \\ \gamma_2 \\ 0 \\ 0 \end{pmatrix} \qquad (3.27)$$

Due to the spin half, one has after a two de Broglie cycles:

$$\vec{r} = \begin{pmatrix} \frac{r}{\sqrt{3}}.(1+\frac{v_2}{c}\alpha_2\sqrt{3}) \\ \frac{r}{\sqrt{3}}.(1+\frac{v_2}{c}\beta_2\sqrt{3}) \\ \frac{r}{\sqrt{3}}.(1+\frac{v_2}{c}\gamma_2\sqrt{3}) \\ 2\lambda_1 \\ 2\lambda_1 \end{pmatrix} \quad \text{and} \quad \vec{R} = \begin{pmatrix} \frac{R}{\sqrt{3}} \\ \frac{R}{\sqrt{3}} \\ \frac{R}{\sqrt{3}} \\ 2\lambda_1 \\ 2\lambda_1 \end{pmatrix} \quad \text{and} \quad \vec{r}_0 = \begin{pmatrix} 0 \\ 0 \\ 0 \\ 2\lambda_1 \\ 2\lambda_1 \end{pmatrix} \qquad (3.28)$$

Since one expects that the motion of particle 2 will produce a drag on the particle 1 along particle 2 direction of motion.

The figure below showcase the geometry associated with these two currents.

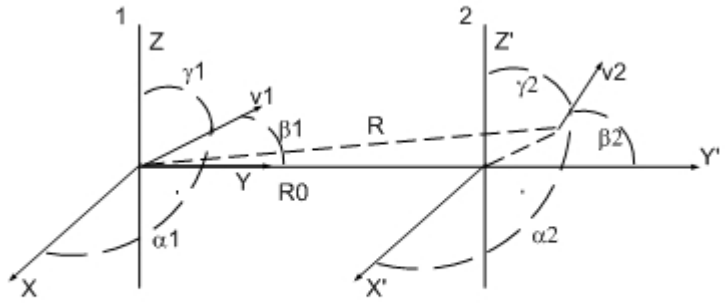


Figure 10. Derivation of Biot-Savart law using spacetime waves.

Notice also that the effect of the ½ spin is to slow down the rate of phase variation along the dimensional time τ in half.

In the case of currents, the velocities are not relativistic and one can make the following approximations to the five-dimensional rotation matrix or metric: $\cosh(\alpha) \cong 1$ and $\sinh(\alpha_i) \cong v_i/c$ where $v_i$ is the velocity along the axis i.

The k-vectors for the two electrons on the static reference frame are given by:

$$\vec{k}_1 \cong \frac{2\pi}{\lambda_1}\begin{bmatrix} 1 & 0 & 0 & -\alpha_1\frac{v_1}{c} & 0 \\ 0 & 1 & 0 & -\beta_1\frac{v_1}{c} & 0 \\ 0 & 0 & 1 & -\gamma_1\frac{v_1}{c} & 0 \\ -\alpha_1\frac{v_1}{c} & -\beta_1\frac{v_1}{c} & -\gamma_1\frac{v_1}{c} & -1 & 0 \\ 0 & 0 & 0 & 0 & -1 \end{bmatrix}\begin{bmatrix} \frac{1}{\sqrt{3}} \\ \frac{1}{\sqrt{3}} \\ \frac{1}{\sqrt{3}} \\ -1 \\ \frac{1}{2} \end{bmatrix} \cong \frac{2\pi}{\lambda_1}\begin{bmatrix} \frac{1}{\sqrt{3}}+\alpha_1\frac{v_1}{c} \\ \frac{1}{\sqrt{3}}+\beta_1\frac{v_1}{c} \\ \frac{1}{\sqrt{3}}+\gamma_1\frac{v_1}{c} \\ -\left(\alpha_1\frac{v_1}{c}+\beta_1\frac{v_1}{c}+\gamma_1\frac{v_1}{c}\right)-1 \\ -\frac{1}{2} \end{bmatrix} \qquad (3.29)$$

Similarly:

$$\vec{k}_2 \cong \frac{2\pi}{\lambda_2}\begin{bmatrix} \frac{1}{\sqrt{3}}+\alpha_2\frac{v_2}{c} \\ \frac{1}{\sqrt{3}}+\beta_2\frac{v_2}{c} \\ \frac{1}{\sqrt{3}}+\gamma_2\frac{v_2}{c} \\ -\alpha_2\frac{v_2}{c}-\beta_2\frac{v_2}{c}-\gamma_2\frac{v_2}{c}-1 \\ -\frac{1}{2} \end{bmatrix} \tag{3.30}$$

The wave intensities at $\vec{r}$ are:

$$\psi_1(x,y,z,r,\Phi) = \frac{\cos(\vec{k}_1.\vec{r})}{1+P.f(\vec{k}_1,\vec{r}-\vec{r}_0)} \tag{3.31}$$

$$\psi_2(x,y,z,r,\Phi) = \frac{M.\cos(\vec{k}_2.(\vec{R}-\vec{r}))}{1+P.f(\vec{k}_2,\vec{R}-\vec{r})} \tag{3.32}$$

Where N= 1000 Avogadro, $\lambda_1$= de Broglie wavelength of a one a.m.u (atomic mass unit) particle, $\lambda_2$=de Broglie wavelength of a 1Kg particle= $\lambda_1$/N.

Now one can calculate:

$$\vec{k}_1.(\vec{r}-\vec{r}_0) \cong \frac{2\pi}{\lambda_1}\begin{bmatrix} \frac{1}{\sqrt{3}}+\alpha_1\frac{v_1}{c} \\ \frac{1}{\sqrt{3}}+\beta_1\frac{v_1}{c} \\ \frac{1}{\sqrt{3}}+\gamma_1\frac{v_1}{c} \\ \left(-\alpha_1\frac{v_1}{c}-\beta_1\frac{v_1}{c}-\gamma_1\frac{v_1}{c}\right)-1 \\ -\frac{1}{2} \end{bmatrix}\begin{pmatrix} \frac{r}{\sqrt{3}}.(1+\frac{v_2}{c}\alpha_2\sqrt{3}) \\ \frac{r}{\sqrt{3}}.(1+\frac{v_2}{c}\beta_2\sqrt{3}) \\ \frac{r}{\sqrt{3}}.(1+\frac{v_2}{c}\gamma_2\sqrt{3}) \\ 0 \\ 0 \end{pmatrix} = \frac{2\pi r}{\lambda_1}\left(1+\frac{\vec{V}_1.\hat{R}}{c}+\frac{\vec{V}_2.\hat{R}}{c}+\frac{\vec{V}_1.\vec{V}_2}{c^2}\right) \tag{3.33}$$

$$\vec{k}_1.\vec{r} \cong \frac{2\pi r}{\lambda_1}\left(1+\frac{\vec{V}_1.\hat{R}}{c}+\frac{\vec{V}_2.\hat{R}}{c}+\frac{\vec{V}_1.\vec{V}_2}{c^2}\right)+2\pi \tag{3.34}$$

$$\nabla\left(\vec{k}_1.(\vec{r}-\vec{r}_0)\right) = \nabla\left(\vec{k}_1.\vec{r}\right) \cong \frac{2\pi}{\lambda_1}\left(1+\frac{\vec{V}_1.\hat{R}}{c}+\frac{\vec{V}_2.\hat{R}}{c}+\frac{\vec{V}_1.\vec{V}_2}{c^2}\right)\hat{R} \tag{3.35}$$

$\nabla\left(P.f(\vec{k}_1,\vec{r}-\vec{r}_0)\right) \cong 0$ due to $\left|\vec{k}_1.(\vec{r}-\vec{r}_0)\right| << 2\pi$.

Similarly:

$$\vec{k}_2.(\vec{R}-\vec{r}) \cong \frac{2\pi}{\lambda_2}\begin{bmatrix} \frac{1}{\sqrt{3}}+\alpha_2\frac{v_2}{c} \\ \frac{1}{\sqrt{3}}+\beta_2\frac{v_2}{c} \\ \frac{1}{\sqrt{3}}+\gamma_2\frac{v_2}{c} \\ \left(-\alpha_2\frac{v_2}{c}-\beta_2\frac{v_2}{c}-\gamma_2\frac{v_2}{c}\right)-1 \\ -\frac{1}{2} \end{bmatrix}\begin{pmatrix} \frac{R}{\sqrt{3}}-\frac{r}{\sqrt{3}}.(1+\frac{v_2}{c}\alpha_2\sqrt{3}) \\ \frac{R}{\sqrt{3}}-\frac{r}{\sqrt{3}}.(1+\frac{v_2}{c}\beta_2\sqrt{3}) \\ \frac{R}{\sqrt{3}}-\frac{r}{\sqrt{3}}.(1+\frac{v_2}{c}\gamma_2\sqrt{3}) \\ 0 \\ 0 \end{pmatrix} \cong \frac{2\pi R}{\lambda_2}\left(1+\frac{\vec{V}_2.\hat{R}}{c}\right) \tag{3.36}$$

(3.37)

$$\nabla\left(f(\vec{k}_2,\vec{R}-\vec{r})\right)\cong\frac{2\pi}{\lambda_2}\begin{bmatrix}\frac{1}{\sqrt{3}}+\alpha_2\frac{v_2}{c}\\ \frac{1}{\sqrt{3}}+\beta_2\frac{v_2}{c}\\ \frac{1}{\sqrt{3}}+\gamma_2\frac{v_2}{c}\\ \left(-\alpha_2\frac{v_2}{c}-\beta_2\frac{v_2}{c}-\gamma_2\frac{v_2}{c}\right)-1\\ -\frac{1}{2}\end{bmatrix}\begin{pmatrix}-\frac{1}{\sqrt{3}}.(1+\frac{v_2}{c}\alpha_2\sqrt{3})\\ -\frac{1}{\sqrt{3}}.(1+\frac{v_2}{c}\beta_2\sqrt{3})\\ -\frac{1}{\sqrt{3}}.(1+\frac{v_2}{c}\gamma_2\sqrt{3})\\ 0\\ 0\end{pmatrix}=-\frac{2\pi}{\lambda_2}\left(1+\frac{\vec{V}_2.\hat{R}}{c}\right)\hat{R}$$

Hence:

$$\nabla\psi_1(x,y,z,r,\Phi)\cong-\frac{\nabla(\vec{k}_1..\vec{r})}{1+P.f(\vec{k}_1,\vec{r}-\vec{r}_0)}\sin(\vec{k}_1.\vec{r}) \tag{3.38}$$

$$\nabla\psi_1(x,y,z,r,\Phi)\cong-\left(\frac{2\pi}{\lambda_1}\right)^2\left(1+\frac{\vec{V}_1.\hat{R}}{c}+\frac{\vec{V}_2.\hat{R}}{c}+\frac{\vec{V}_1.\vec{V}_2}{c^2}\right)^2 r\hat{R} \tag{3.39}$$

And

(3.40)

$$\nabla\psi_2(\vec{r},r,\Phi)\cong-\frac{P\nabla(f(\vec{k}_2,\vec{R}-\vec{r}))}{\left(1+P.f(\vec{k}_2,\vec{R}-\vec{r})\right)^2}=-\frac{1}{P\frac{2\pi}{\lambda_2}.\left(1+\frac{\vec{V}_2.\hat{R}}{c}\right)}\frac{\hat{R}}{R^2}\cong-\left(\frac{\lambda_2}{2\pi P}\right)\left(1-\frac{\vec{V}_2.\hat{R}}{c}\right)\frac{\hat{R}}{R^2}$$

Thus,

(3.41)

$$r\cong-\frac{\left(\frac{\lambda_2}{2\pi P}\right)\left(1-\frac{\vec{V}_2.\hat{R}}{c}\right)\frac{\hat{R}}{R^2}}{\left(\frac{2\pi}{\lambda_1}\right)^2\left(1+\frac{\vec{V}_1.\hat{R}}{c}+\frac{\vec{V}_2.\hat{R}}{c}+\frac{\vec{V}_1.\vec{V}_2}{c^2}\right)^2}\cong-\left(\lambda_1^2\lambda_2\right)\frac{\left(1-\frac{\vec{V}_2.\hat{R}}{c}\right)\left(\hat{R}.\hat{R}-2\frac{\vec{V}_1.\hat{R}}{c}-2\frac{\vec{V}_2.\hat{R}}{c}-2\frac{\vec{V}_1.\vec{V}_2}{c^2}\right)}{(2\pi)^3P}\frac{\hat{R}}{R^2}$$

$$r_{ee}\cong-\left(\lambda_1^2\lambda_2\right)\frac{\left(\hat{R}.\hat{R}-2\frac{\vec{V}_1.\hat{R}}{c}-2\frac{\vec{V}_2.\hat{R}}{c}-2\frac{\vec{V}_1.\vec{V}_2}{c^2}-2\frac{\vec{V}_2.\hat{R}}{c}+2\left(\frac{\vec{V}_1.\hat{R}}{c}\right)\left(\frac{\vec{V}_2.\hat{R}}{c}\right)+2\left(\frac{\vec{V}_2.\hat{R}}{c}\right)\left(\frac{\vec{V}_2.\hat{R}}{c}\right)+2\left(\frac{\vec{V}_1.\vec{V}_2}{c^2}\right)\left(\frac{\vec{V}_2.\hat{R}}{c}\right)\right)}{(2\pi)^3P}\frac{\hat{R}}{R^2} \tag{3.42a}$$

$$r_{ep}\cong+\left(\lambda_1^2\lambda_2\right)\frac{\left(\hat{R}.\hat{R}-2\frac{\vec{V}_1.\hat{R}}{c}\right)}{(2\pi)^3P}\frac{\hat{R}}{R^2}\qquad\text{since v2=0}\qquad(3.42b)$$

$$r_{pe}\cong\left(\lambda_1^2\lambda_2\right)\frac{\left(\hat{R}.\hat{R}-2\frac{\vec{V}_2.\hat{R}}{c}-2\frac{\vec{V}_2.\hat{R}}{c}+2\left(\frac{\vec{V}_2.\hat{R}}{c}\right)\left(\frac{\vec{V}_2.\hat{R}}{c}\right)\right)}{(2\pi)^3P}\frac{\hat{R}}{R^2}\qquad\text{since v1=0}\qquad(3.42c)$$

$$r_{pp}\cong\left(\lambda_1^2\lambda_2\right)\frac{\left(\hat{R}.\hat{R}\right)}{(2\pi)^3P}\frac{\hat{R}}{R^2}\qquad\text{since v1=v2=0}\qquad(3.42d)$$

(3.42f)

$$r_{total} \cong r_{ee} + r_{ep} + r_{pe} + r_{pp} = -\left(\lambda_1^{\,2}\lambda_2\right)\frac{\left(2\left(\frac{\vec{V}_1.\hat{R}}{c}\right)\left(\frac{\vec{V}_2.\hat{R}}{c}\right) - 2\left(\frac{\vec{V}_1.\vec{V}_2}{c^2}\right)\left(1 - \left(\frac{\vec{V}_2.\hat{R}}{c}\right)\right)\right)}{(2\pi)^3 P}\frac{\hat{R}}{R^2}$$

Where p stands for proton and e for electron.

$$r \cong -\left(\lambda_1^{\,2}\lambda_2\right)\frac{\left(-2\frac{\vec{V}_1.\vec{V}_2}{c^2} + 2\left(\frac{\vec{V}_1.\hat{R}}{c}\right)\left(\frac{\vec{V}_2.\hat{R}}{c}\right)\right)}{(2\pi)^3 P}\frac{\hat{R}}{R^2} \tag{3.43}$$

$$r \cong 2\left(\lambda_1^{\,2}\lambda_2\right)\frac{\left(\left[V_1 \otimes \left(V_2 \otimes \hat{R}\right)\right].\hat{R}\right)}{(2\pi)^3 P c^2}\frac{\hat{R}}{R^2} \tag{3.44}$$

Where non-velocity dependent and single velocity dependent contributions where neglected due to the counterbalancing wave contributions from static positively charged centers.

The force is given by:

$$\vec{F} = c^2\frac{\partial \tan(\alpha)}{\partial r} = c^2\frac{r}{2\lambda_1^2} = \frac{\lambda_2}{(2\pi)^3 P}\left(\left[V_1 \otimes \left(V_2 \otimes \hat{R}\right)\right]\hat{R}\right)\frac{\vec{R}}{R^3} = \frac{\lambda_2 \nu_1.\nu_2}{(2\pi)^3 P}\left(\left[d\hat{l}_1 \otimes \left(d\hat{l}_2 \otimes \hat{R}\right)\right]\hat{R}\right)\frac{\vec{R}}{R^3} \tag{3.45}$$

Where one took into consideration that a particle with spin half has a cycle of 2 $\lambda_1$ instead of $\lambda_1$.

The Biot-Savart law can be written as:

$$d\vec{F} = \frac{\mu_0 I_1.I_2}{4\pi}\frac{(d\vec{l}_1.d\vec{l}_2)\vec{x}_{12}}{|\vec{x}_{12}|^3} \tag{3.46}$$

Comparing the two equations one obtains:

$$\frac{\mu_0}{4\pi} = \frac{\lambda_2}{(2\pi)^3 q_e^{\,2} P} \tag{3.47}$$

Thus

$$\mu_0 = \frac{\lambda_2}{2\pi^2 q_e^{\,2} P} \tag{3.48}$$

From equation (3.24)

$$\varepsilon_0 = \frac{2P\pi^2 N q_e^{\,2}}{c^2\lambda_1}$$

Thus

$$\mu_0.\varepsilon_0 = \frac{\lambda_2}{2P\pi^2 q_e^{\,2}}\frac{2P\pi^2 N q_e^{\,2}}{c^2\lambda_1} = \frac{1}{c^2} \tag{3.49}$$

Thus one recovers the relationship between $\mu_0$ and $\varepsilon_0$.

### 3.3 Grand Unification Supersymmetry

As the dimensional age of the universe becomes smaller, the relative strength of gravitation interaction increases. Conversely, one expects that as the universe expands gravity will become weaker and weaker. This and the four-dimensional light speed expanding hyperspherical universe topology explain the acceleration of expansion without the need of anti-gravitational dark matter.

For gravitation the spring coefficient is given by:

$$F = m_{neutron} * a_x = m_{neutron} c^2 \frac{\partial \tan(\theta)}{\partial \lambda} = \frac{m_{neutron} c^2}{\lambda^2_1} \frac{8.56610^4 \lambda_1}{R_0} x = \kappa_g x \quad (3.50)$$

Similarly for electrostatic interaction, one has:

$$F = m_{neutron} * a_x = m_{neutron} c^2 \frac{\partial \tan(\theta)}{\partial \lambda} = \frac{m_{neutron} c^2}{\lambda^2_1} x = \kappa_e x \quad (3.51)$$

$$\text{Thus } \frac{\kappa_g}{\kappa_e} = \frac{8.56610^4 \lambda_1}{R_0} \quad (3.52)$$

Thus when $R_0$ was smaller than $8.566\ 10^4$ times $\lambda_1$ (3.8E-19s), gravitational and electromagnetic interactions had equal strength. They were certainly indistinguishable when the radius of the universe was one de Broglie wavelength long. This section is called Grand unification supersymmetry, because condition (3.52) plays the role of the envisioned group theoretical supersymmetry of the grand unification force in future theories. Of course, it has a geometrical interpretation. At that exact radius, an elastic spring constant of the fabric of space allows for a change in the local normal such that it is parallel to the redirection of k-vector of a freely moving dilator. This is not what most scientists in this field expected but science is not about expectations.

# 4. Hypergeometrical Standard Model

A new model for matter is proposed. In this initial model, the elements, protons, electrons and neutrons and their antimatter counterparties are recast as being derived from a single particle. This particle is expressed in geometrical terms as being a coherence between two 4D deformation stationary states from a rotating 4D double potential well. This coherence is called a dilator. As the dilator oscillates between sides of the potential well, it creates a traveling modulation of the metric or 5D spacetime waves or dilatons. Spin is modeled not as an intrinsic degree of freedom, but as an extrinsic tumbling or rotation of the dilator. **Since the dilaton frequency is defined just by the gap between the fundamental dilator states, it frequency does not depends upon the mass of the dilator**. Dilatons travel through the 4D space. 3D projections are known as de Broglie matter waves. Planck's constant is the connection between the 3D dilaton projection wavelength and the particle 3D linear momentum. **Planck's constant ensures that for the 3D observed mass and velocity, the de Broglie wavelength will match it fundamental dilaton 3D projection.** Mass is considered to be proportional to dilator maximum 4D volume. Calibration is made to replicate Gauss' electrostatics law, Newton's gravitational law and Biot-Savart law of magnetism. Since mass is proportional to a 4D volume and volume depends upon lengths, which are Lorentz invariant , the 4D-mass volume representation is also Lorentz invariant. 4D-mass is defined as being the total mass or 4D volume displaced in an oscillation cycle. Since the dilator oscillates between states corresponding to an electron and a proton, its 4D mass will be one atomic mass unit. 3D-mass is the mass or 4D displacement volume perceived in the 3D Space at given phases of the de Broglie expansion.

Dilators with spin zero are modeled to couple with superficial wave, and thus their position changes from one de Broglie cycle to the next just by the displacement governed by a new quantum Lagrangian principle. Its propagation direction continues to be perpendicular to the 3D universe hypersurface. Dilators with non-zero spin are modeled to couple with volumetric wave, and their position changes from one de Broglie cycle to the next just by the displacement governed by the Lagrangian principle. In addition, its propagation direction is redirected by the angle covered by this transition. Since the change in angle is defined with respect to the last step k-vector, charged particles are to sense a much higher acceleration than zero spin particles (matter). **This is the proposed reason behind the strength difference between gravitation and electromagnetic Forces.**

Here is the Hyperon data sheet:

| Particle | Symbol | Rest Mass(Mev/$c^2$) | Decay Reaction | Spin | **Coherence Lifetime** |
|---|---|---|---|---|---|
| NeutrinoElectron | $\nu_e$ | 0.0000022 | | 1/2 | |
| NeutrinoMuon | $\nu_\mu$ | 0.17 | | 1/2 | |
| NeutrinoTau | $\nu_\tau$ | 15.5 | $\mu^+ + \nu_\mu$ | 1/2 | |
| KaonMinus | $\kappa^-$ | 493.7 | $\mu^- - \nu_\mu$ | 1/2 | |
| KaonPlus | $\kappa^+$ | 493.7 | $\mu^+ + \nu_\mu$ | 1/2 | |
| KaonPlus | $\kappa^+$ | 493.7 | $\boldsymbol{\pi^+ + \pi^0}$ | 1/2 | |
| KaonZeroShort | $K^0_S$ | 497.7 | $\boldsymbol{\pi^0 + \pi^0}$ | 1/2 | |
| KaonZeroLong | $K^0_L$ | 497.7 | $\boldsymbol{\pi^+} + e^- + \nu_e$ | 1/2 | |
| MuonMinus | $\mu^-$ | 105.7 | $e^- - \nu_e + \nu_\mu$ | 1/2 | |
| MuonPlus | $\mu^+$ | 105.7 | $e^+ + \nu_e - \nu_\mu$ | 1/2 | |
| Electron | $e^-$ | 0.510998918 | $e^-$ | 1/2 | Stable |
| PionMinus | $\boldsymbol{\pi^-}$ | 139.57018 | $e^- + \nu_e$ | 1/2 | |
| PionPlus | $\boldsymbol{\pi^+}$ | 139.57018 | $e^+ - \nu_e$ | 1/2 | |
| PionZero | $\boldsymbol{\pi^0}$ | 134.9766 | $e^+ + e^- + hw$ | 1/2 | |
| Proton | **P** | 938.3 | Unobserved | 1/2 | Stable[1] |
| Neutron | **N** | 939.6 | $\mathbf{p} + \mathbf{e^-} - \boldsymbol{\nu_e}$ | 1/2 | 885.7±0.8[2] |
| DeltaPlusPlus | $\boldsymbol{\Delta^{++}}$ | 1232 | $\boldsymbol{\pi^+ + p}$ | 3/2 | $6\times10^{-24}$ |
| DeltaPlus | $\boldsymbol{\Delta^+}$ | 1232 | $\boldsymbol{\pi^+ + n}$ | 3/2 | $6\times10^{-24}$ |
| DeltaPlus | $\boldsymbol{\Delta^+}$ | 1232 | $\boldsymbol{\pi^0 + p}$ | 3/2 | $6\times10^{-24}$ |
| DeltaZero | $\boldsymbol{\Delta^0}$ | 1232 | $\boldsymbol{\pi^0 + n}$ | 3/2 | $6\times10^{-24}$ |
| DeltaZero | $\boldsymbol{\Delta^0}$ | 1232 | $\boldsymbol{\pi^- + p}$ | 3/2 | $6\times10^{-24}$ |
| DeltaMinus | $\boldsymbol{\Delta^-}$ | 1232 | $\boldsymbol{\pi^- + n}$ | 3/2 | $6\times10^{-24}$ |
| LambdaZero | $\boldsymbol{\Lambda^0}$ | 1115.7 | $\boldsymbol{\pi^- + p}$ | 1/2 | $2.60\times10^{-10}$ |
| LambdaZero | $\boldsymbol{\Lambda^0}$ | 1115.7 | $\boldsymbol{\pi^o + n}$ | 1/2 | $2.60\times10^{-10}$ |
| SigmaPlus | $\boldsymbol{\Sigma^+}$ | 1189.4 | $\boldsymbol{\pi^0 + p}$ | 1/2 | $0.8\times10^{-10}$ |
| SigmaPlus | $\boldsymbol{\Sigma^+}$ | 1189.4 | $\boldsymbol{\pi^+ + n}$ | 1/2 | $0.8\times10^{-10}$ |
| SigmaZero | $\boldsymbol{\Sigma^0}$ | 1192.5 | $\boldsymbol{\Lambda^0 + \gamma}$ | 1/2 | $6\times10^{-20}$ |
| SigmaMinus | $\boldsymbol{\Sigma^-}$ | 1197.4 | $\boldsymbol{\pi^- + n}$ | 1/2 | $1.5\times10^{-10}$ |

| | | | | | |
|---|---|---|---|---|---|
| Xi Zero | $\Xi^0$ | 1315 | $\Lambda^0 + \pi^0$ | 1/2 | $2.9\times10^{-10}$ |
| Xi Minus | $\Xi^-$ | 1321 | $\Lambda^0 + \pi^-$ | 1/2 | $1.6\times10^{-10}$ |
| OmegaMinus | $\Omega^-$ | 1672 | $\Lambda^0 + K^-$ | 3/2 | $0.82\times10^{-10}$ |
| OmegaMinus | $\Omega^-$ | 1672 | $\Xi^0 + \pi^-$ | 3/2 | $0.82\times10^{-10}$ |

The Fundamental Dilator is modeled as a coherence between two 4D deformational stationary states of a 4D double potential.

The quantum numbers, associated with the 4D deformational states, are modeled as axes' lengths of a 4D ellipsoid of revolution. Negative values correspond to 180 degrees in phase with respect to a dilator with a positive axis. This means that when the positive dilator is expanding the 4D space, the negative dilator is shrinking 4D space.

## Electron and Proton Models were shown before.

## Electron Neutrino Model

Here is the Electron Neutrino model. Notice that there are no colors associated with the neutrino states since they have zero 3D volume. Since their frequency is not a perfect match to the Fundamental Dilator coherence, their interactions average to zero.

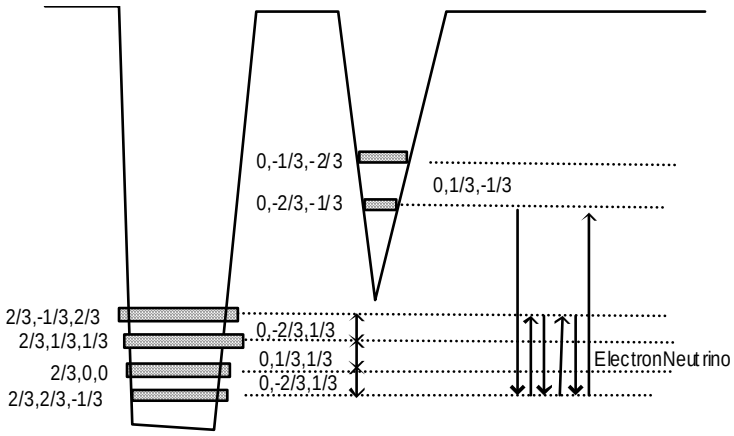


Figure 11. Electron Neutrino coherence

The Electron Neutrino corresponds to a 360 degrees rotation of Proton (2/3.2/3.-1/3) state 4D volume around the X axis.

Electron Neutrino is a Majorama particle since it is clear that half of it applied to an anti-proton state would result in a Proton state and vice-versa.

## Muon Neutrino Model

Here is the Muon Neutrino model. Notice that there are no colors associated with the neutrino states since they have zero 3D volume. The Muon Neutrino corresponds to a rotation around the X axis of a two dimensional coherence between states (0,-2/3,-1/3) and (0,-1/3,-2/3). Since their frequency is not a perfect match to the Fundamental Dilator coherence, their interaction average to zero.

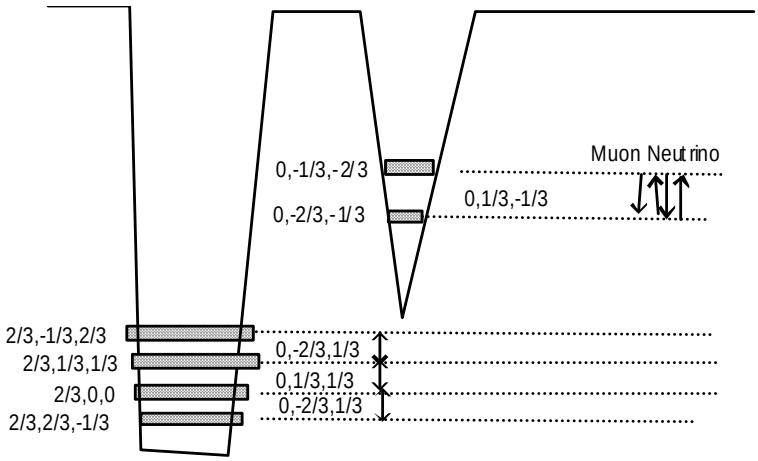


Figure 12. Muon Neutrino coherence

## Neutron Model

| Particle | Symbol | Rest Mass ($Mev/c^2$) | Decay Reaction | Spin | **Coherence Lifetime** |
|---|---|---|---|---|---|
| Neutron | **N** | 939.6 | $\mathbf{p + e^- - \nu_e}$ | 1/2 | $885.7 \pm 0.8$[2] |

Below is the Neutron model. It is worthwhile to notice that the Electron-Proton and Proton-Electron transitions (transmutation coherences) are not in phase with the tumbling process and thus lead to a mismatch between the Neutron overall tumbling and a number of full rotations. This means that due to those sub-coherences, there is kinetic energy stored in the form of a local fabric of space twisting. The angle error at the end of the coherence is the sum of those two contributions. The electron and the proton coherences are by definition in phase with the tumbling process.

The shift in phase is such that the electron/proton fabric of space twisting is 43.90266/-0.07294 degrees for a neutron at rest, respectively. This is the fabric of space twisting that would result in the observed relative velocities after neutron decaying. Notice that twisting the fabric of space results in an increase in the mass or FS overlap of the 4D volume displacement associated with different states, and thus explains the extra mass involved in the neutron formation. The same reasoning is applicable to all particles and elements. The elements and isotopes are modeled as simple coherences involving only the fundamental dilator (electron and proton) and these two transmutation coherences.

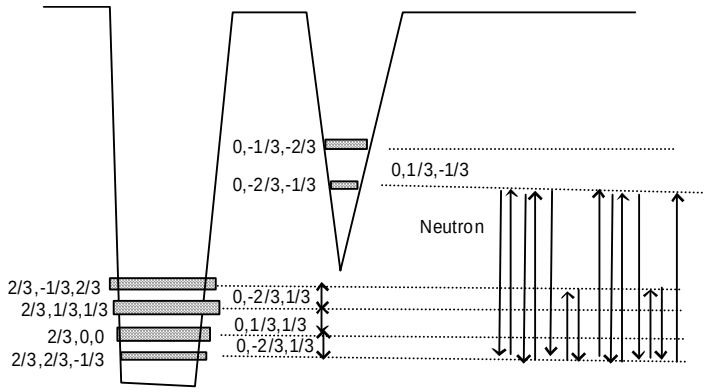


Figure 13. Neutron coherence

Where p=(2/3,2/3,-1/3),p*=(2/3,-1/3,2/3),e=(0,-2/3,-1/3),e*=(0,-1/3,-2/3). Transmutation note (Electron-Proton Transition) contains angular momentum, that is, they correspond to a spinning rotation around the axis perpendicular to R and one of the 3D axes.

Using that dephasing angle, all the stable isotopes lined up in a meaningful pattern scanning the first quadrant (0-p/4) or virtual velocities smaller than the speed of light. Nuclide information from http://ie.lbl.gov/toi/. The dephasing is giving by 180*(Z+N*Θ – round( Z+N*Θ)) where Θ=0.24290 or 43.72 degrees.

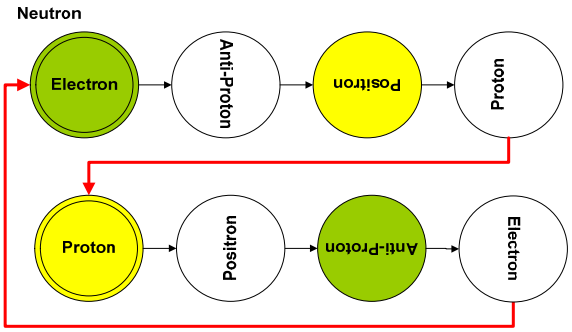


Figure 14. Neutron diagram

The extra energy or mass associated with the neutron is due to the dephasing created by the Electron-Proton Transition and vice-versa. The total angle is balanced between the two 3D footprints (electron and proton masses) to be 42.77/-0.07294 degrees, thus resulting in a dephasing angle by Electron-Proton Transmutation of around 21.4 degrees.

Thus the available kinetic energy after neutron decay is the difference in twisting between these two coherences. Since one is considering a Neutron (or any other particle) in its own reference frame, to total 3D Stress has to add up to zero. This is similar to consider the momentum conservation after the dissociation. This also means that Nuclear Energy is stored in local Fabric of Space deformations.

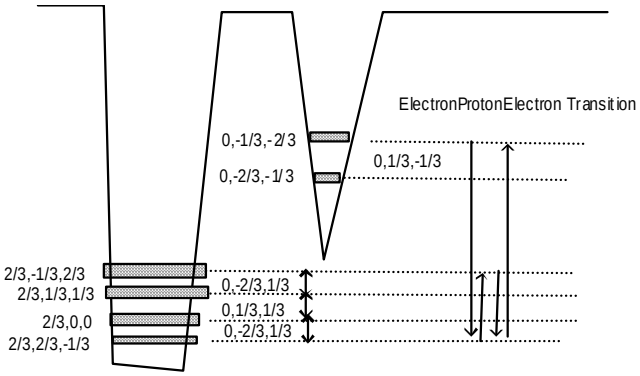


Figure 15. Electron-Proton-Proton-Electron transmutation note

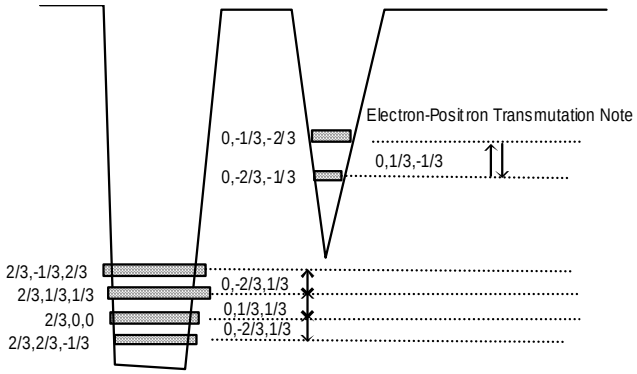


Figure 16. Electron-positron transmutation note.

# Pions – Plus, Minus and Zero

Pion Minus Model

| Particle | Symbol | Rest Mass (Mev/$c^2$) | Decay Reaction | Spin |
|---|---|---|---|---|
| PionMinus | $\pi^-$ | 139.57018 | $e^- + \nu_e$ | 1/2 |

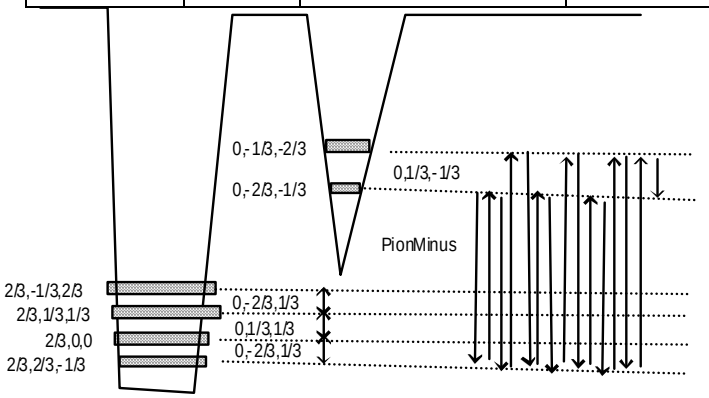


Figure 17. Pion Minus Coherence.

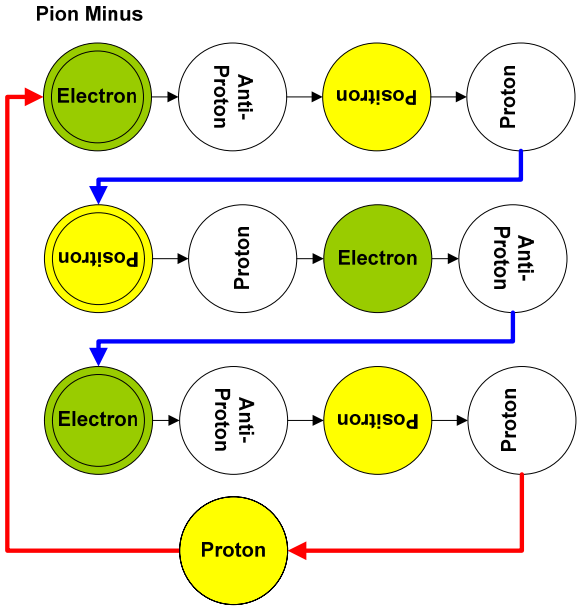


Figure 18. Pion Minus diagram.

Pion Plus Model

| Particle | Symbol | Rest Mass (Mev/$c^2$) | Decay Reaction | Spin |
|---|---|---|---|---|
| PionPlus | $\pi^+$ | 139.57018 | $e^+ - \nu_e$ | 1/2 |

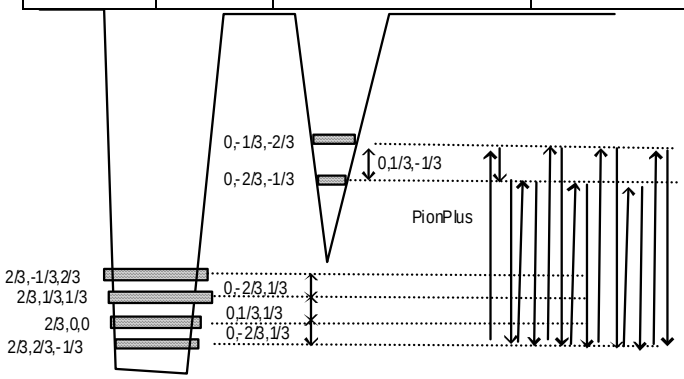


Figure 19. Pion Plus Coherence.

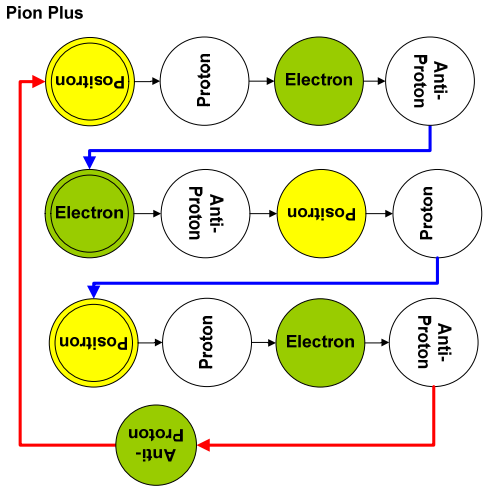


Figure 20. Pion Plus diagram.

Pion Zero

| Particle | Symbol | Rest Mass (Mev/$c^2$) | Decay Reaction | Spin |
|---|---|---|---|---|
| PionZero | $\pi^0$ | 134.9766 | $e^+ + e^- + hw$ | 1/2 |

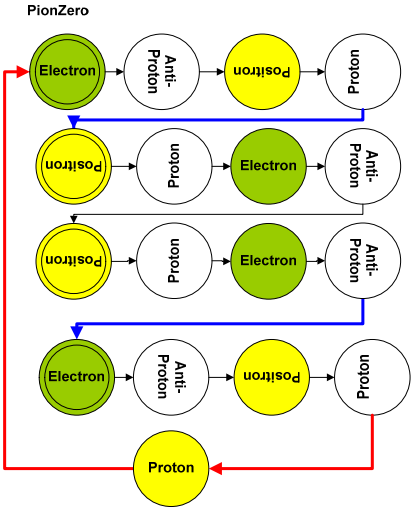


Figure 21. Pion Zero diagram.

DeltaZero= $\pi^0$ + n = $\pi^-$ + p

| Particle | Symbol | Rest Mass (Mev/$c^2$) | Decay Reaction | Spin |
|---|---|---|---|---|
| DeltaZero | $\Delta^0$ | 1232 | $\pi^0$ + **n** | 3/2 |
| DeltaZero | $\Delta^0$ | 1232 | $\pi^-$ + **p** | 3/2 |
| LambdaZero | $\Lambda^0$ | 1115.7 | $\pi^-$ + **p** | 1/2 |
| LambdaZero | $\Lambda^0$ | 1115.7 | $\pi^o$ + **n** | 1/2 |

Delta Zero and Lambda Zero particles differ only by the spin assignments on their sub-coherences and have the same diagram, thus I will only show the Delta Zero.

Decay Pathway: $\Delta^0 \rightarrow \pi^0$ + n and $\Delta^0 \rightarrow \pi^-$ + p

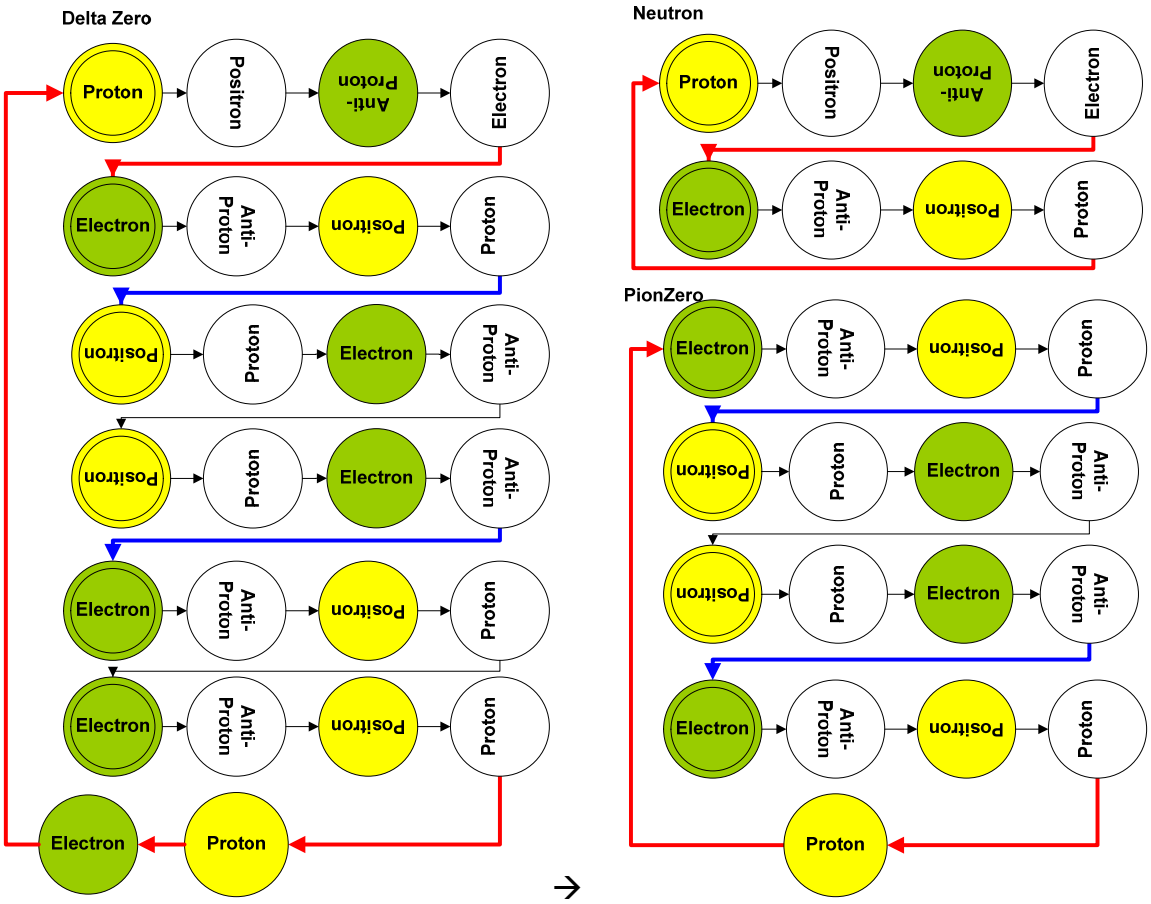


Figure 22. Delta Zero decay diagram.

If one considers that this decay channel has two counter-spinning Electron-Proton transmutation notes (spin ¼ and – ¼).

The next diagram is clarifies prior claims that a Neutron is equivalent to a dimer. The double Proton-Electron transitions were performed first for sake of simplicity. The Pion Minus excited state is pentameric. Since the initial phase of the coherence cannot be determined, the state is equivalent to five shifted states with a 0.2 occupation number each. Scattering experiments would indicate the existence of five "quarks". The relaxed Pion Minus state would insinuate the existence of three "quarks".

Under this paradigm it becomes clear how scattering experiments could be misinterpreted to yield support to the concept of quarks. The impossibility to separate the shifted states can be easily misunderstood as supporting a gluonic field and the concept that quarks are inseparable.

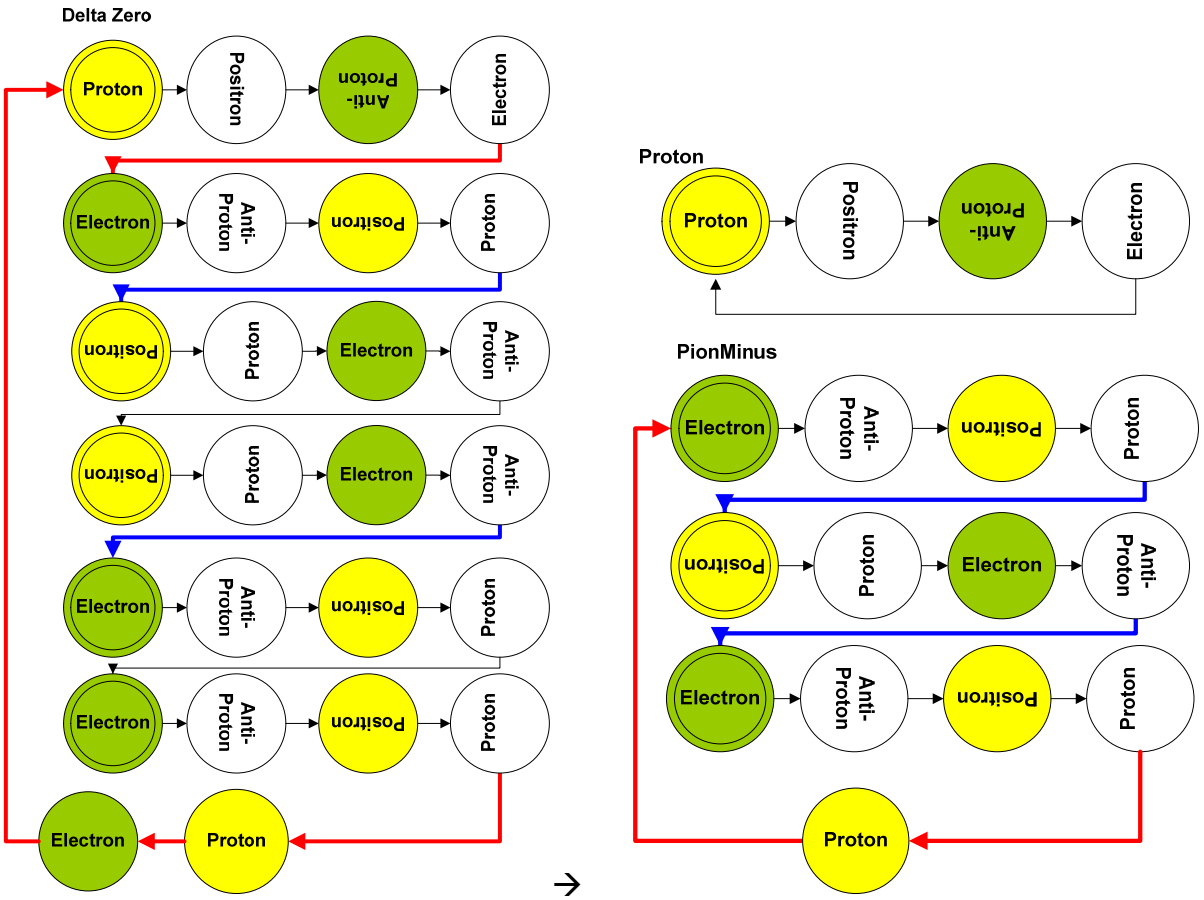


Figure 23. Delta Zero decay diagram.

It is also evident that helicity is a natural result of the model. The sequence of dimensional chords is such that as the pentamer or trimer or dimer travels along time or R, it pseudo-rotates.

In relation with Majorama conjectures, Neutrinos and AntiNeutrinos are the same particles and their effect depends upon which state they are interacting with (electron or positron). Worth noticing also is that the Pion Zero is its own anti-particle (anti-Pion Zero) or a Majorama particle.

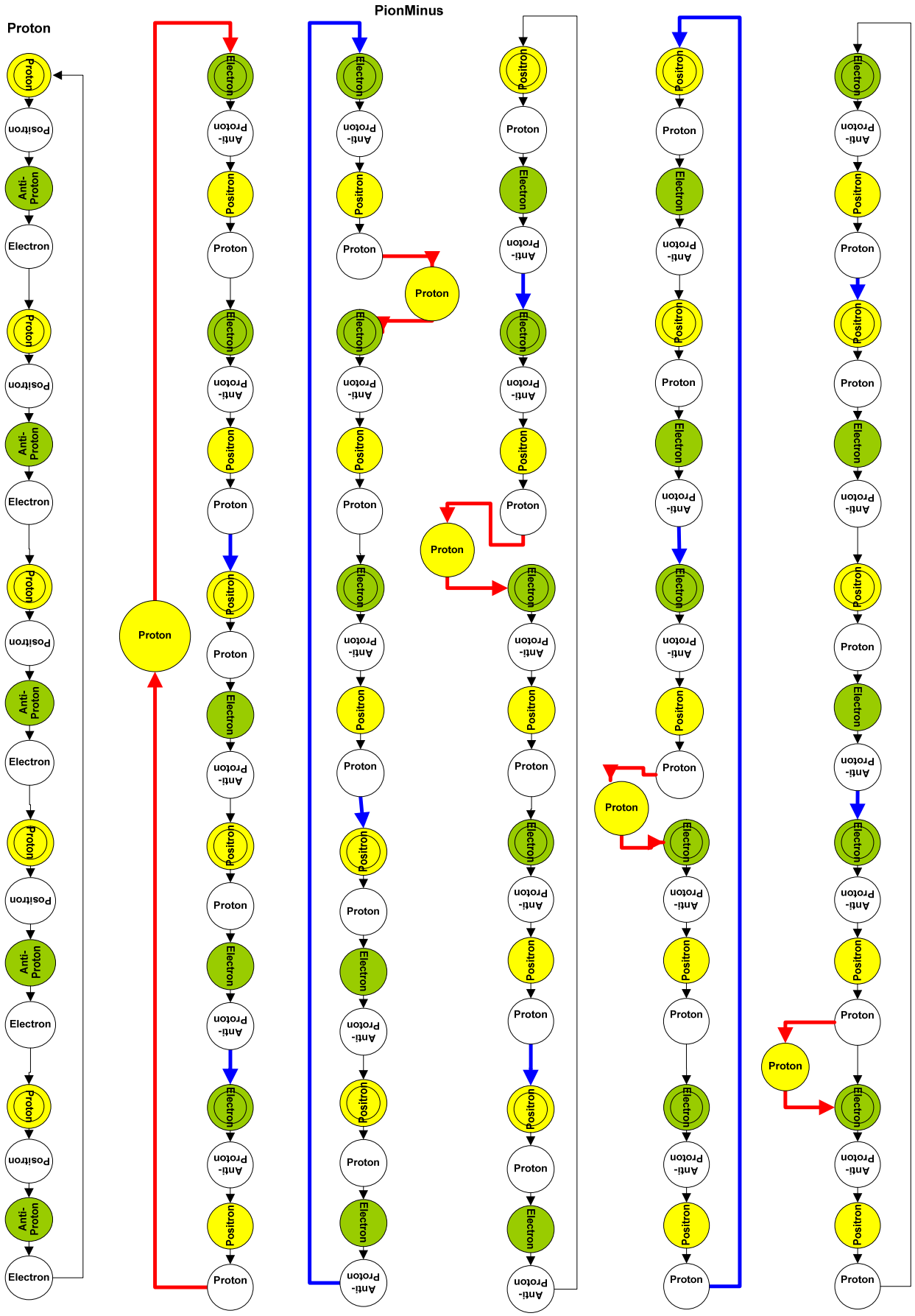
Proton
PionMinus
Proton
Positron
Anti-Proton
Electron
Anti-Proton
Positron
Proton
Electron
Anti-Proton
Positron
Proton
Electron
Anti-Proton
Positron

Trimeric Prion Minus Plus Proton

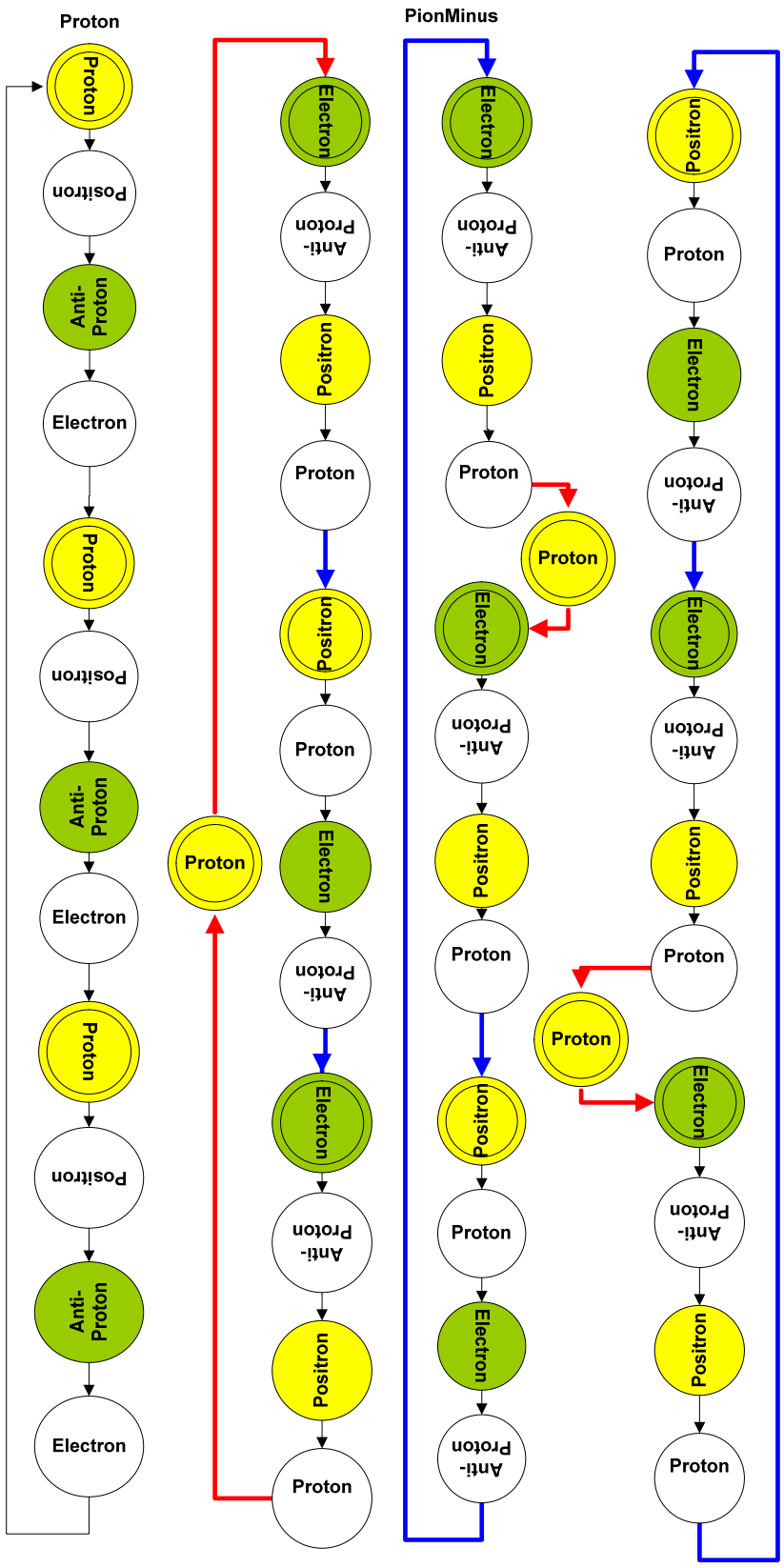


Figure 25. Delta Zero decay diagram with trimeric pion minus.

The trimeric character of pion minus is due to the uncertainty on which phase is in phase with the FS.

Sigma Zero= $\Lambda^0 + \gamma$

| Particle | Symbol | Rest Mass (Mev/$c^2$) | Decay Reaction | Spin |
|---|---|---|---|---|
| SigmaZero | $\Sigma^0$ | 1192.5 | $\Lambda^0 + \gamma$ | 1/2 |

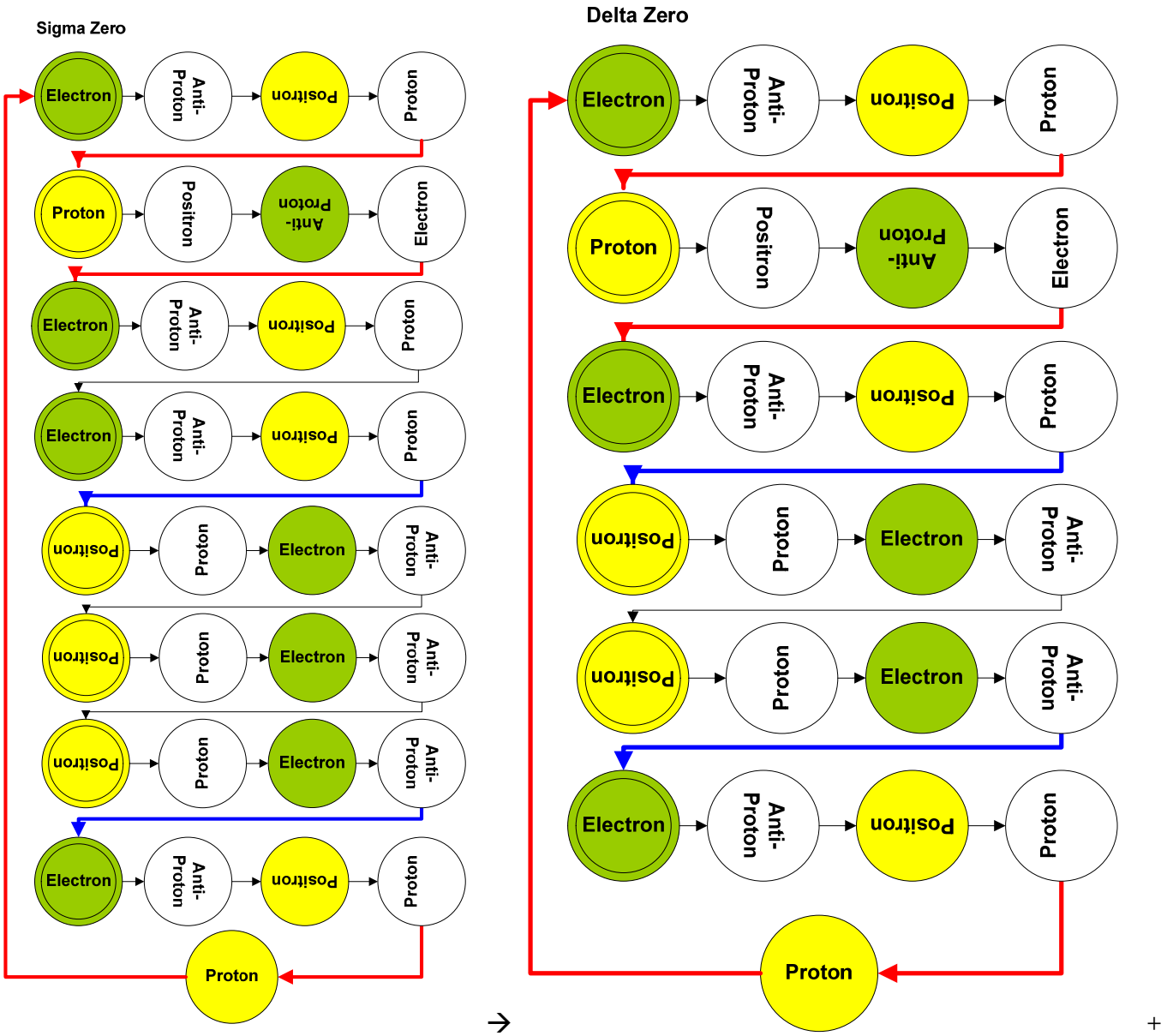


Figure 26. Sigma Zero decay diagram.

DeltaPlusPlus

| Particle | Symbol | Rest Mass (Mev/$c^2$) | Decay Reaction | Spin | **Coherence Lifetime** |
|---|---|---|---|---|---|
| DeltaPlusPlus | $\Delta^{++}$ | 1232 | $\pi^+ + p$ | 3/2 | $6\times10^{-24}$ |

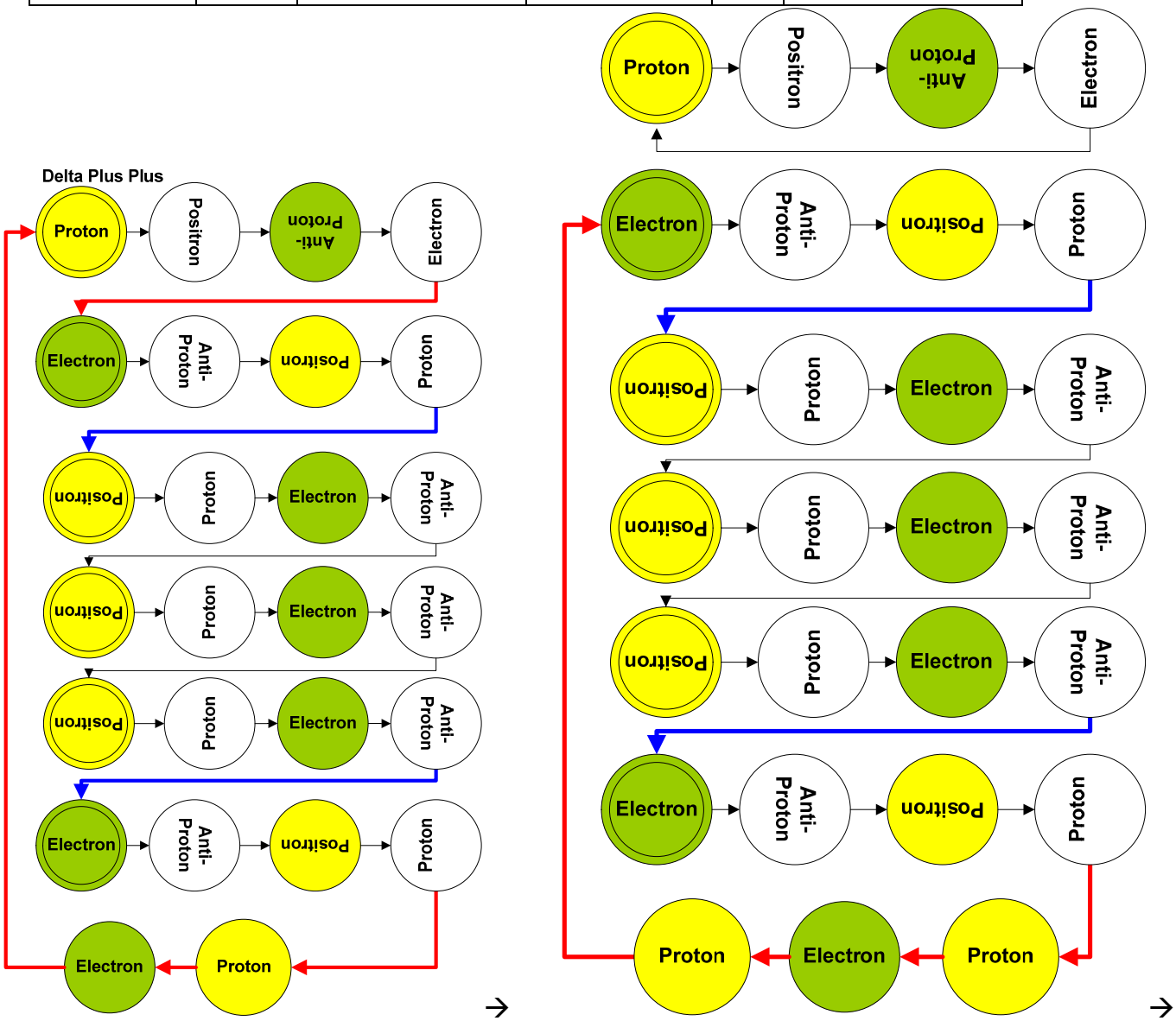


Figure 27. Delta Plus Plus decay diagram.

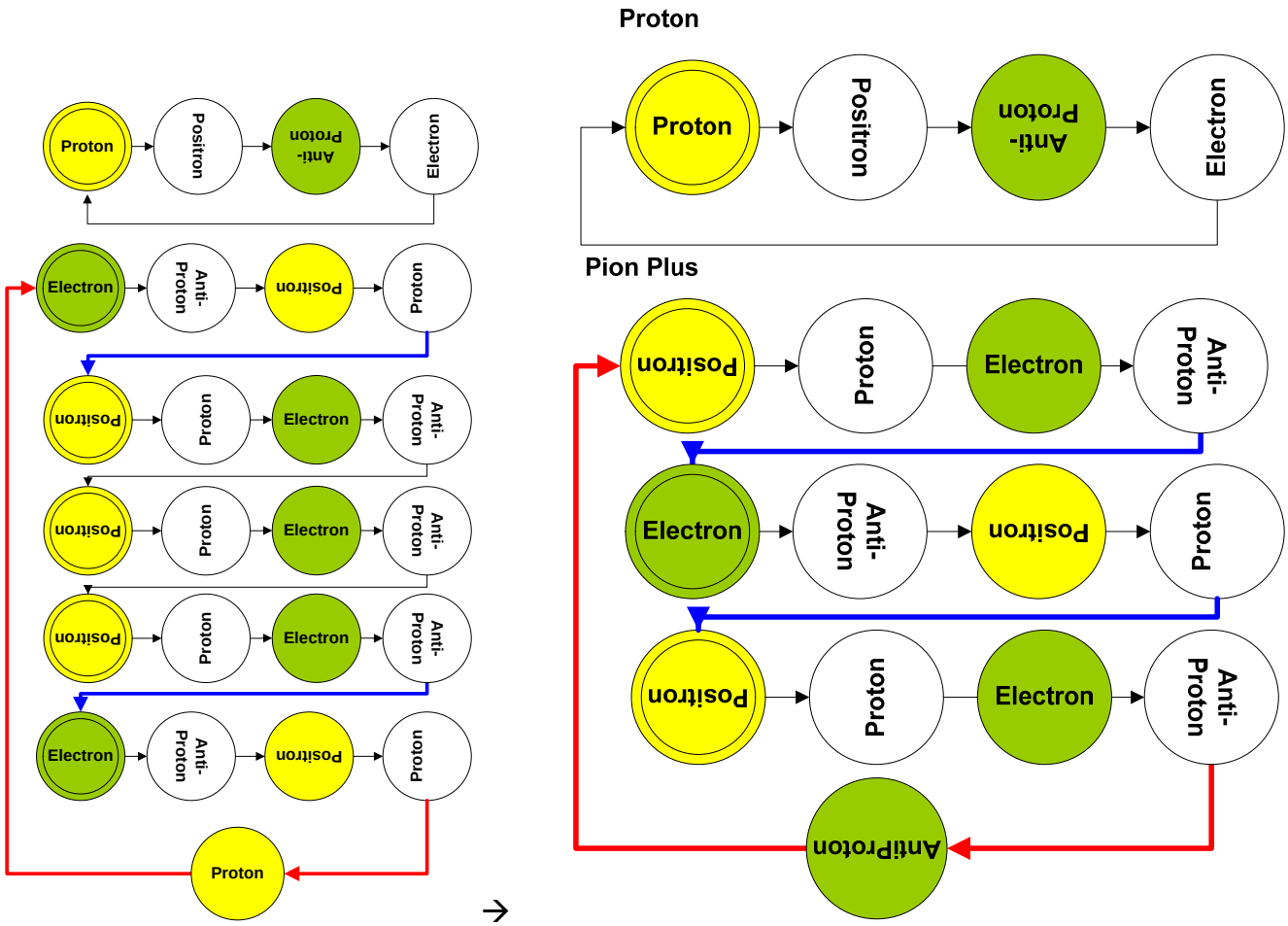


Since

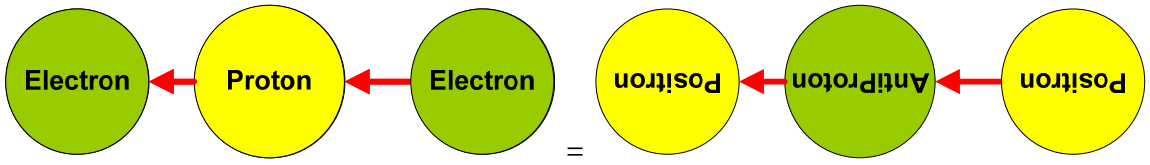


Figure 28. Delta Plus Plus  decay diagram.

Figure 36. Omega Minus diagram.

| Particle | Symbol | Rest Mass (Mev/$c^2$) | Decay Reaction | Spin |
|---|---|---|---|---|
| PionMinus | $\pi^-$ | 139.57018 | $e^- + \nu_e$ | 1/2 |
| PionMinus | $\pi^-$ | 139.57018 | $\mu^- - \nu_\mu$ | 1/2 |
| MuonMinus | $\mu^-$ | 105.7 | $e^- - \nu_e + \nu_\mu$ | 1/2 |

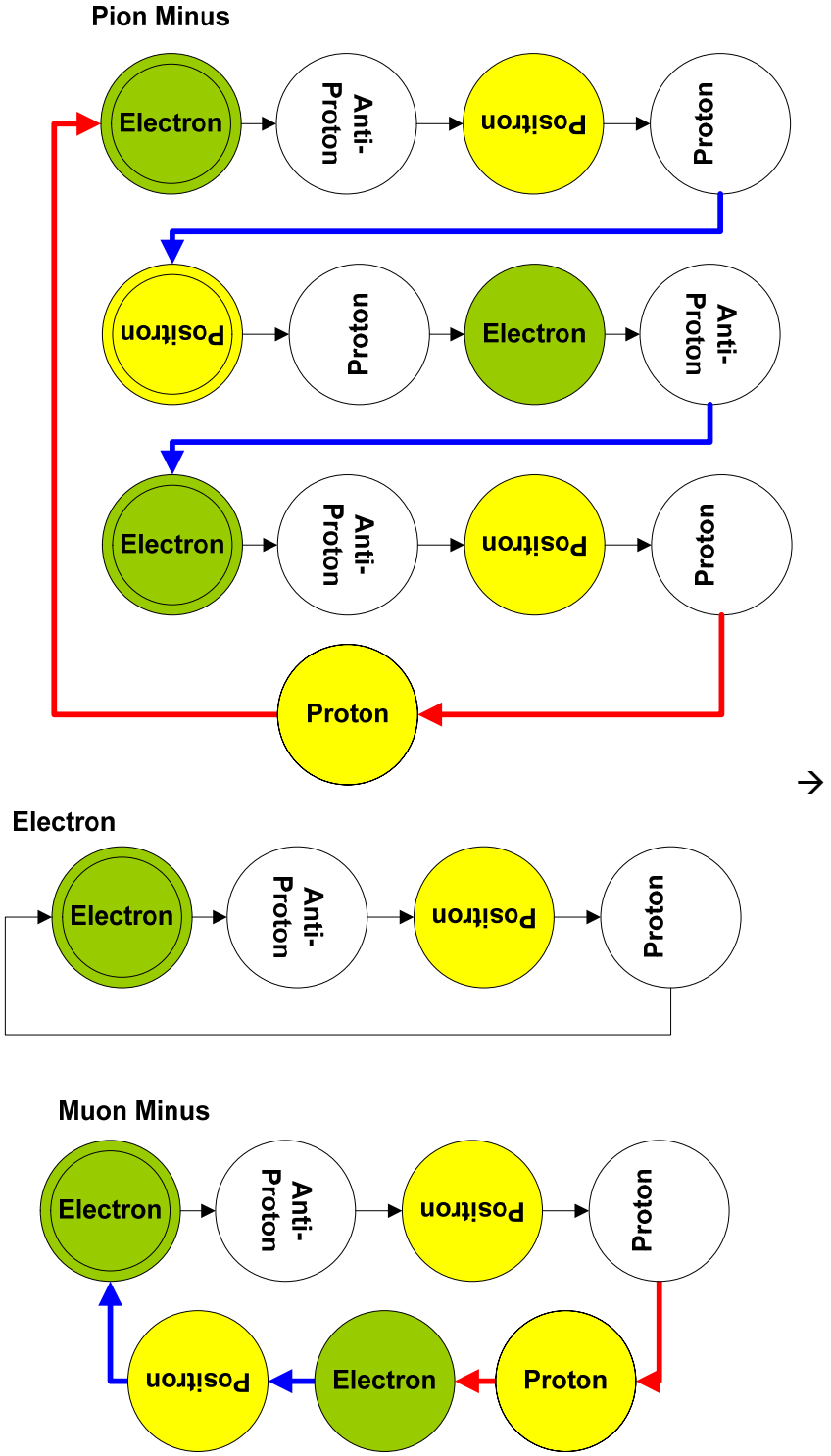


Figure 29. Pion Minus and related decay products diagram. This is not a decay diagram.

| Particle | Symbol | Rest Mass(Mev/$c^2$) | Decay Reaction | Spin |
|---|---|---|---|---|
| KaonMinus | $\kappa^-$ | 493.7 | $\pi^- + \pi^0$ | 1/2 |
| KaonMinus | $\kappa^-$ | 493.7 | $\mu^- + \nu_e - \nu_\mu = e^- - \nu_e + \nu_e + \nu_\mu - \nu_\mu$ | 1/2 |
| MuonMinus | $\mu^-$ | 105.7 | $e^- - \nu_e + \nu_\mu$ | 1/2 |

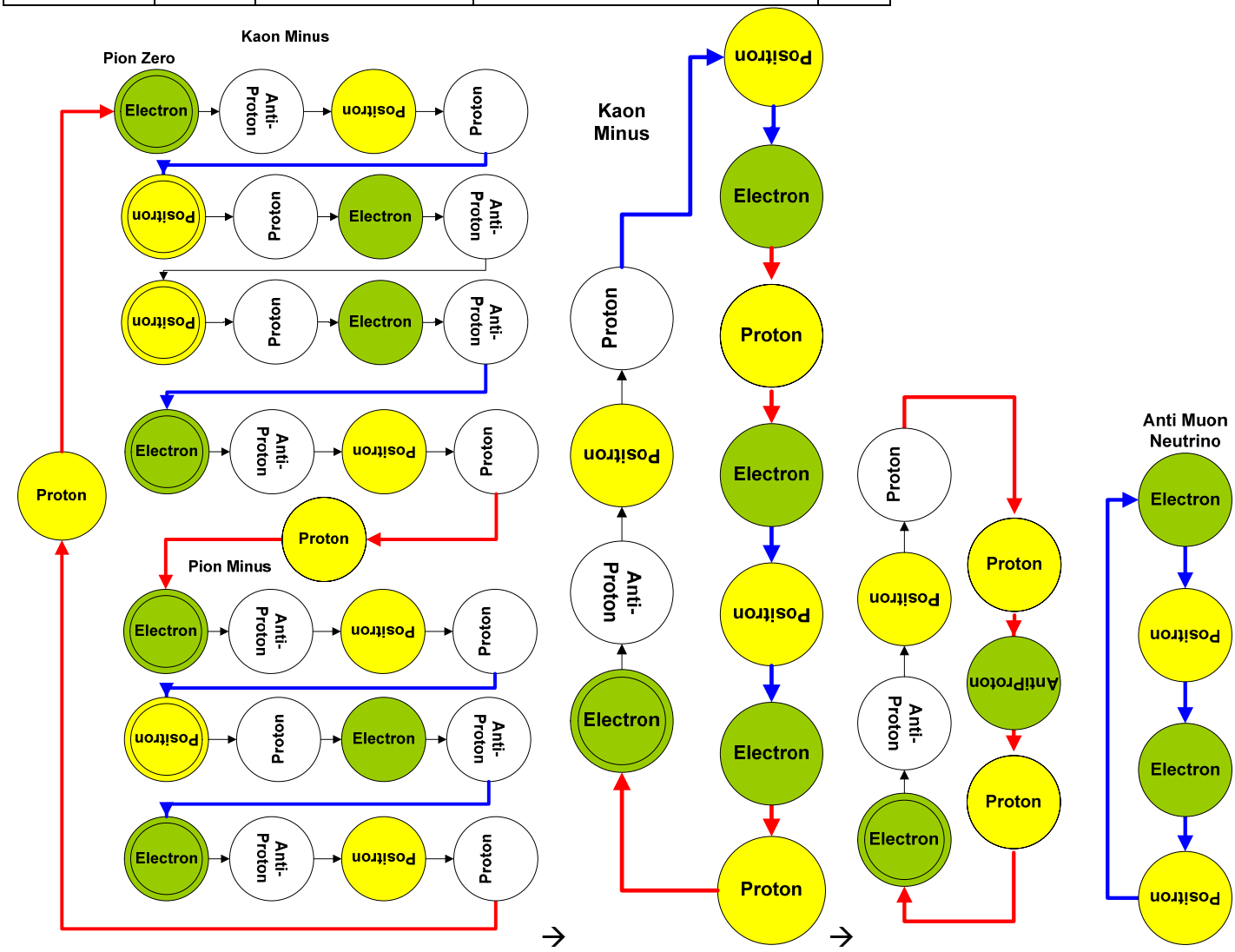


Figure 30. Kaon Minus decay diagram.

| Particle | Symbol | Rest Mass(Mev/$c^2$) | Decay Reaction | Spin |
|---|---|---|---|---|
| KaonPlus | $\kappa^+$ | 493.7 | $\pi^+ + \pi^0$ | 1/2 |
| KaonPlus | $\kappa^+$ | 493.7 | $\mu^+ - \nu_e + \nu_\mu = e^+ + \nu_e - \nu_\mu - \nu_e + \nu_\mu$ | 1/2 |
| MuonPlus | $\mu^+$ | 105.7 | $e^+ + \nu_e - \nu_\mu$ | 1/2 |

| Particle | Symbol | Rest Mass(Mev/$c^2$) | Decay Reaction | Spin |
|---|---|---|---|---|
| NeutrinoTau | $\nu_\tau$ | 15.5 | $\mu^+ + \nu_\mu = e^+ + \nu_e - \nu_\mu + \nu_\mu$ | 1/2 |

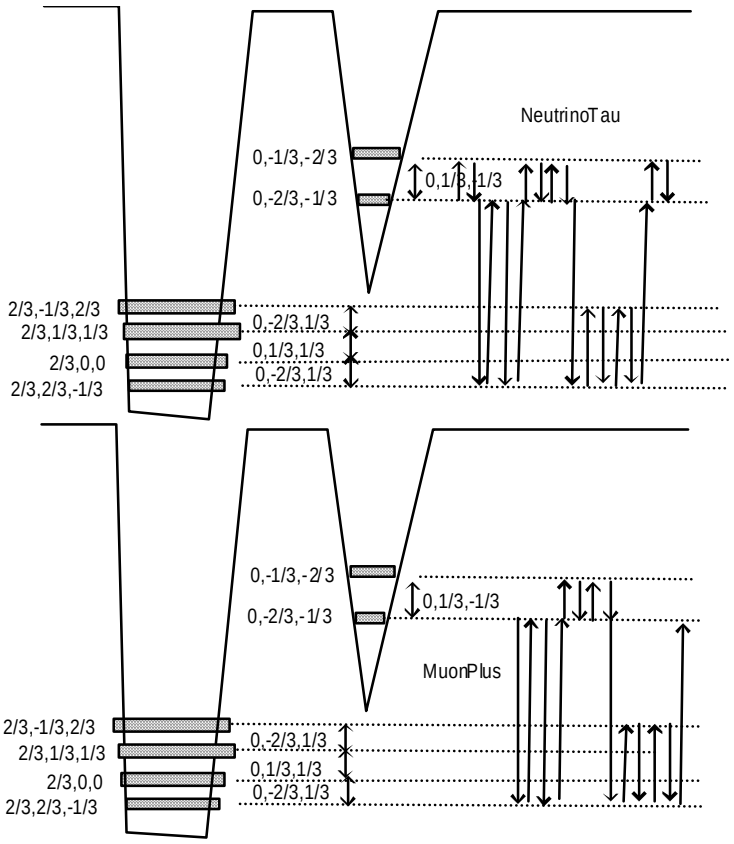


Figure 31. Neutrino Tau and Muon Plus coherence diagrams.

A complete description of all Hyperons and isotopes is available from the blog site.

# 5. Coherent Nuclear Fusion

Let's not be greed at this first analysis. Let's study the following reaction:

D + D → T (1.01 MeV) + p (3.02 MeV)

Where D stands for deuterium and T for Tritium, p for proton. This reaction has 50% yield under normal fusion conditions.

The advantage of having all charged particle as products is that one can use magneto-hydrodynamics energy extraction. If one can make the products to follow specific directions (directional nuclear fusion), one can use coils to extract energy by induction.

Below is the Hypergeometrical Standard Model representation of Deuterium.

Out of a proton and one neutron on can create only one coherence:

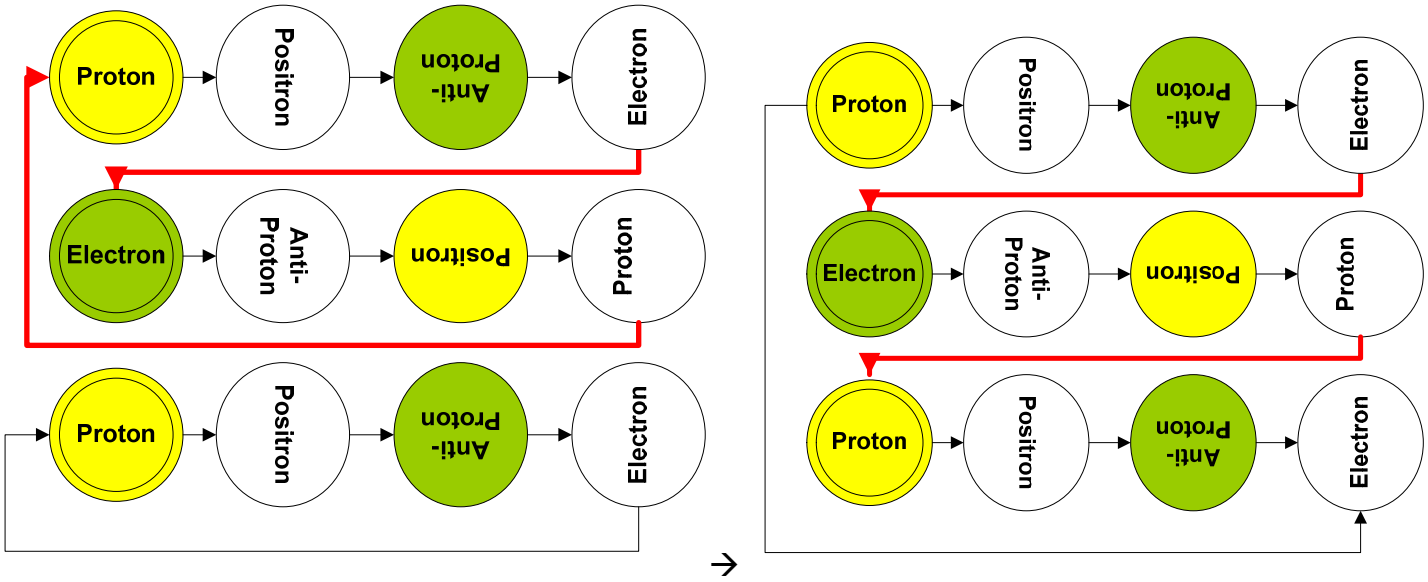


Figure 32. Deuterium diagram.

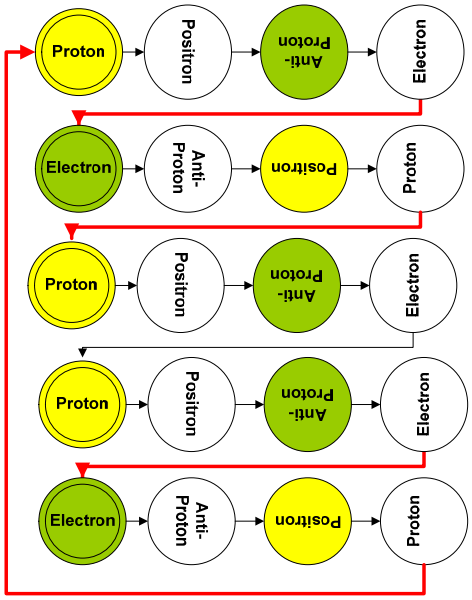


Figure 33. Double Deuterium diagram.

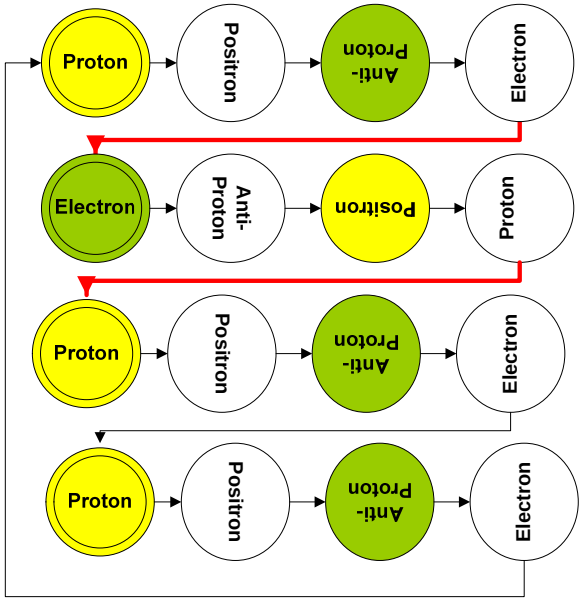


Figure 49. Helium 3 diagram.

$^{3}$He has the following configuration:

The other product channel is given by:

$$D + D \rightarrow {}^{3}He \ (0.82\ MeV) + n \ (2.45\ MeV)$$

Now we can write the equations:

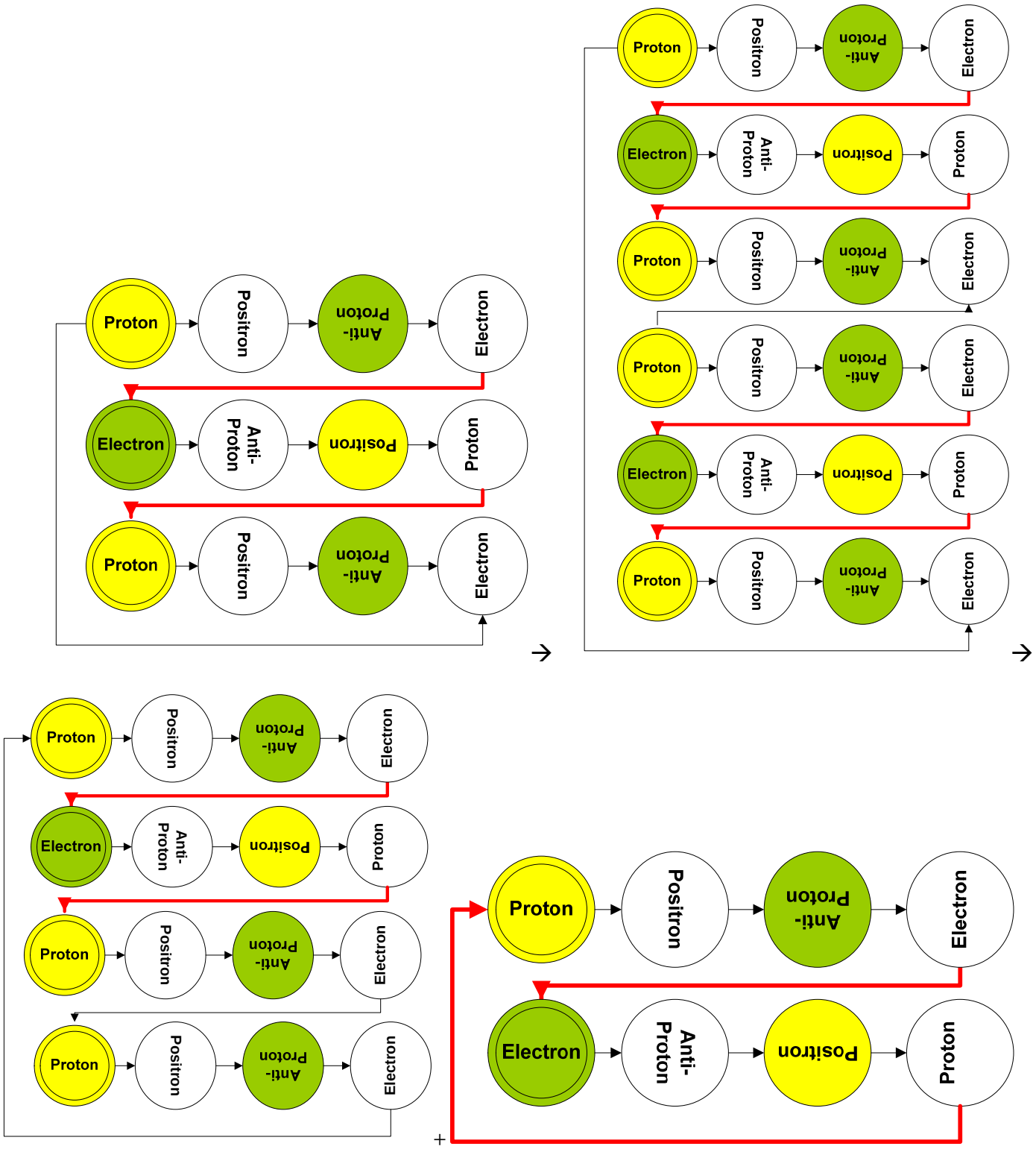


Figure 34. Nuclear Fusion diagram.

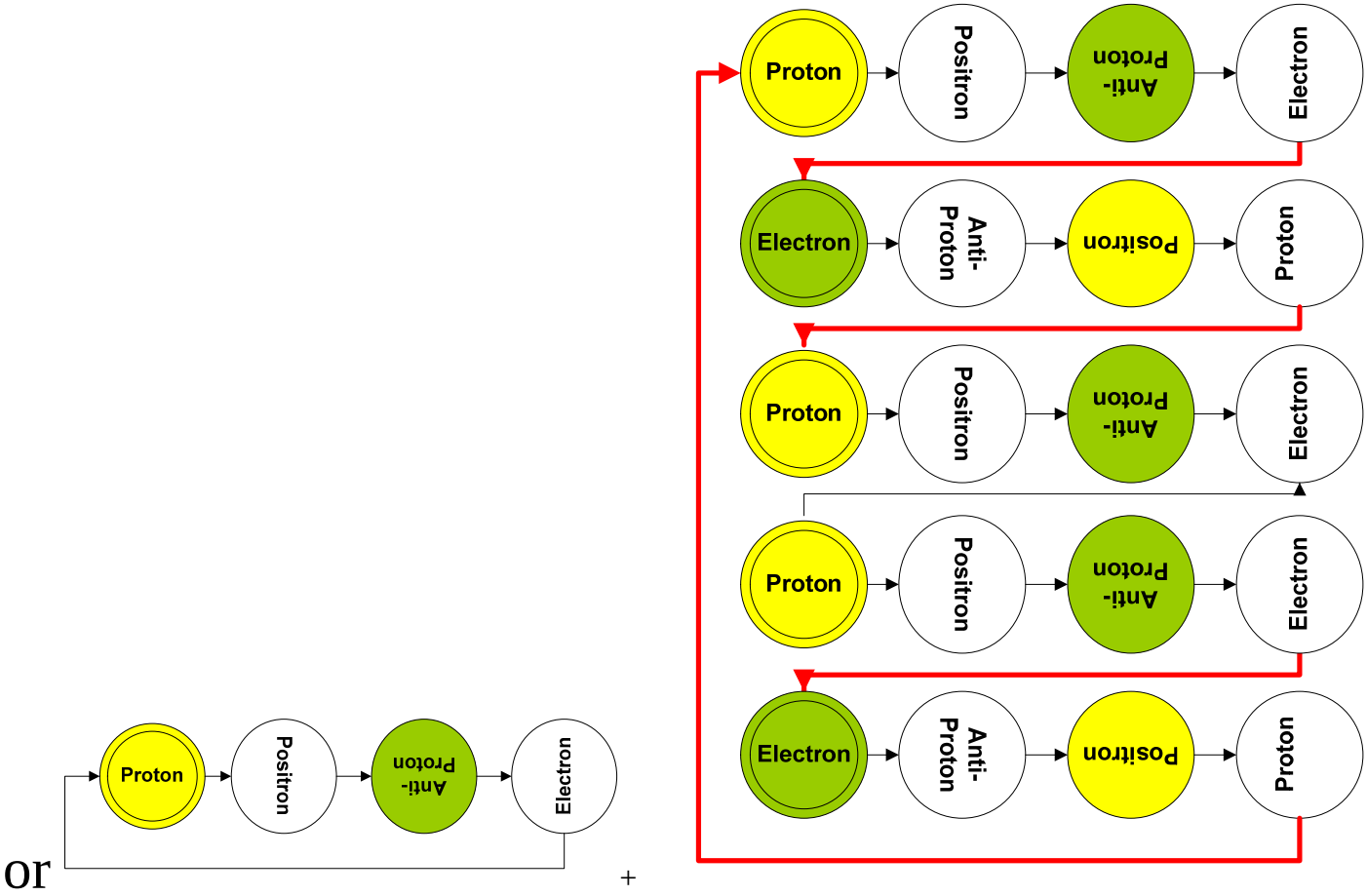


Figure 35. Nuclear Fusion products diagram.

Which settles the correct configuration for tritium.

The Hypergeometrical Standard Model uses the transmutation notes Electron-Proton and Proton-Electron to explain the internal Fabric of Space strain associated with each isotope.

We propose the usage of phase matching to increase the quantum yield of the reaction by realizing that a product direction in an angle with respect to R (the radial expansion direction) corresponds to a local velocity.

**Another extremely important consideration is that the reactant beams should be polarized.. The electromagnetic analogy is that one cannot perform nonlinear optics with scrambled polarization electromagnetic fields.**

This means that there is an specific angle (velocity) for which this reaction yield increases significantly. This also means that a careful prepared experiment should be performed where two deuterium beams intersect each other at an specific angle and at varying velocities while products yield are measured along their phase matching (defined by momentum conservation) conditions.

The calculation depends upon the evaluation of the deformation susceptibility of the Fabric of Space, using all known isotope masses and lifetimes. Precise calculation of the appropriate angle (relative velocity) will be presented elsewhere.

Careful process optimization should create the same gains one have in nonlinear optics.

A coherent fusion process would result in the same revolution one had with the invention of nonlinear optics or lasers. The only difference is that in this case it would be the birth of Nonlinear Hadronics.

# 6. Conclusions:

The hypergeometrical theory, a model that considers the interference of four-dimensional wave on the hypersurface of a hyperspherical expanding universe was introduced.

The complexity of the present description of the universe in our sciences[4-6] is assigned to the fact that one is dealing with four-dimensional projections of a five dimensional process. Our inability to realize that made the description unnecessarily complex.

These are the ingredients for a new and simple formulation of Physics:

- A new quantum Lagrangian principle (QLP) was proposed.
- Quantum gravity, electrostatics and electromagnetism were derived using the same equations (QLP), same framework. The theory is inherently quantum mechanical.
- The quantum version of this theory is readily achieved just by eliminating the high mass or short wavelength approximation on equation (3.9). It is outside the scope of this paper to implement hypergeometrical universe quantum algorithms. In a fully geometric theory, there are no energy or mass quanta. Motion is quantized by the QLP. All the other quantizations can be recovered from that.
- Two fundamental parameters of the universe were calculated from the first principles (permittivity and magnetic susceptibility of vacuum).
- Biot-Savart law was derived from the first principles.
- Grand unification supersymmetry conditions for the time when all forces were equal were derived from simple geometrical considerations.
- The fabric of space can be considered to be the regions of the hypersphere where the normal to its local space is pointing in the radial direction. Any region where that happens has a distinct and yet undistinguishable character. It is distinct because it is pointing in the direction of the universe expansion, but it is indistinguishable within the four-dimensional (relativistic) perspective. All reference frames are equivalent within a four-dimensional perspective. They become distinct but not distinguishable under a five-dimensional analysis.
- The natural frequency of spacetime oscillations is derived to be 32.14 KHz.
- Mach's non-local gravitational interaction explanation for inertia is replaced by a hypergeometrical local fabric of space distortion argument.
- Mach's and Newton's absolute times are assignable to the cosmological time. That time is absolute but can only be measured by observing the expansion of the four-dimensional hyperspherical universe.
- 3D masses were defined in terms of Fabric of Space overlap of a 4D displacement volume at specific phases of the hypergeometrical universe expansion. 4D masses account for all 4D displacement volume created within a de Broglie expansion cycle
- Pseudo time-quantization was proposed.
- A fundamental dilator corresponding to both the proton and the electron was proposed. Particles were modeled as coherences between two 4D deformation states of a rotating 4D double potential well.
- Dilatons from the fundamental dilator were proposed to be light speed traveling metric modulations generated as the dilator tunnels from one state to the other, thus changing character from electron to proton and vice-versa. Anti-matter was proposed to be the same dilator just with a negative phase.

- Since all non-exotic matter (elements, electrons, neutrons, protons, anti-elements, anti-electrons, anti-neutrons and anti-protons) were proposed to be composed of the same dilator, a cosmological coherence is derived.
- Exotic matter (hyperons) is proposed to be the more complex coherences shown in Section 4. Nuclear energy is proposed to be stored in deformations of the fabric of space resulting from mismatch of tunneling and tumbling processes within a complex coherence period. The mismatching would result in a tilted state at the de Broglie phases of the Cosmological Coherence. It is proposed that interaction of these particles with the Universe through the QLP, requires that the beginning and final states to be flat on the 3D hypersurface and that any distortion to be distributed among sub-coherences. The amount of tilting on the individual sub-coherences is recovered at the moment of decay.
- Higher degrees of internal tilting can be achieved by non-fundamental sub-coherences. The higher the degree of internal tilting the lower the element or isotope lifetime.
- The only "force" is due to dilaton-dilator interactions subject to the quantum Lagrangian principle. There is no need for intermediating virtual particles to convey different forces.
- Particle decay, as opposed to collisional reactions, can be explained by nonlinear optics methods or standard barrier tunneling methods – quantum chemistry methodology. Of course, to create quantum chemistry methodology one has to have the Schrodinger equation for the 4D deformation rotating double well potential. This is outside the scope of this paper.
- There is a dilaton bath from which one can envision virtual dilators popping into existence, but it is not clear they are needed at all. Current science does not have the dilaton field, thus under those condition, virtual particles are need to explain nuclear chemistry. Notice that a dilator field is a matter field, that is, it is a function of the proximity of matter and not a property of empty space. It decays as one goes away from matter and thus it doesn't blow up as vacuum zero point fluctuations would. This is at the heart of the challenge to the action-at-distance paradox. The photon decay could be due to dephasing of the electronic coherence due to interaction with the dilaton black body field from the **detectors themselves**. Since the radiation arriving from the detector on the emitting molecule is polarized (by the polarizers), the outgoing photon will know its polarization at the moment of emission and not at the moment of interaction with the polarizers. **This would eliminate the need of infinite velocity and thus eliminates the action-at-distance paradox**.
- The black body radiation due to dilators thermal fluctuations is not polarized and normally average to nothing. Thermal fluctuations are uncorrelated and isotropic. Any coherent motion will have a corresponding dilaton coherence along their 4D trajectory and a de Broglie projection in the 3D universe. This 3D de Broglie projection is real, that is, it is independent upon a single electron and at the same time it is dependent upon each and every electron in the coherent flow. The double slit experiment is done with a monochromatic flow of electrons passing through two slits. Due to the QLP, electrons will travel or surf the 4D dilaton field. That will have a 3D projection, which means that the electron will also surf the 3D projection of this dilaton field. We propose that the electron does not pass the two slits at the same time. It surfs a de Broglie dilaton projection that will create an interferometric pattern after the slits. Since the electron follows the dilaton field before and after the slits, it will follow the interferometric pattern and deposit accordingly. **Thus the electron in the double slit experiment does not need to pass through both slits at the same time**.
- Dilatons and standard collisional excitation should suffice in this theory. In the same way that electronic transitions can be created by collisions, dilator collisions can create 4D deformation transitions. These transitions, if accompanied with the creation of new coherences will interact with the existing universe otherwise they would just disappear. The appropriate description of the 4D deformational rotating double potential well and the dilator rotational dynamics will be described elsewhere.

- A refinement on the fundamental dilator model is to consider it a four-dimensional ellipsoid of revolution with a FS intersection of the 4D volume proportional to the particle mass and three axes' length quantum numbers equal to the corresponding quark composition. This is a zero 4D Volume sum rule for all the particles in the universe. Matter is energy and energy cannot be destroyed. 4D displacement volumes can! They have signs and any cosmogenesis theory basic on them will be able to **reduce the whole universe to a fluctuation of zero**. A simple hypergeometrical universe cosmogenesis theory will be presented in a companion paper
- Since quarks are modeled as quantum numbers (axis lengths) of a volume, they cannot be separated in the same way one cannot separate the X dimension from a three-dimensional object. Structured scattering, which has been used as an indication of the existence of quarks, can be easily understood as an indication of the existence of a form or shape, that is, particles are not spheres. Other dimensions of the standard model are modeled as rotations. Spin is modeled as a rotation perpendicular to radial direction and one spatial coordinate (x, y or z). Three/two additional dimensions are captured as rotational degrees of freedom for rotation along the three/two spatial axes.
- Planck's constant has a new meaning within this theory. It is the proportionality constant that ensures that the de Broglie wavelength, relating the observed 3D mass and 3D velocities, matches the 3D projection of the 4D dilaton. Notice that the 4D dilaton wavelength (frequency) depends only upon the gap between the two states of the fundamental dilator. This mapping is done through the linear momentum equation $h=m.v.\lambda$.

## Cosmological Conclusions:

The hyperspherical expanding universe has profound cosmological implications:

- The expanding hypersphere clearly shows in geometrical terms that any position (cosmological angle) in the hypersurface (3-D universe) has a Hubble receding velocity.
- The HubbleVel, the Hubble cosmological expansion velocity at a cosmological angle $\theta$ (see Figure 1) is given by
    - $HubbleVel = c\theta$
    - This means that the three-dimensional space is expanding at the Hubble cosmological expansion velocity (speed of light per radian) as the hypersphere moves outwards along the radial time direction.
    - The corresponding elicited motions to all interactions in the universe are just side-drifts from a light-speed travel along the radial time direction. This explains why the speed of light is the limiting speed in our Universe. **It is the maximum velocity a transversal wave can travel. The transversal wave is a de Broglie wave (projection of the 4D dilator generated wave) traveling along the 3D hypersurface. Under those conditions, the dilators would be traveling on the interference pattern of two perpendicular lightspeed wave fronts and would travel along the line making 45 degrees angle with the radial direction.**

## Conclusions about Time

- This model contains one absolute time, the Cosmological Time and time projections for each inertial frame of reference.
- Although absolute, one cannot measure time using the Cosmological Time, unless one observes directly the Hyperspherical Expansion of The Universe.
- Our universe corresponds to the $X\tau$ cross-section shown in figure 1. There one can only measure the relative angle between $\tau$ and $\tau$', and thus only the relative passage of time.

Hence time can be both **Absolute** and **Relative** and both Einstein and Newton were right.

## The Passage of Time

The passage of time has been analyzed through Lorentz transformations in Relativity. Experiments using atomic clocks have been performed to show that time follows Lorentz transforms. In the Hypergeometrical Theory we showed that a single dilaton dilator interaction accounts for both Gravitation and Electromagnetism. At each de Broglie step in the hyperspherical expansion, dilator change their k-vectors by some angle α. For an observer traveling at a different speed with respect to the Fabric of Space (angle $\alpha_1$) that angle α' would be calculated as:

$$\tan(\alpha') = \frac{\tan(\alpha') + \tan(\alpha_1)}{1 + \tan(\alpha').\tan(\alpha_1)}$$

as $\alpha_1$ approaches 45 degrees (speed of light), the absolute incremental angle change decreases. When one reaches the speed of light the incremental angle shift per de Broglie step goes to zero. Absolute time continues its flow as usual.

The other velocity (local Fabric of Space deformation angle) dependency is the dilator (hyperon or isotope) coherence lifetime. That lifetime is proportional to the accumulated deformation angle due to the intra-coherence transmutation notes. Since that observation of that angle will also follow the same angle addition equation, the particle lifetimes will also behave according to the expectations from the Lorentz transformation.

Notice that matter dynamics depends upon the rate of angle change as a function of radial expansion, while particle lifetime depends just upon the angle (not is derivative).

This is a fortuitous coincidence for Relativity. The here proposed unification and hypergeometrical standard model shed light into the underlying reasons for the slowing down of time.

Notice that time has nothing to do with the slowing down of matter dynamics and coherence decay.

## Astronomical Conclusions:

- The entire Universe is contained in a very thin three-dimensional hypersurface of a four-dimensional hypersphere of radius c*[Age of The Universe].
- The average radius of curvature of this hypersurface is exactly the speed of light times the age of the Universe, or R=15 billion light-years or so.
- The visible Universe volume is given by: $VisibleUniverseVolume = \frac{4\pi R^3}{3}$.
- Beyond the visible Universe lies the Never-to-be-Seen-Universe, whose linear dimension is actually (2π-2) times the dimensional time radius of the hypersphere. 3π/2R of the Universe linear dimension can never be reached
- Of course, the four-dimensional light speed expanding hypersurface topology also explains why the Big Bang radiation comes from all directions and why one cannot ever locate a simple point where the Big Bang occurred. The Big Bang will always seem to have occurred in any direction if one looks far enough (the dimensional age of the Universe) and that is the result of four-dimensional explosion dynamics.
- The other topology derived conclusion is that if one could "see and measure velocity using Cosmological Time" farther than the dimensional time radius of the Universe, galaxies would be traveling at speeds faster than the speed of light with respect to us. This wouldn't be the case if we measure any velocity using cross-reference time τ. Under those circumstances the maximum velocity is always c.

- The fact that it is impossible to "see" any farther than the dimensional radius of the Universe means that the postulate of Relativity remains semi-solid. If one travels far enough but not as far as the age of dimensional radius of the Universe, one still could travel at absolute speeds faster than the speed of light.
- The highest absolute receding speed of this Universe is $\pi c$, which is the real speed bump in the whole Universe. Absolute receding speeds are measure with respect to the Cosmological Time $\Phi$.
- Since the receding speed of the Big Bang is equal to the speed of light, all its electromagnetic energy is Doppler shifted by the time they arrive at us, thus one cannot ever observe the Big Bang with a telescope. On the other hand, one can probe the initial dynamics by looking as far as one can with a large telescope.
- The Cosmic Microwave Background is likely to be Doppler Shifted Gamma Radiation and not Blackbody Equilibrium Radiation.
- Another corollary of this theory is the Hubble conclusion about an expanding hyperspherical Universe. The speed of light divided by the **average** numerical value for the Hubble constant is the inverse of the Age of the Universe (e.g. 16.4 Billion years, 55 Km/s per megaparsec with one megaparsec = 3 million light years). The averaging is necessary since if one looks at any direction, there will be debris from the Big Bang (Galaxies) of different sizes traveling towards and from your direction.
- The topology offers the revolutionary perception that while we see ourselves at rest we are actually traveling at the speed of light in a direction perpendicular to all the three dimensions we can perceive in our daily life. General Relativity and present Cosmology has no qualms associating a Black Hole with a disturbance of spacetime continuum. Since we could easily fall into a Black Hole, it is not surprising that we should be modeled as a disturbance of the spacetime continuum in a similar manner. Like any disturbance, there is a natural propagation velocity, in our case that velocity is c (the speed of light).
- One can easily see that the Big Bang occurred when the Universe was an infinitesimally small circle across each one of the three dimensions, thus it spanned the whole Universe. It occurred on all places at the same time. This is the basis for the non-locality of the Big Bang in a three-dimensional Universe projection. This means that in our Universe, the Big Bang occurred exactly where we are no matter where we are. The heat, horrendous explosion and debris has long since left this region and now one only can see the beginning of the Universe if one looks very far away to see the debris that traveled the age of the Universe and are only now reaching us. This is a quite surprising and elegant conclusion.
- Due to the topology of a four-dimensional Big Bang, the center of the Universe is a location in the radial direction and not in 3D space.
- Unlike motions along other directions of the four dimensional space, travel along the radial time occurs only at the speed of light.
- The visible Universe corresponds to a hyper-cap in this hypersphere. The hyper-cap radius is also the age of the Universe, which is also the average radius of curvature of the hypersphere. Thus the Universe is not only finite but also curved: a perfect circle.
- Despite of that one cannot travel around it (due to its expansion at the speed of light) and due to the limit imposed on the highest traveling speed in this Universe. Finite, circular but impossible to traverse.
- In addition, the hypersphere model makes any point in the Universe equivalent to another; in the same way that no point on the surface of an expanding balloon is closer to the origin of times (its center or the point in space defined by the balloon when it was very small).
- The fact that we cannot see the past or travel there is because it does not exist any longer, due to the extremely thin character of the hyperspherical Universe. It is only a de Broglie wavelength thick. Needless to say, one cannot either travel to the future because it doesn't exist yet. We can only reach the future when it is the present, since we are traveling there even as we speak.

- Beyond the Big Bang lies more of the same (Universe), albeit invisible Universe. The furthest visible part of the Universe is the Big Bang, that doesn't mean that one could traveling faster than the speed of light go there and see it firsthand. It only means that if we travel at the speed of light in any direction, the cosmic microwave background will Doppler shift into gamma rays (a possible tremendous inconvenience for light speed travelers) and one will be able to actually see the beginning. From Figure 1, it is clear that the hypersphere is uniform and that traveling in any direction wouldn't bring us into the past. The hypersphere travels inexorably into the future.
- It becomes clear that the Hubble expansion theory has to be modified to accommodate a four-dimensional Big Bang. The change is that in a four-dimensional explosion the Big Bang occurred in each and every point of the initial circumference, that is, the Big Bang occurred in each and every point of the Universe at the same time. From each and every point, energy and matter were ejected by tremendous forces. This means, that at any given point of the Universe there is a three dimensional isotropic expansion and thus the average Hubble constant is equal to the inverse of the dimensional age of the Universe times the speed of light. In a three-dimensional Big Bang, matter would expand radially from a single point, thus the Universe would be highly anisotropic and the Hubble constant would be a constant.
- Finally, the relativistic effects and inertia are due to local distortions of the curvature of this hyperspherical surface. The highest distortion one can create is to travel at the speed of light. That corresponds to having one's proper dimensional time vector $\tau$ at 45 degrees with the three-dimensional space. Different regions of the hypersurface have different tangents with respect to an originating point, thus flow of observed time will depend upon how fast and how far you travel. One does have receding velocities that are larger than the speed of light, indicating the Relativity is a local approximation of Universe dynamics.

## Grand Unification Conclusions

- The meaning of physical existence is being phase-matched along the radial direction.
- Quarks are modeled as positive and negative axes' length of the ellipsoid of revolution. A negative axis length means that the four-dimensional wave generated along that axis direction has a negative phase (180 degrees phase shift). The directionality of waves will only play a role when one discusses polarized matter. This is supported by the grand unification equations presented in section 3.
- Section 3 indicates that the conversion of matter to antimatter is done through half muon neutrinos interaction with matter. Cross-section for neutrino splitting might be low, thus explaining why there is an asymmetry in the proportions of matter and antimatter in the Universe.
- The light speed, fast expanding hypersphere model of the Universe allows for the existence of an infinite number of other hyperspherical expanding Universes, separated by dimensional time intervals. The source of "matter and energy" will be explained in the Cosmogenesis paper of this series. Although there is an allowance, it will be described that the Big Bang occurred simultaneously with Dimensional Transitions. This seems to preclude the coexistence of Hyperspherical Universes.
- The fate of the Universe is continuous expansion. It will become clear how the Universe recycles itself and what is the meaning of recycling in the Cosmogenesis paper.

## Solar Neutrino Deficit Conclusion:

The proposed model for neutrinos (Electron Neutrino, Muon Neutrino and Tau Neutrino) indicates an alternative explanation for the Solar Neutrino Puzzle. The missing electron neutrinos could be due to an electron/muon neutrino capture event and not due to neutrino oscillations. Neutrino oscillations defy energy conservation, due to the different neutrino masses.

## Fundamental Conclusion:

A last conclusion worth mentioning is a modification of Newton's first law:

**In the absence of interactions, a body (locally deformed FS region) will drift within the hypersurface (3-D universe) until τ and R are parallel again or conversely until it reaches a point where its drift velocity equals the Hubble velocity of that region of space.**

**This is the Hypergeometrical Universe Newton's First Law.**

Notice that the apparent motion will still exist since the fabric of space is expanding and any place in the 3D universe has a Hubble expansion velocity. Although moving relatively to its original position, the body remains static with respect to the fabric of space ( $\rho$ parallel to R). At that point, the local deformation ceases to exist and the body drifts with the expansion at the Hubble velocity. In other words, motion is a way for 4D space to relax; in the same way a tsunami is the means for the sea to regain a common level.

## Coherent Fusion Conclusion:

The Hypergeometrical Standard Model provide the means to envision a new process of nuclear fusion where yields are much higher. The conceptual basis for the concept of Coherent Hadronics is the direct result of the fundamental dilator and the hyperspherical expansion universe topology. The fundamental dilator model for matter implies that particles are coherences of a malleable Fabric of Space, and thus can be subject to nonlinear processes.

Current approaches to nuclear fusion uses a nuclear chemistry approach, where a barrier has to be overcome for the reaction to occur. The realization that particles could be modeled as coherences, thus similar to electromagnetic waves, allows for a change in paradigm. Instead of overcoming a barrier by extremely high temperatures, we might be able to create the products by fine tuning phase matching conditions in a 4D dynamics space.

The experimental setup for coherent nuclear fusion hadronics would be composed of an accelerator with hadron bunching, and magnetic lensing for controlled focusing. Upon focusing at the phase-matching velocity, maximum nuclear fusion yields would occur and nuclear fusion products would be released at the appropriate directions and velocities.

**REFERENCES**


[1] Pereira, Marco – Hypergeometrical Universe – http://Hypergeometricaluniverse.blogspot.com

[2] The Flying Orchestra – Marco Pereira – To be published

[3] Schwarzschild, Bertram. "**WMAP Spacecraft Maps the Entire Cosmic Microwave Sky With Unprecedented Precision**.", Physics Today. Vol. 56, No. 4 (April 2003): 21.

[4] Pauli W 1958 Theory of Relativity, London: Pergamon Press

[5] Landau L D and Lifshitz E M 1975, The Classical Theory of Fields, Oxford: Pergamon Press.

[6] Classical Electrodynamics – J.D. Jackson (1975-John Wiley & Sons).

[7] Quantization in Astrophysics, Brownian Motion, and Supersymmetry, editors: Florentin Smarandache; V. Christianto, ISBN 819021909X

[8] Pereira, Marco - Hypergeometrical Cosmogenesis, to be published elsewhere.

[9] Hyperon Polarization and Magnetic Moments, Joseph Lach – Fermilab-Conf-93/381

# Interpretation of solution of radial biquaternion Klein-Gordon equation, and comparison with EQPET/TSC model

V. Christianto[1], & F. Smarandache[2]
[1] http://www.sciprint.org, email: admin@sciprint.org
[2] Dept. of Mathematics, Univ. of New Mexico, Gallup, USA,
email: fsmarandache@yahoo.com

In the preceding article we argue that biquaternionic extension of Klein-Gordon equation has numerical solution with sinusoidal form, which differs appreciably from conventional Yukawa potential. In the present article we interpret and compare this result from the viewpoint of EQPET/TSC model described by Takahashi [1]. Further observation is of course recommended in order to refute or verify this proposition.

## Introduction

In the preceding article [2] we argue that biquaternionic extension of radial Klein-Gordon equation (radialBQKGE) has numerical solution with sinusoidal form, which differs appreciably from conventional Yukawa potential. We also argue that this biquaternionic extension of KGE may be useful in particular to explore new effects in the context of low-energy reaction (LENR) [3].

Interestingly, Takahashi [1] has discussed key experimental results in condensed matter nuclear effects in the light of EQPET/TSC. We argue here that the potential model used in his paper (STTBA) may be comparable to our derived sinusoidal potential from radial biquaternion KGE [2]. While we don't offer yet numerical prediction, our qualitative comparison may be interested to verified further in experiments.

## Solution of radial biquaternionic KGE (radial BQKGE)

In our preceding paper [2], we argue that it is possible to write biquaternionic extension of Klein-Gordon equation as follows:

$$\left(\Diamond\overline{\Diamond} + m^2\right)\varphi(x,t) = 0\,, \tag{1}$$

Provided we use this definition [2][3]:

$$\Diamond = \nabla^q + i\nabla^q = \left(-i\frac{\partial}{\partial t} + e_1\frac{\partial}{\partial x} + e_2\frac{\partial}{\partial y} + e_3\frac{\partial}{\partial z}\right) + i\left(-i\frac{\partial}{\partial T} + e_1\frac{\partial}{\partial X} + e_2\frac{\partial}{\partial Y} + e_3\frac{\partial}{\partial Z}\right) \tag{2}$$

Where $e_1$, $e_2$, $e_3$ are *quaternion imaginary units* obeying (with ordinary quaternion symbols: $e_1$=i, $e_2$=j , $e_3$ =k) [3][4]:

$$i^2 = j^2 = k^2 = -1\,,\; ij = -ji = k\,,$$
$$jk = -kj = i\,,\; ki = -ik = j\,. \tag{3}$$

And quaternion *Nabla operator* is defined as [1]:

$$\nabla^q = -i\frac{\partial}{\partial t} + e_1\frac{\partial}{\partial x} + e_2\frac{\partial}{\partial y} + e_3\frac{\partial}{\partial z} \tag{4}$$

By using polar coordinates transformation [5], we get this for the 1-dimensional situation:

$$\left(\frac{\partial}{\partial r}\left(\frac{\partial}{\partial r}\right)-i\frac{\partial}{\partial r}\left(\frac{\partial}{\partial r}\right)+m^2\right)\varphi(x,t)=0\,, \tag{5}$$

The solution is given by [2]:

$$y=k_1.\sin\left(\frac{|m|r}{\sqrt{-i-1}}\right)+k_2.\cos\left(\frac{|m|r}{\sqrt{-i-1}}\right) \tag{6}$$

Therefore, we may conclude that numerical solution of radial biquaternionic extension of Klein-Gordon equation yields different potential compared to the well-known Yukawa potential [2]:

$$u(r)=-\frac{g^2}{r}e^{-mr} \tag{7}$$

In the next section we will discuss an interpretation of this new potential (6) compared to the findings discussed by Takahashi [1] from condensed matter nuclear experiments.

**Comparison with Takahashi's EQPET/TSC/STTBA model**

Takahashi reported some findings from condensed matter nuclear experiments, including intense production of helium-4 ($^4$He) atoms by electrolysis and laser irradiation experiments.

Furthermore he [1] analysed those experimental results using EQPET (Electronic Quasi-Particle Expansion Theory). Formation of TSC (Tetrahedral symmetric condensate) were modelled with numerical estimations by STTBA (Sudden Tall Thin Barrier Approximation). This STTBA model includes strong interaction with negative potential near the center (where r→ 0). See Figure 1.

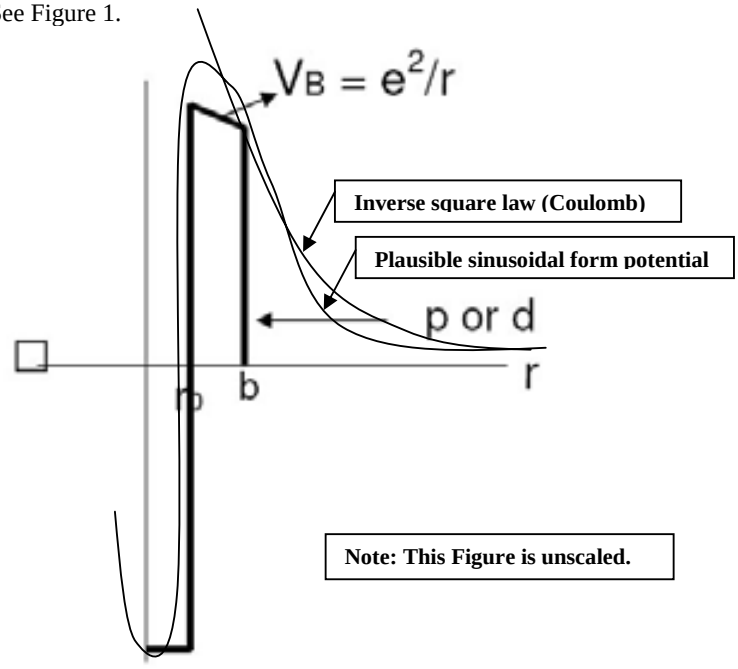


Figure 1. Potential for Coulomb barrier reversal for STTBA. Source [1]

Takahashi described that Gamow integral of STTBA is given by:

$$\Gamma_n = 0.218(\mu^{1/2})\int_{r_0}^{b}(V_b - E_d)^{1/2}\, dr \quad (8)$$

Using b=5.6 fm and $r_0$=5 fm, he obtained [1]:

$$P_{4d} = 0.77 \quad (9)$$

And

$$V_B = 0.257 MeV \quad (10)$$

While his EQPET model gave significant underestimation for 4D fusion rate when rigid constraint of motion in 3D space attained, by introducing different values of $\lambda_{4d}$ can improve the result. [1]. Therefore we may conclude that STTBA can offer good approximation of condensed matter nuclear reaction (LENR). [5]

Interestingly, the STTBA lacks sufficient theoretical basis, therefore one can expect that a sinusoidal form (or combined sinusoidal waves such as in Fourier method) may offer better result which agrees with experiments. However this issue will be discussed elsewhere.

Nonetheless, we recommend further observation in order to refute or verify this proposition of new type of potential derived from biquaternion radial Klein-Gordon equation.

**Acknowledgment**
VC would like to thank to Prof. C. Castro for numerous discussions.

## References

**[1]** Takahashi, A., "A theoretical summary of condensed matter nuclear effects," submitted to Siena WS on Anomalies in Metal-D/H Systems, Siena, May 2005 (http://lenr-canr.org).

**[2]** V. Christianto & F. Smarandache, "Numerical solution of radial biquaternion Klein-Gordon equation," in this volume (Oct. 2007). To appear at *Progress in Physics* Vol. 4 no. 1 (Jan. 2008).

**[3]** Yefremov, A., F. Smarandache & V. Christianto, "Yang-Mills field from quaternion space geometry, and its Klein-Gordon representation," *Progress in Physics* vol 3 no 3 (2007) www.ptep-online.com

**[4]** Christianto, V., "A new wave quantum relativistic equation from quaternionic representation of Maxwell-Dirac equation as an alternative to Barut-Dirac equation," *Electronic Journal of Theoretical Physics*, Vol. 3 no. 12 (2006), www.ejtp.com

**[5]** Storms, E., http://www.lenr-canr.org

**[6]** Nishikawa, M., "A derivation of electroweak unified and quantum gravity theory without assuming Higgs particle," arXiv:hep-th/0407057 (2004) p.15

**[7]** Maxima from http://maxima.sourceforge.net. (Using Lisp GNU Common Lisp).

*First version: 28th Nov. 2007.*

# A note on computer solution of wireless energy transmitted using magnetic resonance

V. Christianto[1], & F. Smarandache[2]
[1] http://www.sciprint.org, email: admin@sciprint.org
[2] Dept. of Mathematics, Univ. of New Mexico, Gallup, USA,
email: fsmarandache@yahoo.com

In the present article we argue that it is possible to find numerical solution of coupled magnetic resonance equation for describing wireless energy transmit, as discussed recently by Karalis (2006) and Kurs *et al.* (2007). The proposed approach may be found useful in order to understand the phenomena of magnetic resonance. Further observation is of course recommended in order to refute or verify this proposition.

## Introduction

In recent years there were some new interests in methods to transmit energy without wire. While it has been known for quite a long-time that this method is possible theoretically (since Maxwell and Hertz [6]), until recently only a few researchers consider this method seriously.

For instance, Karalis et al [1] and also Kurs et al. [2] have presented these experiments and reported that efficiency of this method remains low. A plausible way to solve this problem is by better understanding of the mechanism of magnetic resonance [3].

In the present article we argue that it is possible to find numerical solution of coupled 1st order ODE for describing wireless energy transmitted using coupled magnetic resonance, as discussed recently by Karalis (2006) and Kurs *et al.* (2007). The proposed approach may be found useful in order to understand the phenomena of magnetic resonance.

Nonetheless, further observation is of course recommended in order to refute or verify this proposition.

## Numerical solution of coupled-magnetic resonance equation

Recently, Kurs *et al*. [2] argue that it is possible to represent the physical system behind wireless energy transmit using coupled-mode theory, as follows:

$$a_m(t) = \left(i\omega_m - \Gamma_m\right)a_m(t) + \sum_{n \neq m} i\kappa_{nm} a_n(t) - F_m(t)\,. \qquad (1)$$

The simplified version of equation (1) for the system of two resonant objects is given by Karalis *et al.* [1, p.2]:

$$\frac{da_1}{dt} = -i\left(\omega_1 - i\Gamma_1\right)a_1 + i\kappa a_2\,, \qquad (2)$$

and

$$\frac{da_2}{dt} = -i\left(\omega_2 - i\Gamma_2\right)a_2 + i\kappa a_1\,. \qquad (3)$$

These equations can be expressed as linear 1st order ODE as follows:

$$f'(t) = -i.\alpha.f(t) + i\kappa.g(t) \qquad (4)$$

and

$$g'(t) = -i.\beta.g(t) + i\kappa.f(t) \quad (5)$$

where

$$\alpha = \left(\omega_1 - i\Gamma_1\right), \quad (6)$$

and

$$\beta = \left(\omega_2 - i\Gamma_2\right) \quad (7)$$

Numerical solution of these coupled-ODE equations can be found using Maxima [4] as follows. First we find test when parameters (6) and (7) are set =1. The solution is:

```
(%i5) 'diff(f(x),x)+%i*f=%i*b*g(x);
(%o5) 'diff(f(x),x,1)+%i*f=%i*b*g(x)
(%i6) 'diff(g(x),x)+%i*g=%i*b*f(x);
(%o6) 'diff(g(x),x,1)+%i*g=%i*b*f(x)
(%i7) desolve([%o5,%o6],[f(x),g(x)]);
```

The solution for f(x) and g(x) are:

$$f(x) = \frac{[i.g(0)b - if(x)]\sin(bx)}{b} - \frac{(g(x) - f(0)b)\cos(bx)}{b} + \frac{g(x)}{b}$$

$$g(x) = \frac{[i.f(0)b - ig(x)]\sin(bx)}{b} - \frac{(f(x) - g(0)b)\cos(bx)}{b} + \frac{f(x)}{b}$$

Translated back to our equations (2) and (3), the solutions for $\alpha = \beta = 1$ are given by:

$$a_1(t) = \frac{[i.a_2(0)\kappa - i.a_1]\sin(\kappa t)}{\kappa} - \frac{(a_2 - a_1(0).\kappa)\cos(\kappa t)}{\kappa} + \frac{a_2}{\kappa} \quad (8a)$$

and

$$a_2(t) = \frac{[i.a_1(0)\kappa - i.a_2]\sin(\kappa t)}{\kappa} - \frac{(a_1 - a_2(0).\kappa)\cos(\kappa t)}{\kappa} + \frac{a_1}{\kappa} \quad (8b)$$

Now we will find numerical solution of equations (4) and (5) when $\alpha \neq \beta \neq 1$. Using Maxima [4], we find:

```
(%i12) 'diff(f(t),t)+%i*a*f(t)=%i*b*g(t);
(%o12) 'diff(f(t),t,1)+%i*a*f(t)=%i*b*g(t)
(%i13) 'diff(g(t),t)+%i*c*g(t)=%i*b*f(t);
(%o13) 'diff(g(t),t,1)+%i*c*g(t)=%i*b*f(t)
(%i14) desolve([%o12,%o13],[f(t),g(t)]);
```

And the solution is found to be quite complicated, as follows:

$$f(x) = e^{-(ic-ia)t/2}\left[\frac{[2i.f(0)c + 2i.g(0)b - f(0)(ic-ia)]\sin(\frac{\sqrt{c^2 - 2ac + 4b^2 + a^2}}{2}t)}{\sqrt{c^2 - 2ac + 4b^2 + a^2}} + \frac{f(0)\cos(\frac{\sqrt{c^2 - 2ac + 4b^2 + a^2}}{2}t)}{\sqrt{c^2 - 2ac + 4b^2 + a^2}}\right]$$

and

$$g(x) = e^{-(ic-ia)t/2}\left[\frac{[2i.f(0)c + 2i.g(0)a - g(0)(ic-ia)]\sin(\frac{\sqrt{c^2-2ac+4b^2+a^2}}{2}t)}{\sqrt{c^2-2ac+4b^2+a^2}} + \frac{g(0)\cos(\frac{\sqrt{c^2-2ac+4b^2+a^2}}{2}t)}{\sqrt{c^2-2ac+4b^2+a^2}}\right]$$

For the Maxima display of the result presented herein, see figure below:

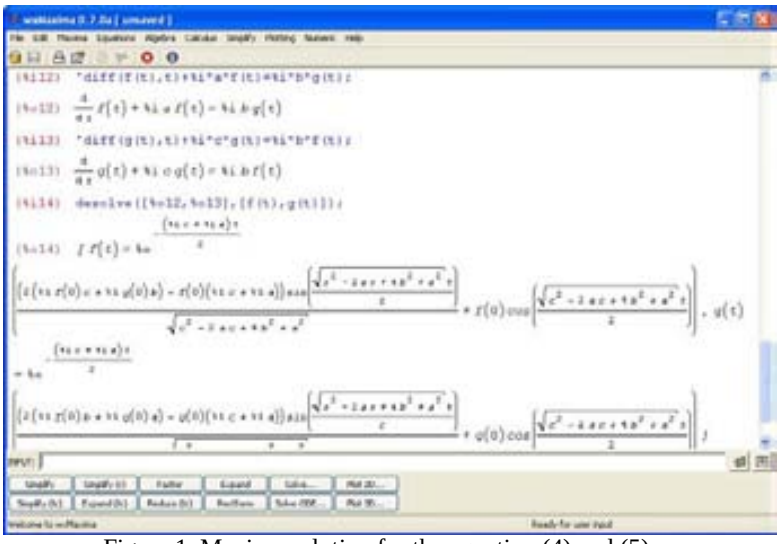

Figure 1. Maxima solution for the equation (4) and (5)

Translated back these results into our equations (2) and (3), the solutions are given by:

$$a_1(t) = e^{-(i\beta-i\alpha)t/2}\left(\frac{[2i.a_1(0)\beta + 2i.a_2(0)\kappa - (i\beta - i\alpha).a_1(0)]\sin(\frac{\xi}{2}t)}{\xi} - \frac{a_1(0).\cos(\frac{\xi}{2}t)}{\xi}\right)$$

and

$$a_2(t) = e^{-(i\beta-i\alpha)t/2}\left(\frac{[2i.a_2(0)\beta + 2i.a_1(0)\kappa - (i\beta - i\alpha).a_2(0)]\sin(\frac{\xi}{2}t)}{\xi} - \frac{a_2(0).\cos(\frac{\xi}{2}t)}{\xi}\right)$$

where we can define a new ‘ratio’:

$$\xi = \sqrt{\beta^2 - 2\alpha\beta + 4\kappa^2 + \alpha^2}$$

It is perhaps quite interesting to remark here that there is no 'distance' effect in these equations. For recent references on other methods to deliver wireless energy, see [7][8].

Nonetheless, further observation is of course recommended in order to refute or verify this proposition .

**Acknowledgment**
VC would like to dedicate this article to R.F.F.

## References

**[1]** Karalis, A., J.D. Joannopoulos, & M. Soljacic, "Wireless non-radiative energy transfer," arXiv:physics/0611063 (2006); [1a] see also R. Johnson, www.eetimes.com/showArticle.jhtml?articleID=194400157

**[2]** Kurs, A., A. Karalis, A., R. Moffatt, J.D. Joannopoulos, P. Fisher & M. Soljacic, "Wireless power transfer via strongly coupled magnetic resonance," *Science* magazine, vol. 317, July 6th, 2007, p.83. www.sciencemag.com

**[3]** Frey, E., & F. Schwabl, "Critical dynamics of magnets," arXiv:cond-mat/9509141 (1995)

**[4]** Maxima from http://maxima.sourceforge.net. (Using Lisp GNU Common Lisp).

**[5]** Christianto, V., "A new wave quantum relativistic equation from quaternionic representation of Maxwell-Dirac equation as an alternative to Barut-Dirac equation," *Electronic Journal of Theoretical Physics*, Vol. 3 no. 12 (2006), www.ejtp.com

**[6]** http://en.wikipedia.org/wiki/Wireless_energy_transfer

**[7]** Meyl, K., "Scalar wave: Wireless Energy Transfer," http://www.k-meyl.de/go/60_Primaerliteratur/Wireless-Energy-Transfer.pdf; [7a] "Energy scavenging for wireless," http://csdl2.computer.org/persagen/DLAbsToc.jsp?resourcePath=/dl/mags/pc/&toc=comp/mags/pc/2005/01/b1toc.xml&DOI=10.1109/MPRV.2005.9

**[8]** Churchill, D.L., *et al*., "Strain Energy Harvesting for Wireless Sensor Networks," Smart Structures and Materials 2003: Modeling, Signal Processing, and Control, *Proc. SPIE*, vol. 5005 (2003), pp. 319–327; www.microstrain.com/white/pdfstrainenergyharvesting.pdf

*First version: 8th Nov. 2007.* 1st revision: *14th Nov. 2007*

# Index

(by Valentin Boju)


accelerating cosmic expansion, 50
action-at-distance, 430
algebraic, 48, 64-65, 139, 144, 209
algebraically
    algebraically simple quantum phases, 97
    algebraically identical to Yang-Mills potential, 218
Allais effect, 50
allowed distances of planets, 293-294
allowed (discretized) elliptical orbits, 295
alpha
    alpha band, 53, 57, 187
    alpha chister of Li, 42
    alpha-corrections in positronium-hyperfine splitting, 206
    alpha decay, 9, 11, 16, 206
    alpha particles, 3-4, 8-9, 11-12, 14, 16-17
    alpha strings, 1, 10
    Alpha Magnetic Spectrometer (AMS), 187
    alpha emission, 11
    inelastic alpha scattering, 42
alternative model, 201
annihilation (particles, mass, linear creation-annihilation of particles), 131, 136, 190-192, 196, 198-202, 204-207, 236, 254, 264, 397
antimeson, 192-194
anomaly, 1, 45, 138
    anomalies, 109, 133-134
    anomalies as support for the new view, 44
    anomalies (related to the burning of hydrogen to oxygen), 81
    anomalies related to the dissociation of water, 45, 82-83
    anomalies found in the electrolysis and plasma electrolysis of water, 83
    free energy (from atomic hydrogen) anomalies, 96
    anomalies challenging reductionism, 132, 136
    anomalous light phenomena, 58, 76
    anomalous phenomenae, 282
    biology as the mother of all anomalies, 137
    (chiral selection) anomaly, 138
    Compton lengths of neutrinos anomalies, 138
    dissociation anomalies, 45, 82-83
    Engineering Anomalies Research, 284
    isotope anomaly, 202
    Langmuir anomaly, thermal dissociation (anomaly), 45, 81, 88-89
    nuclear physics anomalies, 138
    othopositronium annihilation anomalies, 198, 201, 205-206
    Quantum Model of Memory – ELF anomaly, 137
    Siena WS on Anomalies, 438
    thermal dissociation (anomaly), 45, 81, 88
antigravity, 135, 188, 196, 200, 287
antimatter, 127, 130-131, 135-136, 184-190, 193, 195-196, 198-200, 203, 242, 287, 382, 401, 409, 434
antiparticle, 186, 189, 201, 397
antiprotonic helium, 193
antiquark, 31, 187, 189, 193-194
architecture – Decorative & Mosaics Work – Ceramics & Urban Sculpture, 333, 367-368, 379
Astrophysics, v, ix, xvi, xix, 45, 62, 73, 104, 108, 127, 130, 147, 262, 286, 289, 293, 435
    astrophysics quantization, 235
Asymptotic Dimension of Digital Spaces, 333-334, 336, 355, 376, 380
Asymptotic-IQCC-dimension, 333-334, 336, 355, 376, 380

Banach space, 357

Baryonium, 198
bifurcations, vi, 72, 151, 153, 158, 164, 166, 181
binding energy, 1-3, 5-6, 9-12, 16-28, 34-35, 62, 81, 86, 88, 95-96
bio (biochemistry, biology, biologically, biomathematics, biomedical, biophysics, biostatistics, biotechnology), iv, xiii, xv, xvii, 33, 45, 47, 49, 51-58, 60-64, 66-68, 71, 74-77, 79-81, 84, 102-103, 106-108, 132, 137-138, 145-146, 148, 236, 242, 265-266, 284, 287, 289, 308, 333, 366-369, 379
biocontrol, 51
biological death, 54
biological system, 49
biology as the mother of all anomalies, 137
field body (or magnetic body), 47
how magnetic body controls biological body, 50
parabiotic life, 49
pre-biotic, 49
quantum biology, 49
symbiosis, 34
biotechnology
VTF-packings in biotechnologies, 366-367
biquaternion, 230, 232, 266
biquaternion differential operator, 7, 218, 230
biquaternion electrodynamics, 219
biquaternion Klein-Gordon equation, vi, 218, 220, 436
radial biquaternion Klein-Gordon equation, vii, 436, 438
biquaternion Navier-Stokes equation, 229-230
biquaternion number, xviii, 217-227
biquaternion Schrödinger equation, vi, 223
biquaternionic Schrödinger representation of Navier-Stokes equations, 231
Black Light Inc. Laboratory, 88
Bohr quantization of radii of planetary orbits, 50, 137
Bose-Einstein condensation, 1, 3, 5
boson, 2, 19, 21-22, 32, 34, 43, 84, 129, 131, 138-139, 148, 159, 161-164, 176, 193, 199, 207
bosons and antibosons help in the decay of unmatter, 193
boson-fermion clusters, link boson clusters, interacting boson-fermion nucleon "clusters", 199
boson pairs, 199
electroweak gauge bosons, 162
exotic weak bosons, 132
fermion and electroweak gauge boson fields, 157
gauge boson states, 160
bosons & fermions unified through a fundamentally different mechanism than the supersymmetry, 182-183
13+1 Higgs boson, 193
Interacting Boson Model-IBM, 199
massive gauge boson, 163, 177
massive vector bosons, 177
mechanism of gauge boson-fermion unification, 178
vector boson masses, 159
mechanism of gauge boson and fermion fields, including classical gravitation, 178-179
boundary, 141, 389
boundary value problem, 164
boundary points, 358, 361
(d – 1)-area of a boundary, 358
(intrinsic) perimeter of an 1-boundary, 358
mantle-core boundary, 81
n-dimensional manifold (without boundary), 248
time-like boundary of a 4-D body, 54
time-like boundary of the space-time sheet, 59
traveling boundary, 385
boundary in/of a theory
Boundary between the family of sq- or Hex-(L; K)-Digital Plane and the family of 2-dim Riemannian, xvii, 353
Holcman-Pugh Boundary between Compact and Noncompact Complete Riemann Manifolds, xvii, 332-334,

350, 354-355, 367, 379
the n-Trans-Riemannian Boundary, 332, 334, 350, 357
(asymptotic) boundary of field theory, 182
Brightsen, 198-200, 203
Brightsen Nucleon Cluster Model, 4, 198
Brightsen's closed-packed cluster model of nuclei, ix
Brightsen pairs of nucleons, 203
Brownian motions, vii, 232, 236, 237-241, 244-245, 253-254, 265-267, 282-286
Brownian motion model of fusion in Hadronic Mechanics, 236

C++, Python & Pascal Programs & Technologies, vii, 332-335, 338-339, 360, 367-369, 374, 376, 380
sq-Superfractals and Hex-Superfractals C++ Programs, 369-374
Python Programs for Juxtaposition Fractals, 374-376
VTF Methods – Riemannian Regression Submanifolds & Nanotech Applications – T-Pascal Programs, 376
calculation for New Energy Development, 111
capacity, 126, 161, 337, 339, 341, 343, 346, 350-351
capacity in a CEBGU=Compartmented Energetic Bank, xvii, 332-336, 344-350, 354-355, 380
capacity of 61-CEBGU-Hex[(3;17), (9; 19)], 346
capacity of 61-CEBGU-Hex[(9; 19), (3;17)], 346
capacity of 61 th Energetic Level Hex[(3;17), (9; 19)], xvii, 346
capacity of 61 th Energetic Level Hex[(9; 19), (3;17)], xvii, 346
cap-polynomial and Asymptotic Dimension of Digital Spaces (CPADDS), 333, 380
cap-polynomial and Polynomial growth of the Digital-Energetic-superstable-Levels, xv, 333, 341-342, 376, 379, 380
Cartan algebra of Poincare algebra, 97
chaos, xiii, xvi, 44, 65, 89-91, 95, 109, 126, 151, 158, 162, 164, 166-167, 177, 181, 183, 286, 290, 302
Chromodynamics Formula, vi, 189, 193, 204
Clifford, 95, 228, 232, 251, 285
Close-Packed Spheron Model of Pauling, 199
cloud, 73, 192, 281
weighted/dynamical cloud, 362, 364-367, 380
clusters, iv, vii, 42, 80, 189, 198-200, 203-205
coarse Baum-Connes conjecture, 333, 343, 380
coherent dilatons controls dilators motions, 396
coherent Nuclear Fusion, 425, 435
cohomology (see homology)
cold fusion, 2, 28-30, 33, 42, 51, 138, 149, 283
Combinatorial Methods, iii, vii, x, xvi, xvii, 332-335, 337, 347-348, 356, 358, 376-378, 380, 443
compact, xvii, 248, 259, 267, 353-354, 366-367, 379, 396
Compartmented Energetic Bank/Generator Unit (CEBGU), xvii, 332-336, 344-350, 354- 355, 380
Compton lengths of neutrinos anomalies, 137
computer, xvii, 57-58, 144, 220-221, 328, 439, 442
computer and Video Games, 368, 380
computer-assisted proofs, xvii, 340
computer-search, xvii
computer viruses, 58
Computer Vision and Image Processing (CVIP), 333, 367, 380
conjecture, 34, 180, 333, 343, 358-359, 379-380, 417
connected sum, 1, 7-8, 11, 27
controlled transition, 45, 91
convex, 347, 357, 360, 378-379
cosmic, cosmic microvawe, cosmic strings, xviii, 48, 50, 65, 90, 135, 137, 147, 149, 169, 187, 301, 386, 396, 433-435
cosmological, cosmological coherence, cosmological constant problem, vi, 108,127, 131, 133, 136-137, 168-170, 172-174, 237-239, 285, 367, 383-386, 388-389, 395-397, 399-400, 429-432
cosmological time, 384
Coulomb problem, 293
Covering, 46, 55, 68, 95, 98-101, 334, 360, 378
Cryptography, 333, 368- 369, 380
curvature, 53, 101, 208-209, 212-213, 218, 237, 239, 251, 253, 266, 270, 286, 332-334, 350, 354-357, 368, 372, 386, 432-434
Inverse Quotient Curvature Coefficients (IQCC), xvii, 332-334, 350-355, 380
QL-DigitCurvature, 341, 355-357

Quasi Constant Curvature, Constant Curvature, 354, 368
dark matter, dark electro-weak force, dark energy, 2, 8, 32-34, 40, 43-44, 48, 50, 52, 54, 56-57, 61, 70, 72-74, 79-81, 95, 97, 102, 104-106, 108, 127, 131, 132, 136-138, 145, 147-148, 284, 289, 391, 409
de-coherence, 1, 2, 4, 6, 34-39, 56, 81
Defence Research Programs, 333, 369, 378, 380
deformation of space-time
Einstein's gravitation theory (Pioneer anomaly, Einstein used mass to deform s-t), 341, 396
Kaluza-Klein used mass to deform s-t &, 396
derivation, derivative, 4, 131, 154, 156, 169, 171, 180, 183, 214, 219, 222-223, 232, 250, 288-289, 295, 302, 343-344, 383, 389,
2-DEG &Quantum dots, 304
5-dimensional
Einstein Gravitational equations in a 5D metric, 382
Kaluza-Klein based 5D Gauge Theories, 382
diffuse interstellar bands, 45, 68, 108
diffusion systems, 236
digital,
Digital Space, iii, vii, x, xvii, 332-356, 368-369, 376, 378-380, 443
digital tape, disk, 327
dilator, 382-386, 389-390, 392-398, 400, 409-412, 429-432, 435
discrete, 263, 265, 289, 313
Arithmetic Discrete Hyperspheres, 336
Discrete and Differentiable VTF Methods, 332, 334, 362, 368, 376
Discrete & Cont. Dynamical Systems, 285
discrete degrees of freedom, 95
discrete distances in the gravitational field of an astronomical body, 296
discrete fiber, 101
discrete frequencies, 75
discrete group of SU(2), 97, 99
discrete group, subgroup, set, symmetries, 55-56, 65, 73, 95, 97, 99, 101
discrete intersections, 48
discrete jumps, 266
discrete levels, 312
discrete lines, 67
Discrete Methods, iii, vii, x, xvii, 332-334
discrete quantum levels, 316
discrete spacetime, 266
discrete energy spectrum, discrete spectrum, 51, 314
discrete states, 109, 321
discrete structures, 266
discrete values of distances of possible planets and galaxies, 295-296
dissociation anomalies, 40
distances of planets in the solar system, 293 (see also V. Perinova, A. Luks, P. Pintr, "Distribution of distances in the solar system," *Chaos, Solitons and Fractals* 34 (2007) 669—676)
distribution of distances, vii, 293
disturbance, disturbing, 237, 386, 433
disturbing zones of a dynamical system, 362, 367, 380
Double Slit Experiment, 430
dynamical, 34, 131, 151, 248, 286, 362, 380
disturbing zones of a dynamical system, 362, 367, 380
dynamical p-Adic length scale of electron, 140
VTG Dynamical Systems (Versor Type Gradient DS), 362, 380
geodesic dynamical system, 366
the dynamical signature, 34
the dynamical system grad f, xvii, 362-366, 377, 380
dynamics of neutrino oscillations, vi, 131, 138, 139

elephant trunks, 45, 73-74
energetic level, 332-336, 340-341, 343-344, 346, 352
Energy Units (Compartmented Energetic Bank/Generator Units-CEBGU), xvii, 332-333, 335, 340-341, 343-350, 352, 354-355
"enveloping mechanism"of Hybrid phenomenon, 348

exact mapping, vii, 229
exotic deuterium, 2, 30-31, 34
exotic (deuterium, weak bosons, meson bonds, leptons, light mesons, excitations of nuclear, color forces, di-neutron, charge states, quarks associated with color bond, counterpart of QCD, anti-quark, nn-state, di-,tri-, and tetra- neutron, negatively charged), 2-4, 7, 13-15, 22, 24, 27-34, 42, 88, 136-138, 189, 193, 202, 207, 382, 430
exotic matter with negative pressure, 137
exotic weak bosons, 2, 32
experimental, experiments, 4-6, 10, 13, 15, 30, 37-38, 45, 72, 74, 80, 86, 89-90, 93, 110, 128, 138, 140, 143, 151, 159, 168-169, 176, 182-183, 187, 189-191, 193, 196, 198-199, 201-204, 209, 214, 240-241, 275, 282-285, 290, 302, 311, 325, 334, 397, 432, 435-439
experimental verification of QED laws of conservation, 202
experimental findings of Mills, 45, 94-95
verifying Unmatter by experiments, vi, 189, 204
extended Red Emissions, 75

factor spaces, 46, 97-98, 101
far-from-equilibrium statistical processes, 182
Feigenbaum (attractor, constant scaling, scenario), Feigenbaum-Sharkovskii-Magnitskii (FSM) paradigm, 158, 164, 166, 176, 180, 183
Fermi, fermions etc, 2-3, 5, 15, 19, 21-22, 31, 74, 84, 95, 109, 128, 139-141, 143, 157, 161-164, 169, 176-179, 181-182, 187-188, 199, 214, 243, 308-313, 435
fermion families, 138
boson-fermion clusters, 199
fermion Higgs, 139
field body, 25, 44, 47, 50-51, 53, 56-58, 65, 73, 138
flight dynamics, 362, 367, 380
fold, folding, folded, 17, 93-95, 97, 99-100, 130, 133
folded configuration, 7
fold fusion, 29
N-fold , N-fold covering, 73, 93
protein folding, 7
fractal, 111, 116-117, 119-126, 136, 138, 145, 166, 177, 183, 236, 238, 240-241, 265-266, 285-286, 288, 290, 302, 332-336, 342, 360, 381 (image)
fractal dimension, 111-114, 119, 126, 360
fractal method, 111-112, 115, 123
juxtaposition fractals (exterior, hybrid, interior, random), xvii, 333-334, 357, 361-362, 368, 374, 376, 380
super-fractals, xvii, 332-336, 353, 368, 380, 381 (image)
fractional [fractional Bohr quantization, fractional dynamics, fractional field theory, fractional quantization, fractional quantization of magnetic (radial) quantum number, fractional spectrum, fractional statistics systems, fractional valued quantum numbers], vi, 45, 88-94, 110, 130-131, 151, 161-163, 167, 176-183, 187
free energy, vi, viii, 44-45, 51, 82-83, 88, 96, 105, 110, 148, 292
fundamental dilator, 382-384, 389, 394-398, 409, 411-412, 429, 431, 435

G-invariant fermionic states, 95
Gamma function, 354, 357
gauge theories, 144, 151-152, 236, 267-268, 270-271, 288-289, 382
Lie-Isotopic Gauge Theory, 267
gauge boson Higgs, 139
generalization of the Bohr's quantization rules, 89-91
geodesic field, 362, 367, 380
geodesic spheres, 99
geometric (al), hypergeometric (al), iii, vii, ix, x, 47, 48, 52, 53, 59, 60-65, 67, 73, 94, 132, 141-142, 158, 181-182, 208, 210, 212, 218, 237-241, 243, 248, 250, 271, 282, 285, 288, 290, 299, 333, 341, 352-354, 357, 377, 382-384,389, 392, 394-398, 404, 409, 425, 428-429, 431, 432, 435
geostrophic flows, 229, 232
giant dipole resonance, 1, 2, 4, 6, 34, 42
gradient,63, 157, 183, 249, 251, 253, 262, 275-276, 277, 400
dynamical system grad f, vii, 362-366, 377, 380
gradual, gradually, 96, 97, 133
graphics, 181, 312, 333, 369, 378
gravitation, gravitational, (acceleration, attraction, collapse, coupling, corrections, effect, energies, field, interaction,

instability, masses, momenta, quadratic g. theory, repulsion, solar-like g. systems, trajectories, structure, wave), 50-51, 55, 59, 72, 94, 128, 132, 135-136, 139, 168, 176-177, 218-219, 237-238, 244, 253, 284, 294-295, 302, 386, 393, 396-397, 399, 400-403, 409, 429
anti-gravitational dark matter, 409
gravitational atom, 294
G-gravitational for two bodies, 403
Gravitational Constant, 94, 127, 173, 295, 400
gravitational corrections to both quantum field theory and renormalization group (RG) equation, 176
hadrons, hadronic, leptohadrons, iii, vii-x, xii, xvi, 27, 33-34, 43, 51, 105, 138-140, 147, 163, 167, 183, 187, 195, 207, 218-219, 232, 236, 241, 243, 245, 274, 280, 282, 284, 287-288, 291-292, 428, 434-435, 443
Hamilton, hamiltonian, 143, 167, 183, 209, 218, 243-245, 274, 278-279
Hamilton-Jacobi reduced equation, 332, 334, 362-363, 368, 378
handle numbers for partonic 2-surfaces, 140
heavier nuclei, 2-6, 8-9, 12, 19, 21, 27
Hertz, Hertz potential, 251-252, 439
hexaquark unmatter, 200
hidden, 111, 197, 199-200, 208, 209
untapped energy' hidden in the formation of elementary particles , viii,
hidden link between micro-systems and large scale systems hierarchy of Planck constants, viii
hidden connection between our Earth and galaxy rotation, viii
hidden electromagnetic field origin of YM fields, 209
Higgs type fields, 135
high resolution standard nearness network, 367
Holcman-Pugh Compactness Riemannian Boundary, xvii, 332-334, 350, 354-355, 367, 379
Holcman-Pugh Kick Method, 332-334, 350, 354-355, 379
holonomy, holonomic, 209, 244-245, 247, 289
holonomy group of spinor connection, 134
homology, cohomology, 100, 101, 367
homology group, 101
homologically non trivial geodesic sphere, 99, 100
real cohomology, 366
homothety, homothetic, quasi-homothetic, 353, 356, 358-359, 361
Hubble Expansion, 434-435
hybrid, 92, 102
hybrid Digital Spaces, xvii, 380
hybrid combinations of quarks and antiquarks, 194
hybrid Juxtaposition Fractals – Python Programs, 361-362
hybrid multi-type-CEBGU, xvii, 332, 348, 350, 354
"enveloping mechanism" of Hybrid phenomenon , xvii, 348
Generalized Hybrid multi-type-CEBGU with an admissible nucleus, 354
hybrid point-distances-spaces (M; p-d) with Ω Scaling Spheroidal Model , 354
Hypergeometrical, Hyperspherical (Hypergeometrical Standard Model, Hypergeometrical Universe, Hyperspherical universe), iii, vii-x, 382-384, 389, 392, 395, 397-398, 404, 409, 425, 428-429, 431-432, 435

Interacting Boson-Fermion Model, 199
imbedding spaces, 45-48, 51, 56, 94-95, 97-98, 100, 134, 144
imbeddings of Robertson-Walker metrics, 135
infinitesimal symmetry, 241
inflationary cosmologies, 135
infrared bands, 44, 67
intrinsic connexity of an Energetic Level, 335
Inverse Quotient Curvature Coefficients (IQCC), 332-334, 350-355
iso-Heisenberg representation, 236, 245, 279
isometry group SU(2), SO(3), 99
iso-Schrödinger equation, 275
Iso-StabilityDiophantine Equations, xvii, 342
Iso-Stable Digital Spaces, xvii, 332, 341, 356
isotope anomaly, 202
isotopic, 241, 242-246, 264-265, 267-284, 288
isotopic compositions, 202, 206
isotopic generalizations, 267
Isotopic Geometries and Isotopic Gauge Theories, 267

isotopic Hilbert space, 268
isotopic inverse, 268
isotopic lift, 236, 242, 244-246, 275
isotopic lift of the Schroedinger and Heisenberg represen-tation, 242
isotopic theory of the strong interactions, vii
isotopic Santilli-Schrödinger equation, vii
Lie-isotopic extension of QM, 241
Lie-Santilli-isotopic theory, 242
Santilli-Lie-isotopic lift , 268, 275
isotopic hermitean conjugate, 268
Jones inclusions, 101
Juxtaposition Combinatorial Measures, 332, 334, 357-360, 377
Juxtaposition Fractals, Hybrid Juxtaposition Fractals, 333-334, 357, 361-362, 374, 376, 380

Kähler coupling strength, 136
Klein-Gordon (equation, representation), vi-vii, ix, 208-209, 213-215, 217-223, 227, 232, 436-438
knotting (of nuclear string, trunks are made up of dark filaments and knots which show evidence of twisted structures), 1, 7-8, 73

Lagrangian, 179, 180, 208, 210, 218, 222, 232, 245, 336, 337, 376, 379, 382-384, 393, 396, 397, 410, 429, 430
Lagrangian density, 154, 178
Quantum Lagrangian Principle, 383-384, 386, 393, 396-397, 410, 429-430
length scales, 303
lepton, 15, 34, 59, 128-129, 134, 140, 170, 176, 181-183, 189, 195, 208, 214, 219
life as a symbiosis, 45, 77
light nuclei, 2, 16, 21, 30, 205
(L; K)-Digital Spaces
(L; K)-Iso-Stable Digital Spaces, 341-342, 345-347, 356, 380
(L; K; Hex, and sqCells-Digital Plane), 337-357
(L; K)-Threshold Stability Formula, 338-339, 343, 345
(L; K)-Value Stability Formula, 338-340
Logarithmic Kick Method & Nanotech Applications, 333, 380

magnetic body, 51, 53, 57-58, 61, 70, 77, 79, 138
how magnetic body controls biological, 50
magnetic resonance, xiii, 243, 439
matrix (S-matrix, density matrix, mixing matrix), 44, 59, 60, 104, 129, 142-143, 146, 149, 174, 209-212, 268, 275, 404-405
matter (antimatter, nonmatter, unmatter),
antimatter, 127, 130-131, 135-136, 184-190, 193, 195-200, 203, 242, 287, 382, 401, 409, 434
nonmatter, 184, 186
unmatter, iii, vi, ix, 130-131, 184-190, 192-196, 198-201, 203-204
maxima, 3, 5, 13, 28, 59, 62, 93, 94, 98, 101, 162, 221-222, 225, 228, 231-232, 274, 341, 346, 349, 361, 401, 438, 440, 441-442
Maxwell theory, 47, 208-209, 214, 219, 222, 238, 251-253, 271, 286, 438-439
Measure (Juxtaposition Combinatorial Measures and applications in Intrinsic Measure Theory), 332, 334, 342, 350, 357-361
mechanism
a fundamentally different mechanism than the supersymmetry, 182, 183
the (L; K)-machine as an “enveloping mechanism”for Hybrid phenomenon, 348
gravitational instability as a mechanism leading to the formation of the helices, 72
mechanism of gauge boson-fermion unification, 178
natural mechanism of the phenomenon of (L; K)-stability, 346
time mirror mechanism, 44, 47, 60-62, 82-83
unification mechanism of gauge boson and fermion fields, including classical gravitation, 178-179
mesoscopic (device, physics, superconductor, systems), xvi, 308-309, 317, 324, 329
metabolic, 44-45, 49-51, 61-63, 66-68, 70, 72, 85, 362, 367
metric structure, 209, 275
metric structure of (L; K)-Digital Spaces, 332, 337
Minkowski factor, 98
model
models beyond the standard model, 151

models for how magnetic body controls biological, 50-51
modified Schrödinger equation, iii, 296, 299, 300
Möller's Atomic Hydrogen Generator (MAHG), 95
muon, 15, 129-131, 189, 193, 394, 410-412, 423-425, 434
muonium, 129-130
Mysterium Cosmographicum, 292

N-atom, 95, 96
nanotechnology, nanotech, vii, x, xvi, 308, 310, 317, 324, 329, 332-334, 362, 364, 366-369, 376
applications of Riemannian Regression Submanifolds in Nanotechnologies, 332-334, 362, 369, 376-377
Nanotech Applications (remote sensing, microrobotics), 332-334, 362, 364, 366-367, 369, 376
VTF-packings in nanotechnologies, 367-368
Natural Frequency of Spacetime Oscillations, 403, 429
Natural Mechanism of the phenomenon of (L; K)-stability, 346
Navier-Stokes equations, 229, 231, 238-241, 260
negative energy signals propagating to geometric past become possible, 141-142
Neutrino (mixing, oscillations), 130-131, 168-170, 172-174, 176, 434
neutrosophy
neutrosophic logic, xix, 188, 197
neutrosophic probability, 188, 197
Nöther currents, 135
nonlinear dynamics and chaos, 45, 65, 89-91, 95, 109, 126, 151, 158, 162, 164, 166-167
nonnucleus, 186
Nottale's theory, 54, 109, 148, 236, 240, 262, 265, 283, 286, 288
Novikov conjectures, 333, 343, 380
Nöther charges related to symmetries, 134
Nöther currents, 135
nuclear binding, 1, 3-5, 16
nuclear physics anomalies, 138
nuclear string, 1-13, 18-21, 27-28, 33-37, 39, 105, 148
numerical
numerical simulation, solution, 4, 66, 74, 84, 151-153, 158, 159, 161, 165,166, 168, 173, 176-183, 216, 217, 220-222, 225-227, 231, 272, 287, 381, 344, 345, 350, 354, 379, 433, 436-440
(numerical invariants of ) the 50 th Stable Energetic Level [3; 17; Hex], 346
(L; K, Hex) Digital Spaces (numerical values), 345-347
Hex[(9; 19), (3;17)] and Hex[(3;17), (9; 19)] (numerical values)
capacity (numerical values), 346
compute the isotopic hermitean conjugate, 268

orbifolorbifold, d singularities, 95, 100
orbital 3-surface, 91-93
ordinary deuterium, 31

p-Adic quantization, phasis, thermodynamics, xv, 3-4, 14, 19, 21-27, 32-34, 40, 44-45, 47-50, 62, 64-66, 74-75, 79, 84-90, 93, 102, 104-105, 138-140, 144-145, 147, 266
packings, packed, ix, 32, 199, 205, 358-360, 362, 378
VTF-packings in biotechnologies, 366-367
VTF-packings in nanotechnologies, 367-368
partonic 3-surfaces, 99
pathological metabolic activity, universal metabolic quanta, 44-45, 362, 367
pattern
pattern (pattern formation), iii, vi, viii, 151-153, 163, 177
pattern recognitions, 333, 337, 369, 378
perimeter
approaching the perimeter, 358
perimeter (intrinsic) of the boundary, 358-360
permittivity of vacuum, 400, 403, 429
Photon assisted tunneling, 314
Pion [pion unmatter, pion like colored states, pion mass, pionium, lepto-pion (or electro-pion), light particles (pions), PionMinus, PionPlus, PionZero, pentameric excited state of Pion Minus, PionPlus coherence, PionPlus model, Pion Zero is its own anti-particle (anti-Pion Zero) or a Majorama particle], 3-5, 15-17, 21, 24, 41, 140, 190- 193, 200, 219, 289, 414-417, 422

pipe inspection microrobotics, 362, 367
Planck constants (gravitational P.c., hierarchy of Planck constants), 50, 55
plasma electrolysis, 45, 83, 86, 87
plasmoids, 44-45, 55, 58, 66, 70-71, 74-80
Poincaré, 97, 134, 177, 244-245, 286
polyhedral symmetries in living matter
polynomial, vii, 299
    cap-polynomial Asymptotic Dimension of Digital Spaces, 332
    cap-polynomial of Digital Spaces, 333, 342
    finitely generated groups with a polynomial dimension growth have Yu's property A, 343
    polynomial growth of the Digital-Energetic-superstable Levels, 332, 341-343, 376
positronium, 129, 131, 193, 195, 198, 201-203, 205-207
    othopositronium, 198
    parapositronium, 201-202
prediction
    prediction for New Energy Development, iii, vi, xv, 111, 126
    prediction of distances of planets in the solar system, 293
problems of QCD: 139
Programming Technologies, 369-376
protonium, 193
pygmy resonances, 2, 4, 6, 39-40
Python & Pascal adjacent Programs & Technologies, 374-376
QCD (Quantum Chromodynamics), 2-4, 6, 15, 18, 21, 22, 25, 33-34, 128, 132, 139-140, 149, 152, 177, 183, 193, 222
    QCD binds nucleons, 2, 21
Q-LDCurv of the Energetic (r+x)stable-Level
quantified space, 335
quantization, 45, 49, 50, 57, 88-94, 97-100, 128-129, 137-138, 152, 165, 240, 244-246, 260, 278-280, 285, 289, 293-294301-302, 313, 324-325, 282-283, 387, 393, 394, 404, 429, 435
quantized (see quantization):
    Astrophysics quantization
    quantized (quantization) Planck constant
Quantum Chromodynamics (see QCD)
quantum critical sub-manifold
quantum dots, 304
quantum dot turnstile, 316
Quantum Lagrangian Principle, 383-384, 386, 393, 396-397, 410, 429-430
quark
    biquark, 194
    triquark, 194
    tetraquark, 194
    pentaquark, 194
    hexaquark, 194
    septiquark, 194
    octoquark, 194
    nonaquark, 194
    decaquark, 194
Quaternion space geometry, iii, 208, 218, 222, 227, 232, 438

radial Klein-Gordon equation, 221
Renormalization Group flow, 159, 166, 176, 183
rescaled range analysis (R/S analysis), 111, 125
RF-SET, 313
Riccati equation, 229-230
Riemann-Cartan-Weil (RCW) geometries, diffusions, 236, 238, 240, 244-245, 249-251, 253-254, 262-263, 265-266, 271, 278
Riemannian context, 332
Riemannian Nonlinear Regression, 362
Riemannian packings, 362
Riemannian Regression Submanifolds, VTF-regression, 332-334, 364-367, 369, 376-377
Riemannian Regression Submanifolds – T Pascal Programs, 376
robotics, microrobotics, 362, 367
rotation, 51, 55-56, 73, 78, 93-98, 100, 105, 127, 139, 149, 209, 237-238, 241, 244, 247, 251, 282, 285, 289-290, 328,

382-383, 385, 388-390, 392-393, 396, 398-399, 405, 409, 411, 413, 417, 429-431
Santilli
Hadronic Mechanics due to Santilli, 236
isotopic Santilli-Schrödinger equation, vii
isotopic theory of the strong interactions due to Santilli, vii
Lie-Santilli-isotopic theory, 242
Santilli-Lie-isotopic lift , 268, 275
scale Relativity, 236, 262, 288
scattered, scattering, vi, xvi, 42, 201, 202, 309, 310, 383, 397, 416, 432
Raman scattering, xvi
Schrödinger (Schroedinger, biquaternion Schrödinger equation, modified Schrödinger equation, Navier-Stokes-Schrödinger equations, Schrödinger equation, Schrödinger field), 93-94, 129, 140-141, 156, 219, 222-226, 228-234, 236, 238- 243, 245, 250, 252-254, 256-258, 260, 262-266, 272, 275, 277-278, 280-284, 286, 288, 295-296, 299-302, 430
Schrödinger uncertainty theorem, 233-234
Security Procedures (CSP), 333, 367, 368, 380
Separation supposition and Compactness Riemannian Boundary, 332-334, 353, 355
sheet (many sheet space-time, many sheet, nuclear space-time sheet, nucleon space-time sheets, neutron space-time sheets, protonic space-time sheets, subsystems as smaller space-time sheets glued to, p-adic space-time sheets, many-sheeted space- time as an implications of TGD, Many-sheeted space-time and TGD; Many-sheeted space-time, universal metabolic quanta, and plasmoids as primitive life forms, Plasma sheet), vi, 13, 23-24, 28, 30-31, 33-34, 44-45, 47, 51, 54, 57-59, 61-63, 70, 75, 77-98, 102, 105-106, 108, 136-137, 139, 141-142, 145, 148, 410
3D-Shockwave universe, 391
single electron devices: 311
single photodetector in microwave range, 316
Smarandache-Christianto potential (see also ‘Yukawa potential’), 222, 437
Solar cells & photovoltaics, 319
solar system, 293-295, 299, 300-302
solitons, 109, 166, 286-287, 290, 302
space
Banach space, 357
isotopic Hilbert space, 268
spacetime anisotropy, 236
space-time fluctuation, 283
spaces with Polynomial growth of the Digital-Energetic-superstable-Levels, 332, 343
spintronics: 320
Stability
sq and Hex-Iso-Stability, 341, 356
sq-Stability Formula & Hex-Stability Formula, 338-339
Stability of the Digital-Energetic Levels, 380
stable
exotic states stable under beta decay, 29
stable nuclei, 1, 7-9, 11-12, 19, 41, 204
Stable Threshold (StabThresh), 338-341, 344-349, 356
Stable Value (StabVal), 339-341, 343, 345-348, 356
standard model, iii, vi-viii, x, 14, 34, 128, 130-131, 133-134, 139, 151, 176-183, 198, 201, 208-209, 214, 382-383, 389, 392, 395, 398, 409, 425, 428, 431, 435
standard model of elementary particles, iii,vi, vii-viii, 176, 208-209, 443
Stochastic Mechanics, Nelson's Stochastic Mechanics, 236, 240, 262, 265, 295
strings, iii, vi, 1-21, 25, 27, 28, 33-37, 39, 52, 74, 99, 101, 104, 105, 133-136, 139, 147, 148, 289, 382
alpha strings, 1, 10
cosmic strings, 99, 101, 104, 136, 147
knotting of nuclear strings, 1, 7, 8
lighter nuclear strings, 1, 8, 10
nuclear string (hypothesis), iii, vi, 1-13, 18-19, 21, 27, 28, 33-37, 39, 105, 148
shorter nuclear string, 1, 7
superstring models, xiii, 382
strong force, 2, 13, 23-25, 33-34, 187, 195, 208, 397
SU(2), SU(3) (color group), SO(3), 101
Super-Fractals, xv, 332-336, 353, 380, 381(image)
susceptibility (magnetic susceptibility of vacuum, deformation susceptibility of the Fabric of Space), 428-429

symmetry, symmetric, 7-8, 20, 52, 55-56,60, 73, 93, 96, 98, 102, 104, 127-129, 133-136, 142-144, 146, 162-163, 165, 167-168, 178-180, 182-183, 198-200, 208-209, 213-214, 217-219, 224, 240-245, 247-248, 256-262, 265, 270-271, 284, 286, 289, 324, 358-362, 378, 382, 395-396, 409, 429, 434-435

tau, 189, 410, 425, 434
technology, technologies (biotechnology, New Energy t., Free Energy t., nanotechnologies, alternative energy t., untapped energy t., energy generating t., production and distribution t., novel biophotonics t., New hydrogen t., measurement of orthopositronium annihilation rate – 1987 experimental verification of QED laws of conservation, stimulating nuclear decays technology, semiconductor t.), iii, viii, x-xiii, xv, xvii, 45, 47, 49, 70, 81, 202, 244, 308, 310, 313, 317, 324, 328-329, 333, 362, 366-367, 369
Programming Technologies, 369-376

Tesla coil, 82, 105, 110
tetra-neutron, 1-3, 5, 12-14, 16, 21, 26-28, 39-40
tetraquark (unmatter), 194
Textile Pictures and Textures (TPT), 333, 369, 381 (image)
thermal dissociation (anomaly), 45, 81, 88-89
thermal noise, 55, 96
Threshold, 76, 136, 153, 157, 177
Threshold Stability Formula, 333, 335, 338-339, 343, 345
TGD framework, 134
time
time quantization, 394, 429
time mirror mechanism, 44, 47, 60-62, 82-83
topological and metric structure of (L; K)-Digital Space
topological structure of the multi-type-CEBGU, 346

(topological structure of) [(3;17; Hex, StabThresh34),(9;19; Hex, $r_1$=53, multi-type StabThresh=12, StabVal1680)], 346
(topological structure of) the 50 th Stable Energetic Level [3; 17; Hex], 345-346
Topological Geometrodynamics (TGD), iii, vi, viii, xv, 3-5, 15-16, 20, 27, 33-34, 36, 39- 40, 43-44, 47, 49-55, 57, 59-60, 74, 76, 78, 82- 83, 90-91, 97, 102-106, 109, 133-148, 289, 443
topological
complexity of the topological struct. of a r- Energetic Level, 355
intrinsic and extrinsic topological structures of the hyperspheres and disks, 333
mixing of different topologies of partonic 2-surfaces, 140
topological structure of a r- Energetic Level-FVWPET-examined, 335
topology
topology of L-Maximal Digital Hex-Spaces, 341
topology of space-time codes, 53
torsion (fields, torsion generating field), 208-209, 218, 232, 236-241, 243-250, 253-254, 258-259, 261-267, 269-271, 275, 282-287, 298-290, 385, 402
translation, 52, 97, 126, 215, 233
Trans-n-Riemannian Boundary, Trans-n-Riemannian Boundary, 332, 334, 350, 357
twisted structures (see: knotting), 73
two-dimensional Coulomb problem, 293

universal metabolic quanta, 44-45, 74
unatom, 185
uncertainty (notations, Schrödinger's uncertainty theorem), 36, 52, 67, 111, 181, 198, 233-234, 419
unenergy, 196
unforce, 196
ungravity, 188, 196
unification, unified
unification mechanism of gauge boson and fermion fields, including classical gravitation, 178-179
gauge bosons & fermions unified through a fundamentally different mechanism than the supersymmetry, 182, 183
un-ion, 185-186
unmatter, unmatter entities inside nuclei, 185-190, 192-196, 198-200, 203-204
unnucleus, 185
upper bound, 27, 37, 93, 95

UV photons, 45, 50, 69, 70, 74, 75, 77, 80

vacuum energy, 168-169, 177, 289
value
    experimental values, 4,
    Stable Value (StabVal), 339-341, 343, 345-348, 356
Verifying Unmatter by experiments, vi, 189, 204
Versor Type Functions (VTF), xvii, 332, 334, 362-368, 376-377
Versor Type Gradient dynamical systems, 362
vibrational dark photons, 96
vibrational modes, 96
viral infection, 362, 367, 380
VTF-foliations, 362, 367, 380
VTF-Methods, 332, 362, 368

wave function, ix, 19, 39, 91, 199, 203, 236, 238, 240, 253, 260, 262, 264-265, 275, 277- 278, 282-284, 296, 298, 310, 321-322
weighted/dynamical cloud, 362, 364-367, 380
wireless energy, wireless energy transmit, vii, 439, 442

Yang-Mills, iii, vi, ix, 208, 210-215, 218-219, 222, 227, 232, 270, 438, 443
Yukawa potential, 214, 216, 218, 220-222, 224, 436-437

- --- -

# Hadron models and related New Energy issues

The present book covers a wide-range of issues from alternative hadron models to their likely implications to New Energy research, including alternative interpretation of low-energy reaction (coldfusion) phenomena.

The authors explored some new approaches to describe novel phenomena in particle physics. M Pitkanen introduces his nuclear string hypothesis derived from his Topological Geometrodynamics theory, while E. Goldfain discusses a number of nonlinear dynamics methods, including bifurcation, pattern formation (complex Ginzburg-Landau equation) to describe elementary particle masses. Fu Yuhua discusses a plausible method for prediction of phenomena related to New Energy development.

F. Smarandache discusses his unmatter hypothesis, and A. Yefremov et al. discuss Yang-Mills field from Quaternion Space Geometry. Diego Rapoport discusses link between Torsion fields and Hadronic Mechanic.

A.H. Phillips discusses semiconductor nanodevices, while V. and A. Boju discuss Digital Discrete and Combinatorial methods and their likely implications to New Energy research. Pavel Pintr et al. describe planetary orbit distance from modified Schrödinger equation, and M. Pereira discusses his new Hypergeometrical description of Standard Model of elementary particles.

The present volume will be suitable for researchers interested in New Energy issues, in particular their link with alternative hadron models and interpretation.

While some of these discussions may be found a bit too theoretical, our view is that once these phenomena can be put into rigorous theoretical framework, thereafter more 'open-minded' physicists may be more ready to consider these New Energy methods more seriously. Our basic proposition in the present book is that considering these new theoretical insights, one can expect there are new methods to generate New Energy technologies which are clearly within reach of human knowledge in the coming years.

ISBN 1-59973-042-1

9 781599 730424 53995>